THE UNIVERSITY
of EDINBURGH

Investigating the Porcine Feto-Maternal Interface Throughout Gestation: Associations with Foetuses of Different Size and Sex

Claire Stenhouse

Thesis presented for the degree of Doctor of Philosophy

Developmental Biology

The University of Edinburgh

2018

Declaration

I declare that the work presented in this thesis is my own, except where otherwise stated. All experiments were designed and planned by myself in collaboration with my supervisors Prof. Cheryl J. Ashworth and Dr. F. Xavier Donadeu. No part of this thesis has been or will be submitted for any other degree, diploma or qualification.

Claire Stenhouse

March 2018

Lay Summary

There is often large variation within litter in the birth weight of piglets, with many litters having a ‘runt’ piglet. These piglets are at a permanent disadvantage compared to their normal-sized littermates. The weight of pig foetuses within the same uterus varies substantially, even during early pregnancy, suggesting that the differences observed after birth could arise early in development. Furthermore, it has been shown in human studies that placentas supplying male and female infants develop differently and respond differently to prenatal stressors but this is not yet fully understood in the pig.

This study investigated changes in the expression of genes and proteins in the pig uterus and placenta throughout pregnancy, in relation to the size and the sex of the foetus. A number of biologically important pathways and functions were investigated including the integrin signalling pathway (important in establishing pregnancy), cell death and division, blood flow in the umbilical artery and blood vessel formation and structure.

Monitoring of umbilical artery blood flow during pregnancy by Doppler ultrasound demonstrated that changes in the resistance of the vessel, the heart rate of the foetus, and the flow of blood changed during pregnancy in a similar way to other species. The size of the litter and the sex of the foetus did not influence uterine artery blood flow but the sex ratio of the litter and the weight of the foetuses did. The pregnant pigs were lightly sedated for about 30 minutes to ensure their movement did not affect the ultrasound traces and so allow reliable monitoring of umbilical artery blood flow. Interestingly, as the time that the mother was sedated increased, at days 60 and 90 pregnancy (length of pig pregnancy is 114 days), the heart rate of the foetuses decreased. This was not observed at days 30 and 45 of pregnancy. It was found that sedating a pregnant mother in early pregnancy decreased the weight of the foetuses in later pregnancy. It is hoped that the development of this method of ultrasound monitoring of uterine artery blood flow in the pig will allow monitoring of UA in ‘runt’ piglets throughout pregnancy.

The structure of placentas and endometrium supplying foetuses of different size and sex throughout pregnancy was investigated. It was found that the area of the placenta which acts as the interface between the foetus and the mother in placentas supplying small foetuses had altered blood vessel structure compared to those supplying normal-sized foetuses. Interestingly, at day 60 of pregnancy there was an increased number of blood vessels in this region in placentas supplying the small foetuses compared to those supplying the normal-sized foetuses. This then switched at day 90 of pregnancy, with placentas supplying the lightest foetuses having fewer blood vessels compared to those supplying the normal-sized foetuses. No relationships between the weight of the foetus and the structure of the endometrium were observed however, endometrial samples supplying females had an increased number of blood vessels at day 45 of pregnancy compared to those supplying males.

Due to the observed differences in the structure of the placenta and endometrium, the abundance of genes involved in the formation of blood vessels was investigated in both tissues. The results of this experiment suggested that the size and sex of a foetus was associated with the abundance of genes and proteins in both the placenta and the endometrium. A number of differences in gene expression were found in the endometrium early in pregnancy, but not in the placenta, which might suggest that embryos which are smaller and of different sex, interact differently with the endometrium from very early in pregnancy. Blood vessel-like structures were formed in the laboratory by treating the cells which make blood vessels with a solution that had been treated with placental and endometrial samples that supply foetuses of different size and sex. This experiment showed that placental and endometrial samples that supplied small foetuses had a decreased ability to make blood vessels compared to those supplying normal-sized foetuses. Placental samples supplying male foetuses could not make blood vessels as well as those supplying female samples. Interestingly, the opposite was observed in the endometrium, with samples supplying female foetuses having

a decreased ability to make blood vessels compared to those supplying male foetuses.

Similarly, the abundance of genes involved in the integrin signalling pathway, and cell death and division was altered in placental and endometrial samples that supply small foetuses compared to normal-sized foetuses, and foetuses of different sex.

This study has confirmed that placentas supplying small foetuses have a different structure and expression of a number of genes involved in integrin signalling pathway, cell death and division and blood vessel formation. It also found an interesting relationship between the size of a foetus and the endometrium, which has not previously been reported. For the first time, this study has shown that embryos of different sex interact differently with the placenta, and more interestingly the endometrium in the pig. Further experiments should be performed to improve the understanding of the processes of foetal growth and their interaction with the placenta and endometrium.

Abstract

Background

Inadequate foetal growth cannot be remedied postnatally, leading to severe consequences for neonatal and adult development. Furthermore, sexual dimorphism in placental development has been suggested in humans although this remains poorly investigated in the pig.

Hypotheses

Intrauterine Growth Restriction (IUGR) occurs due to aberrant conceptus attachment, which leads to alterations in angiogenesis and vascularity of the feto-maternal interface. Altered gene expression and vascularity will be observed at the feto-maternal interface in male foetuses compared to female foetuses. Increased apoptosis and decreased proliferation will be observed in the feto-maternal interface associated with the lightest foetuses compared to the closest to mean litter weight (CTMLW) foetuses.

Aims

This thesis aimed to investigate the association between foetal size and sex and: integrin signalling; apoptotic and proliferation pathways; umbilical arterial (UA) blood flow; and angiogenesis and vascularity at the feto-maternal interface. This was performed by the collection of placental and endometrial samples associated with conceptuses or foetuses of different size (lightest and CTMLW) and sex at gestational day (GD) 18, 30, 45, 60 and 90.

Results – Integrin Subunits, Secreted Phosphoprotein 1 (SPP1) and Fibronectin (FN)

Integrin receptors exist as heterodimers consisting of an α and a β subunit at the porcine feto-maternal interface. They bind to a number of ligands including secreted phosphoprotein 1 (SPP1) and fibronectin (FN), and play a central role

in the establishment of pregnancy. The mRNA expression of the integrin subunits (ITG) *ITGα2*, *ITGαV*, *ITGβ1*, *ITGβ3*, *ITGβ5*, *ITGβ6* and *ITGβ8*, and the ligands *SPP1* and *FN* was quantified by qPCR in placental and endometrial samples supplying foetuses of different size and sex throughout gestation. Temporal changes in mRNA expression were observed in both tissues. At GD45, placental samples supplying the lightest foetuses had increased *ITGα2* expression compared to those supplying the CTMLW foetuses (P=0.07). Endometrial samples supplying the lightest foetuses had decreased expression of *ITGβ1* and *SPP1* at GD45 and 60 respectively (P≤0.05). Placental samples associated with female foetuses had decreased expression of *ITGβ6* and *FN* (P≤0.05) compared to those supplying male foetuses at GD45 and 90 respectively. *FN* and *ITGβ3*expression was increased in endometrial samples supplying female foetuses compared to their male littermates at GD30 and 60 respectively (P≤0.05). In contrast, *SPP1* expression was decreased in endometrial samples supplying female foetuses compared to their male littermates at GD60 (P≤0.05). SPP1 protein staining per uterine gland was assessed throughout gestation by immunofluorescence. Whilst temporal changes in staining were observed, with a similar profile to the mRNA expression data, no associations between foetal size or sex, and uterine gland staining were observed.

Results – Apoptosis and Proliferation

The mRNA expression of candidate genes involved in apoptosis or proliferation (*Bax*, *Bcl2*, *P53* and *Ki67*) was quantified by qPCR. Temporal changes were observed in both tissues. Placentas associated with the lightest foetuses had decreased *P53* and *Ki67* expression compared to the CTMLW foetuses at GD45. However, at GD60, *P53* expression was increased in placentas supplying the lightest foetuses compared to CTMLW foetuses. Intriguingly, endometrial *P53* expression was increased in samples associated with the lightest foetuses compared to the CTMLW foetuses at GD45. A trend towards females having decreased placental *Bax* expression was observed at

GD45 (P=0.06). At GD60 the expression of *Bcl2*, *P53* and *Ki67* was decreased in endometrial samples associated with females compared to their male littermates. At GD30, *Bax* expression was increased in endometrial samples associated with female foetuses compared to their male littermates. TUNEL staining revealed an increased prevalence of apoptotic cells in placentas at GD60 compared to GD45 however, no association between foetal size or sex, and apoptotic cell number was observed.

Results – Doppler Ultrasound

Human IUGR is diagnosed prenatally by alterations in UA blood flow, detected by Doppler ultrasound. Doppler ultrasound was used under moderate sedation over a 30-minute period to monitor umbilical arterial (UA) blood flow in the right uterine horn of Large White X Landrace gilts at GD30, 45, 60 and 90. Gilts were scanned prior to euthanasia to examine relationships between litter size, sex ratio and five UA parameters of interest. In GD90 gilts where scans were obtained from all foetuses in the scanned horn, relationships between individual foetal weight and sex were examined. A subset of the gilts were sedated, scanned and recovered (SSR) earlier in gestation to assess the influence of sedation on later foetal development by comparing with control litters that had not been sedated previously. Temporal changes were observed in all UA parameters (P≤0.001). At GD60 and 90 foetal heart rate decreased with increasing duration of sedation (P≤0.001). Sex ratio and foetal weight were associated with UA blood flow whereas litter size and foetal sex were not. SSR at GD30 and 45 was associated with decreased foetal weight at GD60 (P≤0.001) and 90 (P=0.06), respectively, when compared to controls. These results suggest that maternal sedation during gestation has a significant effect on foetal development, the mechanisms of which warrant further investigation.

Results – Angiogenesis and Vascularity

Angiogenesis is essential for foetal and placental development and has been shown to be inadequately regulated in instances of complicated pregnancies. Immunohistochemistry on placental (GD45, 60 and 90) and endometrial (GD18, 30, 45, 60 and 90) samples for the endothelial cell marker Platelet and Endothelial Cell Adhesion Molecule 1 (CD31) was performed to assess placental and endometrial vascularity. At GD60, the percentage staining in the chorioallantoic membrane (CAM) of placentas supplying the lightest foetuses was increased compared to those supplying the CTMLW foetuses (P=0.06). The direction of this relationship switched at GD90, with placentas supplying the lightest foetuses having decreased percentage CD31 staining in the CAM compared to those supplying the CTMLW foetuses (P≤0.05). No association between foetal sex and placental vascularity was observed. At GD60, a trend for both the total (P=0.07) and mean number of blood vessels (BV) (P=0.07) to be decreased in endometrial samples supplying the lightest foetuses compared to the CTMLW foetuses was observed. Similarly, a trend towards a decrease in the mean number of uterine glands in endometrial samples supplying the lightest compared to the CTMLW foetuses was observed at GD90 (P=0.08). The total number of uterine glands (P≤0.05), total number of BV (P≤0.05) and mean number of BV (P≤0.05) were increased in endometrial samples supplying female foetuses compared to male foetuses at GD45.

The mRNA expression of candidate genes which are quantitative trait loci (QTL) associated or have a central role in angiogenesis and foetal development, including: Uteroferrin (*ACP5*), CD31, Hypoxia Inducible Factor 1 Alpha Subunit (*HIF1A*), Heparanase (*HPSE*), Prostaglandin F2α Receptor (*PTGFR*) and Vascular Endothelial Growth Factor A (*VEGFA)* were investigated by qPCR. Temporal changes in expression were observed in both tissues. *ACP5* expression was increased (GD60), whilst *HIF1A* (GD90) were decreased in placentas supplying the lightest foetuses compared to the CTMLW foetuses. *CD31* expression was decreased at GD45, and increased at GD60, in placental samples supplying the lightest foetuses compared to the CTMLW foetuses. Decreased expression of *CD31* (GD60), *HPSE* and *VEGFA*

(GD90), alongside increased *HIF1A* (GD45) expression were observed in endometrial samples supplying the lightest foetuses compared to the CTMLW foetuses. Decreased expression of *CD31*, *PTGFR* and *VEGFA* was observed in endometrial samples associated with male compared to female foetuses at GD30. At GD60, the direction of these differences in endometrial expression was reversed, with increased expression of *ACP5*, *CD31* and *VEGFA* in endometrial samples associated with male foetuses compared to their female littermates.

Results – *In vitro* Angiogenic Potential of Placental and Endometrial Samples

Matrigel branching assays were used to assess the angiogenic potential of GD45 and 60 placental and endometrial conditioned media on endothelial cell branching *in vitro*. Conditioned media from GD45 placental and endometrial samples increased endothelial cell branching *in vitro* compared to treatment with media from GD60 samples. Endothelial cell branching was impaired in response to treatment with conditioned media from placental and endometrial samples associated with the lightest foetuses compared to the CTMLW foetuses at both GD. At GD60, conditioned media from female placentas had increased endothelial cell branching compared to those supplying males. Interestingly, the inverse of this was observed in the endometrium, with samples supplying females having a decreased ability to induce endothelial cell branching compared with males.

Conclusion

This thesis has presented novel findings of associations between foetal size and sex, and placental and endometrial integrin signalling, apoptosis and proliferation, and angiogenesis and vascularity. Currently, this is the first suggestion in the literature that foetal size, and more intriguingly foetal sex, may have a strong influence on the activity of the endometrium. The

mechanisms behind these findings warrant further investigation. Switches in the direction of differences at the feto-maternal interface between foetuses of different size were observed throughout gestation, notably between GD45 and 60, highlighting the dynamic nature of the feto-maternal interface and suggesting this as a potential window that could be manipulated by the industry to attempt to rescue the postnatal phenotype of IUGR piglets.

Acknowledgements

First and foremost, I would like to thank my primary supervisor Prof. Cheryl Ashworth for giving me the opportunity to work with her on this interesting project. It is amazing to think that her enthusiasm for lactation in reproductive biology lectures all those years ago led us to where we are today. It has been challenging road but without her unwavering, continuous support and belief in my abilities, none of this would have been possible. Although our paths are beginning to diverge, I have no doubt our friendship will continue for many years to come and I will look back fondly on our time working together and speculating about all things pig related.

I would like to thank my second supervisor Dr Xavier Donadeu, and my thesis committee Dr Clare Pridans and Dr Liam Morrison for their advice, support and for keeping me on track.

None of this would have been possible without the support of the other Ashworth group members. I would like to thank Charis Hogg for her technical support and ability to fix anything - I would not be the scientist I am today without you. Research has lost an outstanding scientist, and I wish her every success in her new career – the teaching world have no idea how lucky they are to have her. It has been a pleasure doing my PhD alongside Selene Jarrett, and I value her friendship and advice immensely. From punting in Oxford, to exploring Missouri we have had many adventures together and I wouldn't change a thing. I also would like to thank Bob Fleming, the honorary Ashworth group member. Although on paper you were not part of the Ashworth group, you more than made up for this in your bioimaging and histology expertise, love of gin and rum and outrageous dance moves.

I would like to thank the other 'Reproductive Biology' group members Yennifer Cortés, Dr Jason Ioannidis, Dr Erin Williams and Dr Xavier Donadeu for their passionate scientific discussions and support. In the west wing, Dr Barry Bradford, Dr Sarah Caughey, Pete Wilson, Dec King, Val Bishop, Stefan Szymkowiak and Sam Eaton have provided essential technical support and lab banter.

Performing the large animal experiments described in this thesis takes a significant amount of planning and organisation. To all the individuals involved in the sample collections, from labelling tubes to guddling in pig reproductive tracts, I couldn't have done it without you. I would like to think all the Dryden Farm staff, especially Peter Tennant and Adrian Ritchie – without them the experiments would not have been possible. Prof. Colin Duncan and Prof. Eddie Clutton were fundamental in the design and optimisation of the Doppler ultrasound experiments and I am grateful to them both for taking time out of their busy schedules to assist. Prof. Aneta Andronowska provided timely assistance with the *in vitro* angiogenesis assays and kindly provided her immortalised endothelial cell line. When the results were finally obtained, Dr Darren Shaw's statistical support was vital in helping to explain and interpret sometimes unexpected results.

The Society for Reproduction and Fertility has been a fantastic source of support throughout my PhD. They not only provided financial support in the form of an academic scholarship to fund my research and travel grants to enable me to attend exciting conferences, but they have enabled me to present my work to the supportive SRF community, prompting interesting and insightful scientific discussions.

I could not have got through this PhD without the support of others who were not directly involved in the project. I would like to thank all of my friends at Roslin, especially Amy Fraser, Lorna Taylor and Lynn McTeir. You have been the best work family I could ever have hoped for and your banter, love, support and friendship have helped me through some difficult times. Outside of Roslin, Zoë Johnson has been my rock and, having followed similar paths from our reproductive biology honours days, I would be lost without her. To all of my friends out with science, especially Jemma Beveridge, Jenni Kenny, Erin Lynch and Nicola Thorburn, your support has meant the world to me.

Lastly, I would like to thank my family. Without you, none of this would be possible.

I dedicate this thesis to my grandfather Alasdair Kennedy, his support and encouragement are the reason I have pursued a career in science.

“I am fond of pigs. Dogs look up to us. Cats look down on us. Pigs treat us as equals.”

— Winston S. Churchill

Conferences Attended

3rd World Congress on Reproductive Biology, September 2nd-4th 2014 (Edinburgh, Scotland).

Society for Reproduction and Fertility Annual Conference, September 1st-2nd 2014 (Edinburgh, Scotland).

Society for Reproduction and Fertility Annual Conference, July 20th-22nd 2015 (Oxford, England) (Oral Presentation).

Society for Reproduction and Fertility Annual Conference, 11th-13th July 2016 (Winchester, England) (Poster Presentation/Oral Presentation by supervised MSc Student).

18th International Congress on Animal Reproduction, June 26th-30th 2016 (Tours, France) (Poster Presentation).

Fertility 2017, 5th-7th January 2017 (Edinburgh, Scotland) (Poster Presentation)

10th International Conference on Pig Reproduction, June 11th-14th 2017 (Columbia, Missouri) (Poster Presentation).

Little Embryos Do Make Big Decisions Symposium, July 7th 2017 (Southampton, England) (Poster Presentation).

Fertility 2018, 3rd-5th January 2018 (Liverpool, England) (Oral Presentation)

Publications

Manuscripts

Stenhouse C, Tennant P, Duncan CW, Ashworth CJ. Impact of gestational age and repeat sedation on umbilical arterial blood flow in sedated gilts using Doppler ultrasound (Published online early 4th May 2018. Reproduction, Fertility and Development).

Stenhouse C, Hogg CO, Ashworth CJ. Associations between Fetal Size, Sex and Placental Angiogenesis in the Pig (Revision under review June 2018. Biology of Reproduction).

Stenhouse C, Hogg CO, Ashworth CJ. Associations between Fetal Size, Sex and both Proliferation and Apoptosis at the Porcine Feto-Maternal Interface (Under Review June 2018. Placenta).

Manuscripts in Preparation:

Stenhouse C, Hogg CO, Ashworth CJ. Associations between Fetal Size, Sex and Endometrial Angiogenesis in the Pig (Working Title).

Stenhouse C, Hogg CO, Ashworth CJ. Foetal size and sex are associated with proliferation and apoptosis at the feto-maternal interface (Working Title).

Stenhouse C, Hogg CO, Ashworth CJ. Associations between Foetal Size, Sex and Fibronectin, SPP1 and Integrin mRNA expression at the porcine feto-maternal interface (Working Title).

Stenhouse C, Hogg CO, Ashworth CJ. Characteristics of litters containing IUGR foetuses throughout gestation (Working Title).

Stenhouse C, Hogg CO, Ashworth CJ. Identification of Appropriate Reference Genes for qPCR analyses of Porcine Placental and Endometrial Samples at Gestational Days 30, 60 and 90 (Working Title)

Abstracts

Ashworth CJ, Avey B, Stenhouse C, Sauter K, Waddell L, Hogg CO, Lisowski Z, Hume D (2016) The effect of macrophage colony-stimulating factor (CSF1) on piglet gonad development. Reproduction Abstracts 3 P051.

Ashworth CJ, Avey B, Stenhouse C, Sauter K, Waddell L, Hogg, CO, Lisowski Z., Hume D (2017) The effect of macrophage colony-stimulating factor (CSF1) on piglet gonad development. 10th International Conference on Pig Reproduction Proceedings P35.

Ashworth CJ, Stenhouse C (2015) Placental Contribution to Fetal Growth, IUGR and Piglet Birth Weight. Proceedings of the XVII ABRAVES Congress, Campinas, Brazil, Volume I, pp 86-87.

Moolnangdeaw A, Stenhouse C, Ashworth, CJ (2016) The role of integrin AVB6 in the regulation of foetal growth in pigs. Reproduction Abstracts 3 O029.

Stenhouse C, and Ashworth CJ (2017) Integrin subunit expression in porcine endometrial tissue supplying small and normal-sized foetuses throughout gestation. Fertility 2017 Conference Handbook P185.

Stenhouse C, Hogg CO, Ashworth CJ (2017) Foetal size and sex influence placental and endometrial mRNA expression of angiogenesis related genes throughout gestation in the pig. Little Embryos Do Make Big Decisions Symposium Abstract Book p15 P1.

Stenhouse C, Hogg CO, Donadeu FX, Ashworth CJ (2015) Investigation into the role of endometrial heparanase, hypoxia-inducible factor 1A, secreted phosphoprotein 1, uteroferrin, and vascular endothelial growth factor A in foetal growth in pigs. Reproduction Abstracts, Society for Reproduction and Fertility Annual Conference, Volume 2, p16, Abstract O027.

Stenhouse C, Hogg CO, Donadeu FX, Ashworth CJ (2016) Alterations in the vasculature of placental but not endometrial tissue associated with small porcine foetuses compared to their normal-sized littermates. Reproduction Abstracts 3 P007.

Stenhouse C, Hogg CO, Donadeu FX, Ashworth CJ (2016) Alterations in the Vasculature of Placental but not Endometrial Tissue Associated with Small Porcine Fetuses Compared to their Normal-Sized Littermates at Gestational Day 60. 18th International Conference on Animal Reproduction Conference Proceedings PW1315.

Stenhouse C, Tennant P, Duncan CW, Ashworth CJ (2017) Foetal heart rate and umbilical arterial resistance index, detected by non-invasive Doppler ultrasound, decrease throughout gestation in pigs. 10th International Conference on Pig Reproduction Proceedings 106.

Table of Contents

Table of Figures

Table of Tables

List of Abbreviations

11βHSD2	11β-Hydroxysteroid dehydrogenase 2
4EBP1/eIF4E	Eukaryotic Translation Initiation Factor 4E
ACP5	Uteroferrin
ACTB	Beta Actin
ACTH	Adrenocorticotrophic Hormone
AGD	Anogenital Distance
AHRR	Aryl-Hydrocarbon Receptor Repressor
Akt	Protein Kinase B
ALF	Allantoic Fluid
AMF	Amniotic Fluid
ANOVA	Analysis of Variance
Apaf1	Apoptotic Protease Activating Factor 1
ASPRs	Aspartyl-tRNA synthetase
B2M1	Beta-2-microglobulin
Bak	Bcl-2 Homologous Antagonist/Killer
Bax	Bcl-2-Associated X Protein
Bcl2	B-cell lymphoma 2
BL	Basal Lamina
BV	Blood Vessel
CAM	Chorioallantoic Membrane
cAMP	Cyclic Adenosine Monophosphate
CD31	Platelet and Endothelial Cell Adhesion Molecule 1
cFLIP	Cellular FLICE (FADD-Like IL-1β-Converting Enzyme)-Inhibitory Protein
CL	Corpus Luteum
COL1A	Collagen type 1 alpha
COX2	Cyclooxygenase 2
CRH	Corticotrophin Releasing Hormone
CRL	Crown-Rump Length
CSF2	Colony Stimulating Factor 2
CTMLW	Closest to Mean Litter Weight
CXCL	Chemokine Ligand
DAPI	4',6-Diamidino-2-Phenylindole
DISC	Death-Inducing Signalling Complex
DMEM-F12	Dulbecco's Modified Eagle's Medium/Nutrient Mixture F-12 Ham
dpc	Days Post-Coitum
E2	Oestradiol
ECGS	Endothelial Cell Growth Supplement
ECM	Extracellular Matrix
EDTA	Ethylenediaminetetraacetic Acid
EDV	End Diastolic Velocity
eEF1A-1	Eukaryotic Translation Elongation Factor 1

EIF5A2	Eukaryotic Translation Initiation Factor 5A2
EIF6	Eukaryotic Translation Initiation Factor 6
ELISA	Enzyme-Linked Immunosorbent Assay
eNOS	Endothelial Nitric Oxide Synthase
ERK	Extracellular Signal–Regulated Kinase
Erk3	Mitogen-activated protein kinase (MAPK6)
FA	Focal Adhesion
FACS	Fluorescent Activated Cell Sorting
FGF	Fibroblast Growth Factor
FHR	Foetal Heart Rate
FN	Fibronectin
Fwd	Forward
G6PD	Glucose-6-Phosphate Dehydrogenase
GA	General Anaesthesia
GAPDH	Glyceraldehyde-3-Phosphate Dehydrogenase
GD	Gestational Day
GE	Glandular Epithelium
hCG	human Chorionic Gonadotrophin
HGPRT	Hypoxanthine-Guanine Phosphoribosyl transferase
HIF1A	Hypoxia Inducible Factor 1 Alpha Subunit
hLW	Hyperprolific Large White
HMBS2	Hydroxymethylbilane Synthase
HNRNPK	Heterogeneous Nuclear Ribonucleoprotein K
HPA	Hypothalamus-Pituitary-Adrenal
HPRT1	Hypoxanthine phosphoribosyltransferase 1
HPSE	Heparanase
HRE	Hypoxia Response Element
HS	Heparan Sulphate
HSCs	Haematopoietic Stem Cells
IGF	Insulin-like Growth Factor
IgG	Immunoglobulin G
IL1B	Interleukin 1 β
INSL3	Insulin Like Peptide 3
ITG	Integrin Subunit
ITIMs	Immunoreceptor Tyrosine-Based Inhibitory Motifs
IUGR	Intrauterine Growth Restriction
IVF	In Vitro Fertilisation
KGF	Keratinocyte Growth Factor
Lad	Ladder
LE	Luminal Epithelium
LIF	Leukaemia Inhibitory Factor
LS	Litter Size
M199	Medium-199
MAPK	Mitogen-Activated Protein Kinase

MLKL	Mixed Kinase Domain-Like
MLW	Mean Litter Weight
MS	Meishan
mTOR	Mammalian Target of Rapamycin
n/a	Not Applicable
NBCS	Newborn Calf Serum
NBW	Normal Body Weight
NOXA	Phorbol-12-Myristate-13-Acetate-Induced Protein 1
NRT	No Reverse Transcription Control
NTC	No Template Control
OD	Optical Density
OPN	Osteopontin
OR	Ovulation Rate
OX	Ovariectomised
P21	Cyclin-Dependent Kinase Inhibitor 1
P4	Progesterone
p53	Tumour Protein 53
PBS	Phosphate Buffered Saline
PCNA	Proliferating Cell Nuclear Antigen
PCR	Polymerase Chain Reaction
PenStrep	Penicillin-Streptomycin
PFA	Paraformaldehyde
PGF2α	Prostaglandin F2α
PGK	Phosphoglycerate Kinase
PGs	Prostaglandins
PI	Ponderal Index
PI3K	Phosphatidylinositol-4,5-Bisphosphate 3-Kinase
PlGF	Placental Growth Factor
PMSG	Pregnant Mare Serum Gonadotrophin
PPARGC1A	Peroxisome proliferator-activated receptor gamma coactivator 1-alpha
PPS	Percentage Prenatal Survival
p-STAT3	phosphorylated Signal Transducer and Activator of Transcription 3
PSV	Peak Systolic Velocity
PTGFR	Prostaglandin F2α Receptor
PUMA	P53 Upregulated Modulator of Apoptosis
qPCR	Quantitative Polymerase Chain Reaction
QTL	Quantitative Trait Loci
Rev	Reverse
RT	Reverse Transcription
RGD	Arginine-Glycine-Asparagine
RI	Resistance Index
RINe	RNA Integrity Number equivalent
RIPK	Receptor Interacting Protein Kinase 1

RPL4	Ribosomal protein L4
RPS6	Ribosomal Protein S6
RT	Reverse Transcription
S.E.M.	Standard Error of the Mean
SA	Surface Area
SC	Sample Collection
SD	Standard Deviation
SDHA	Succinate dehydrogenase complex, subunit A
SGA	Small for Gestational Age
SIBLING	Small Integrin-Binding Ligand, N-Linked Glycoproteins
SIRT2	Sirtuin 2
SPP1	Secreted Phosphoprotein 1
Sqrt	Square Root
Sry	Sex Determining Region on the Y Chromosome
SSR	Sedate, Scan, Recovery
TA	Transabdominal
TAE	Tris Base, Acetic acid and EDTA
TAMV	Timed Average Mean Velocity
TBP1	TATA box binding protein
Tdt	Terminal deoxynucleotidyl transferase
TLN	Talin
TLW	Total Litter Weight
TNF	Tumour Necrosis Factor
TOP2B	Topoisomerase II beta
TR	Transrectal
TRAP	Tartrate-Resistant Acid Phosphatase
TUNEL	Terminal deoxynucleotidyl transferase dUTP nick end labelling
UA	Umbilical Arterial
VEGF	Vascular Endothelial Growth Factor
vWF	von Willebrand Factor
Wnt	Wingless-Type MMTV Integration Site Family
XIAP	X-linked inhibitor of apoptosis protein
YWHAZ	Tyrosine 3-Monooxygenase/Tryptophan 5-Monooxygenase Activation Protein Zeta
ZFP	Zinc Finger Protein

1 General Introduction

1.1 Importance of Improving Pig Reproduction for the Porcine Industry

The human population is projected to reach 9.8 billion by 2050 (https://www.un.org/development/desa/en/news/population/world-population-prospects-2017.html accessed 13th March 2018) and this, coupled with increased meat consumption as countries become more affluent (Kearney, 2010), will undoubtedly place a strain on the available meat resources. Pork is a valuable source of protein and nutrients (Wyness, 2016), and is the most highly consumed meat worldwide (http://www.fao.org/home/en/ accessed 14th March 2018). To meet the increasing human nutritional demands it is therefore essential to optimise and increase pig production.

The number of live born piglets per year, piglets weaned per sow per year and the number of litters farrowed per sow per year are economically important traits for the pig industry (Koketsu *et al.*, 2017). In the U.K., the average values for these traits are 23.97-26.8, 12.11-13.3 and 2.28-2.3 respectively, depending upon the breeding system used (December 2017 figures https://pork.ahdb.org.uk/prices-stats/costings-herd-performance/ accessed 14th March 2018). To increase pig production, genetic selection for favourable traits such as litter size (LS) and ovulation rate (OR) has been utilised with an aim to increase the number of piglets weaned per sow per year (Bee, 2007). This strategy has been successful in increasing the number of live born piglets. For example, an increase in the number of live born piglets from 11.2 to 14.8 in Denmark and 10.8-11.4 in the U.K. was observed between 1996 and 2011 (Rutherford *et al.*, 2013). Unfortunately, it has also increased the within-litter variation in piglet size, and the prevalence of low-birthweight piglets (Quiniou *et al.*, 2002). Further, it has been suggested that as LS increases, individual piglet weight at birth decreases (Bauer *et al.*, 1998; Quiniou *et al.*, 2002). Considering this, the pig industry aims to improve the within-litter uniformity in piglet weight at birth without compromising individual birth weight, whilst

increasing the number of piglets weaned per sow per year, which would be financially advantageous to the agricultural industry (Bee, 2007).

Investigations must be performed to determine when within-litter variation in piglet size arises during gestation, and the mechanisms governing this, to achieve the desired LS, whilst reducing within-litter variation in piglet size.

1.2 Female Pig reproduction

Puberty occurs in the female pig at around 150-220 days and is characterised by their first oestrous cycle, although mating is not usually performed until the third oestrous cycle (Soede *et al.*, 2011). The oocytes are released into the oviduct where they can be fertilised (Figure 1.1). The female pig has a bicornuate uterus, composed of two uterine horns, two ovaries and oviducts, a cervix, vagina and vulva (Ashworth, 2006) (Figure 1.1). At the ends of the uterine horns are two ovaries which contain follicles that house the oocytes (gametes). The oestrous cycle in the pig is approximately 21 days long, composed of a follicular phase, after which ovulation occurs, followed by a luteal phase (Soede *et al.*, 2011). Within this 21-day cycle, oestrus, when the pig is receptive to mating, can be observed for approximately 48 hours which corresponds to ovulation. Pigs are a spontaneous polyovulatory species therefore, multiple oocytes are ovulated from both ovaries during ovulation, with 15-30 oocytes ovulated each cycle (Soede *et al.*, 2011). In addition, OR is influenced by breed (Christenson, 1993), nutrition (Prunier and Quesnel, 2000; Cárdenas and Pope, 2002; Hazeleger *et al.*, 2005) and maturity, with gilts having a lower OR than sows (Soede *et al.*, 2011).

1.2.1 Pregnancy

1.2.1.1 Fertilisation and Embryo Development

The sperm travel through the reproductive tract towards the oviduct where they can fertilise the oocytes, forming the one-cell embryo (zygote) (Figure 1.2). The ovulated oocytes will reach the ampulla region of the oviduct, the site of

fertilisation, within an hour of ovulation occurring where they remain viable until 8-12 hours post-ovulation. Pigs have an exceptionally high fertilisation rate of >90% (Wright *et al.*, 1983; McGeady *et al.*, 2018). However, considering the short viability of the oocytes, this success rate is heavily influenced by timing of insemination (Soede *et al.*, 1995). Following fertilisation, the zygote undergoes rapid cell division which leads to the formation of the morula (16 cells). Once the embryo has reached the morula stage it enters the uterus and undergoes compaction, forming the blastocyst approximately five days after fertilisation. The blastocyst contains cells which will go on to produce both the placenta (the trophectoderm) and all cell lineages in the developing embryo (the inner cell mass) (Figure 1.2). The blastocyst hatches from the zona pellucida and expands further. Initially, the hatched spherical blastocyst changes into a tubular form, which is followed by elongation of the trophectoderm to form a filamentous embryo (Figure 1.2). This elongation step is characterised by changes in the structure of the cytoskeleton (Geisert *et al.*, 1982; Albertini *et al.*, 1987; Mattson *et al.*, 1990). Once the conceptuses undergo elongation, they migrate freely around the uterus before evenly spacing themselves (Perry and Rowlands, 1962; Anderson and Parker, 1976), beginning the attachment process (Figure 1.3).

Gastrulation is the process by which the blastocyst differentiates into three distinct somatic cell layers (ectoderm, mesoderm and endoderm) and is a highly conserved process across species (Mikawa *et al.*, 2004; Solnica-Krezel and Sepich, 2012). It has been demonstrated that gastrulation occurs during the initiation of elongation of the porcine conceptuses (Wolf *et al.*, 2011) and, in contrast to mice and humans (Fléchon *et al.*, 2004; Blomberg *et al.*, 2006), it is not dependent on implantation (Hyttel *et al.*, 2011). Following completion of gastrulation (process reviewed by Hyttel *et al.*, 2011), the embryo contains the three somatic cell layers and the germ cell lineage (primordial germ cells). Organ development is very similar to that of the human foetus, and by approximately gestational day (GD) 35, the basis of all the organs have formed. Foetal growth is initially slow followed by exponential growth in late gestation, when the placenta is no longer undergoing rapid development

(Figure 1.5) (Marrable, 1971; McPherson *et al.*, 2004; Ji *et al.*, 2005). In contrast to some other species, the porcine liver undergoes rapid development in early gestation, slowing its growth rate in late gestation (Dyce *et al.*, 1996; Bazer *et al.*, 2001).

Whilst there is a high fertilisation rate in the pig (>90%), there is a significant amount of prenatal death (30-50% of conceptuses) (Pope, 1994; Ford *et al.*, 2002; Geisert and Schmitt, 2002). Much of the prenatal death occurs before GD30 (20-30% of conceptuses), with a suggestion that the majority of the prenatal death occurs between GD12-18 (Stroband and Van der Lende, 1990; Pope, 1994; Ford *et al.*, 2002; Geisert and Schmitt, 2002). There is then a second wave of prenatal loss between GD50 and 90 (10‑15% of conceptuses) (Ford *et al.*, 2002; Vonnahme *et al.*, 2002; Vallet *et al.*, 2011), which is hypothesised to occur due to inadequate uterine capacity (Webel and Dziuk, 1974).

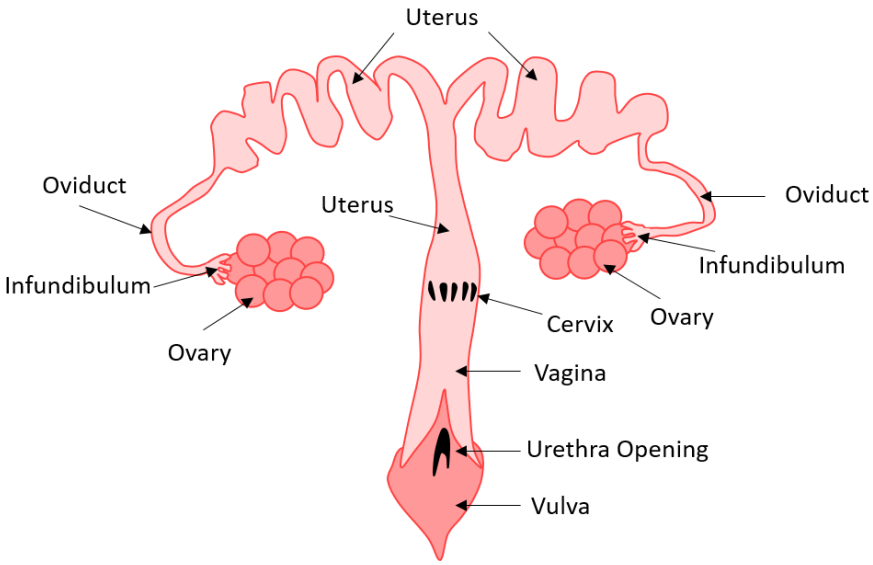

Figure 1.1: Structure of Pig Female Reproductive Tract.

At the ends of the uterine horns, are two ovaries which contain the oocytes which allow the mother to pass genetic material to her offspring. Oocytes are released from the ovaries, and collected in the infundibulum, where they are channelled into the oviduct. Oocytes can be fertilised by sperm here, and embryos are then transferred to the uterus where they implant and develop until 114 days of gestation when parturition occurs. The uterus is connected to the vagina by the cervix. The vulva is externalised and changes in its appearance can be used to indicate when the pig is in oestrus. The reproductive tract kept in position by the broad ligament (connective tissue), which runs continuously from the spine around the abdominal cavity. Redrawn and adapted from Lorenzen *et al.*, (2015).

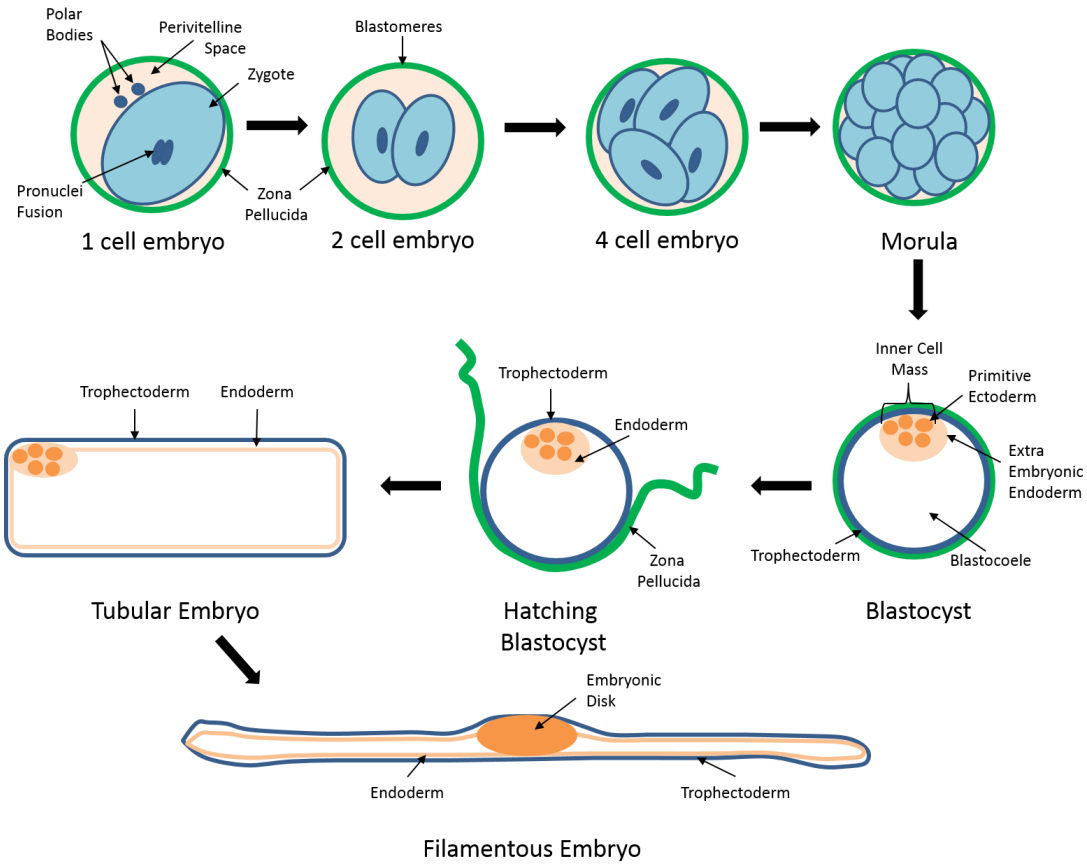

Figure 1.2: Preimplantation Embryonic Development in the Pig.

After mating or insemination, the sperm travel to the oviduct where fertilisation of the ovulated oocyte occurs, to form the one-cell embryo. Rapid cell division occurs leading to the formation of the morula (16 cells). Once the embryo has reached the morula stage it enters the uterus and undergoes compaction, ultimately leading to the formation of the blastocyst at five days post-fertilisation. The blastocyst hatches from the zona pellucida and can then expand further and begin migration. Initially the hatched spherical blastocyst changes formation into a tubular form, which is followed by elongation of the trophectoderm to form a filamentous embryo. Redrawn from Bazer *et al.*, (2009).

1.2.1.2 Establishment and Recognition of Pregnancy

Gestation in the pig lasts for approximately 114 days. During the peri-implantation period (~GD11 and 15), the elongating porcine conceptus secretes oestradiol-17β (E2). E2 induces a switch in the mode of prostaglandin F2α (PGF2α) secretion from an endocrine approach (uterine venous drainage), to an exocrine approach (uterine luminal secretion), allowing it to act directly on the uterus (Bazer and Thatcher, 1977). As PGF2α in the absence of E2 induces luteolysis (McCracken *et al.*, 1999), this change in mode of secretion prevents the regression of the *corpus luteum* (CL), maintaining progesterone (P4) production and allowing the establishment and maintenance of pregnancy (Bazer, 2013; Ziecik *et al.*, 2017).

In addition to preventing luteolysis, embryonic E2 secretion induces transcriptional changes in the endometrium to prepare for implantation between GD13 and 15 (Bazer, 2013). Secreted phosphoprotein 1 (SPP1) (White *et al.*, 2005) (discussed in chapter 4) and fibroblast growth factor 7 (FGF7, also known as keratinocyte growth factor (KGF)) (Ka *et al.*, 2000, 2001, 2007) uterine luminal epithelial (LE) secretion is induced by conceptus secreted E2, and is known to induce cell proliferation, adhesion and migration during the peri-implantation period. Several other molecules have been demonstrated to be expressed at the feto-maternal interface during implantation including epidermal growth factor (EGF), insulin-like growth factor-1 (IGF1) (Ashworth *et al.*, 2005), leukaemia inhibitory factor (LIF) (Blitek *et al.*, 2012), vascular endothelial growth factor (VEGF), and colony stimulating factor 2 (CSF2) and their receptors (reviewed by Jeong and Song, 2014). These molecules have been suggested to have a role in apoptosis, proliferation and angiogenesis, which are discussed in more detail later in this thesis. In addition to the secretion of E2, the conceptus has also been demonstrated to secrete interleukin 1 beta (IL1B) during this period. This molecule plays a central role in the regulation of conceptus elongation, and the conceptus secreted E2 regulates the response of the uterus to IL1B (Ross *et al.*, 2003; Geisert *et al.*, 2017).

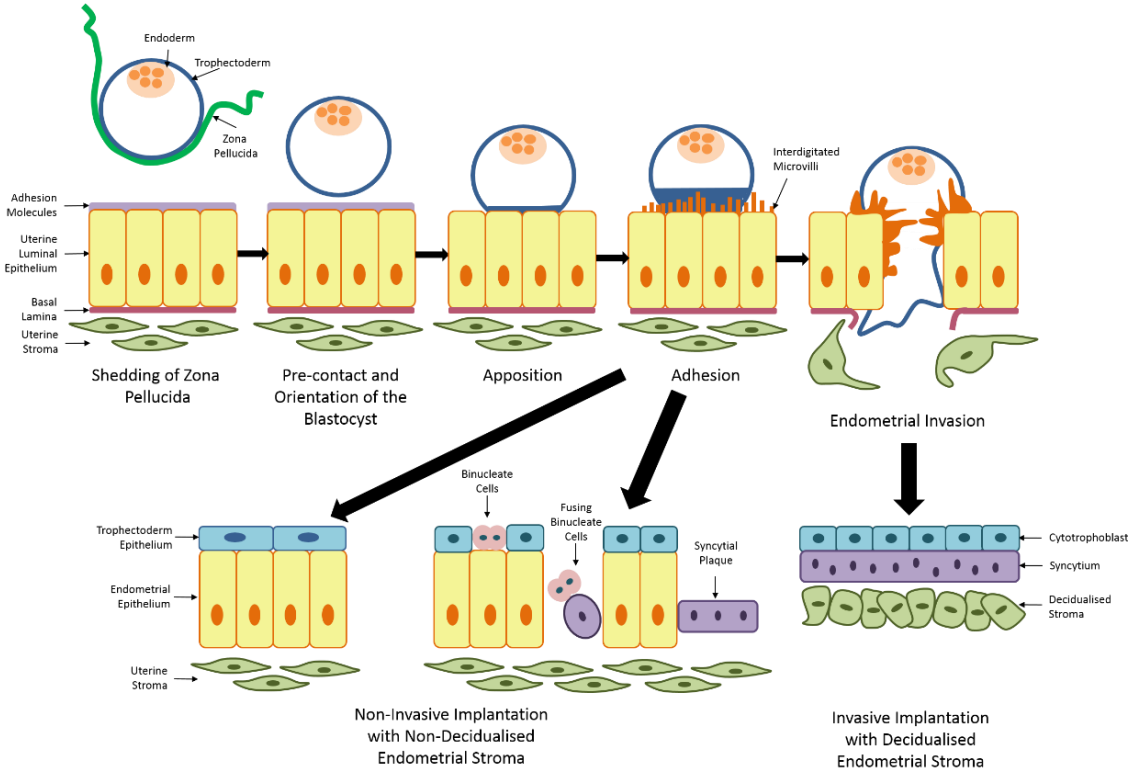

Figure 1.3: Implantation in Species with Invasive and Non-Invasive Placentation.

The blastocyst hatches from the zona pellucida, allowing expansion and elongation to occur in domestic animals. During the apposition phase, the blastocysts migrate around the uterus and optimise their orientation with the inner cell mass positioned at the mesometrial side. During this stage in ruminants, villi extend into the superficial ducts of the uterine glands which improves the adhesion of the blastocyst to the endometrium, whilst improving nutrient transfer. Following apposition, the trophectoderm cells attach to the underlying uterine luminal epithelium, and in some species to the glandular epithelium. In ruminants, during this stage interdigitation occurs between the uterine luminal epithelial cells and the trophectoderm for the later development of the placentomes. In some ruminant species, the trophectoderm cells differentiate intro giant trophoblast cells which are binuclear. In the pig, the resulting interface is non-invasive and composed of a layer of trophectoderm epithelial cells, the uterine luminal epithelial cells, with the uterine stromal cells below this. In ruminants, which exhibit an intermediate level of implantation, in addition to what is observed in the pig, syncytial plaques are also present. In species like humans where implantation is fully invasive, the uterine stromal cells undergo decidualisation and the blastocyst invades the uterine luminal epithelium, with the resulting interface having cytotrophoblasts, a syncytium and decidualised endometrial stromal cells. Redrawn from Bazer *et al.*, (2009).

1.2.1.3 Placentation

1.2.1.3.1 Placentation types.

Internal foetal development is a strategy used by most mammalian species which has the benefit of protecting the foetus(es) from fluctuations in environmental conditions such as temperature, and from predation (Maltepe and Fisher, 2015), improving the survival rate of the offspring compared to species which undergo external foetal development. However, internal foetal development requires significant maternal investment (Boehlert *et al.*, 1991; Qualls and Shine, 1995; Maltepe and Fisher, 2015). Mammalian species have an amnion membrane which encapsulates the developing embryo. They also have two additional membranes, the chorion and allantois, which form the placenta and umbilical cord (Maltepe and Fisher, 2015). In the pig, an allanto-chorionic membrane, also known as the chorioallantoic membrane (CAM) forms from the fusion of the mesoderm covering the allantois with the mesoderm lining the chorion (Perry, 1981).

Despite the striking similarities that exist between mammalian species during pregnancy, placentation varies substantially (Figure 1.4) (Enders and Blankenship, 1999; Enders and Carter, 2004; Montiel *et al.*, 2013). Humans exhibit invasive haemochorionic placentation, whereby the trophectoderm cells are in direct contact with maternal blood. Endotheliochorionic placentation is partially invasive, with only the wall of the maternal vessel and the interstitial membrane separating foetal tissues from the maternal blood and is observed in dogs and cats. The pig has an epitheliochorial placenta which is the least invasive type of placenta, with three layers separating the foetal tissue from the maternal blood.

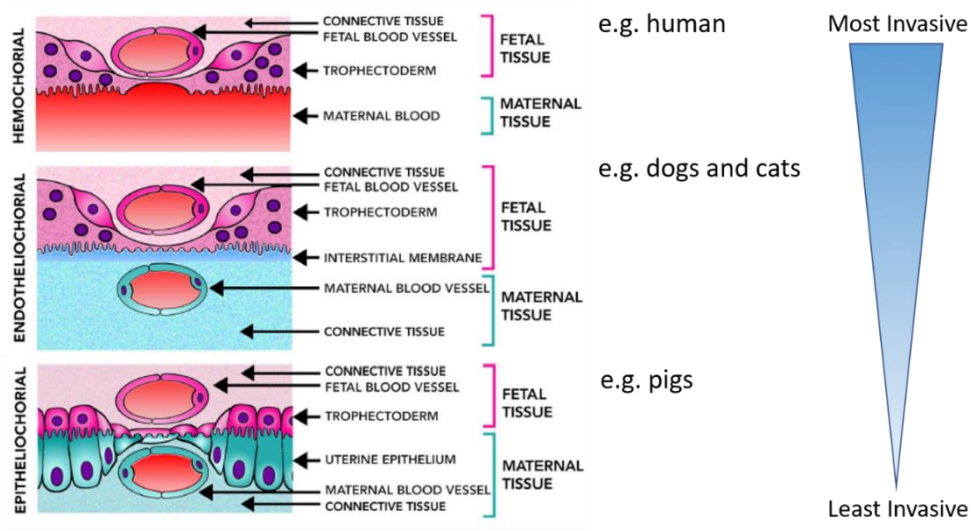

Figure 1.4: Illustration of the Variation in Placental Invasiveness between Species.

Haemochorial placentas are highly invasive with the foetal trophectoderm cells being in direct contact with maternal blood. Endotheliochorial placentas have an intermediate level of invasiveness, with foetal tissues being in close proximity to maternal blood, separated only by the wall of the maternal blood vessel and the interstitial membrane. Epitheliochorial placentas are the least invasive, with the wall of the maternal vessel, connective tissue and uterine epithelium separating the maternal blood from the trophectoderm cells. Adapted from Montiel *et al.*, (2013).

1.2.1.3.2 Uterine Structure

The endometrium is essential in the establishment and maintenance of a successful pregnancy. The uterus has a layer of smooth muscle, termed the myometrium. Inside this, the endometrium lines the inside of the uterine horn forming a lumen. The endometrium is composed of two types of epithelium: the luminal epithelium (LE) and glandular epithelium (GE) and stromal cells (Figure 1.7). Uterine glands secrete nutrients into the uterine lumen, and they undergo morphological changes throughout gestation to increase the availability of nutrients to the developing foetus (Spencer and Bazer, 2004). These nutrients are collectively known as the histotroph and are the sole source of nutrition for the conceptus prior to the development of the placenta.

1.2.1.3.3 Placental Development in the Pig

Following implantation and the maternal recognition of pregnancy, the trophectoderm layer begins to form the placenta. Between GD17 and 22, fluids accumulate around the foetus to push the allantois towards the endometrium, so that nutrients can transfer from the histotroph to the foetus (Knight *et al.*, 1977; Goldstein *et al.*, 1980). Throughout gestation these fluids are essential for foetal development. The foetus is buoyant in amniotic fluid (AMF), which is important to ensure symmetrical growth and to protect the foetus (Figure 1.6). AMF has a dynamic composition throughout gestation and is a central source of nutrition to the developing foetus. Further, this fluid is important in ensuring the developing skin of the foetus does not adhere to the amnion. Surrounding the amniotic sac is the allantoic fluid (ALF) contained within the CAM and this fluid is essential for the transport of nutrients, especially iron (Bazer *et al.*, 2012a).

At approximately GD30, the pig placenta forms dome-like structures called areolae at the placental regions adjacent to each uterine gland (Friess *et al.*, 1981). These structures absorb secretions from the maternal endometrium, known as the histotroph, to transport nutrients to the developing foetus (Friess *et al.*, 1981; Ducsay *et al.*, 1982). The placenta undergoes significant

proliferation from approximately GD20 to 60 to increase in size (Marrable, 1971; Knight *et al.*, 1977; Wu *et al.*, 2005; Wright *et al.*, 2016), after which its growth plateaus (Figure 1.5). As described in 1.2.1.3.1, the pig placenta is non-invasive therefore, to maximise the surface area (SA) available for exchange, a folded bilayer forms (Dantzer, 1985; Rootwelt *et al.*, 2012, 2013) (Figure 1.7).

It has been suggested that during the initial period of development of the microfolds of the bilayer (GD32-37), the placenta does not increase in weight (Wright *et al.*, 2016). This strategy, whereby placental remodelling is of greater importance than increasing in weight, is important to increase the SA available for nutrient transfer, allowing foetal growth and development to take place. In early gestation, the placental regions adjacent to the foetus have high vascularity whereas areas not adjacent to the foetus have decreased vascularity (Flood, 1973; Wright *et al.*, 2016). In contrast to the regions of high vascularity where fold formation can be observed from GD27, the regions with low vascularity do not develop folds until GD32-37. As the growth rate of the placenta decreases, the foetus increases its growth rate (Figure 1.5). Therefore, the placental SA must increase to facilitate increased nutrient exchange between the mother and the foetus (Leiser and Dantzer, 1994; Vallet and Freking, 2007). It does this by increasing the width of the microfolds from GD65 to 105 (Vallet and Freking, 2007).

The tissue at the ends of the placentas become necrotic from as early as GD27 (Flood, 1973; Wright *et al.*, 2016), and are therefore known as the ‘necrotic tips’. These regions have very few blood vessels, meaning that minimal nutrient exchange occurs (Wright *et al.*, 2016), and become increasingly necrotic throughout gestation, eventually losing all vascularity (Ashdown and Marrable, 1967; Flood, 1973; Wright *et al.*, 2016).

The growth and development of the placenta is related to uterine capacity (the number of foetuses the uterus can accommodate), placental vascular development and LS (Knight *et al.*, 1977; Vallet and Freking, 2007). It has been suggested that as LS increases, piglet weight at birth decreases (Bauer *et al.*, 1998; Quiniou *et al.*, 2002), which is thought to occur due to uterine crowding.

Further, it has been suggested that uterine crowding decreases placental weight (Vallet and Freking, 2007; Foxcroft *et al.*, 2009; Mesa *et al.*, 2012; Rootwelt *et al.*, 2012, 2013). Variations exist in placental growth between breeds, with breeds with increased LS and improved within-litter uniformity having increased placental vascularity compared to breeds with decreased LS and poor within-litter uniformity (Vonnahme *et al.*, 2002).

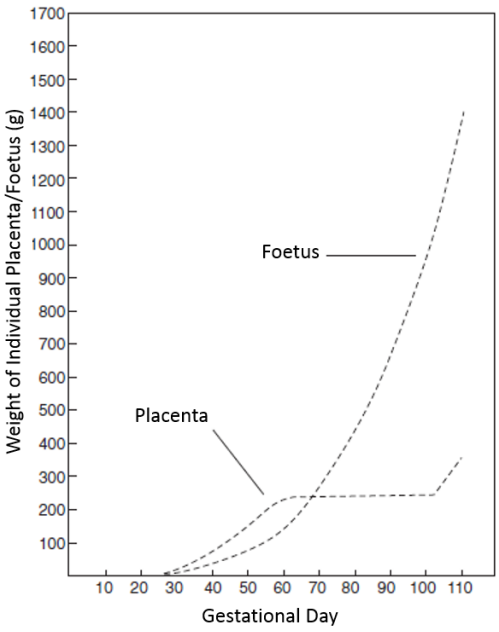

Figure 1.5: Placental and Foetal Growth Trajectories in the Pig.

The placenta initially develops at a faster rate than the foetus. Placental growth plateaus in mid-gestation, when foetal growth begins to grow exponentially. Adapted from Marrable, (1971).

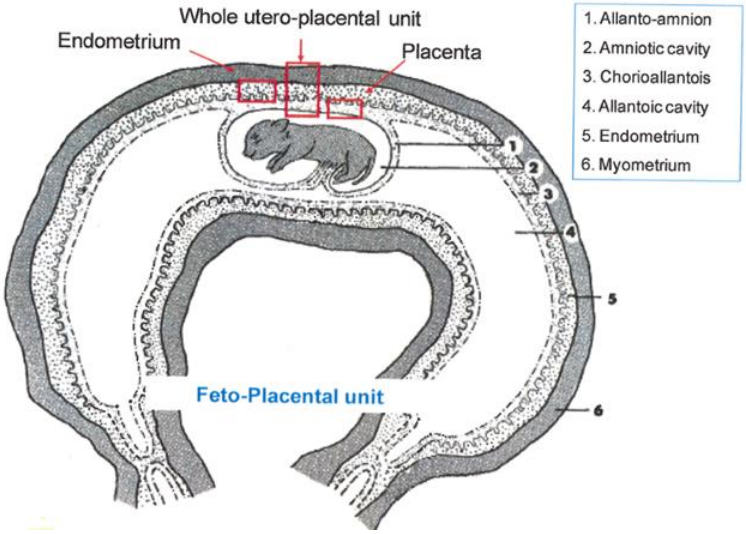

Figure 1.6: Illustration of the Porcine Feto-Placental Unit.

Each foetus in the pig uterus is contained within its own feto-placental unit. The foetus is contained in an amniotic sac, containing amniotic fluid, inside an allantoic sac, containing allantoic fluid. The chorioallantois is in direct contact with the underlying endometrium, which is located on top of a smooth muscle layer (myometrium). Adapted from Rice *et al.*, (1991).

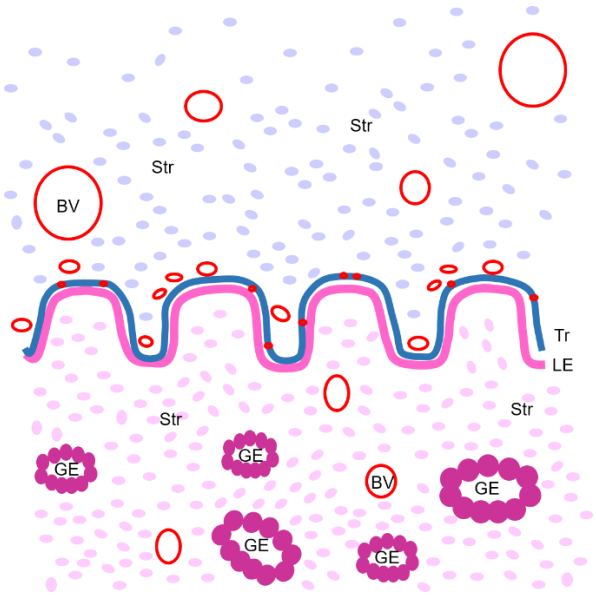

Figure 1.7: Illustration of the Structure of the Porcine Feto-Maternal Interface.

Pink and blue coloured items reflect uterine and placental tissues respectively. The endometrium is composed of stromal tissue (Str), blood vessels (BV) and epithelial cells. Two types of epithelium exist in the endometrium: the luminal epithelium (LE) and the glandular epithelium (GE). The foetal trophectoderm (Tr) cells are in close proximity to the LE. In mid and late gestation, the folds at this interface increase in depth and their vascularity (BV indicated as red circles) also increases thereby increasing the surface area available to ensure adequate transfer of nutrients from the maternal histotroph, secreted by the GE, to the developing foetus. The placenta is highly vascularised, with many BV.

1.2.1.3.4 Placental Angiogenesis

Vasculogenesis and angiogenesis are the two key processes by which blood vessels can be formed *in vivo* (Zygmunt *et al.*, 2003). Vasculogenesis describes the process of formation of new blood vessels in the developing embryo by the differentiation of angioblasts, undifferentiated precursors cells from the mesodermal lineage, into endothelial cells, which proceed to form vascular networks. In contrast to this, angiogenesis describes the development of new vessels from pre-existing blood vessels by either sprouting or intussusception (Carmeliet, 2000; Vailhé *et al.*, 2001; Zygmunt *et al.*, 2003).

One of the first events in the development of the feto-maternal interface is the establishment of placental and foetal circulatory systems (Reynolds and Redmer, 1995; Magness, 1998; Charnock-Jones *et al.*, 2004; Kaufmann *et al.*, 2004; Reynolds *et al.*, 2005a, b). As described in 1.2.1.3.1, the pig has an epitheliochorial placenta, where three layers separate the maternal and foetal circulations throughout gestation (Montiel *et al.*, 2013). Despite the superficial nature of the placenta, with no trophoblast invasion of uterine vessels observed, the maternal and foetal tissues are tightly interdigitated for the duration of gestation. To allow sufficient nutrient transfer between the mother and the foetus, extensive angiogenesis must occur at the feto-maternal interface. At the pig feto-maternal interface, there are two keys stages of gestation when angiogenesis occurs. The first occurs at GD13-18 (Keys *et al.*, 1986), which corresponds to the period of conceptus attachment. The second wave of angiogenesis occurs at approximately GD50 (Vonnahme *et al.*, 2001), which corresponds to the period when placental growth is beginning to plateau and the foetus is about to undertake the period of exponential growth (Figure 1.5). The placental capillary bed continues to increase to accommodate foetal nutrient demand until term (Bazer *et al.*, 2012a).

As gestation progresses, in cows (Reynolds *et al.*, 1986; Reynolds and Ferrell, 1987), sheep (Rudolph and Heymann, 1970; Bell *et al.*, 1986), pigs (described in Chapter 6), and humans (Konje *et al.*, 2003), it has been shown that uterine and umbilical blood flow increase to accommodate increasing foetal demand

(Reynolds and Redmer, 1995). This increase in blood flow is an important mechanism to increase nutrient transfer to the foetus (Reynolds *et al.*, 1986; Molina *et al.*, 1991). Additionally in the pig, each individual feto-placental unit must increase the available attachment area and the density of the vascular supply available for the mother to meet the increasing requirements of the growing foetuses (Tayade *et al.*, 2007a).

Placental efficiency is usually defined as the weight of the foetus/piglet per mass of placenta (Wilson and Ford, 2001; Wooding and Burton, 2008). Efficient placentas have been shown to be shorter with a denser vascular supply when compared with less efficient placentas (van Rens and van der Lende, 2004). It has been demonstrated that highly prolific pig breeds, such as Meishan (MS), have smaller placentas with an increased vascular density contributing to increased placental efficiency compared to the less prolific commercial European breeds (Wilson *et al.*, 1998; Wilson and Ford, 2001). Further, it has been shown that smaller more efficient placentas have increased vascularity, and vascular endothelial growth factor (VEGF) mRNA and protein expression compared to less efficient placentas (Vonnahme *et al.*, 2001). Large within-litter variation in placental efficiency has been observed and is proposed as a significant contributor to the large within-litter variation in birthweight observed in pigs (Wilson and Ford, 2001; Bell and Ehrhardt, 2002; Reynolds *et al.*, 2006; Yuan *et al.*, 2015). Appropriate regulation of placental angiogenesis is therefore essential for the establishment and maintenance of pregnancy, and appropriate regulation of foetal growth.

1.3 IUGR

1.3.1 Human

Low birthweight infants are at increased risk of mortality and morbidity and can be classified as small for gestational age (SGA) or intrauterine growth restricted (IUGR). Many definitions are used to define IUGR and SGA in the literature. SGA infants have a weight below the 10th percentile or weigh less than two standard deviations below the ‘expected’ weight in the given

population (Ananth and Vintzileos, 2009; Bamfo and Odibo, 2011; Sharma *et al.*, 2016). SGA infants exhibit normal organ allometry and are thought to be 'small but perfectly formed', having reached their genetic potential. In stark contrast, IUGR infants are not considered to have reached their genetic potential and often exhibit asymmetric organ growth, with the growth of the brain spared at the expense of other less essential organs (McMillen *et al.*, 2001; Stephens *et al.*, 2015). Often in the literature SGA and IUGR are used interchangeably, and the weight criteria used to define each classification vary significantly, which can lead to challenges when interpreting the literature in this field. A wide range of criteria are present in the literature for the definition of IUGR ranging from below <25 % to <1 % of the expected weight for gestational age (Seeds and Peng, 1998; Chauhan and Magann, 2006; Suhag and Berghella, 2013). Whilst some groups would describe infants which weight below the tenth percentile to be growth restricted, they may be SGA rather than growth restricted. To overcome this, it has been suggested that using more discriminating percentile criteria such as below the fifth to third percentile increases the likelihood of identifying growth restricted infants with an increased risk of mortality and morbidity (McIntire *et al.*, 1999).

SGA has a high prevalence worldwide (Black, 2015), with a much greater incidence in developing countries compared to developed countries (Suhag and Berghella, 2013; Chiavaroli *et al.*, 2016; Reeves and Galan, 2017). Similarly, depending on the definition of IUGR used, it is estimated that between 3 and 15% of pregnancies are affected by IUGR (Romo *et al.*, 2009; Gardosi, 2011). The high prevalence of low birth weight infants in the population makes it a leading cause of perinatal mortality and morbidity (World Health Organisation, 2006). Therefore, it is essential that investigations are performed to improve the understanding of the mechanisms governing foetal growth.

It has been demonstrated that IUGR infants have an increased risk of pre- and neo-natal mortality compared to normally-grown infants (Bamfo and Odibo, 2011; Chen *et al.*, 2011; Gardosi, 2011; Unterscheider *et al.*, 2014; Sangamam, 2015; Reeves and Galan, 2017). Growth-restricted offspring have

an increased incidence of obesity and diabetes, hypertension, stroke, metabolic disease, cerebral palsy, cardiovascular disease, and psychiatric and neurodevelopmental disorders compared to normally-grown infants in both childhood and adulthood, which is programmed prenatally (Barker, 2004, 2006; Calkins *et al.*, 2011; Hennington and Alexander, 2013; Nielsen *et al.*, 2013; Von Beckerath *et al.*, 2013; Demicheva and Crispi, 2014; Murray *et al.*, 2015).

IUGR is attributed to inadequate nutrient and oxygen supply, which is termed placental insufficiency (Usha and Sarita, 2011). Placental insufficiency is thought to be attributed to a placental vascular dysfunction (Chaddha *et al.*, 2004; Junaid *et al.*, 2014), as it has been suggested that IUGR may occur due to decreased maternal-foetal blood flow and/or impaired angiogenesis at the feto-maternal interface (Wootton *et al.*, 1977; Konje *et al.*, 2003; Reynolds *et al.*, 2006) which results in decreased nutrient and oxygen transport to the developing foetus. Based on the plethora of information regarding the alterations in placental vascularity in compromised pregnancies, it has been suggested that placental blood flow is a promising target for IUGR and pre-eclamptic pregnancies (Godfrey, 2002; Wu *et al.*, 2004; Ahmad and Ahmed, 2005; Wareing *et al.*, 2005; Downing, 2010; Sasser and Baylis, 2010; Satterfield *et al.*, 2010; Panda *et al.*, 2014; Paauw *et al.*, 2017). Considering this, in human clinical practice non-invasive Doppler ultrasound is heavily utilised to identify and monitor umbilical arterial (UA) blood flow in IUGR pregnancies, ensuring that clinical interventions occur at the optimal time (Detti *et al.*, 2002).

Placental insufficiency in IUGR has been demonstrated to induce foetal hypoxia, which in turn has drastic consequences for the developing foetus. In response to the hypoxic, nutrient depleted conditions, the foetus redistributes its cardiac output to ensure an adequate blood supply to the essential organs, notably the brain, at the expense of less essential organs such as the liver, skeletal muscle and kidney (McMillen *et al.*, 2001; Stephens *et al.*, 2015). This phenomenon is called brain sparing (Cohen *et al.*, 2015).

1.3.2 Experimental Models

Commonly rats, mice, guinea pigs and rabbits are used for investigation into the mechanisms governing IUGR. These animals have several advantages compared to other species including their small size, short gestation lengths and the ability to induce the phenotype in multiple offspring (Swanson and David, 2015). In these species, nutrient or protein restriction has been demonstrated to be an effective method to induce foetal growth restriction (Girard *et al.*, 1977; Resnick *et al.*, 1982; Woodall *et al.*, 1996, 1999; Lingas *et al.*, 1999; Roberts *et al.*, 2001; Bhasin *et al.*, 2009; Elias *et al.*, 2016). Further, performing a unilateral ovariectomy to induce uterine crowding (Coe *et al.*, 2008) and ligation (Wigglesworth, 1974; Jones and Parer, 1983; Tolcos and Rees, 1997; Eixarch *et al.*, 2011; Janot *et al.*, 2014) or occlusion (Tanaka *et al.*, 1994; Herrera *et al.*, 2016a) of the uterine artery reduce blood flow to the developing foetuses, inducing growth restriction. In mice it has been demonstrated that knocking out extracellular signal-regulated kinase 3 (Erk3) (Klinger *et al.*, 2009), vascular endothelial growth factor (VEGF) (Carmeliet *et al.*, 1996), endothelial nitric oxide synthase (eNOS) (Kusinski *et al.*, 2012) and the placental specific knock out of insulin growth factor 2 (IGF2) (Constância *et al.*, 2002) successfully induces foetal growth restriction. Despite the advantages of using these models, there are also several disadvantages associated with these species including differences in maturity at birth, differences in placentation and their small size which can make both surgical and non-surgical procedures challenging (Swanson and David, 2015).

Experimental models of growth restriction have been developed in the sheep as, despite the difference in placentation type, the sheep is considered a good animal model for human pregnancy (Barry and Anthony, 2008). Like humans, sheep usually only have singleton or twin pregnancies, and their offspring are of a similar physiological maturity at birth (Swanson and David, 2015). Experimentally, growth restriction has been induced in the sheep using carunculectomy (removal of caruncles to reduce placental growth) (Owens *et al.*, 1986; McMillen *et al.*, 2001; Phillips *et al.*, 2001), undernutrition (Vincent *et*

al., 1985; Parr *et al.*, 1986; Vonnahme *et al.*, 2003), overfeeding adolescents (Wallace *et al.*, 1996) and heat stress (Galan *et al.*, 1999). Manipulations can be performed with relative ease in the sheep, and foetuses tolerate them well (Coutelle and Rodeck, 2002). Further, due to the length of gestation, manipulations can be performed at specific stages of gestation reflecting key stages of foetal and/or placental development.

The major disadvantage with using these models is that they all require experimental manipulation. Therefore, whilst they provide considerable information regarding the mechanisms governing foetal growth, they do not accurately reflect the naturally occurring growth restriction observed in humans. Herrera *et al.*, (2016b) recently demonstrated that, as with human pregnancies, ewes that conceived and gestated at high altitudes exhibited marked growth restriction compared to those at low altitudes; providing an opportunity to investigate growth restriction in the sheep without invasive modifications.

1.3.3 Pig

1.3.3.1 Phenotype of IUGR in Pigs

Whilst the previously discussed experimental models of IUGR have contributed significantly to the understanding of the mechanisms governing foetal growth, they have been experimentally induced therefore they may not accurately reflect naturally occurring growth restriction. The pig has a high incidence of naturally occurring IUGR, with many litters having a growth restricted piglet or ‘runt’ piglet that can weigh less than a half or a third of the weight of their largest littermates (Widdowson, 1971). It is estimated that growth restricted piglets, with a weight of less than 1.1kg at birth, contribute to 25% of the total number of piglets born (Wu *et al.*, 2010). This makes the pig a readily available animal model which has several advantages for research compared to the use of the previously discussed models (Swindle *et al.*, 2012). Further, the pig is an excellent model for the study of foetal growth and development due to the striking similarities with human development.

Many definitions for IUGR in the pig exist (Ashworth *et al.*, 2001) including piglets weighing less than 1.1kg at birth (Wu *et al.*, 2010), weighing less than two standard deviations of the mean body weight for age, weighing less than two-thirds of the mean litter weight, the smallest of each litter or a low weight statistical outlier from the population (Royston *et al.*, 1982; van der Lende *et al.*, 1990).

IUGR in the pig severely impacts upon neonatal and adult development, with piglets exhibiting increased morbidity and mortality (Wu *et al.*, 2006). Postnatally it has been demonstrated that important organs have impaired development and function in IUGR piglets, with these piglets having smaller livers, kidneys, small intestine and skeletal muscle as a percentage of body weight (Ritacco *et al.*, 1997; Bauer *et al.*, 2000; Wang *et al.*, 2008). The adaptation of IUGR piglets to extra-uterine life is compromised, with these piglets struggling to compete for available colostrum, having increased susceptibility to disease and decreased energy reserves compared to their normally-grown littermates (Hayashi *et al.*, 1987; Wu *et al.*, 2006; Bee, 2007). Due to this, it is unsurprising that growth restricted piglets heavily contribute to pre-weaning mortality statistics, with Wu *et al.*, (2010) suggesting they account for 76% piglet death pre-weaning. The small percentage of growth restricted piglets that do survive are a significant burden to the agricultural industry (Wu *et al.*, 2006). The alterations in organ development, accompanied by the increased disease susceptibility cause several health problems for these piglets. Their growth rate continues to be slower than that of their normally-grown littermates, with a decreased mature carcass weight (Quiniou *et al.*, 2002; Tilley *et al.*, 2007). Further, the quality of the carcass and meat produced from these piglets is reduced, with a high fat content, altered protein and mineral content and aberrant development of the muscle fibres (Wigmore and Stickland, 1983; Greenwood *et al.*, 2000; Bee, 2004, 2007; Wu *et al.*, 2006). Growth restricted piglets have impaired reproductive performance compared to their normally-grown littermates (Wu *et al.*, 2006). Female IUGR piglets have delayed follicular development, with an increased number of primordial follicles, accompanied by a decrease in the prevalence of both primary and

secondary follicles at birth (Da Silva-Buttkus *et al.*, 2003). Further, it has been demonstrated that female piglets with slower growth rates are older when first mating occurs (Tummaruk *et al.*, 2000). Male IUGR piglets have also been shown to have impaired gonadal development and reproductive performance. Testicular development is impaired, with decreased numbers of germ cells (Smit *et al.*, 2013), Leydig cells and Sertoli cells compared to normally-grown piglets (Smit *et al.*, 2013; Lin *et al.*, 2017). Further, it has been demonstrated that semen volume and the number of spermatozoa per ejaculate are decreased in IUGR piglets compared to normally-grown piglets (Lin *et al.*, 2017), demonstrating that this decrease in cell number has a functional effect on male fertility. This severe phenotype develops *in utero* and cannot be rectified postnatally. Considering the high prevalence and severity of the phenotype, it is essential to improve the understanding of the mechanisms associated with impaired foetal growth in the lightest foetuses compared to their normal-sized littermates (Ashworth *et al.*, 2001).

It has been suggested that IUGR in the pig may be programmed from an early stage of gestation, with significant within-litter variation in foetal size observed from as early as GD30-35 (Pettigrew *et al.*, 1986; Wise *et al.*, 1997; Finch *et al.*, 2002; Foxcroft and Town, 2004; Foxcroft *et al.*, 2006). Due to the large within-litter variation in birth weight, and high incidence of growth restriction, the pig is a readily available model to investigate the mechanisms governing foetal growth. As pigs are a litter bearing species, each foetus has its own feto-placental unit (Figure 1.6), allowing direct comparison between samples associated with foetuses of different size within the same uterus, without the confounding factors of maternal genotype, nutrition or husbandry practice. Further, as samples can be obtained throughout gestation, this allows investigation into the temporal profile of the development of the phenotype.

1.3.3.2 Foetal Size is Associated with Placental Development

As described previously, foetal and placental weight decrease with increasing LS, suggesting that uterine capacity is a limiting factor governing their growth.

Within-litter it has been suggested that lighter foetuses have less space for growth in the late stages of gestation when exponential foetal growth occurs, compared to normal and larger sized foetuses (Wright *et al.*, 2016). Wright *et al.*, (2016) demonstrated that foetal size is not associated with the width of the bilayer in early gestation (from formation to GD42) or the structure of the highly vascular region of the placenta adjacent to the foetus from GD22-42. However, distinct differences in the less vascular zone of the placenta were observed, with narrower areas of less vascular placenta that were lighter present in placentas associated with smaller foetuses compared to those associated with normal sized foetuses.

In mid-late gestation, an association between foetal size and folding at the feto-placental interface has been suggested. Michael *et al.*, (1983) proposed an inverse relationship between placental SA and foetal weight, with an increased macroscopic SA observed in placentas supplying small foetuses in late gestation (GD70-112) compared to normally-sized foetuses. Further, Vallet and Freking, (2007) observed significantly wider folds at GD65, 85 and 105 in placentas supplying the smallest foetuses compared to the largest foetuses. They demonstrated that the stroma above the CAM decreased in size at a faster rate in the placentas associated with the smallest foetuses compared to the largest foetuses. Similar patterns were observed by Vallet and Freking, (2007) at GD45 although they were not found to be statistically significant, although this may be attributed to the smaller sample size in this group. It is thought that to compensate for having smaller placentas, the width of the folds at the feto-maternal interface supplying small foetuses increase at a faster rate to form wider folds, thereby providing a larger SA for exchange and improving the efficiency of the placenta. To accommodate the substantial remodelling of the feto-maternal interface, it would be expected that significant angiogenesis, apoptosis and proliferation would occur.

Chen *et al.*, (2015) also suggested this, reporting increased apoptosis and oxidative stress at the feto-maternal interface in instances of IUGR, which in turn would be hypothesised to have striking effects on placental and foetal growth and development. Further, they suggested that cellular proliferation is

decreased in placentas associated with IUGR in late gestation, which may contribute to the decreased placenta size associated with IUGR foetuses (Blomberg *et al.*, 2010). Intriguingly, the mRNA expression of endothelial nitric oxide synthase (*eNOS*), which is pro-angiogenic, was increased in IUGR placentas at GD50 compared to control placentas (Blomberg *et al.*, 2010). This may suggest that at this stage of gestation the placentas supplying IUGR foetuses are trying to increase the vascularity at the feto-placental interface to compensate for having a decreased nutrient supply.

Several biochemical differences in placentas associated with IUGR foetuses compared to their normal-sized littermates have been reported. It has been suggested that placentas supplying IUGR foetuses have decreased glucocorticoid receptor expression compared to those supplying normal-sized foetuses (McNeil *et al.*, 2007). Further, the expression of specific amino acids and amino acid transporters are decreased in placentas supplying growth restricted foetuses compared to those supplying their normally-grown littermates (Ashworth *et al.*, 2001, 2013; Finch *et al.*, 2004; Wu *et al.*, 2008). Considering the importance of amino acids in development (Wu *et al.*, 1999), supplementation of the premating and/or gestating diet with amino acids has the potential to improve LS and foetal growth in the pig (Wu *et al.*, 1996, 2010, 2017; Gao *et al.*, 2012). For example, it has been demonstrated that supplementing the diet of gestating pigs with arginine between GD14 and 25 increased placental growth, the number of live foetuses, the vascularity of the placenta and augmented folding of the bilayer of at the feto-maternal interface at GD60 (Li *et al.*, 2014; Seo *et al.*, 2014). Similarly, arginine supplementation in early gestation (GD14-28) increased the number of foetuses by three at GD70 (Bérard and Bee, 2010), which translated to an additional piglet at farrowing (Ramaekers *et al.*, 2006). Importantly, it has been suggested that arginine supplementation between GD25-90 increases birth weight and decreases the prevalence of low birth weight piglets (Dallanora *et al.*, 2017).

1.4 Sexual dimorphism in Placental Development

1.4.1 Human

Sex determination begins very early in development, with the sex determining region on the Y chromosome (Sry), an important gene in sex determination, undergoing transcription at the 2-cell stage in human embryo development (Ao *et al.*, 1994; Ingemarsson, 2003). In humans, it has been demonstrated that sex influences birth weight, with males being heavier than females, a characteristic that can be observed from an early stage of gestation (Lubchenco *et al.*, 1963; Pedersen, 1980; Zegher *et al.*, 1999; Widnes *et al.*, 2017). Considering this suggested difference in growth rate and presumed nutrient requirements, male foetuses may be more susceptible than female foetuses to adverse environmental conditions, resulting in an impaired nutrient supply to the foetus.

The concept that male foetuses are at a disadvantage in response to adverse environmental conditions has been suggested in the literature, and sexual dimorphism in susceptibility to disease has been observed postnatally (Eriksson *et al.*, 2010; Gabory *et al.*, 2013; Sandman *et al.*, 2013). Male pregnancies are more likely to have complications and adverse outcomes than female pregnancies (Kraemer, 2000; Ingemarsson, 2003; Vatten and Skjærven, 2004; Boklage, 2005; Di Renzo *et al.*, 2007; Eriksson *et al.*, 2010). Further, in pregnancies complicated by preeclampsia or IUGR, it has been shown that male infants exhibit increased perinatal mortality and morbidity compared to females that have been subjected to the same conditions (Challis *et al.* 2013; Muralimanoharan *et al.* 2013).

As described previously, the placenta is derived from the trophectoderm of the conceptus so the placenta can be considered to be male or female (Clifton, 2010). Further, it has been suggested that placentas associated with males are heavier with increased efficiency than those associated with females (Ishikawa *et al.*, 2003; Widnes *et al.*, 2017). As sexual dimorphism in disease susceptibility has been reported in humans, investigations have been carried out into the association between foetal sex and placental development

(Rosenfeld, 2015; Kalisch-Smith *et al.*, 2017a). It has been demonstrated that foetal sex is associated with the placental expression of genes involved in the inflammatory response (Challis *et al.*, 2013). Inflammation has an important role in the establishment of pregnancy (Dekel *et al.*, 2010, 2014) therefore, this could contribute to the sexual dimorphism in disease susceptibility and response to adverse conditions. It has also been suggested that placentas associated with female foetuses have increased expression of genes involved in placental development, growth and pregnancy recognition compared to those associated with males (Buckberry *et al.*, 2014).

1.4.2 Rats

Sexual dimorphism in placental development has recently been investigated in the rat (Kalisch-Smith *et al.*, 2017b). In contrast to the increased growth rate observed in male compared to female foetuses early in gestation in humans, foetal sex was not found to influence cell number, trophoblast outgrowth, number of trophoblasts or the expression of trophoblast stemness and differentiation markers. However, at GD15 placentas supplying female foetuses had a decreased labyrinthine volume, foetal and maternal blood space volume and reduced SA of the foetal blood space compared to male placentas. Intriguingly, these differences were not observed in the GD13 or GD20 placentas, highlighting the dynamic nature of the placenta and that multiple stages of gestation must be investigated to fully understand the relationship between the sex of a foetus and the function of the feto-maternal interface. In this study, male foetuses were not heavier than female foetuses until GD20 however, this decrease in foetal weight in female foetuses may be linked to the alterations in placental structure observed in mid-gestation.

1.4.3 Cow

To date, limited investigations into the presence of sexual dimorphism at the feto-maternal interface have been performed in large animals. In bovine blastocysts, sexual dimorphism in gene expression, notably of genes located

on the X or Y chromosome (Bermejo-Alvarez *et al.*, 2009), and in the metabolic profiles of amino acids (Sturmey *et al.*, 2010) has been reported. Forde *et al.*, (2016) furthered this research and demonstrated sexual dimorphism in the utilisation of amino acids by bovine conceptuses at GD19. In this study, Forde *et al.*, (2016) demonstrated that >5000 transcripts were differentially expressed in conceptuses of different sex at GD19 highlighting the early development of sexual dimorphism in foetal development.

1.4.4 Pig

As observed in humans, it has been suggested that porcine male conceptuses have an increased growth rate compared to female conceptuses from GD10 (Cassar *et al.*, 1994). In both obese pigs with leptin resistance and lean pigs, it has been demonstrated that organ development and metabolic responses are increased in female foetuses compared to male foetuses at GD62 (Torres-Rovira *et al.*, 2013), which could indicate increased postnatal survival and development of females. It has been proposed that male new-born piglets have a survival disadvantage compared to their female littermates (Baxter *et al.*, 2012). However, whether this difference arises prenatally due to sexual dimorphism in placental development has not been determined in the pig.

1.5 General Hypothesis and Aims

It is hypothesised that IUGR in the pig occurs due to aberrant conceptus attachment, which leads to alterations in angiogenesis and vascularity of the feto-maternal interface. Further, it is hypothesised that impaired gene expression and vascularity will be observed at the feto-maternal interface associated with male foetuses compared to female foetuses.

The aim of the research presented in this thesis was to investigate the association between foetal size, sex and integrin signalling, apoptosis and proliferation, umbilical arterial (UA) blood flow, and angiogenesis and vascularity at the feto-maternal interface to gain an integrated understanding of the feto-placental units associated with small- and normal-sized pig foetuses. This was performed by the collection and analysis of placental and endometrial samples associated with foetuses of different size (lightest and closest to mean litter weight (CTMLW)) at five key stages of gestation (GD18, 30, 45, 60 and 90).

2 General Materials and Methods

2.1 DNA Methodology

2.1.1 DNA Isolation

Small pieces of tissue (≤25mg) were cut from the snap-frozen samples of interest with a scalpel and stored in a nuclease-free tube (Sarstedt, Leicester, U.K.) on dry ice until required. DNA extractions were performed using the DNeasy Blood and Tissue Kit (Qiagen, Manchester, U.K.). All centrifugation steps were performed using an Eppendorf 5415D centrifuge (Eppendorf, Arlington, Stevenage, U.K.).

Samples were lysed by incubation with 180µl Buffer ATL and 20µl Proteinase K at 55^{o}C, with gentle agitation overnight. The lysate was mixed by vortexing with 200µl Buffer AL, and 200µl 100% Ethanol (Fisher Scientific, Loughborough, U.K.) was added. This was mixed by vortexing and the lysate was transferred to a DNeasy spin column. This was centrifuged at ≥6000g for 1 minute and the flow-through and collection tube were discarded. The spin column was placed into a fresh 2ml collection tube, and the membrane was washed by the addition of 500µl Buffer AW1. This was centrifuged at ≥6000g for 1 minute, and the flow-through and collection tube were discarded. An additional wash step was performed by the addition of 500µl Buffer AW2, followed by centrifugation for 3 minutes at ≥6000g. The spin column was transferred to a nuclease-free 1.5ml collection tube, where the DNA was eluted by the addition of 100µl of Buffer AE directly to the membrane. Following incubation for 1 minute at room temperature, the spin column was centrifuged at ≥6000g for 1 minute. The elution step was then repeated to maximise DNA yield.

2.1.2 Quantification of DNA by Spectrophotometry

The Nanodrop ND-1000 (Labtech International Ltd, Heathfield, U.K.) was used to determine the concentration of the DNA samples generated in 2.1.1 by spectrophotometry, using the elution buffer to calibrate the spectrophotometer.

The concentration of DNA in 1µl of sample was measured in ng/µl. In addition to the concentration, the optical density (OD) 260/280nm and OD 260/230nm ratios were calculated. A 260/280 ratio of ~1.8 was used to indicate that the DNA was pure. The 260/230 ratio acted as an additional measurement of the purity of the nucleic acid, and a range of 1.8-2.2 indicated that the sample was pure.

2.1.3 Polymerase Chain Reaction (PCR)

All primers were synthesised by Life Technologies (ThermoFisher Scientific, Altrincham, U.K.). Neat stocks of 100µM were created by reconstituting the primers in nuclease-free water (Life Technologies, ThermoFisher Scientific). These were diluted in nuclease-free water to form 5µM working stocks which were used for the PCRs.

For the reaction, 7µl nuclease-free water, 5µl 10 X PCR Buffer, 1µl dNTP mix (10 mM), 1µl FastStart Taq (all solutions from Roche FastStart Taq kit, Indianapolis, Indiana, U.S.A.) and 5µl of both forward and reverse primers (5µM stock) were added to 1µg of sample DNA. A No Template Control (NTC) using nuclease-free water instead of DNA was run as a negative control, and positive controls were run wherever possible. The PCR conditions had an initial step of 95^{o}C for 4 min 30 seconds, which was followed by 30 cycles of 95^{o}C for 30 seconds, 60^{o}C for 30 seconds and 72^{o}C for 30 seconds, with a final extension of 72^{o}C for 4 min 30 seconds followed by an indefinite hold at 4^{o}C. Samples were processed in 96-well microplates (NUNC, ThermoFisher Scientific) using a 96-well thermocycler (TProfessional, Biometra, Goettingen, Germany).

2.1.4 Agarose Gel

PCR products were visualised by electrophoresis using agarose gels. These were prepared in 1X TAE buffer, from a 50X TAE stock (Tris Base (484g), glacial acetic acid (114.5ml) and 5M EDTA pH 8.0 (200ml), dissolved in 1l of

deionised water (dH_2O) and made up to 2l with dH_2O). The percentage of gel varied depending on the size of the expected PCR product (Table 2.1). The agarose (Bioline, London, U.K.) was melted in a conical flask containing TAE buffer using a microwave. Following this, 10µl of DNA stain (SYBR Safe, Invitrogen, ThermoFisher Scientific) per 100ml gel volume was added to the agarose solution and the gel was allowed to set in a gel tray with a gel comb. The gel was placed in a gel tank containing 1X TAE buffer where, following removal of the comb, 5µl of the PCR product was loaded into each well of a gel, mixed with 3µl of blue/orange loading buffer (Promega, Southampton, U.K.). A set of size markers were run alongside the samples (PCR Markers, Promega) to allow determination of the size of the PCR product produced. A current of approximately 100V was applied to the gel with a power pack (NBL Gene Sciences Limited, Cramlington, U.K.) and the DNA migrated towards the anode at a rate proportional to the fragment size. The gel was then visualised under U.V. light (Gel Logic 200, Kodak, Hemel Hempstead, Hertfordshire, U.K.).

Percentage Agarose in 1 X TAE (%)	Optimum Resolution for Linear DNA (base pairs)
0.5	1,000–30,000
0.7	800–12,000
1.0	500–10,000
1.2	400–7,000
1.5	200–3,000
2.0	50–2,000

Table 2.1: Resolution of Linear DNA on Agarose Gels

2.2 RNA Methodology

2.2.1 RNA-Later Like Solution

To make an RNA-Later like solution, 700g Ammonium sulphate (SLS, Nottingham, U.K.) was dissolved in 935ml of RNase free water with heat and stirring. Once dissolved, 25ml of 1M Sodium Citrate (Fisher Scientific) and 40ml of 0.5M ethylenediaminetetraacetic acid (EDTA) were added. The

solution was then adjusted to pH 5.2 using concentrated sulphuric acid and stored at room temperature until required.

2.2.2 Preservation of Tissues for RNA Isolation

Following dissection of the uterus (described in chapter 3), the tissue samples of interest were dissected and snap frozen in cryovials (Starlab, Milton Keynes, U.K.) in liquid nitrogen. The samples were stored at -80^{o}C until required.

2.2.3 RNA Isolation from Tissue

All reagents used for RNA isolation were from the RNeasy Mini-Kit (Qiagen) unless otherwise stated. A small fragment of each sample (≤30mg) was cut with a scalpel and placed into a 1.5ml nuclease-free tube (Sarstedt) and stored on dry ice until homogenisation was performed. Each sample was added to 1ml of RNA-Bee (AMS Biotechnology, Abingdon, U.K.) in Lysing Matrix D tubes (MP Biomedicals, Illkirch, France) and homogenised using a Fast Prep (Thermo Electron Corporation, Ohio, U.S.A.) for 20 seconds at speed 4.0. The homogenate was transferred to a fresh nuclease-free 1.5ml tube and centrifuged at 12000g for 10 minutes at 4^{o}C (5415R, Eppendorf). The supernatant was transferred to a 1.5ml nuclease-free tube and stored at room temperature for 5 minutes. Chloroform (200µl; Fisher Scientific) was added, and the tube was shaken vigorously for 30 seconds. The tube was stored on wet ice for 10 minutes, before centrifugation at 12000g for 15 minutes at 4^{o}C. Approximately 500µl of the aqueous phase was transferred to a fresh 1.5ml nuclease-free tube, where it was mixed by pipetting with 500µl of 70% Ethanol (Fisher Scientific). Half of the solution (500µl) was transferred to an RNeasy spin column placed in a 2ml collection tube and was centrifuged for 15 seconds at ≥8000g (5415D, Eppendorf). The flow-through was discarded and the column was placed back into the 2ml collection tube. The remainder of the sample (~500µl) was added to the spin column and the centrifugation step was repeated. The flow-through was discarded and the spin column was placed back into the 2ml collection tube. Buffer RW1 (350µl) was added to the spin

column and it was centrifuged for 15 seconds at ≥8000g. The flow-through was discarded and the column was placed back in the 2ml collection tube. The RNase-free DNase stock solution (Qiagen) was prepared by reconstituting the DNase 1 vial in 550µl of nuclease-free water and mixing gently by inversion. The DNase incubation mix was prepared by adding 10µl of the DNase stock solution to 70µl Buffer RDD (supplied in kit). The solution was added to the filter in the RNeasy spin column and incubated at room temperature (~20-30^{o}C) for 15 minutes. Buffer RW1 (350µl) was added to the spin column and it was centrifuged for 15 seconds at ≥8000g. The flow-through was discarded and the spin column was placed back into the 2ml collection tube. Buffer RPE (500µl) was added to the spin column and it was centrifuged for 15 seconds at ≥8000g. The flow-through was discarded and the spin column was placed back into the 2ml collection tube. A further 500µl of Buffer RPE was added to the spin column and it was centrifuged for 2 minutes at ≥8000g. The spin column was transferred to a fresh nuclease-free 2ml collection tube and centrifuged at maximum speed (16100g) for 1 minute to dry the membrane and purge any remaining Buffer RPE. The spin column was transferred to a fresh nuclease-free 1.5ml tube, where 30µl nuclease-free water was added to the membrane of the spin column to elute the RNA. This was centrifuged for 1 minute at ≥8000g. A further 30µl nuclease-free water was added to the membrane of the spin column and the centrifugation step was repeated. The solution was vortexed to mix the two eluates and an aliquot of the sample was placed into a separate 1.5ml nuclease-free tube, for assessment of RNA quantity and quality (2.2.5 and 2.2.6). The remainder of the sample was placed on dry ice and stored at -80^{o}C until required for reverse transcription (2.2.7).

2.2.4 RNA Isolation from Adherent Cells

All reagents used for RNA Isolation were from the RNeasy Mini-Kit (Qiagen) unless otherwise stated. Adherent cells of interest were grown until ~80% confluency in a T25 flask (Eppendorf), at which time they were washed with Phosphate Buffered Saline (PBS) without Calcium and Magnesium (Life Technologies, ThermoFisher Scientific). TryPLE (Life Technologies,

ThermoFisher Scientific) (5ml) was added to the flask for 6 minutes with gentle agitation to dissociate the cells from the flask. After the incubation, 5ml of media containing serum was added to the flask. The solution was transferred to a 15ml falcon tube and centrifuged for 5 minutes at 400g at room temperature (Sorvall RT7, ThermoFisher Scientific). The supernatant was discarded, the pellet was resuspended in 600µl of Buffer RLT, and the cell suspension was transferred to a 1.5ml nuclease-free tube (Sarstedt). To lyse the cells, the suspension was briefly vortexed and centrifuged for 3 minutes at full speed (5415D, Eppendorf). Following this, the supernatant was transferred to a fresh nuclease-free 1.5ml tube, to which 600µl of 70% Ethanol (Fisher Scientific) was added and mixed by pipetting. To the RNeasy spin column, 700µl of the sample was added and centrifuged for 15 seconds at ≥8000g. The flow through was discarded and the process repeated with the remainder of the sample. To wash the column, 700µl Buffer RW1was added to the column, which was centrifuged for 15 seconds at ≥8000g. The flow through was discarded and 500µl Buffer RPE added to the column. Again, the column was centrifuged for 15 seconds at ≥8000g and the flow through discarded. To the column, a further 500µl RPE Buffer was added and the column was centrifuged for 2 minutes at ≥8000g. The flow through was discarded and the column was placed into a fresh collection tube, which was centrifuged at full speed to dry the membrane. The column was placed into a fresh 1.5ml nuclease-free tube and the RNA was eluted from the membrane by the addition of 30µl nuclease-free water. This was centrifuged for 1 minute at ≥8000g and the elution step repeated once more to maximise the RNA yield. The two eluates were vortexed to mix, and an aliquot of the sample was placed into a separate 1.5ml nuclease-free tube, for assessment of RNA quantity and quality (2.2.5 and 2.2.6). The remainder of the sample was stored at -80^{o}C until required for reverse transcription (2.2.7).

2.2.5 Quantitation of RNA by Spectrophotometry

The Nanodrop ND-1000 (Labtech International Ltd) was used to determine the concentration of the RNA samples generated in 2.2.3 and 2.2.4. The nuclease-

free water used to elute the RNA from the spin column was used to calibrate the spectrophotometer. A 260/280 ratio of ~2.0 was used to indicate that the RNA was pure. If the 260/280 ratio was considerably less than 2.0, this indicated the presence of contaminants (protein or phenol). The 260/230 ratio is an additional measurement of the purity of the nucleic acid, and a range of 1.8-2.2 would indicate that the sample was pure.

2.2.6 RNA Quality Assessment by Electrophoresis

Electrophoresis was performed using the tapestation and RNA screentapes to assess RNA concentration and integrity as per the manufacturer's instructions (Agilent Technologies, Edinburgh, U.K.) on an Agilent 2200 Tapestation (Agilent Technologies). From the electropherograms produced, an RNA Integrity Number equivalent (RINe) value was generated. The RINe value generated by the software ranged between 1 and 10, where 10 represented the highest quality RNA sample. Mean and the range of RINe values obtained from the placental and endometrial samples are summarised in Table 2.2. Generally, samples with RINe values of ≥7 were considered to be of good quality and were used for this study. Due to difficulties associated with obtaining RNA of acceptable quality from placentas, the acceptable threshold for RNA quality used was decreased to RINe≥6.5. For samples where the RNA quality was below this threshold, the extraction and quality assessment was repeated at least twice more, and if it still did not meet the criteria the sample was excluded from the analysis. The number of samples within each group of interest are summarised in Table 2.3.

2.2.7 Reverse Transcription

All reagents were supplied with SuperScript III (Invitrogen) unless otherwise stated. The RNA concentration calculated by spectrophotometry (2.2.5) was used to calculate the specific weight of RNA that would be used for the reverse transcription reaction. The weight of RNA used for each experiment was consistent between samples, to allow comparison of gene expression levels

when performing quantitative PCR. The reaction was performed in a 200µl PCR tube (Axygen, Union City, U.S.A.). The RNA sample (0.3µg) was added to 1µl of Random Primers (250ng/µl; Promega), 1µl of dNTPs (10mM; Invitrogen), and nuclease-free water was used to make the total volume up to 13µl. The tubes were gently mixed and centrifuged briefly. A thermocycler (TProfessional; Biometra) was used to incubate the samples for 5 minutes at 65^{o}C, and then cool them to 4^{o}C for a minimum of 2 minutes.

Following this, 4µl of First Strand Buffer, 1µl DTT, 1µl RNase Inhibitor (40 units/µl; Promega), and 1µl SuperScript III were added to the PCR tube. A No Reverse Transcription (NRT) control was set up to check for genomic contamination, where 4µl of First Strand Buffer, 1µl DTT, 1µl RNase Inhibitor (40 units/µl; Promega) and 1µl of nuclease-free water were added. The tubes were briefly centrifuged and placed back into the thermocycler, where they were heated to 25^{o}C for 5 minutes, 50^{o}C for 60 minutes and 70^{o}C for 15 minutes. The samples were then stored at -20^{o}C until required. The reverse transcription reactions were performed in duplicate and pooled for each sample.

GD	Placenta		Endometrium	
	Mean	Range	Mean	Range
18	n/a	n/a	8.63	7.8-9.3
30	7.83	7.2-9.0	7.74	7.0-8.3
45	7.12	6.5-8.5	7.80	7.1-8.6
60	7.34	6.9-7.8	7.64	7.0-8.5
90	7.04	6.5-8.0	7.80	6.6-8.5

Table 2.2: Summary of Placental and Endometrial RINe Values.

Summary of the RNA Integrity Number equivalent (RINe) value obtained when assessing RNA quality for placental and endometrial samples within Gestational Day (GD) of interest.

GD	Tissue	Lightest	CTMLW	Male	Female
18	Endometrium	5	5	n/a	n/a
30	Placenta	6	6	7	5
	Endometrium	5	5	7	4
45	Placenta	6	6	10	11
	Endometrium	4	3	11	6
60	Placenta	6	5	11	12
	Endometrium	6	8	16	14
90	Placenta	7	4	10	9
	Endometrium	6	5	11	11

Table 2.3: Summary of Number of Samples Obtained RNA of Acceptable Quality.

The number of samples quoted here represents the RNA samples within group which had a RINe value of acceptable quality. This reflects the maximum number of samples per group, as during the statistical analysis on the qPCR results, any outliers were excluded. Abbreviations: GD=Gestational Day, CTMLW=Closest to Mean Litter Weight, n/a=not applicable.

2.2.8 Quantitative PCR

All primers were synthesised by Life Technologies (ThermoFisher Scientific). Neat stocks of 100μM were created by reconstituting the primers in nuclease-free water. These were diluted in nuclease-free water (Life Technologies, ThermoFisher Scientific) to form 5μM working stocks which were used for the experiments

2.2.8.1 Preparation of cDNA for qPCR

The cDNA samples prepared in 2.2.7 from the RNA isolated from the samples snap-frozen in liquid nitrogen were then used for quantitative PCR (qPCR). A pool of cDNA to produce a standard curve was created by taking a small volume of each of the undiluted samples and placing them in a 1.5ml nuclease-free tube (Sarstedt). The pool was then diluted 1:5 with nuclease-free water (Life Technologies, ThermoFisher Scientific) and mixed. A series of dilutions were performed with nuclease-free water (Life Technologies, ThermoFisher Scientific) to obtain a standard curve (1:10, 1:20, 1:40, 1:80, 1:160, 1:320 and 1:640). A standard curve was generated for each tissue and was used for all qPCRs on that tissue within an experiment to allow accurate comparison of the results. The samples were diluted 1:25 with nuclease-free water in a 1.5ml nuclease-free tube.

2.2.8.2 qPCR Protocol

Platinum SYBR Green qPCR Supermix-UDG (Invitrogen) was used to perform the qPCRs. A master mix was prepared and added to the required wells of a 96 well plate (NUNC, ThermoFisher Scientific), to give the following volumes per well: 12.5μl Platinum SYBR Green qPCR Supermix-UDG, 0.1μl ROX reference dye, 2μl forward primer (5μM working stock solution), 2μl reverse primer (5μM working stock solution), and 3.4μl nuclease-free water (20μl of master mix per well). All samples, standards and controls were measured in duplicate. An NTC, NRT control, and a standard curve were run on every plate. To the master mix, 5μl of diluted cDNA, standard or control was added to each

well. The plate was sealed with optical caps and centrifuged at (≤500g) (Perfect Spin Vertical Plate Centrifuge) for ~1 minute. The plate was placed in a Stratagene MX3005P qPCR machine (Agilent Technologies) and the desired program was set up using the Stratagene MxPro software. The plate was heated to 50^{o}C for 2 minutes, followed by a further 2 minutes at 95^{o}C. This was followed by 40 cycles of 15 seconds at 95^{o}C and 30 seconds at 60^{o}C. A final cycle of 1 minute at 95^{o}C, followed by 30 seconds at 60^{o}C and 30 seconds at 95^{o}C was performed.

2.2.8.3 Analysis of Output Generated by MxPro

Data were collected from all wells and following completion of the PCR, the wells in the plate were labelled with the software as NTC, NRT, standards or unknowns (samples of interest). To generate the standard curve on the program, a relative value was assigned to each standard curve dilution (5, 2.5, 1.25, 0.625, 0.3125, 0.15625, 0.078125 and 0.039063 for the 1:5, 1:10, 1:20, 1:40, 1:80, 1:160, 1:320 and 1:640 standards respectively).

The dissociation peak was checked at the end of each reaction to ensure that the PCR products produced were homogeneous and that the reaction was optimal and specific. The threshold for the efficiency of the standard curve was set to between 90-110%, with an RSq value of ≥0.990, indicating that the line was a good fit. The standard curve was visualised in a plot containing the samples of interest, to check that the line produced was linear and that the samples were contained within the range of the curve. The amplification plots were used to visualise the duplicates for each sample. The cycle threshold (Ct) indicated the cycle where the fluorescence levels for each sample crossed the threshold. If the difference in the Ct value was ≥0.5 for duplicates, the qPCR for that sample was repeated in duplicate again.

The data collected were exported as a text file from MxPro, which was then imported into qBase+ (Biogazelle, Zwijnaarde, Belgium) for analysis. For each sample, reference genes that were identified as stable (2.2.8.4) were run to allow normalisation of the data. A target and run specific strategy was

employed and the results, normalised to the two reference genes, were scaled to the minimum sample.

2.2.8.4 Selection of Appropriate Reference Genes for Normalisation

To allow appropriate normalisation of qPCR data, it is essential to have appropriate internal control genes, or reference genes, which have stable expression in the tissue of interest. Reference genes are essential to account for variability between samples that occurs during the previous steps in the preparation of the samples, e.g. during reverse transcription. Normalisation of the expression obtained from target genes of interest to the expression of reference genes ensures that any variation in amplification observed is reliable and cannot be explained by differences in the preparation.

For this study, 11 reference genes were identified to test from previous publications in the pig (Table 2.4). To assess the stability of these reference genes, a subset of samples were identified. This group of 10 samples contained samples from gestational days (GD) 30 (n=2), 60 (n=4) and 90 (n=4) supplying the lightest and closest to mean litter weight foetuses, of both sexes. This was performed for both placental and endometrial samples individually.

PCRs were performed (2.1.3) to ensure that the primers generated a single product with the desired amplicon size. The primers were tested on pooled cDNA using a gradient PCR block (TProfessional; Biometra), testing 6 annealing temperatures (55^{o}C, 56^{o}C, 58.2^{o}C, 60.6^{o}C, 63.0^{o}C and 64.7^{o}C). Electrophoresis was performed (2.1.4) and the gel was visualised. From this experiment, a product of the desired size and intensity was visible at 60^{o}C annealing temperature in all cases, therefore qPCRs were performed using this annealing temperature.

The 11 primer sets were tested on both the placental and endometrial samples and the standard curve for both tissue types (2.2.8.1). The qPCR was performed (2.2.8.2) and the text file from MxPro was imported in qBase+ (Biogazelle). A geNorm analysis was performed to identify both the most stable

reference gene from the tested primers and the optimal number of reference genes to be used in relation to the number of target genes of interest.

The geNorm M function on qBase+ defines the stability of the reference genes by calculating the average pairwise variation of a particular gene with all other control genes. Additionally, the average expression stability value (M) where stepwise exclusion of the genes which were the least stable (highest M values) was performed. This generates a graph with the least stable reference gene on the left, and the most stable reference gene on the right. Genes with an M value below the threshold of 1.5 were considered to have stable expression. A number of reference genes were considered stable in both tissues, with M values of ≤1.5 (Figure 2.1). These analyses revealed that TATA box binding protein (*TBP1*) and Hypoxanthine phosphoribosyltransferase 1 (*HPRT1*), and *TBP1* and Topoisomerase II beta (*TOP2B*) were the most stable reference genes for the placenta and endometrial samples respectively (Figure 2.1). These references genes were run all samples for each experiment and on occasions, these genes were not considered stable when the genes had been run on all samples. If this was the case other reference genes which were considered stable in the geNorm M analysis were trialled.

The geNorm V function on qBase+ allowed identification of the optimal number of reference genes required. This application of the software calculates the pairwise variation (*Vn/n+1*) where n represents the number of genes. A *V* value of ≤0.15 was proposed as a threshold, below which no additional references genes were required to be included (Vandesompele *et al.*, 2002). From these analyses, the optimal number of reference genes required for both tissues was two (Figure 2.1).

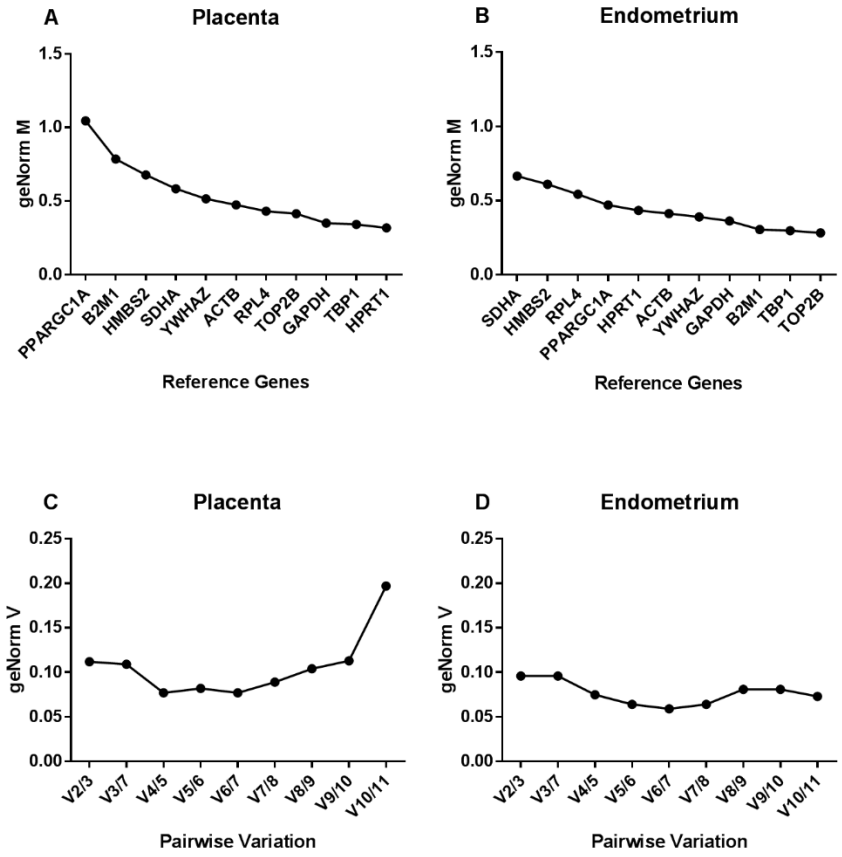

Figure 2.1: Summary of Identification of Stable Reference Genes in Placental and Endometrial Samples.

The geNorm function of qBase+ was used to identify the most stable reference genes in placental (A and C) and endometrial (B and D) samples. *TBP1* and *HPRT1*, and *TBP1* and *TOP2B* were identified as the most stable reference genes for placental and endometrial samples respectively (A and B). The geNorm V function calculated the pairwise variation (*Vn/n+1*) where n represents the number of genes (C and D). The results of this analysis indicated that the optimal number of reference genes required for normalisation was 2 in both placental (C) and endometrial (D) samples.

Gene Symbol	Gene Name	Accession Number	Function	Primer Sequence (5'→ 3')		Amplicon Size (bp)	Reference
ACTB	Beta-actin	DQ845171	Involved in cell motility, structure, and integrity	Fwd	CACGCCATCCTGCGTCTGGA	100	Nygard *et al.*, (2007)
				Rev	AGCACCGTGTTGGCGTAGAG		
B2M1	Beta-2-microglobulin	DQ845172	Cytoskeletal protein involved in cell locomotion	Fwd	CAAGATAGTTAAGTGGGATCGAGAC	161	Nygard *et al.*, (2007)
				Rev	TGGTAACATCAATACGATTTCTGA		
GAPDH	Glyceraldehyde-3-phosphate dehydrogenase	DQ845173	Involved in carbohydrate metabolism	Fwd	ACACTCACTCTTCTACCTTTG	90	Nygard *et al.*, (2007)
				Rev	CAAATTCATTGTCGTACCAG		
HMBS2	Hydroxymethylbilane synthase	DQ845174	Involved in haeme biosynthesis	Fwd	AGGATGGGCAACTCTACCTG	83	Nygard *et al.*, (2007)
				Rev	GATGGTGGCCTGCATAGTCT		
HPRT1	Hypoxanthine phosphoribosyltransferase 1	DQ845175	Involved in purine ribonucleoside salvage	Fwd	GGACTTGAATCATGTTTGTG	91	Nygard *et al.*, (2007)
				Rev	CAGATGTTTCCAAACTCAAC		
PPARGC1A	Peroxisome proliferator-activated receptor gamma coactivator 1-alpha	XM021074733.1	Regulator of mitochondrial biogenesis	Fwd	CCTGCATGAGTGTGTGCTCT	137	Erkens *et al.*, (2006)
				Rev	CTCAGAGTCGTTGCACA		
RPL4	Ribosomal protein L4	DQ845176	Structural constituent of ribosome	Fwd	CAAGAGTAACTACAACCTTC	122	Nygard *et al.*, (2007)
				Rev	GAACTCTACGATGAATCTTC		
SDHA	Succinate dehydrogenase complex, subunit A	DQ845177	Involved in Tricarboxylic acid cycle	Fwd	CTACAAGGGGCAGGTTCTGA	141	Nygard *et al.*, (2007)
				Rev	AAGACAACGAGGTCCAGGAG		
TBP1	TATA box binding protein	DQ845178	Involved in transcription	Fwd	AACAGTTCAGTAGTTATGAGCCAGA	153	Nygard *et al.*, (2007)
				Rev	AGATGTTCTCAAACGCTTCG		

			initiation from RNA polymerase II promotor				
TOP2B	Topoisomerase II beta	NM_001258386.1	Involved in chromosome condensation and chromatid separation	Fwd	AACTGGATGATGCTAATGATGCT	107	Erkens *et al.*, (2006)
				Rev	TGGAAAAACTCCGTATCTGTCTC		
YWHAZ	Tyrosine 3-monooxygenase /tryptophan 5-monooxygenase activation protein, zeta polypeptide	DQ845179	Involved in protein domain specific binding	Fwd	TGATGATAAGAAAGGGATTGTGG	203	Nygard *et al.*, (2007)
				Rev	GTTCAGCAATGGCTTCATCA		

Table 2.4: Reference Gene Primer Details.

Abbreviations: bp=base pairs; Fwd=Forward; Rev=Reverse.

2.3 Histological Methodology

2.3.1 Tissue Preservation and Processing for Histology

From the placental and endometrial samples of interest, small pieces of tissue were placed in a falcon tube containing approximately 15ml of Bouin's fixative (Sigma Aldrich, St Louis, Missouri, U.S.A.). The samples were left at room temperature for 24 hours. Following this, the samples were changed into 70% Ethanol (Genta Medical, York, U.K.), and the 70% Ethanol was changed daily for a minimum of one week.

After fixation, the samples were transferred into labelled tissue processing cassettes (Simport, Beloecil, Canada). The tissue samples were processed using a tissue processor (ASP3005, Leica, Milton Keynes, U.K.). Samples were incubated in 70% Ethanol (Genta Medical) for 2 hours, followed by two 1 hour incubations in 95% Ethanol (Genta Medical). They were then incubated for 4 hours in 100% Ethanol (Genta Medical), with two changes in that period. Finally, the tissues were incubated three times for 2 hours each in Xylene (Genta Medical) followed by three incubations for 2 hours each in molten paraffin wax.

Following processing, the cassettes were opened, and the samples were placed in a mould containing a thin cushion of molten paraffin wax that was allowed to partially solidify. The cassette was placed on top of the mould, which was then filled with paraffin wax (~55^{o}C) using an embedding station (Histocore Arcadia, Leica) The samples were left to cool for approximately 2 hours and were removed from their moulds.

2.3.2 Microtome Sectioning of Paraffin Embedded Tissues

Sections were generated from the paraffin embedded samples using a microtome (Microm HM325, ThermoFisher Scientific) with disposable blades (MB-35, ThermoFisher Scientific). Sections were cut at a thickness of 5µm and floated into a water bath (37^{o}C). The sections were transferred to polysine coated slides (ThermoFisher Scientific) and left to dry flat at room temperature

for approximately 20 minutes. Following this, the sections were allowed to adhere to the slides in an oven (55^{o}C) for a minimum of 2 hours.

2.3.3 Immunohistochemistry of Paraffin Embedded Sections

For immunohistochemistry of paraffin embedded sections, the Vectastain Elite ABC Kit (Vector Laboratories, Peterborough, U.K.) was used. For antibodies raised in mouse and rabbit, the PK6102 and PK6101 kits were used respectively.

2.3.3.1 Preparation of Solutions Required

- 0.3% Hydrogen Peroxide in Methanol.
  The stock 30% Hydrogen Peroxide (Sigma Aldrich) was diluted 1:100 in Methanol (Fisher Scientific) prior to use.
- Citrate Based Antigen unmasking solution (Vector Laboratories)
  The concentrated solution was diluted 1:100 with dH_20 prior to use.
- Novared peroxidase substrate (Vector Laboratories).
  This solution was created by adding: 150µl reagent 1; 100µl reagent 2; 100µl reagent 3 and 100µl hydrogen peroxide solution to 5ml dH_20. The solution was thoroughly mixed by vortexing after the addition of each component.
- Dulbecco's Phosphate Buffered Saline (PBS) (1 X PBS)
  PBS tablets (Oxoid, ThermoFisher Scientific) were dissolved in dH_20 and the pH adjusted to pH7.4 using 1M HCl. Each tablet was dissolved in 100ml dH_2O and scaled up depending on the final volume of PBS required. Each tablet was composed of NaCl 8g/l, KCl 0.2g/l, KH_2PO_4 1.15g/l, Na_2HPO_4 0.24 g/l.
- 0.3% Tween-20 in PBS
  To 1 litre of PBS, 3ml of Tween-20 (Amresco, Solon, Ohio, U.S.A.) was added.
- Harris Haematoxylin (Leica)

This was filtered using 240mm filter paper (GE Healthcare, Little Chalfont, Buckinghamshire, U.K.) prior to use.

- Scotts Tap Water substitute
  In 1 litre of dH_20, 2g sodium hydrogen carbonate (BDH Laboratory Supplies, Poole, U.K.) and 20g magnesium sulphate-7-hydrate (SLS) were dissolved.
- Blocking Solution
  To 10ml PBS, 150µl of normal serum (supplied in ABC Kit) was added.
- Biotinylated secondary antibody
  To 10ml PBS, 150µl of normal serum (supplied in ABC Kit) and 50µl of biotinylated antibody was added.
- Vectastain Elite ABC reagent
  To 5ml PBS, 100µl reagent was added followed by the addition of 100µl reagent B. The solution was mixed after the addition of each component and was left to incubate at room temperature for a minimum of 30 minutes before use.

2.3.3.2 Immunohistochemistry Protocol

The paraffin wax was removed from the sections by performing three 5 minute washes in Xylene (Genta Medical). The sections were rehydrated by treatment with 100% Ethanol (Fisher Scientific) twice for 5 minutes, 95% Ethanol for 2 minutes and washed with tap water for 5 minutes. To permeabilise the tissues, the slides were treated twice for 5 minutes in 0.3% Tween-20 in PBS.

To reverse epitope masking, often caused by the fixation process, heat-mediated antigen retrieval was performed by placing slides in a plastic slide container containing 250ml diluted antigen unmasking solution for approximately 30 minutes at 121^{o}C in an autoclave (Little Sister Ses 200, Eschmann, Lancing, U.K.). The slides were cooled by washing with tap water. To block for endogenous peroxidase activity, slides were treated with 0.3% Hydrogen Peroxide in Methanol for 30 minutes at room temperature and washed for 5 minutes in PBS. To decrease the prevalence of background

staining, non-specific antibody binding sites were blocked by incubating the slides for a minimum of 30 minutes in blocking solution. The primary antibody of interest was diluted in PBS and applied to the section overnight at 4^{o}C in a humidity chamber. Simultaneously, an additional slide was incubated with immunoglobulin G (IgG) (Vector Laboratories) from the species in which the primary antibody was raised, at an equivalent protein concentration to the primary antibody of interest.

Following a 5 minute wash in PBS, the sections were incubated with the biotinylated antibody for 30 minutes, followed by a further 5 minute wash in PBS. The Vectastain Elite ABC reagent was applied to the slides for 30 minutes, and they were washed for 5 minutes in PBS. Novared peroxidase substrate was applied to the sections until the desired intensity of staining had developed. This was optimised for each antibody of interest. Following a 5 minute wash in tap water, the slides were counterstained with haematoxylin, to stain the nuclei of the cells in the section, for 30 seconds and excess haematoxylin was removed by washing in tap water. The sections were then treated with Scott's tap water for 2 minutes, washed again in tap water, and dehydrated by treatment with 70% Ethanol for 30 seconds, twice with 95% Ethanol for 30 seconds, and 100% Ethanol twice for 1 minute. Following this, the slides were treated with 50/50 Ethanol/Xylene for 1 minute, followed by three 1 minute treatments with Xylene. ClearVue mountant (Shandon, ThermoFisher Scientific) was used to mount the slides with glass coverslips and they were left to cure for a minimum of 24 hours prior to imaging.

2.3.4 Immunofluorescence of Paraffin Embedded Sections

2.3.4.1 Preparation of Solutions Required

- 1 X PBS. As described in 2.3.3.1.
- 0.3% Tween-20 in PBS. As described in 2.3.3.1.
- Citrate Based Antigen unmasking solution (Vector laboratories H3300) The concentrated solution was diluted 1:100 with dH_20 prior to use.
- Antibody Dilution Buffer

To a falcon tube 2 parts by volume PBS was added. To this, 1% Bovine Serum Albumin (Sigma Aldrich), 0.3% Tween-20 (Amresco) and 1 part by volume Glycerol (Fisher Scientific) were added.

- Blocking Solution
  Antibody dilution buffer was supplemented with 10% Normal Goat Serum (Sigma Aldrich).

2.3.4.2 Immunofluorescence Protocol

Paraffin sections were dewaxed and rehydrated (2.3.3.2) and treated twice for 5 minutes each with 0.3% Tween-20 in PBS, after which heat-mediated antigen retrieval was performed. To reduce background staining, non-specific antibody binding sites were blocked by incubating the slides for a minimum of 1 hour in blocking solution (antibody dilution buffer supplemented with 10% normal goat serum). The slides were washed for 5 minutes in PBS before incubating at 4^{o}C overnight in primary antibody diluted in antibody dilution buffer. As a negative control, IgG (Vector Laboratories) from the species in which the primary antibody was raised was diluted in antibody dilution buffer and the section was incubated overnight at 4^{o}C. Following this, all slides were washed three times for 5 minutes in PBS, in a plastic slide container covered with aluminium foil to protect the slides from the light.

An Alexa Fluor (Invitrogen) fluorescent secondary antibody against the species and isotype of interest, e.g. goat anti-rabbit IgG, was prepared in antibody dilution buffer containing 10% normal goat serum. The slides were incubated in secondary antibody in a light-proof humidity chamber for 1 hour at room temperature. After this incubation, the slides were washed three times for 5 minutes in PBS.

The sections were counterstained, to allow recognition of the cell nuclei, with Propidium Iodide (10ng/ml) (Sigma Aldrich) for 3 minutes at room temperature, in a plastic slide container covered with aluminium foil to protect the slides from the light. After this, the sections were washed with dH_2O three times for 5

minutes, in a plastic slide container covered with tinfoil to protect the slides from the light.

Excess moisture was blotted from the slides with tissue paper and the slides were placed on a slide tray in a light-proof box. A drop of ProLong Gold Antifade reagent (Invitrogen) was added to the sections and they were covered with glass coverslips. The slides were left in the dark at room temperature to cure for a minimum of 48 hours prior to imaging. Once cured, the edge of the coverslips were sealed with nail polish to increase the length of time the samples maintained their fluorescence.

2.3.5 Immunocytochemistry of Adherent Cells

2.3.5.1 Preparation of Solutions

- 4% Paraformaldehyde (PFA)

  To 50ml autoclaved PBS, 2g paraformaldehyde (Sigma Aldrich) was added in a sterile beaker on a hot plate with stirring. Once the paraformaldehyde had dissolved, 1 drop of 5M sodium hydroxide was added. The pH was adjusted to 7.2 with the addition of 37% hydrochloric acid. The solution was then filtered with 240mm filter paper (Whatman, GE Healthcare) into 50ml falcon tubes and stored on ice until required.
- 1 X PBS. As described in 2.3.3.1.
- 5% Normal Goat Serum in PBS

  To 100ml PBS, 5ml Normal Goat Serum (Sigma Aldrich) was added.
- 0.3% Triton-X in PBS

  To a 50ml falcon tube containing 10ml PBS, 30µl of Triton-X (Sigma Aldrich) was added.
- 4',6-diamidino-2-phenylindole (DAPI)

  To 50ml PBS, 0.8µl of 1mg/ml neat DAPI stock (Novus Biologicals LLC, Littleton, Colorado, U.S.A.) was added to form a working stock of 6ng/ml. The bottle was wrapped in tinfoil and stored at 4^{o}C until required.

2.3.5.2 Immunocytochemistry Protocol

The adherent cells of interest were pre-grown on poly-D-lysine coated glass coverslips (Neuvitro, Vancouver, Washington, U.S.A.) in a 12 well plate (Eppendorf). When the cells were at ~80% confluency, 3ml of pre-warmed 4% PFA was added to the wells and the cells were incubated with this at room temperature for 2 mins. The culture medium containing PFA was removed and the cells were gently washed twice for two minutes in PBS, taking care to prevent the cells being dislodged. Following this, the cells were fixed by incubating in warm 4% PFA at room temperature for 15 minutes. After this, three washes for 5 minutes in PBS were performed. Methanol (1ml; Fisher Scientific), which had been stored at -20^{o}C, was added to the wells and the plates were incubated at -20^{o}C for 10 minutes. The methanol was removed, and the cells were permeabilised by incubating with 0.3% Triton-X in PBS for 5 minutes at room temperature. This step was followed by three 1 minute washes in PBS.

To prevent background staining, the cells were incubated in a protein block solution (Springbio, Pleasanton, California, U.S.A.) for 60 minutes at room temperature. The protein block was removed, and the cells were incubated overnight at 4°C with the primary antibody diluted in PBS with 5% normal goat serum. An IgG negative control (Vector Laboratories) of the species in which the primary antibody of interest was raised and which had an equivocal protein concentration to the primary antibody of interest, and a secondary antibody only (PBS with 5% normal goat serum) control was set up and incubated overnight at 4^{o}C.

A further three 5 minute washes in PBS were performed before incubation with the fluorescence-labelled secondary antibody (Alexa Fluor, Invitrogen) diluted in PBS with 5% normal goat serum. This incubation was performed at room temperature in a light-proof box for 60 minutes. The coverslips were washed twice for 5 minutes in PBS, before counterstaining with 6ng/ml DAPI solution for 10 minutes. The coverslips were rinsed with dH_2O before mounting with ProLong Gold Antifade reagent (Invitrogen) using specialised concaved slides (Marienfeld, Lauda-Königshofen, Germany). The slides were allowed to cure

in the dark for a minimum of 48 hours prior to imaging. Once cured, the edge of the coverslips were sealed with nail polish to increase the length of time the samples maintained their fluorescence.

2.4 Cell Culture Media

All media was sterile filtered using a 0.22µm syringe filter (Merck Millipore, Cork, Ireland).

2.4.1 Components

- Dulbecco's Modified Eagle's Medium/Nutrient Mixture F-12 Ham (DMEM-F12) with 15mM HEPES and sodium bicarbonate, without L-glutamine and phenol red (Sigma Aldrich).
- L-glutamine (200mM; Sigma Aldrich)
- Heat-inactivated Newborn Calf Serum (NBCS; Gibco, ThermoFisher Scientific).
- Penicillin-Streptomycin (PenStrep; 10,000 U/ml penicillin, 10,000µg/ml streptomycin) (Gibco, ThermoFisher Scientific).
- Medium-199 (M199) with Earle’s salts, L-glutamine and sodium bicarbonate (Sigma Aldrich).
- Endothelial Cell Growth Supplement from Bovine Neural Tissue (Sigma Aldrich). Resuspended 15mg in 1.5ml M199.

2.4.2 Media Composition

Medium for Tissue Culture – DMEM-F12 + 10% NBCS + PenStrep

To every 500ml of medium, 12.5ml L-glutamine was added. In a sterile 50ml falcon tube, 500µl PenStrep was added to 5ml NBCS and 44.5ml of DMEM-F12.

Medium for Culture of G-1410 Endothelial Cells – M199 + 10% NBCS + PenStrep + ECGS

In a sterile 50ml falcon tube, 44ml M199 was supplemented with 5ml of NBCS, 500µl PenStrep and 500µl ECGS.

Medium for Serum Starvation – M199 + PenStrep

In a sterile 50ml falcon tube, 500µl PenStrep was added to 49.5ml of M199.

Medium for Matrigel Branching Assays – DMEM-F12 + 10% NBCS + PenStrep

To every 500ml of medium, 12.5ml L-glutamine was added. In a sterile 50ml falcon tube, 500µl PenStrep was added to 5ml NBCS and 44.5ml of DMEM-F12.

2.5 Statistical Analysis

All statistical analyses were performed using Minitab 17 (Pennsylvania, U.S.A.) or GenStat 13.1 (VSN International Ltd., Oxford, UK). Throughout, the following workflow of statistical analysis was performed unless otherwise stated (Figure 2.2). Any data transformations performed are detailed in each chapter. The mean value for each parameter for each sample was calculated. The normality of the distribution of the data was assessed for each parameter by an Anderson-Darling test, both with all gestational days (GD) investigated combined and within GD. Following this, a Grubbs outlier test was performed to identify any outliers and the distribution of the data was reassessed after each exclusion. If the data did not have a normal distribution, log10 or square root (sqrt) transformations were performed.

2.5.1 Assessment of Temporal Changes

For each experiment, the influence of GD was assessed. If the data with all GD combined had a normal distribution, an analysis of variance (ANOVA) was performed, with and without a block for gilt. The block for gilt (maternal ID) was

fitted into the statistical test to account for any variations observed solely because of litter. Due to this, more confidence is placed throughout this thesis on the results which achieved statistical significance in the presence of a block for gilt. If the data with all GD combined did not have a normal distribution in the same transformation, a Kruskal-Wallis test was performed to identify temporal changes.

2.5.2 Assessment of Influence of Foetal Size

Associations between foetal size and each parameter were assessed at GD18-90 and GD30-90 in endometrial and placental samples respectively. Analyses were performed using samples associated with the closest to mean litter weight (CTMLW) and the lightest foetus at GD18 and 30. At GD45, 60 and 90, samples were taken from the CTMLW and lightest foetus of both sex. For the analysis of the influence of foetal size on each parameter at GD45-90, two analyses were performed: 1) the CTMLW and lightest foetus of both sex and 2) the true CTMLW and true lightest foetus, regardless of sex. Generally, due to both of the lightest foetuses not being growth restricted, fewer significant results were obtained performing the first analysis. It was deemed that the second analysis was more appropriate and informative therefore, throughout this thesis, only the true CTMLW and true lightest foetus comparison has been presented at GD18, 30, 45, 60 and 90 (unless otherwise stated). If the data had a normal distribution, ANOVA for foetal size, with and without a block for gilt was performed with all GD combined, and within GD. If the data did not have a normal distribution, a Mann-Whitney test was performed for foetal size within GD.

2.5.3 Assessment of Influence of Foetal Sex

Associations between foetal sex and each parameter were investigated at GD30, 45, 60 and 90 in both placental and endometrial samples. Analyses were performed using the data from samples associated with the overall lightest and CTMLW foetus at GD30, and the lightest and CTMLW foetuses of

both sex at GD45-90. If the data had a normal distribution, ANOVA for foetal sex, with and without a block for gilt was performed with all GD combined, and within GD. If the data did not have a normal distribution, a Mann-Whitney test was performed for foetal sex within GD.

2.5.4 Assessment of Sex X Size Interactions

Where possible, the presence of sex x size interactions in the overall CTMLW and overall lightest foetal comparisons was assessed. This was performed if the data were normally distributed by a two-way ANOVA, with and without a block for gilt. This was not usually possible at GD45, as only one of the overall lightest foetuses was male.

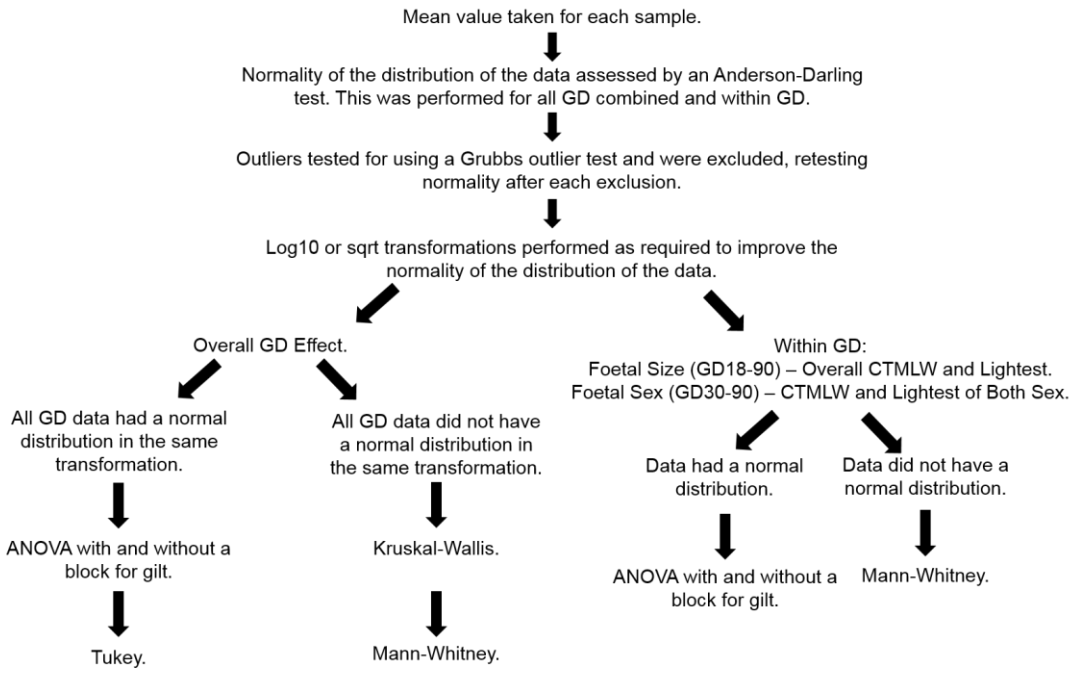

Figure 2.2: General Workflow for Statistical Analyses Performed.

Flow diagram showing the general workflow of statistical analyses performed. All statistical analyses were performed using Minitab 17 (Pennsylvania, U.S.A.) or GenStat 13.1 (VSN International Ltd., Oxford, UK). Any exceptions from this general approach, including any data transformations performed are detailed in the specific chapter. For each experiment, the gestational day (GD) and associations between foetal size (closest to mean litter weight (CTMLW) and lightest) and sex were assessed.

3 Sample Collection Data Analysis

3.1 Introduction

3.1.1 Association between General Litter Characteristics and Foetal Weight

As litter size increases, foetal weight decreases in rats (Barr *et al.*, 1970; Jensh *et al.*, 1970; Chahoud and Paumgartten, 2005, 2009; McLaurin and Mactutus, 2015), mice (Healy *et al.*, 1961; Ishikawa *et al.*, 2006) and rabbits (Pálos *et al.*, 1996; Prayaga and Eady, 2001; Poigner *et al.*, 2010). In contrast to these findings, some controversy exists regarding the relationship between litter size and foetal weight in the pig. Whilst Bauer *et al.*, (1998) suggest an inverse relationship between litter size and foetal weight, Finch *et al.*, (2002) demonstrated no relationship between litter size and mean litter weight (MLW), or weight of the lightest and heaviest foetuses at gestational day (GD) 30 and 100 in Meishan or Large White X Landrace gilts. Although, an inverse relationship was observed between litter size and both the MLW and weight of the lightest piglet in the litter at birth in Meishan gilts (Finch *et al.*, 2002). In addition to the overall effect of litter size, it has been suggested that the number of foetuses present in the individual uterine horn has an effect on foetal weight in rodents (Barr *et al.*, 1970) and pigs (Waldorf *et al.*, 1957), highlighting the importance of the foetuses located in close proximity on foetal development.

3.1.2 Uterine Position

Investigations into the influence of uterine position on foetal weight have been performed in litter bearing species. In the rabbit, it has been suggested that the foetuses located at the ovarian and cervical end of the uterine horn are heavier than those located in the middle of the uterine horn (Pálos *et al.*, 1996; Poigner *et al.*, 2010; Bautista *et al.*, 2015). Uterine position has been suggested to influence foetal weight in mice in a temporal manner. At GD14, foetuses located at the ovarian and cervical ends of the uterine horn were the lightest (v. Domarus *et al.*, 1986) whereas at GD19 foetuses located at the cervical and ovarian end of the uterine horn were the lightest and heaviest

respectively (Healy *et al.*, 1961; Louton *et al.*, 1988). In the rat, it has been suggested that the uterine position effect is dependent on the number of foetuses in the uterine horn. The average litter size in the rat varies depending on the strain but is commonly between 10 and 12 pups (Chahoud and Paumgartten, 2009; McLaurin and Mactutus, 2015). If the uterine horn contains more than eight foetuses, the foetuses located in the middle of the uterine horn are heavier than those located at the ovarian and cervical ends of the uterine horn (Barr *et al.*, 1969, 1970; Barr and Brent, 1970; Jensh *et al.*, 1970; McLaurin and Mactutus, 2015). In contrast, when there are less than four foetuses present in the uterine horn, foetuses located at the cervical end of the uterine horn were heaviest and those at the ovarian end were the lightest (McLaurin and Mactutus, 2015).

Contradicting reports in the literature exist regarding the influence of uterine horn position on porcine foetal weight. Rohde Parfet *et al.*, (1990a) demonstrated a tendency for piglets which are located at the ovarian end (and adjacent to the ovarian end) of the uterine horn to be heavier at birth. Similar findings were presented by Jang *et al.*, (2014) who found that foetuses at the ovarian end of the uterine horn, and immediately adjacent to the foetuses located at the ovarian end were heavier and longer than foetuses located in the middle of the horn at GD58. They demonstrated that at GD101 and 108 foetuses located at the ovarian end were heavier and longer than foetuses located in the middle of the uterine horn and those adjacent to the foetuses at the cervical end, and foetuses located at the cervical end of the uterine horn had an intermediate weight and length. Jang *et al.*, (2014) suggested that uterine position does not influence foetal growth until after GD43, as they did not observe an association between foetal size and position at this GD or earlier. This hypothesis was also suggested by Knight *et al.*, (1977) who demonstrated no association between uterine position and foetal weight or crown-rump length (CRL) prior to GD35 of gestation, with an effect observed from GD45 onwards. Wise *et al.*, (1997) demonstrated no association between uterine position and foetal weight in early gestation (GD30), but in late gestation (GD70 and 104) the heaviest and lightest foetuses were located at

the ovarian and cervical ends of the uterine horn respectively. Finch *et al.*, (2002) also did not find an association between uterine position and foetal weight at GD30 however, in contrast to the previously detailed studies, did not observe a relationship at GD100. Further, their investigations demonstrated that intrauterine growth restricted (IUGR) and small for gestational age (SGA) foetuses were found throughout the uterine horn throughout gestation. It has been shown on occasions where less than five foetuses are present in the uterine horn, uterine position is not associated with foetal weight in the pig (Perry and Rowell, 1969). Whereas, on occasions where there are more than five foetuses in the uterine horn, foetuses located at cervical end were lighter than those located at the ovarian end of the uterine horn (Perry and Rowell, 1969). Further, it has been suggested that the foetuses located in the middle of the uterine horn are smaller than those located at the ends of the uterine horns (Perry and Rowell, 1969).

3.1.3 Influence of Sex of Foetuses in the Litter

3.1.3.1 Androgen Exposure

In several mammalian species, it has been demonstrated that male foetuses produce testosterone at an earlier stage of gestation and in greater quantities than female foetuses, whereas female foetuses produce large quantities of oestradiol (E2) in late gestation (described by Ryan and Vandenbergh, 2002). Steroids are known to be transported between foetuses in litter bearing species (Clemens *et al.*, 1978; vom Saal and Bronson, 1978; Vomachka and Lisk, 1986; vom Saal, 1988; Krohmer and Baum, 1989; vom Saal *et al.*, 1990; Clark *et al.*, 1991, 1992; Even *et al.*, 1992; Drickamer, 1996). Therefore, the sex ratio of a litter and sex of adjacent foetuses can influence the exposure of foetuses to sex steroids, for example a female foetus in a male biased litter or with two male neighbours will be exposed to increased androgens during gestation (vom Saal and Bronson, 1980a; vom Saal *et al.*, 1990; Clark *et al.*, 1991), whereas a female foetus with two female neighbours or from a female biased litter would be exposed to increased E2 (vom Saal, 1983; vom Saal *et*

al., 1999). This is turn could have a significant effect on the development of the reproductive system, which could influence reproductive success postnatally. In addition to the inter-foetal transport of sex steroids, it has been demonstrated that substantial transport of insulin like peptide 3 (INSL3), produced by male foetuses to promote testicular descent, occurs between male and female foetuses, at GD30 and 45 in the pig (Vernunft *et al.*, 2016). This finding suggests that hormone transport occurs between foetuses from an early stage of gestation.

Anogenital distance (AGD) is known to reflect prenatal exposure to androgens (Dean and Sharpe, 2013; Thankamony *et al.*, 2016), which regulate the migration of the genital orifice during development. In the pig, Rohde Parfet *et al.*, (1990a) suggested that the number of neighbours of the same sex had no influence on AGD. In addition, it has been suggested that the sex of adjacent foetuses does not influence foetal testosterone levels (Wise and Christenson, 1992). However, the findings of Drickamer *et al.*, (1997) contradict this, with a positive correlation observed between the proportion of males in the litter and gilt AGD. This would suggest that females from male biased litters are exposed to a greater amount of androgens than females in a female biased, or equally balanced litter, which in turn may induce the differences in reproductive behaviour and outcome observed in females from male biased litters (discussed below).

3.1.3.2 Sex Ratio of Litters

Female piglets from male biased litters have decreased reproductive success, with an increased number of inseminations required to conceive (Drickamer *et al.*, 1997), despite reaching puberty earlier (Lamberson *et al.*, 1988). From an industry perspective, it has been demonstrated that gilts from litters with >70% males produced fewer piglets (Huhn *et al.*, 2002) therefore, breeding with gilts from heavily male biased litters should be avoided. Some controversy exists regarding the influence of litter sex ratio on the number of stillborn piglets. Górecki, (2003) suggest that perinatal mortality is increased in female biased

litters. Huhn *et al.*, (2002) however suggested that males are more likely to be still born than their female littermates, and that litters from gilts from male biased litters (>60% male) had an increased number of piglets which had to be culled. Further evidence for the role of sex ratio on female reproductive success was provided by Drickamer *et al.*, (1999) who suggest that the number of teats was inversely related to the proportion of males in the litter, which would limit the number of suckling piglets, thereby limiting the number of piglets weaned per sow per year. Also, it has been suggested that the proportion of females in the litter is positively associated with litter size (Górecki, 2003), which is a beneficial trait to the pig industry. Considering this, the association between foetal sex ratio and the feto-maternal interface in the pig should be investigated further.

3.1.3.3 Sex of the Neighbours

The influence of the sex of the adjacent (neighbour) foetuses has been extensively investigated in litter bearing species (reviewed by (vom Saal, 1989; Ryan and Vandenbergh, 2002). To date, a significant amount of research has been performed in rodents although the majority of studies have compared foetuses with zero and two male neighbours, with limited investigation of foetuses with one male neighbour (

Table 3.1).

Jang *et al.*, (2014) investigated the influence of neighbour sex on foetal weight and CRL in the pig at GD43, 58, 73, 91, 101 and 108. Generally, neighbour sex had no influence on foetal weight or CRL. Similar findings were observed by Rohde Parfet *et al.*, (1990), who found that the number of neighbours of the same sex has no influence on birth weight or postnatal survival. However, Tarraf and Knight, (1995) found that female foetuses with two male neighbours are heavier than those with no male neighbours at GD40, 60, 80 and 100. Additionally, female foetuses with two male neighbours have been suggested to be longer (increased CRL) compared to female foetuses with no male neighbours at GD73 (Jang *et al.*, 2014). Finch *et al.*, (2002) made an

interesting observation at GD100 that none of the IUGR foetuses in their study had two neighbours of the opposite sex. In contrast to this idea, Wise and Christenson, (1992) suggested that foetuses with two neighbours of the opposite sex are lighter than those with no or one neighbour of the opposite sex.

Male piglets that had two male neighbours *in utero* had increased weight gain from post-natal day 175-270 when challenged with restricted feeding compared to males with no or one male neighbours, which could suggest that it is advantageous postnatally to develop in close proximity to foetuses of the same sex prenatally (Rohde Parfet *et al.*, 1990a). Rohde Parfet *et al.*, (1988, 1990a, b) demonstrated that the number of male neighbours influenced female reproductive outcome and sexual behaviour postnatally. Whilst no influence on aggressiveness or ovulation rate (OR) were observed, female pigs with two male neighbours had a shorter oestrous cycle length compared to female pigs with male neighbours (Rohde Parfet *et al.*, 1988) and reached puberty sooner (Rohde Parfet *et al.*, 1990b) than females which had no or one male neighbour. In mice it has been demonstrated that females with two male neighbours are more aggressive (vom Saal and Bronson, 1978). This has been suggested to a certain extent in the pig, with females with no male neighbours participating in and winning fewer fights than those with one or two male neighbours (Rohde Parfet *et al.*, 1990b). Gilts with no male neighbours were found to be more sexually receptive than those with one or two male neighbours (Rohde Parfet *et al.*, 1990b). Receptivity in the pig is known to be regulated by E2 (Signoret, 1971; Beach, 1976; Ford, 1985), which could suggest that females with no male neighbours have altered sensitivity to E2, which could have the potential to alter reproductive success. Considering the mixed reports in the literature of the influence of neighbour sex on foetal weight, further investigations should be performed.

3.1.4 Asymmetric Organ Growth

As described in the general introduction, placental insufficiency in IUGR pregnancies has been demonstrated to induce foetal hypoxia, which in turn has drastic consequences for the developing foetus. In response to the hypoxic and nutrient depleted conditions, the foetus redistributes its cardiac output to ensure an adequate blood supply to the essential organs, notably the brain, at the expense of less essential organs such as the liver, skeletal muscle and kidney (McMillen *et al.*, 2001; Stephens *et al.*, 2015). This phenomenon is called brain sparing and is well characterised in human IUGR (Cohen *et al.*, 2015). Importantly, it has been suggested that the degree of asymmetric organ growth is related to the onset, intensity and duration of the placental insufficiency (Miller *et al.*, 2016). Using a foetal sheep model Jones Jr *et al.*, (1977) demonstrated that the consumption of oxygen by the brain can be maintained in low oxygen conditions. Despite this mechanism of brain sparing, brains from IUGR human pregnancies have abnormal development, with neurodevelopmental defects including decreased brain volume, structure, cell number, impaired myelination and reduced brain connectivity (Miller *et al.*, 2016).

Experimentally induced sheep models of IUGR have demonstrated that brain growth is spared at the expense of other organs, notably the kidney and liver (McMillen *et al.*, 2001; Carr *et al.*, 2012). Asymmetric organ growth has been demonstrated in growth restricted newborn piglets (Bauer *et al.*, 1998, 2003), indicated by an increased brain weight to liver weight ratio, which reflects a small decrease in brain weight compared with a large decrease in the liver weight observed in the growth restricted piglets compared to their normal sized littermates. Bauer *et al.*, (2007) investigated the cerebral utilisation of oxygen in normal and IUGR piglets in response to asphyxia and hypoxia and demonstrated that growth restricted piglets have improved cerebral oxygen utilisation compared to normal body weight foetuses. This suggests programming of the response to hypoxic challenges exists in growth restricted piglets, with an increased ability to maintain the oxygen supply to the brain. Using a unilateral oviduct ligation model to induce uterine crowding and growth

restriction Town *et al.*, (2004) demonstrated that in the resulting foetuses at GD90, brain sparing was observed. Despite the organ allometry analyses performed in newborn piglets, the timing of the development of this brain sparing phenotype in the naturally-occurring growth restricted piglet during gestation remains poorly understood.

3.1.5 Selection of Gestational Days

In this thesis, five key gestational days have been selected to investigate the relationship between foetal size, sex and the structure and function of the porcine feto-maternal interface. Considering the hypothesis that IUGR in the pig occurs due to aberrant conceptus attachment, it was important that an early stage of pregnancy was investigated. As described in 1.2.1, the porcine conceptus has a long pre-implantation stage, with attachment beginning around day 11-12. As this study is interested in exploring the relationship between the conceptus and the endometrium, it was decided to investigate GD18 as by this day of pregnancy all of the conceptuses which are going to attach will have attached and the endometrial samples associated with each individual conceptus can be easily identified.

During pregnancy, temporal changes in the rate of foetal and placental growth can be observed (Figure 1.5). Samples associated with foetuses of different size and sex at GD30 were utilised as at this stage of pregnancy placental growth occurs at a faster rate than foetal growth (Figure 1.5). In addition, it has previously been demonstrated that significant variation in foetal size can be observed at GD30 (Pettigrew *et al.*, 1986; Wise *et al.*, 1997; Finch *et al.*, 2002; Foxcroft and Town, 2004; Foxcroft *et al.*, 2006), which is reflective of the post-natal within-litter variation in piglet size observed. The third gestational day selected for investigation in this thesis was GD45, as at this GD both the placenta and the foetus are growing at an increased rate compared to GD30 (Figure 1.5).

After the initially fast period of placental growth, the growth rate of the porcine placenta plateaus in mid-gestation (Figure 1.5) whereby instead of continuing

to increase in weight, the structure of the placenta undergoes extensive remodelling to increase the surface area available for nutrient exchange with the developing foetus (Vallet and Freking, 2007). In addition, whilst the placental growth rate is decreased, the foetus is undergoing rapid growth, placing large demands upon the placenta. Considering this, GD60 was selected for investigation as it was anticipated that large differences would be observed between foetuses of different size and sex at this dynamic stage of pregnancy. For the final day of pregnancy, a late GD (GD90) was selected in order to be reflective of the phenotype observed at term. At this stage of pregnancy, the foetus is still maintaining an exponential growth rate (Figure 1.5) whilst the placenta is continuing to undergo extensive remodelling to maintain nutrient transfer to the developing foetus.

3.2 **Aims**

The aims of the research described in this chapter were:

i. To investigate temporal changes in foetal weight, CRL, Ponderal Index (PI), allantoic fluid (ALF) and amniotic fluid (AMF) volumes at GD30, 45, 60 and 90.
ii. To investigate the relationship between foetal weight and CRL, PI, ALF and AMF volume, and organ weight at GD30, 45, 60 and 90.
iii. To investigate the relationship between foetal sex and foetal weight, CRL, PI, ALF and AMF volumes, and organ weight at GD30, 45, 60 and 90.
iv. To investigate the influence of litter sex ratio on foetal weight and CRL, PI, ALF and AMF volume at GD30, 45, 60 and 90.
v. To investigate the influence of neighbour sex on foetal weight, CRL, PI, ALF and AMF volumes, and organ weight at GD30, 45, 60 and 90.
vi. To investigate the association between uterine position and foetal weight, CRL, PI, ALF and AMF volumes at GD30, 45, 60 and 90.

Sex (M = Male; F = Female)	Variable	Number of Male Neighbours		Reference
		0	2	
M and F	Oestradiol	Increased	Decreased	vom Saal, (1988)
M and F	Testosterone	Decreased	Increased	vom Saal and Bronson, (1978); vom Saal *et al.*, (1990)
M and F	Post-weaning body weight	Decreased	Increased	Kinsley *et al.*, (1986)
F	Anogenital Distance (AGD)	Decreased	Increased	Gandelman *et al.*, (1977); McDermott *et al.*, (1978); vom Saal and Bronson, (1978); Vandenbergh and Huggett, (1995)
F	Male Offspring	Decreased	Increased	Vandenbergh and Huggett, (1995)
M and F	Aggressiveness	Less	More	Gandelman *et al.*, (1977); vom Saal and Bronson, (1978); Drickamer, (1996)
F	Mating and Impregnation	Earlier	Later	Vom Saal, (1989)
F	Mounting by other F	Less likely	More likely	Rines and vom Saal, (1984); Quadagno *et al.*, (1987)
M	Sexual Activity	Increased	Decreased	vom Saal, (1983)
M	Parental Behaviour	Decreased	Increased	vom Saal, (1983, 1988)
F	Sexual Attractiveness	Increased	Decreased	vom Saal and Bronson, (1978, 1980)
F	Sexual Receptivity	Increased	Decreased	Rines and vom Saal, (1984)
F	Oestrous Cycle Length	Shorter	Longer	vom Saal and Bronson, (1980b); vom Saal, (1981); Vom Saal, (1989)
M	Prostate Weight	Increased	Decreased	vom saal, (1989)
F	Vaginal Opening	Earlier	Later	(McDermott *et al.*, 1978; Vom Saal, 1989)

Table 3.1: Summary of Influence of Number of Male Neighbours on Postnatal Behaviour, Physiology and Morphology in Mice.

3.3 Materials and Methods

3.3.1 General Animals/Experimental Design

All procedures were performed with approval from The Roslin Institute (University of Edinburgh) Animal Welfare and Ethical Review Board and in accordance with the U.K. Animals (Scientific Procedures) Act, 1986.

Samples were collected from Large White X Landrace gilts (age 11-14 months; n=41) in three animal experiments (Figure 3.1). Gilts were observed daily for signs of oestrus and were housed in groups of 6-8 animals per pen. Oestrous cyclicity and ovarian function were controlled in accordance with routine normal practice at The Roslin Institute Large Animal Unit. In a subset of gilts (distribution between the gestational days investigated; indicated in Table 3.6) oestrus was synchronized by daily feeding of 20mg Altrenogest (Regumate, Hoechst Roussel Vet Ltd., Milton Keynes, U.K.) for 18 days followed by injection of Pregnant Mare Serum Gonadotrophin (PMSG) and human chorionic gonadotrophin (hCG) as described by Lillico *et al.*, (2013). All gilts were inseminated twice daily for the duration of oestrus with semen from a Large White sire. The distribution of the sires used between the GD investigated is detailed in Table 3.6. The first day of insemination was assigned as GD0 and gilts were euthanised at the GD of interest with sodium pentobarbitone 20% w/v (Henry Schein Animal Health, Dumfries, U.K.) at a dose of 0.4ml/kg by intravenous injection via a cannula inserted in the ear vein. Following confirmation of death, mid-ventral incision revealed the reproductive tract. The tract was lifted from the body cavity and placed in a dissecting tray, and excess broad ligament was removed. Throughout the dissection, all instruments and containers were nuclease free, or regularly cleaned with RNase Zap (Life Technologies, ThermoFisher Scientific, Altrincham, U.K.). The ovaries were removed from the tract and the *corpora lutea* (CL) dissected and quantified to give the OR.

3.3.2 GD18 Sample Collections

The uterine tract was rinsed with saline and string was used to tie the end of the right and left uterine horns at the bifurcation. The uterine horns were cut between the two pieces of string and each uterine horn was placed in a floatation device (Figure 3.2) containing an RNA-Later® like solution (2.2.1) to preserve the integrity of the RNA. Using dissection scissors, the uterine horn was opened along the mesometrial side and the conceptuses floated upwards in the solution. The conceptuses were removed from the floatation device with forceps and weighed in a cryovial (Starlab, Milton Keynes, U.K.). The conceptuses were then preserved for later isolation of nucleic acids (2.2.2). Nucleic acids were not isolated from these samples for the research performed in this thesis as the samples are part of a larger project. Therefore, the sex of the conceptuses has not yet been determined. The uterine lumen was occluded between each conceptus to ensure that endometrial samples associated with particular conceptuses could be identified.

The lightest and the closest to the mean litter weight (CTMLW) conceptus was identified based on weight, and endometrial samples were taken from each conceptus of interest. Samples were snap-frozen in liquid nitrogen and stored at -80^{o}C for RNA extraction, or fixed in Bouin's (Sigma Aldrich, St Louis, Missouri, U.S.A.) for histology. RNA (2.2) and tissue processing (2.3) were performed.

3.3.3 GD30, 45, 60 and 90 Sample Collections

The uterine horns were dissected, from the ovary towards the cervix, with Cheryl Ashworth and myself dissecting the left and right uterine horns respectively throughout the sample collections. The allantoic sac was burst and the ALF collected and measured. Following this, the amniotic sac was burst and the AMF collected and measured. The umbilicus for each foetus was cut and the foetus was placed in an RNase-free container. Foetuses were identified as 'live' based on their morphology, and any foetuses that were defined as 'dead' or if there was evidence of resorption were recorded. GD90

foetuses are protected under the U.K. Animals (Scientific Procedures) Act, 1986 which meant that cardiac injection with sodium pentobarbitone had to be performed following removal from the uterine tract to ensure the foetus was no longer alive. Each foetus was weighed and the CRL measured. CRL was measured using digital callipers at GD30, and a piece of string and a ruler at the other GD investigated. Using the weight and CRL, PI for each foetus was calculated using the equation:

$$Ponderal\ Index\ (PI) = \frac{Mass\ (kg)}{Height\ (m)\text{^}3}$$

The uterine lumen was occluded between each feto-placental unit by tying with string to ensure that placental tissues associated with particular foetuses could be identified. At GD45, 60 and 90 foetal sex was determined visually at the point of sample collection. Gonads were dissected, and one was snap frozen for nucleic acid isolation and the other was fixed in Bouin's for histology. At GD30, it was not possible to determine foetal sex visually, so part of the foetus was snap-frozen for nucleic acid isolation. DNA was isolated from the GD45, 60 and 90 gonads and the part GD30 foetuses (2.1.1) and was quantified by spectrophotometry (2.1.2). PCR was performed for the Sry region of the Y chromosome (forward primer 5'-GAAAGCGGACGATTACAGCC -3'; reverse primer 5'-TTGCGACGAGGTCGGTATTT-3') (2.1.3). Primers for the homologous zfx/zfy regions of the sex chromosomes served as a positive control (forward primer 5'-ATAATCACATGGAGAGCCACAAGCT-3'; reverse primer 5'-GCACTTCTTTGGTATCTGAGAAAGT-3') (Oliver *et al.*, 2011). A no template control and postnatal porcine testicular and ovarian DNA were run as controls. The PCR products were visualised by electrophoresis on a 1.2% (wt/vol) agarose 1 X SybrSafe (ThermoFisher, Altrincham, U.K.) gel (2.1.4).

The percentage of males in the litter was calculated using the following equation:

$$Percentage\ Males = \left(\frac{Number\ of\ Male\ Foetuses}{Number\ of\ Live\ Foetuses}\right) \times 100$$

The lightest and the CTMLW foetus (GD30), of both sex (GD45, 60 and 90) were identified based on foetal weight. From the anti-mesometrial side, placental and endometrial samples were taken from each feto-placental unit of interest. Samples were snap-frozen in liquid nitrogen and stored at -80^{o}C for RNA extraction, or fixed in Bouin's (Sigma Aldrich, St Louis, Missouri, U.S.A.) for histology. RNA (2.2) and tissue processing (2.3) were performed. Samples were also obtained from the heaviest conceptus/foetus (GD18, 30), of both sex (GD45, 60 and 90) although these samples have not been utilised in the current study.

The foetal livers (GD30, 45, 60 and 90), brains (GD45, 60 and 90), and gonads (GD60 and 90) were dissected from the foetuses and weighed from the foetuses of interest in the third sample collection (GD30, 45, 60 and 90 n=4, 6, 5, and 4 litters respectively) (Figure 3.1). An attempt was made to weigh the foetal gonads at GD45 however the balance was not sensitive enough. The liver, brain and combined gonad weight were expressed as a percentage of foetal weight and the brain: liver and brain: gonad ratios were calculated.

To assess the influence of uterine position on foetal weight, CRL, PI, ALF and AMF volume, initially foetuses were identified as being located in the middle or end (cervical or ovarian end) and the values for each variable were compared. The mean value for each parameter for each gilt was calculated, and the deviation from the gilt mean was calculated. The analyses performed were repeated using the deviation from the gilt mean data. In addition, the proportion of the distance along the horn for each foetus was calculated using a scale from 0-1, with 0 denoting foetuses located at the cervical end of the uterine horn, and 1 denoting foetuses located at the ovarian end. (Ashworth, 1991; Finch *et al.*, 2002). The deviation from the gilt mean was plotted against the position of the foetus in the uterine horn (0-1).

To assess the influence of sex of the adjacent (neighbour) foetuses on foetal and organ weight, CRL, PI, ALF and AMF volume, each foetus was assigned a value of 0, 1 or 2 as described by Jang *et al.*, (2014), which denotes the number of neighbours they have of the same sex (Figure 3.3). A male foetus

would have 0 male (M), 1M or 2M neighbours, and a female foetus would have 0 female (F), 1F, or 2F neighbours. Males and females were separated for this analysis and the foetuses at the cervical and ovarian ends of both uterine horns were excluded.

3.3.4 Percentage Prenatal Survival

The percentage prenatal survival (PPS) was calculated using the following equation at all GD investigated:

$$Percentage\ Prenatal\ Survival = \left(\frac{Number\ of\ Live\ Foetuses}{Ovulation\ Rate\ (OR)}\right) \times 100$$

The ovulation rate, determined by the number of CL present, reflects the maximum number of conceptuses that could be present based on the assumption that one oocyte was released from each follicle during ovulation.

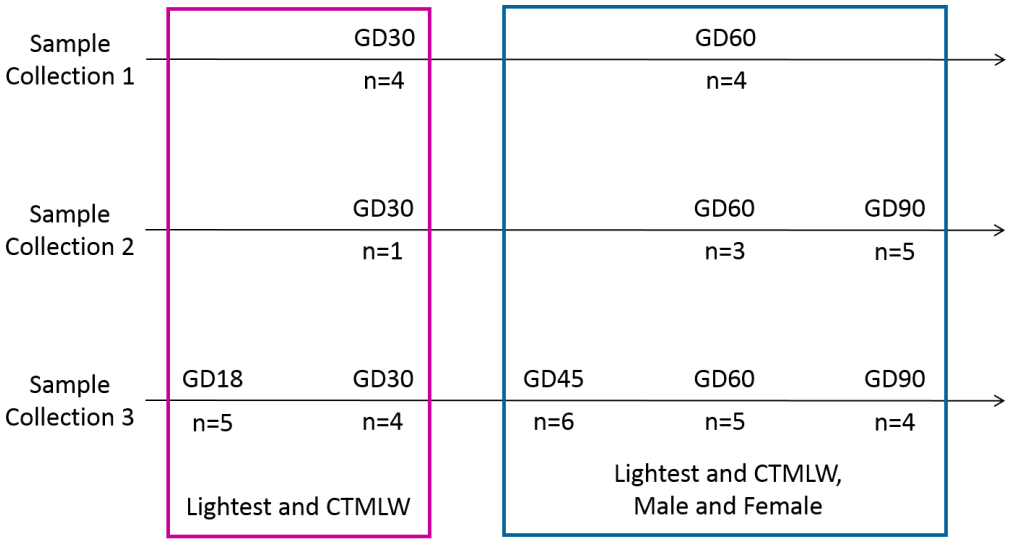

Figure 3.1: Distribution of Sample Collections.

The placental and endometrial samples utilised for this thesis were collected over three sample collections. At gestational day (GD) 18 and 30, samples were collected that supplied the lightest and closest to mean litter weight (CTMLW) foetus, regardless of sex. GD30 foetuses were sexed after the collections by PCR. At GD45, 60, and 90, samples were collected that supplied the lightest and CTMLW foetus of both sex.

Figure 3.2: Floatation Device used for GD18 Sample Collections.

Floatation device containing an RNA-Later® like solution and a representative gestational day (GD18) uterine horn, opened along the anti-mesometrial side.

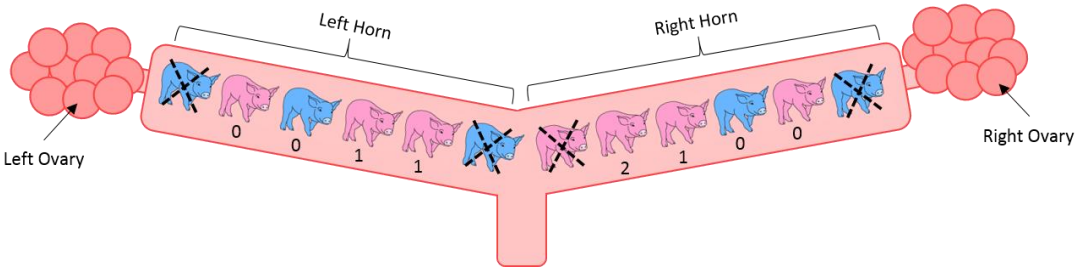

Figure 3.3: Illustration of Neighbour Sex Categorisation.

Once all GD30, 45, 60, and 90 foetuses were sexed, identification of the sex of the adjacent foetuses (or neighbours) was possible. Foetuses located at the cervical and ovarian ends of the uterine horns were not assigned a value for the number of neighbours but were included for the identification of neighbour sex for the adjacent foetus. Foetuses were assigned a value of 0, 1, or 2 indicating that they had 0, 1, or 2 neighbours of the same sex.

3.3.5 Statistical Analysis

Unless stated otherwise, statistical analyses were performed following the general protocol outlined in 2.5. Mean values were taken for each parameter (foetal weight, CRL, PI, and ALF and AMF volume) and the normality of the data was assessed, and transformations performed as required (2.5) (Table 3.2).

3.3.5.1 General Litter Characteristics

Pearson's correlations were performed to investigate the relationship between the number of live foetuses and the: PPS; percentage males in the litter; MLW; total litter weight (TLW); weight of the lightest foetus; and the within litter standard deviation (SD) in foetal weight. Following this, Pearson's correlation was performed to assess the relationship between the number of live foetuses in each uterine horn (right or left) and mean foetal weight within uterine horn. Similarly, Pearson's correlations were performed to determine if there was an association between maternal weight on the day of sample collection and the: number of live foetuses; MLW; and TLW. Pearson's correlations were performed to investigate the association between foetal weight and CRL, within GD and within sample collection within GD.

3.3.5.2 Temporal Changes

Foetal weight data had a normal distribution and an ANOVA for GD, with and without a block for gilt, with a post-hoc Tukey test was performed. To assess temporal changes in CRL, PI, and ALF and AMF volume, Kruskal-Wallis was performed.

3.3.5.3 Foetal Size

Regressions were performed to assess the relationship between foetal weight, and ALF and AMF volumes at GD30-90. As stated in 3.3.3, at GD45, 60 and 90 samples were collected from the lightest and CTMLW foetuses of both sex.

Throughout this thesis, the size analysis presented is the true lightest foetus compared with the true CTMLW foetus only, as it was demonstrated that comparing the CTMLW and the lightest foetuses of both sex masked differences in the data sets. The normality of the foetal weight, CRL, PI, ALF and AMF volumes data were assessed, and transformations were performed as required (Table 3.3). Statistical analysis for the association between the variable of interest and foetal size was performed as described in 2.5.

3.3.5.4 Foetal Sex

Within GD, ANOVA for foetal sex, with and without a block for gilt was performed for all parameters with a normal data distribution (Table 3.2). For data which did not have a normal data distribution, a Mann-Whitney for sex within GD was performed**.**

3.3.5.5 Sex Ratio of the Litter

The mean values were calculated for weight, CRL, PI, ALF and AMF volumes per litter. The relationship between percentage males in the litter and each of these parameters was assessed by Pearson's correlation.

3.3.5.6 Sex of the Neighbour

The normality of the foetal weight, CRL, PI, ALF and AMF volumes data were assessed, and transformations were performed as required (Table 3.4). ANOVA with and without a block for gilt, with post-hoc t-tests were performed to assess the influence of neighbour sex on the parameters of interest. For data without a normal data distribution, Kruskal-Wallis and Mann-Whitney tests were performed.

GD	Foetal Weight	CRL	PI	ALF Volume	AMF Volume
30	Normal	Not Normal	Log10	Normal	Sqrt
45	Normal	Normal	Not Normal	Log10	Not Normal
60	Normal	Not Normal	Not Normal	Sqrt	Normal
90	Normal	Not Normal	Not Normal	Sqrt	Sqrt

Table 3.2: Normality of Data Distribution for Foetal Weight, CRL, PI, ALF and AMF.

Log10 and Square Root (Sqrt) transformations were carried out where appropriate, with the aim of improving the normality of the distribution of the data. Abbreviations: GD=Gestational day, CRL=Crown-Rump Length, PI=Ponderal Index, ALF=Allantoic Fluid, AMF=Amniotic Fluid.

GD	Conceptus/Foetal Weight	CRL	PI	ALF Volume	AMF Volume
18	Log10	n/a	n/a	n/a	n/a
30	Normal	Normal	Normal	Normal	Normal
45	Normal	Normal	Normal	Normal	Normal
60	Normal	Not Normal	Not Normal	Log10	Normal
90	Normal	Not Normal	Normal	Normal	Normal

Table 3.3: Normality of Data Distribution used for Size Analysis.

Log10 and Square Root (Sqrt) transformations were carried out where required, to improve the normality of the distribution of the data. Abbreviations: GD=Gestational day, CRL=Crown-Rump Length, PI=Ponderal Index, ALF=Allantoic Fluid, AMF=Amniotic Fluid, n/a=not applicable.

GD	Foetal Weight	CRL	PI	ALF Volume	AMF Volume
30	Normal	Not Normal	Log10	Normal	Sqrt
45	Normal	Normal	Not Normal	Log10	Not Normal
60	Normal	Not Normal	Not Normal	Sqrt	Normal
90	Normal	Not Normal	Not Normal	Sqrt	Sqrt

Table 3.4: Normality of Data Distribution used for Sex of Neighbour Analysis.

Log10 and Square Root (Sqrt) transformations were carried out where required, to improve the normality of the distribution of the data. Abbreviations: GD=Gestational day, CRL=Crown-Rump Length, PI=Ponderal Index, ALF=Allantoic Fluid, AMF=Amniotic Fluid.

3.3.5.7 Uterine Position

Statistical analysis was performed as detailed in 2.5 to compare the foetuses at the end of the uterine horns with the foetuses at the middle of the uterine horn. The normality of the distribution of the raw data, and any transformations required are summarised in Table 3.5. ANOVA for uterine horn position was performed, with and without a block for gilt for the data which had a normal distribution. This was performed for: 1) end foetuses, which described foetuses at the cervical or ovarian end of the uterine horns, compared with the foetuses in the middle of the uterine horn, and 2) for cervical and ovarian end foetuses separated, compared with foetuses located in the middle of the uterine horn. For the variables which did not have a normal data distribution in the end compared with middle analysis, and the three locations analysis, a Mann-Whitney and Kruskal-Wallis test respectively was performed. This analysis was performed for the variables individually and the deviation from gilt mean analysis. In the deviation from gilt mean analysis, gilt was not accounted for in the statistical analysis.

3.3.5.8 Differences in Organ Weights

All organ weights, organ as a percentage of foetal weight, and brain: organ ratios at GD45, 60, and 90 had a normal data distribution. At GD30, Log10 transformation was required for liver weight and liver as a percentage of foetal weight. Regressions were performed to assess the relationship between foetal weight and brain, liver, and combined gonadal weight. Following this, the organ weights, organ as a percentage of foetal weight, and brain: organ ratios were compared between the CTMLW and lightest groups within GD by ANOVA with and without a block for gilt, as described in 2.5. The association between foetal sex and the parameters of interest was investigated using the same method. The relationship between neighbour sex and the parameters of interest was assessed by ANOVA with and without a block for gilt, and t-tests.

Variable	GD30	GD45	GD60	GD90
ALF Volume	Normal	Log10	Log10	Sqrt
AMF Volume	Sqrt	Not Normal	Normal	Sqrt
CRL	Not Normal	Normal	Not Normal	Not Normal
Weight	Normal	Normal	Normal	Normal
PI	Log10	Not Normal	Not Normal	Not Normal
Deviation from Gilt Mean ALF Volume	Normal	Not Normal	Sqrt	Sqrt
Deviation from Gilt Mean AMF Volume	Normal	Not Normal	Normal	Normal
Deviation from Gilt Mean CRL	Normal	Not Normal	Not Normal	Normal
Deviation from Gilt Mean Weight	Normal	Not Normal	Not Normal	Not Normal
Deviation from Gilt Mean PI	Normal	Not Normal	Not Normal	Log10

Table 3.5: Normality of Data Distribution for Uterine Position Analyses.

Log10 and Square Root (Sqrt) transformations were carried out where appropriate, with the aim of improving the normality of the distribution of the data. Abbreviations used: GD=Gestational Day, CRL=Crown-Rump Length, PI=Ponderal Index, ALF=Allantoic Fluid, AMF=Amniotic Fluid, Sqrt=Square Root Transformation.

3.4 Results

3.4.1 General Litter Characteristics

As detailed in 3.3, during the sample collection process a large amount of information was collected from each animal. Information regarding the litters investigated is summarised in Table 3.6 and includes OR, PMSG treatment, sires used, range in GD used, litter size, PPS, percentage of males in the litter (sex ratio), MLW and TLW, within litter SD in foetal weight, and lightest and CTMLW foetal weight.

The within-litter ranges for foetal weight, CRL, PI, ALF and AMF volumes are illustrated in Supplementary Figure 1-Supplementary Figure 5. Pearson's correlations were performed between the number of live foetuses and mean MLW, TLW, weight of the lightest foetuses and within litter SD in foetal weight (

Table 3.7). No statistically significant relationships between the number of conceptuses or foetuses and MLW, TLW, weight of the lightest conceptuses or foetuses, and within litter SD in conceptus or foetal weight were observed. A negative relationship between number of live foetuses and MLW was observed at GD60 (P≤0.001). In contrast, a positive relationship between number of live foetuses and TLW was observed at GD30 (P≤0.001) and 60 (P=0.004). At GD45, a positive relationship between number of live foetuses and within litter SD in foetal weight was observed (P=0.023). At GD60, a negative relationship was observed between the number of live foetuses and the weight of the lightest foetus (P≤0.001). A negative relationship between number of foetuses in the individual uterine horn (right or left) and foetal weight was observed at GD30 (P=0.02) and 60 (P≤0.001), but not at GD18, 45 or 90 (Figure 3.4).

Pearson's correlations were performed between maternal weight at the time of sample collection and the number of foetuses, PPS, MLW and TLW (Supplementary Table 1). An inverse relationship between number of foetuses and maternal weight was observed at GD18 (P=0.052), and between MLW and maternal weight at GD30 (P=0.038). Whilst at GD60, a positive

relationship between maternal weight and the number of foetuses (P=0.046) and the MLW (P=0.005) was observed.

The relationship between foetal weight and CRL within GD was investigated (Figure 3.5). At GD30 (Correlation coefficient=0.618, P≤0.001), 45 (Correlation coefficient=0.882, P≤0.001) and 90 (Correlation coefficient 0.658, P≤0.001), a positive relationship between foetal weight and CRL was observed for the foetuses from the three sample collections combined. This relationship was not statistically significant in the GD60 group however, the scatterplot of the data revealed two distinct populations of foetuses, which reflected the sample collection groups (Figure 3.5C). Considering this, a Pearson's correlation was performed within sample collection to assess the relationship between foetal weight and CRL, and revealed that within the individual sample collections at GD60, a statistically significant relationship was observed (Figure 3.5H-J).

At GD30, a positive relationship between number of live foetuses and PPS was observed (Correlation coefficient=0.918, P≤0.001), which was not present at the other GD investigated. Further, a positive correlation was observed between number of live foetuses and percentage of males in the litter at GD60 (Correlation coefficient=0.695, P=0.01), which was not observed at the other GD investigated.

3.4.2 Temporal Changes

To investigate temporal changes in foetal weight, CRL, PI, ALF and AMF volume, the mean values were calculated within GD (Figure 3.6). Foetal weight increased with advancing GD (ANOVA with and without Gilt Block FP≤0.001; Figure 3.6A). Foetal weight did not significantly increase between GD30 and 45, but did increase significantly between GD45 and 60, and GD60 and 90. A gradual increase in CRL (Kruskal-Wallis P≤0.001; Figure 3.6B) and AMF volume (Kruskal-Wallis P≤0.001; Figure 3.6E) was observed with advancing GD. In contrast, PI decreased (Kruskal-Wallis P≤0.001; Figure 3.6C) with advancing GD. ALF volume fluctuated throughout gestation (Kruskal-Wallis P≤0.001; Figure 3.6D). A moderate ALF volume was observed at GD30, before

decreasing to the lowest observed level at GD45. ALF volume peaked at GD60, before decreasing back to an intermediate volume at GD90.

Table 3.6: Summary of Litter Characteristics.

Parameter	GD18 (n=5) (PMSG=1/5)		GD30 (n=9) (PMSG=4/9)		GD45 (n=6) (PMSG=1/6)		GD60 (n=12) (PMSG=4/12)		GD90 (n=9) (PMSG=3/9)	
	Mean ± S.E.M.	Range	Mean ± S.E.M.	Range	Mean ± S.E.M.	Range	Mean ± S.E.M.	Range	Mean ± S.E.M.	Range
Gestational Day (GD)	18.4 ± 0.245	18-19	30 ± 0.147	29-30	45 ± 0.516	43-46	60.333 ± 0.284	58-62	90.333 ± 0.289	89-92
Ovulation Rate (OR)	31.6 ± 9.678	19-70	19.889 ± 1.438	13-27	21.5 ± 2.814	14-33	21 ± 2.677	15-49	21.889 ± 2.124	15-37
Litter Size	26 ± 5.367	11-44	13 ± 2.128	6-24	16.5 ± 1.455	12-20	14.083 ± 1.003	9-19	14 ± 0.833	11-20
Prenatal Survival (%)	94.559 ± 19.436	42.308-152.632	63.843 ± 7.708	35.294-100	80.382 ± 7.599	57.143-93.333	71.728 ± 5.420	36.735-90	66.385 ± 4.024	54.054-93.333
Total Litter Weight (TLW) (g)	5.755± 1.927	1.084-10.749	17.821 ± 2.415	9.022-29.540	343.110 ± 36.872	191.11-465.24	1658.008 ± 71.495	1305.910-2137.160	8855.500 ± 625.739	6467.490-13151.890
Mean Litter Weight (MLW) (g)	0.209± 0.057	0.099-0.410	1.442 ± 0.092	1.138-2.061	20.815 ± 1.603	15.923-25.780	121.564 ± 5.579	89.186-150.056	630.091 ± 21.798	539.381-759.266
Mean Within-Litter SD in Foetal Weight (g)	0.121± 0.039	0.036-0.233	0.184 ± 0.023	0.087-0.271	1.939 ± 0.320	0.927-3.038	12.238 ± 0.905	7.367-17.296	122.457 ± 14.893	40.253-205.243
Weight CTMLW Foetuses (g)	0.212± 0.059	0.100-0.422	1.458 ± 0.088	1.17-2.058	20.793 ± 1.577	15.920-25.660	121.858 ± 5.817	86.96-150.24	626.778 ± 22.916	544.88-756.75

Weight Lightest Foetuses (g)	0.069± 0.014	0.043-0.120	1.117 ± 0.096	0.65-1.661	17.827 ± 1.849	11.240 - 23.890	95.763 ± 7.648	45.76-128.71	382.05 ± 32.328	248.95-532.75
Percentage Males in Litter (%)	n/a	n/a	57.480 ± 5.777	25-83.333	47.009 ± 9.177	30-80	51.922 ± 14.989	33.333-72.222	56.162 ± 4.960	33.333-76.923
Sires Used	Champion Boy x 4 Candidus x 1		Champion Boy x 6 Candidus x 1 Krosus & Tates x 1 Unknown x 1		Champion Boy x 4 Candidus x 1 Snobb x 1		Champion Boy x 9 Snobb x 2 Field Marshall x 1		Champion Boy x 5 Snobb x 2 Unknown x 2	

Table 3.6: Summary of Litter Characteristics.

This table indicates the mean ± S.E.M. and range of values obtained for each characteristic within GD. Abbreviations used: PMSG=Pregnant Mare Serum Gonadotrophin, GD=Gestational Day, SD=Standard Deviation, S.E.M.=the standard error of the mean.

GD	Mean Litter Weight		Total Litter Weight		Lightest Foetal Weight		Within-Litter SD in Foetal Weight	
	Correlation Coefficient	P Value	Correlation Coefficient	P Value	Correlation Coefficient	P Value	Correlation Coefficient	P Value
18	0.204	0.742	0.693	0.194	0.789	0.112	0.519	0.370
30	-0.588	**0.096**	0.970	**≤0.001**	-0.576	0.105	-0.175	0.652
45	-0.029	0.956	0.739	**0.093**	-0.157	0.766	0.875	**0.023**
60	-0.877	**≤0.001**	0.761	**0.004**	-0.862	**≤0.001**	0.094	0.772
90	-0.035	0.929	0.129	0.741	0.336	0.376	-0.168	0.665

Table 3.7: Summary of Pearson's Correlations between Number of Live Conceptuses/Foetuses and Mean Litter Weight, Total Litter Weight, Lightest Foetal Weight, and Within-Litter SD in Foetal Weight.

Abbreviations: GD=Gestational Day, SD=Standard Deviation, P=Probability Value. P≤0.1 are indicated in bold.

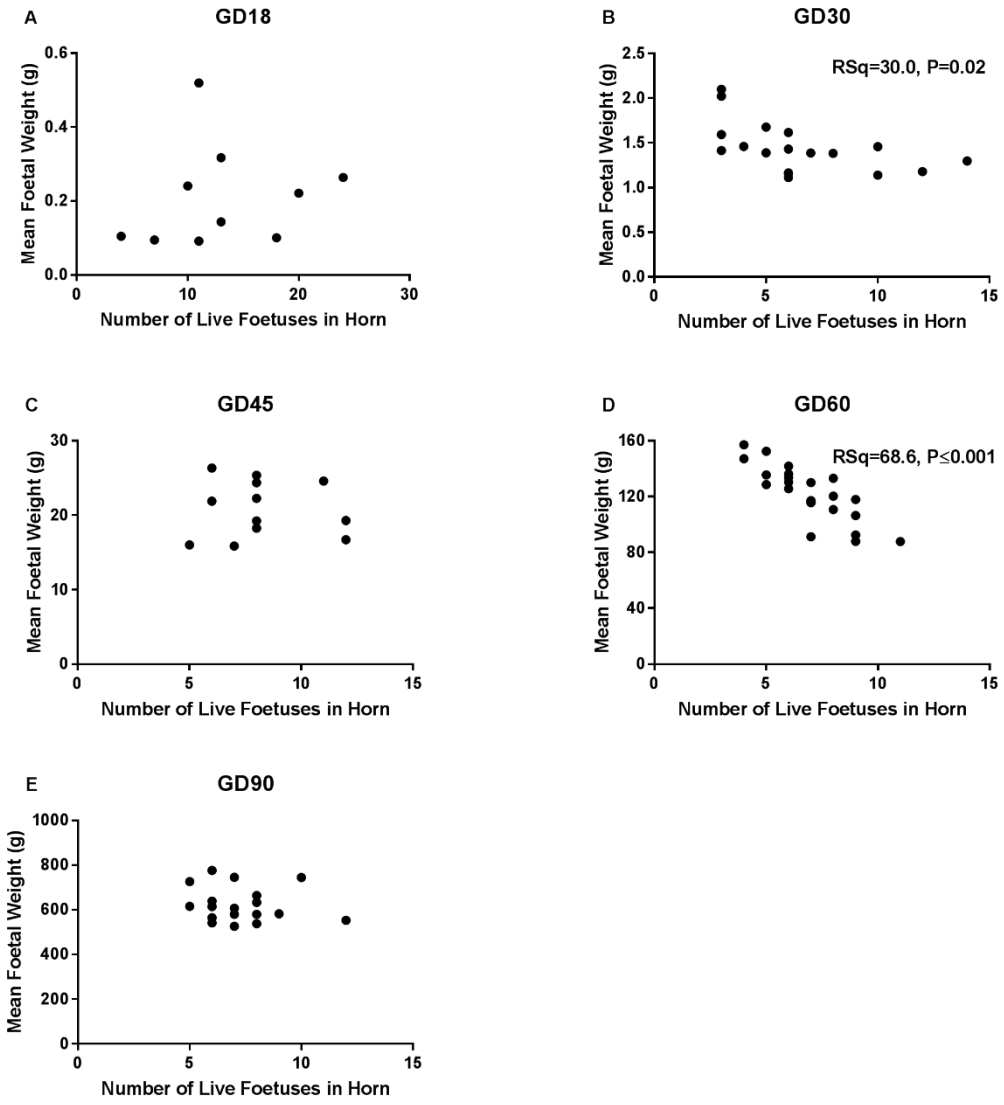

Figure 3.4: An Inverse Relationship between the Number of Live Foetuses in the Uterine Horn and Mean Foetal Weight was observed.

A negative relationship between number of foetuses in the uterine horn and foetal weight was observed at GD30 (RSq=30%, P=0.02; A) and 60 (RSq=68.6%, P≤0.001; C). No statistically significant relationship was observed at GD18 (A), GD45 (C) or 90 (E).

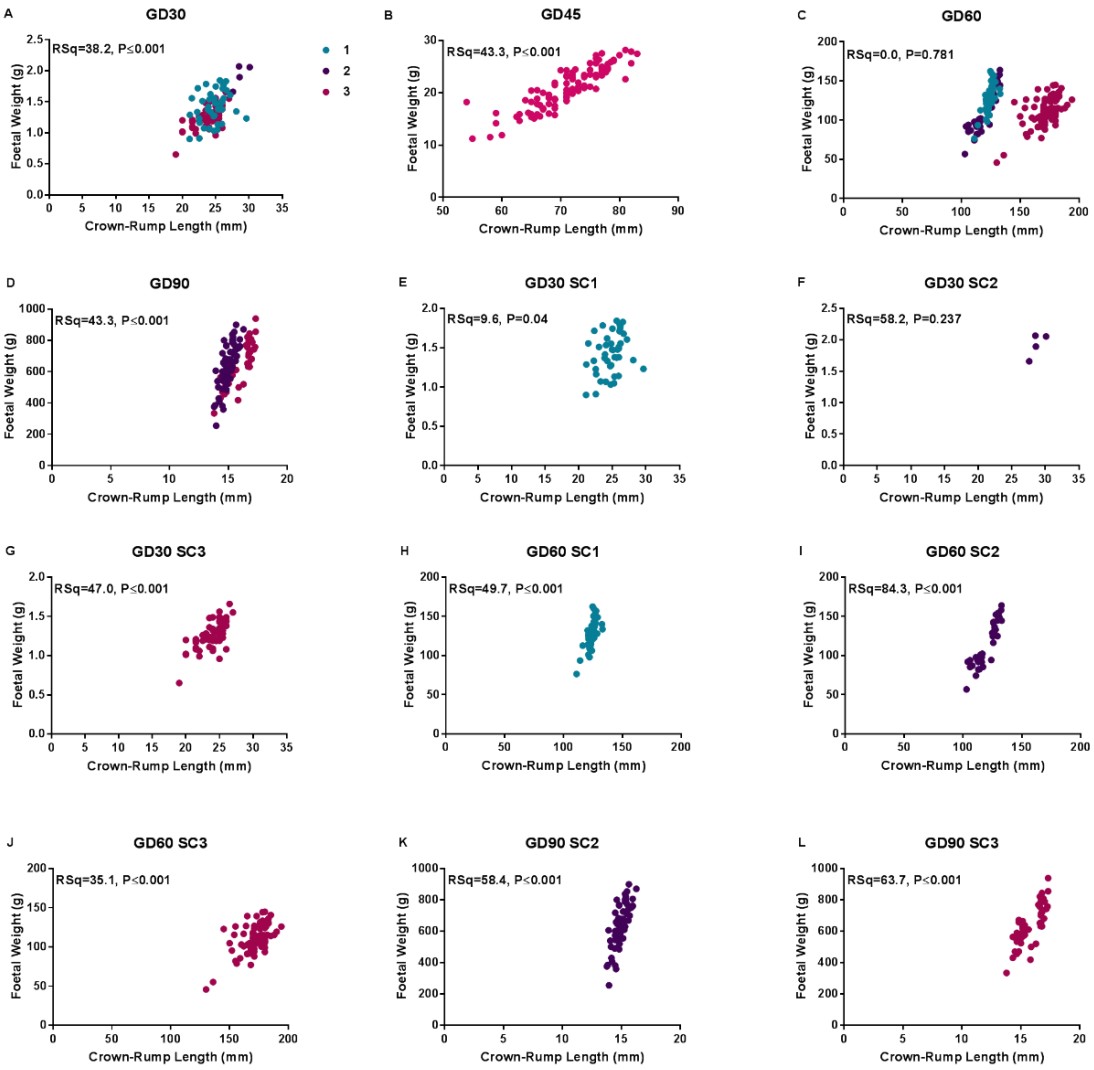

Figure 3.5: Foetal Weight was correlated to CRL throughout Gestation.

A, B, C, and D illustrates the relationship between foetal weight and crown-rump length (CRL) within gestational day (GD) 30, 45, 60, and 90 respectively. Teal = Sample Collection (SC) 1, Purple = SC2, and Magenta = SC3. E, F, and G illustrates the relationship between foetal weight and CRL within sample collection 1, 2, and 3 respectively at GD30. H, I, and J illustrates the relationship between foetal weight and CRL within sample collection 1, 2, and 3 respectively at GD60. K and L illustrates the relationship between foetal weight and CRL within sample collection 2, and 3 respectively at GD90. RSq values and P values from the Pearson's correlations are indicated on the individual graphs.

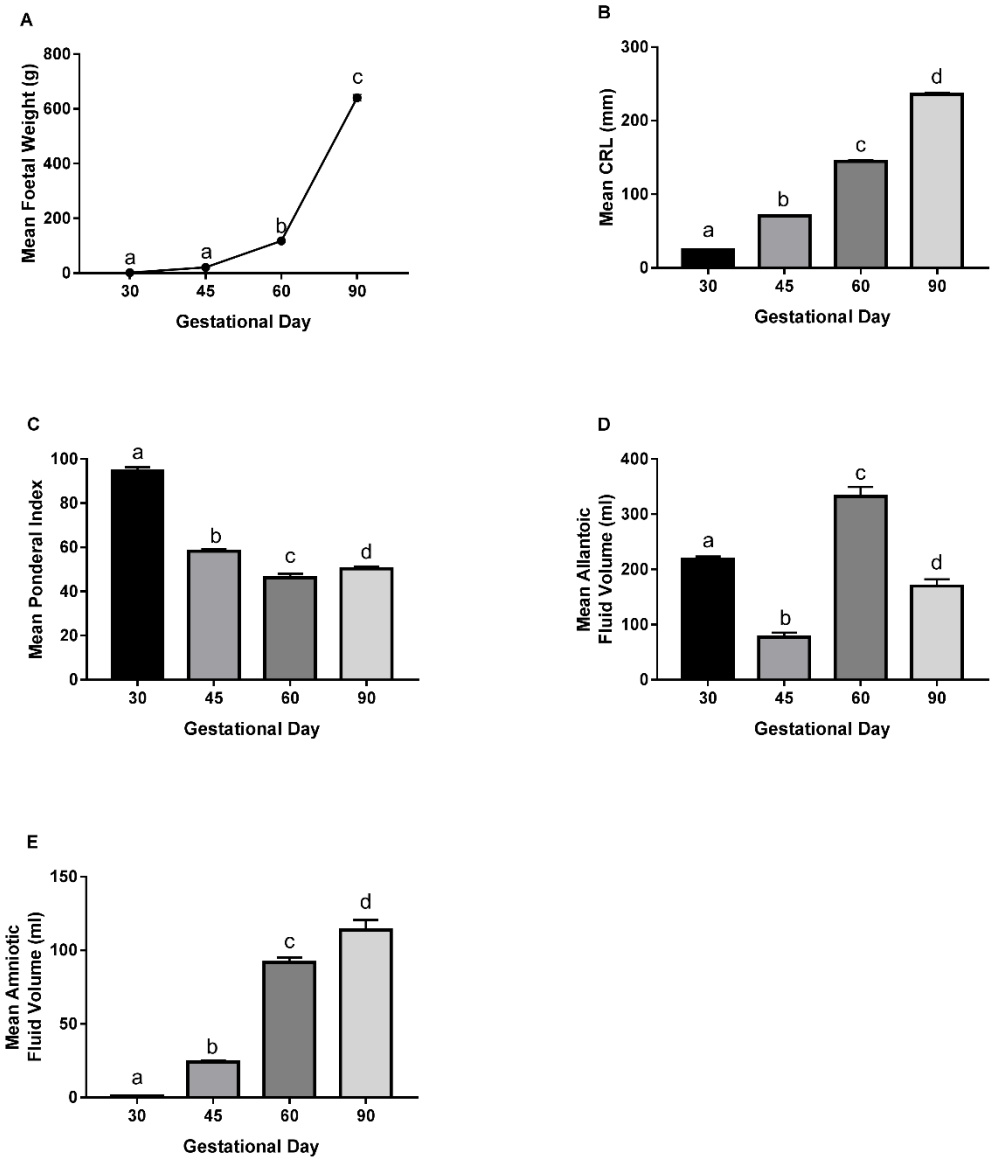

Figure 3.6: Temporal Changes in Foetal Weight, CRL, PI, Allantoic and Amniotic Fluid Volumes were observed.

A: Foetal weight increased with advancing gestational day (GD) (ANOVA with and without Gilt Block FPr≤0.001). A gradual increase in CRL (Kruskal-Wallis P≤0.001; B) and amniotic fluid volume (Kruskal-Wallis P≤0.001; E) was observed with advancing GD. C: PI decreased (Kruskal-Wallis P≤0.001) with advancing GD. D: Allantoic fluid volume fluctuated throughout gestation (Kruskal-Wallis P≤0.001). Error bars represent S.E.M. Letters indicate that group means differ from one another.

3.4.3 Foetal Size

Regressions between foetal weight, and ALF and AMF volumes revealed positive relationships (Table 3.8). However, when comparing the ALF and AMF volumes between the CTMLW and lightest foetuses no statistically significant relationships were observed (Table 3.9). As expected, foetal weight was lower in the lightest conceptuses or foetuses compared to the CTMLW conceptuses or foetuses throughout gestation (GD18 ANOVA without Gilt Block FPr≤0.05; with Gilt Block FPr=0.004; GD30 ANOVA without Gilt Block FPr=0.019, with Gilt Block FPr≤0.001; GD45 ANOVA with Gilt Block FPr=0.023; GD60 ANOVA without Gilt Block FPr=0.054, with Gilt Block FPr≤0.001; GD90 ANOVA with and without Gilt Block FPr≤0.001. Figure 3.7). CRL was shorter in the lightest foetuses compared to the CTMLW foetuses throughout gestation (Figure 3.8), reaching statistical significance at GD30 (ANOVA with Gilt Block FPr=0.074), GD60 (ANOVA with Gilt Block FPr=0.064), and GD90 (Mann-Whitney P=0.048). PI was decreased in the lightest foetuses compared to the CTMLW foetuses at GD90 (ANOVA with Gilt Block FPr=0.07; Figure 3.11).

Parameter	Foetal Weight							
	GD30		GD45		GD60		GD90	
	RSq (%)	P	RSq (%)	P	RSq (%)	P	RSq (%)	P
ALF Volume	30.1	**0.07**	24.5	**≤0.001**	0.95	0.2331	5.5	**0.017**
AMF Volume	61.2	**0.009**	23.7	**≤0.001**	4.2	**0.01**	3.6	**0.06**

Table 3.8: Summary of Regression Information between Foetal Weight, and Allantoic and Amniotic Fluid Volumes.

Abbreviations: GD=Gestational Day, ALF=Allantoic Fluid, AMF=Amniotic Fluid. P≤0.1 indicated in bold.

Parameter	GD30 (Mean ± S.E.M. (n))		GD45 (Mean ± S.E.M. (n))		GD60 (Mean ± S.E.M. (n))		GD90 (Mean ± S.E.M. (n))	
	CTMLW	Lightest	CTMLW	Lightest	CTMLW	Lightest	CTMLW	Lightest
ALF Volume	218.875 ± 12.513 (8)	217.222 ± 15.051 (9)	65.1667 ± 23.913 (6)	52.5 ± 13.226 (4)	320.222 ± 59.760 (9)	279.182 ± 60.259 (11)	181.125 ± 34.963 (9)	172.5 ± 31.993 (4)
AMF Volume	1.109 ± 0.220 (9)	0.863 ± 0.203 (8)	18.667 ± 4.529 (6)	19.517 ± 3.844 (6)	96.222 ± 13.430 (9)	89.546 ± 16.455 (11)	83.571 ± 16.484 (7)	92.6 ± 31.714 (5)

Table 3.9: No Association between Foetal Weight Classification and Allantoic or Amniotic Fluid Volume were Observed.

Abbreviations: GD=Gestational Day, ALF=Allantoic Fluid, AMF=Amniotic Fluid, CTMLW=Closest to Mean Litter Weight, S.E.M.=Standard Error of the Mean, n=number of foetuses.

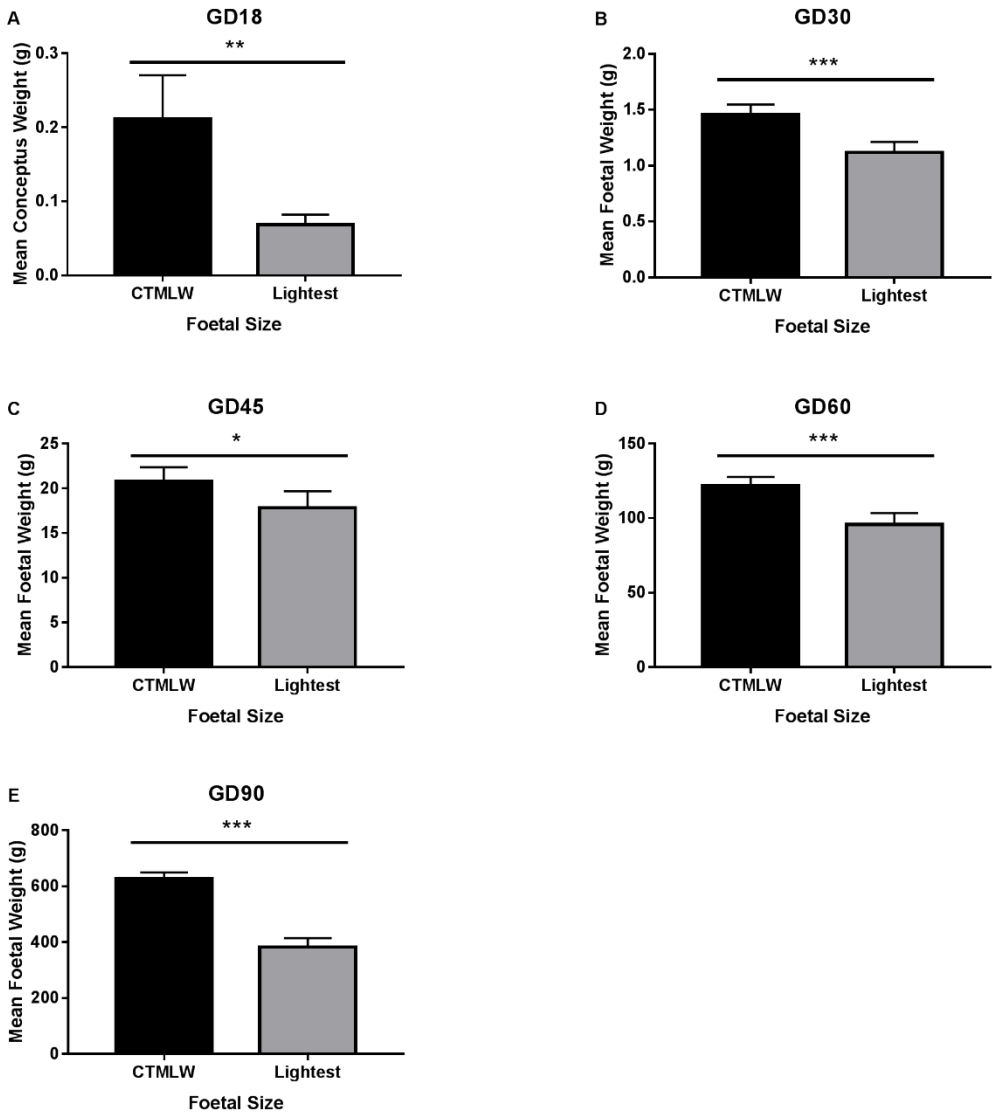

Figure 3.7: Illustration of the Difference in Conceptus/Foetal Weight between the CTMLW and Lightest Conceptuses or Foetuses within GD.

Foetal weight was lower in the lightest foetuses compared to the closest to mean litter weight (CTMLW) foetuses throughout gestation. A: Gestational Day (GD) 18 (ANOVA without Gilt Block FPr≤0.05; with Gilt Block FPr=0.004). B: GD30 (ANOVA without Gilt Block FPr≤0.05, with Gilt Block FPr≤0.001). C: GD45 (ANOVA with Gilt Block FPr≤0.05). D: GD60 (ANOVA without Gilt Block FPr≤0.05, with Gilt Block FPr≤0.001). E: GD90 ANOVA with and without Gilt Block FPr≤0.001). Mean values presented. *FPr≤0.05. ***FPr/P≤0.001. Error bars represent S.E.M.

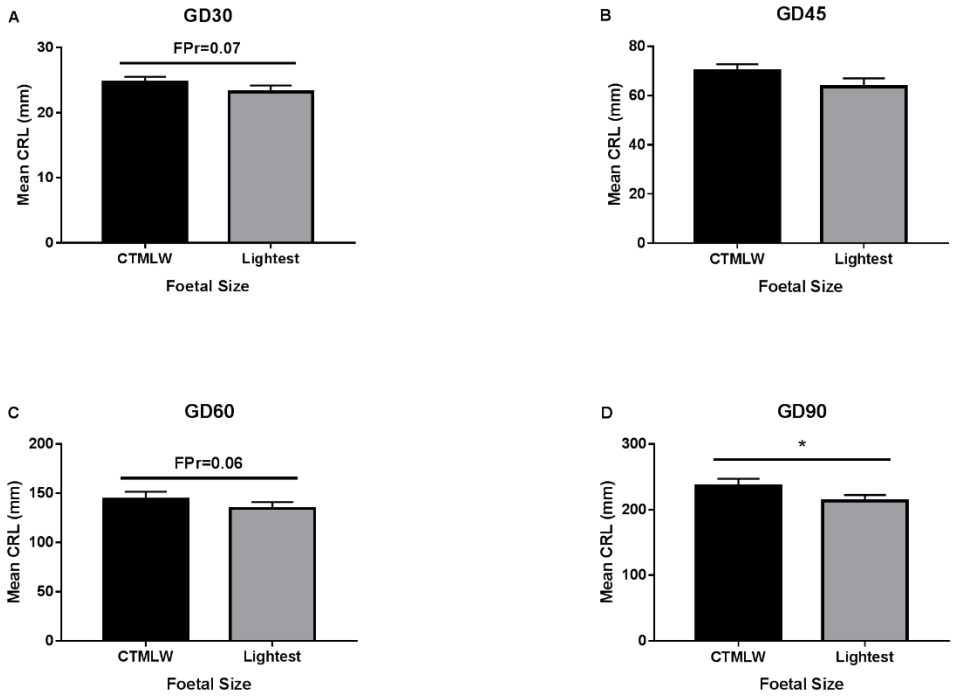

Figure 3.8: Illustration of the Difference in CRL between the CTMLW and Lightest Foetuses within GD.

A: Crown-Rump Length (CRL) was shorter in the lightest foetuses compared to the closest to mean litter weight (CTMLW) foetuses at gestational day (GD) 30 (ANOVA with Gilt Block FPr=0.07). B: CRL was decreased in the lightest foetuses compared to the CTMLW foetuses (not statistically significant). C and D: CRL was decreased in the lightest foetuses compared to the CTMLW foetuses at GD60 (ANOVA with Gilt Block FPr=0.06) and 90 (Mann-Whitney P≤0.05). Mean values presented. *FPr≤0.05. Error bars represent S.E.M.

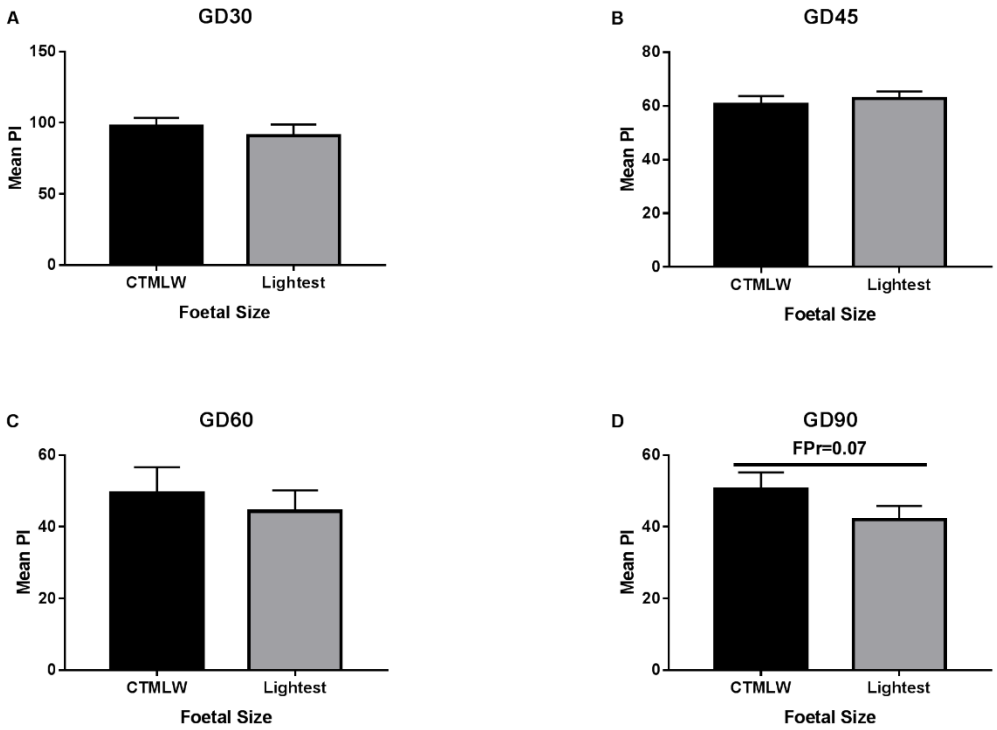

Figure 3.9: The PI was decreased at GD90 in the Lightest Compared to the CTMLW Foetuses.

No statistically significant relationship between foetal size and PI (Ponderal Index) was observed at gestational day (GD) 30 (A), 45 (B), or 60 (C). PI was decreased in the lightest foetuses compared to the closest to mean litter weight (CTMLW) foetuses at GD90 (ANOVA with Gilt Block FPr=0.07). Error bars represent S.E.M.

3.4.4 Foetal Sex

3.4.4.1 Porcine Foetuses were sexed by PCR for the Sry Region of the Y chromosome

To assess the association between foetal sex and the parameters investigated throughout this thesis, a PCR for the Sry region of the Y chromosome was utilised. This PCR was successfully used to sex foetuses at GD30, 45, 60 and 90 (Figure 3.10).

3.4.4.2 Male vs Female Growth Trajectory.

Throughout gestation, male foetuses were heavier than their female littermates (Figure 3.11A-D), (GD30 ANOVA without Gilt Block FPr = 0.064; GD45 ANOVA with Gilt Block FPr= 0.057; GD60 ANOVA with Gilt Block FPr≤0.001, GD90 ANOVA without Gilt Block FPr=0.029; with Gilt Block FPr=0.026). At GD30 and 90, male foetuses were longer (increased CRL) than their female littermates (Mann-Whitney P=0.08; Figure 3.11E). Male foetuses had an increased AMF volume compared to their female littermates at GD30 (ANOVA without Gilt Block FPr=0.024; with Gilt Block FPr=0.08) and 90 (ANOVA without Gilt Block FPr=0.063; with Gilt Block FPr=0.08; Figure 3.11H). No associations between foetal sex and PI or ALF volume were observed.

3.4.5 Sex Ratio of the Litter

The percentage of males in the litter was calculated at GD30, 45, 60 and 90, and varied considerably between litters (Figure 3.12). Considering this, the relationship between percentage males in the litter and foetal weight, CRL, PI, ALF and AMF volume was investigated (Figure 3.13). Percentage males in the litter was positively associated with AMF volume at GD30 (RSq=79.9%, P=0.003. Figure 3.13A) and foetal weight at GD90 (RSq=62.5%, P=0.01. Figure 3.13C). In contrast, at GD60 a trend towards a negative relationship between percentage males in the litter and foetal weight was observed (RSq=29.9%, P=0.06. Figure 3.13B).

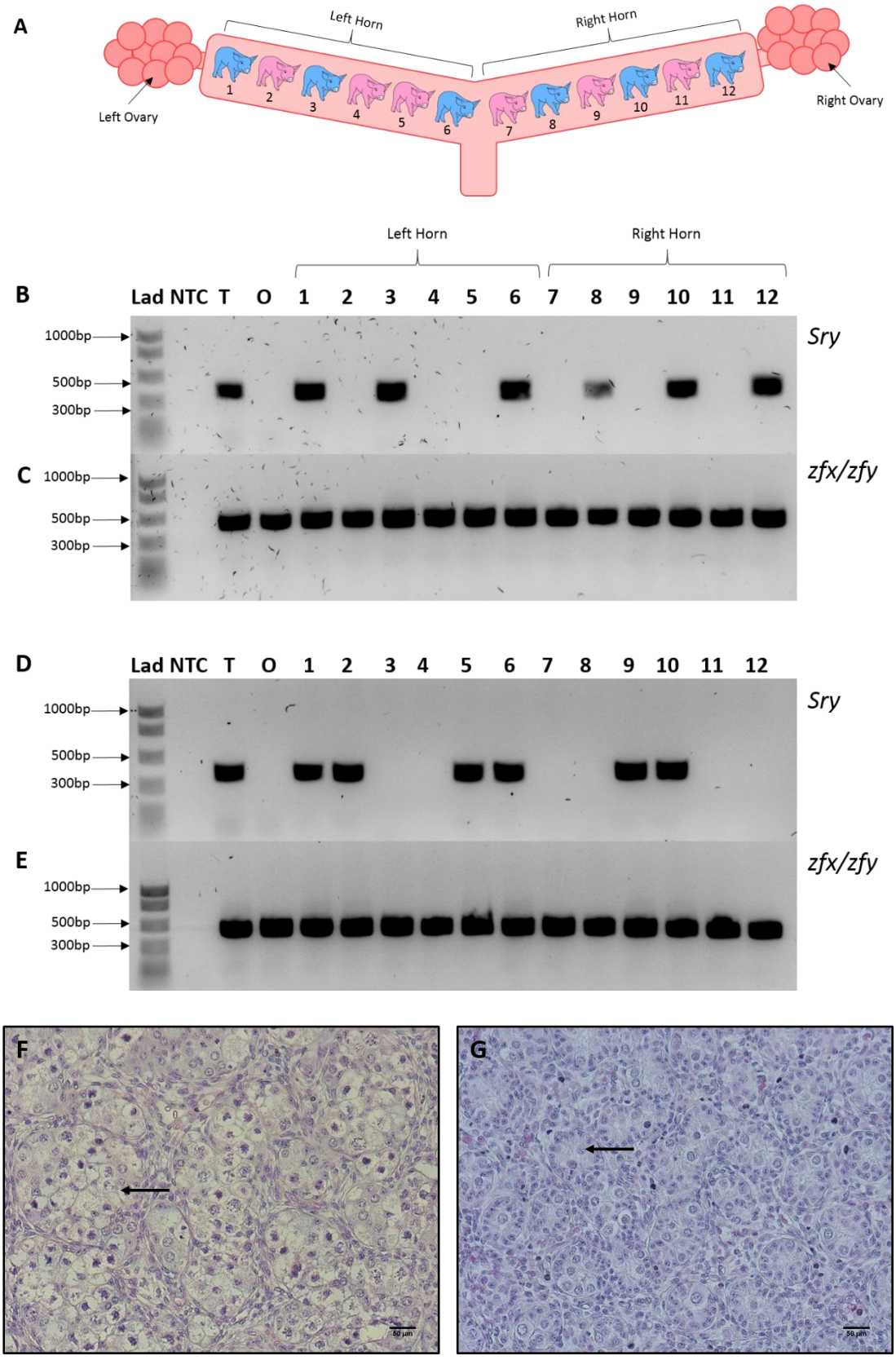

Figure 3.10: PCR for Sry can be used to Sex Porcine Foetuses from GD30.

Figure 3.10: PCR for Sry can be used to Sex Porcine Foetuses from GD30.

A: Schematic diagram of porcine uterus to illustrate the GD30 PCR results from B. Blue and pink piglets indicate male and female foetuses respectively. B-F: PCR products run on 1.5% TAE gel by electrophoresis. B and C: A representative GD30 litter. D and E: Samples from the lightest and closest to mean litter weight (CTMLW) male and female foetuses from 4 litters in the following order: lightest male, CTMLW male, lightest female and CTMLW female. B and D: PCR products using primers for the Sry region of the Y chromosome, with a band indicating that the foetus is male. C and E: PCR products from the control PCR using primers for a homologous region present on the X and Y chromosome (zfx/zfy) to demonstrate that DNA is present in all samples. Haematoxylin and eosin stained GD60 ovary (F) and testes (G) confirmed PCR result. Arrows indicate forming nests and seminiferous tubules in the ovary and testes respectively. Abbreviations: Lad=ladder, NTC=no template control, O=postnatal ovarian control DNA, T=postnatal testicular control DNA. Scale bars represent 50µm.

Figure 3.11: Male Foetuses are Heavier, Longer and have an Increased Amniotic Fluid Volume Compared to their Female Littermates.

Throughout gestation, male foetuses were heavier than their female littermates (A-D), (A: GD30 ANOVA without Gilt Block FPr=0.06; B: GD45 ANOVA with Gilt Block FPr= 0.057; C: GD60 ANOVA with Gilt Block FPr≤0.001; D: GD90 ANOVA with and without Gilt Block FPr≤0.05). E: At GD30 and 90, male foetuses had longer CRL than their female littermates (Mann-Whitney GD30 and 90 P=0.08). F and G: No associations between foetal sex and PI or allantoic fluid volume were observed. H: Male foetuses had an increased volume of amniotic fluid compared to their female littermates at GD30 (ANOVA without Gilt Block FPr≤0.05; with Gilt Block FPr=0.08) and 90 (ANOVA without Gilt Block FPr=0.06; with Gilt Block FPr=0.08). Error bars represent S.E.M. *FPr/P≤0.05. ***FPr/P≤0.001.

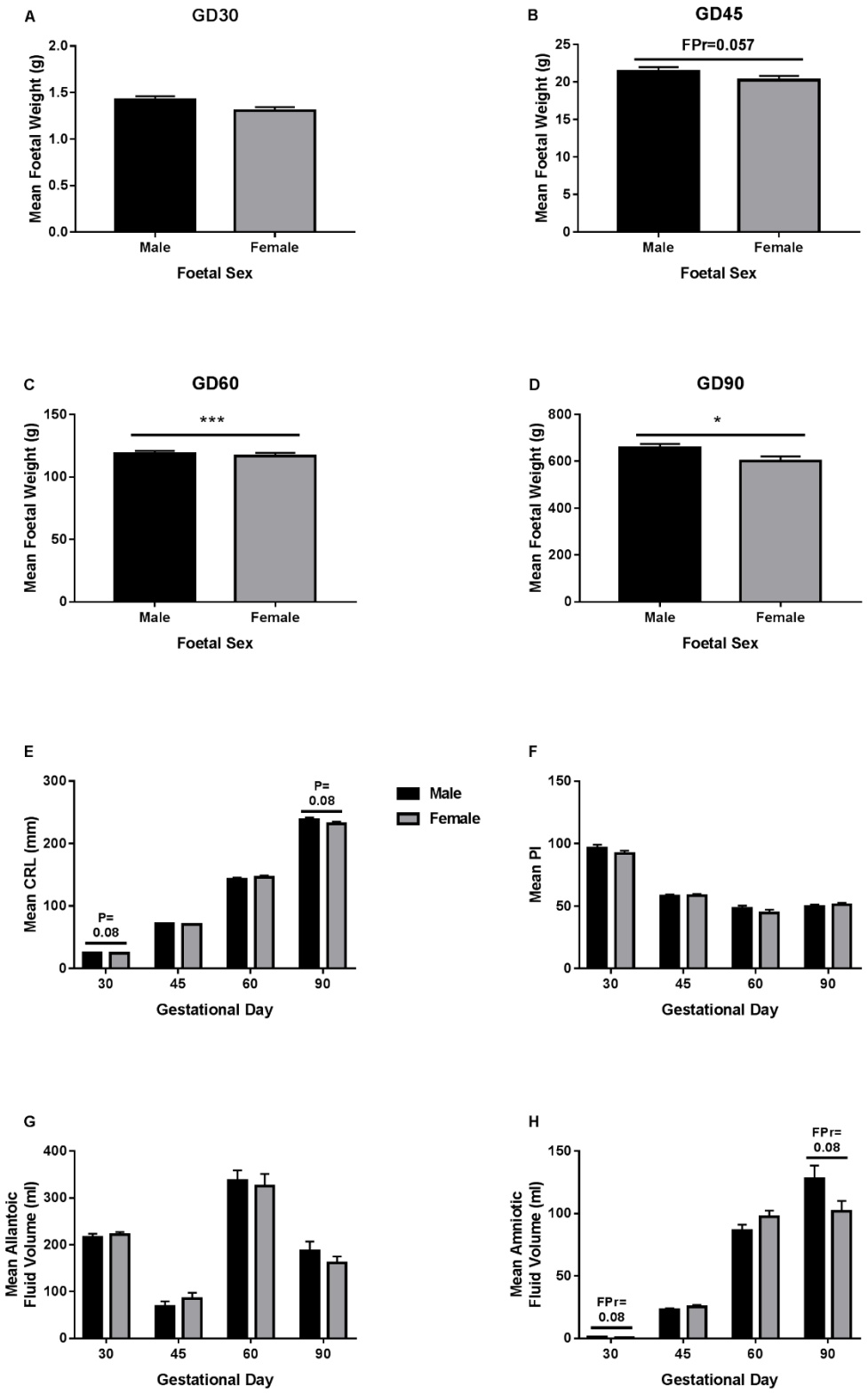

Figure 3.11: Male Foetuses are Heavier, Longer and have an Increased Amniotic Fluid Volume Compared to their Female Littermates.

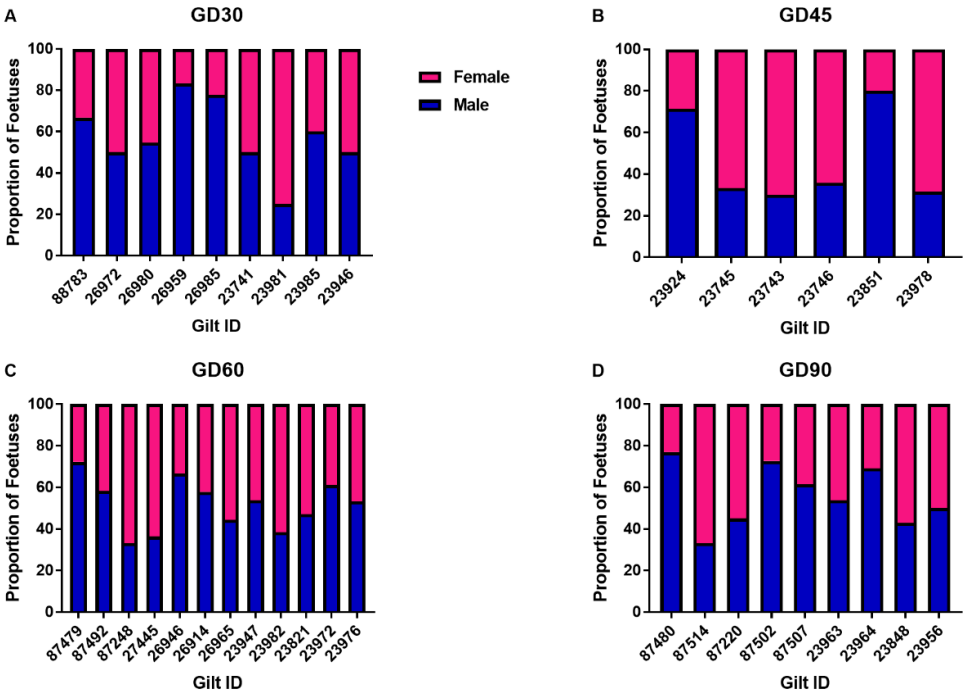

Figure 3.12: Illustration of the Range of Sex Ratio within GD.

Within litter, the percentage of foetuses of each sex was calculated. A, B, C and D illustrates the sex ratio of gestational day (GD) 30, 45, 60 and 90 respectively. Females and males indicated in pink and blue respectively.

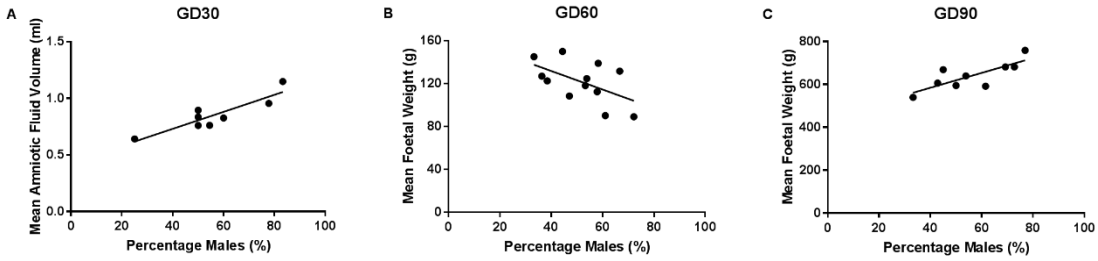

Figure 3.13: Percentage Male Foetuses in the Litter is Associated with Amniotic Fluid Volume at GD30, and Foetal Weight at GD60 and 90.

The relationship between percentage males in the litter and foetal weight, CRL, PI, allantoic and amniotic fluid volume was investigated. A, B and C illustrate the significant results of interest. Percentage males in the litter was positively associated with amniotic fluid volume at GD30 (RSq=79.9%, P=0.003; A) and foetal weight at GD90 (RSq=62.5%, P=0.01; C). In contrast, at GD60 a trend towards a negative relationship between percentage males in the litter and foetal weight was observed (RSq=29.9%, P=0.06; B).

3.4.6 Sex of the Neighbour

The relationship between the sex of a foetus's neighbour and foetal weight, CRL, PI, ALF and AMF volume was investigated (Figure 3.15-Figure 3.18). Table 3.10 summarises the sex of the neighbour for the CTMLW and lightest foetuses of interest, excluding foetuses located at the ovarian and cervical ends of the uterine horn. 1M foetuses were heavier than 0M foetuses at GD30 (t-test P=0.01. Figure 3.15A), 45 (overall effect: ANOVA without Gilt Block FPr=0.029, t-test P=0.08. Figure 3.15C), and 60 (t-test P=0.09. Figure 3.15E). At GD30, a trend towards decreased foetal weight in 2M foetuses was also observed (t-test P=0.09). In contrast, at GD30 0F foetuses were heavier than 1F (t-test P=0.02) or 2F (P=0.035) foetuses (overall effect: ANOVA without Gilt Block FPr=0.028) (Figure 3.15B). However, at GD60 2F foetuses were heavier than 0F (t-test P=0.02) or 1F (t-test P=0.05) foetuses. The sex of the neighbour did not influence male weight at GD90 (Figure 3.15G), or female weight at GD45 (Figure 3.15D) or GD90 (Figure 3.15H).

Sex of the neighbour did not influence CRL of male foetuses at GD60 (Figure 3.16E) or 90 (Figure 3.16G), or female foetuses at GD45 (Figure 3.16D) or 90 (Figure 3.16H). 2M foetuses were shorter than 1M foetuses at GD30 (Mann-Whitney P=0.06. Figure 3.16A) and at GD45, 0M foetuses were shorter than 1M or 2M foetuses (overall effect ANOVA without Gilt Block FPr=0.074. t-test P≤0.05. Figure 3.16C). At GD30, 0F foetuses were longer (overall effect: Kruskal-Wallis P=0.081) than those with 1F (Mann-Whitney P=0.085) or 2F (Mann-Whitney P=0.014) foetuses (Figure 3.16B). This was reversed at GD60 (overall effect: Kruskal-Wallis: P=0.011), with 0F (Mann-Whitney test P=0.013) and 1F (Mann-Whitney test P=0.008) foetuses being longer than 2F foetuses (Figure 3.16F).

Sex of the neighbour was not associated with PI of male foetuses at GD30, 60 or 90 (Figure 3.17A, E, or G) or female foetuses at GD30 (Figure 3.17B). At GD45 (overall effect: Kruskal-Wallis P=0.012), 0M foetuses had a lower PI than 2M foetuses (Mann-Whitney P=0.004) (Figure 3.17C). In addition, 2M foetuses had a lower PI than 1M foetuses (Mann-Whitney P=0.055). A trend towards decreased PI in 2F foetuses compared to 1F foetuses was observed

(Mann-Whitney P=0.08. Figure 3.17D). At GD60, a trend towards 0F foetuses having increased PI compared to 1F foetuses was observed (Mann-Whitney P=0.06. Figure 3.17F). This was reversed at GD90, with 0F foetuses having a decreased PI compared to 1F foetuses (Mann-Whitney P=0.04. Figure 3.17H).

Sex of the neighbour had little influence on ALF volume in either sex (Figure 3.18). However, at GD90 2F foetuses had less ALF compared to 1F foetuses (t-test P=0.045. Figure 3.18H). Additionally, sex of the neighbour was not associated with AMF volume in either sex at the four GD investigated (data not presented).

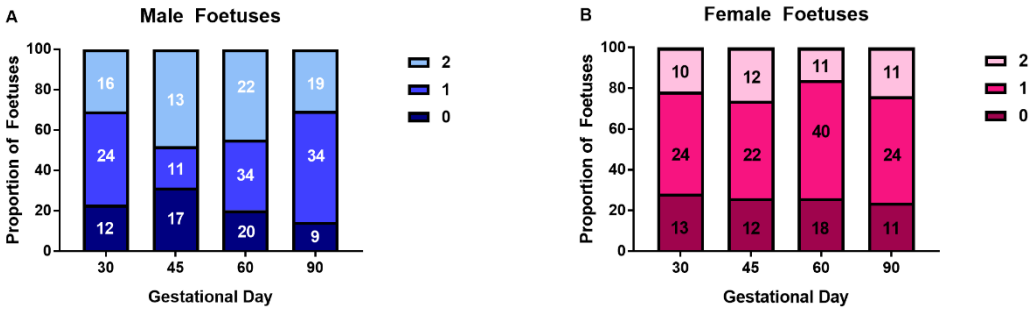

Figure 3.14: Proportion of Male and Female Foetuses with Neighbours of the Same Sex.

The sex of the neighbours of each foetus, excluding the foetuses at the end of the uterine horns which only have one neighbour, was calculated. Each foetus was assigned a value of 0, 1 or 2 which denotes that they had 0, 1 or 2 neighbours of the same sex. Male (A) and female (B) foetuses were separated for this analysis. Number on the bars indicate the number of foetuses within this category used for the analyses.

GD	CTMLW			Lightest		
	0	**1**	**2**	**0**	**1**	**2**
30	2	5	1	0	6	1
45	0	4	1	4	1	1
60	0	8	3	2	7	2
90	1	3	2	3	4	2
Total	*3*	*20*	*7*	*9*	*18*	*6*

Table 3.10: Summary of the Number of Neighbours (0, 1 or 2) of the Same Sex for the CTMLW and Lightest Foetuses within GD.

Abbreviations used: GD=Gestational Day, CTMLW=Closest to Mean Litter Weight.

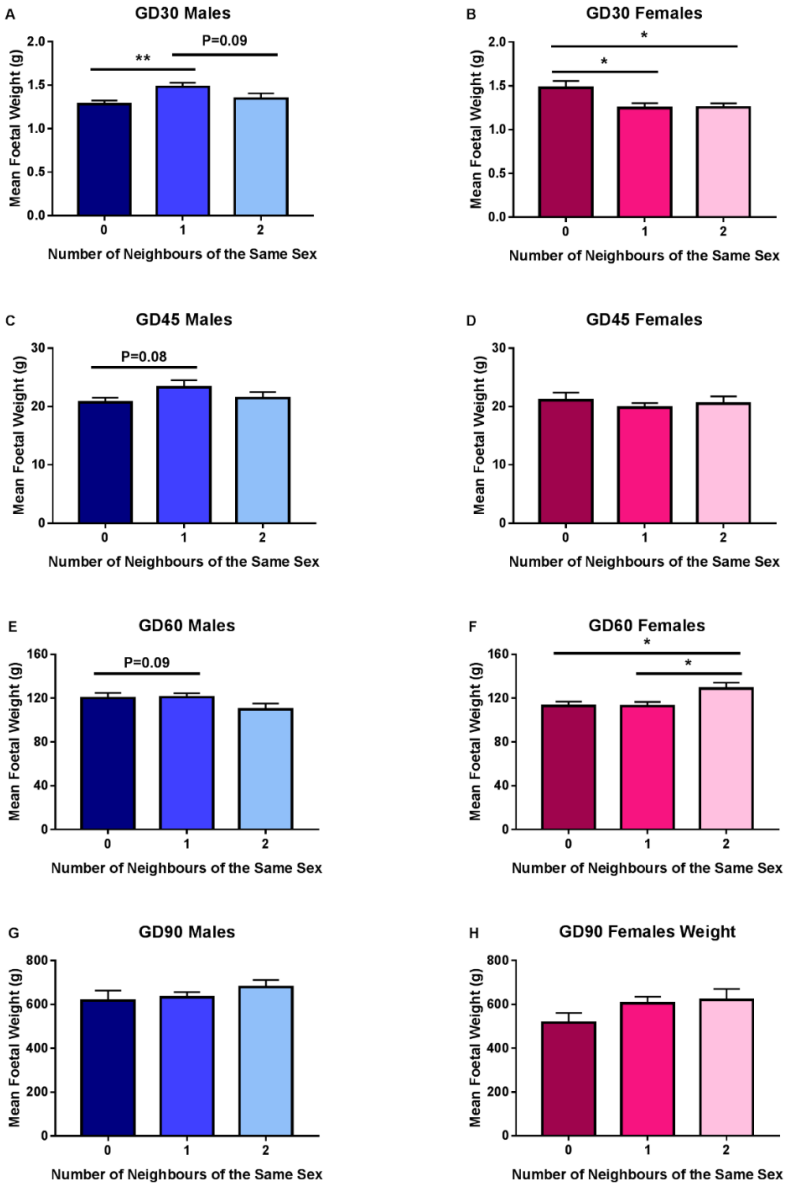

Figure 3.15: Sex of the Neighbour Influences Foetal Weight.

The sex of the neighbour was not associated with male foetal weight at GD90 (G), or female weight at GD45 (D) or GD90 (H). Male foetuses with one neighbour of each sex were heavier than male foetuses with two female neighbours at GD30 (t-test P=0.01. A), 45 (overall effect: ANOVA without Gilt Block FPr≤0.05, t-test P=0.08. C), and 60 (t-test P=0.09. E). At GD30, a trend towards decreased foetal weight in male foetuses with two male neighbours was observed (t-test P=0.09) (A). At GD30 female foetuses with two male neighbours were heavier than females with one (t-test P=0.02) or two female neighbours (P≤0.05) (overall effect: ANOVA without Gilt Block FPr≤0.05) (B). At GD60 female foetuses with two female neighbours were heavier than female foetuses with one (t-test P≤0.05) or two (t-test P≤0.05) male neighbours. Error bars represent S.E.M. **FPr/P≤0.01. *FPr/P≤0.05.

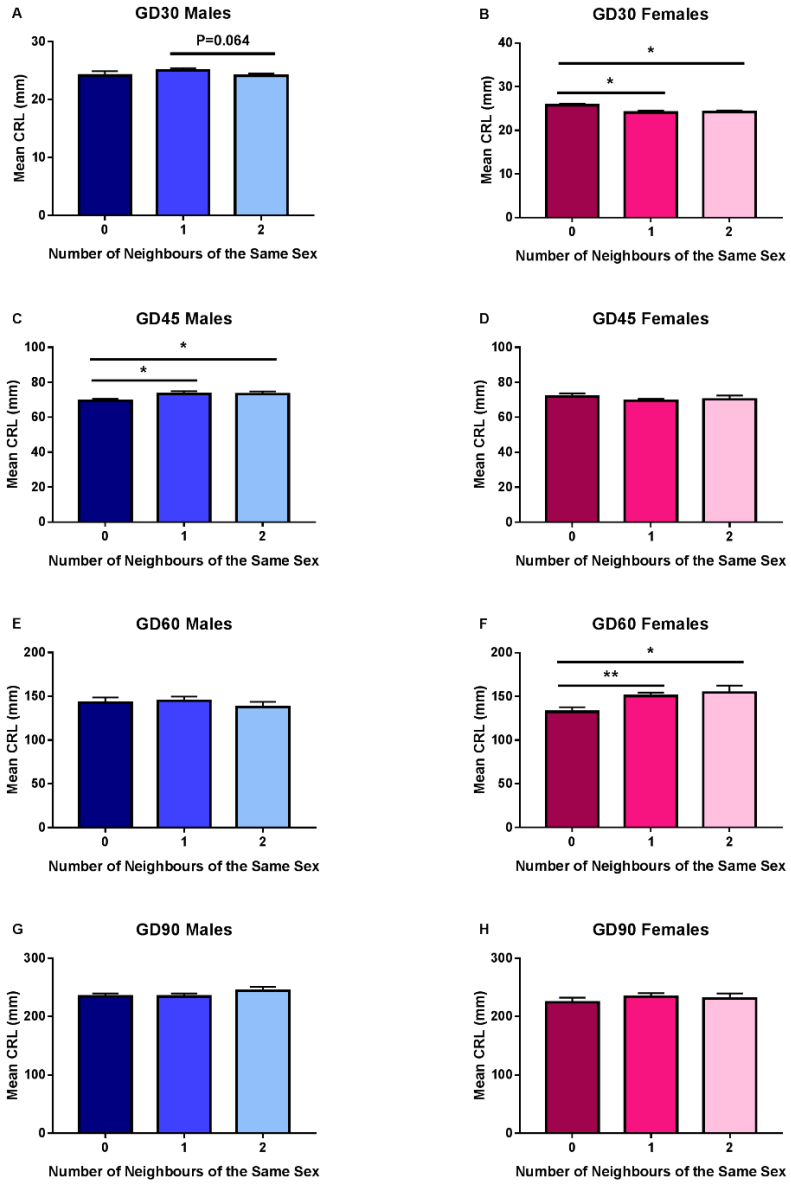

Figure 3.16: Sex of the Neighbour Influences Foetal CRL.

A: Male foetuses with two male neighbours were shorter than those with one male neighbour at GD30 (Mann-Whitney P=0.06). C: At GD45, male foetuses with two female neighbours were shorter than male foetuses with one or two male neighbours (overall effect ANOVA without Gilt Block FPr=0.07. t-test P≤0.05). B: At GD30, female foetuses with two male neighbours were longer (overall effect: Kruskal-Wallis P=0.08) than those with one (Mann-Whitney P=0.085) or two (Mann-Whitney P P≤0.01) female neighbours. F: At GD60 females with one (Mann-Whitney test P≤0.01) or two (Mann-Whitney test P≤0.01) male neighbours were longer than those with two female neighbours (overall effect: Kruskal-Wallis P≤0.01). Sex of the neighbour did not influence CRL of male foetuses at GD60 (E) or 90 (G), or female foetuses at GD45 (D) or 90 (H). Error bars represent S.E.M. **FPr/P≤0.01. *FPr/P≤0.05.

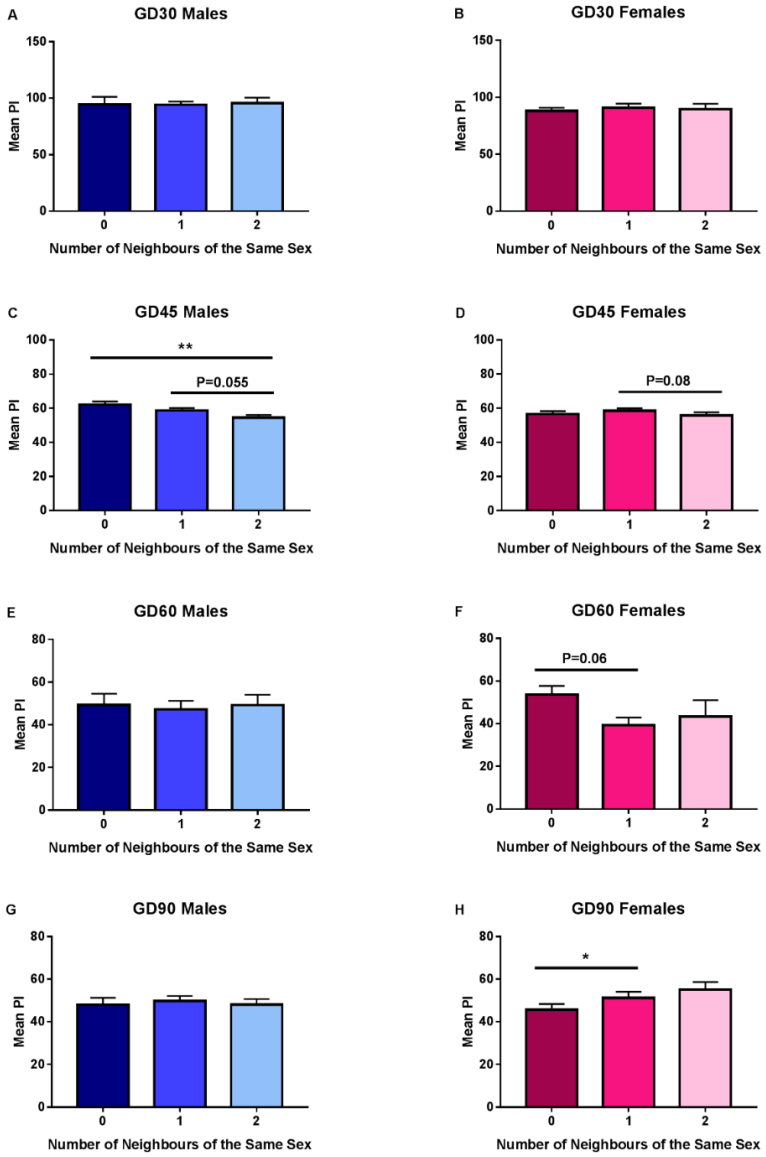

Figure 3.17: Sex of the Neighbour Influences Foetal PI.

Sex of the neighbour was not associated with PI of male foetuses at GD30, 60 or 90 (A, E, or G) or female foetuses at GD30 (B). C: At GD45 (overall effect: Kruskal-Wallis P≤0.01), male foetuses with two female neighbours had a lower PI than those with two male neighbours (Mann-Whitney P≤0.01). In addition, male foetuses with two male neighbours had a lower PI than those with one male neighbour (Mann-Whitney P≤0.05). D: A trend towards decreased PI in female foetuses with two female neighbours compared to those with one female neighbour was observed (Mann-Whitney P=0.08). F: At GD60, a trend towards female foetuses with two male neighbours having increased PI compared to those with 1 male neighbour was observed (Mann-Whitney P=0.06). H: At GD90, females with two male neighbours have a decreased PI compared to those with one male neighbour (Mann-Whitney P≤0.05. Figure 13H). Error bars represent S.E.M. **FPr/P≤0.01. *FPr/P≤0.05.

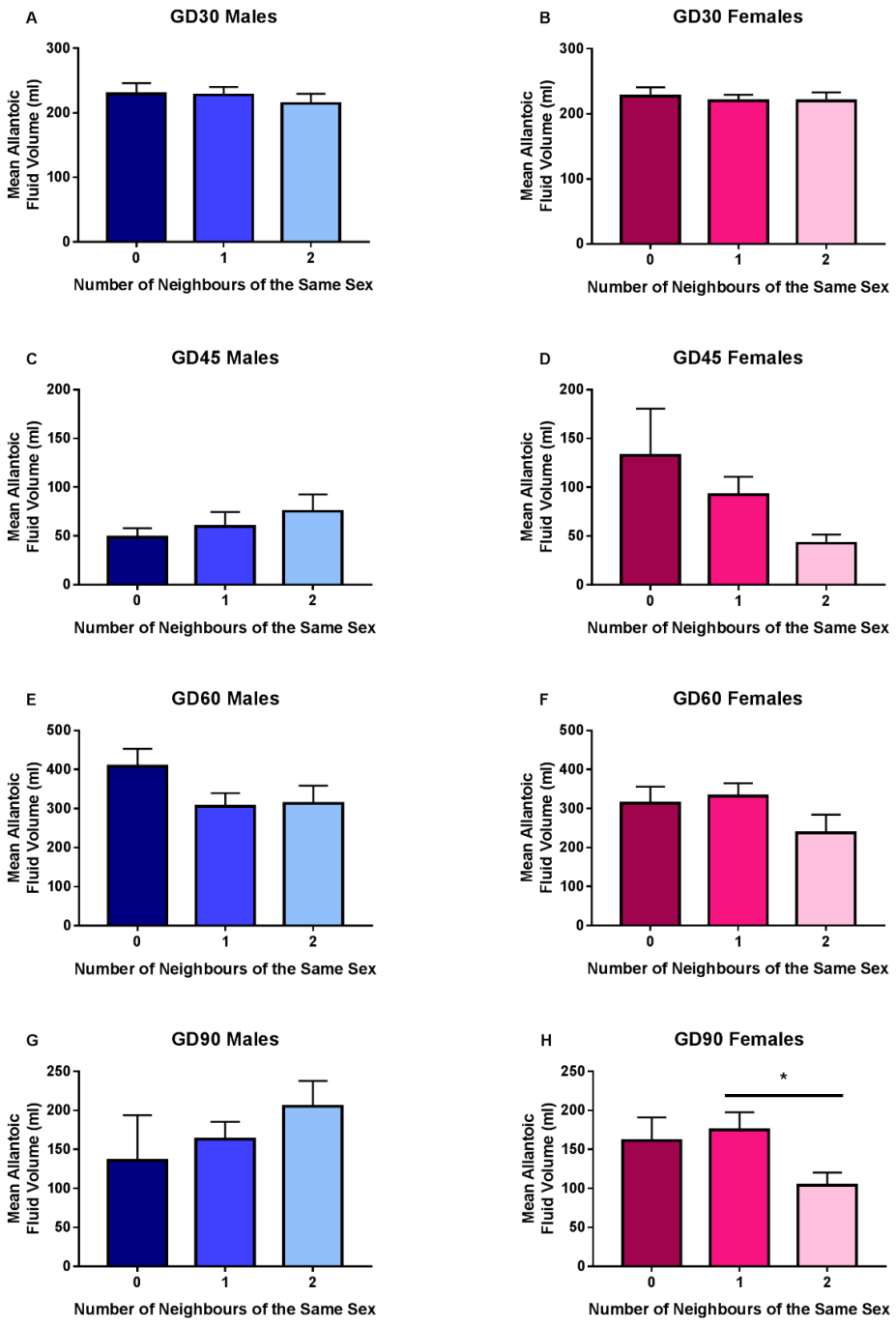

Figure 3.18: Sex of the Neighbour is Associated with Allantoic Fluid Volume in Female Foetuses at GD90.

Sex of the neighbour was associated with allantoic fluid volume at GD90 in female foetuses, with those with two female neighbours having less allantoic fluid compared to those with one neighbour (t-test P≤0.05. H). No other associations between sex of the neighbour and allantoic fluid volume in either sex at any of the GD investigated were observed. Error bars represent S.E.M. *FPr/P≤0.05.

3.4.7 Uterine Position

Analyses were performed to investigate the association between uterine position and foetal weight, CRL, PI, and ALF and AMF volume. The proportion of the length along the uterine horn for each foetus (0 = cervical end; 1 = ovarian end) was calculated and the deviation from the gilt mean (denoted 1) for each parameter was plotted (Supplementary Figure 6-Supplementary Figure 9). Additionally, the data values and deviation from gilt mean for each variable for the foetuses at the end of the uterine horns (cervical and ovarian combined) were compared with the foetuses at the middle of the uterine horn (Supplementary Table 2-Supplementary Table 3).

The influence of uterine position was investigated further by separating the end foetuses into those which are located at the cervical end and those which were found at the ovarian end of the uterine horn. A trend towards an association between foetal weight and uterine position was observed at GD30 (ANOVA with Gilt Block FPr=0.07; Figure 3.19A), with foetuses located at the cervical end of the uterine horn being the heaviest of the three groups investigated. Similarly, at GD45 foetuses located at the cervical end were the heaviest, and foetuses located at the ovarian end of the uterine horn were the lightest (ANOVA with Gilt Block FPr=0.05; Figure 3.20A). In contrast, at GD60 (ANOVA without Gilt Block FPr=0.07; Figure 3.21A) and 90 (ANOVA without Gilt Block FPr=0.079, with Gilt Block FPr=0.036. Figure 3.22A), the foetuses at the ovarian end of the uterine horn were the heaviest. No relationship between CRL or PI and uterine position were observed at GD30 (Figure 3.19), 45 (Figure 3.20), 60 (Figure 3.21) or 90 (Figure 3.22). AMF volume was associated with uterine position at GD60, with foetuses located at the cervical end of the uterine horn having increased AMF volume compared to foetuses located in the middle and at the ovarian end of the uterine horn (ANOVA without Gilt Block FPr=0.02; with Gilt Block FPr=0.01; Figure 3.21E). At GD90, foetuses located at the cervical end of the uterine horn had a decreased ALF volume compared to foetuses located in the middle and at the ovarian end of the uterine horn (ANOVA without Gilt Block FPr=0.024; with Gilt Block FPr=0.005; Figure 3.22E).

The analysis was repeated using the deviation from the gilt mean for each variable of interest (results of interest illustrated in Figure 3.23). As described for the raw data analysis, an association between foetal weight and uterine position was observed at GD30 (ANOVA without Gilt Block FPr=0.027; Figure 3.23A) and GD90 (Kruskal-Wallis P=0.01; Figure 3.23B). An association between uterine position and PI in the deviation from gilt mean analysis was observed (Kruskal-Wallis P=0.082; Figure 3.23C), with increased deviation from gilt mean observed in foetuses located at the ovarian end of the uterine horn. Decreased deviation from gilt mean for ALF volume at GD90 (ANOVA without Gilt Block FPr=0.004; Figure 3.23D), and increased deviation from gilt mean for AMF volume at GD60 (ANOVA without Gilt Block FPr=0.005; Figure 3.23F) was observed in foetuses located at the cervical end of the uterine horn. At GD45, decreased deviation from gilt mean for AMF volume was observed in foetuses located at the ovarian end of the uterine horn than those located in the cervical and middle portion of the uterine horn (Kruskal-Wallis P=0.058; Figure 3.23E).

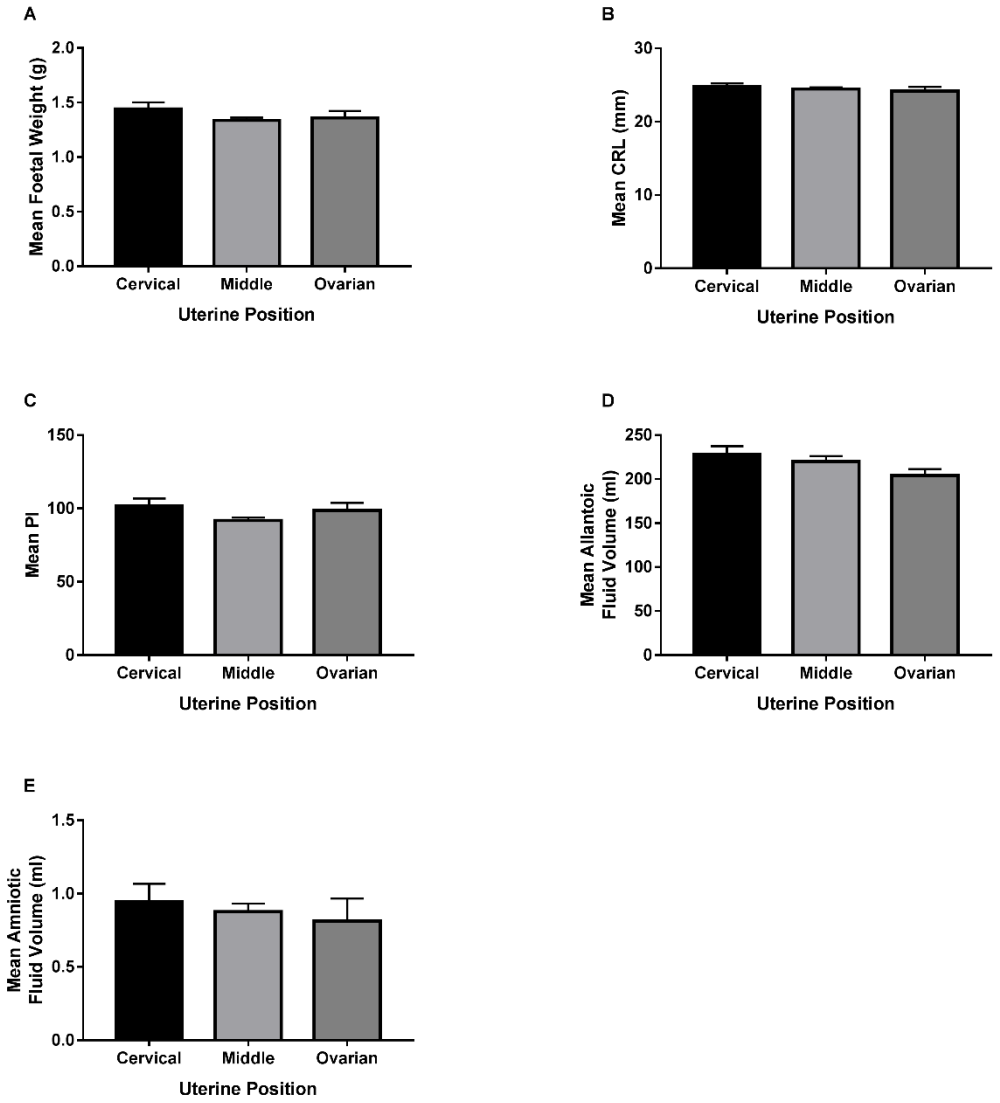

Figure 3.19: A Trend towards an Association between Uterine Position and Foetal Weight was observed at GD30.

A: A trend towards an association between foetal weight and uterine position was observed at GD30 (ANOVA with Gilt Block FPr=0.07), with foetuses located at the cervical end of the uterine horn being the heaviest of the three groups investigated. No relationship between CRL (B), PI (C), allantoic fluid volume (D), or amniotic fluid volume (E), and uterine position were observed at GD30. Error bars represent S.E.M.

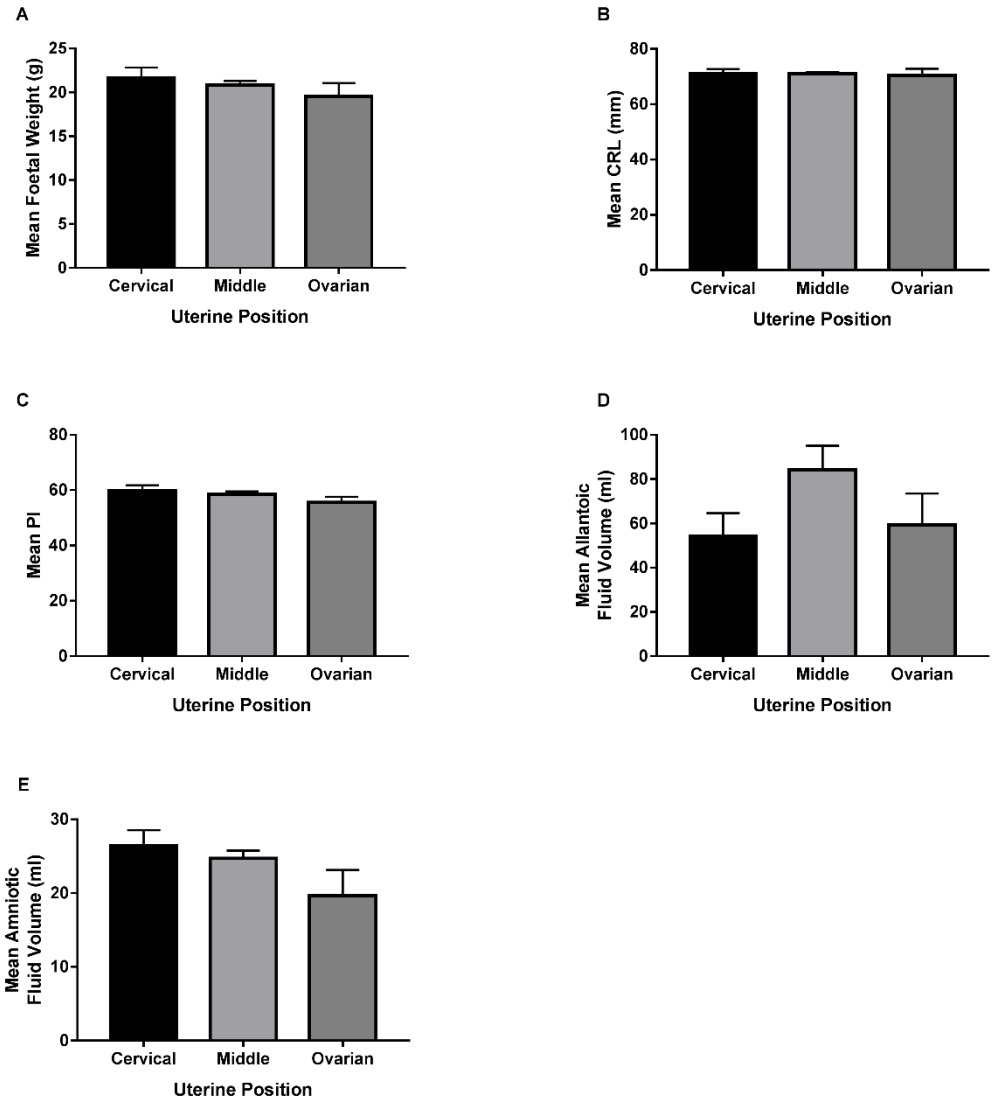

Figure 3.20: An Association between Uterine Position and Foetal Weight was observed at GD45.

A: Foetuses located at the cervical end were the heaviest, and foetuses located at the ovarian end of the uterine horn were the lightest (ANOVA with Gilt Block FPr≤0.05). No relationship between CRL (B), PI (C), allantoic fluid volume (D), or amniotic fluid volume (E), and uterine position were observed at GD45. Error bars represent S.E.M.

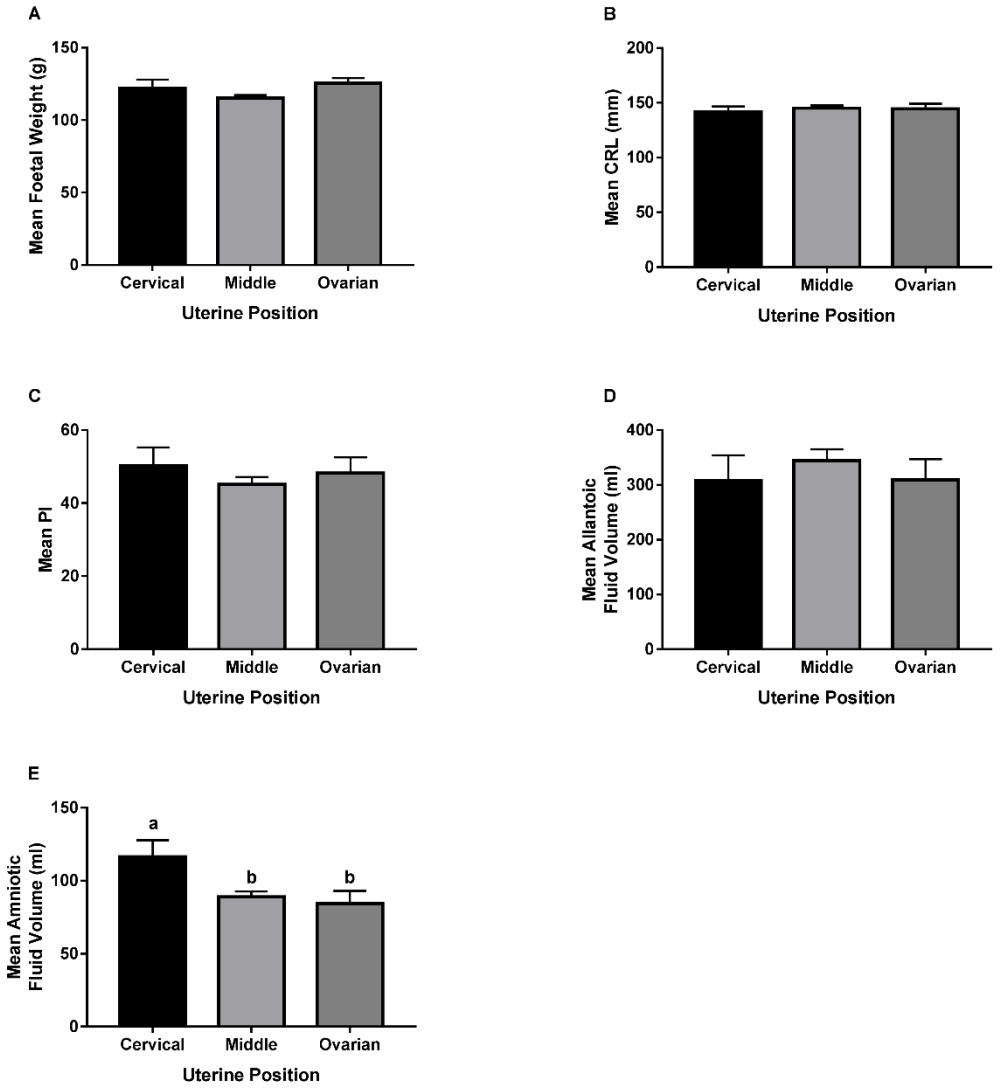

Figure 3.21: Foetuses Located at the Cervical End of the Uterine Horn Have Increased Amniotic Fluid compared to the Middle and Ovarian End of the Uterine Horn at GD60.

A: An indication towards a relationship between uterine position and foetal weight was observed (ANOVA without Gilt Block FPr=0.07) which was not statistically significant with the addition of a block for gilt. No association between uterine position and CRL (B), PI (C), or allantoic fluid volume (D) was observed. E: Amniotic fluid volume was associated with uterine position (ANOVA without Gilt Block FPr≤0.05; with Gilt Block FPr≤0.01), with foetuses located at the cervical end of the uterine horn having increased amniotic fluid compared to foetuses located in the middle and at the ovarian end of the uterine horn. Error bars represent S.E.M. Letters indicate that group means differ from one another, tested by post-hoc Tukey.

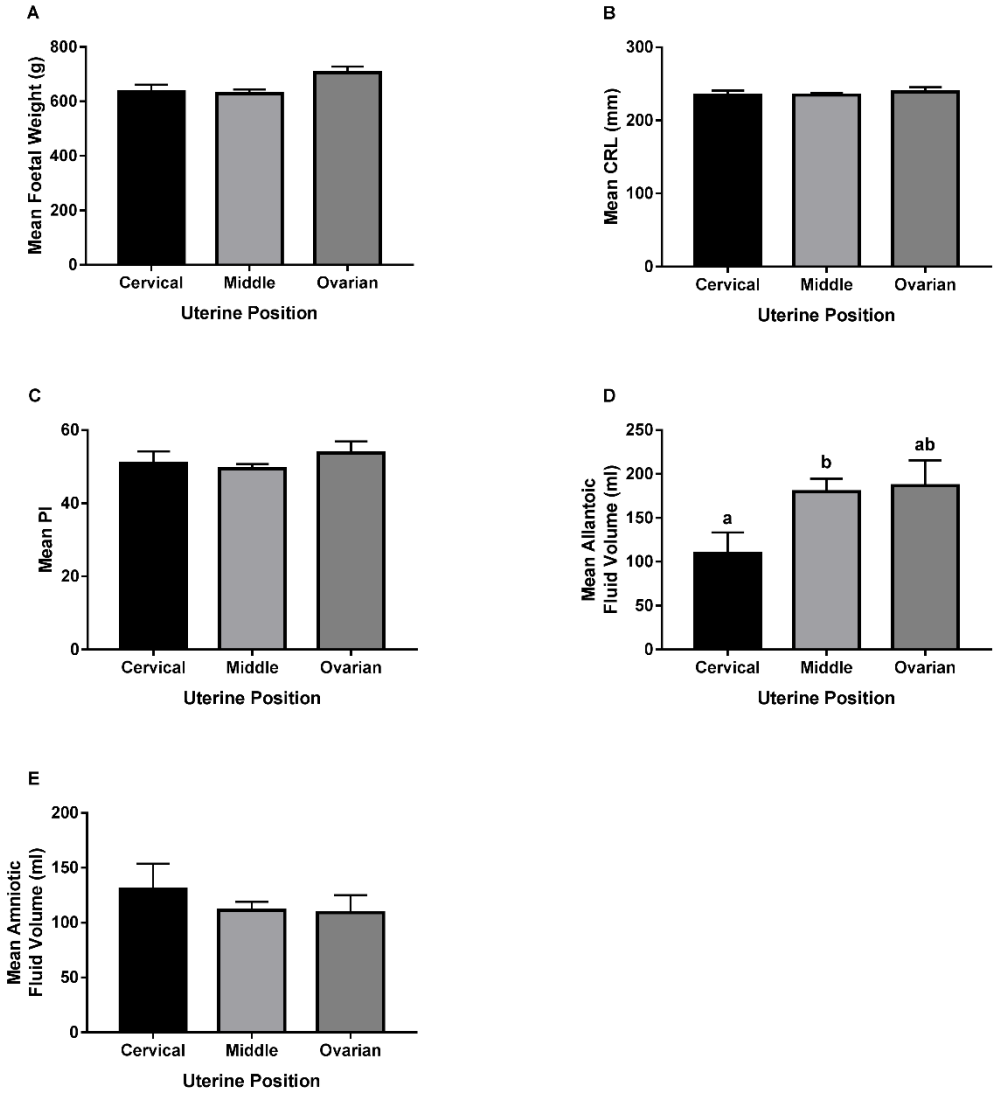

Figure 3.22: An Association between Foetal Weight and Allantoic Fluid Volume, and Uterine Position was observed at GD90.

A: An association between foetal weight and uterine position was observed (ANOVA without Gilt Block FPr=0.08, with Gilt Block FPr≤0.05), with the heaviest foetuses being located at the ovarian end of the uterine horn. No association between CRL (B), PI (C), or amniotic fluid volume (E), and uterine position was observed. D: Foetuses located at the cervical end of the uterine horn had a decreased allantoic fluid volume compared to foetuses located in the middle and at the ovarian end of the uterine horn (ANOVA without Gilt Block FPr≤0.05; with Gilt Block FPr≤0.01). Error bars represent S.E.M. Letters indicate that group means differ from one another, tested by post-hoc Tukey.

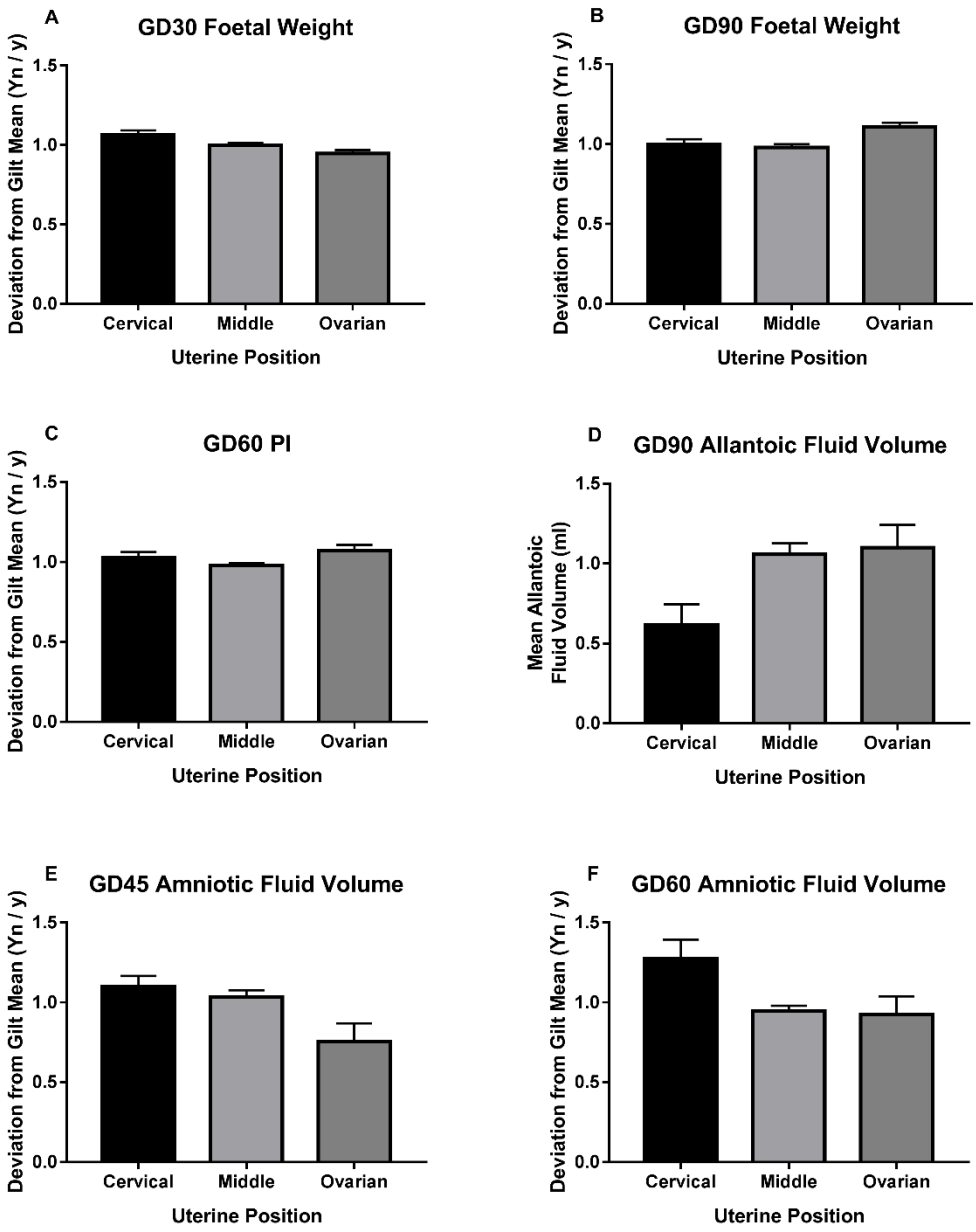

Figure 3.23: Significant Associations were observed between Uterine Position and Foetal Weight, PI, Allantoic and Amniotic Fluid Volumes.

An association between foetal weight and uterine position was observed at GD30 (ANOVA with and without Gilt Block FPr≤0.05; A) and GD90 (Kruskal-Wallis P=0.01; B). C: A trend towards an association between uterine position and deviation from PI gilt mean was observed (Kruskal-Wallis P=0.08). D: Decreased deviation from gilt mean for allantoic fluid volume at GD90 (ANOVA with and without Gilt Block FP≤0.01) was observed in foetuses located at the cervical end of the uterine horn. E: At GD45, decreased deviation from gilt mean for amniotic fluid volume was observed (Kruskal-Wallis P=0.06). F: Increased deviation from gilt mean for amniotic fluid volume (ANOVA with and without Gilt Block FPr≤0.01) was observed in foetuses located at the cervical end of the uterine horn at GD60. Error bars represent S.E.M.

3.4.8 Differences in Organ Weights

3.4.8.1 Evidence for Brain Sparing was observed in the Lightest Foetuses

Regressions were performed to assess the relationship between foetal weight and brain, liver and combined gonadal weight (Figure 3.24 and Table 3.11). A positive relationship between foetal weight and liver weight at GD45 (P≤0.001) and 60 (P≤0.001), and brain weight at GD45 (P≤0.001) was observed. Following this, the brain, liver and combined gonadal weight were compared between the CTMLW and lightest groups within GD (Figure 3.25). At GD30 and 45, foetal size was not associated with liver weight, or liver and brain weight respectively. At GD60, the lightest foetuses had decreased liver weight compared to the CTMLW foetuses (ANOVA without Gilt Block FPr=0.081; with Gilt Block FPr=0.053. Figure 3.25C). At GD90, there was an indication that livers were heavier in the lightest foetuses compared to the CTMLW foetuses (ANOVA without Gilt Block FPr=0.088), although this was not statistically significant with the addition of a block for gilt. Brain and gonad weights were not associated with foetal size at GD60 or 90.

As detailed previously, there is evidence in the literature to suggest asymmetric organ growth, otherwise known as the brain 'sparing' effect, in runt piglets. Considering this, the brain: liver and brain: gonad ratio for the lightest and CTMLW foetuses was calculated at GD45, 60 and 90, and GD60 and 90 respectively (Figure 3.26). At GD60, the brain: liver ratio was increased in the lightest foetuses compared to the CTMLW foetuses (ANOVA with Gilt Block FPr=0.053; Figure 3.26A). This difference was reversed at GD90 (ANOVA without Gilt Block FPr=0.008; with Gilt Block FPr=0.059), with the lightest foetuses having a decreased brain: liver ratio compared to the CTMLW foetuses (Figure 3.26A). A trend towards increased liver as a percentage of foetal weight was observed in the lightest foetuses compared to the CTMLW foetuses at GD90 (ANOVA without Gilt Block FPr=0.015; with Gilt Block FPr=0.069; Figure 3.26C). In contrast, the brain to gonad ratio (Figure 3.26B) and brain as a percentage of foetal weight (Figure 3.26D) were not associated with foetal weight. However, gonads as a percentage of foetal weight was

increased in the lightest foetuses compared to the CTMLW foetuses at GD90 (ANOVA without Gilt Block FPr=0.064; with Gilt Block FPr=0.054; Figure 3.26E).

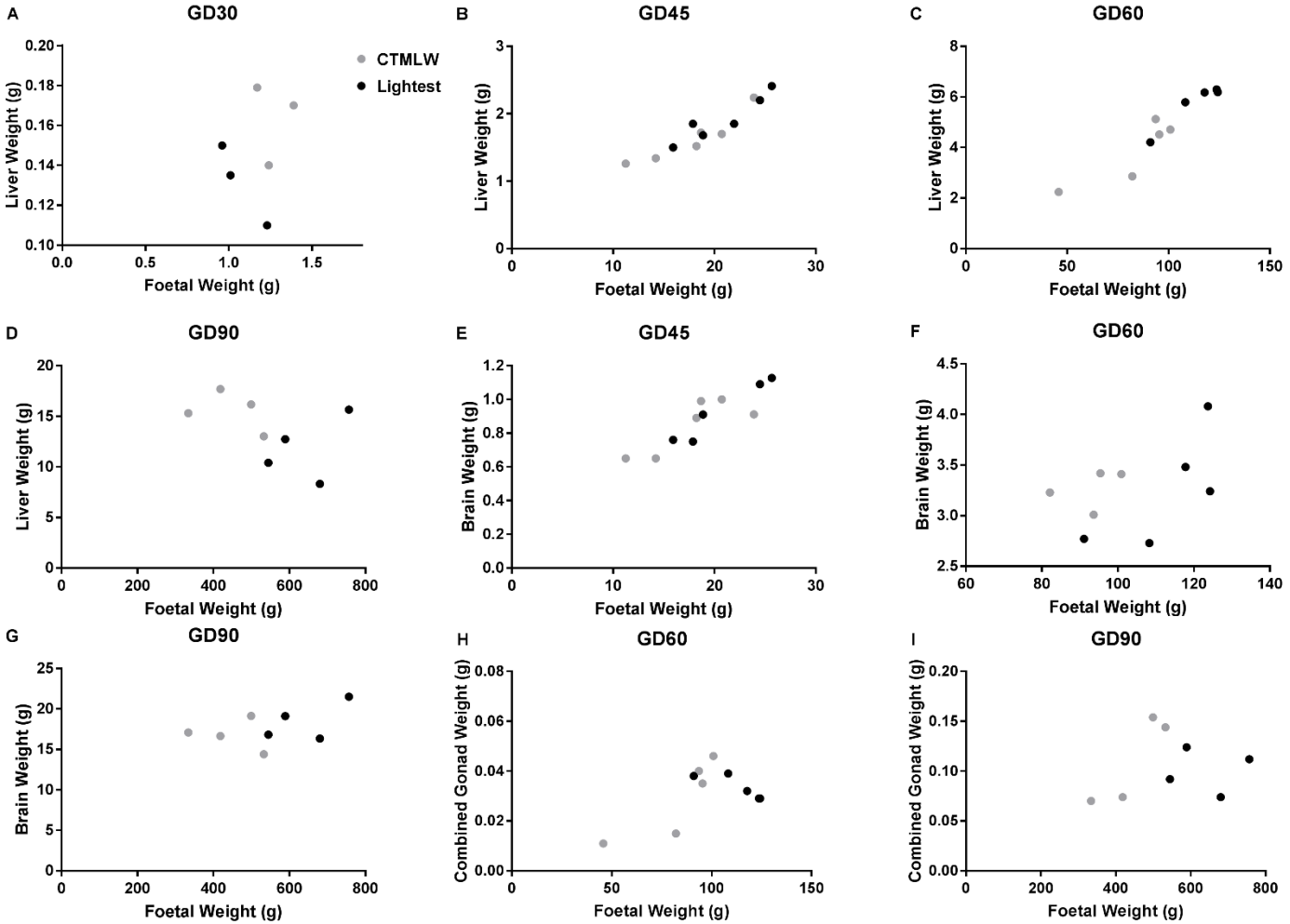

Figure 3.24: Scatterplot Illustrating the Relationship between Foetal and Organ Weight Within GD.

Organ	GD30		GD45		GD60		GD90	
	RSq (%)	P	RSq (%)	P	RSq (%)	P	RSq (%)	P
Liver	3.4	0.728	88.4	≤0.001	89.3	≤0.001	19.1	0.279
Brain	n/a		80.0	≤0.001	23.6	0.185	19.9	0.268
Gonad	n/a		n/a		28.6	0.112	4.7	0.608

Table 3.11: Summary of Regressions between Foetal and Organ Weights within GD.

Linear regressions were performed between organ weight and foetal weight within GD. This analysis suggested a positive relationship between foetal weight and brain and liver weight at GD45, and liver weight at GD60.

Figure 3.24: Scatterplot Illustrating the Relationship between Foetal and Organ Weight Within GD.

The weight of foetal livers (A-D), brains (E-G), and gonads (H and I) from the lightest and closest to mean litter weight (CTMLW) were plotted against foetal weight within Gestational Day (GD).

Figure 3.25: Foetal Liver Weight is decreased in the lightest foetuses compared to the CTMLW foetuses at GD60.

The brain, liver and combined gonadal weight was compared between the closest to mean litter weight (CTMLW) and lightest groups within GD. At GD30 and 45 foetal size was not associated with liver weight (A), or liver (B) and brain (E) weight respectively. C: At GD60, the lightest foetuses had decreased liver weight compared to the CTMLW foetuses (ANOVA without Gilt Block FPr=0.08; with Gilt Block FPr≤0.05). D: At GD90, there was an indication that livers were heavier in the lightest foetuses compared to the CTMLW foetuses (ANOVA without Gilt Block FPr=0.088), although this was not statistically significant with the addition of a block for gilt. Brain and gonad weights were not associated with foetal size at GD60 (F and H) or 90 (G and I).

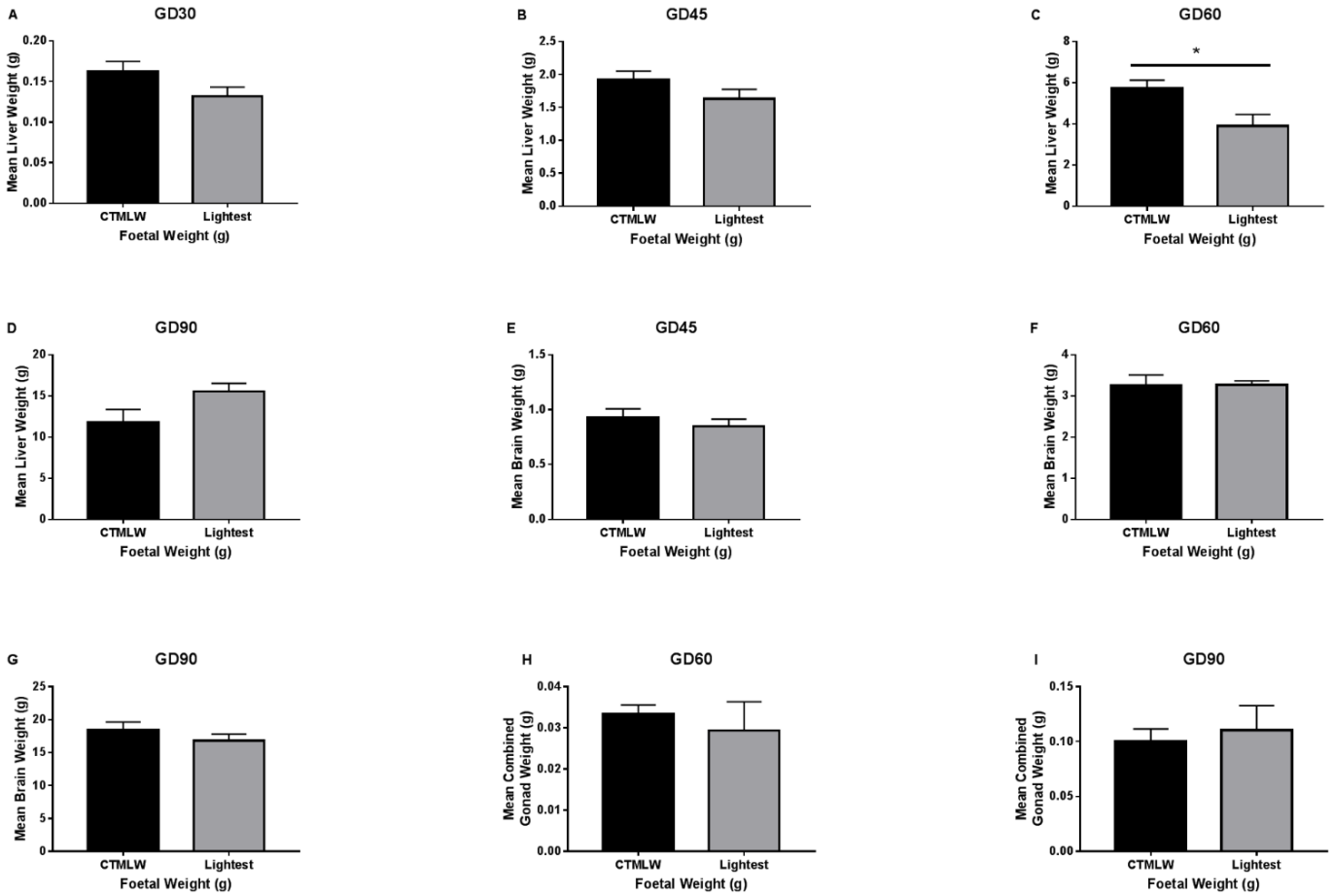

Figure 3.25: Foetal Liver Weight is decreased in the lightest foetuses compared to the CTMLW foetuses at GD60.

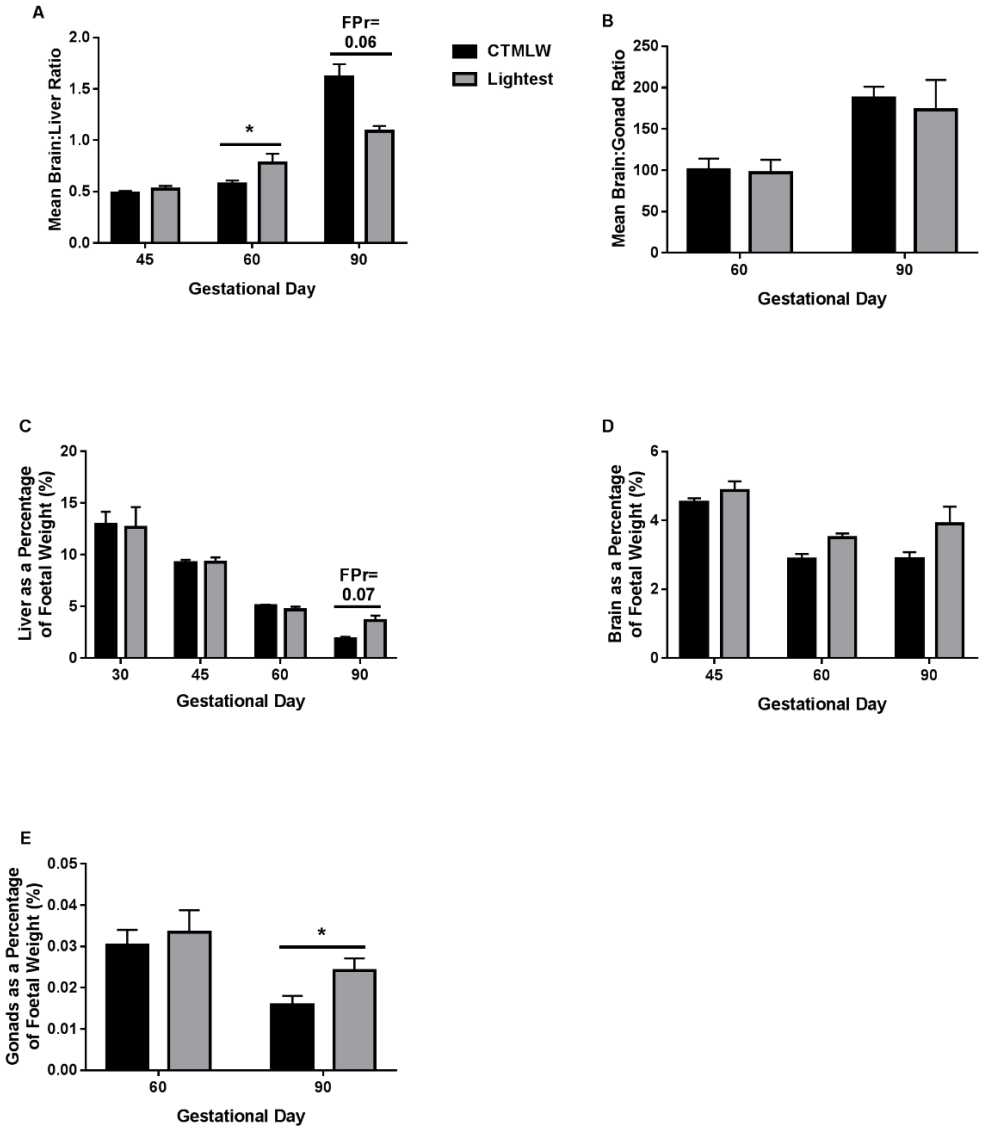

Figure 3.26: Brain: Liver Ratio, and Liver and Gonads as a Percentage of Foetal Weight are Associated with Foetal Weight.

A: At GD60, the brain: liver ratio was increased in the lightest foetuses compared to the closest to mean litter weight (CTMLW) foetuses (ANOVA with Gilt Block FPr≤0.05). At GD90 the lightest foetuses had a decreased brain: liver ratio compared to the CTMLW foetuses (ANOVA without Gilt Block FPr≤0.01; with Gilt Block FPr=0.059). C: A trend towards increased liver as a percentage of foetal weight was observed in the lightest foetuses compared to the CTMLW foetuses at GD90 (ANOVA without Gilt Block FPr≤0.05; with Gilt Block FPr=0.069). The brain to gonad ratio (B) and brain as a percentage of foetal weight (D) were not associated with foetal weight. E: Gonads as a percentage of foetal weight was increased in the lightest foetuses compared to the CTMLW foetuses at GD90 (ANOVA without Gilt Block FPr=0.064; with Gilt Block FPr=0.054). Error bars represent S.E.M. *FPr/P≤0.05.

3.4.8.2 Ovaries are lighter than Testes at GD60 and 90

Foetal sex was not associated with liver weight at any GD investigated (Figure 3.27A-D). Similarly, no association between brain weight and foetal sex was observed at GD45, 60 or 90 (Figure 3.27E-G). At GD60 (ANOVA without Gilt Block FPr=0.03; with Gilt Block FPr=0.04) and 90 (ANOVA without Gilt Block FPr=0.089; with Gilt Block FPr=0.097), gonad weight was decreased in female foetuses compared to male foetuses (Figure 3.27H and I). Liver (Figure 3.28A) and brain (Figure 3.28B) as a percentage of foetal weight were not associated with foetal sex. Similarly, brain: liver ratio (Figure 3.28D) and brain: gonad ratio (Figure 3.28E) were not associated with foetal sex. In contrast, gonads as a percentage of foetal weight was decreased in female foetuses compared to male foetuses at GD60 (ANOVA with and without Gilt Block FPr≤0.05) and 90 (ANOVA with and without Gilt Block FPr=0.057) (Figure 3.28C).

3.4.8.3 Sex of the Neighbour Influenced Liver Weight

Considering the influence of sex of the neighbour detailed in 3.4.6, the association between sex of the neighbour and organ weight was investigated.

Table 3.12 and Table 3.13 summarise the mean values obtained for males (0M, 1M, and 2M) and females (0F, 1F, and 2F) respectively. Sex of the neighbour had a limited influence on organ weight in both males and females. At GD45, 0M foetuses had smaller livers than 1M foetuses (ANOVA without Gilt Block FPr=0.044. t-test P=0.03). At GD90, liver weight increased with increasing number of female neighbours in female foetuses (ANOVA with Gilt Block FPr=0.024) however, the 0F and 2F groups had a small number of foetuses.

Figure 3.27: Ovaries are lighter than Testes at GD60 and 90.

No association between foetal sex and liver weight was observed at GD30 (A), 45 (B), 60 (C), and 90 (D). Similarly, no association between foetal sex and brain weight was observed at GD45 (E), 60 (F), and 90 (G). At GD60 (ANOVA without Gilt Block FPr=0.03; with Gilt Block FPr=0.035. H), and 90 (ANOVA without Gilt Block FPr=0.089; with Gilt Block FPr=0.097. I), the mean combined gonad weight was decreased in female foetuses compared to male foetuses. Gonads as a percentage of body weight was also lower in female foetuses compared to male foetuses at GD60 (ANOVA with and without Gilt Block FPr≤0.05. H), and 90 (ANOVA with and without Gilt Block FPr=0.057). Error bars represent S.E.M. *FPr/P≤0.05.

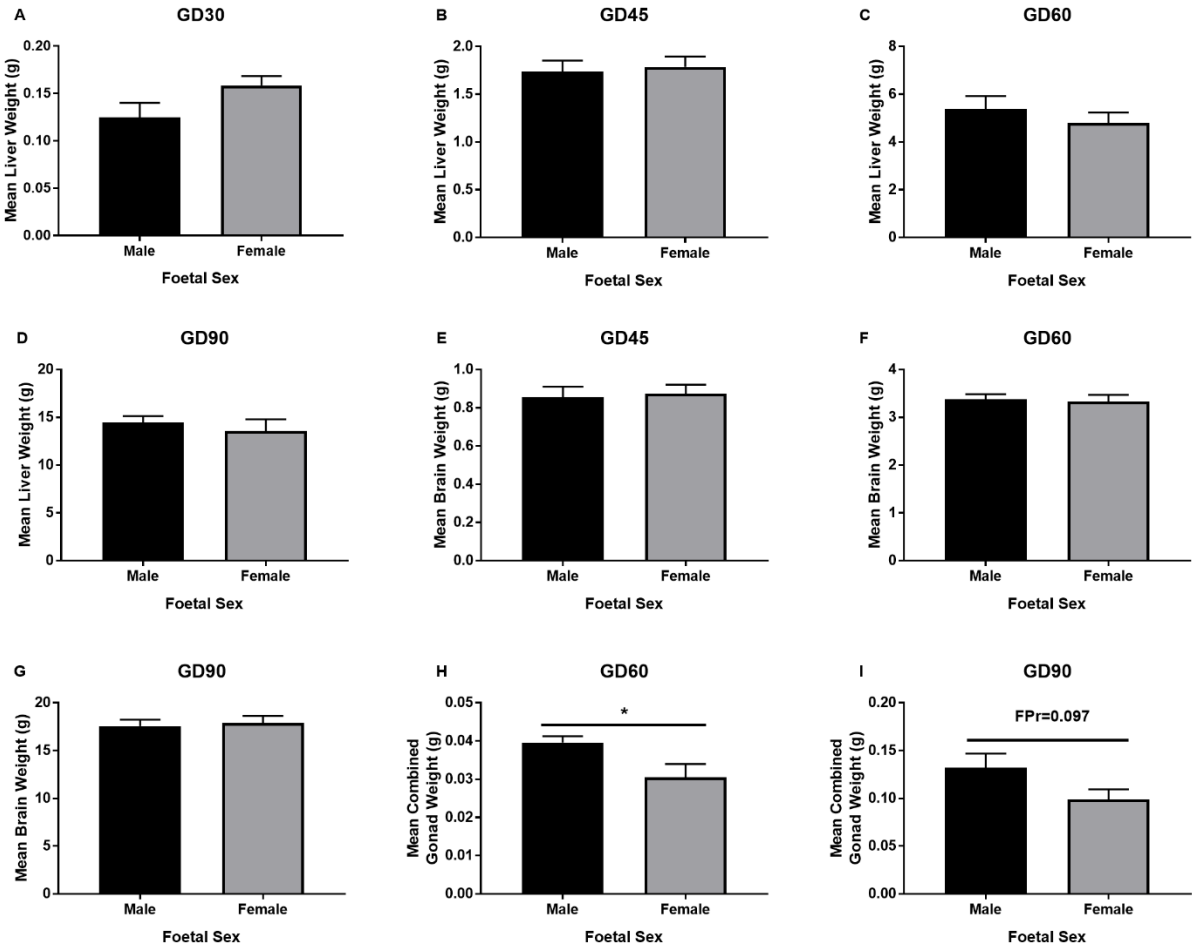

Figure 3.27: Ovaries are lighter than Testes at GD60 and 90.

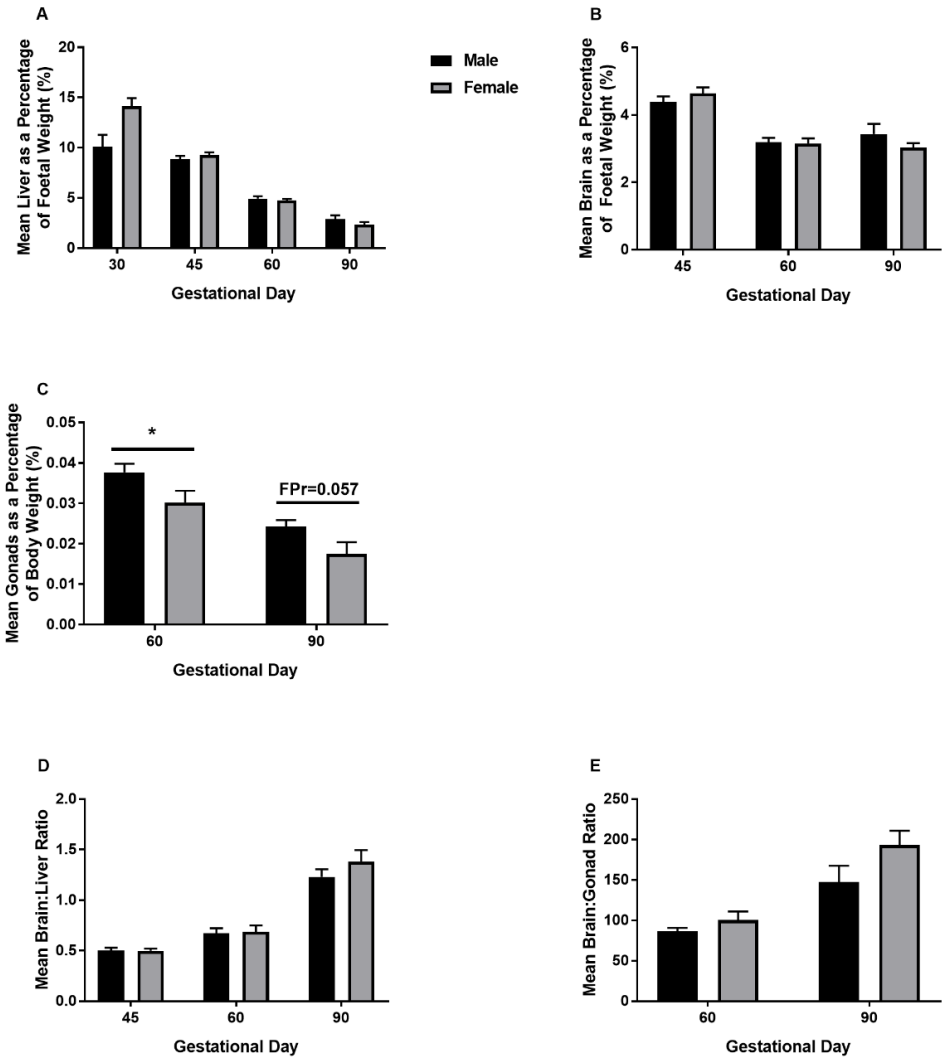

Figure 3.28: Gonad weight as a Percentage of Body Weight is lower in Females Compared to Males.

Liver (A) and brain (B) as a percentage of foetal weight were not associated with foetal sex. Similarly, brain: liver ratio (D) and brain: gonad ratio (E) were not associated with foetal sex. C: Gonads as a percentage of foetal weight was decreased in female foetuses compared to male foetuses at GD60 (ANOVA with and without Gilt Block FPr≤0.05) and 90 (ANOVA with and without Gilt Block FPr=0.057). Error bars represent S.E.M. *FPr/P≤0.05.

Variable	Males (mean ± S.E.M. (n))											
	GD30			GD45			GD60			GD90		
	0	1	2	0	1	2	0	1	2	0	1	2
Liver Weight (g)	n/a	0.11 (1)	0.12 ± 0.02 (2)	1.854 ± 0.129 (8)	2.302 ± 0.252 (6)	2.41 (1)	5.187 ± 0.588 (5)	6.118 ± 0.803 (6)	5.18 ± 1.000 (2)	17.69 (1)	14.428 ± 0.621 (6)	14.05 ± 0.830 (2)
Liver as a Percentage of Body Weight (%)	n/a	8.943 (1)	8.871 ± 2.419 (2)	9.537 ± 0.438 (8)	9.546 ± 0.570 (6)	9.392 (1)	4.721 ± 0.278 (5)	5.069 ± 0.302 (6)	4.587 ± 0.659 (2)	4.229 (1)	2.769 ± 0.408 (6)	2.528 ± 0.320 (2)
Brain Weight (g)	n/a			0.82 ± 0.062 (8)	1.001 ± 0.026 (6)	1.127 (1)	3.436 ± 0.147 (5)	3.337 ± 0.193 (6)	3.415 ± 0.065 (2)	16.65 (1)	17.033 ± 0.646 (6)	18.395 ± 2.315 (2)
Brain as a Percentage of Body Weight (%)	n/a			4.190 ± 0.191 (8)	4.247 ± 0.176 (6)	4.392 (1)	3.201 ± 0.210 (5)	2.889 ± 0.200 (6)	3.051 ± 0.097 (2)	3.980 (1)	3.241 ± 0.426 (6)	3.269 ± 0.191 (2)
Combined Gonad Weight (g)	n/a			n/a			0.040 ± 0.002 (5)	0.047 ± 0.005 (6)	0.036 ± 0.004 (2)	0.074 (1)	0.130 ± 0.015 (6)	0.139 ± 0.002 (2)
Gonads as a Percentage of Body weight (%)	n/a			n/a			0.037 ± 0.003 (5)	0.040 ± 0.002 (6)	0.032 ± 0.005 (2)	0.018 (1)	0.024 ± 0.002 (6)	0.025 ± 0.002 (2)

Table 3.12: Summary of Organ Weights in Male Foetuses with 0, 1 and 2 Neighbours of the Same Sex.

The mean values ± standard error of the mean (S.E.M.) were calculated for each variable of interest for male foetuses with 0, 1 or 2 neighbours of the same sex within gestational day (GD). (n) Denotes the number of foetuses. n/a=not applicable.

Variable	Females (mean ± S.E.M. (n))											
	GD30			GD45			GD60			GD90		
	0	1	2	0	1	2	0	1	2	0	1	2
Liver Weight (g)	0.757 ± 0.315 (3)	0.15 (1)	0.131 ± 0.001 (2)	1.983 ± 0.174 (7)	1.81 ± 0.118 (8)	1.725 ± 0.205 (2)	4.85 ± 0.240 (2)	5.082 ± 0.497 (10)	6.54 ± 0.780 (2)	8.33 (1)	15.828 ± 1.481 (4)	17.33 ± 2.510 (2)
Liver as a Percentage of Body Weight (%)	50.642 ± 19.462 (3)	15.625 (1)	9.601 ± 0.876 (2)	9.233 ± 0.480 (7)	9.387 ± 0.304 (8)	8.858 ± 0.520 (2)	4.671 ± 0.268 (2)	4.842 ± 0.178 (10)	5.148 ± 0.298 (2)	1.225 (1)	2.736 ± 0.404 (4)	2.338 ± 0.017 (2)
Brain Weight (g)	n/a			0.952 ± 0.058 (7)	0.889 ± 0.066 (8)	0.905 ± 0.015 (2)	3.645 ± 0.125 (2)	3.247 ± 0.134 (9)	3.655 ± 0.135 (2)	16.348 (1)	18.035 ± 1.487 (4)	20.44 ± 1.250 (2)
Brain as a Percentage of Body Weight (%)	n/a			4.505 ± 0.289 (7)	4.578 ± 0.068 (8)	4.676 ± 0.206 (2)	3.508 ± 0.092 (2)	3.032 ± 0.153 (10)	2.892 ± 0.072 (2)	2.404 (1)	3.049 ± 0.202 (4)	2.793 ± 0.256 (2)
Combined Gonad Weight (g)	n/a			n/a			0.030 ± 0.004 (2)	0.031 ± 0.003 (10)	0.040 ± 0.005 (2)	0.074 (1)	0.107 ± 0.018 (4)	0.090 ± 0.023 (2)
Gonads as a Percentage of Body weight (%)	n/a			n/a			0.028 ± 0.004 (2)	0.030 ± 0.003 (10)	0.311 ± 0.002 (2)	0.011 (1)	0.019 ± 0.006 (4)	0.120 ± 0.001 (2)

Table 3.13: Summary of Organ Weights in Female Foetuses with 0, 1 and 2 Neighbours of the Same Sex.

The mean values ± standard error of the mean (S.E.M.) were calculated for each variable of interest for female foetuses with 0, 1 or 2 neighbours of the same sex within gestational day (GD). (n) Denotes the number of foetuses. n/a=not applicable.

3.5 Discussion

The results of the data collected at the time of sample collection have been summarised in this chapter, providing a valuable opportunity to advance our understanding of relationships between litter size, foetal size and sex and foetal fluid values at key stages of gestation. Intriguingly, the data highlighted the importance of the sex of foetuses in the uterus on foetal development, an area which will be discussed throughout this thesis.

3.5.1 General Litter Characteristics

It has previously been suggested in the pig that an inverse relationship exists between litter size and foetal weight, and between litter size and the weight of the lightest foetus (Bauer *et al.*, 1998). Although, as described in 3.1.1, some controversy exists in this field with others not observing an association between litter size and MLW or the weight of the lightest foetus (Finch *et al.*, 2002). The results presented in this chapter have demonstrated that a negative relationship between the number of live foetuses and MLW is present at GD60 in the pig, suggesting that as the number of foetuses increases, the foetuses are smaller. As this was not observed earlier in gestation, this may suggest that foetal growth is limited by uterine space by GD60. At this GD, a negative relationship was also observed between the number of live foetuses and the weight of the lightest foetus. Considering the controversy surrounding this topic, the influence of the local environment, i.e. the number of foetuses in the individual uterine horn, was investigated instead. This, as described in 3.1.1, has been proposed to be more influential on foetal development than the overall litter size (Waldorf *et al.*, 1957). Intriguingly, a negative relationship between number of foetuses in the uterine horn and foetal weight was observed at GD30 and 60, but no relationship was observed at GD45 or 90. Currently there is not obvious explanation for the temporal changes in this relationship. Although it is intriguing that these differences coincide with the two waves of prenatal loss in the pig: the early stage - between GD12 and 30 (Geisert and Schmitt, 2002; Ross *et al.*, 2009; Bidarimath and Tayade, 2017);

and the later stage - between GD50 and 90 (Vonnahme *et al.*, 2002; Vallet *et al.*, 2011).

Correlations were observed between foetal weight and CRL, which supports the previous findings of Jang *et al.*, (2014) in the pig. Intriguingly, whilst a linear relationship was observed between foetal weight and CRL with all three sample collections combined at GD30, this was not observed at GD60. The linear relationship was observed within sample collection but the foetuses from the third sample collection consistently had a longer CRL than those from the other two sample collections. A suggestion for this was also observed at GD90 however, the sample collection group was not as distinctly separated. The reason for this striking difference in CRL is not clear at this time but may reflect a genotype difference in foetal growth, as this was only observed in the final sample collection. Whilst all the gilts were from the same herd and were of comparable maturity when mated, the animals were transported from the herd (PIC, Germany) to the Roslin Institute Large Animal Facility immediately prior to each sample collection taking place. As it was not observed in the other GD investigated, and was in the final sample collections rather than the initial sample collections, it is unlikely to be a technical issue in the measurement of CRL at this GD.

3.5.2 Temporal Changes

Unsurprisingly, as gestation proceeded, an increase in foetal weight and CRL was observed. Foetal weight and CRL both increased significantly in late gestation, following a similar profile to the previously described literature suggesting that exponential foetal growth occurs after GD70 (Marrable, 1971; McPherson *et al.*, 2004; Ji *et al.*, 2005).

ALF volume is known to fluctuate significantly during gestation in the pig (Bazer *et al.*, 2012a), and is known to significantly increase between GD20 and 30 (Knight *et al.*, 1977; Goldstein *et al.*, 1980). This is essential in placentation as it induces expansion of the chorioallantoic membrane to increase the surface area, pushing the membrane into direct contact with the underlying uterine

endometrium. Consequently, ALF volume can be used as a proxy for placental size. The volume of ALF then decreases around GD40 (Goldstein *et al.*, 1980), prior to a major increase in fluid volume where it peaks between GD55-70 (Knight *et al.*, 1977; Goldstein *et al.*, 1980). This corresponds to the period of dramatic remodelling of the chorioallantoic membrane (described in general introduction), reflecting a similar role in mid-pregnancy to that observed in early pregnancy. Following this, ALF volume then decreases until term (Knight *et al.*, 1977; Goldstein *et al.*, 1980). The previously detailed temporal profile for ALF volume described is reassuringly reflected in the current study.

In contrast to the fluctuations in ALF volume observed, AMF volume gradually increased with advancing gestation, as previously described in the literature (McCance and Dickerson, 1957; Knight *et al.*, 1977). This gradual increase in AMF volume reflects the important function of AMF described in general introduction.

3.5.3 Foetal Size

As anticipated, the foetuses in the lightest group were lighter and shorter throughout gestation compared to those in the CTMLW foetuses group. PI describes the corpulence, or leanness, of an individual and is commonly used in clinical practice to identify asymmetrical organ growth in instances of growth restriction (Khoury *et al.*, 1990). In instances of asymmetric organ growth in humans, the PI is lower than normally grown individuals. At GD90, PI was decreased suggesting the presence of asymmetric organ growth in the lightest foetuses, discussed further in 3.5.7, and that the foetuses are leaner than the CTMLW foetuses. It has been suggested that neonates that are ‘short and stocky’ have a survival advantage over ‘long and lean’ individuals (Mellor and Matheson, 1979; Leymaster and Jenkins, 1993; Morris *et al.*, 1998), which would suggest that the decrease in PI observed in the lighter foetuses at GD90 in the current study may reflect a postnatal survival disadvantage for the piglet.

3.5.4 Foetal Sex

Throughout gestation, male foetuses were heavier than their female littermates, although at GD30 this was only statistically significant without the addition of a block for gilt. This finding is similar to that of (Jang *et al.*, 2014), who found that male foetuses were heavier than female foetuses at GD43, 58, 73, 108, suggesting that male foetuses grow at a faster rate than their female littermates from early in gestation. Previously it has been suggested that male porcine conceptuses have an increased growth rate compared to female conceptuses at GD10 (Cassar *et al.*, 1994). The results presented in this chapter suggest that CRL is increased in male foetuses compared to female foetuses at GD30 and 90, which has been suggested previously by Poore and Fowden, (2004) and Jang *et al.*, (2014) at GD58 and postnatally respectively. AMF volume was increased at GD30 and 90 in male foetuses compared to female foetuses. As described in the general introduction, AMF functions as a nutrient store for the developing foetus (Bazer *et al.*, 2012a). As males have been demonstrated in this thesis to be heavier throughout gestation than their female littermates, it could be hypothesised that they require an increased supply of nutrients, and therefore have an increased volume of AMF. In humans, it has been suggested that the levels of the angiogenic cytokine angiogenin in AMF in male pregnancies is decreased compared to those in female pregnancies (Poggi *et al.*, 2004). Given the hypothesis that angiogenesis is impaired in placentas supplying male foetuses compared to female foetuses, discussed in chapters 6-8, this is an interesting finding.

ALF volume can be used as a proxy for placental size. In this study, despite males being consistently heavier than female foetuses, ALF volume was not associated with foetal sex. This provides potential evidence for sexual dimorphism in placental function, which will be investigated throughout this thesis.

3.5.5 Influence of Sex of Foetuses in the Litter

As described in 3.1.3.2, the sex ratio of a litter can influence reproductive behaviour and outcome, making it an area of considerable commercial interest. In this study, there was a positive relationship between percentage of males in the litter and AMF volume at GD30, and foetal weight at GD90. This relationship between percentage of males in the litter and AMF volume at GD30 presumably reflects that male foetuses had an increased AMF volume at this GD. Similarly, at GD90 this difference presumably reflects that male foetuses are significantly heavier than female foetuses. To assess the influence of male and female foetuses on foetal development, investigating the relationship between sex of adjacent foetuses and the variables of interest would provide more information. As described in 3.1.3.3, conflicting reports describing the relationship between the sex of a foetus's neighbour and foetal development in the pig exist. It was previously suggested by Jang *et al.*, (2014) that female foetuses with two male neighbours were longer than female foetuses with no male neighbours at GD73. This finding was observed in the current study at GD60, with female neighbours with one or two male neighbours having an increased CRL compared to female foetuses with two female neighbours, and it also had an effect at GD30. Unlike the findings of Jang *et al.*, (2014), the CRL of male foetuses was also influence by neighbour sex in a temporal manner, with an association between CRL and neighbour sex observed at GD30 and 45 but not GD60 or 90.

In contrast to the previous investigations, the results of this study have demonstrated that the weight of male foetuses is influenced by neighbour sex, with male foetuses with no or one male neighbours being heavier than those with two female neighbours. Considering the previous literature investigating this area (3.1.3.3), it could be suggested that signalling of hormones, such as testosterone and INSL3, is responsible for this difference. Current investigations in the Ashworth laboratory aim to investigate the foetal plasma levels of hormones of interest in the foetuses utilised in this study.

A previous study by Tarraf and Knight, (1995) indicated that female foetuses with two male neighbours are heavier than those with no male neighbours

GD40, 60, 80 and 100. This was not observed in the current study, where a temporal relationship was observed between neighbour sex and the weight of female foetuses, with female foetuses with two male neighbours being heavier at GD30, compared to GD60 when female foetuses with two female neighbours were heavier than those with no or one female neighbour. An intermediate phenotype was suggested by Jang *et al.*, (2014) at GD43 whereby female foetuses with one male neighbour were lighter than those with no or two male neighbours. The sex of the neighbour was not found to be associated with foetal weight in male or female foetuses at GD90, which would support the findings of Rohde Parfet *et al.*, (1990b) who suggested that the number of neighbours of the same sex had no influence on birth weight. Further, the finding in this study that the sex of the neighbours was not associated with AMF volume, and had little influence on ALF volume, support the findings of Tarraf and Knight, (1995).

3.5.6 Uterine Position

Conflicting reports exist in the literature regarding the influence of uterine position on foetal weight (3.1.2). At GD30, a trend towards foetuses positioned at the cervical end of the uterine horn being heavier than those located in the middle or at the ovarian end of the uterine horn was observed. This relationship achieved statistical significance at GD45, where foetuses located at the cervical end were the heaviest, and foetuses located at the ovarian end of the uterine horn were the lightest. It has previously been suggested that uterine position does not influence foetal weight in the pig until after GD43 (Knight *et al.*, 1977; Wise *et al.*, 1997; Finch *et al.*, 2002; Jang *et al.*, 2014), which is supported by the current results. In this chapter, foetuses located at the ovarian end of the uterine horn were the heaviest at GD60 and 90. Similar findings were observed by Rohde Parfet *et al.*, (1990a) at term, Wise *et al.*, (1997) at GD70 and 104, and Jang *et al.*, (2014) at GD58, 101 and 108. However, the results presented by Finch *et al.*, (2002) do not support these findings.

It has been shown on occasions where less than five foetuses are present in the uterine horn, uterine position is not associated with foetal weight (Perry and Rowell, 1969). In contrast, on occasions where there are more than five foetuses in the uterine horn, foetuses located at cervical end were lighter than those located at the ovarian end of the uterine horn (Perry and Rowell, 1969). As described in 3.5.1, it was demonstrated that number of foetuses present in the uterine horn did influence foetal weight therefore, this discrepancy in findings in the literature may be due to this effect. The mechanisms behind the increased size observed at the ovarian end of the uterine horn in late gestation are poorly understood. It could be hypothesised that the vasculature of the uterus influences this, as is the case in mice (vom Saal and Dhar, 1992). However, the porcine uterine vasculature has a highly variable structure (Perry and Rowell, 1969; Père and Etienne, 2000) which has previously been suggested to not be associated to foetal weight (Perry and Rowell, 1969). Alternatively, considering the structure of the uterus illustrated in the general introduction, the foetuses located at the ovarian ends of the uterine horn may have increased space available for growth.

At GD90, foetuses located at the cervical end of the uterine horn were shown to have a decreased ALF volume compared to foetuses located in the middle and at the ovarian end of the uterine horn. As detailed previously, ALF volume can be used as a proxy for placental size. This decrease would indicate that placentas at the cervical end of the uterine horn are smaller and this difference in ALF volume, reassuringly, is partially reflected in the foetal weight data.

3.5.7 Differences in Organ Weight

In this chapter, it has been demonstrated that brain weight was not associated with foetal weight at GD45, 60 or 90. As described previously, an increased brain: liver ratio indicates that brain sparing has occurred, which has been illustrated in newborn IUGR piglets (Bauer *et al.*, 1998, 2003). Whilst the maintenance of brain weight at GD45 may suggest that brain sparing has occurred at this stage of gestation, liver weight was not decreased, resulting

in an increase in the brain: liver ratio, in the lightest foetuses compared to the CTMLW foetuses until GD60 of pregnancy. This is an interesting finding as it suggests a slight delay in the development of the asymmetric organ growth phenotype associated with growth restriction in the pig, which may be explained by the asynchronous growth of these organs, with the porcine foetal liver growing rapidly in early gestation (Dyce *et al.*, 1996; Bazer *et al.*, 2001).

Despite limited investigations into gonadal development in the pig, a recent study by Pontelo *et al.*, (2018) investigated the relationship between gonadal weight and anatomical measurements in the pig. In this chapter, it was demonstrated that testes were heavier than ovaries at GD60 and 90, which supports the results of Pontelo *et al.*, (2018) who demonstrated that testes were heavier than ovaries at GD50, 80 and 106. In both male and female foetuses, gonad weight was positively correlated to foetal weight, and gonadal weight as a percentage of body weight was negatively correlated to foetal weight at GD50, 80 and 106 (Pontelo *et al.*, 2018). Whilst this finding is interesting, only 'normal-sized' foetuses were selected for investigation in this study, with foetuses that were noticeably smaller than the rest of the litter were excluded from the analysis. Gonads as a percentage of foetal weight were demonstrated by Pontelo *et al.*, (2018), to represent a larger proportion of foetal weight at GD50, which was decreased at GD80 and 106, reinforcing the previous findings (Colenbrander *et al.*, 1979; van Vorstenbosch *et al.*, 1982). In this chapter, no association between foetal weight and gonadal weight was observed at GD60 and 90 however, gonads as a percentage of foetal weight was higher in the lightest foetuses compared to the CTMLW foetuses at GD90. This is an interesting finding and it is hoped that the current investigations in the Ashworth laboratory into gonadal development in IUGR piglets should improve the understanding of the mechanisms behind this phenotype.

3.6 Conclusion

This chapter has described the origin and collection of the biological material investigated in subsequent chapters. The data presented in this chapter have

highlighted the association between GD, foetal size and sex, and several parameters of interest, which has provided a rationale to investigate the association between both foetal size and sex, and the development and function of the feto-maternal interface.

4 Investigating the Association between Integrin Expression, and Foetal Size and Sex at the Feto-Maternal Interface

4.1 Introduction

4.1.1 Integrin Receptors

Integrins are glycoprotein transmembrane receptors which exist as heterodimers composed of non-covalently linked α and β subunits (Giancotti and Ruoslahti, 1999). To date, 18 α and 8 β integrin subunits (ITG) have been characterised, which have been reported to form 24 different heterodimers (Humphries, 2006) (Figure 4.1). It has been demonstrated that the ITGαV combines with the greatest number of β subunits, forming the following heterodimers: αVβ1, αVβ3, αVβ5, αVβ6, and αVβ8 (Humphries, 2006).

Integrins have been demonstrated to play a central role in cell adhesion and the formation of focal adhesions (FA), cell migration, proliferation and the development of the actin cytoskeleton (Irving and Lala, 1995; Schwartz and Assoian, 2001; Gallant *et al.*, 2005; Delon and Brown, 2007). Previous studies have demonstrated that specific integrin heterodimers can bind to peptides containing an Arg-Gly-Asp (RGD) region, with the RGD region binding at the interface between the α and β integrin subunits (Humphries, 2006).

4.1.2 Ligands for the Integrin Receptors

Several ligands exist which have been demonstrated to bind to integrin receptors, which are commonly extracellular matrix (ECM) proteins or have a role in cell adhesion. Examples of these ligands include, but are not limited to, thrombospondin, laminin, collagen, fibrinogen, fibrillin, vitronectin, secreted phosphoprotein 1 (SPP1, also known as osteopontin (OPN)) and fibronectin (FN) (Humphries, 2006). In this thesis, SPP1 and FN are of particular interest due to their roles in reproduction, outlined in 4.1.3.

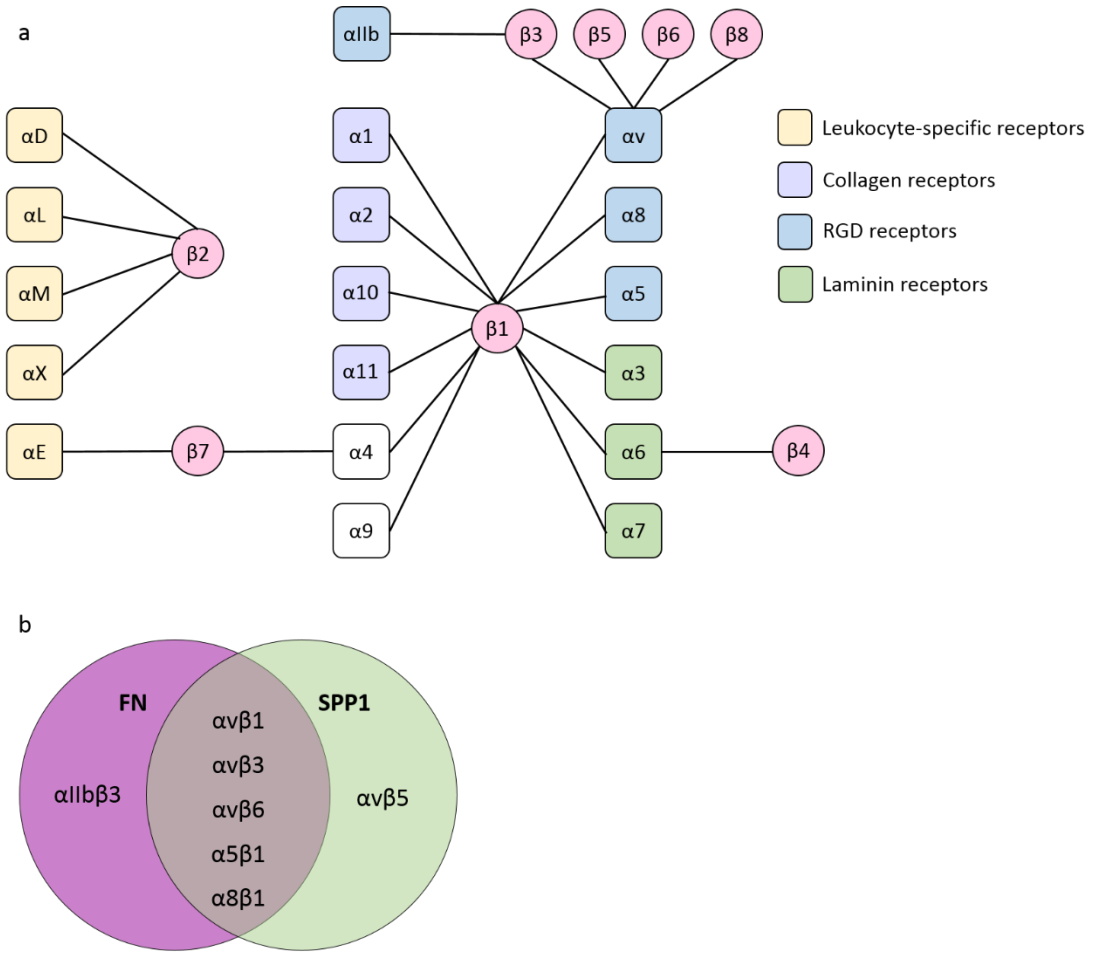

Figure 4.1: Integrin α and β Subunits Combine to Form Heterodimers.

Integrin receptors are heterodimers composed of an α and β subunit. A: This diagram illustrates the classification of integrin heterodimers. The α subunits indicated in yellow are leukocyte specific, purple form collagen receptors, blue bind to the Arg-Gly-Asp (RGD) sequence on their ligands such as secreted phosphoprotein 1 (SPP1) and fibronectin (FN) and green bind to laminin receptors. The β subunits are indicated in pink. B: Venn diagram detailing the potential RGD-binding integrin heterodimers that FN and SPP1 can bind to. Notably, the majority of the receptors detailed bind to both ligands of interest, and 4 of the 7 heterodimers contain the αV subunit. Adapted from (Srichai and Zent, 2010). Information from Humphries, (2006) and Srichai and Zent, (2010).

SPP1 is a member of the SIBLING (small integrin-binding ligand, N-linked glycoproteins) family of glycoproteins (Bellahcène *et al.*, 2008; Staines *et al.*, 2012). This family of glycoproteins are well characterised in bone and have been demonstrated to regulate cell adhesion processes by binding to integrins (Fisher *et al.*, 2001). The glycoprotein FN has a dimeric structure composed of two covalently linked subunits, each approximately 250kDA in size (Bachman *et al.*, 2015). FN has been demonstrated to bind to a number of integrin receptors (Humphries, 2006).

Both SPP1 and FN contain an RGD binding site (Bellahcène *et al.*, 2008; Staines *et al.*, 2012; Bachman *et al.*, 2015) which, as detailed previously, allows binding to specific integrin heterodimers. The binding of these glycoproteins is important for regulation of the structure of the ECM (Giancotti and Ruoslahti, 1999; Singh *et al.*, 2010). Post-translational modifications, including phosphorylation, proteolytic cleavage and glycosylation of SPP1 (Zhang *et al.*, 1992; Bazer *et al.*, 2012b) and FN (Paul and Hynes, 1984; Ruoslahti, 1988) are known to be essential in regulating their biological activity.

4.1.3 Role of Integrins and their Ligands in the Establishment of Pregnancy

The process of implantation requires significant remodelling of the ECM at the interface between the conceptus and the mother (Carson *et al.*, 2000; White *et al.*, 2006). As described previously, large variation in placentation type exists between species. Integrin signalling is implicated in attachment and early embryo development in several species including mouse (Sutherland *et al.*, 1993; Fassler and Meyer, 1995; Schultz and Armant, 1995; Stephens *et al.*, 1995; Schultz *et al.*, 1997; Hodivala-Dilke *et al.*, 1999; Illera *et al.*, 2000), humans (Feinberg *et al.*, 1991; Lessey *et al.*, 1994; Ruck *et al.*, 1994; Campbell *et al.*, 1995; Yoshimura *et al.*, 1995; Shiokawa *et al.*, 1996, 1999; Bloor *et al.*, 2002; Kao *et al.*, 2002; Zheng *et al.*, 2006; Germeyer *et al.*, 2014), sheep (Johnson *et al.*, 1999a, 2001a; Burghardt *et al.*, 2009), cow (Kimmins and MacLaren, 1999), goat (Guillomot, 1999), pig (Denker, 1993; Aplin *et al.*, 1994;

Bowen *et al.*, 1996; Yelich *et al.*, 1997; Burghardt *et al.*, 2002; White *et al.*, 2005; Rashev *et al.*, 2005; Lin *et al.*, 2007; Erikson *et al.*, 2009a; Vélez *et al.*, 2015, 2017; Frank *et al.*, 2017), rhesus monkey (Qin *et al.*, 2003), baboon (Fazleabas *et al.*, 1997) and rabbit (Illera *et al.*, 2003). More specifically, heterodimers containing ITGαV have been heavily implicated in conceptus attachment (Aplin, 1997).

In species which have non-invasive placentation, including cattle, pigs and sheep, it has been demonstrated that ITGαV is expressed on the apical surface of the endometrial luminal epithelium (LE) (Bowen *et al.*, 1996; Johnson *et al.*, 1999a; Kimmins and MacLaren, 1999). In addition, it has been demonstrated in humans that the integrin receptor αVβ3 is important in defining the window of implantation (Lessey *et al.*, 1994, 1996). Investigations in mice demonstrated that αVβ3 is expressed by the trophoblast from gestational day (GD) 4 (Sutherland *et al.*, 1993) and the α5β1 receptor translocates to the apical membrane surface at GD7 (Schultz *et al.*, 1997); implicating integrin receptors and their ligands in implantation and subsequent trophoblast invasion. Investigations into the role of ITGβ1 have suggested its critical role in blastocyst development and differentiation after embryo attachment by binding to FN (Yoshimura *et al.*, 1995; Shiokawa *et al.*, 1996, 1999).

To further investigate the potential role of integrins in the establishment of pregnancy in the mouse, a number of integrin knockout lines have been generated (reviewed by Hynes, (1996) and Srichai and Zent, (2010)). Hodivala-Dilke *et al.*, (1999) generated a line of β3 deficient mice which were viable and fertile however, a decrease in overall litter size, and pre- and post-natal offspring survival was observed. A number of defects were observed in placental development including haemorrhage in the labyrinth, increased necrosis and increased thickness of cell layers in the labyrinth. In the mouse, knock out of ITGαV resulted in peri-implantation lethality (Hynes, 1996). This research was taken further in rabbits and mice, with uterine injection with antibodies against ITGαV and ITGβ3 resulting in a decreased number of implantation sites (Illera *et al.*, 2000, 2003); highlighting the importance of

signalling through the αvβ3 receptor during implantation. When ITGβ1 was knocked out, the homozygous mutants reached the blastocyst stage, despite having defective inner cell mass morphogenesis, but they did not implant (Fassler and Meyer, 1995; Stephens *et al.*, 1995). Knockout mice for ITGα2 and ITGβ5 were viable and fertile (Srichai and Zent, 2010) whereas, the ITGβ8 knockout was embryonic lethal with defective vascular systems and impaired placental vascularisation observed (Zhu *et al.*, 2002).

4.1.3.1 The Role of Integrins in the Establishment and Maintenance of Pregnancy in the Pig

During the period of implantation in the pig, αVβ3 and αVβ6 are expressed on the apical surface of the uterine LE and the trophectoderm respectively (White *et al.*, 2005; Erikson *et al.*, 2009a). ITGαV has been shown to play a central role in the formation of FA-mediated attachment between the trophectoderm and uterine LE in the pig, with expression found in conjunction with talin (TLN) at the apical surface of both tissues (Johnson *et al.*, 2001a; Erikson *et al.*, 2009a).

Frank *et al.*, (2017) demonstrated that knockdown of *ITGαV* expression in porcine trophectoderm cells decreased cell attachment in response to SPP1. An ovariectomised (OX) pig model was utilised to investigate the influence of sex steroids on ITG expression. Administration of oestradiol (E2) and progesterone (P4) was not found to influence the endometrial expression of *ITGαV*, *ITGβ3* and *ITGβ6*. These data reinforce the results of Bowen *et al.*, (1996), who also found that sex steroids did not influence the uterine expression of these subunits in pigs. Johnson *et al.*, (2001) had similar findings in the sheep. Porcine trophoblast and uterine LE cells have been shown to express *ITGαV*, *ITGα2*, *ITGα5*, *ITGβ1*, *ITGβ3,* and *ITGβ6* (Bowen *et al.*, 1996; Erikson *et al.*, 2009a; Frank *et al.*, 2017). Frank *et al.*, (2017) demonstrated that porcine trophoblast cells utilise integrin heterodimers containing the ITGαV to bind to SPP1 during implantation. At GD25, substantial aggregates of the ITGαV and ITGβ3, and SPP1 were observed at the interface between

the uterine LE and trophoblast cells, reinforcing the previous findings of Erikson *et al.*, (2009a). It has been suggested that mechanical forces are generated at the feto-maternal interface between the attaching elongating filamentous conceptuses and the uterine LE which leads to the formation of FAs, indicated by the observed aggregates. These aggregates are not observed by mid-gestation (GD50), and this loss of FAs is believed to occur due to the extensive folding of the feto-maternal interface during this period (Vallet and Freking, 2007).

In situ hybridisation illustrated that *ITGαV*, *ITGβ3* and *ITGβ6* are expressed in the LE of both cyclic and pregnant pigs (Frank *et al.*, 2017). Quantification of these results did not find any difference in their expression between cyclic and pregnant pigs, or between the GD investigated (13, 15, 20, 25, 30, 45 and 60), suggesting that these subunits are not upregulated on an mRNA level during attachment. Similar results were observed by Bowen *et al.*, (1996), who demonstrated that the protein expression of integrin subunits (α1, α3, α4, α5, αV, β1 and β3) was not different between cyclic and pregnant animals at days 0 to 15. Bowen *et al.*, (1996) also demonstrated that whilst the protein levels of ITGα4, ITGα5 and ITGβ1 increased between day 0 and 15, ITGα1 and ITGα3 had low and ITGαV and ITGβ3 had high LE expression at GD0-15. This study demonstrated that ITGα4, ITGα5, ITGαV, ITGβ1 and ITGβ3 subunits are all expressed at the interface during the attachment process (GD12-15), suggesting that they may have a role in regulating implantation in the pig. Yelich *et al.*, (1997) demonstrated that the *ITGβ1* is expressed by porcine conceptuses at GD10-12 (range in developmental stage: 2mm-filamentous). Whilst no relationship between foetal size and mRNA expression was observed, expression peaked in 7-8mm conceptuses, before decreasing during conceptus elongation.

Based on these expression data, and the previously published literature (Humphries, 2006), Frank *et al.*, (2017) suggested that α5β1, αVβ3, αVβ6, and αVβ1 receptors may be able to bind to SPP1 on trophoblast cells. Similarly, they indicated that FN may bind to one of three receptors α5β1, αVβ3, or αIIβ3, and Collagen, type I, alpha 1 (COL1A1) would only bind to α2β1. An intricate

siRNA knockdown experiment highlighted the role of the ITGαV in implantation, with decreased adherence to FN and SPP1 and fewer aggregates of porcine trophoblasts following knockdown of ITGαV.

4.1.3.2 Secreted Phosphoprotein 1 in Reproduction

4.1.3.2.1 Relationship between SPP1 and Porcine Reproductive Outcome

The gene for SPP1 is found on chromosome 8 in the pig, in a region which has been shown to be under a quantitative trait loci (QTL) peak for prenatal survival and litter size (King *et al.*, 2003; Hernández *et al.*, 2014). Due to the location under this QTL, SPP1 has been compared between highly prolific breeds, for example Meishan (MS), and commercial European breeds which have a lower prolificacy, for example Large White. It has been demonstrated that highly prolific pigs have decreased ovarian expression of SPP1 (Fernandez-Rodriguez *et al.*, 2011) than breeds with lower prolificacy. The relationship between SPP1 and reproductive potential has also been investigated by Korwin-Kossakowska *et al.*, (2013), who demonstrated that a number of polymorphisms in SPP1 exist in the pig, and that the uterine and oviductal expression levels of these variants are related to a number of characteristics including litter weight, number of active nipples, body weight at mating and cervical length. Han *et al.*, (2012) also demonstrated a relationship between polymorphisms in SPP1 and carcass traits, including growth rate, in a population of Landrace X Jeju pigs. Increased SPP1 protein and mRNA were observed in endometrial samples, but not placental samples, from MS compared to hyperprolific Large White (hLW) gilts (Hernández *et al.*, 2013). Overall, the findings of these studies have demonstrated the importance to the pig industry of improving the understanding of the mechanisms behind the relationship of SPP1 and these highly desirable traits.

4.1.3.2.2 Role of SPP1 in the Establishment and Maintenance of Pregnancy

In response to conceptus secreted E2 in the peri-implantation period, the uterine LE has been shown to significantly increase the secretion of SPP1in several species including sheep (Johnson *et al.*, 1999a, b; Dunlap *et al.*, 2008), humans (Mirkin *et al.*, 2005), rabbits (Apparao *et al.*, 2003), rat (Girotti and Zingg, 2003), and mice (White *et al.*, 2006; Chaen *et al.*, 2012; Qi *et al.*, 2014).

In the mouse, SPP1 is regulated by E2 alone (White *et al.*, 2006; Chaen *et al.*, 2012; Qi *et al.*, 2014). Qi *et al.*, (2014) demonstrated an increase in *SPP1* expression in the mouse uterus at GD4, followed by increased expression at the implantation sites specifically on GD5 and 8, suggesting a potential role of SPP1 in implantation. Similarly, White *et al.*, (2006) found that SPP1 is expressed along the apical surface of the LE and in macrophages in the uterine stroma, which may illustrate that SPP1 in these cells contributes to the remodelling of the uterine stroma during trophoblast invasion. Qi *et al.*, (2014) knocked down SPP1 *in vitro*, which decreased blastocyst adhesion, highlighting a potential role of SPP1 in implantation in the mouse. Both *in vitro* and *in vivo*, it has been demonstrated in the mouse that decidualisation induces the expression of SPP1, which is driven by P4 (Qi *et al.*, 2014). Kang *et al.*, (2014) utilised *in vitro* models of implantation using Ishikawa cells and demonstrated that αVβ3 binds to SPP1, allowing the attachment of mouse blastocysts to the Ishikawa cells in culture.

A decidualisation-like response was observed in the ovine uterus, with SPP1 expression increasing in the stratum compactum stroma in both caruncular and non-caruncular regions (Johnson *et al.*, 2003a). P4 supplementation to OX ewes upregulated the expression of *SPP1* in the glandular epithelium (GE) and uterine stroma, suggesting that P4 regulates SPP1 expression in the ovine uterus (Dunlap *et al.*, 2008). SPP1 has been heavily implicated in regulating conceptus attachment in the sheep, with supplementation of SPP1 to ovine trophectoderm cells inducing attachment *in vitro* (Johnson *et al.*, 2001a; Dunlap *et al.*, 2008). Johnson *et al.*, (2001) demonstrated that SPP1 leads to the accumulation of TLN and α-actinin on the apical surface of cells in contact

with beads coated with SPP1 in response to RGD binding, suggesting the formation of FAs. SPP1 is expressed along the apical surface of the uterine LE, GE and on trophectoderm cells for the duration of gestation (Johnson *et al.*, 2003b; Burghardt *et al.*, 2009). *SPP1* is expressed in immune cells in the stratum compactum of the endometrium in both cyclic and pregnant ewes (Johnson *et al.*, 1999a, b) and its GE expression in pregnant ewes during preimplantation suggests that SPP1 could mediate adhesion between the LE and trophectoderm during implantation.

During implantation in the pig, αVβ3 and αVβ6 are expressed on the apical surface of the uterine LE and the trophectoderm respectively (White *et al.*, 2005; Erikson *et al.*, 2009a). It has been demonstrated in the pig that SPP1 is highly expressed in the areas of the uterine LE adjacent to the attaching conceptus and that this expression is induced by conceptus secreted E2 (White *et al.*, 2005; Steinhauser *et al.*, 2017). The LE expression extends to the whole uterine LE by GD20 where it remains until at least GD90 (latest stage of investigation) (Garlow *et al.*, 2002; Steinhauser *et al.*, 2017). SPP1 is not expressed in the LE regions or GE cells found adjacent to the areolae throughout gestation (investigated until GD85), but is expressed in GE from GD35-85 (Steinhauser *et al.*, 2017). Whilst the GE cells in contact with the areolae did not express SPP1, they do express the P4 receptor, suggesting that P4 does not stimulate histotroph secretion from cells that express the P4 receptor (Steinhauser *et al.*, 2017).

White *et al.*, (2005) illustrated that oestrogen administration modestly upregulates SPP1 mRNA and protein expression in a uniform manner along the entire uterine LE both at day 15 and 90 of pseudopregnancy. In the pseudopregnant group at day 90, SPP1 was expressed by the GE to a similar degree to that observed in the pregnant group. This may indicate that *corpora luteal* P4 production, which is known to influence the secretion of proteins by the GE in the pig (Knight *et al.*, 1973, 1974a, b; Roberts and Bazer, 1988), is responsible for regulating the production of SPP1 by the endometrium following implantation. In contrast, Bailey *et al.*, (2010) demonstrated that exogenous administration of P4 to OX gilts did not induce *SPP1* expression,

and SPP1 protein was not present in the GE, indicating that P4 alone does not induce SPP1 production in gilts. Similarly, Frank *et al.*, (2017) demonstrated with the use of OX gilts, that administration of E2 and P4 did not influence endometrial expression of *ITGαV*, *ITGβ3* and *ITGβ6*.

In summary, during the preimplantation period conceptus secreted E2 induces SPP1 expression by the uterine LE (White *et al.*, 2005). SPP1 then acts as a bridge during attachment, binding to the αVβ3 receptor on the apical surface of the uterine LE and the αVβ6 receptor on the trophectoderm (White *et al.*, 2005; Erikson *et al.*, 2009a) (Figure 4.2), where it is expressed for the remainder of gestation. SPP1 increases the

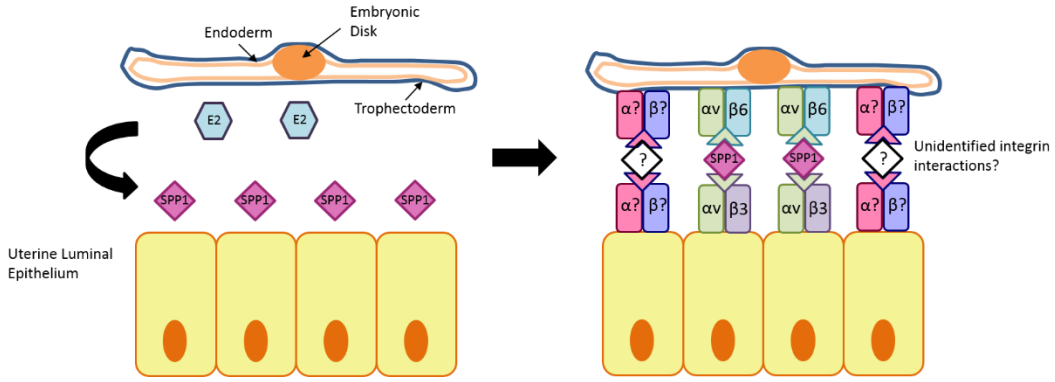

Figure 4.2: Proposed Role of SPP1 and Integrin Receptors in Porcine Conceptus Attachment.

Oestradiol (E2) secreted by the elongating conceptus induces the expression of secreted phosphoprotein 1 (SPP1) by the uterine luminal epithelium (LE). SPP1 then acts as a bridge during attachment, binding to the αVβ3 receptor on the apical surface of the uterine LE and the αVβ6 receptor on the trophectoderm.

prevalence of ECM proteins, leading to the formation of FAs at the feto-maternal interface, which regulate adhesion and signalling between the conceptus and the uterus (Johnson *et al.*, 2001a; Erikson *et al.*, 2009a). Uterine GE expression of SPP1 is induced between GD30 and 40 (Frank *et al.*, 2017; Steinhauser *et al.*, 2017), which is believed to occur in response to P4. However, whilst there is evidence to suggest both P4 and oestrogens play a central role in the production of SPP1, there is also evidence from studies

described above which administered sex steroids to OX pigs suggesting that SPP1 production in the pig may be influenced by the interaction between multiple pathways and factors.

A number of *in vitro* experiments have been performed to attempt to improve the understanding of the role of SPP1 in pregnancy. Supplementation with SPP1 (Hao *et al.*, 2008) or the use of hydrogels supplemented with SPP1 or conjugated to the RGD peptide (Laughlin *et al.*, 2017) improves *in vitro* porcine conceptus development. Similar results were noted in the mouse, with supplementation of SPP1 enabling blastocyst hatching and adhesion (Qi *et al.*, 2014). Further, SPP1 can promote porcine trophectoderm cell migration, but not proliferation, and the attachment of porcine trophectoderm cells to uterine LE cells *in vitro* (Erikson *et al.*, 2009a). This binding ability is impaired when RGD binding is blocked, suggesting that SPP1 binds to RGD integrin receptors at the feto-maternal interface. Immunofluorescence revealed that TLN and ITGαV are expressed in the FAs, and SPP1, ITGαV, ITGβ3 and α-actinin were expressed at the interface, specifically at the sites of conceptus attachment. Importantly, the authors clearly demonstrated in this study that the trophectoderm expresses αVβ6, the uterine LE expresses αVβ3, and that SPP1 binds to these receptors during the attachment process (Figure 4.2).

Weintraub *et al.*, (2004) utilised a biallelic and single allelic mouse knock-out of SPP1 to investigate the influence on embryo number and size at 10.5, 15.5 and 19.5 days post-coitum (dpc). Litter size was not altered by the mutation however, the $SPP1^{-/-}$ embryos were smaller than wildtype embryos at all GD investigated, highlighting a potential role of SPP1 in regulating foetal growth. Due to the involvement of SPP1 in implantation in mice (White *et al.*, 2006), the decreased pregnancy rate observed in both the $SPP1^{-/-}$ and $SPP1^{+/-}$ groups compared to wildtype mice is not surprising. As pregnancy was achieved, and the mice were viable, this may indicate that SPP1 is not essential in mice for the establishment and maintenance of pregnancy.

4.1.3.3 Role of FN in the Establishment and Maintenance of Pregnancy

FN has been under considerable investigation in several species to determine its role in the establishment of pregnancy. Expression of FN is upregulated in the uterus of GD6 rats, with localisation of its expression to the mesometrium of the subepithelial stroma (Rider *et al.*, 1992). FN has been implicated in trophoblast invasion in humans (Feinberg *et al.*, 1991; Zheng *et al.*, 2006), mice (Schultz and Armant, 1995) and rhesus monkeys (Qin *et al.*, 2003), by binding to ITGα5 (Zheng *et al.*, 2006), ITGβ1 and ITGβ3 (Sutherland *et al.*, 1993). In the sheep, it has been suggested that FN improves trophoblast adhesion, with the effect augmented further following the addition of chemokine ligand (CXCL) 9 and 10 (Imakawa *et al.*, 2006), although the mechanisms behind this require further investigation. Mouse trophoblast cells cannot bind to FN by the RGD site *in vitro* until GD7 (Schultz and Armant, 1995; Yelian *et al.*, 1995), which suggests that binding of FN through integrin receptors may play a role in regulating implantation in the mouse.

George *et al.*, (1993) utilised a knock out model for FN to investigate its role in placentation and embryo development. Heterozygote mice were viable and, despite having a 50% decrease in plasma FN, appeared phenotypically normal. In contrast, the homozygous knockout embryos implanted successfully and began gastrulation. However, defects in the mesoderm led to defective development of the neural tube and vascular system, ultimately leading to embryonic death.

4.1.3.3.1 Potential Role of FN in Porcine Pregnancy

FN has previously been implicated in the establishment of pregnancy in the pig (Bowen *et al.*, 1996; Rashev *et al.*, 2005; Vélez *et al.*, 2015, 2017). FN and two of the potential receptors for FN, αVβ3 and α5β1, have been shown to be expressed in both conceptus and endometrial tissues during implantation and early pregnancy (Rashev *et al.*, 2005; Erikson *et al.*, 2009a; Vélez *et al.*, 2015, 2017). Rashev *et al.*, (2005) demonstrated that FN and α5β1 are localised to the trophectoderm and the surface epithelium of the endometrium, with

elevated expression observed in areas of contact between the embryo and the endometrium. The abundance of FN staining at the apical surface of the trophectoderm increases between GD20 and 35, highlighting a potential role in placental development. In the endometrium, FN was demonstrated to be intensely expressed at the apical and basal regions of the surface and GE (Rashev *et al.*, 2005). In the endometrial stroma, FN had diffuse expression at GD20, before forming compact fibrils at GD30 in areas in close proximity to the surface epithelium. At the early GD investigated (GD15 and 20), α5β1 staining of the extra-embryonic endoderm and trophectoderm were observed. With advancing GD, an increase in the intensity of α5β1 staining was observed, with intense staining observed at the apical and basal regions of the trophectoderm and uterine surface epithelium.

Vélez *et al.*, (2015, 2017) found intense expression of both αVβ3 and FN at the placental interface from GD17 to 60, after which (GD70, 80 and 114) the staining intensity significantly decreased. Maternal P4 levels followed a similar profile until GD70 where P4 level peaked and staining for αVβ3 and FN decreased. The authors proposed that P4 may be able to play a role in the regulation of αVβ3 and FN until GD70, after which alternative adhesion molecules may have a more significant role at the feto-maternal interface. Bowen *et al.*, (1996) demonstrated that ITGα4, ITGα5, ITGαV, ITGβ1 and ITGβ3 and FN were all expressed at the interface during the attachment process (GD12-15), suggesting that FN-Integrin signalling may have a role in regulating implantation in the pig.

4.1.4 Hypotheses

During the process of implantation, significant remodelling of the ECM at the interface between the conceptus and the mother occurs. It is hypothesised that intrauterine growth restriction (IUGR) occurs due to inadequate conceptus attachment. Due to the previously detailed literature implicating integrin receptors and their ligands in both the establishment and maintenance of pregnancy, it is hypothesised that their expression will be decreased in placental and endometrial samples associated with the lightest conceptuses or foetuses compared to their normal-sized litter mates throughout gestation. In addition, it is hypothesised that decreased expression of the integrin receptors and their ligands will be observed in placental and endometrial samples supplying male foetuses compared to their female littermates.

4.2 Aims

i. To investigate gestational changes in placental and endometrial mRNA expression of the integrin subunits *ITGα2*, *ITGαV*, *ITGβ1*, *ITGβ3*, *ITGβ5*, *ITGβ6* and *ITGβ8* at GD18 (endometrium only), 30, 45, 60 and 90.

ii. To investigate the association between conceptus or foetal size and the mRNA expression of the above integrin subunits at the feto-maternal interface at GD18, 30, 45, 60 and 90.

iii. To investigate the association between foetal sex and the mRNA expression of the above integrin subunits at the feto-maternal interface at GD30, 45, 60 and 90.

iv. To investigate gestational changes in uterine gland SPP1 protein expression.

v. To investigate the association between foetal size and sex and uterine gland SPP1 protein expression at GD30, 45, 60 and 90.

4.3 Materials and Methods

4.3.1 Assessment of *SPP1*, *FN* and Integrin Subunit mRNA Expression by qPCR

The RNA extracted from placental (GD30, 45, 60 and 90; n=6, 6, 6 and 8 litters respectively), and endometrial (GD18, 30, 45, 60 and 90; n=5, 5, 6, 6 and 6 litters respectively) samples described in 2.2.3 were utilised. Complementary DNA was synthesised (as described in 2.2.7) and diluted 1:25 with nuclease free water. The candidates of interest were *SPP1*, *FN*, and the integrin subunits (ITG) *ITGα2*, *ITGαV*, *ITGβ1*, *ITGβ3*, *ITGβ5*, *ITGβ6* and *ITGβ8*. The primer sequences for these candidates are detailed in Table 4.1. All qPCRs were performed for 40 cycles with an annealing temperature of 60^{o}C (2.2.8.2).

The GeNorm experiment (2.2.8.4) identified that multiple genes were stable in both tissues and that the optimal number of reference genes for each tissue based on use of the most stable reference genes was two. Placental mRNA expression was normalised using the reference genes *TBP1* (TATA box binding protein) and *HPRT1* (Hypoxanthine phosphoribosyltransferase 1). Endometrial *SPP1* and *FN* expression were normalised using the reference genes *TBP1* and *YWHAZ* (Tyrosine 3-monooxygenase/tryptophan 5-monooxygenase activation protein, zeta polypeptide), and endometrial ITG expression was normalised using the reference genes *TBP1* and *TOP2B* (Topoisomerase II beta). These reference genes were run for all samples; the primer sequences for these are detailed in Table 2.4. All data were scaled to the minimum sample and imported into qBase+ (Biogazelle) and data for each candidate gene were normalised to the reference gene expression.

Gene Symbol	Gene Name	Accession Number	Primer Sequence (5'→ 3')		Amplicon Size	Reference
ITGα2	Integrin Subunit Alpha 2	NM001244272.2	Fwd	CATGCCAGATCCCTTCATCT	153	Frank *et al.*, 2017
			Rev	CGCTTAAGGCTTGGAAACTG		
ITGαV	Integrin Subunit Alpha V	NM001083932.1	Fwd	CGAGGACTTTGGGAATGGTTT	111	King *et al.*, 2011
			Rev	CAGTGGCAGCGACAGAAAATC		
ITGβ1	Integrin Subunit Beta 1	NM213968.1	Fwd	CTGCGAGTGTGATAATTTCAACTGT	112	King *et al.*, 2011
			Rev	GAACAGTCACAGGCGCTGC		
ITGβ3	Integrin Subunit Beta 3	NM214002.1	Fwd	TGATGCCATCATGCAGGCTAC	123	King *et al.*, 2011
			Rev	CTGCCAGCCTTCCATCCA		
ITGβ5	Integrin Subunit Beta 5	NM001246669.1	Fwd	GAACGAGGCCAACGAGTACAC	101	King *et al.*, 2011
			Rev	CAAAGATGAGGTTGATGTTGTT		
ITGβ6	Integrin Subunit Beta 6	NM001097423.1	Fwd	TCCAGCTGATCATCTCAGCTTATG	147	King *et al.*, 2011
			Rev	TCATGTGAGAGCATTTCTTTTGGT		
ITGβ8	Integrin Subunit Beta 8	NM001097424.1	Fwd	AATACTGTGAAAAGGATGACTTTTCTTGT	109	King *et al.*, 2011
			Rev	CCTTCCCAGCCCCTGAAG		
SPP1	Secreted Phosphoprotein 1	X16575	Fwd	TTGGACAGCCAAGAGAAGGACAGT	121	Hernandez *et al.*, 2013
			Rev	GCTCATTGCTCCCATCATAGGTCTTG		
FN	Fibronectin	AY839862.1	Fwd	CGGGAGGAAAAGGACAGTTCA	82	n/a
			Rev	GCCAGGAAGCTGAATACCGT		

Table 4.1: Primer Sequences for qPCR of Candidate Genes.

This table summarises the gene abbreviation and name, accession number, primer sequences (Fwd = Forward, Rev = Reverse), amplicon size and the source of the primer sequences. N/A indicates that the primer pair were designed specifically for this experiment using NCBI Primer Blast.

4.3.2 Analysis of SPP1 Uterine Gland Staining

Immunofluorescence was performed as described in 2.3.4. For the primary antibody, a cocktail of whole rabbit anti-human recombinant SPP1 serum (1:100) (LF-166 and LF-124, kindly provided by Dr Larry W. Fisher, National Institutes of Health, U.S.A.) (Fisher *et al.*, 1995), or RIgG (1:200 dilution) as a negative control were used. Slides were imaged at x20 magnification using a fluorescent microscope (DMLB, Leica, Milton Keynes, U.K.), with the cyan (1482) and green (598) thresholds kept constant throughout the imaging process. Image analysis was performed using ImageJ. Images were split into red, green and blue channels. On the green channel, the threshold was adjusted to reflect the staining present and, using the free hand drawing tool, each uterine gland was drawn around. The percentage staining per uterine gland was quantified on two sections per sample, for a minimum of 20 uterine glands per section. The mean percentage staining was taken per uterine gland was calculated for each sample and this was used for the statistical analysis.

4.3.3 Statistical Analysis

Statistical analyses were performed following the general protocol outlined in 2.5. The normality of the data was assessed, and transformations performed as required.

4.3.3.1 Assessment of SPP1, FN and Integrin Subunit mRNA Expression by qPCR

The normalised mean value for each placental and endometrial sample was taken. Log10 transformation was required for many of the data from the candidates of interest in both tissues for the data to have a normal distribution. Placental *ITGβ1* expression data had a normal distribution without transformation. *ITGβ8* endometrial expression data did not have a normal distribution with all GD combined. Within GD, endometrial *ITGβ8* expression data had a normal distribution at GD18, 30 and 60 without transformation, and had a normal distribution following log10 transformation at GD45 and 90.

ANOVA was performed, with and without a block for gilt, to determine if there was a GD effect within tissue. To test for the GD effect in *ITGβ8* endometrial expression, a Kruskal-Wallis was performed. Within GD, ANOVA was performed with and without a block for gilt. This analysis was carried out comparing the true lightest with the true closest to mean litter weight (CTMLW) samples to determine if there was an association with conceptus or foetal size (GD18-90), and using the lightest and CTMLW foetuses of both sex to determine if there was an association with foetal sex (GD30-90). The true lightest compared with the true CTMLW conceptuses or foetuses' dataset by two-way ANOVA, with and without a block for gilt, to assess the presence of sex x size interactions within GD. This was performed at GD30, 60 and 90. This was not performed on GD18 or 45 samples, as the sex of the GD18 conceptuses was unknown and because there was only one true lightest male on GD45. Pearson's correlations between the α and β subunit expressions were performed within GD for both tissues.

4.3.3.2 Analysis of SPP1 Uterine Gland Staining

The GD90 data had a normal distribution without transformation however GD30, 45 and 60 data required log10 transformation to have a normal distribution. To investigate the effect of GD, as the data did not have a normal distribution within the same transformation for all GD combined, a Kruskal-Wallis was performed. Within GD, ANOVA was performed with and without a block for gilt. This analysis was carried out comparing the true lightest with the true CTMLW endometrial samples to determine if there was an association with foetal size, and using the lightest and CTMLW foetuses of both sex to determine if there was an association with foetal sex.

4.4 Results

4.4.1 mRNA Expression

4.4.1.1.1 Amplification Efficiencies and RSq from Placental and Endometrial qPCRs

qPCR was performed for the candidates of interest the integrin subunits *ITGα2*, *ITGαV*, *ITGβ1*, *ITGβ3*, *ITGβ5*, *ITGβ6* and *ITGβ8*, and two ligands of interest *SPP1* and *FN*. The data were normalised to stable reference genes. The amplification efficiencies, RSq, slope and intercept values for each gene for both tissues are detailed in Table 4.2.

4.4.1.2 Temporal Changes in mRNA Expression

4.4.1.2.1 Temporal Changes in Placental mRNA Expression were observed

No significant day effect was observed in the placental expression of *ITGβ5* (ANOVA without Gilt Block FPr=0.037; Figure 4.3E) or *SPP1* (Figure 4.3I). An overall day effect was observed in the placental expression of *ITGα2* (ANOVA without Gilt Block FPr=0.03; with Gilt Block FPr=0.015; Figure 4.3A), with GD30 placentas having decreased expression compared to the other GD investigated. The placental expression of *ITGαV* was influenced by GD (ANOVA without Gilt Block FPr = 0.013; with Gilt Block FPr= 0.02; Figure 4.3B), with decreased expression observed at GD60 compared to GD30 and 45. An overall GD effect was observed in the placental expression of *ITGβ1* (ANOVA with and without Gilt Block FPr≤0.001), with increased expression observed at GD45 and 90 compared to GD30 and 60. The placental expression of *ITGβ3* was decreased at GD60 and 90 compared to GD45 (overall GD effect ANOVA without Gilt Block FPr=0.005, with Gilt Block FPr=0.028; Figure 4.3D). Temporal changes in the placental expression of *ITGβ6* were observed (ANOVA without Gilt Block FPr≤0.001, with Gilt Block FPr=0.007; Figure 4.3F), with low expression observed at GD30, which significantly increased at GD45. A slight, non-significant increase in placental expression was observed between GD45 and 60, followed by a significant increase in expression to its peak expression level at GD90. Placental *ITGβ8*

expression increased with advancing gestation (ANOVA without Gilt Block FPr≤0.001, with Gilt Block FPr=0.007), with a significant increase observed between GD30 and 45 (Figure 4.3G). Placental *FN* expression varied throughout gestation (Kruskal-Wallis P=0.002; Figure 4.3H).

4.4.1.2.2 Temporal Changes in Endometrial mRNA Expression were observed

Several significant temporal changes were observed in endometrial mRNA expression (Figure 4.4). A significant overall GD effect was observed in *ITGα2* endometrial expression (ANOVA without Gilt Block FPr=0.083; with Gilt Block FPr=0.022; Figure 4.4A). The endometrial expression of *ITGαV* (ANOVA with and without Gilt Block FPr≤0.001; Figure 4.4B) and *ITGβ3* (ANOVA without Gilt Block FPr≤0.001; with Gilt Block FPr=0.003) were decreased at GD30 compared to the other GD investigated. During gestation, the endometrial *ITGβ1* expression (ANOVA without Gilt Block FPr≤0.001, with Gilt Block FPr=0.003; Figure 4.4C) and *ITGβ8* (Kruskal-Wallis P≤0.001; Figure 4.4G) fluctuated. Endometrial *ITGβ5* also expression fluctuated throughout gestation (ANOVA with and without Gilt Block FPr≤0.001; Figure 4.4E), with decreased expression observed at GD30, 60 and 90 compared to GD18 and 45. Endometrial *ITGβ6* expression was increased in mid and late gestation compared to early gestation, with a notable increase in expression observed between GD30 and 45 (ANOVA with and without Gilt Block FPr≤0.001; Figure 4.4F). A decrease in endometrial *FN* expression was observed between GD60 and 90 (ANOVA without Gilt Block FPr=0.026; Figure 4.4H), although this was not statistically significant with the addition of a block for gilt. The endometrial expression of *SPP1* increased with advancing gestation (ANOVA with and without gilt block FPr≤0.001; Figure 4.4I).

Gene	Placenta				Endometrium			
	Amplification Efficiency (%)	**RSq**	**Slope**	**Intercept**	**Amplification Efficiency (%)**	**RSq**	**Slope**	**Intercept**
ITGα2	92.6	0.991	-3.512	22.055	90.3	0.996	-3.578	23.527
ITGαV	91.9	0.991	-3.533	25.653	95.5	0.991	-3.434	24.742
ITGβ1	94.5	0.993	-3.460	26.475	104.2	0.991	-3.224	28.247
ITGβ3	91.4	0.994	-3.548	29.146	91.4	0.992	-3.547	27.323
ITGβ5	90.4	0.996	-3.574	26.433	91.2	0.992	-3.553	27.791
ITGβ6	90.7	0.995	-3.568	28.043	92.4	0.991	-3.518	28.421
ITGβ8	90.7	0.994	-3.566	30.511	92.2	0.995	-3.524	28.012
SPP1	96.9	0.993	-3.399	20.560	97.8	0.991	-3.376	15.788
FN	90.0	0.996	-3.588	22.220	90.6	0.991	-3.571	27.152
TBP1	102.6	0.991	-3.261	27.199	97.4	0.990	-3.385	28.393
HPRT1	99.5	0.991	-3.335	26.933	N/A	N/A	N/A	N/A
TOP2B	N/A	N/A	N/A	N/A	99.5	0.990	-3.334	28.671
YWHAZ	N/A	N/A	N/A	N/A	92.6	0.990	-3.513	21.871

Table 4.2: Quantitative Polymerase Chain Reaction Calibration Curve Data for Placental and Endometrial qPCRs.

Abbreviations used: ITG=integrin subunit; SPP1=Secreted Phosphoprotein 1; FN=Fibronectin; TBP1=TATA box binding protein; HPRT1=Hypoxanthine phosphoribosyltransferase 1; TOP2B= Topoisomerase II beta; YWHAZ=Tyrosine 3-monooxygenase/tryptophan 5-monooxygenase activation protein, zeta polypeptide, n/a=not applicable.

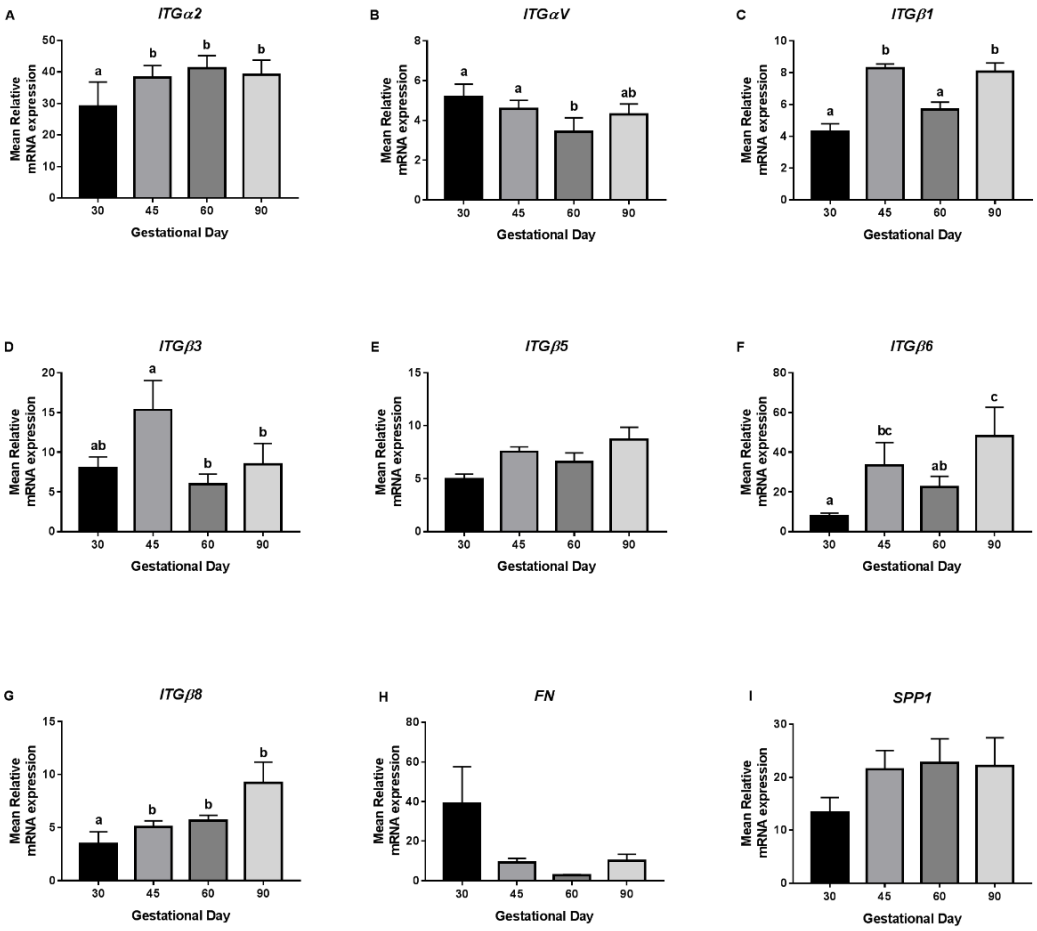

Figure 4.3: Temporal Changes in *Integrin Subunit* and *FN*, but not *SPP1* Placental mRNA Expression were observed.

The mean values normalised to the expression of stable reference genes are plotted here. A: GD30 placentas had decreased *ITGα2* expression compared to the other GD investigated (ANOVA with and without Gilt Block FPr≤0.05). B: Decreased *ITGαV* expression was observed at GD60 compared to GD30 and 45 (ANOVA with and without Gilt Block FPr≤0.05). C: Increased *ITGβ1* expression was observed at GD45 and 90 compared to GD30 and 60 (ANOVA with and without Gilt Block FPr≤0.001). D: Placental *ITGβ3* expression was decreased at GD60 and 90 compared to GD45 (overall GD effect ANOVA without Gilt Block FPr≤0.01, with Gilt Block FPr≤0.05). E: No statistically significant day effect was observed in the placental expression of *ITGβ5*. *ITGβ6* (ANOVA without Gilt Block FPr≤0.001, with Gilt Block FPr≤0.01; F) and *FN* (Kruskal-Wallis P≤0.01; H) expression fluctuated throughout gestation. G: *ITGβ8* increased with advancing gestation (ANOVA without Gilt Block FPr≤0.001, with Gilt Block FPr≤0.01), with a significant increase observed between GD30 and 45. I: No statistically significant day effect was observed in the placental expression of *SPP1*. Error bars represent S.E.M. Letters indicate that group means differ from one another, tested by post-hoc Tukey.

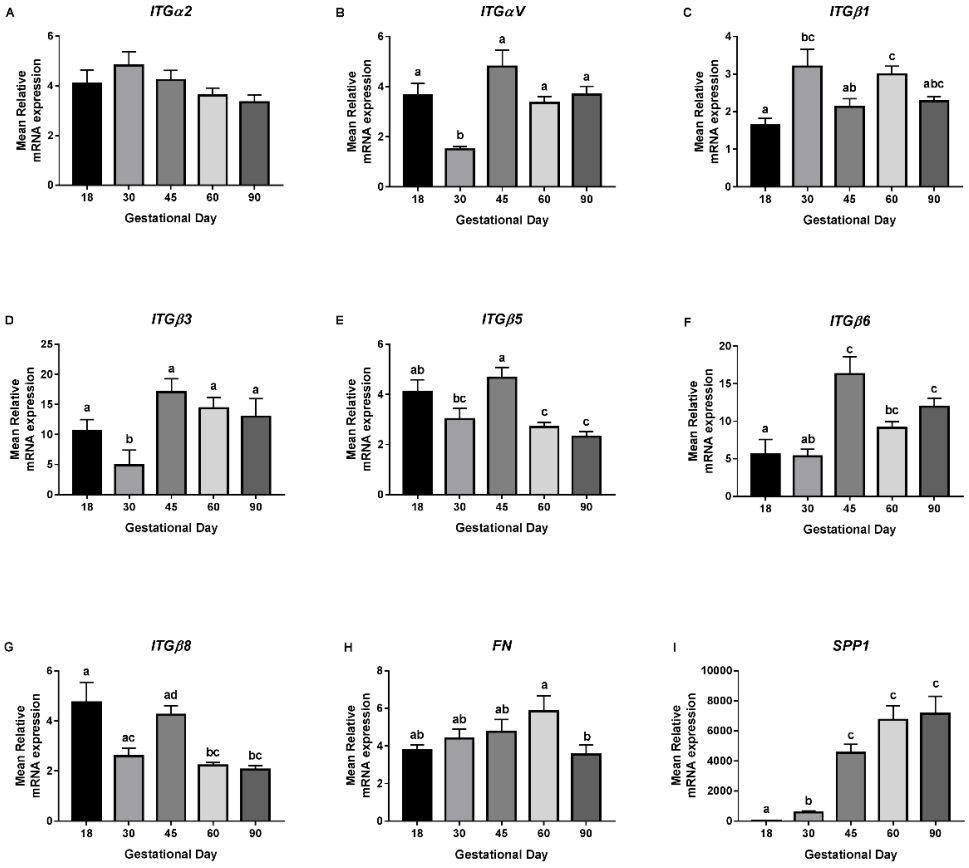

Figure 4.4: Temporal Changes in *Integrin Subunit*, *FN* and *SPP1* Endometrial mRNA Expression were observed.

The mean values normalised to the expression of stable reference genes are plotted here. A: An overall GD effect was observed in *ITGα2* endometrial expression (ANOVA with Gilt Block FPr≤0.05). The expression of *ITGαV* (ANOVA with and without Gilt Block FPr≤0.001; B) and *ITGβ3* (ANOVA without Gilt Block FPr≤0.001; with Gilt Block FPr≤0.01; D) were decreased at GD30 compared to the other GD investigated. During gestation, the endometrial expression of *ITGβ1* (ANOVA without Gilt Block FPr≤0.001, with Gilt Block FPr≤0.01; C) and *ITGβ8* (Kruskal-Wallis P≤0.001; G) fluctuated. E: Endometrial *ITGβ5* expression fluctuated throughout gestation with decreased expression observed at GD30, 60 and 90 compared to GD18 and 45 (ANOVA with and without Gilt Block FPr≤0.001). F: *ITGβ6* endometrial expression was increased in mid and late gestation compared to early gestation, with a significant increase in expression observed between GD30 and 45 (ANOVA with and without Gilt Block FPr≤0.001). H: Decreased endometrial *FN* expression was observed between GD60 and 90 (ANOVA without Gilt Block FPr≤0.05), although this was not statistically significant with the addition of a block for gilt. I: *SPP1* endometrial expression increased with advancing gestation (ANOVA with and without gilt block FPr≤0.001). Error bars represent S.E.M. Letters indicate that group means differ from one another (Tukey or Mann-Whitney).

4.4.1.3 Association between Foetal Size and mRNA Expression

4.4.1.3.1 A Trend towards an Association between Foetal Size and Placental mRNA Expression of *ITGα2* was observed.

The association between foetal size and the placental mRNA expression of the integrin subunits of interest, *FN* and *SPP1* was investigated at GD30, 45, 60 and 90. No statistically significant associations between foetal size and placental expression of *ITGαV* (ANOVA without Gilt Block GD30 FPr=0.089; Figure 4.5B), *ITGβ1* (Figure 4.5C), *ITGβ3* (Figure 4.5D), *ITGβ5* (Figure 4.5E), *ITGβ6* (Figure 4.5F), *ITGβ8* (Figure 4.5G), *FN* (Figure 4.5H) or *SPP1* (Figure 4.5I) were observed. At GD45 (ANOVA with Gilt Block FPr=0.07; Figure 4.5A), placental samples supplying the lightest foetuses had increased *ITGα2* expression compared to those supplying the CTMLW foetuses. The direction of this difference switched at GD90 (ANOVA without Gilt Block FPr=0.022; with Gilt Block FPr=0.092; Figure 4.5A), with placental samples supplying the lightest foetuses having decreased *ITGα2* expression compared to those supplying the CTMLW foetuses.

4.4.1.3.2 An Association between Foetal Size and *ITGβ1* and *SPP1* Endometrial mRNA Expression was observed.

The association between conceptus or foetal size and the endometrial mRNA expression of the integrin subunits of interest, *FN* and *SPP1* was investigated at GD18, 30, 45, 60 and 90. No statistically significant associations between conceptus or foetal size and endometrial expression of *ITGα2* (Figure 4.6A), *ITGαV* (Figure 4.6B), *ITGβ3* (ANOVA GD90 with Gilt Block FPr=0.097; Figure 4.6D) or *ITGβ6* (Figure 4.6F) were observed. *ITGβ1* expression was decreased in endometrial samples supplying the lightest foetuses compared to the CTMLW foetuses at GD45 (ANOVA without Gilt Block FPr=0.027, with Gilt Block FPr=0.045; Figure 4.6C). At GD30, a trend towards endometrial samples supplying the lightest foetuses having increased *ITGβ5* expression compared to samples supplying the CTMLW foetuses was observed (ANOVA with Gilt Block FPr = 0.069; Figure 4.6E). There was an indication at GD45

that endometrial samples supplying the lightest foetuses had decreased expression of *ITGβ5* (ANOVA without Gilt Block FPr=0.038; Figure 4.6E). However, this was not significant with the addition of a block for gilt. A trend towards increased expression of *ITGβ8* (ANOVA without Gilt Block FPr=0.004; with Gilt Block FPr=0.087; Figure 4.6G) was observed in endometrial samples supplying the lightest compared to the CTMLW conceptuses at GD18. In contrast, *FN* endometrial expression was decreased at GD18 in endometrial samples supplying the lightest compared to the CTMLW conceptuses (ANOVA without Gilt Block FPr=0.049; Figure 4.6H), although this was not statistically significant with the addition of a block for gilt. An overall size effect in *SPP1* expression was observed (ANOVA with Gilt Block FPr=0.02; Figure 4.6I), with a statistically significant decrease observed in endometrial samples supplying the lightest foetuses compared to the CTMLW foetuses at GD60 (ANOVA without Gilt Block FPr=0.015; with Gilt Block FPr=0.028).

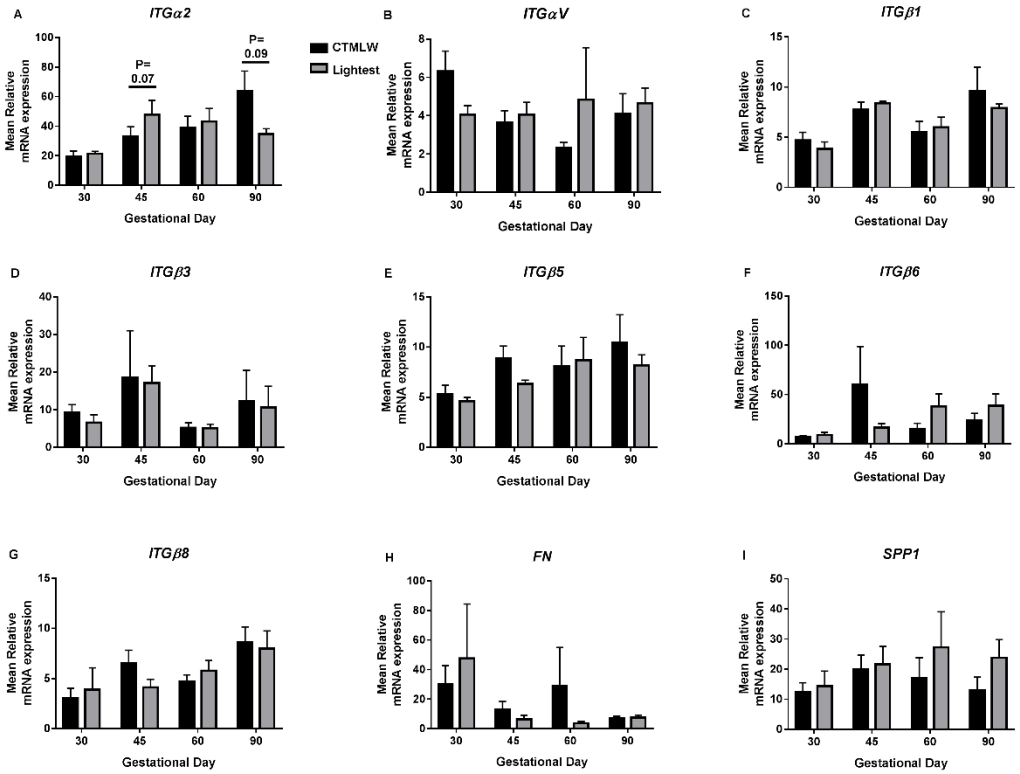

Figure 4.5: A Trend towards an Association between Foetal Size and Placental mRNA Expression of *ITGα2* was observed.

The mean values normalised to the expression of stable reference genes are plotted here. A: At GD45 (ANOVA with Gilt Block FPr=0.07), a trend towards increased *ITGα2* expression in placental samples supplying the lightest foetuses compared to those supplying the closest to mean litter weight (CTMLW) foetuses was observed. The direction of this difference switched at GD90 (ANOVA without Gilt Block FPr≤0.05; with Gilt Block FPr=0.09), with placental samples supplying the lightest foetuses having decreased *ITGα2* expression compared to those supplying the CTMLW foetuses. No statistically significant associations between foetal sex and placental expression of *ITGαV* (B), *ITGβ1* (C), *ITGβ3* (D), *ITGβ5* (E), *ITGβ6* (F), *ITGβ8* (G), *FN* (H) or *SPP1* (I) were observed. Error bars represent S.E.M.

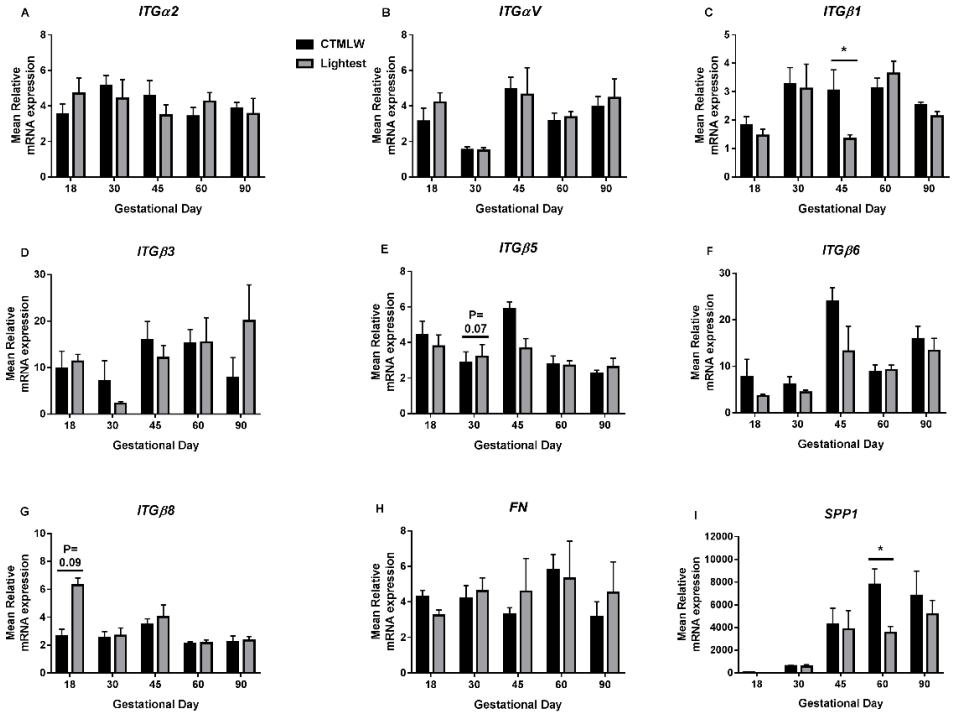

Figure 4.6: An Association between Foetal Size and *ITGβ1* and *SPP1* Endometrial mRNA Expression was observed.

The mean values normalised to the expression of stable reference genes are plotted here. No statistically significant associations between foetal size and endometrial expression of *ITGα2* (A), *ITGαV* (B), *ITGβ3* (ANOVA GD90 with Gilt Block FPr=0.097; D) or *ITGβ6* (F) were observed. C: Decreased *ITGβ*1 expression was observed in endometrial samples supplying the lightest foetuses compared to the closest to mean litter weight (CTMLW) foetuses at GD45 (ANOVA with and without Gilt Block FPr≤0.05). E: At GD30, a trend towards endometrial samples having increased *ITGβ5* expression compared to samples supplying the CTMLW foetuses was observed (ANOVA with Gilt Block FPr=0.07. At GD45, there was an indication of endometrial samples supplying the lightest foetuses having decreased *ITGβ5* expression (ANOVA without Gilt Block FPr≤0.05). However, this was not significant with the addition of a block for gilt. G: A trend towards increased expression of *ITGβ8* (ANOVA without Gilt Block FPr≤0.01; with Gilt Block FPr=0.087) was observed in endometrial samples supplying the lightest compared to the CTMLW conceptuses at GD18. H: *FN* endometrial expression was decreased at GD18 in endometrial samples supplying the lightest compared to the CTMLW conceptuses (ANOVA without Gilt Block FPr≤0.05). However, this was not significant with the addition of a block for gilt. I: An overall size effect in *SPP1* expression was observed (ANOVA with gilt block FPr≤0.05), with a significant decrease observed in endometrial samples supplying the lightest foetuses compared to the CTMLW foetuses at GD60 (ANOVA with and without Gilt Block FPr≤0.05. Error bars represent S.E.M. *FPr/P≤0.05.

4.4.1.4 Association between Foetal Sex and mRNA Expression

4.4.1.4.1 An Association between Foetal Sex and Placental *ITGβ6* and *FN* mRNA Expression was observed.

The association between foetal sex and the placental mRNA expression of the integrin subunits of interest, *FN* and *SPP1* was investigated at GD30, 45, 60 and 90. No statistically significant associations between foetal sex and placental expression were observed for *ITGα2* (ANOVA GD60 without Gilt Block FPr=0.076; Figure 4.7A), *ITGαV* (Figure 4.7B), *ITGβ1* (Figure 4.7C), *ITGβ3* (Figure 4.7D), *ITGβ5* (Figure 4.7E), *ITGβ8* (ANOVA GD45 without Gilt Block FPr=0.044; Figure 4.7G) or *SPP1* (Figure 4.7I). A significant association between foetal sex and *ITGβ6* (ANOVA GD45 without Gilt Block FPr=0.046, with Gilt Block FPr=0.053; Figure 4.7F) and *FN* (ANOVA GD90 with Gilt Block FPr=0.052; Figure 4.7H) expression was observed, with females having decreased expression at GD45 and 90 for *ITGβ6* and *FN* respectively.

4.4.1.4.2 Associations between Foetal Sex and Endometrial *ITGβ3*, *FN* and *SPP1* Expression were observed.

The association between foetal sex and the endometrial mRNA expression of the integrin subunits of interest, *FN* and *SPP1* was investigated at GD18, 30, 45, 60 and 90. No statistically significant associations between foetal sex and endometrial expression were observed for *ITGα2* (Figure 4.8A), *ITGαV* (Figure 4.8B), *ITGβ1* (Figure 4.8C), *ITGβ5* (Figure 4.8E), *ITGβ6* (Figure 4.8F) or *ITGβ8* (Figure 4.8G). Endometrial samples supplying females at GD60 had increased *ITGβ3* expression compared to their male littermates (ANOVA without Gilt Block FPr=0.033; with Gilt Block FPr=0.02; Figure 4.8D). At GD30, *FN* expression was increased in endometrial samples supplying females compared to their male littermates (ANOVA with Gilt Block FPr=0.045; Figure 4.8H). A trend towards decreased endometrial *FN* expression in samples associated with females compared to males was observed at GD60 (ANOVA without Gilt Block FPr=0.07). However, this difference was lost with the addition of a block for gilt. *SPP1* endometrial expression was decreased in

samples supplying female foetuses compared to their male littermates at GD60 (ANOVA without Gilt Block FPr=0.071; with Gilt Block FPr=0.020; Figure 4.8I).

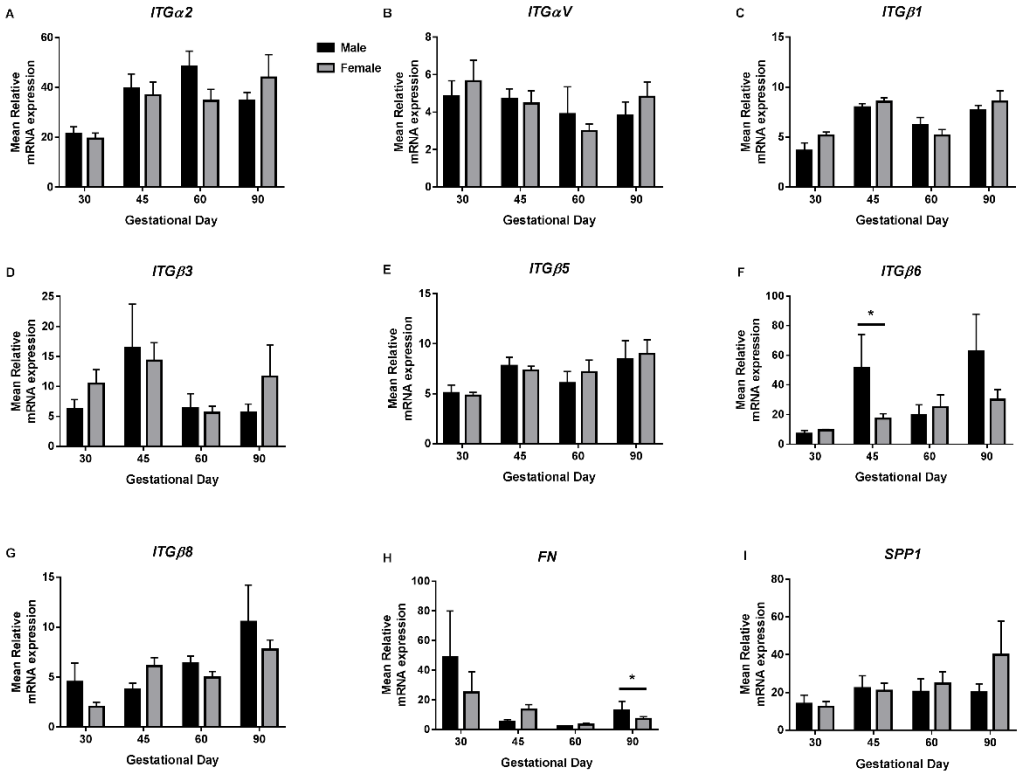

Figure 4.7: Associations between Foetal Sex and Placental *ITGβ6* and *FN* mRNA Expression.

The mean values normalised to the expression of stable reference genes are plotted here. No statistically significant associations between foetal sex and placental expression were observed for *ITGα2* (ANOVA GD60 without Gilt Block FPr=0.076; Figure 4.7A), *ITGαV* (B), *ITGβ1* (C), *ITGβ3* (D), *ITGβ5* (E), *ITGβ8* (ANOVA GD45 without Gilt Block FPr≤0.05; G) or *SPP1* (I). A significant association between foetal sex and *ITGβ6* was observed (ANOVA GD45 with and without Gilt Block FPr≤0.05; F) and *FN* (ANOVA GD90 with Gilt Block FPr≤0.05; H), with females having decreased expression at GD45 and 90 for *ITGβ6* and *FN* respectively. Error bars represent S.E.M. *FPr/P≤0.05.

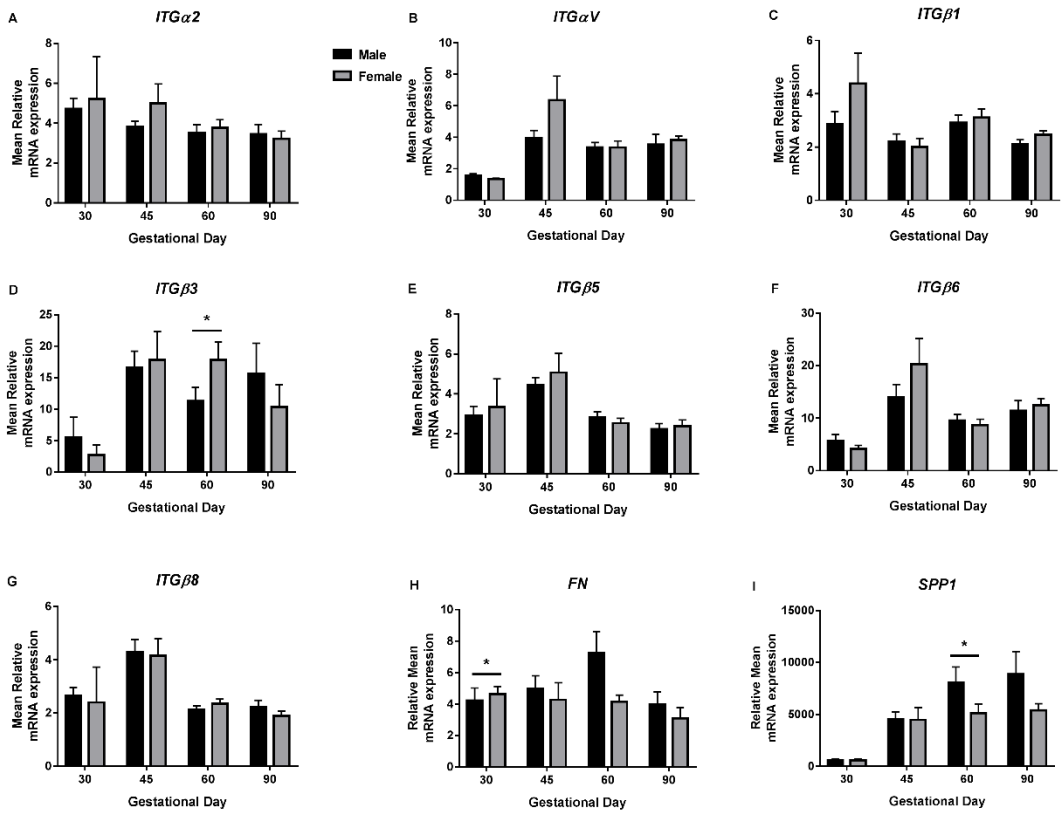

Figure 4.8: Associations between Foetal Sex and Endometrial *ITGβ3*, *FN* and *SPP1* Expression were observed.

The mean values normalised to the expression of stable reference genes are plotted here. No statistically significant associations between foetal sex and endometrial expression were observed for *ITGα2* (A), *ITGαV* (B), *ITGβ1* (C), *ITGβ5* (E), *ITGβ6* (F) or *ITGβ8* (G). D: Endometrial samples supplying females at GD60 had increased *ITGβ3* expression compared to their male littermates (ANOVA with and without Gilt Block FPr≤0.05). H: At GD30, endometrial *FN* expression was increased in samples supplying females compared to their male littermates (ANOVA with Gilt Block FPr≤0.05). A trend towards decreased endometrial *FN* expression in samples associated with females compared to males was observed at GD60 (ANOVA without Gilt Block FPr=0.07). However, this difference was lost with the addition of a block for gilt. I: *SPP1* endometrial expression was decreased in samples supplying female foetuses compared to their male littermates at GD60 (ANOVA without Gilt Block FPr=0.07; with Gilt Block FPr≤0.05). Error bars represent S.E.M. *FPr/P≤0.05.

4.4.1.5 Sex x Size Interactions in mRNA Expression

4.4.1.5.1 Sex x Size Interactions in Placental mRNA Expression of *ITGβ1, ITGβ3* and *ITGα2* were observed.

The data were analysed by two-way ANOVA, with and without a block for gilt, to assess the presence of sex x size interactions within GD. This was performed at GD30, 60 and 90 for all integrin subunits, *FN* and *SPP1* however, due to limitations in the GD45 data set with only one overall lightest male present, this analysis was not performed at GD45. The three sex x size interactions with statistically significant results are presented in Figure 4.9. A sex x size interaction was observed in placental GD60 *ITGβ1* (ANOVA with Gilt Block FPr=0.073; Figure 4.9A), GD60 *ITGβ3* (ANOVA with and without Gilt Block FPr=0.023; Figure 4.9B) and GD90 *ITGα2* (ANOVA without gilt block FPr=0.022; Figure 4.9C) expression.

4.4.1.5.2 Sex x Size Interactions in Endometrial mRNA Expression of *ITGβ1 and ITGβ8* were observed.

The data were analysed by two-way ANOVA, with and without a block for gilt, to assess the presence of sex x size interactions within GD. This was performed at GD30, 60 and 90 for all integrin subunits, *FN* and *SPP1* but, due to limitations in the GD45 data set with only one overall lightest male present, this analysis was not performed at GD45. A sex x size interaction was observed in endometrial *ITGβ8* expression at GD60 (ANOVA with Gilt Block FPr=0.056; Figure 4.10A) and *ITGβ1* expression at GD90 (ANOVA with Gilt Block FPr=0.04; Figure 4.10B).

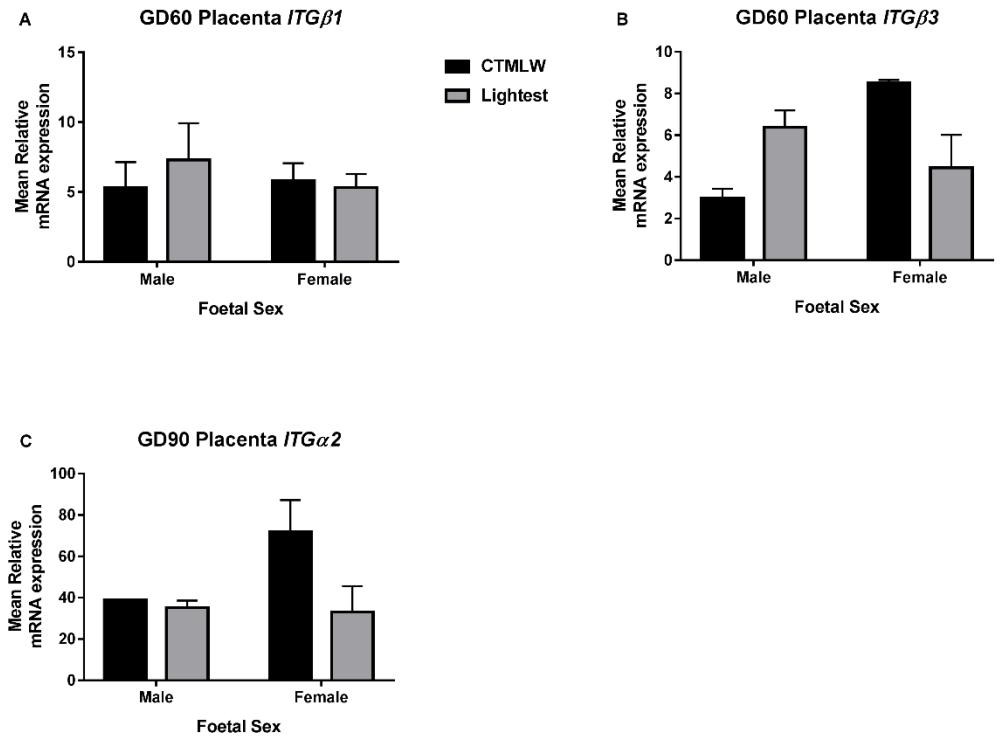

Figure 4.9: Sex x Size Interactions in Placental mRNA Expression of *ITGβ1*, *ITGβ3* and *ITGα2* were observed.

qPCR was performed on cDNA from porcine placental samples supplying the lightest and the closest to mean litter weight (CTMLW) foetuses of both sex at GD30, 60, and 90. The mean values normalised to the expression of stable reference genes are plotted here for each sex x size treatment group. The data were analysed by two-way ANOVA, with and without a block for gilt, to assess the presence of sex x size interactions within GD. The three sex x size interactions of interest are presented here. A: A trend towards a significant sex x size interaction was observed in placental GD60 *ITGβ1* expression (ANOVA with Gilt Block FPr=0.073). A significant sex x size interaction was observed for *ITGβ3* expression at GD60 (ANOVA with and without Gilt Block FPr≤0.05; B), and for *ITGα2* expression at GD90 (ANOVA without gilt block FPr≤0.05; C). Error bars represent S.E.M.

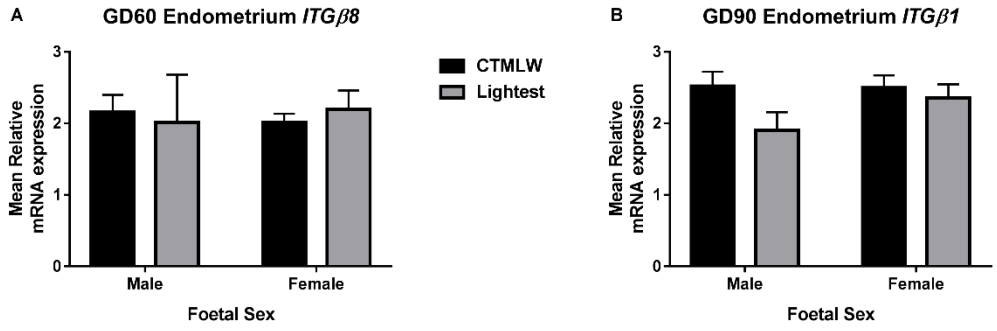

Figure 4.10: Sex x Size Interactions in Endometrial mRNA Expression of *ITGβ1* and *ITGβ8* were observed.

qPCR was performed on cDNA from porcine endometrial samples supplying the lightest and the closest to mean litter weight (CTMLW) foetuses of both sex at GD30, 60, and 90. The mean values normalised to the expression of stable reference genes are plotted here for each sex x size treatment group. The data were analysed by two-way ANOVA, with and without a block for gilt, to assess the presence of sex x size interactions within GD. The two sex x size interactions of interest are presented here. A sex x size interaction was observed in endometrial *ITGβ8* expression at GD60 (ANOVA with Gilt Block FPr=0.056; A) and *ITGβ1* expression at GD90 (ANOVA with Gilt Block FPr=0.04; B). Error bars represent S.E.M.

4.4.1.6 Correlations between Integrin Subunit mRNA Expression

4.4.1.6.1 Correlations between Integrin α Subunits Expression with Integrin β Subunits in Placental Samples were observed.

Correlations were performed within GD for the mRNA expression for each of the α subunits against each of the β subunits to give an indication of quantitative associations between heterodimers at each stage of gestation (Table 4.3).

GD	α Subunit	β Subunit	RSq (%)	P Value
30	2	5	79.18	≤0.001
60	2	1	17.80	0.045
60	V	1	17.65	0.046
60	V	5	32.81	0.005
60	V	6	20.70	0.030
90	2	1	44.92	0.002
90	2	3	29.92	0.020
90	V	5	29.83	0.020
90	V	6	39.93	0.005
90	V	8	26.58	0.024

Table 4.3: Correlations between the Placental mRNA Expression of Integrin α and β Subunits Revealed Positive Relationships.

The normalised expression value for each placental mRNA expression for each sample for each α and β subunit were correlated against one another within gestational day (GD). Correlations which had a P value of ≤0.09 are presented here.

4.4.1.6.2 Correlations between Integrin α Subunits Expression with Integrin β Subunits in Endometrial Samples were observed.

Correlations were performed within GD for the mRNA expression for each of the α subunits against each of the β subunits to give an indication of quantitative associations between heterodimers at each stage of gestation (Table 4.4).

GD	α Subunit	β Subunit	RSq (%)	P Value
18	V	3	35.97	0.067
18	V	8	52.51	0.065
30	2	8	52.51	0.068
30	V	3	59.32	0.015
30	V	6	69.53	0.005
45	2	8	18.38	0.086
45	V	3	34.04	0.014
45	V	5	46.99	0.002
45	V	6	69.24	≤0.001
60	2	1	46.26	≤0.001
60	V	6	70.75	≤0.001
90	2	1	20.50	0.034
90	2	5	18.81	0.044
90	2	6	38.11	0.002
90	V	6	48.92	≤0.001
90	V	8	13.73	0.090

Table 4.4: Correlations between the Endometrial mRNA Expression of Integrin α and β Subunits Revealed Positive Relationships.

The normalised expression value for each placental mRNA expression for each sample for each α and β subunit were correlated against one another within gestational day (GD). Correlations which had a P value of ≤0.09 are presented here.

4.4.2 Uterine Gland SPP1 Staining

4.4.2.1 Temporal Changes in Uterine Gland SPP1 Staining

The percentage SPP1 staining per uterine gland was quantified at GD30, 45, 60 and 90. Temporal changes in the percentage staining of SPP1 were observed (Kruskal-Wallis P≤0.001; Figure 4.11A). The intensity of SPP1 uterine gland staining observed at GD30 was low, before gradually increasing for the remainder of gestation.

4.4.2.2 Association between Foetal Size and Uterine Gland SPP1 Staining

To determine if there was a relationship between foetal size and uterine gland SPP1 staining, the endometrial samples supplying the lightest foetuses were compared with those supplying the CTMLW foetuses at GD30, 45, 60 and 90 (Figure 4.11B). No association between foetal size and SPP1 staining was observed.

4.4.2.3 Association between Foetal Sex and Uterine Gland SPP1 Staining

To determine if there was a relationship between foetal sex and uterine gland SPP1 staining, the endometrial samples supplying male foetuses were compared with those supplying female foetuses at GD30, 45, 60 and 90 (Figure 4.11C). No association between foetal sex and SPP1 staining was observed.

4.4.2.4 Sex x Size Interactions in Uterine Gland SPP1 Staining

The data were analysed by two-way ANOVA, with and without a block for gilt, to assess the presence of sex x size interactions within GD. This was performed at GD30, 60 and 90 but, due to limitations in the GD45 data set with only one overall lightest male present, this analysis was not performed at GD45. No statistically significant sex x size interactions in uterine gland SPP1 staining were observed (Figure 4.11D, E, and F).

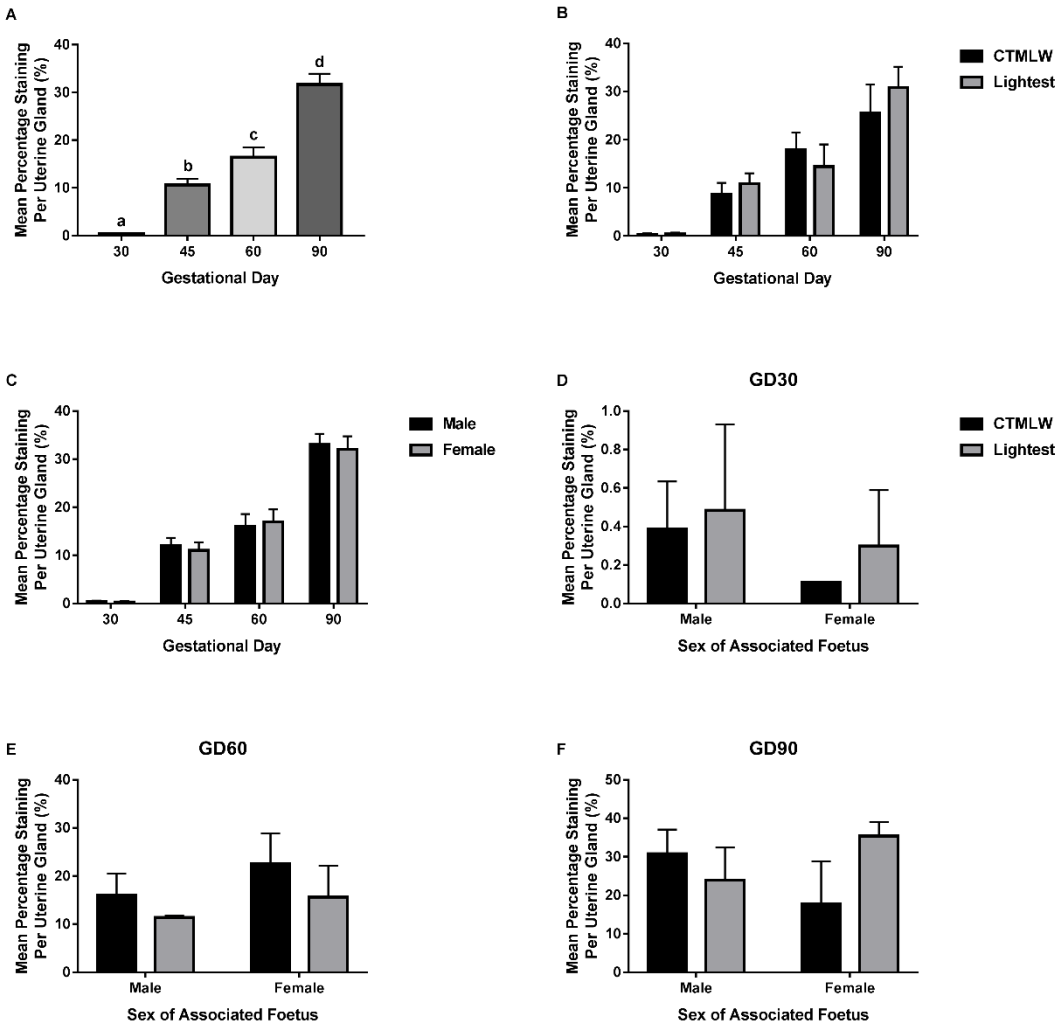

Figure 4.11: No Association between Foetal Size or Sex and SPP1 uterine gland Staining was observed.

Immunofluorescence was performed for SPP1 on endometrial samples at GD30, 45, 60 and 90. A: Temporal changes in SPP1 percentage staining per uterine gland were observed, with a gradual increase in uterine gland SPP1 staining intensity observed with advancing GD. No association between foetal size (B) or sex (C) and SPP1 percentage staining per uterine gland was observed. No statistically significant sex x size interactions were observed at GD30 (D), 60 (E) or 90 (F). Mean values presented. Error bars represent S.E.M. Letters indicate group means differ, post-hoc Mann Whitney. Abbreviations used: GD=gestational day, CTMLW=closest to mean litter weight.

4.5 Discussion

The experiments described in this chapter have demonstrated that foetal size and sex are associated with the mRNA expression of integrin subunits and their ligands at the feto-maternal interface in the pig (Table 4.5 and Table 4.6). This is the first evidence that foetal sex may have a strong influence on uterine expression of integrins and their ligands in the pig, and the mechanisms behind this warrant much further investigation.

4.5.1 Temporal Changes in Placental and Endometrial mRNA Expression and Endometrial SPP1 Uterine Gland Staining

The results presented in this chapter demonstrated the dynamic nature of the feto-maternal interface, with large temporal changes in mRNA expression observed in the expression of integrin subunits and their ligands. A significant decrease in the endometrial expression of *ITGαV* and *ITGβ3* at GD30 compared to the other GD investigated was observed. Additionally, fluctuations in *ITGβ6* expression were noted, with increased expression observed at GD45 compared to GD18 and 30. Lin *et al.*, (2007) suggest that *ITGαV* has high endometrial expression at GD18 compared to GD12 and 25. On a protein level, similar findings were observed which indicate that the ITGαV and ITGβ3 had high expression at GD18, before decreasing towards GD25, in a similar manner to what was observed on an mRNA level in the current study. In contrast to our findings, it has been suggested by Frank *et al.*, (2017) that LE mRNA expression of these integrin subunits is not influenced by GD investigated. It is important when comparing these papers to note that the techniques used are very different, with Frank *et al.*, (2017) specifically investigating LE mRNA expression by *in situ* hybridisation in contrast to the current study which investigated whole tissue expression by qPCR.

On a protein level, the αvβ3 receptor has been demonstrated to be highly expressed at the feto-maternal interface from GD17 to 70, before decreasing significantly (Vélez *et al.*, 2015, 2017). This difference was not noted in the current study however mRNA was utilised from whole tissue rather than

performing immunohistochemistry on the interface specifically which may mask this difference. In this study it has been demonstrated that *ITGαV*, *ITGβ3* and *ITGβ6* are all highly expressed in the endometrium at GD45, which corresponds to an increase in the expression of SPP1 both on an mRNA level and in uterine gland protein expression. Throughout this thesis, evidence is put forward to suggest that this period of gestation is highly dynamic therefore, an increase in the expression of receptors and ligands involved in cell adhesion may not be surprising during this dynamic period to ensure adequate placental attachment is maintained. In addition, P4 is believed to influence the secretion of the histotroph (reviewed by Spencer *et al.*, 2004) and, as detailed in 4.1.3.2, has been proposed to regulate uterine gland SPP1 expression. However, a recent study proposed that SPP1 GE expression in the pig is not induced by P4 alone and may instead be influenced by the interaction between multiple pathways and factors (Steinhauser *et al.*, 2017). Further investigation into the mechanisms governing production of SPP1 and other components of the histotroph, may improve the understanding of the feto-maternal interface.

This study illustrated novel temporal changes in the placental expression of *ITGα2*, *ITGαV*, *ITGβ1*, *ITGβ3*, *ITGβ6* and *ITGβ8*. To date, there have been limited investigations into the expression of these receptors in the porcine placenta during gestation, with the majority of studies focussing on their expression during implantation and early gestation. In the current study, a decrease in placental *ITGαV* expression was observed at GD60 compared to GD30 and 45, and a decrease in *ITGβ3* expression was observed at GD60 and 90 compared to GD45. These findings support those of Vélez *et al.*, (2015, 2017) who demonstrated intense protein staining for αVβ3 at the placental interface from GD17 to 60, after which (GD70, 80 and 114) the staining intensity decreased significantly. Intriguingly, P4 in both serum and placental extracts mirrored the temporal profile of αVβ3 staining. The authors have proposed an interesting hypothesis that P4 may be able to play a role in the regulation of αVβ3 and FN until GD70, after which alternative adhesion molecules may have a more significant role.

Placental *FN* expression fluctuated during pregnancy, with the highest expression observed at GD30. This reinforces the findings of Rashev *et al.*, (2005), who demonstrated an increase in porcine trophectoderm FN protein expression between GD20 and 35. In the current study, endometrial *FN* expression decreased between GD60 and 90, which adds weight to the findings of Vélez *et al.*, (2015, 2017) where intense staining for FN was observed at the feto-maternal interface from GD17-70, after which the intensity significantly decreased.

Reassuringly, in this study the SPP1 uterine gland protein staining followed a similar expression profile to the mRNA data. Previous studies have demonstrated that *SPP1* is not induced in the uterine gland until between GD30 and 35 of pregnancy (Garlow *et al.*, 2002; Frank *et al.*, 2017; Steinhauser *et al.*, 2017). In the current sample set, some diffuse SPP1 staining was noted in the uterine gland of some endometrial samples at GD18 however, the staining was not directly comparable with the remainder of the GD investigate so they were not included in the analysis. SPP1 uterine gland staining was low at GD30, which is comparable with the previous reports in the literature, before increasing with advancing GD. Garlow *et al.*, (2002) demonstrated that endometrial *SPP1* increased between GD25 and 30, and remained elevated through until GD85. The current data support this finding, with an increase in endometrial *SPP1* observed between GD18 and 30, followed by a further increase between GD30 and 45, after which it remained strongly expressed for the remainder of gestation.

4.5.2 Foetal Size was Associated with Placental and Endometrial mRNA Expression

As detailed in 4.1.3, integrin signalling has been heavily implicated in the establishment and maintenance of pregnancy by regulating adhesion at the feto-maternal interface. This study demonstrated an association between mRNA expression of integrins and their ligands, and foetal size at the feto-maternal interface. Intriguingly, foetal size was associated with endometrial

expression of the candidate genes to a greater extent than placental expression.

Placentas supplying the lightest foetuses had increased *ITGα2* expression compared to the CTMLW foetuses at GD45, and the direction of this difference switched at GD90. This switch in the direction of differences in gene expression highlights the dynamic nature of the placenta and the importance of investigating the feto-maternal interface at multiple GDs when researching foetal growth. ITGα2 binds to a number of ECM ligands including collagen, laminin and thrombospondin (Humphries, 2006). In the pig it has been demonstrated that the expression of *ITGα2* is upregulated at GD45, compared to GD25 (Liu *et al.*, 2015), which the temporal data presented in the chapter support. This increase in gene expression has been proposed to be linked to the development of the folds of the placental bilayer by increasing cell adhesion. During gestation it is known that the folded bilayer of the placenta is drastically remodelled to meet the demands of the growing foetus. Vallet and Freking, (2007) investigated the remodelling of the CAM, or folded bilayer, throughout gestation in the pig and demonstrated that the width of the bilayer increased significantly at GD65, 85 and 105 in placentas supplying the smallest foetuses in the litter compared to the largest. They also demonstrated that the stroma above the CAM decreased in size at a faster rate in the placentas supplying the smallest foetuses compared to the largest foetuses. Considering this, the switch in the direction of the difference of *ITGα2* expression is of significant interest and in the future the mRNA and protein expression of this integrin subunit should be investigated at the feto-maternal interface throughout gestation by *in situ* hybridisation and immunohistochemistry respectively.

Endometrial samples supplying the lightest foetuses had significantly decreased expression of *ITGβ1* and *SPP1* expression at GD45 and 60 respectively. A trend towards significantly decreased expression of *ITGβ5* and increased *ITGβ8* was observed at GD45 and 18 respectively. In humans, it has been shown that extravillous trophoblast cells in term placentas which supplied IUGR foetuses had decreased expression of α2β1, α3β1 and α5β1

integrin receptors compared to those which supplied normal-sized foetuses (Zygmunt *et al.*, 1997). In the current study, endometrial samples supplying the lightest foetuses had decreased *ITGβ1* expression at GD45 compared to those supplying their normal-sized littermates; reinforcing that ITGβ1 and its ligands may have a role in regulation of foetal growth in the pig. Further, the α5β1 receptor has been suggested to bind both FN and SPP1 at the feto-maternal interface in the pig (Frank *et al.*, 2017). Whilst no decrease in the expression of *SPP1* or *FN* were observed in the endometrial samples supplying the lightest foetuses compared to their normal-sized littermates at GD45, a decrease in the expression of *SPP1* was observed at GD60.

In the current study, no relationships between foetal size or sex and uterine gland SPP1 protein staining were observed. In contrast to this, Hernandez *et al.*, (2013) observed that SPP1 protein was increased in uterine glands associated with small foetuses compared to their normal-sized littermates in hLW and MS pigs at GD41. Whilst this was not observed in the current study, it is important to note that this was a different breed of pig and a different GD, in a period which has been identified throughout this thesis as being highly dynamic. The breed effect is extremely important when comparing integrin expression and their ligands as differences exist between prolific and European commercial breeds in the expression of SPP1, as detailed in 4.1.3.2.1. Hernandez *et al.*, (2013) demonstrated that MS and hLW SPP1 protein staining was increased in the LE associated with small MS foetuses compared to their normal-sized littermates but, this was not observed in hLW foetuses. Additionally, SPP1 protein expression was found to be increased in placentas supplying small hLW foetuses compared to their normal-sized littermates but, this was not observed in MS. On an mRNA level, similar discrepancies between breeds was observed, with decreased *SPP1* expression in endometrial samples supplying small foetuses compared to their normal-sized littermates at GD41 in hLW but not MS. The difference observed in the hLW foetuses at GD41 observed by Hernandez *et al.*, (2013) were observed in the current study at GD60. Reassuringly, in the current study foetal

size did not influence placental *SPP1* expression, reinforcing the findings of Hernandez *et al.*, (2013).

Further, Li *et al.*, (2013) suggested that in cases of human monochorionic twins with discordant growth, the placenta supplying the smaller twin had decreased SPP1 protein and mRNA expression; suggesting a potential role of SPP1 in the regulation of foetal growth. Weintraub *et al.*, (2004) utilised a biallelic and single allelic mouse knock-out of SPP1 to investigate the influence on embryo number and size at 10.5, 15.5 and 19.5 days post-coitum. The mutation did not alter litter size however, the $SPP1^{-/-}$ embryos were smaller than wildtype embryos at all GD investigated, again suggesting a role of SPP1 in the regulation of foetal growth. A specific mechanism behind this decrease in foetal size observed by Weintraub *et al.*, (2004) may be that uteroplacental blood flow is impaired in SPP1 null mice. Myers *et al.*, (2003) analysed the arterial physiology in SPP1 null mice and demonstrated that the $SPP1^{-/-}$ mice had impaired organisation of collagen in arterial walls. The heart rate and circulating lymphocytes were both found to be increased, whereas blood pressure was decreased in SPP1 null mice compared to wildtype mice. Considering these findings, it may be hypothesised that the vasculature of the placenta would also be impaired in these mice, which in turn could cause decreased blood flow to the developing foetus.

4.5.3 Foetal Sex was Associated with Placental and Endometrial mRNA Expression

As detailed in the general introduction, emerging evidence in humans has suggested that sexual dimorphism in placental development is responsible for sexual dimorphism to disease susceptibility postnatally. It has been proposed that male newborn piglets have a survival disadvantage compared to their female littermates Baxter *et al.*, (2012). However, whether this difference arises prenatally due to sexual dimorphism in placental development has not been determined in the pig.

This study has demonstrated for the first time that placental *ITGβ6* and *FN* expression is decreased in placentas supplying females compared to their male littermates at GD45 and 90 respectively. In endometrial samples, *FN* and *ITGβ3* expression were increased in samples associated with females compared to their male littermates at GD30 and 60 respectively. In addition, *SPP1* expression was decreased in endometrial samples supplying females compared to their male littermates at GD60.

Currently, the suggestion of sexual dimorphism in placental or endometrial integrin expression in any species has not been explored. However, in a recent RNA sequencing experiment using human placentas from 10.5-13.5 weeks it was identified that placentas supplying female foetuses had increased *ITGβ8* expression compared to those supplying males (Gonzalez *et al.*, 2018). Considering this, and the findings presented in this chapter, further studies should be performed to investigate the interaction between foetal sex and integrin signalling throughout gestation.

Males have been demonstrated in this thesis to have a different growth trajectory than female foetuses throughout gestation and were consistently heavier than their female littermates (Chapter 3). As males are heavier, it could be suggested that they would place an increased demand on the placenta for nutrients. To accommodate this, it may be hypothesised that placental expression of *ITGβ6* and *FN* increases to augment adhesion, thereby allowing a better exchange of nutrients from the histotroph to the foetus. In contrast, endometrial expression of *FN* and *ITGβ3* were increased in samples associated with female foetuses compared with their male littermates at GD30 and 60 respectively. The differential expression of *FN* in the endometrium at GD30 may indicate the presence of differential signalling between the conceptus and the endometrium in early gestation.

Tissue	Gestational Day				
	18	30	45	60	90
Placenta	n/a	ns	*ITGα2*	ns	*ITGα2*
Endometrium	ns	*ITGB5*	*ITGβ1*	*SPP1*	ns

Table 4.5: Summary of Results which showed statistically significant effects of foetal size.

Green=Increased; Red=Decreased in samples associated with the lightest foetuses compared to their Closest to Mean Litter Weight (CTMLW) littermates. Abbreviations: ITG=Integrin Subunit, SPP1=Secreted Phosphoprotein 1, ns=not significant, n/a=not applicable.

Tissue	Gestational Day			
	30	45	60	90
Placenta	ns	*ITGβ6*	ns	ns
Endometrium	ns	ns	*SPP1* *ITGβ3*	ns

Table 4.6: Summary of Results which showed statistically significant effects of foetal sex.

Green=Increased; Red=Decreased in samples associated with the male foetuses compared to their female littermates. Abbreviations: ITG=Integrin Subunit, SPP1=Secreted Phosphoprotein 1, ns=not significant, n/a=not applicable.

4.5.4 General Discussion

SPP1 has been implicated as a negative regulator of haematopoietic stem cells (HSCs) in the mouse (Nilsson *et al.*, 2005; Stier *et al.*, 2005). Further, SPP1 has been demonstrated to bind with HSCs *in vitro* through binding to integrin receptors containing ITGβ1, with exogenous SPP1 administration decreasing HSC proliferation (Nilsson *et al.*, 2005). In the current study, endometrial SPP1 expression was decreased in samples supplying both the lightest and female foetuses compared to their normal-sized and male littermates respectively at GD60. It has previously been suggested that the placenta is a source of HSCs (Gekas *et al.*, 2005; Dzierzak and Robin, 2010), and it has been demonstrated in the mouse that oestrogen signalling induces HSC cell division, and that HSCs divide more frequently in females than males (Nakada *et al.*, 2014). In light of the differences in endometrial SPP1 expression observed it would be interesting to investigate haematopoiesis at this stage of gestation using *in vitro* colony forming unit assays.

Binding of SPP1 to the αVβ3 receptor has been demonstrated to activate the Akt (Protein Kinase B)/eNOS (endothelial nitric oxide synthase) signalling pathway, leading to increased proliferation, migration and tube formation of endothelial cells *in vitro* (Dai *et al.*, 2009; Wang *et al.*, 2011). Dunlap *et al.*, (2008) demonstrated in the sheep a relationship between uterine von Willebrand Factor (vWF) staining and SPP1, and that uterine arterial endothelial cells produce SPP1 during angiogenesis *in vitro*. Analysis of GD9, 12 and 15 porcine endometrial samples identified the presence of a 32kDA fragment of SPP1, which is known to bind to the cell surface of endothelial cells (Erikson *et al.*, 2009b; Bayless *et al.*, 2010). In these studies, *in vitro* experiments using blood samples from newborn piglets demonstrated that SPP1 has a positive effect on the migration and adhesion of endothelial cells, suggesting a potential role in regulating placental and endometrial angiogenesis. At the pig feto-maternal interface, there are two keys stages of gestation when angiogenesis occurs. The first is at ~GD13-18 (Keys *et al.*, 1986), which corresponds to the period of conceptus attachment, and the second wave of angiogenesis occurs at approximately GD50 (Vonnahme *et*

al., 2001), which corresponds to the period when placental growth is beginning to plateau and the foetus is about to undergo exponential growth. Therefore, considering the role of SPP1 and αVβ3 during implantation (Erikson *et al.*, 2009a; Frank *et al.*, 2017) and the differences in endometrial *SPP1* observed at GD60, it could be hypothesised that SPP1 has an additional role in inducing angiogenesis during this period, which should be investigated further.

As detailed in 4.1.3, mouse integrin, SPP1 and FN knockout mice have been generated which have highlighted the role of integrin signalling in placental and embryonic development. Similarly, uterine injection with antibodies against ITGαV and ITGβ3 in mice and rabbits resulted in fewer implantation sites (Illera *et al.*, 2000, 2003); highlighting the importance of signalling through this receptor during implantation. An intricate siRNA knockdown experiment highlighted the role of the ITGαV in implantation, with decreased adherence to FN and SPP1, decreased number of aggregates, and decreased spreading ability of the cells on SPP1 observed in porcine trophoblast cells with the ITGαV knockdown (Frank *et al.*, 2017). Despite these studies, relevant *in vivo* knockdown and/or knockout experiments in the sheep and pig have not been performed which, due to the differences in implantation between mice and domestic animals, would further improve the understanding of the role of integrin signalling in development.

The experiments performed in this study have investigated the mRNA expression of the candidate genes of interest. It is important to remember that the mRNA expression levels do not necessarily translate to the protein levels present (Maier *et al.*, 2009; Koussounadis *et al.*, 2015). Hernandez *et al.*, (2013) suggested that there might be breed specific differences in SPP1 post-translational modifications, outlined by the differences in SPP1 protein at the feto-maternal interface in foetus of different size between hLW and MS pigs. Therefore, it is essential to fully understand the mechanisms governing foetal growth that both mRNA and protein are investigated. Due to time limitations and problems with antibody validation, it was not possible to examine the protein expression of all candidates in all tissues in this thesis however, it will be important in the future to validate the results of interest on a protein level.

Whilst foetal size and sex were not found to influence uterine gland SPP1 staining, they may influence uterine LE or placental protein staining. A semi-quantitative approach was devised to attempt to quantify LE staining at GD60 and 90 (Appendix; Supplementary Figure 10-Supplementary Figure 11). Unfortunately, this method appeared to be subjective therefore an alternative approach should be devised for more accurate analysis of this staining in relation to foetal size and sex. Due to the expression of integrin receptors and their ligands by the uterine LE, the LE thickness was quantified in SPP1 stained endometrial samples to determine if there was a relationship between LE thickness and 1) percentage prenatal survival, 2) litter size, 3) foetal weight (actual weight and lightest/CTMLW classification), and 4) foetal sex (Supplementary Figure 12).

4.6 **Conclusion**

In this study a comprehensive temporal analysis of the mRNA expression of key integrin subunits, *FN* and *SPP1* throughout gestation in both placental and endometrial samples was performed, identifying previously undescribed temporal changes in integrin expression. The investigations identified that the placental expression of *ITGα2* and the endometrial expression of *ITGβ1* and *SPP1* are associated with foetal size. Novel associations between foetal sex and the expression of *ITGβ3*, *ITGβ6, SPP1* and *FN* at the feto-maternal interface have been observed. The results presented in this chapter are intriguing and the mechanisms behind these differences warrant further investigation, especially during preimplantation development and early pregnancy.

5 Apoptosis and Proliferation at the Feto-Maternal Interface

5.1 Introduction

5.1.1 Apoptosis

Programmed cell death is an essential part of prenatal development and the maintenance of tissue homeostasis postnatally (Fuchs and Steller, 2011). Whilst multiple forms of programmed cell death exist, apoptosis is the best characterised. Cells which undergo apoptosis have a characteristic morphology defined by the maintenance of the integrity of the plasma membrane, cell shrinkage, pyknosis and karyorrhexis and the formation of apoptotic bodies (Elmore, 2007). Apoptosis can be divided into two pathways, the extrinsic and the intrinsic apoptotic pathways, which are also known as the death-receptor and stress pathways respectively (Cory and Adams, 2002).

The extrinsic apoptosis pathway acts through binding of pro-apoptotic ligands to death receptors, which are tumour necrosis factor (TNF) transmembrane receptors that contain a 'death domain' composed of a conserved region of approximately 80 amino acids (Ashkenazi and Dixit, 1998; Locksley *et al.*, 2001) (Figure 5.1). Several ligands can bind to these transmembrane receptors to activate the apoptotic cascade including Fas ligand (FasL) to the Fas receptor (FasR) and TNFα to TNF receptor 1 (TNFR1) (Smith *et al.*, 1994; Nagata and Golstein, 1995; Nagata, 1997). Following binding of the ligand to the death receptor, adaptor proteins which recognise the death domain are recruited, for example in FasL/FasR signalling, the adaptor protein Fas-associated death domain (FADD) is recruited. The adaptor proteins then recruit inactive caspase 8 (procaspase 8) to form a complex known as the death inducing signalling complex (DISC) (Scott *et al.*, 2009), which leads to activation of procaspase 8. The activation of caspase 8 is important as the active from proceeds to activate procaspase 3 and 7, ultimately leading to cell death (Fuentes-Prior and Salvesen, 2004).

The intrinsic apoptosis pathway is tightly regulated by the B-cell lymphoma 2 (Bcl2) family of proteins (Cory and Adams, 2002). This family consists of both pro- and anti-apoptotic proteins and the balance and interaction between these family members is essential for ensuring appropriate regulation of cell death. Examples of pro-apoptotic Bcl2 family members include Bcl-2-associated X protein (Bax) and Bcl-2 homologous antagonist/killer (Bak), and anti-apoptotic Bcl2 family members include Bcl2 and Bcl2-xL. In response to cell stressors, for example DNA damage, tumour suppressor protein 53 (P53) is upregulated which initiates a cascade of events (Figure 5.1). P53 increases the expression of P53 upregulated modulator of apoptosis (PUMA) and Phorbol-12-myristate-13-acetate-induced protein 1 (NOXA), which have sequence homology with a specific region characteristic of the Bcl2 family, the Bcl-2 homology 3 (BH3) domain. PUMA transduces the apoptotic signals to the mitochondrion, where it binds to several anti-apoptotic Bcl2 family members, preventing the inhibitory effects that they usually have on pro-apoptotic Bcl2 family members. NOXA is not thought to play as dominant a role as PUMA in the regulation of P53 dependent apoptosis, as it selectively interacts with Bcl2 the family members Mcl-1 and A1 (Chen *et al.*, 2005; Ploner *et al.*, 2008). In addition to the central role of PUMA in regulating P53 dependent apoptosis, PUMA is also thought to be activated by transcription factors to induce cell death in a P53 independent manner (Jeffers *et al.*, 2003; Yu and Zhang, 2003, 2009). Further, it has been shown that the promoter for Bax contains four motifs which correspond to P53 binding sites (Toshiyuki and Reed, 1995), suggesting a direct effect of P53 on Bax.

Anti-apoptotic Bcl2 family members, for example Bcl2, are localised to the outer membrane of mitochondrion and function to maintain their structural integrity. Following the induction of P53 dependent apoptosis, Bcl2 no longer maintains the structural integrity of the outer membrane and Bax and Bak homo-oligomerise to form pores in the outer mitochondrial membrane, allowing the release of apoptotic proteins such as cytochrome C into the cytoplasm (Westphal *et al.*, 2011). This release of cytochrome C activates the protein apoptotic protease-activating factor-1 (Apaf-1), that forms a complex which

can recruit and activate caspases. This happens in a sequential manner, initially with the initiator caspase 9 to form the apoptosome, followed by effector caspases 3 and 7 (Zou *et al.*, 1997; Bratton *et al.*, 2001).

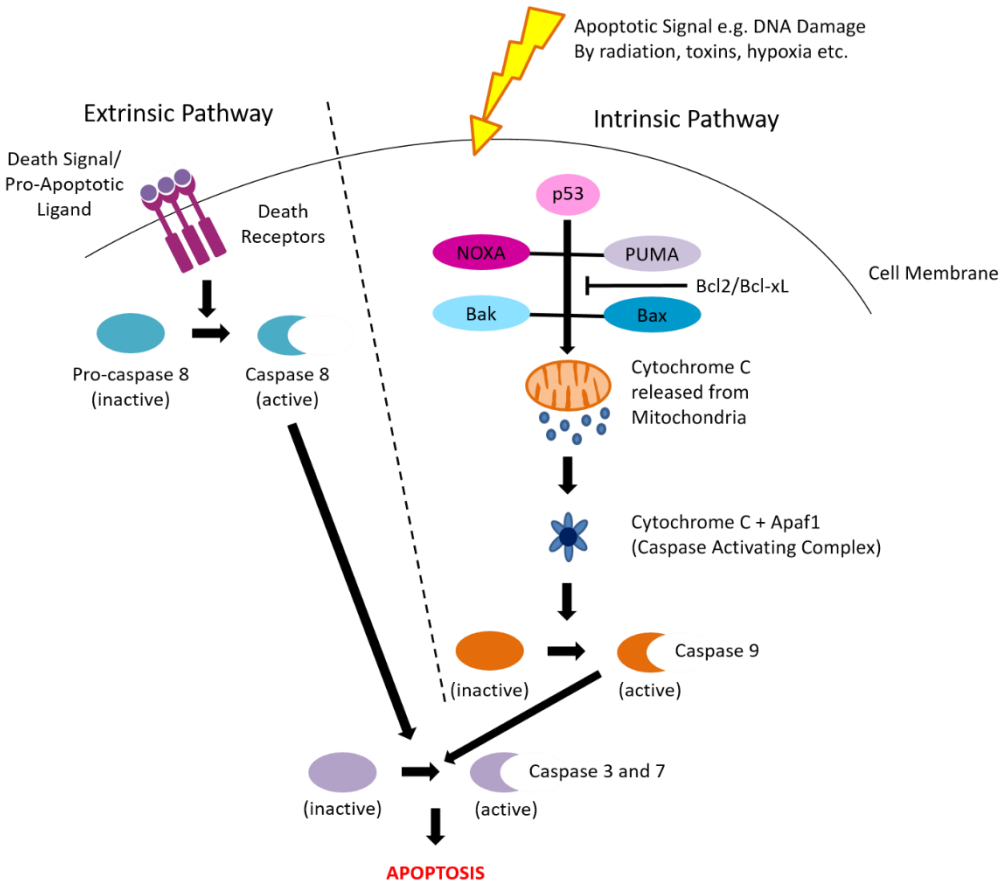

Figure 5.1: Extrinsic and Intrinsic Apoptosis Pathways.

Extrinsic cell death occurs by ligands containing a death motif binding to transmembrane death receptors, which induces the recruitment of adaptor proteins. The adaptor proteins then recruit inactive caspase 8 (procaspase 8) to form a complex known as the death inducing signalling complex (DISC), in turn activating procaspase 8. The active caspase 8 proceeds to activate procaspase 3 and 7, leading to apoptosis. The intrinsic cell death pathway is tightly regulated by the Bcl2 family of proteins. In response to an apoptotic signal, the tumour suppressor protein P53 is activated which increases the expression of P53 upregulated modulator of apoptosis (PUMA) and Phorbol-12-myristate-13-acetate-induced protein 1 (NOXA). PUMA transduces the apoptotic signals to the mitochondrion, where it binds to several anti-apoptotic Bcl2 family members, including Bcl2 and Bcl2-xL, preventing their usual inhibitory effects on pro-apoptotic Bcl2 family members Bax and Bak. Following the induction of P53 dependent apoptosis, Bcl2 no longer maintains the structural integrity of the outer mitochondrial membrane and Bax and Bak homo-oligomerise to form pores in the outer mitochondrial membrane, allowing the release of apoptotic proteins such as cytochrome C into the cytoplasm. This release of cytochrome C activates the protein apoptotic protease-activating factor-1 (Apaf-1), that forms a complex which can sequentially activate caspases, initially with the initiator caspase 9, followed by effector caspases 3 and 7.

5.1.2 Proliferation

Cell proliferation describes the process by which cell number increases, by the cell increasing in size before dividing equally to form two daughter cells (reviewed by Golias *et al.*, 2004; Berridge, 2014). Cells which are not undergoing proliferation are described as resting, or in the zero growth (G0) stage of the cell cycle (Figure 5.2). Growth factors stimulate the resting cell to enter the cell cycle, where the cell can be described as entering the first growth (G1) phase. The G1 phase is primarily controlled by growth factors, accompanied by cell cycle signalling in the form of cyclin D and E. After the restriction point in the cell cycle, which occurs at the end of the G1 phase, the cell is committed to undergo the remainder of the cell cycle, which is regulated exclusively by cell cycle signalling. The cell then undergoes DNA synthesis (S phase), where the chromosomes are duplicated, and then enters the second growth phase (G2). Following this, the cell undergoes mitosis (M Phase) to produce two daughter cells which themselves are in the G0 cell cycle phase. The M phase is subdivided into a series of sequential steps: prophase, metaphase, anaphase, telophase, followed by cytokinesis, to ensure the cell divides into two equally sized cells, which contain the same information as the mother cell. This process is tightly regulated, maintaining a delicate balance between increasing cell number, cell death, and the differentiation of cells *in vivo*.

As described above, the entry of the cell into the G1 phase of the cell cycle is regulated by growth factors. Growth factors bind to their corresponding receptors, initiating a signalling cascade which eventually induces cell proliferation and migration. Several pathways have been demonstrated to induce cell proliferation, examples of which are illustrated in Figure 5.3. Due to the importance of the cell cycle in the maintenance of tissue homeostasis, several methods to investigate proliferation have been utilised (Romar *et al.*, 2016). However, in samples that have been fixed or frozen the options to investigate proliferating cells are more limited. Ki67 (or MKI67) is expressed in the active stages of the cell cycle, but not the G0 phase therefore it can be used to investigate cell proliferation (Bologna-Molina *et al.*, 2013). An

alternative method can be to investigate Proliferating Cell Nuclear Antigen (PCNA), which allows identification of cells in the S phase of the cell cycle (Bologna-Molina *et al.*, 2013).

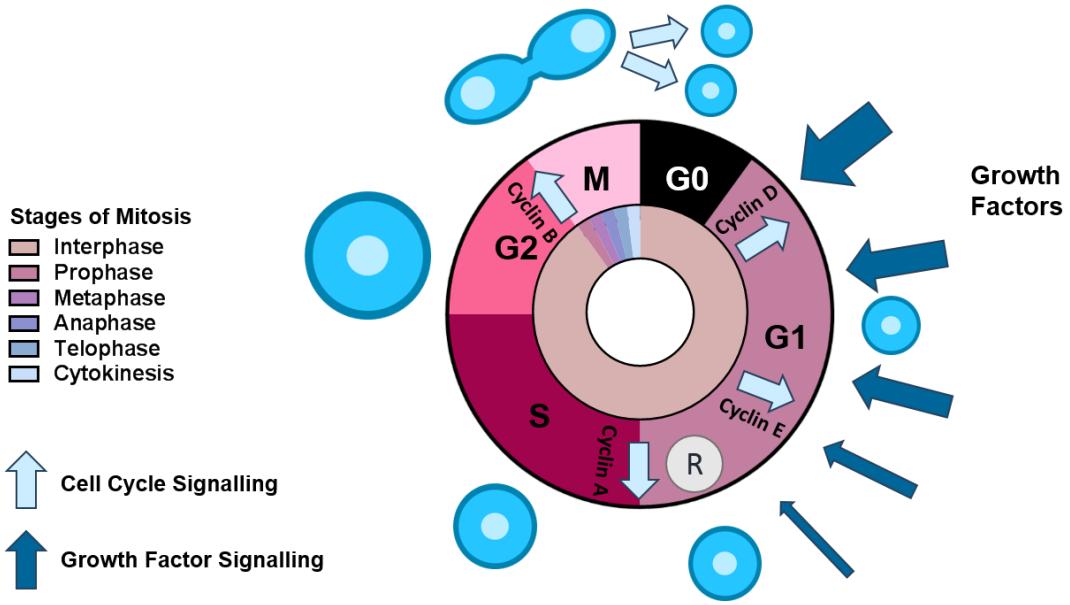

Figure 5.2: Operation of the Growth Factor and Cell Cycle Signalling Systems during Different Phases of the Cell Cycle.

Cells which are not undergoing proliferation are described as resting, or in the zero growth (G0) stage of the cell cycle. Growth factors (dark blue arrows) stimulate the resting cell to enter the cell cycle, where the cell can be described as entering the first growth (or G1) phase. The G1 phase is primarily controlled by growth factors, accompanied by cell cycle signalling (light blue arrows) in the form of cyclin D and E After the restriction point in the cell cycle (R) which occurs at the end of the G1 phase, the cell is committed to undergo the remainder of the cell cycle, which is regulated exclusively by cell cycle signalling. During the cell cycle, the cell significantly increases in size, whilst remaining in the interphase stage of mitosis. When the cell has reached the appropriate size and maturity, it undergoes the remaining stages of mitosis to produce two daughter cells which are in the G0 cell cycle phase. Redrawn and modified from Berridge, (2014).

5.1.3 Apoptosis and Proliferation in Pregnancy

5.1.3.1 Role of Apoptosis and Proliferation in Pregnancy

As outlined in the general introduction, the establishment and maintenance of pregnancy requires significant changes in uterine structure and function. Apoptosis is well characterised in the human placenta and has been demonstrated to be essential for trophoblast invasion, differentiation and survival (Marzusch *et al.*, 1995; Huppertz and Kaufmann, 1999; Mayhew *et al.*, 1999; Levy *et al.*, 2000; Straszewski-Chavez *et al.*, 2005; Huppertz *et al.*, 2006; Heazell and Crocker, 2008; Kang and Rosenwaks, 2018). Dysregulated apoptosis has been linked to pregnancy complications including gestational trophoblast disease (Halperin *et al.*, 2000; Chiu *et al.*, 2001), preeclampsia (Allaire *et al.*, 2000; Leung *et al.*, 2001; Levy, 2005; Cali *et al.*, 2013; Can *et al.*, 2014) and intrauterine growth restriction (IUGR) (Smith *et al.*, 1997; Ishihara *et al.*, 2002; Jeschke *et al.*, 2006; Karowicz-Bilińska *et al.*, 2007; Heazell *et al.*, 2011; Longtine *et al.*, 2012; Börzsönyi *et al.*, 2013; Cali *et al.*, 2013) highlighting the importance of appropriately regulated cell death at the feto-maternal interface in foetal and placental development.

Knockout mouse models have been utilised to improve the understanding of the functions of apoptotic genes in pregnancy. Bax knockout mice were viable, although cell lineage specific alterations in cell death were observed in the offspring (Knudson *et al.*, 1995). Female Bax knockout mice were fertile although an accumulation of atretic follicles, with atrophic granulosa cells was noted. In contrast, knockout males were infertile, with highly disorganised seminiferous tubules and no mature spermatozoa present. The phenotype of Bcl2 null mice is more severe, with growth restriction observed at birth and early mortality observed in postnatal life due to immunodeficiency and renal failure from polycystic kidneys (Nakayama *et al.*, 1993; Veis *et al.*, 1993). When both Bax and Bak were knocked out, only 10% of embryos survived and those that did survive had defective central nervous system (CNS) and haematopoietic systems (Lindsten *et al.*, 2000). Uterine specific P53 knockout mice had an elevated rate of preterm birth compared to control mice, which was demonstrated to occur through activation of the Cyclooxygenase-2

(COX2)/Prostaglandin F2α (PGF2α) signalling pathway (Hirota *et al.*, 2010). Sexual dimorphism has been demonstrated in P53 knockout mice, with decreased implantation rate, pregnancy rate and litter size observed when matings were carried out using female P53 null mice, but not with male P53 null mice (Hu *et al.*, 2007). Hu *et al.*, (2007) also demonstrated that Leukaemia Inhibitory Factor (LIF) expression is regulated by P53. LIF is known to play a central role in the pig uterus, with the endometrium secreting LIF during the preimplantation period, peaking at gestational day (GD) 12 (Anegon *et al.*, 1994; Blitek *et al.*, 2012), which binds to the LIF receptor expressed by the conceptus. Therefore, it could be hypothesised that endometrial P53 expression may play a role in regulating implantation in the pig via Lif signalling.

5.1.3.2 Specific Role of Apoptosis and Proliferation in Porcine Pregnancy

Due to the extensive remodelling that occurs at the porcine feto-maternal interface, it is not surprising that apoptosis and proliferation at this site are thought to be vital for the establishment and maintenance of pregnancy.

Several transcriptomic analyses have identified potential roles of apoptosis and proliferation during gestation in the pig. An increased number of genes involved in apoptosis and proliferation was observed when comparing gene expression of pregnant endometrium with non-pregnant endometrium at GD14, suggesting a potential role of these processes in implantation (Østrup *et al.*, 2010). It has been demonstrated, by deep sequencing, that at GD14 endometrial samples highly express genes associated with proliferation, apoptosis and anti-apoptosis (Samborski *et al.*, 2013a). The high expression of both apoptotic and anti-apoptotic genes highlights the tight regulation of endometrial apoptosis during this critical stage of pregnancy, with conceptus secreted molecules potentially regulating endometrial apoptosis and proliferation to allow the establishment of pregnancy, and subsequent placentation. Samborski *et al.*, (2013b) demonstrated increased expression of

genes involved in apoptosis and proliferation in the pregnant porcine endometrium at GD12 compared to control animals. Similarly, Kiewisz *et al.*, (2014) found that cell death and survival was one of the top 15 molecular pathways identified when performing a transcriptomic analysis on endometrial samples at GD12 and 16 compared to cyclic animals. At GD16, cellular growth and proliferation was also one of the top 15 pathways identified.

Cristofolini *et al.*, (2013) identified apoptotic cells throughout gestation in the porcine placenta and, at GD60, apoptotic bodies were observed in phagocytes present in the endometrial stroma. The apoptotic index, which describes the relationship between the number of cells with fragmented DNA and the number of total cells, in placental villi was high at GD28, before decreasing to a low level at GD60, and increasing to the highest detected level at GD114. The initially high levels of apoptosis in early pregnancy presumably reflects the extensive remodelling that occurs at the feto-maternal interface to establish pregnancy and begin placental development. The decrease in apoptotic index in mid-pregnancy corresponds to the plateauing of placental growth, whilst foetal growth is starting to occur exponentially. An exceptionally high apoptotic index was observed at GD114, coinciding with parturition in the pig, which presumably would assist with the expulsion of foetal tissues during farrowing. Okano *et al.*, (2007) has reported extensive apoptosis in the porcine uterus at 13 days post-partum, suggesting a role of apoptosis in remodelling the uterus during uterine involution. A similar role of apoptosis in parturition has been suggested in both Holstein and Nelore breeds of cattle (Martins *et al.*, 2004). These findings suggest the critical nature of appropriate and regulated apoptosis for the prevention of abortion and preterm labour and thus maintenance of a successful pregnancy.

Cellular FLICE (FADD-like IL-1β-converting enzyme)-Inhibitory proteins (c-FLIP) proteins are important inhibitors of extrinsic apoptosis, which function by suppressing the activation of caspase 8 and 10 (Safa, 2012). Previously c-FLIP mRNA and protein has been identified in human placentas in early and late gestation and has been proposed to play a central role in regulating cell survival in the human placenta (Ka and Hunt, 2006). In addition, c-FLIP has

been demonstrated to be moderately expressed in many structures in both placental and endometrial porcine samples at GD28 and 60, with weaker staining observed at GD114 (Cristofolini *et al.*, 2013). The expression of c-FLIP, which inhibits extrinsic apoptosis, suggests that intrinsic apoptosis occurs at the porcine feto-maternal interface. Cristofolini *et al.*, (2013) also indicated that Bax is expressed at the feto-maternal interface in early and late gestation, which would provide further evidence for the activation of the intrinsic apoptotic pathway in these periods of gestation. Merkis *et al.*, (2010) demonstrated that FasL is moderately expressed on a protein level in the placental villi and uterine connective tissue and glands at GD55, but this was not observed at GD30 or 114; suggesting potential temporal regulation of apoptosis at the feto-maternal interface.

FasL and FasR have been demonstrated to play a central role in apoptosis by the extrinsic pathway (Caulfield and Lathem, 2014). Tayade *et al.*, (2006) demonstrated increased *FasL* expression in pregnant porcine endometrial samples at GD15-23 compared to non-pregnant control endometrium. In addition, *FasL* and *FasR* expression were increased in endometrial samples associated with arresting conceptuses compared to healthy conceptuses at GD21 and 23. In the corresponding trophoblast cells, FasR was also found to be increased in samples associated with arresting conceptuses compared to healthy conceptuses. However, *FasL* expression was decreased in trophoblasts associated with arresting conceptuses compared to healthy conceptuses.

Appropriately regulated proliferation is essential for the establishment and maintenance of a successful pregnancy. Growth factors have a central role in the establishment and maintenance of pregnancy and it has been demonstrated that several of these factors can influence proliferation at the feto-maternal interface. Supplementary Table 4 contains examples of factors which have been suggested to play a role in regulating proliferation by interacting pathways at the porcine feto-maternal interface. Importantly, it has been demonstrated that Epidermal Growth Factor (EGF), Insulin-like Growth Factor-1 (IGF1), Vascular Endothelial Growth Factor (VEGF) and Colony

Stimulating Factor 2 (CSF2) and their receptors are expressed at the feto-maternal interface during implantation (reviewed by Jeong and Song, 2014). Recent publications have demonstrated that these factors activate Phosphatidylinositol-3 kinase (PI3K)- protein kinase B (AKT) and Mitogen-activated Protein Kinase (MAPK) signalling pathways to induce proliferation and/or migration of porcine trophectoderm cells *in vitro* (Figure 5.3; Supplementary Table 4). In response to binding of IGF1, VEGF and CSF2 to their corresponding receptors, cross-talk is observed between the PI3K and extracellular signal-regulated kinase 1/2 (ERK1/2) MAPK signalling pathways. However, in response to EGF binding, the PI3K and ERK1/2 MAPK signalling pathways do not interact with one another. Jeong *et al* demonstrated, by the use of inhibitors of these signalling pathways, that these factors are critical for regulating the proliferation and migration of trophectoderm cells, accompanied by changes in gene expression, during early pregnancy. These findings suggest a central role of these pathways in regulating proliferation at the porcine feto-maternal interface.

5.1.4 Evidence for the Role of Apoptosis and Proliferation in IUGR

As described above, appropriate regulation of apoptosis and proliferation are essential for regulating the establishment and maintenance of pregnancy in several species. Considering this, dysregulation of apoptosis and proliferation at the feto-placental interface could be hypothesised to play a role in pregnancy pathology.

In human IUGR, aberrant regulation of apoptosis has been heavily implicated (reviewed by Heazell and Crocker, 2008; Scifres and Nelson, 2009). Placentas associated with IUGR infants at term have increased apoptosis compared to those supplying normally-grown infants (Smith *et al.*, 1997; Barrio *et al.*, 2003). More specifically, Karowicz-Bilińska *et al.*, (2007) found decreased Bcl2 (anti-apoptotic) trophoblast protein expression, accompanied by increased trophoblast and decidual protein expression of Bax (pro-apoptotic) in IUGR placentas compared to those supplying normally-grown infants. Börzsönyi *et*

al., (2013) performed quantitative polymerase chain reaction (qPCR) and demonstrated, from a whole tissue perspective, decreased *Bcl2* expression, but no alterations in *Bax* expression, in term placental samples supplying IUGR infants compared to those supplying normally-grown infants. The authors demonstrated no correlation between the 'degree of growth restriction' observed at birth and placental *Bax* or *Bcl2* expression. In addition to these valuable studies, apoptosis in cytotrophoblasts and synctiotrophoblasts in human term IUGR placentas has been investigated. It has been demonstrated on both an mRNA and protein level that P53, P21 and Bax, but not Bcl2 or Mdm2 expression are increased in term human IUGR placentas, specifically in synctiotrophoblasts, compared to those supplying normally-grown infants (Heazell *et al.*, 2011).

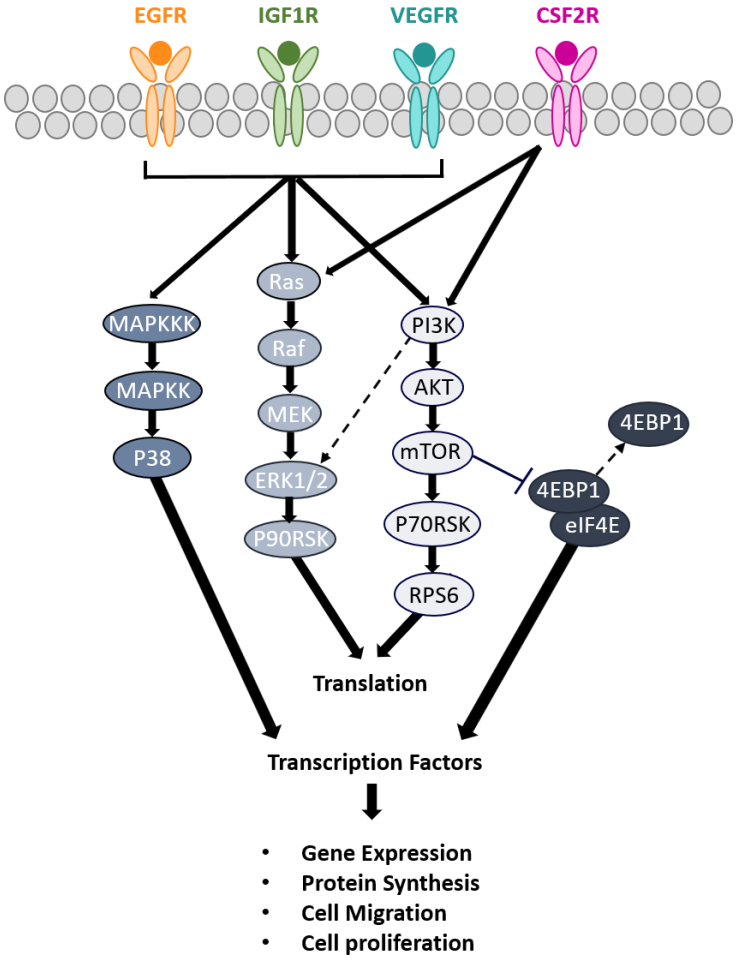

Figure 5.3: EGF, IGF1, VEGF and CSF2 binding to their receptors activate porcine trophectoderm proliferation and migration.

EGF, IGF1, VEGF and CSF2 activate PI3K-AKT and MAPK signalling pathways to induce proliferation and/or migration of porcine trophectoderm cells *in vitro*. In response to binding of IGF1, VEGF and CSF2 to their corresponding receptors, cross-talk is observed between the PI3K- and ERK1/2 MAPK signalling pathways. However, in response to EGF binding, the PI3K and ERK1/2 MAPK signalling pathways do not interact with one another. These factors are critical for regulating the proliferation and migration of trophectoderm cells, accompanied by changes in gene expression, during the early stages of pregnancy in the pig; suggesting a central role of these pathways in regulating proliferation at the porcine feto-maternal interface. Abbreviations used: EGF(R)=Epidermal Growth Factor (Receptor); IGF1(R)=Insulin-Like Growth Factor 1 (Receptor); VEGF(R)=Vascular Endothelial Growth Factor (Receptor), CSF2(R)=Colony Stimulating Factor 2 (Receptor); MAPK(KK)=Mitogen-activated protein kinase (kinase kinase); ERK1/2=extracellular signal-regulated kinase 1/2; PI3K=Phosphatidylinositol-3 kinase; AKT=protein kinase B; mTOR=mechanistic target of rapamycin; RPS6=Ribosomal Protein S6; 4EBP1=4E Binding Protein 1; eIF4E=Eukaryotic Translation Initiation Factor 4E. Redrawn from Jeong and Song, (2014).

Ishihara *et al.*, (2002) and Barrio *et al.*, (2003) also suggest, by Terminal deoxynucleotidyl transferase dUTP nick end labelling (TUNEL) staining, that increased apoptosis is present in both cytotrophoblasts and synctiotrophoblasts in IUGR placentas although, in contrast to Heazell *et al.*, (2011), Ishihara *et al.*, (2002) observed decreased Bcl2 protein expression in synctiotrophoblasts of placentas supplying IUGR infants compared to normally-grown infants. Jeschke *et al.*, (2006) instead investigated proliferation and P53 staining, and demonstrated that whilst proliferation was not altered, P53 staining was decreased in the cytotrophoblasts of placentas associated with IUGR infants compared to normally-grown infants. Longtine *et al.*, (2012) suggest that placentas supplying IUGR infants have increased cytotrophoblast apoptosis compared to placentas supplying normal-sized infants.

Whilst extensive research has been performed investigating placental apoptosis in instances of IUGR in term human placentas, to date there have been limited investigations into this area in the pig. Proteomic analysis of porcine placental and endometrial samples associated with IUGR and normal body weight (NBW) foetuses at GD60, 90 and 110 revealed alterations in the apoptotic and proliferation pathways (Chen *et al.*, 2015). Placental expression of CTSZ (proteinase) and CSTB (protease inhibitor) were upregulated in placentas supplying IUGR foetuses compared to NBW foetuses at GD90, suggesting increased apoptosis and increased expression of inhibitors that are attempting to protect against apoptosis. The expression of serpins (ACT2, ACT3 and serpin A3-6) were upregulated in endometrial samples associated with IUGR foetuses compared to NBW foetuses, indicating increased apoptotic stress at the feto-maternal interface. In addition, components of the proliferation pathway were downregulated in placentas (Eukaryotic Translation Initiation Factor 5A2 (EIF5A2), Eukaryotic Translation Initiation Factor 6 (EIF6), Aspartyl-tRNA synthetase (AspRs), and Zinc Finger Protein 420 (ZFP 420)) and endometrium (Eukaryotic Translation Elongation Factor 1 (eEF1A-1), and Heterogeneous Nuclear Ribonucleoprotein K (HNRNPK)) associated with IUGR foetuses compared to those associated with NBW foetuses.

The increased expression of components of the apoptotic pathways demonstrated by Chen *et al.*, (2015), indicates heightened apoptosis and oxidative stress at the feto-maternal interface in instances of IUGR, which in turn would be hypothesised to have striking effects on placental and foetal growth and development. In addition, the decreased expression of components of the proliferation pathway suggests that placentas associated with IUGR are proliferating less, which may contribute to the decreased placental size associated with IUGR foetuses (Blomberg *et al.*, 2010). It is known that remodelling of the placental bilayer occurs to increase the surface area available for exchange with the developing foetus, with the width of the bilayer increasing from GD65 to 105 (Vallet and Freking, 2007). Further, the authors demonstrated a significantly wider bilayer in GD65, 85 and 105 placentas supplying the smallest foetuses compared to the largest foetuses. They also demonstrated that the stroma above the CAM decreased in size at a faster rate in the placentas supplying the smallest foetuses compared to the largest foetuses. The data observed at GD45 followed the same pattern however it was not statistically significant, which may be attributed to the smaller sample size in this group. Considering this, it is thought that to compensate for having smaller placentas, the width of the bilayers of placentas supplying small foetuses increase at a faster rate to form larger folds, thereby providing a larger area for exchange and improving the efficiency of the placenta. To accommodate this remodelling event at the feto-maternal interface, it would be expected that significant apoptosis and proliferation would occur.

5.2 Hypotheses

It is hypothesised that the expression of candidate genes involved in apoptosis will be increased, and the expression of proliferation associated genes will be decreased in placental and endometrial samples associated with the lightest foetuses compared to their normal-sized littermates. In addition, it is hypothesised that the expression of candidate genes involved in apoptosis will be increased, and the expression of proliferation associated genes will be decreased in placental and endometrial samples supplying male foetuses compared to their female littermates.

5.3 Aims

The aims of the research described in this chapter were:

i. To investigate the expression of candidate genes (*Bax*, *Bcl2*, *Bax: Bcl2* Ratio, *P53* and *Ki67*) involved in apoptosis and proliferation throughout gestation by qPCR on placental and endometrial samples at GD18, 30, 45, 60 and 90.
ii. To investigate the relationship between foetal size and apoptosis and proliferation at the feto-maternal interface by performing qPCR for the candidate genes (*Bax*, *Bcl2*, *Bax:Bcl2* Ratio, *P53* and *Ki67*) on placental and endometrial samples supplying the lightest and closest to mean litter weight (CTMLW) conceptuses or foetuses at GD18, 30, 45, 60 and 90.
iii. To investigate the relationship between foetal sex and apoptosis and proliferation at the feto-maternal interface by performing qPCR for the candidate genes (*Bax*, *Bcl2*, *Bax: Bcl2* Ratio, *P53* and *Ki67*) on placental and endometrial samples supplying male and female foetuses at GD30, 45, 60 and 90.
iv. To investigate temporal changes in placental apoptosis by TUNEL staining of placental samples at GD45 and 60.
v. To investigate the relationship between foetal size and apoptosis by TUNEL staining of placental samples at GD45 and 60.

vi. To investigate the relationship between foetal sex and apoptosis by TUNEL staining of placental samples at GD60.

5.4 Materials and Methods

5.4.1 qPCR

The RNA extracted from placental (GD30, 45, 60 and 90; n=6, 6, 6 and 8 litters respectively), and endometrial (GD18, 30, 45, 60 and 90; n=5, 5, 6, 6 and 6 litters respectively) samples described in 2.2.3 were utilised. Complementary DNA was synthesised as described in 2.2.7 and diluted 1:25 with nuclease free water. The candidates of interest were *Bax*, *Bcl2*, *P53* and *Ki67*. The ratio of *Bax: Bcl2* expression was calculated using the normalised values for each sample. The primer sequences for these candidates are detailed in Table 5.1. All qPCRs were performed for 40 cycles with an annealing temperature of 60^{o}C (2.2.8.2).

The GeNorm experiment (2.2.8.4) identified that multiple genes were stable in both tissues and that the optimal number of reference genes for each tissue based on use of the most stable reference genes was two. The most stable reference genes for this experiment were *TBP1* (TATA box binding protein) and *HPRT1* (Hypoxanthine phosphoribosyltransferase 1) for the placenta and *TBP1* and *YWHAZ* (Tyrosine 3-monooxygenase/tryptophan 5-monooxygenase activation protein, zeta polypeptide) for the endometrium. The primer sequences are detailed in Table 2.4 and the reference genes were run for all samples. All data were scaled to the minimum sample and were imported into qBase+ (Biogazelle) and data for each candidate gene were normalised to the reference gene expression.

Gene Symbol	Gene Name	Accession Number	Primer Sequence (5'→ 3')		Amplicon Size (bp)	Reference
Bax	BCL2 associated X	XM_003127290.5	Fwd	CCGAAATGTTTGCTGACG	154	Zhao *et al.*, (2014)
			Rev	AGCCGATCTCGAAGGAAGT		
Bcl2	B-cell lymphoma 2	XM_021099593.1	Fwd	GATAACGGAGGCTGGGATGC	147	n/a
			Rev	CTTATGGCCCAGATAGGCACC		
P53	Tumour protein p53	NM_213824.3	Fwd	GCCACTGGATGGCGAGTATT	84	n/a
			Rev	TCCAAGGCGTCATTCAGCTC		
Ki67	Ki67	NM_001101827.1	Fwd	AGTCTGTAAGGAAAGCCACCC	119	n/a
			Rev	ACAAAGCCCAAGCAGACAGG		

Table 5.1: Primer Sequences for qPCR of Candidate Genes.

This table summarises the gene abbreviation and name, accession number, primer sequences (Fwd = Forward, Rev = Reverse), amplicon size and the source of the primer sequences. bp=base pairs. n/a indicates that the primer pair were designed specifically for this experiment using NCBI Primer Blast.

5.4.2 TUNEL Staining

To investigate apoptosis in the Bouin's fixed paraffin embedded GD45 and 60 placental samples, a TUNEL assay was performed. This assay allows identification of single- and double-stranded breaks associated with apoptosis by enzymatically labelling the free 3'-OH termini with modified nucleotides by use of terminal deoxynucleotidyl transferase (TdT). Normal or proliferating nuclei do not stain with this method, allowing specific identification of the cells that have undergone apoptosis.

For this experiment, placental samples supplying the true lightest and true closest to mean litter weight (CTMLW) foetuses at GD45 and 60 (n=4 and 6 litters respectively) were used. The TUNEL assay was performed using the ApopTag plus Peroxidase *In Situ* Apoptosis Detection Kit (S7101, (Merck Millipore, Cork, Ireland) as per the manufacturer's instructions. As a positive control, a slide of normal female rat mammary gland 3-5 days post-weaning was used (provided with the kit). As a negative control, CTMLW female GD45 and GD60 placental sections were treated with PBS instead of TDT enzyme.

The slides were imaged using the NanoZoomer slide scanner (Hamamatsu, Welwyn Garden City, U.K.). The placental stromal and the chorioallantoic membrane (CAM) regions were not directly comparable with one another therefore 6 images were taken of both regions at x20 magnification from 2 sections per sample from the slide scans. For the stromal image analysis, positively stained cells and negative cells were counted in each image and the data were expressed as the number of positive cells per total number of cells counted. As the images were all taken at the same magnification, they occupied the same area. For the CAM, the positively stained cells in the CAM region were counted and the area of the CAM region in each image was measured. This was then expressed as the number of positively stained cells per 10,000μm^2 area to allow direct comparison between samples.

5.4.3 Statistical Analysis

Statistical analyses were performed following the general protocol outlined in 2.5. Mean values were taken for each parameter and the normality of the data was assessed, with transformations performed as required.

5.4.3.1 Analysis of mRNA Expression Data for Candidate Genes involved in Apoptosis and Proliferation

Log10 transformations were required for placental *Ki67*, *Bax*, and *Bax: Bcl2* ratio, and endometrial *Ki67*, *P53* and *Bcl2* expression data on all GD investigated. Placental *P53* and endometrial *Bax* and *Bax: Bcl2* ratio expression data did not require log10 transformation. Placental *Bcl2* expression required log10 transformation at GD30, 45 and 90 however, at GD60 these data did not have a normal data distribution, regardless of transformation. A two-way ANOVA for sex x size, with and without a block for gilt was performed to investigate the presence of sex x size interactions on GD30, 60 and 90 on occasions where the data had a normal distribution.

5.4.3.2 Analysis of TUNEL Stained Placentas

All data had a normal distribution except for the GD45 stromal data which required log10 transformation.

5.5 Results

5.5.1 mRNA Results

5.5.1.1 Amplification Efficiencies and RSq from Placental and Endometrial qPCRs

qPCR was performed for the candidates of interest *Bax*, *Bcl2*, *P53* and *Ki67*, and the data were normalised to the reference genes *TBP1* and *HPRT1*, and *TBP1* and *YWHAZ* for the placental and endometrial samples respectively. The amplification efficiencies, RSq, slope and intercept values for each gene are detailed in

Table 5.2.

5.5.1.2 Temporal Changes in mRNA Expression

5.5.1.2.1 Temporal Changes were observed in Placental mRNA Expression

Temporal changes were observed in placental expression of all of the candidates investigated (Figure 5.4). *Bax* (ANOVA with and without Gilt Block FPr≤0.001, Figure 5.4A) and *Bcl2* (Kruskal-Wallis P≤0.001; Figure 5.4B) expression fluctuated significantly throughout gestation, with the lowest expression observed at GD30, the highest expression at GD45 and 90, and an intermediate expression level observed at GD60. The ratio of *Bax: Bcl2* expression was increased at GD30 compared to the other GD investigated (ANOVA without Gilt Block FPr=0.035), although this was not statistically significant with the addition of a block for gilt (Figure 5.4C). *P53* expression was low at GD30, with a statistically significant increase in expression observed between GD30 and 45, with intermediate expression observed at GD60 and 90 (ANOVA without Gilt Block FPr≤0.001; with Gilt Block FPr=0.003; Figure 5.4D). *Ki67* expression modestly fluctuated throughout gestation (ANOVA without Gilt Block FPr=0.003; with Gilt Block FPr=0.025; Figure 5.4E), with a statistically significant decrease in expression observed between GD45 and 60.

5.5.1.2.2 Temporal Changes in Endometrial mRNA Expression of *Bcl2*, *Bax: Bcl2* Ratio and *P53*, but not *Bax* or *Ki67,* were observed

No temporal changes in endometrial expression of *Bax* (Figure 5.5A) or *Ki67* (Figure 5.5E) were observed. Increased *Bcl2* expression was observed in GD18 endometrial samples compared to the other GD investigated (ANOVA with and without Gilt Block FPr≤0.001; Figure 5.5B). The *Bax: Bcl2* ratio was decreased at GD18 compared to GD30, 45 and 90 (ANOVA without Gilt Block FPr≤0.001; with Gilt Block FPr=0.022; Figure 5.5C). The endometrial expression of *P53* decreased with advancing gestation (ANOVA without Gilt Block FPr=0.002; with Gilt Block FPr=0.009; Figure 5.5D), with a statistically significant decrease observed between GD18 and 45.

Gene	Placenta				Endometrium			
	Amplification Efficiency (%)	**RSq**	**Slope**	**Intercept**	**Amplification Efficiency (%)**	**RSq**	**Slope**	**Intercept**
Bax	93.2	0.995	-3.497	28.180	92.8	0.992	-3.507	28.840
Bcl2	90.5	0.991	-3.573	30.988	92.8	0.991	-3.509	29.805
P53	95.4	0.991	-3.437	27.044	96.6	0.990	-3.406	28.152
Ki67	90.8	0.993	-3.563	26.530	91.0	0.994	-3.559	26.243
TBP1	102.9	0.990	-3.254	27.211	105.6	0.991	-3.194	28.209
HPRT1	96.8	0.991	-3.402	27.002	N/A	N/A	N/A	N/A
YWHAZ	N/A	N/A	N/A	N/A	92.6	0.990	-3.513	21.871

Table 5.2: Summary of Amplification Efficiencies and RSq Values from Placental and Endometrial qPCRs.

Abbreviations used: *Bax*=BCL2 associated X, *Bcl2*=B-cell lymphoma 2, *P53*=Tumour protein p53, *TBP1*=TATA box binding protein, *HPRT1*=Hypoxanthine phosphoribosyltransferase 1, and *YWHAZ*=Tyrosine 3-monooxygenase/tryptophan 5-monooxygenase activation protein, zeta polypeptide, N/A=not applicable.

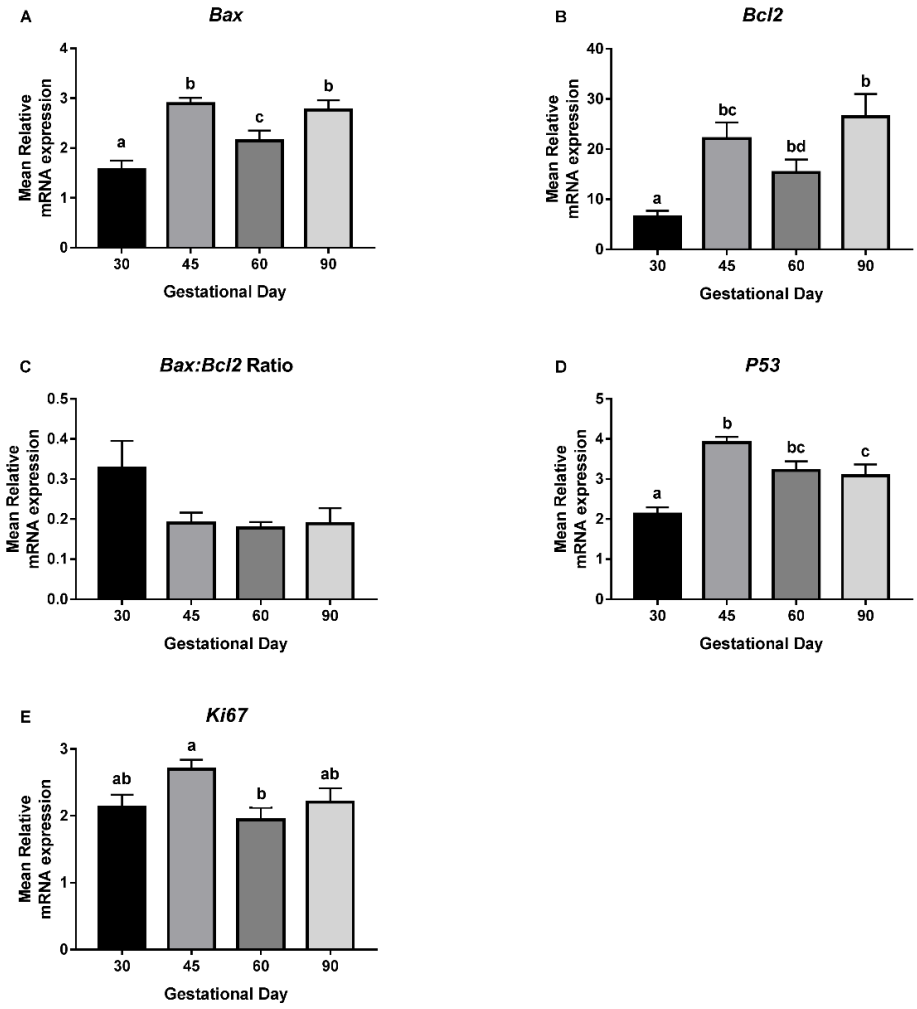

Figure 5.4: Temporal Changes in Placental mRNA Expression were observed.

The mean values, normalised to the expression of stable reference genes are plotted here. *Bax* (ANOVA with and without Gilt Block FPr≤0.001; A) and *Bcl2* (Kruskal-Wallis P≤0.001; B) expression fluctuated throughout gestation, with the lowest expression observed at gestational day (GD) 30, the highest expression at GD45 and 90, and an intermediate expression level observed at GD60. C: The ratio of *Bax: Bcl2* expression was increased at GD30 compared to the other GD investigated (ANOVA without Gilt Block FPr≤0.05), although this was not statistically significant with the addition of a block for gilt. D: *P53* expression was low at GD30, with a statistically significant increase in expression observed between GD30 and 45, and intermediate expression observed at GD60 and 90 (ANOVA without Gilt Block FPr≤0.001; with Gilt Block FPr≤0.01). E: *Ki67* expression modestly fluctuated throughout gestation (ANOVA without Gilt Block FPr≤0.01; with Gilt Block FPr FPr≤0.05), with a statistically significant decrease in expression observed between GD45 and 60. Error bars represent S.E.M. Letters indicate that group means differ from one another (Tukey/Mann-Whitney).

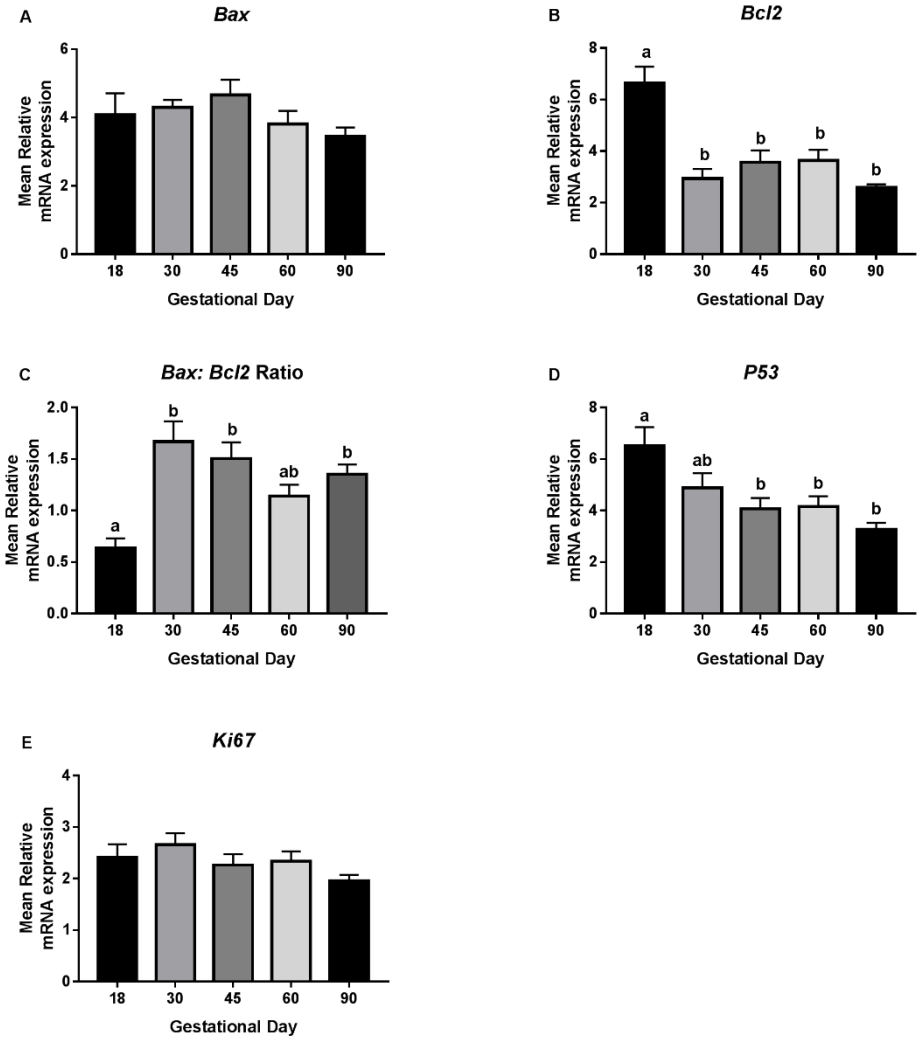

Figure 5.5: Temporal Changes in *Bcl2*, *Bax: Bcl2* Ratio and *P53*, but not *Bax* or *Ki67* Endometrial mRNA Expression were observed.

The mean values, normalised to the expression of stable reference genes are plotted here. No temporal changes in *Bax* (A) or *Ki67* (E) expression were observed. B: Increased *Bcl2* expression was observed in gestational day (GD) 18 endometrial samples compared to the other GD investigated (ANOVA with and without Gilt Block FPr≤0.001). C: The *Bax: Bcl2* ratio was decreased at GD18 compared to GD30, 45, and 90 (ANOVA without Gilt Block FPr≤0.001; with Gilt Block FPr≤0.05). D: The endometrial expression of *P53* decreased with advancing gestation (ANOVA with and without Gilt Block FPr≤0.01), with a statistically significant decrease observed between GD18 and 45. Error bars represent S.E.M. Letters indicate that group means differ from one another, tested by post-hoc Tukey.

5.5.1.3 Association between Foetal Size and mRNA Expression

5.5.1.3.1 An Association between Foetal Size and Placental *P53* and *Ki67* Expression was observed

To address the question of whether there is a relationship between foetal size and the placental expression of the candidate genes, placentas supplying the lightest foetuses were compared with those supplying the CTMLW foetuses within GD (Figure 5.6). No association between foetal size and the placental expression of *Bax*, *Bcl2* or the *Bax: Bcl2* ratio was observed (Figure 5.6A-C). *P53* expression was decreased in placental samples associated with the lightest foetuses compared to the CTMLW foetuses at GD45 (ANOVA without Gilt Block FPr=0.04; with Gilt Block FPr=0.074; Figure 5.6D). Intriguingly, the direction of this difference switched at GD60 (ANOVA with Gilt Block FPr=0.08), with placentas associated with the lightest foetuses having increased *P53* expression compared to the CTMLW foetuses. At GD45, the expression of *Ki67* was also decreased in placentas supplying the lightest foetuses compared to the CTMLW foetuses (ANOVA without Gilt Block FPr=0.033; with Gilt Block FPr=0.071; Figure 5.6E).

5.5.1.3.2 An Association between Foetal Size and Endometrial *P53* Expression was observed at GD45.

The expression of the candidate genes in endometrial samples supplying the lightest conceptus or foetus were compared with those supplying the CTMLW conceptus or foetus within GD (Figure 5.7). No association between foetal size and endometrial expression of *Bax* (Figure 5.7A), *Bcl2* (Figure 5.7B), *Bax: Bcl2* Ratio (Figure 5.7C), or *Ki67* (Figure 5.7E) was observed. Increased *P53* expression was observed in endometrial samples supplying the lightest foetuses compared to the CTMLW foetuses at GD45 (ANOVA without Gilt Block FPr=0.007; with Gilt Block FPr=0.04; Figure 5.7D).

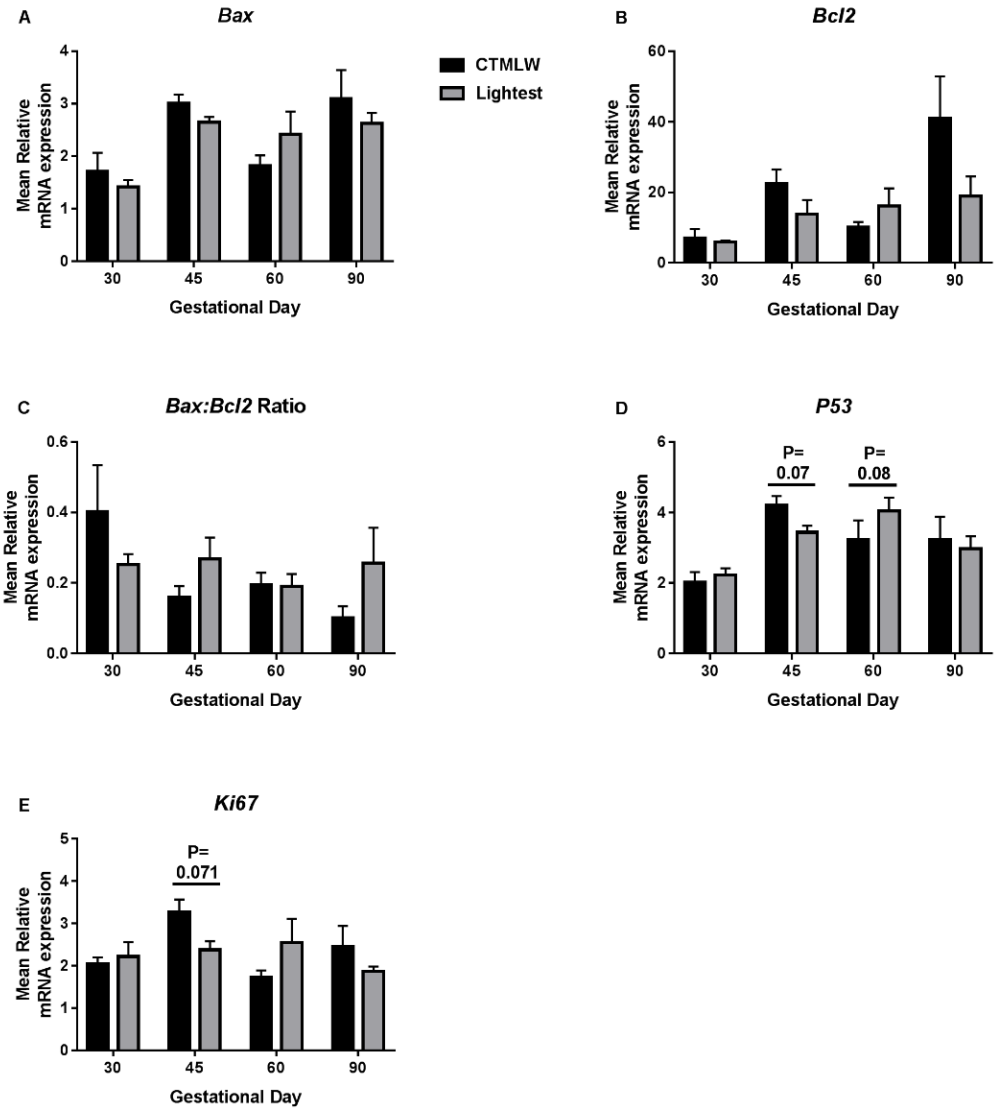

Figure 5.6: An Association between Foetal Size and Placental *P53* and *Ki67* Expression was observed.

The mean values, normalised to the expression of stable reference genes are plotted here. No relationship between foetal size and the placental expression of *Bax* (A), *Bcl2* (B), or the *Bax: Bcl2* ratio (C) were observed. D: The expression of *P53* was decreased in placental samples associated with the lightest foetuses compared to the closest to mean litter weight (CTMLW) foetuses at gestational day (GD) 45 (ANOVA without Gilt Block FPr≤0.05; with Gilt Block FPr=0.07). The direction of this difference switched at GD60 (ANOVA with Gilt Block FPr=0.08), with placentas associated with the lightest foetuses having increased *P53* expression compared to the CTMLW foetuses. E: At GD45, the expression of *Ki67* was decreased in placentas supplying the lightest foetuses compared to the CTMLW foetuses (ANOVA without Gilt Block FPr≤0.05; with Gilt Block FPr=0.07). Error bars represent S.E.M.

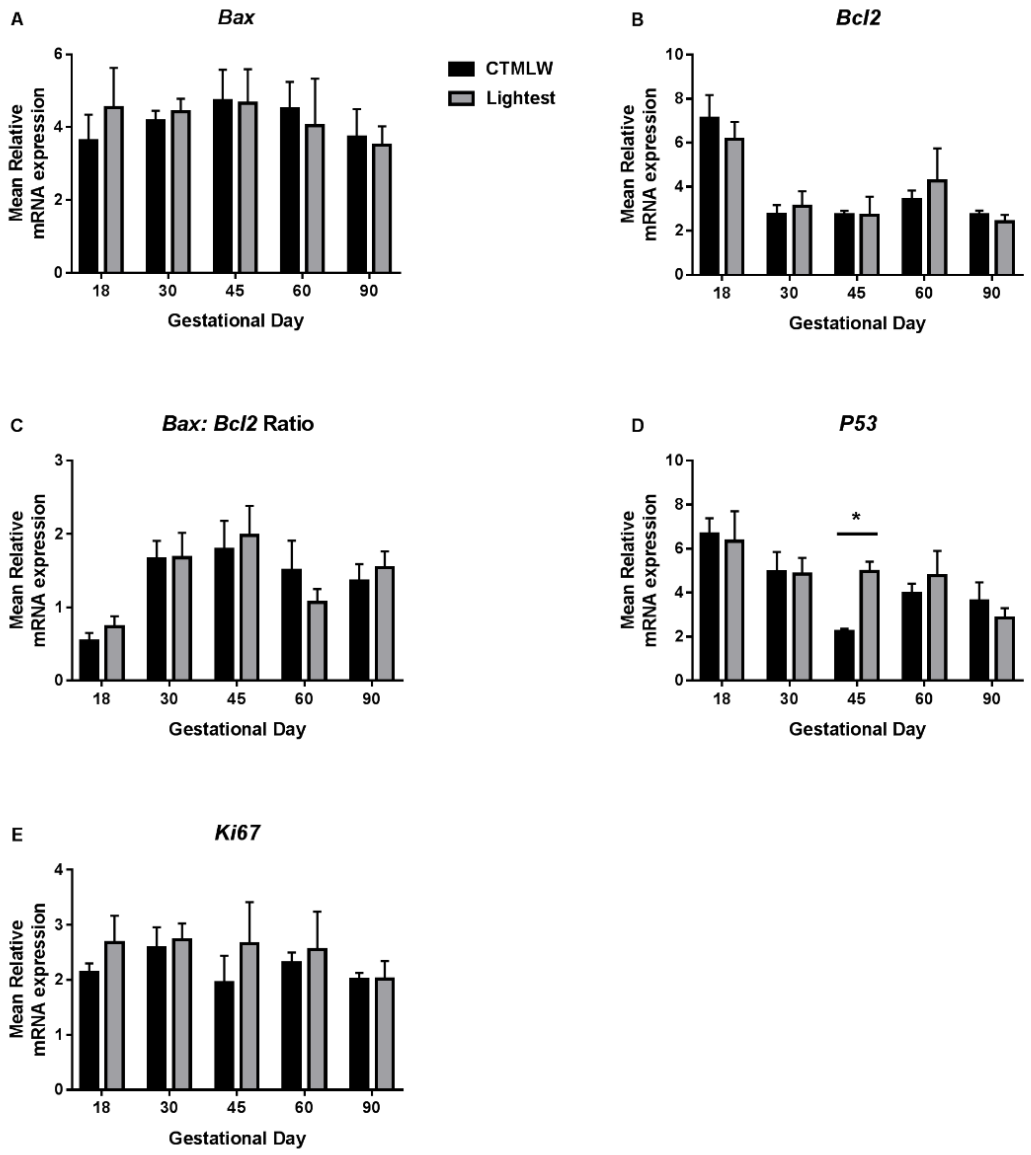

Figure 5.7: An Association between Foetal Size and Endometrial *P53* Expression was observed at GD45.

The mean values, normalised to the expression of stable reference genes are plotted here. No association between conceptus or foetal size and endometrial expression of *Bax* (A), *Bcl2* (B), *Bax: Bcl2* Ratio (C) or *Ki67* (E) were observed. D: The expression of P53 was increased in endometrial samples supplying the lightest foetuses compared to the closest to mean litter weight (CTMLW) foetuses at gestational day (GD) 45 (ANOVA without Gilt Block FPr≤0.01; with Gilt Block FPr≤0.05). Error bars represent S.E.M. *FPr≤0.05.

5.5.1.4 Association between Foetal Sex and mRNA Expression

5.5.1.4.1 A Trend towards an Association between Foetal Sex and Placental *Bax* Expression was observed.

The influence of foetal sex on placental mRNA expression was investigated within GD by comparing the mean expression of samples supplying males with those supplying females (Figure 5.8). A trend towards decreased *Bax* expression in placental samples associated with female foetuses compared to their male littermates was observed at GD45 (ANOVA without Gilt Block FPr=0.055; with Gilt Block FPr=0.063; Figure 5.8A). *Bcl2* expression was decreased at GD30 in placentas associated with female foetuses compared to males (ANOVA without Gilt Block FPr=0.05; Figure 5.8B). Although, this was not statistically significant with the addition of a block for gilt. No statistically significant associations between foetal sex and placental *Bax: Bcl2* Ratio (Figure 5.8C), *P53* (Figure 5.8D) or *Ki67* (Figure 5.8E) expression were observed.

5.5.1.4.2 An Association between Foetal Sex and Endometrial *Bax*, *Bcl2*, *P53*, and *Ki67* Expression was observed.

The influence of foetal sex on endometrial mRNA expression was investigated within GD by comparing the mean expression of samples supplying males with those supplying females (Figure 5.9). *Bax* expression was increased in endometrial samples supplying female foetuses compared to those supplying male foetuses at GD30 (ANOVA with Gilt Block FPr=0.047; Figure 5.9A). An indication of decreased *Bax* expression in endometrial samples supplying female foetuses compared to male foetuses was observed at GD60 (ANOVA without Gilt Block FPr=0.075). However, this difference was lost with the addition of a block for gilt. Endometrial samples supplying female foetuses had decreased *Bcl2* expression compared to those supplying male foetuses at GD60 (ANOVA without Gilt Block FPr=0.017; with Gilt Block FPr=0.009; Figure 5.9B). The *Bax: Bcl2* ratio was increased in endometrial samples supplying female foetuses compared to male foetuses at GD45 (ANOVA without Gilt

Block FPr=0.033; Figure 5.9C). This difference was not statistically significant with the addition of a block for gilt. The expression of *P53* (ANOVA without Gilt Block FPr=0.002; with Gilt Block FPr=0.006; Figure 5.9D) and *Ki67* (ANOVA with Gilt Block FPr=0.052; Figure 5.9E) were decreased in endometrial samples supplying female foetuses compared to those supplying male foetuses at GD60.

5.5.1.5 Sex x Size Interactions

To investigate the presence of sex x size interactions in mRNA expression, a two-way ANOVA for sex x size, with and without a block for gilt were performed at GD30, 60 and 90 for each candidate for the lightest and CTMLW foetus. Only the analyses which were significant following the addition of a block for gilt are described below. As described previously this was not performed at GD45 due to the small sample size available for the male comparison. In addition, some of the other sub-sets are particularly limited, especially at GD90 due to problems obtaining RNA of acceptable quality, therefore the relevance and importance of these findings should not be over-interpreted.

5.5.1.5.1 Sex x Size Interactions in Placental *Bax* and *Bcl2* Expression were observed

A sex x size interaction in placental *Bax* expression was observed at GD90 (ANOVA with Gilt Block FPr=0.048), with placentas supplying the CTMLW male and lightest females (mean: 1.62 and 3.12 respectively; n=1 in each group) having decreased expression compared to the other two groups (lightest males: (mean±S.E.M.) 2.522±0.338; CTMLW females 3.583±0.212; n=3 and 5 respectively). At GD30, a sex x size interaction in placental *Bcl2* expression was observed (ANOVA with Gilt Block FPr=0.029), with the CTMLW males (10.7±3.809; n=3) having increased expression compared to the other groups investigated (lightest males: 6.38±1.481, n=4; CTMLW females 3.557±0.606, n=3; lightest females 4.825±0.363, n=2).

5.5.1.5.2 Sex x Size Interaction in Endometrial *Bax: Bcl2* Ratio was observed

A sex x size interaction in endometrial *Bax: Bcl2* ratio was observed at GD60 (ANOVA with Gilt Block FPr=0.051) with the CTMLW females (mean: 2.470, n=1) having increased expression compared to the other groups (CTMLW males: 1.178±0.354; lightest males 1.132±0.363; lightest females 1.004±0.164; n=3 for all groups). At GD90, a sex x size interaction was observed (ANOVA with Gilt Block FPr=0.024), with the lightest females having increased expression (1.688±0.453; n=3) compared to the other three groups (CTMLW males: 1.303±0.419, n=3; lightest males: 1.391±0.054, n=3; CTMLW females 1.435±0.145, n=2).

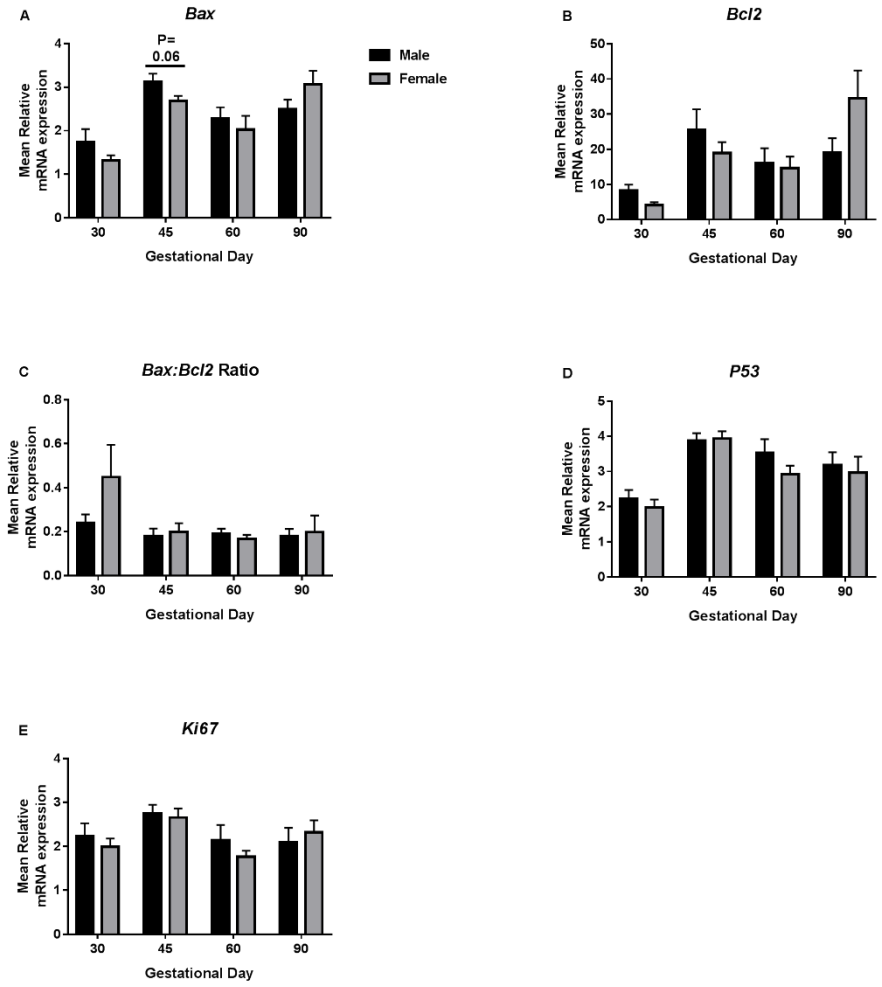

Figure 5.8: A Trend towards an Association between Foetal Sex and Placental *Bax* mRNA Expression was observed.

The mean values, normalised to the expression of stable reference genes are plotted here. A: A trend towards decreased *Bax* expression in placental samples associated with female foetuses compared to their male littermates was observed at GD45 (ANOVA without Gilt Block FPr=0.055; with Gilt Block FPr=0.063). B: *Bcl2* expression was decreased at GD30 in placentas associated with female foetuses compared to males (ANOVA without Gilt Block FPr≤0.05) although, this was not statistically significant with the addition of a block for gilt. No statistically significant associations between foetal sex and placental *Bax: Bcl2* Ratio (C), *P53* (D) or *Ki67* (E) expression were observed. Error bars represent S.E.M.

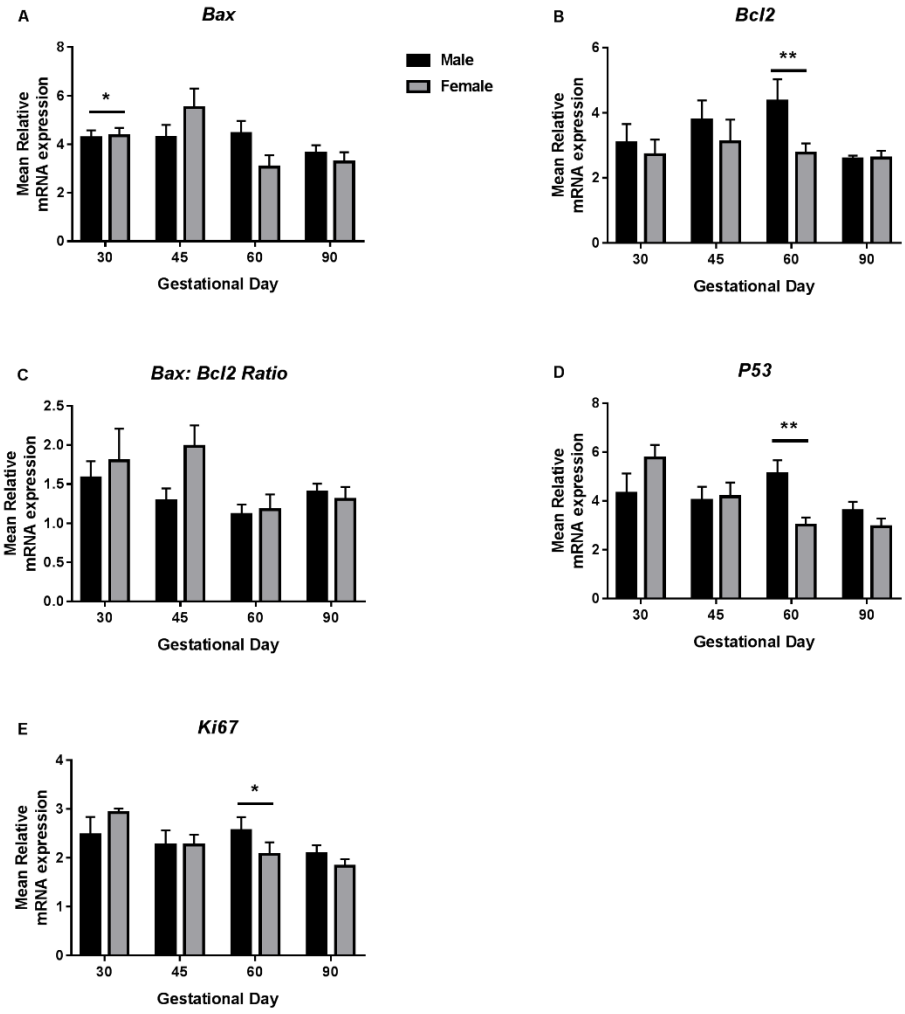

Figure 5.9: An Association between Foetal Sex and Endometrial *Bax*, *Bcl2*, *P53* and *Ki67* Expression was observed.

The mean values, normalised to the expression of stable reference genes are plotted here. A: *Bax* expression was increased in endometrial samples supplying female foetuses compared to those supplying male foetuses at GD30 (ANOVA with Gilt Block FPr≤0.05). B: Endometrial samples supplying female foetuses had decreased *Bcl2* expression compared to those supplying male foetuses at GD60 (ANOVA without Gilt Block FPr≤0.05; with Gilt Block FPr≤0.01). C: The *Bax: Bcl2* ratio was increased in endometrial samples supplying female foetuses compared to male foetuses at GD45 (ANOVA without Gilt Block FPr≤0.05). However, this difference was not statistically significant with the addition of a block for gilt. *P53* (ANOVA with and without Gilt Block FPr≤0.01; D) and *Ki67* (ANOVA with Gilt Block FPr≤0.05; E) expression were decreased in endometrial samples supplying female foetuses compared to those supplying male foetuses at GD60. Error bars represent S.E.M. *FPr≤0.05. **FPr≤0.01.

5.5.2 TUNEL Staining

5.5.2.1 Temporal Changes

As described in 3.2, one of the broad objectives of this chapter was to investigate gestational changes in placental apoptosis. GD45 and 60 placentas were TUNEL stained to identify apoptotic cells. An increased number of TUNEL stained cells, indicating increased placental apoptosis, were observed in both the stroma (Mann-Whitney $P \leq 0.001$; Figure 5.10C, D, K, H and Figure 5.11A) and CAM (ANOVA without Gilt $FPr \leq 0.001$; with Gilt $FPr = 0.017$; Figure 5.10K, L, O and P and Figure 5.11B) at GD60 compared to GD45.

5.5.2.2 Foetal Size was not associated with Placental TUNEL Staining at GD45 or 60

To address the question of whether there is a relationship between foetal size and placental apoptosis, TUNEL stained placentas supplying the lightest foetuses were compared with those supplying the CTMLW foetuses within GD at GD45 and 60 (Figure 5.11C-F). No statistically significant relationships were observed between the number of TUNEL stained cells and foetal size, in the placental stroma or CAM at either GD.

5.5.2.3 Foetal Sex was not associated with Placental TUNEL Staining at GD60

The relationship between foetal sex and placental apoptosis was investigated at GD60, by comparing TUNEL stained placentas supplying male and female foetuses. No statistically significant associations were observed between foetal sex and TUNEL staining in the stroma or CAM at GD60 (Figure 5.11G and H).

5.5.2.4 A Sex x Size Interaction in Placental CAM TUNEL Staining at GD60 was observed

To investigate the presence of sex x size interactions, two-way ANOVA for sex x size was performed on the GD60 stroma and CAM data (n=3 in each sex x size group). No statistically significant sex x size interactions were observed in the stromal data. However, a sex x size interaction was observed in the CAM data (ANOVA without Gilt Block FPr=0.044; with Gilt Block FPr=0.016). Placentas supplying the CTMLW males (mean±S.E.M; 21.048±7.988) and the lightest females (24.735±7.679) had an increased number of TUNEL stained cells per 10,000μm^2 CAM area than those supplying the CTMLW females (18.333±9.522) and lightest males (14.661±7.599).

Figure 5.10: Representative TUNEL Stained GD45 and 60 Placentas.

Placental samples were Terminal deoxynucleotidyl transferase dUTP nick end labelling (TUNEL) stained to investigate the prevalence of apoptotic cells in placental samples at gestational day (GD) 45 and 60. A negative control using PBS instead of TDT enzyme was performed on GD45 (A and E) and GD60 (I and M) placental samples. Normal female rat mammary gland sections at 3-5 days post-weaning were used as a positive control (B, F, J, and N). Representative TUNEL stromal staining from placentas supplying the closest to mean litter weight (CTMLW) (C) and lightest foetuses (D) at GD45. Representative TUNEL stromal staining from placentas supplying the CTMLW (G) and lightest foetuses (H) at GD60. Representative TUNEL chorioallantoic membrane (CAM) staining from placentas supplying the CTMLW (K) and lightest foetuses (L) at GD45. Representative TUNEL CAM staining from placentas supplying the CTMLW (P) and lightest foetuses (P) at GD60. Scale bar represents 100µm.

Figure 5.11: Temporal Changes, but no Association between Foetal Size or Sex and TUNEL Staining were observed.

To investigate the relationship between gestational day (GD), foetal size and sex, and placental apoptosis, placental samples were Terminal deoxynucleotidyl transferase dUTP nick end labelling (TUNEL) stained to investigate the prevalence of apoptotic cells in placental samples at GD45 and 60. An increased number of TUNEL stained cells, indicating an increase in placental apoptosis, were observed in both the stroma (Mann-Whitney $P \leq 0.001$; A) and CAM (ANOVA without Gilt $FPr \leq 0.001$; with Gilt $FPr \leq 0.05$; B) at GD60 compared to GD45. No statistically significant relationships were observed between the number of TUNEL stained cells and foetal size in the placental stroma (C and E) or CAM (D and F) at GD45 or 60. No statistically significant associations were observed between foetal sex and TUNEL stained in the stroma or CAM at GD60 (G and H).

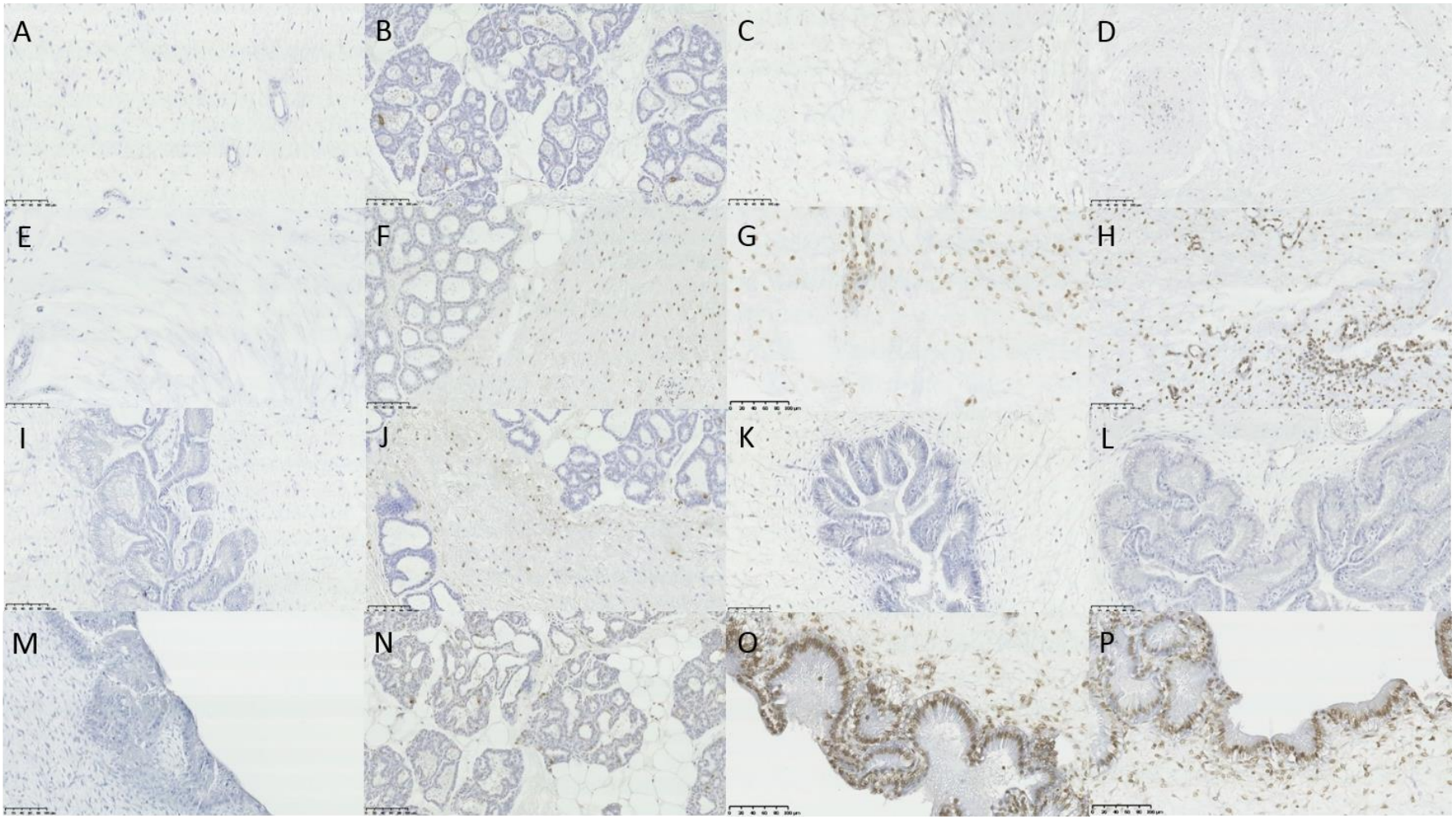

Figure 5.10: Representative TUNEL Stained GD45 and 60 Placentas.

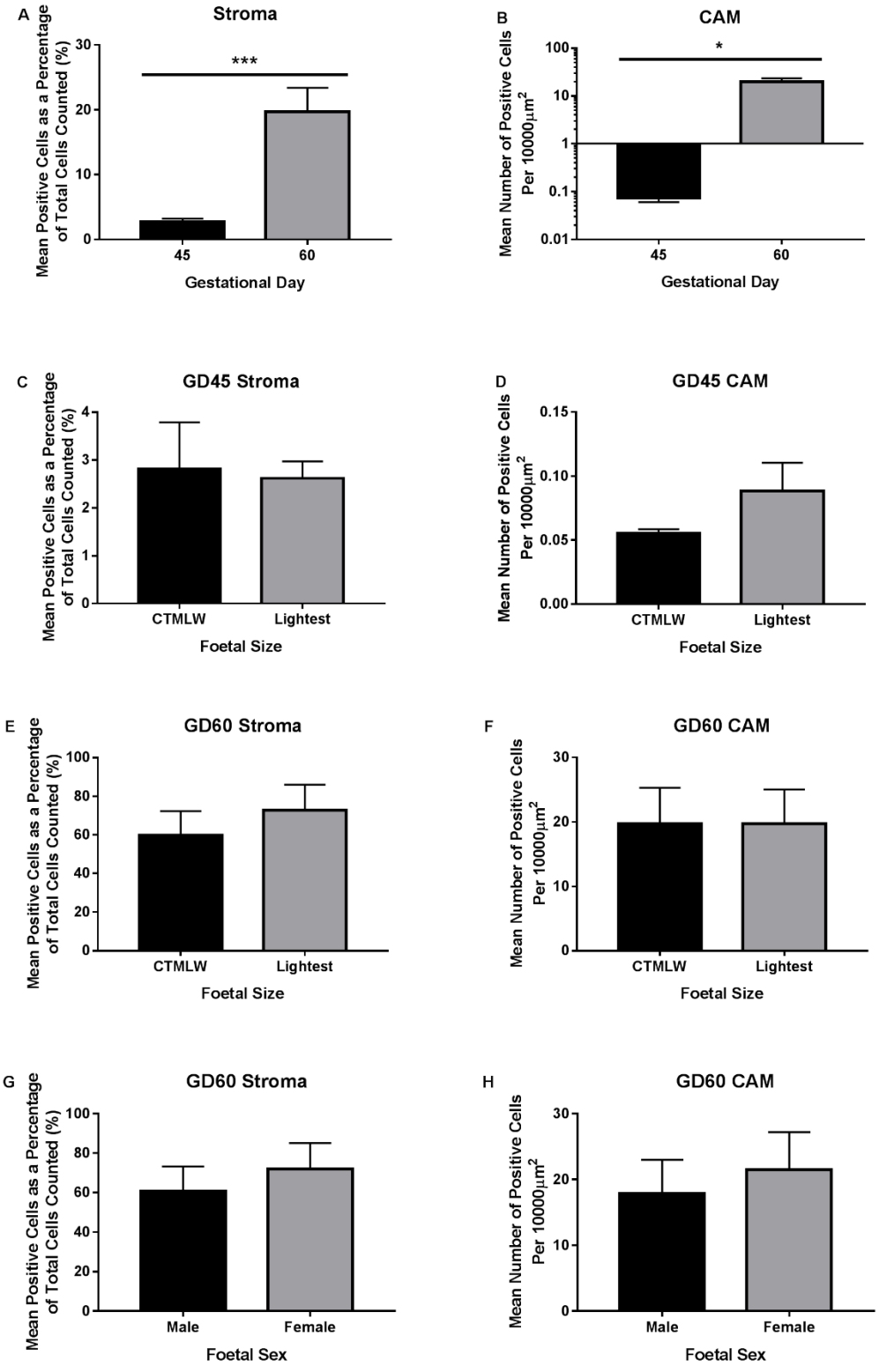

Figure 5.11: Temporal Changes, but no Association between Foetal Size or Sex and TUNEL Staining were observed.

5.6 Discussion

The experiments in this chapter have highlighted novel relationships between foetal size, and more intriguingly foetal sex, and apoptosis and proliferation at the porcine feto-maternal interface (

Table 5.3 and Table 5.4).

5.6.1 Temporal Changes

Temporal changes in mRNA expression were observed in both tissues investigated, with different temporal profiles in expression were observed between the two tissues. Placental *Bax* and *Bcl2* expression fluctuated significantly throughout gestation, with the lowest expression observed at GD30 and the highest expression at GD45 and 90. As detailed in 5.1.3, temporal changes in the activation of intrinsic and extrinsic apoptosis has been suggested at the porcine feto-maternal interface (Merkis *et al.*, 2010; Cristofolini *et al.*, 2013). The temporal changes in *Bax* and *Bcl2* presumably reflect the dynamic nature of the placenta, and potentially changes in cell death pathway activation; although this requires further investigation.

Ki67 expression modestly fluctuated throughout gestation, with a statistically significant decrease in expression observed between GD45 and 60. This decrease in proliferation may reflect the change in the relationship between the placenta and the developing foetus that occurs at this point. At GD45, placental growth occurs at a greater rate than foetal growth whereas, at GD60, placental growth begins to plateau whilst the foetus undergoes exponential growth. Therefore, the decrease in cell proliferation may reflect the decrease in placental growth rate.

When investigating endometrial gene expression, both the pro-apoptotic *P53* and the anti-apoptotic *Bcl2* had high expression at GD18, demonstrating the tight regulation of the apoptotic pathways at the feto-maternal interface. This reinforces the findings of Samborski *et al.*, (2013a) who demonstrated that GD14 porcine endometrial samples have high expression of both anti- and pro-apoptotic, and proliferation associated genes. The high expression of these genes during this period of gestation suggests a role for apoptosis and

proliferation in the establishment of pregnancy. Whilst the endometrial expression of *Bcl2* was greatest at GD18, *Bax* expression remained relatively constant throughout gestation, although it was expressed at a higher abundance than *Bcl2* at GD30-90 which was reflected in the *Bax: Bcl2* ratio. *P53* endometrial expression decreased gradually with advancing gestation, with a statistically significant decrease observed between GD18 and 45 in contrast to the placenta which had low expression at GD30, with a statistically significant increase in expression observed between GD30 and 45, with intermediate expression observed at GD60 and 90. These temporal, and tissue specific changes in *P53* expression may be explained by the significant remodelling of the placenta to meet increasing foetal demand.

TUNEL staining demonstrated an increase in placental apoptosis at GD60 compared to GD45 however this experiment was performed on a limited sample set. Therefore, analysis of TUNEL stained placental and endometrial samples supplying foetuses of different size and sex throughout gestation should be performed to provide a comprehensive overview of apoptosis at the feto-maternal interface.

5.6.2 Foetal Size was Associated with Altered Apoptosis and Proliferation at the Feto-Maternal Interface

As discussed in 5.1.3, aberrant regulation of apoptosis has been heavily implicated in human IUGR. In the current study, placental *Ki67* expression was decreased, suggesting decreased proliferation, in samples associated with the lightest foetuses compared to the CTMLW at GD45. Chen *et al.*, (2015) suggested in a proteomics analysis that components of the proliferation pathway were downregulated in placental and endometrial samples associated with IUGR foetuses compared to those associated with NBW foetuses at GD60, 90, and 110. Future analyses investigating the gene and protein expression of the candidates suggested by Chen *et al.*, (2015) alongside other growth factors which are known to influence proliferation at the feto-maternal interface (Supplementary Table 4) would vastly improve the

understanding of the association between foetal size and proliferation at the feto-maternal interface. In addition, primary endometrial LE, GE, stromal and myometrial cells, and conceptus trophectoderm cells could be isolated (Wang *et al.*, 2000; Ka *et al.*, 2001) and their proliferative ability investigated *in vitro* (Romar *et al.*, 2016).

The increased expression of *P53* observed in GD60 placentas associated with the lightest foetuses compared to those supplying the CTMLW foetuses reinforces the previous findings of Chen *et al.*, (2015) who demonstrated increased apoptotic stress in placentas associated with IUGR foetuses compared to NBW foetuses at GD60, 90 and 110. In contrast, at GD45, placental and endometrial *P53* expression were decreased in samples associated with the lightest foetuses compared to the CTMLW foetuses. At GD45, placental growth occurs at a greater rate than foetal growth however, at GD60, placental growth begins to plateau whilst the foetus is undergoing exponential growth. Therefore, this period of development is likely to be highly dynamic which may reflect the changes in gene expression observed between GD45 and 60. As detailed in 5.1.3, temporal changes in the activation of intrinsic and extrinsic apoptosis has been suggested at the porcine feto-maternal interface (Merkis *et al.*, 2010; Cristofolini *et al.*, 2013). Considering this, further assessment of components of both the intrinsic and extrinsic pathway should be performed to ensure that placentas supplying the lightest foetuses are utilising the same programmed cell death pathway as those supplying the CTMLW foetuses.

Whilst this chapter has investigated *Bax*, *Bcl2* and *P53*, which are involved in the intrinsic apoptosis pathway, recent literature has suggested the presence of additional methods of programmed cell death. Examples of additional programmed cell death pathways include: anoikis, pyroptosis, necroptosis, ferroptosis, autophagic cell death, entosis, netosis, and parthanatos (Tait *et al.*, 2014; Ke *et al.*, 2016). In contrast to apoptosis, following activation of the necroptotic cell death pathway, the cell membrane is ruptured which leads to the release of the cytoplasmic contents. During necroptosis, caspase 8 activates receptor interacting protein kinase 1 (RIPK1), RIPK3, and the mixed

kinase domain-like (MLKL) to induce cell death. Sirtuin 2 (SIRT2) and RIPK1, key components of the necroptosis pathway, are expressed in growth restricted human placentas (Hannan *et al.*, 2017). This work highlights that additional methods of cell death may exist in the placenta, the mechanisms of which remain poorly understood. Whilst temporal changes in the activation of intrinsic and extrinsic apoptosis have been suggested at the porcine feto-maternal interface (Merkis *et al.*, 2010; Cristofolini *et al.*, 2013), additional forms of cell death such as necroptosis have not yet been investigated and may further the understanding of the mechanisms which regulate remodelling of the feto-maternal interface.

5.6.3 Foetal Sex was Associated with Altered Apoptosis and Proliferation at the Feto-Maternal Interface

As stated previously, several recent studies have described the existence of sexual dimorphism in placental development and function, with males generally considered to be disadvantaged. In this chapter, foetal sex was associated with placental and endometrial mRNA expression of candidate genes involved in apoptosis and proliferation.

The expression of the pro-apoptotic gene *Bax* was increased in endometrial samples supplying female foetuses compared to those supplying male foetuses at GD30. Interestingly, this was not observed in the placenta, where instead a trend towards decreased *Bax* expression in placental samples associated with female foetuses compared to their male littermates observed at GD45. In the current study, it was demonstrated that foetal sex was associated with the endometrial expression of apoptotic genes in early gestation, but not the placental expression. This suggests that early signalling events between the conceptus and the endometrium may regulate this. Female mouse embryos have been shown to have increased resilience to oxidative induced heat stress than male embryos (Pérez-Crespo *et al.*, 2005) and it has been suggested that female bovine embryos have increased mRNA expression of X-linked inhibitor of apoptosis protein (XIAP) (Jiménez *et al.*,

2003). In addition, other X-linked genes including glucose-6-phosphate dehydrogenase (G6PD), hypoxanthine-guanine phosphoribosyltransferase (HGPRT) and phosphoglycerate kinase (PGK) have been demonstrated to have increased expression in mouse and bovine female blastocysts compared to males (Krietsch *et al.*, 1982; Williams, 1986; Gutiérrez-Adán *et al.*, 2000). Sexual dimorphism in glucose metabolism has previously been demonstrated in both bovine and mouse (Williams, 1986; Bredbacka and Bredbacka, 1996; Lane and Gardner, 1996; Gutiérrez-Adán *et al.*, 2000; Larson *et al.*, 2001), with increased glucose uptake and metabolism observed in female embryos compared to males. Interestingly, this increased metabolism of glucose in female embryos has been demonstrated to augment interferon tau production in female bovine embryos, suggesting a potential sex-specific alteration in implantation itself (Larson *et al.*, 2001). It has been proposed by Gutiérrez-Adán *et al.*, (2001) that, as XIAP is expressed upstream near HGPRT, the increased uptake of glucose by female embryos, which translates to females having increased resilience to hyperglycaemia, compared to males may be explained by decreased apoptosis through this signalling. Porcine conceptuses are known to metabolise a significant amount of maternal derived glucose into fructose, which can then be used to synthesise glucosamine. Glucosamine has been demonstrated to induce mTOR signalling (Wen *et al.*, 2005), which in turn induces proliferation of trophectoderm cells and the synthesis of hyaluronic acid, which is a significant component of the feto-maternal interface (Kim *et al.*, 2012). Vickers *et al.*, (2011) reported that maternal supplementation of fructose to rats resulted in sex-specific alterations in placental development and sugar metabolism postnatally, with female offspring being more adversely affected by this prenatal challenge than male offspring. Considering the results of these investigations and the results presented in this chapter, it would be interesting to investigate glucose and fructose metabolism in relation to apoptosis and conceptus sex at the feto-maternal interface in early gestation in the pig.

In contrast to the GD30 analysis, at GD60 endometrial samples supplying female foetuses had decreased expression of the anti-apoptotic *Bcl2*, the pro-

apoptotic *P53*, and the proliferation marker *Ki67* compared to those supplying male foetuses. Males have been demonstrated in this thesis be heavier than their female littermates throughout gestation (Chapter 3). As males are heavier with a faster growth rate, it could be suggested that they would place an increased demand on the placenta for nutrients. It could be hypothesised that increased remodelling of the feto-maternal interface is required to accommodate the increasing demands being placed on placentas supplying male foetuses compared to those supplying female foetuses. This would require increased apoptosis and proliferation, reflecting the relationship between foetal sex and gene expression illustrated in this study.

To date, there have been limited investigations into the relationship between foetal sex and placental and endometrial expression of apoptosis and proliferation related genes. During human pregnancy, hCG is secreted by synctiotrophoblasts and cytotrophoblasts (Snegovskikh *et al.*, 2007) and it has been suggested to play a role in regulating trophoblast invasion by ERK1/2 signalling (Prast *et al.*, 2008). In humans, maternal serum hCG concentration is increased if they are carrying a female compared to a male foetus (Adibi *et al.*, 2015) although, despite the differences in maternal hCG levels, foetal sex was not found to influence Bcl2 or Bax protein staining in term placentas (Gol and Tuna, 2009). In instances of preeclampsia, it has been demonstrated that placentas supplying male foetuses have increased apoptotic activity, with a greater number of TUNEL positive cells, and increased expression of PUMA and Bax than placentas supplying females (Muralimanoharan *et al.*, 2013). In the current study, foetal sex was not associated with placental TUNEL staining at GD60. However, the current experiment was performed on a small sample set at only one GD and, given the considerable temporal changes in gene expression patterns observed, further analyses on both placental and endometrial samples should be performed.

5.6.4 Limitations of TUNEL Staining

TUNEL staining is considered an appropriate method for the detection of apoptotic cells in tissue sections (Didenko, 2011). In this thesis, discrepancies between the qPCR data investigating the p53 apoptosis pathway and the TUNEL staining results were observed. As stated above, the discrepancy may be attributed to the small sample size in the TUNEL staining experiment. In addition, there are a number of limitations associated with the technique. The method of TUNEL staining is not able to specifically label cells that have undergone apoptosis and instead will label all free 3'-hydroxyl termini present in the sample. This means that it will label necrotic cells (Ansari *et al.*, 1993) and cells undergoing DNA repair (Kanoh *et al.*, 1999). In addition, there are some reports in the literature of histological processes including fixation (Huerta *et al.*, 2007), sectioning (Sloop *et al.*, 1999) altering the staining results obtained. Considering this, an important future experiment would be to perform immunohistochemistry or western blots for the candidates of interest in the p53 pathway.

5.7 Conclusion

The experiments in this chapter have highlighted novel relationships between foetal size, and more intriguingly foetal sex, and placental and endometrial apoptosis and proliferation. It is hoped that further investigation into the roles of these processes at the feto-maternal interface will further the understanding of the mechanisms governing foetal growth.

Tissue	Gestational Day				
	18	30	45	60	90
Placenta	n/a	ns	*P53* *Ki67*	*P53*	ns
Endometrium	ns	ns	*P53*	ns	ns

Table 5.3: Summary of Results which showed statistically significant effects of foetal size.

Green=Increased; Red=Decreased in samples associated with the lightest foetuses compared to their Closest to Mean Litter Weight (CTMLW) littermates. Abbreviations: P53=tumour suppressor protein 53, ns=not significant, n/a=not applicable.

Tissue	Gestational Day			
	30	45	60	90
Placenta	ns	*Bax*	*Bcl2* *P53* *Ki67*	ns
Endometrium	*Bax*	ns	*Bcl2* *P53* *Ki67*	ns

Table 5.4: Summary of Results which showed statistically significant effects of foetal sex.

Green=Increased; Red=Decreased in samples associated with the male foetuses compared to their female littermates. Abbreviations: P53=tumour suppressor protein 53, Bax=Bcl-2-associated X protein, Bcl2= B-cell lymphoma 2

6 The Use of Doppler Ultrasound in Pregnant Gilts to Assess Umbilical Arterial Blood Flow

The work presented in this chapter was accepted for publication by *Reproduction, Fertility and Development* on 20th February 2018. The manuscript is entitled “Doppler ultrasound can be used to monitor umbilical arterial blood flow in lightly sedated pigs at multiple gestational ages”. This manuscript has four authors: Claire Stenhouse (CS), Peter Tennant (PT), W. Colin Duncan (WCD) and Cheryl J. Ashworth (CJA). CS, CJA and PT devised and performed the experiment. WCD provided the Doppler ultrasound machine, training for the operation and interpretation of the data obtained. CJA performed the ultrasound and CS operated the Doppler ultrasound machine throughout the experiment. CS performed all data analysis. CS prepared the manuscript with assistance from CJA. All authors approved the final version of the manuscript.

6.1 Chapter Introduction

It is estimated that 3-15% and 5-8% of human pregnancies worldwide are affected by intrauterine growth restriction (IUGR) (Romo *et al.*, 2009; Gardosi, 2011) and preeclampsia (Muralimanoharan *et al.*, 2013) respectively, making them two of the leading causes of perinatal mortality and morbidity. Considering this, it is essential that clinicians can identify compromised pregnancies early in gestation to allow regular monitoring of maternal and foetal health throughout the remainder of gestation. This ensures interventions occur at the optimal time to decrease perinatal mortality and morbidity.

6.1.1 What is Doppler Ultrasound?

Doppler ultrasound is a non-invasive method of estimating blood vessel flow using the Doppler principle (Harville *et al.*, 2008), whereby the frequency of sound waves changes when either the source or the receiver moves. Conventional ultrasound uses sound waves to produce images, whereas

colour Doppler ultrasound can superimpose information regarding blood flow onto the conventional anatomical display. In Doppler ultrasound, a hand-held device (transducer; source of the sound waves) connected to the control panel is applied to the abdomen and a series of pulses are transmitted (Dickey, 1997). The echo, or returning sound wave, from tissue is the same from pulse to pulse. When the receiver hits moving blood, there will be a difference in the time taken for the echo to return which results in a shift in the Doppler frequency. This shift is dependent on the rate of blood flow, thereby allowing measurement of blood flow through the vessel of interest. This information produces a colour display which can be superimposed onto the conventional ultrasound image. An illustration of the echo received is produced in the form of a waveform, allowing measurements of the blood flow to be taken at different stages of the cardiac cycle.

In clinical practice, Doppler ultrasound can be used on non-sedated pregnant women throughout gestation to monitor both umbilical and uterine blood flow. The waveforms produced (Figure 6.1) can be used to calculate several parameters, examples of which include: Peak Systolic Velocity (PSV); End Diastolic Velocity (EDV); A/B Ratio; Resistance Index (RI); and the Pulsatility Index (PI) (Thompson *et al.*, 1988). The A/B Ratio, RI and PI are calculated using the following equations:

$$A/B\ Ratio = \frac{PSV}{EDV}$$

$$RI = \frac{PSV - EDV}{PSV}$$

$$PI = \frac{PSV - EDV}{Mean\ Velocity}$$

These parameters fall into two categories: angle dependent and angle-independent. Velocity measurements are categorised as angle-dependent measurements, whereby to obtain a truly accurate measurement of the velocity present, the angle of the ultrasound beam needs to be as close to zero degrees as possible (McDicken, 1991; Detti *et al.*, 2002). As the angle

increases, the accuracy of determining the velocity decreases. Considering this, angle independent parameters (the A/B ratio, RI and PI) are commonly used in clinical practice to ensure consistency between clinicians. These parameters provide an indication of vascular resistance, which in turn provides information regarding the arterial blood flow and placental vascular resistance.

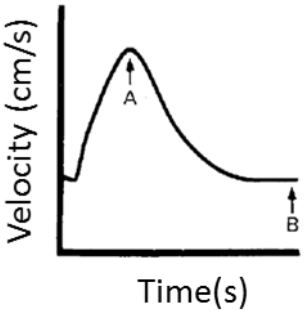

Figure 6.1: Profile of the umbilical arterial waveform obtained by Doppler ultrasound.

Adapted from Thompson *et al.*, (1988). A: Peak Systolic Velocity (PSV). B: End Diastolic Velocity (EDV). The ratio of the PSV to EDV (A/B Ratio) is commonly used when monitoring umbilical arterial blood flow. s=seconds

A number of temporal changes in vascularity can be observed by Doppler ultrasound to allow identification and further monitoring of IUGR pregnancies (Baschat *et al.*, 2001; Ferrazzi *et al.*, 2002). These changes can be categorised into 'early' and 'late', whereby 'early' changes reflect alterations in the middle cerebral artery and the umbilical artery (UA) and 'late' changes reflect UA reverse diastolic blood flow and abnormalities in the blood flow of the ductus venosus and aorta. The reduction, complete absence or reversal of end diastolic blood flow results in increased RI, PI and A/B Ratios.

It is hypothesised that due to placental insufficiency associated with IUGR, the foetus shifts the available blood flow to its most vital organs, namely the brain and heart, to spare their growth at the expense of the other organs (Giussani, 2011). Doppler ultrasound parameters reinforce this theory, with a decrease in the PI of the middle cerebral artery reported in IUGR foetuses (Johnson *et al.*, 2001b). The ratio of middle cerebral arterial and UA PI is thought to be the

most precise index for the prediction of IUGR prior to 34 weeks of gestation. Little investigation into the monitoring of IUGR and preeclamptic pregnancies by Doppler ultrasound has occurred after 34 weeks of gestation as often intervention occurs prior to this.

Baschat *et al.*, (2001) demonstrated that the alterations in UA blood flow and middle cerebral arterial blood flow precede deteriorations in biophysical profile scores. Biophysical profile scores describe foetal breathing and movement and amniotic fluid volume to identify if the foetus is in distress and requires intervention (Manning *et al.*, 1980, 1990). It is thought that the combination of serial UA and middle cerebral arterial Doppler measurements with the biophysical profile scores is the optimal method to enhance perinatal survival in IUGR pregnancies, by ensuring that clinical interventions occur at the optimal time (Detti *et al.*, 2002).

6.1.2 Previous Large Animal Studies using Doppler Ultrasound to Measure Uterine and Umbilical Blood Flow

As described above, Doppler ultrasound has been extremely useful in a clinical setting to monitor UA and uterine arterial blood flow in high-risk compromised pregnancies. Initially in veterinary research, Doppler ultrasound was used to investigate the cyclic changes in uterine blood flow in cows (Bollwein *et al.*, 2000) and mares (Bollwein *et al.*, 1998) (Table 6.1). Following this, Doppler ultrasound has been used increasingly to investigate changes in uterine and UA blood flow throughout gestation in mares and cows (Table 6.1). Bollwein *et al.*, (1998) developed a transrectal method for performing Doppler ultrasound which allowed analysis of uterine and umbilical vascularity non-invasively. These studies have vastly improved the knowledge of uterine and umbilical blood flow in these species and, due to the high number of pregnancy complications found in both species, it is hoped that the technique could be used to monitor pregnancies with increased risk of complications.

As described previously, sheep are considered a relevant large animal model for the study of mammalian foetal growth and development (Vuguin, 2007;

Barry and Anthony, 2008; Swanson and David, 2015). Until recently, assessment of uterine blood flow in cyclic and pregnant ewes has been performed using invasive techniques or under general anaesthesia (GA) whilst performing surgery (Tchirikov *et al.*, 2001; Acharya *et al.*, 2004, 2007; Gibson *et al.*, 2004; Sprague *et al.*, 2009; Abi-Nader *et al.*, 2010). Whilst these methods have provided insights into changes in uterine blood flow during pregnancy, the biological importance of the findings of these studies should not be extrapolated due to the invasiveness of the methods used. The results obtained may not be reflective of the normal environment the uterine tract would be subjected to during gestation. Considering this, Elmetwally *et al.*, (2016) developed a non-invasive method to perform transrectal and transabdominal Doppler ultrasound, without the use of sedation, in pregnant sheep and goats (Table 6.1). This study indicated that non-invasive ultrasound could be used to perform serial measurements of uterine vessels within the same ewe over gestation, highlighting the potential of this technique to improve the knowledge of the mechanisms governing foetal growth and placental and umbilical blood flow.

6.1.3 Previous Studies Using Doppler Ultrasound on Pregnant Pigs

Despite the large number of studies which have investigated the use of Doppler ultrasound to measure uterine and umbilical arteries in women, cows and mares, currently only two papers have reported the use of Doppler ultrasound in pregnant pigs. Brüssow *et al.*, (2012) used a laparoscopy guided approach on pregnant Landrace gilts to investigate umbilical blood flow for approximately 45-90 minutes under GA (Ketamine and Azaperone). In this study it was suggested that transabdominal non-invasive Doppler ultrasound would not be possible in pigs due to the presence of multiple foetuses in close proximity to one another therefore they opted to develop a laparoscopy-based approach. This study investigated the relationship between Doppler ultrasound data and foetal size (small, medium and large) at gestational days (GD) 36, 42 and 51. A decrease in foetal heart rate (FHR) between GD36 and 45 was observed in this study. Foetal size had a minimal influence on the parameters

investigated, with only the systolic pulse duration tending to be longer in large compared with small foetuses at GD36. Similar gestational changes in UA blood flow were observed by Harris *et al.*, (2013), with FHR decreasing with advancing gestation. RI and PI increased from GD39 to 55, were similar at GD55 and 66, before decreasing back to a level comparable with GD39. This study did not investigate the influence of foetal size on the Doppler ultrasound parameters and instead investigated the impact of maternal activity during gestation. In contrast to the Brüssow *et al.*, (2012) paper, no sedative was used in this study and instead the mammary glands were gently rubbed, having a calming effect on the gilts. However, this did limit the number of foetuses used in the study, with measurements only obtained from two foetuses from each gilt, and presumably the quality of the traces obtained would be poorer due to the influence of maternal movement.

Prior to the recent Doppler ultrasound papers, there have been a limited number of studies using more invasive techniques to investigate uterine and umbilical blood flow during gestation in the pig. Reynolds *et al.*, (1985) investigated uterine and umbilical blood flow in Yorkshire sows at GD70, 90 and 110 under GA (sodium thiamylal; maintained with an oxygen and halothane (fluothane) mixture). Using the Ford and Christenson, (1979) method for measuring uterine blood flow, an electromagnetic transducer was placed around the middle uterine artery of the exposed uterine horn. FHR and both uterine and umbilical blood flow remained constant throughout gestation. Interestingly, a negative correlation between umbilical blood flow and foetal number was observed. Père and Etienne, (2000) used ultrasonic transit time flow probes around the middle artery of each uterine horn to investigate changes in uterine blood flow during gestation (GD44-111). Their results suggest that uterine blood flow increases in a linear manner throughout gestation. Additionally, they showed an inverse relationship between the number of foetuses and uterine blood flow per foetus, indicating that uterine blood flow does not increase as the number of foetuses in the litter increases, consolidating the Reynolds *et al.*, (1985) results.

Although Doppler ultrasound is used routinely in clinical practice to identify compromised pregnancies, and many investigations have been carried out in cows and mares with the aim of developing a similar set of criteria, to date investigations into uterine and umbilical blood flow in pregnant pigs are limited. The broad objective of this study was to determine if non-invasive Doppler ultrasound can be performed on pregnant gilts, under light sedation, to investigate UA blood flow.

Table 6.1: Examples of previous uterine and umbilical arterial Doppler ultrasound studies in large animal models.

Animal	P or C	Artery	Method	Aim(s)	Main Findings	Reference
Horse	P	Uterine Umbilical	TR	To use Doppler ultrasound to non-invasively examine umbilical and uterine blood flow in the arteries ipsi- and contra-lateral to the foetus throughout gestation. To establish normal values that could be a reference for the identification of pregnancies with an increased risk of complications.	No difference was observed between ipsilateral and contralateral uterine vessels RI and volume of blood flow. RI decreased dramatically by around 50% throughout gestation and volume of blood flow increased 398-fold during gestation in the uterine vessels. Total oestrogen from maternal plasma was related to RI and volume of blood flow in uterine arteries. There was a non-linear relationship between week of gestation and umbilical RI values.	Bollwein *et al.*, (2004)
Heifer	P	Uterine	TR	To determine if vascular perfusion of the endometrium is mediated by the contact between the conceptus and the endometrium. (Pregnant compared with cyclic days 0-18; in pregnant between horns and with and without the embryo proper and foetus at GD0-60).	Vascularity increased in both uterine horns in non-pregnant but not pregnant heifers between days 14-18. In pregnant heifers, endometrial vascularity increased in the ipsilateral horn between GD18 and 20. A modest increase in vascularity between GD18 and 22 was detected in the contralateral horn, although a much greater increase was observed after GD32. At GD42, similar vascularity was observed between the two horns, before decreasing between GD42 and 60 in the contralateral horn.	Silva and Ginther, (2010)

Table 6.1: Examples of previous uterine and umbilical arterial Doppler ultrasound studies in large animal models.

Animal	P or C	Artery	Method	Aim(s)	Main Findings	Reference
Cow	P	Uterine	TR	To perform Doppler ultrasound once weekly from GD30-270 to examine changes over gestation in RI, TAMV, volume, A/B ratio and PI. To relate birth weight and calf sex to the parameters measured throughout gestation.	RI, PI, and A/B Ratio were negatively correlated to all other parameters investigated. RI, PI, and A/B Ratio were lower, and velocity and volume indices were higher in the uterine arteries ipsilateral to the foetus, when compared to the contralateral artery. RI, PI, and A/B Ratio decreased, and velocity, area and volume increased with advancing GD. Birth weight had a positive correlation with the volume of blood flow and a negative relationship with RI. No sex effects were observed in any of the parameters investigated throughout gestation.	Panarace *et al.*, (2006)
Goat	P	Umbilical	TA	To determine the normal FHR, RI and PI values for singleton and multiple pregnancies for future monitoring of pregnancies throughout gestation (GD40, 55, 70, 85, 100, 115, 130 and 145 investigated).	The number of foetuses present did not influence FHR, RI, or PI. FHR decreased with advancing GD. PI decreased until GD85 where it plateaued until parturition. RI decreased until GD130, before increasing towards parturition.	Serin *et al.*, (2010)

Table 6.1: Examples of previous uterine and umbilical arterial Doppler ultrasound studies in large animal models.

Animal	P or C	Artery	Method	Aim(s)	Main Findings	Reference
Cow	C	Uterine	TR	To develop a non-invasive reproducible method to assess changes in the uterine arterial blood flow (right and left) during two consecutive oestrous cycles.	A difference in the TAMV but not the RI between the right and left uterine arteries was observed, which was not related to the ovary that contained the CL/dominant follicle. This method was reproducible, and no differences were observed between the two oestrous cycles investigated. TAMV and RI were influenced by day of the oestrous cycle. Plasma oestrogen levels were positively correlated with TAMV and negatively correlated with RI.	Bollwein *et al.*, (2000)
Horse	C	Uterine	TR	To develop a non-invasive reproducible method to assess blood flow in the uterine arteries of mares. To assess differences in uterine blood flow between mares, over the course of the oestrous cycle and over multiple oestrous cycles. (Days 0, 5, 10, 15 and 20 during 4 oestrous cycles).	No difference was observed in RI between the right and left uterine arteries. RI values were correlated with mares and day of the oestrous cycle. RI was increased in multiparous mares compared to maidens however there were only 2 animals in the multiparous group. RI was influenced by day of the oestrous cycle. No differences were detected within mares between the RI values measured in the 4 oestrous cycles investigated.	Bollwein *et al.*, (1998)

Table 6.1: Examples of previous uterine and umbilical arterial Doppler ultrasound studies in large animal models.

Animal	P or C	Artery	Method	Aim(s)	Main Findings	Reference
Cow	Pregnant	Uterine	TR	To use Doppler ultrasound to non-invasively examine uterine blood flow in the arteries ipsi- and contralateral to the foetus throughout gestation (once per month for 10 months).	Decrease in RI during the first 8 months of gestation. RI values negatively correlated TAMV, vessel diameter and volume of blood flow. TAMV increased during the first two trimesters of pregnancy. Vessel diameter increased throughout gestation. TAMV, vessel diameter and volume of blood flow were higher, and RI was lower in the artery ipsilateral to the foetus.	Bollwein *et al.*, (2002)
Horse	Pregnant/ Cyclic	Uterine	TR	To use Doppler ultrasound to examine differences in uterine blood flow (right and left arteries) during the oestrous cycle and early pregnancy (2 cycles and 2 early pregnancies in each mare).	From day 11, TAMV was increased and RI was decreased in the uterine vessels in pregnant mares compared to those on day 11 of the oestrous cycle. During the oestrous cycle, no difference was observed in TAMV or RI between the right and left arteries. TAMV values were increased and RI was decreased between GD15-29 in the uterine artery ipsilateral to the conceptus compared to the contralateral artery.	Bollwein *et al.*, (2003)

Animal	P or C	Artery	Method	Aim(s)	Main Findings	Reference
Sheep and Goat	P	Uterine	TR,TA	To use Doppler ultrasound to non-invasively examine uterine blood flow (volume, TAMV, RI, PI, A/B Ratio, PSV, blood flow acceleration) throughout gestation. (2 weeks after mating at 2-week intervals).	Blood flow volume, PSV and TAMV increased with advancing GD in both species. RI, PI, and A/B ratio decreased with GD. Blood flow acceleration increased until week 14 and 16 in goat and sheep respectively. This then decreased until parturition.	Elmetwally *et al.*, (2016)
Sheep	P	Umbilical	TA	To relate umbilical arterial blood flow to foetal growth trajectories and placental biometry in a model of growth restriction at weekly intervals from GD83-126.	Doppler indices (PI, RI and A/B Ratio) were increased in growth restricted pregnancies compared to controls from GD83.	Carr *et al.*, (2012)

Table 6.1: Examples of previous uterine and umbilical arterial Doppler ultrasound studies in large animal models.

Abbreviations used: P or C = Pregnant or Cyclic TAMV = Timed Average Mean Velocity; RI = Resistance Index; CL = Corpus Luteum; A/B Ratio = Ratio of Peak Systolic Velocity (PSV) to End Diastolic Velocity (EDV); PI = Pulsatility Index; GD = Gestational Day, TR=Trans-rectal, TA=Trans-abdominal.

6.2 Chapter Aims

The aims of the research described in this chapter were:

i. To develop and optimise a Doppler ultrasound protocol to investigate UA blood flow in sedated pregnant gilts.
ii. To investigate gestational changes in foetal heart rate (FHR) and UA blood flow parameters.
iii. To determine if the number of foetuses in the uterus or the sex ratio of the litter influence UA blood flow.
iv. To scan every foetus in the right uterine horn and relate the parameters from ii to foetal size and sex.
v. To sedate, scan and recover (SSR) pregnant gilts prior to the terminal procedure to allow monitoring of UA blood flow within the same litter on two gestational days.

6.3 Accepted Manuscript

CSIRO PUBLISHING
Reproduction, Fertility and Development
https://doi.org/10.1071/RD17298

Doppler ultrasound can be used to monitor umbilical arterial blood flow in lightly sedated pigs at multiple gestational ages

Claire Stenhouse[A], *Peter Tennant*[A], *W. Colin Duncan*[B] *and Cheryl J. Ashworth*[A,C]

[A]Developmental Biology Division, The Roslin Institute and Royal (Dick) School of Veterinary Studies, University of Edinburgh, Easter Bush Campus, Edinburgh, EH25 9RG, UK.

[B]Centre for Reproductive Health, The Queen's Medical Research Institute, University of Edinburgh, Edinburgh, EH16 4TJ, UK.
[C]Corresponding author. Email: cheryl.ashworth@roslin.ed.ac.uk

Abstract. Doppler ultrasound was performed under moderate sedation (ketamine and azaperone) for 30 min to monitor umbilical arterial (UA) blood flow in one uterine horn of Large White Landrace gilts (n = 23) at Gestational Days (GD) 30, 45, 60 and 90. Gilts were scanned before they were killed to examine relationships between litter size, sex ratio and five UA parameters (peak systolic velocity (PSV), end diastolic velocity (EDV), A/B (PSV to EDV) ratio, fetal heart rate (FHR) and resistance index (RI)). In gilts in which scans were obtained from all fetuses in the scanned horn, relationships between UA parameters, and fetal weight and sex were examined. A subset of gilts were sedated, scanned and recovered (SSR) earlier in gestation (GD30 or GD45) to assess the effects of sedation on later fetal development by comparison with control litters (no previous sedation). Temporal changes were observed in all UA parameters ($P \leq 0.001$). At GD60 and GD90, FHR decreased with increasing duration of sedation ($P \leq 0.001$). Sex ratio and fetal weight affected UA blood flow, whereas litter size and fetal sex did not. SSR at GD30 and GD45 was associated with decreased fetal weight at GD60 ($P \leq 0.001$) and GD90 ($P = 0.06$) respectively, compared with controls. These results suggest maternal sedation during gestation affects fetal development, which should be investigated further. Measuring UA blood flow in growth-restricted porcine fetuses throughout gestation may be feasible.

Additional keywords: gestation, gilt, sedation.

Received 28 July 2017, accepted 28 March 2018, published online 4 May 2018

Introduction

Increased litter size has been a focus of recent pig genetic selection programs as an effective means to increase the profitability of the pig industry (Bee 2007). This has increased the within-litter variation in birthweight observed, with many litters containing an intrauterine growth-restricted (IUGR) piglet (Ashworth et al. 2001; Wu et al. 2006; Bee 2007; Vallet et al. 2014; Yuan et al. 2015). The decrease in birthweight observed in the IUGR piglet has severe consequences for postnatal development, with several disadvantageous phenotypes observed, including impaired adaptation to extrauterine life, a permanently reduced growth rate, altered organ growth and development, decreased reproductive performance and increased disease susceptibility (Wu et al. 2006).

It is essential that the umbilical cord and placenta function efficiently throughout gestation to support the growing fetus, with inadequate placental function being associated with adverse pregnancy outcomes, including pre-eclampsia and IUGR (Baschat 2003). It is hypothesised that due to the placental insufficiency associated with IUGR, the fetus redirects available blood flow to its most vital organs, namely the brain and heart, to spare their growth at the expense of other organs (Giussani 2011). In human clinical practice, non-invasive Doppler ultrasound is widely used to identify and monitor umbilical arterial (UA) blood flow in IUGR pregnancies, ensuring that clinical interventions occur at the optimal time (Detti et al. 2002). The waveforms produced by Doppler ultrasound can be used to calculate several parameters, including peak systolic velocity (PSV), end diastolic velocity (EDV), the A/B ratio (or PSV to EDV (S/D) ratio), resistance index (RI) and the pulsatility index (PI; Thompson et al. 1988; Berkley et al. 2012). These parameters fall into two categories: angle dependent and angle independent. Velocity measurements are categorised as angle-dependent measurements, whereby to obtain a truly accurate measurement of the velocity present, the angle of the ultrasound beam needs to be as close to 08 as possible (McDicken 1991; Detti et al. 2002). As the angle

increases, the accuracy of determining the velocity decreases. Considering this, angle-independent parameters, such as the A/B ratio, RI and PI, are commonly used in clinical practice (Trudinger et al. 1985; Detti et al. 2002; Berkley et al. 2012). These parameters provide an indication of vascular resistance, which, in turn, provides information regarding arterial blood flow and placental vascular resistance.

In large animals, Doppler ultrasound has been used to investigate uterine, umbilical and fetal vessels in cattle (Bollwein et al. 2002; Panarace et al. 2006; Silva and Ginther 2010), goats (Serin et al. 2010; Elmetwally et al. 2016), horses (Bollwein et al. 2000, 2004) and sheep (Elmetwally et al. 2016). There have also been limited investigations into gestational changes in UA blood flow in the pig (Brüssow et al. 2012; Harris et al. 2013). It has been suggested that an invasive laparoscopic approach is the most effective method to monitor UA blood flow in the pig (Brüssow et al. 2012), although the effect of general anaesthesia is unknown. In addition, the relationship between UA blood flow and fetal growth and development in the pig is poorly understood.

The aim of the present study was to relate several parameters (including litter size, fetal weight and sex and the sex ratio of the litter) to UA blood flow parameters throughout gestation in the pig, in a non-invasive manner, under light sedation. In addition, this protocol was used to monitor gestational changes within the same pregnancy, with an additional objective of investigating the effect of light sedation in early gestation on later fetal development.

Materials and methods

All procedures were performed with approval from The Roslin Institute (University of Edinburgh) Animal Welfare and Ethical Review Board and in accordance with the UK Animals (Scientific Procedures) Act, 1986.

Experimental animals

In all, 23 Large White Landrace gilts (age 11–14 months; mean weight at death 188.76 kg) were included in this study. All gilts were observed daily for signs of oestrus and were housed six to eight animals per pen, unless stated otherwise. Oestrous cyclicity and ovarian function were controlled in accordance with routine normal practice at The Roslin Institute Large Animal Unit. In a subset of gilts (n = 5), oestrus was synchronised by daily feeding of 20 mg altrenogest (Regumate; Hoechst Roussel Vet) for 18 days followed by injection of pregnant mare's serum gonadotrophin (PMSG) and human chorionic gonadotrophin (hCG), as described by Lillico et al. (2013). All gilts were inseminated twice daily for the duration of oestrus with semen from one of two sires (Large White). The first day of insemination was assigned as Gestational Day (GD) 0. The average ovulation rate (determined by the number of corpora lutea present) and percentage prenatal survival (determined as the number of live fetuses present divided by the ovulation rate multiplied by 100) was 20.5% and 66.75% respectively.

Doppler ultrasound procedure

Gilts were sedated by intramuscular injection with 1 mg/kg ketamine (Henry Schein Animal Health) and 2 mg/kg azaperone (Henry Schein Animal Health). Once the animals were sedated (~10–15 min after drug administration), they were positioned in lateral recumbency on their left side. The presumed right uterine horn was scanned by a single operator from the cervix towards the ovary using a Philips iU22 colour Doppler ultrasound machine, with an L9-3 transducer probe (Philips Healthcare). The scanning procedure lasted for approximately 30 min. UA traces were obtained from the fetuses and the following parameters were measured: fetal heart rate (FHR), PSV, EDV, RI and the A/B ratio (PSV : EDV). The number of fetuses and waveform data collected are summarised in Table 1.

Experiment 1: temporal changes in UA blood flow

Pregnant gilts were used in this study at GD30 (range GD29–30; n = 3), GD45 (range GD43–46; n = 6), GD60 (range GD60–61; n = 5) and GD90 (range GD89–92; n = 9). Following completion of the scanning procedure, the gilts were killed with 0.4 mL kg 1 of 20% w/v sodium pentobarbitone (Henry Schein Animal Health), injected intravenously via a cannula inserted in the ear vein.

A subset of pregnant gilts at GD60 (n = 4) and GD90 (n = 3) were sedated, scanned and allowed to regain consciousness (recovered; SSR) at GD30 (range GD29–33; n = 4) and GD45 (range GD43–44; n = 3) respectively. The sedation and scanning procedure was performed as described above. Following this, sedated gilts were hoisted onto a surgical trolley and transferred to a recovery pen. Once the animals had fully recovered, they were transferred to a shed where they were housed individually, in close proximity to other pregnant gilts, for the remainder of the experiment. These animals were killed immediately after the second scanning procedure. To assess

temporal changes in UA blood flow, the SSR traces at GD30 and GD45 were combined with those of the killed animals (GD30, n = 7 litters; GD45, n = 9 litters; GD60, n = 5 litters; GD90, n = 9 litters).

Experiment 2: effect of litter size and sex ratio of the litter on UA blood flow

Following confirmation of death, the reproductive tract was revealed by a mid-ventral incision. The tract was lifted from the body cavity and placed on a dissecting tray. Both uterine horns were dissected, from the ovaries towards the cervix, allowing determination of whether traces were obtained from all fetuses in the right uterine horn. All fetuses were identified as 'live' or 'dead' based on their morphology at the time of dissection. Fetuses were weighed and, at GD45, GD60 and GD90, fetal sex was determined morphologically. DNA was isolated from the GD30 fetuses using the DNeasy Blood and Tissue DNA extraction kit (Qiagen), and polymerase chain reaction (PCR) was performed for the SRY region of the Y chromosome (forward primer, 5^0-GAAAGCGGACGATTACAGCC-3^0; reverse primer, 5^0-TTGCGACGAGGTCGGTATTT-3^0). Primers for the homologous zfx/zfy regions of the sex chromosomes served as a positive control (forward primer 5^0-ATAATCACA TGGAGAGCCACAAGCT-3^0; reverse primer 5^0-GCACT TCTTTGGTATCTGAGAAAGT-3^0; Oliver et al. 2011). For the reaction, 7mL nuclease-free water, 5 mL of 10 PCR Buffer, 1 mL dNTP mix (10 mM), 1 mL FastStart Taq (all solutions from the Roche FastStart Taq kit; Sigma Aldrich) and 5 mL of both forward and reverse primers (5 mM stock) were added to 1 mg sample DNA. A no-template control and postnatal porcine testicular and ovarian DNA were run as controls. The PCR conditions had an initial step of 958C for 4 min 30 s, which was followed by 30 cycles of 958C for 30 s, 608C for 30 s and 728C for 30 s, with a final extension at 728C for 4 min 30 s and an indefinite hold at 48C. Samples were processed in 96-well microplates (NUNC; Thermofisher) on a 96-well thermocycler (Biometra). The PCR products were then analysed on a 1.2% (w/v) agarose 1 SybrSafe (Thermofisher) gel with 1 Tris–acetic acid–EDTA buffer. This allowed the results to be related to the number of live fetuses and the sex ratio of the litter at all GD.

Experiment 3: effects of fetal size and sex on UA blood flow

As described in Experiment 2, fetal weight and sex was recorded for all fetuses in all killed litters at all GD investigated. In a subset of the killed GD90 litters (n = 4), UA waveforms were obtained from all fetuses in the right uterine horn, which allowed the parameters obtained to be related to fetal size and sex.

Experiment 4: effect of sedation

The difference in time since the first fetal trace measurement to each subsequent trace measured was calculated within gilt to determine whether the fetuses were affected by maternal sedation over the scanning period. The mean FHR for each fetus was then related to the time since the first fetal trace measurement. To determine whether the sedation in early gestation for the SSR procedure affected fetal development later in gestation, fetal weight, the number of live fetuses in the uterus and the sex ratio of the litters in the SSR gilts were compared with GD-matched control gilts that had not been subjected to the SSR procedure (n = 8 and 4 control and SSR GD60 litters respectively; n = 6 and 3 control and SSR GD90 litters respectively).

Statistical analysis

All statistical analyses were performed using Minitab 17 or GenStat 13.1 (VSN International). The mean value for each parameter was calculated for each fetus and normality was assessed. Outliers were tested for using a Grubbs outlier test and were excluded systematically, with normality within each group being reassessed following each exclusion. Log-transformed data were used for PSV at GD45, GD60 and GD90, as well as for EDV at GD45 and GD90, to improve the distribution of the data. Non-parametric tests were used whenever the data were found to be not normally distributed after transformation.

Temporal changes in FHR were analysed by one-way analysis of variance (ANOVA) followed by Tukey analysis. The gilt term was blocked to account for the common maternal environment. For the remainder of the parameters, where the data did not have a normal distribution with the four GD combined, a Kruskal–Wallis test was used to investigate temporal changes. Linear regressions were performed within GD for all parameters against the number of live fetuses and percentage of males in the litter (sex ratio). Two-sample t-tests were performed to determine whether fetal sex affected any of the parameters investigated. A restricted maximum likelihood (REML) variance component analysis was performed with gilt fitted as a random effect to identify the effects

of fetal weight on FHR, PSV, EDV, A/B ratio and RI. The difference in time from the first fetal trace measurement to each subsequent trace measured was calculated within gilt. The results were grouped by GD and gilt was fitted as a random effect in a REML variance component analysis to account for the variation attributed to gilt within GD. Similarly, two-way ANOVA (GD treatment (SSR or control)) with a block for gilt was performed to compare the number of live fetuses, the percentage of males in the litter and the s.d. in fetal weight in SSR and control litters. The weight of the SSR and control fetuses were compared within GD (Mann–Whitney at GD60; ANOVA with gilt block at GD90) and fetal weight was then compared within sex (two-way ANOVA (sex treatment) with gilt block). In all cases, $P \leq 0.05$ was considered significant. Data are presented as the mean s.e.m.

Table 1. Measurements of umbilical arterial parameters per gestational day

Unless indicated otherwise, data show mean values, with the range in parentheses. GD, Gestational Day; FHR, fetal heart rate; PSV, peak systolic velocity;
EDV, end diastolic velocity; A/B ratio, PSV : EDV ratio; RI, resistance index

	Parameter	No. fetuses	No. litters	No. waveforms per fetus	No. fetuses per litter
GD30	FHR (b.p.m.)	18	7	5.78 (1–16)	2.57 (1–4)
	PSV (cm s ^{1})	18	7	6.06 (1–17)	2.57 (1–4)
	EDV (cm s ^{1})	15	7	6.06 (1–17)	2.14 (1–4)
	A/B ratio	18	7	6.06 (1–17)	2.57 (1–4)
	RI	17	7	6.06 (1–17)	2.43 (1–4)
GD45	FHR (b.p.m.)	39	9	7.15 (2–15)	4.33 (2–7)
	PSV (cm s ^{1})	39	9	7.69 (2–16)	4.33 (2–7)
	EDV (cm s ^{1})	35	9	7.69 (2–16)	3.89 (1–7)
	A/B ratio	39	9	7.69 (2–16)	4.33 (2–7)
	RI	37	9	7.69 (2–16)	4.11 (1–7)
GD60	FHR (b.p.m.)	29	5	8.07 (1–22)	6.00 (5–7)
	PSV (cm s ^{1})	31	5	8.29 (3–22)	6.20 (5–7)
	EDV (cm s ^{1})	29	5	8.29 (3–22)	5.80 (4–7)
	A/B ratio	30	5	8.29 (3–22)	6.00 (4–7)
	RI	30	5	8.29 (3–22)	6.00 (5–7)
GD90	FHR (b.p.m.)	45	9	6.73 (1–19)	6.00 (3–8)
	PSV (cm s ^{1})	48	7	7.11 (1–23)	7.00 (5–10)
	EDV (cm s ^{1})	50	7	7.11 (1–23)	7.00 (5–10)
	A/B ratio	55	9	7.11 (1–23)	6.11 (3–10)
	RI	55	9	7.11 (1–23)	6.11 (3–10)

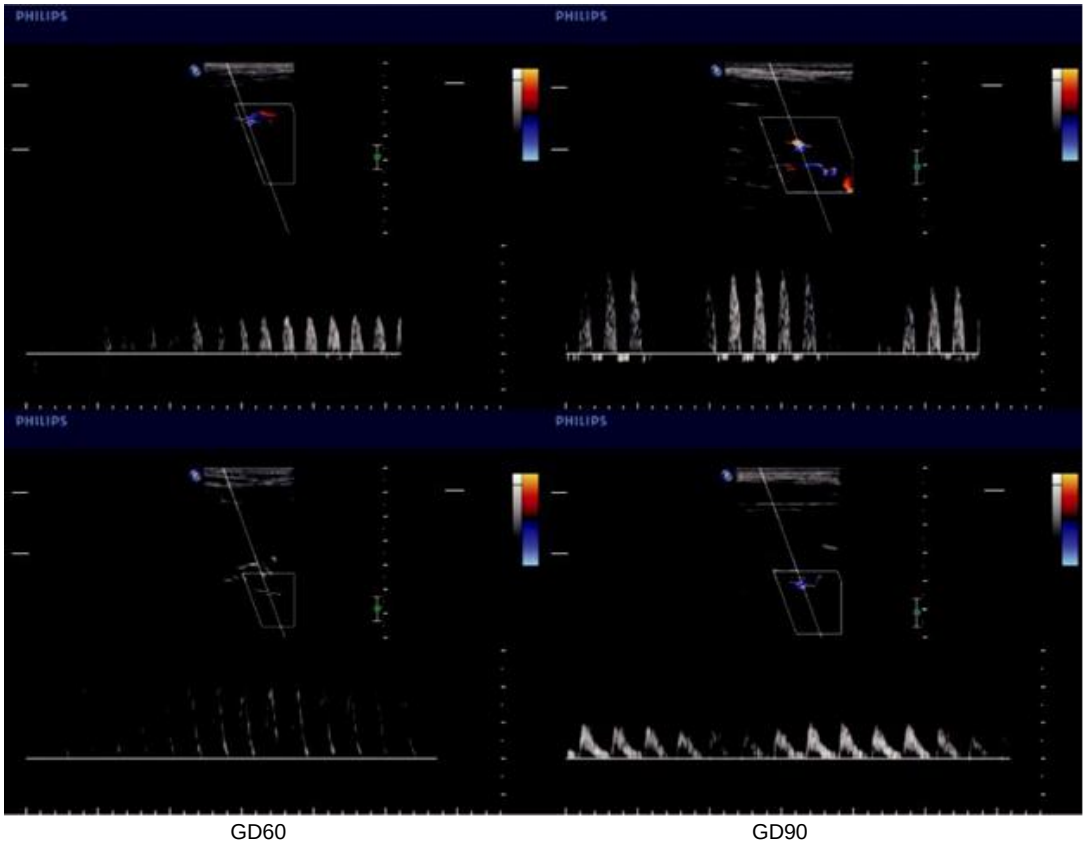

Fig. 1. Representative umbilical arterial waveforms produced at Gestational Day (GD) 30, GD45, GD60 and GD90. Pregnant gilts were sedated and non-invasive Doppler ultrasound was performed on umbilical arteries. Representative Doppler ultrasound images were obtained using the Philips iU22 colour Doppler ultrasound machine.

Results

Experiment 1: temporal changes in FHR, PSV, EDV, RI and A/B ratio

UA waveforms were obtained at all GD studied (Fig. 1). Temporal changes were observed in all parameters investigated, with a decrease in FHR, A/B ratio and RI (all $P \leq 0.001$), and an increase in PSV and EDV (all $P \leq 0.001$; Fig. 2) with advancing gestation. FHR decreased gradually with advancing gestation, but the largest differences in the other parameters occurred between GD60 and GD90, reflecting the presence of diastolic blood flow at GD90 but not at earlier GD.

Experiment 2: effects of litter sex ratio and litter size on UA blood flow

The number of fetuses in the litter or right uterine horn did not affect any of the parameters investigated within GD (Table 2). A negative relationship between the percentage of males in the litter and EDV at GD30 ($P = 0.077$) and GD60 ($P \leq 0.05$) was observed. In addition, a positive relationship was observed at GD30 between the percentage of males in the litter and both the A/B ratio ($P \leq 0.05$) and RI ($P \leq 0.05$).

Experiment 3: effects of fetal weight and sex on UA blood flow

In four of the GD90 litters, UA waveforms were obtained from all fetuses in the right uterine horn, allowing relationships between UA parameters and both fetal size and sex to be explored. FHR did not differ significantly between male (n = 16) and female (n = 10) fetuses (135.0 3.0 and 132.9 3.2 b.p.m. respectively; Fig. 3a). Similarly, no differ-ences were observed between male (n = 16) and female (n = 9) fetuses in PSV (69.29 6.54 and 81.45 7.88 cm s 1 respectively) or EDV (15.03 2.24 and 16.54 1.88 cm s 1 respectively; Fig. 3b, c). Sex did not affect the A/B ratio (5.62 0.62 and 5.12 0.45 in male (n = 16) and female (n = 9) fetuses respectively) or RI (0.79 0.02 and 0.79 0.02 respectively; Fig. 3d, e). Fetal weight was negatively related to FHR ($P = 0.089$), A/B ratio ($P \leq 0.05$) and RI ($P \leq 0.05$).

Experiment 4: effects of sedation on FHR and later fetal development

A significant decrease in FHR over the sedation period was observed at GD60 and GD90 ($P \leq 0.001$), but not at GD30 or GD45 (Fig. 4). The mean decrease in FHR at GD30, GD45, GD60 and GD90 was 8.7 4.6, 5.3 6.2, 18.4 5.7 and 20.6 10.3 b.p.m. respectively. The SSR process at GD30 and GD45 did not affect the number of live fetuses or the sex ratio of the litter at GD60 and GD90 compared with control fetuses whose dams had not been sedated previously. Intriguingly, fetal weight was significantly lower in GD60 SSR fetuses compared with control GD60 fetuses ($P \leq 0.001$; Fig. 5a, c). A similar trend was observed at GD90 ($P = 0.061$; Fig. 5b, d). Analysis of the s.d. in fetal weight within the litter revealed a lower s.d. in SSR litters compared with controls at GD90, but not at GD60 ($P \leq 0.05$; Fig. 5e).

Discussion

The broad objective of the present study was to determine whether non-invasive Doppler ultrasound could be used to monitor UA blood flow in pregnant gilts under light sedation. To our knowledge, this is the first report of the use of Doppler ultrasound at this early stage of gestation in the pig. This method was successfully used to obtain traces at all GD analysed, and highlighted novel temporal changes in all parameters investi-gated. The length of the sedation period affected FHR at GD60 and GD90, but not earlier in gestation, suggesting that fetuses in late gestation may be more affected by maternal sedation, albeit with modest numbers. Pregnant gilts were subjected to an SSR procedure to allow measurements on two GD within the same litter. Interestingly, the most striking finding from the present study was that approximately 30 min light sedation in early gestation decreased fetal weight in later gestation, highlighting surprising potential long-term programming effects that warrant further investigation.

Similar temporal changes in UA blood flow parameters have been reported in sheep and goats (Serin et al. 2010; Carr et al. 2012). The two published studies describing pig UA blood flow parameters (Brüssow et al. 2012; Harris et al. 2013) both reported a decrease in FHR as gestation proceeded, but only Harris et al. (2013) observed temporal changes in RI and PI between GD39 and GD81. Changes in FHR observed in both studies follow a similar pattern to those seen in the present study, but not all parameters studied exhibited the same temporal trends in the three studies. The three experiments were performed under different sedation conditions, with Harris et al. (2013) using non-sedated gilts, 'rubbing' the udder of the gilts to produce a 'calming' effect in the animals, whereas Brüssow et al. (2012) performed the procedure by scanning the exposed uterus directly while the pig was under general anaesthesia. Comparison of the mean

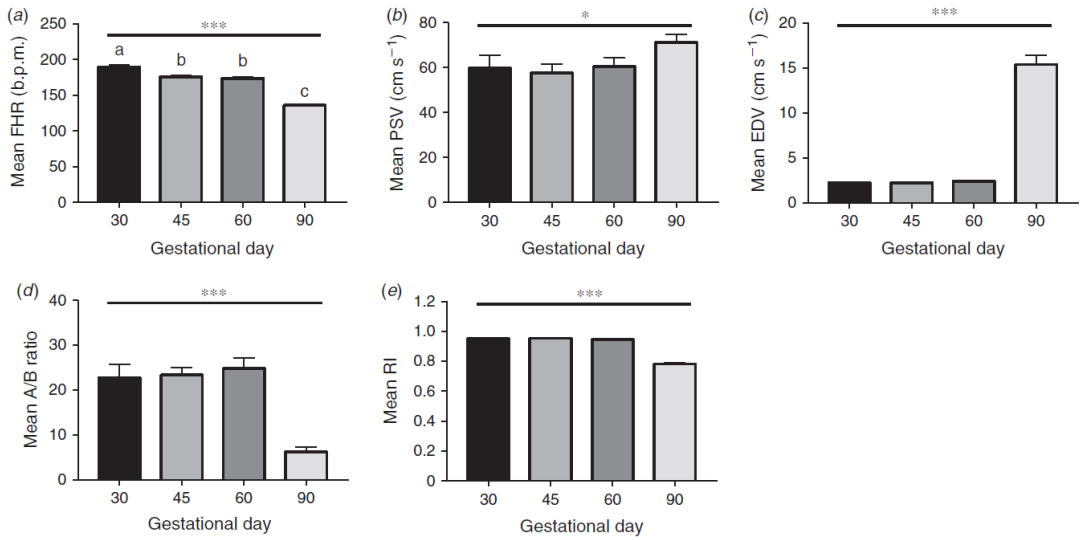

Fig. 2. Temporal changes in umbilical arterial blood flow parameters. Non-invasive Doppler ultrasound was performed on sedated pregnant gilts at Gestational Day (GD) 30, GD45, GD60 and GD90. Mean values for each parameter were calculated for each image to give a mean value per fetus. These values were then used to calculate the mean within each GD. Data show the mean s.e.m. (a) Fetal heart rate (FHR) decreased with advancing gestation (ANOVA with block for gilt; different letters indicate significant differences between groups determined by Tukey analysis). (b) Peak systolic velocity (PSV) and (c) end diastolic velocity (EDV) increased with advancing gestation (Kruskal–Wallis). (d) The A/B ratio (PSV : EDV) and (e) resistance index (RI) decreased with advancing gestation (Kruskal–Wallis). *P ≤ 0.05, ***P ≤ 0.001.

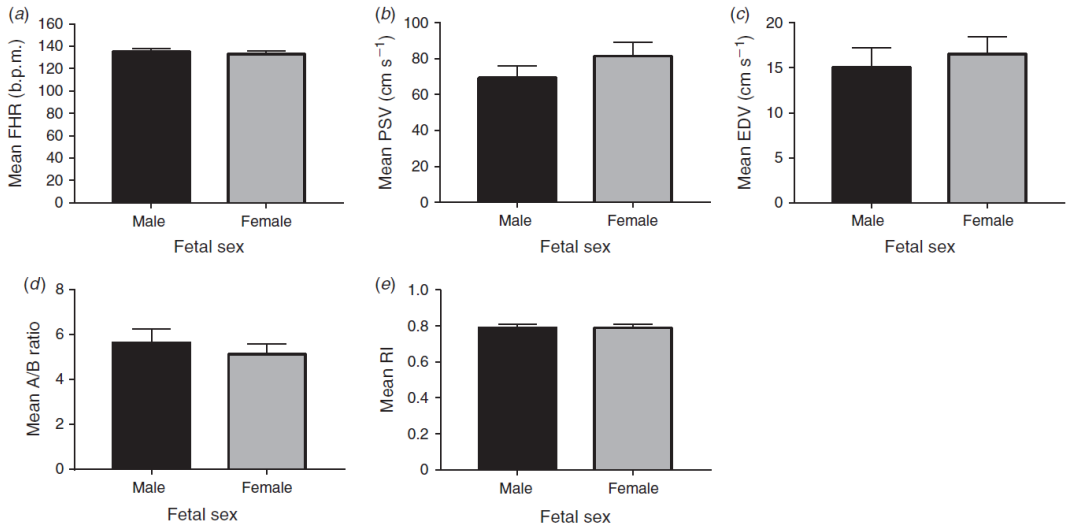

Fig. 3. Fetal sex did not affect (a) fetal heart rate (FHR), (b) peak systolic velocity (PSV), (c) end diastolic velocity (EDV), (d) the A/B ratio (PSV : EDV) or (e) the resistance index at Gestational Day 90. Mean values for each parameter were calculated for each image to give a mean value per fetus. These values were used to calculate the mean within each sex. Data show the mean s.e.m.

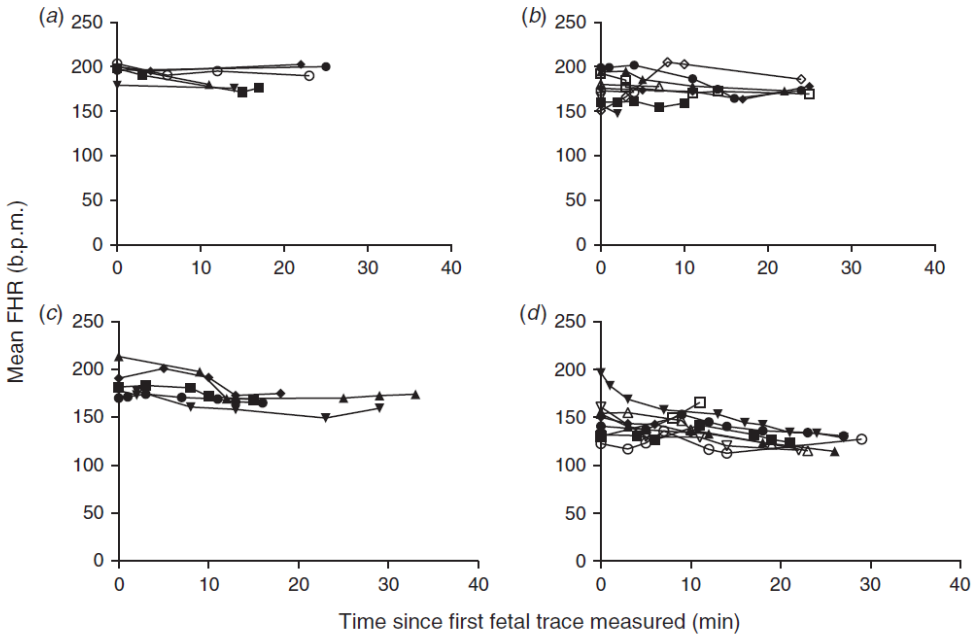

Fig. 4. Mean fetal heart rate (FHR) over the sedation period within gestational day (GD): (a) GD30, (b) GD45, (c) GD60 and (d) GD90. Pregnant gilts were sedated and non-invasive Doppler ultrasound was performed on umbilical arteries. To determine whether the sedation process had an effect on FHR, time since the first fetal trace was measured and plotted against FHR. The results were grouped by GD, as shown, and gilt was fitted as a random effect in a restricted maximum likelihood (REML) variance component analysis to account for the variation attributed to gilt within GD. Each symbol represents a different gilt.

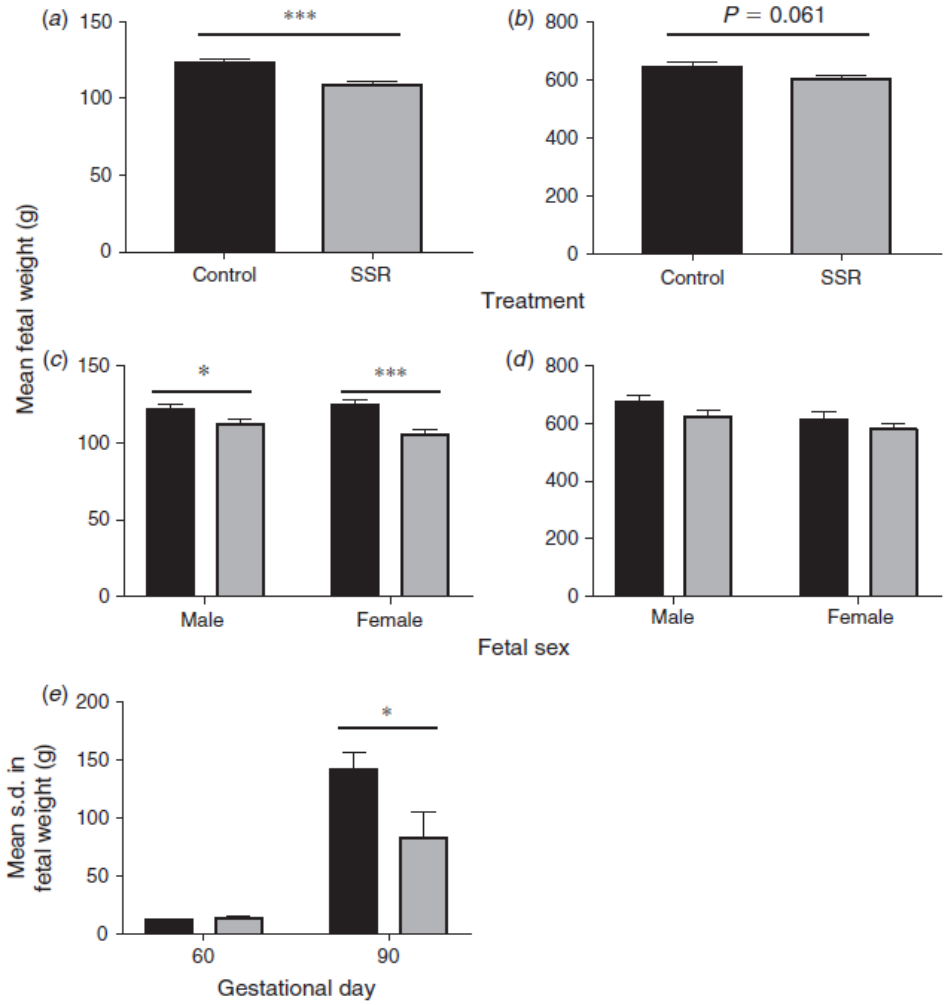

Fig. 5. (a–d) Fetal weight and (e) the s.d. of fetal weight in litters that had been sedated in early gestation and control litters. Non-invasive Doppler ultrasound was performed on sedated pregnant gilts at Gestational Day (GD) 30 and GD45. Following this, the gilts were allowed to recover (sedated, scanned and recovered; SSR) before undergoing the procedure for a second time in late gestation (GD60 or GD90) as a terminal procedure. The weight of the control (black) and SSR (grey) fetuses was compared within GD (Mann–Whitney at GD60; ANOVA with gilt block at GD90) and fetal weight was then compared within sex (two-way ANOVA (sex x treatment) with gilt block). In all cases, $P \leq 0.05$ was considered significant. Control litters were those that had not been subjected to the SSR procedure. (a, b) Fetal weight at GD60 (a) and GD90 (b). (c, d) Fetal weight at GD60 (c) and GD90 (d) within sex. Data are the mean ± s.e.m. (n = 8 and 4 control and SSR GD60 litters respectively; n¼6 and 3 control and SSR GD90 litters respectively). *$P \leq 0.05$, ** $P \leq 0.01$, *** $P \leq 0.001$.

FHR values reported in these studies with the values obtained in the present experiment suggests that increasing the level of sedation decreases the mean FHR observed at all stages of gestation studied.

The sex ratio of pig litters is an area of significant interest to the pig industry, with gilts from female- biased litters having an increased number of teats, a higher fertility rate and an increased conception rate on their first breeding attempt than gilts from male-biased litters (Drickamer et al. 1997; Górecki 2003). It has also been proposed that male piglets are disadvantaged, with male piglets being crushed by the sow more than females, more males dying from disease-related causes than females and males having impaired thermoregulation compared with females (Baxter et al. 2012). In the present study, the percentage of males in the litter affected EDV, the A/B ratio and RI, highlighting that the sex ratio of the litter could affect UA blood flow. Recent studies have revealed that sexual dimorphism exists in human placentas (for reviews, see Adibi et al. 2017; Kalisch-Smith et al. 2017). In addition, it has been shown that male babies have increased perinatal mortality and morbidity when human pregnancy is complicated by pre-eclampsia and IUGR (Challis et al. 2013; Muralimanoharan et al. 2013). Similarly, fetal sex has been shown to affect the expression of placental genes and the inflammatory response in humans, which is thought to be attributed to sexual dimorphism in placental function (Ghidini and Salafia 2005; Challis et al. 2013). It has also been shown in the pig that placental and endometrial gene expression and vascularity are associated with both fetal size and sex (C. Stenhouse, C. O. Hogg and C. J. Ashworth, unpubl. obs.). Widnes et al. (2017) reported that in humans, UA PI is increased in females compared with males, although these authors did not suggest that fetal sex affected any of the other parameters investigated. Therefore, if differences are observed in placental and endometrial tissue supplying fetuses of different sex, this may indicate that the uterine environment of a male-biased litter would be very different to that of a female-biased litter, which may explain the relationships between the sex ratio of the litter and UA blood flow parameters measured in the present study.

Surprisingly, light sedation in early gestation decreased fetal weight in later gestation. This, alongside the decrease in FHR over the sedation period, suggests that sedation during gestation could have significant effects on fetal development. The mechanisms behind this decrease in fetal weight warrant much further investigation. It has previously been suggested that azaperone has a vasodilatory effect, and can therefore result in a decrease in blood pressure and body temperature

(Van Woerkens et al. 1990; Hall and Clarke 1991; Brodbelt and Taylor 1999; Hodgkinson 2007). Although care was taken to ensure that the gilts were kept warm throughout the process, temperature and blood pressure were not monitored in the present study. In addition, there is some evidence suggesting that azaperone can promote activation of the hypothalamic– pituitary–adrenal (HPA) axis. Das et al. (2016) investigated the effects of azaperone- and azaperone plus ketamine-induced general anaesthesia on plasma cortisol levels in pigs. Administration of azaperone led to a prolonged and significant increase in plasma cortisol within 45 min of drug administration for the remaining 255 min of the experiment, and this effect was increased further with the addition of ketamine (Das et al. 2016). This may indicate that cortisol mediates the observed physiological effects of azaperone, suggesting that azaperone may promote an increased stress response in pigs.

Considering this information, it could be hypothesised that sedation with azaperone and ketamine promoted a decrease in body temperature and blood pressure, activating the maternal HPA axis and increasing cortisol production by the adrenal cortex. Although cortisol is metabolised by 11b-hydroxysteroid dehydrogenase 2 into inactive corticosterone at the placenta from GD24 in the pig (Klemcke 2003), not all the available cortisol will be converted into inactive corticosterone, leading to an increase in the levels of maternal cortisol crossing the placenta to affect the fetus. This would ultimately act as a stressful environment for the fetus, leading to the observed decreased fetal weight in late gestation, and potentially having effects postnatally. Interestingly, it has previously been suggested that there is an inverse relationship between fetal plasma cortisol and fetal size (Klemcke and Christenson 1997), indicating that lighter fetuses may have a higher baseline stress response. To test the proposed mechanism of action in the future, it would be useful to monitor maternal rectal and surface temperature, blood pressure and salivary cortisol at regular intervals throughout the Doppler process.

In conclusion, we have demonstrated that Doppler ultrasound can be used to non-invasively monitor UA blood flow in the pregnant pig from GD30. Our results have indicated, for

the first time, that fetal weight and the sex ratio of the litter could affect UA blood flow in the pig. Intriguingly, sedation with azaperone and ketamine had a significant effect on fetal development; the mechanisms and long-term effects of this warrant much further investigation and could have clinical relevance. It is hoped that further optimisation of Doppler ultrasound under light sedation would allow evaluation of UA blood flow parameters in relation to fetal growth and development, especially in IUGR fetuses.

Conflicts of interest

The authors declare no conflicts of interest.

Acknowledgements

The authors thank the staff of The Roslin Institute Large Animal Unit for skilled assistance, Eddie Clutton for helpful discussions and advice and Darren Shaw for statistical advice. The Roslin Institute receives Institute Strategic Grant funding from the Biotechnology and Biological Sciences Research Council (BBSRC) (BBS/E/D/30002276). C. Stenhouse is in receipt of a studentship from the University of Edinburgh.

References

Adibi, J., Burton, G. J., Clifton, V., Collins, S., Frias, A. E., Gierman, L., Grigsby, P., Jones, H., Lee, C., Maloyan, A., Markert, U. R., Morales-Prieto, D. M., Murthi, P., Myatt, L., Pollheimer, J., Roberts, V., Robinson, W., Salafia, C., Schabel, M., Shah, D., Sled, J., Vaillancourt, C., Weber, M., and O'Tierney-Ginn, P. F. (2017). IFPA meeting 2016 workshop report II: placental imaging, placenta and development of other organs, sexual dimorphism in placental function and trophoblast cell lines. Placenta 60(Suppl. 1), S10–S14. doi:10.1016/J.PLACENTA.2017.02.021

Ashworth, C. J., Finch, A. M., Page, K. R., Nwagwu, M. O., and McArdle, H. J. (2001). Causes and consequences of fetal growth retardation in pigs.
Reprod. Suppl. 58, 233–246.

Baschat, A. A. (2003). Integrated fetal testing in growth restriction: combining multivessel Doppler and biophysical parameters. Ultrasound Obstet. Gynecol. 21, 1–8. doi:10.1002/UOG.21

Baxter, E. M., Jarvis, S., Palarea-Albaladejo, J., and Edwards, S. A. (2012). The weaker sex? The propensity for male-biased piglet mortality. PLoS One 7, e30318. doi:10.1371/JOURNAL.PONE.0030318

Bee, G. (2007). Birth weight of litters as a source of variation in postnatal growth, and carcass and meat quality. Adv. Pork Prod. 18, 191–196.

Berkley, E., Chauhan, S. P., and Abuhamad, A. (2012). Doppler assessment of the fetus with intrauterine growth restriction. Am. J. Obstet. Gynecol. 206, 300–308. doi:10.1016/J.AJOG.2012.01.022

Bollwein, H., Meyer, H. H. D., Maierl, J., Weber, F., Baumgartner, U., and Stolla, R. (2000). Transrectal Doppler sonography of uterine blood flow in cows during the estrous cycle. Theriogenology 53, 1541–1552. doi:10.1016/S0093-691X(00)00296-X

Bollwein, H., Baumgartner, U., and Stolla, R. (2002). Transrectal Doppler sonography of uterine blood flow in cows during pregnancy. Therio-genology 57, 2053–2061. doi:10.1016/S0093-691X(02)00706-9

Bollwein, H., Weber, F., Wosche´e, I., and Stolla, R. (2004). Transrectal Doppler sonography of uterine and umbilical blood flow during pregnancy in mares. Theriogenology 61, 499–509. doi:10.1016/S0093-691X (03)00225-5

Brodbelt, D. C., and Taylor, P. M. (1999). Comparison of two combinations of sedatives before anaesthetising pigs with halothane and nitrous oxide. Vet. Rec. 145, 283–287. doi:10.1136/VR.145.10.283

Brüssow, K. P., Kurth, J., Vernunft, A., Becker, F., Tuchscherer, A., and Kanitz, W. (2012). Laparoscopy guided Doppler ultrasound measure-ment of fetal blood flow indices during early to mid-gestation in pigs. J. Reprod. Dev. 58, 243–247. doi:10.1262/JRD.11-059T

Carr, D. J., Aitken, R. P., Milne, J. S., David, A. L., and Wallace, J. M. (2012). Fetoplacental biometry and umbilical artery Doppler velocimetry in the overnourished adolescent model of fetal growth restriction. Am. J. Obstet. Gynecol. 207, 141.e6–15. doi:10.1016/J.AJOG.2012.05.008

Challis, J., Newnham, J., Petraglia, F., Yeganegi, M., and Bocking, A. (2013). Fetal sex and preterm birth. Placenta 34, 95–99. doi:10.1016/J. PLACENTA.2012.11.007

Das, G., Vernunft, A., Gors, S., Kanitz, E., Weitzel, J. M., Brüssow, K. P., and Metges, C. C. (2016). Effects of general anesthesia with ketamine in combination with the neuroleptic sedatives xylazine or azaperone on plasma

metabolites and hormones in pigs. J. Anim. Sci. 94, 3229–3239. doi:10.2527/JAS.2016-0365

Detti, L., Akiyama, M., and Mari, G. (2002). Doppler blood flow in obstetrics. Curr. Opin. Obstet. Gynecol. 14, 587–593. doi:10.1097/00001703-200212000-00003

Drickamer, L. C., Arthur, R. D., and Rosenthal, T. L. (1997). Conception failure in swine: importance of the sex ratio of a female's birth litter and tests of other factors. J. Anim. Sci. 75, 2192–2196. doi:10.2527/1997. 7582192X

Elmetwally, M., Rohn, K., and Meinecke-Tillmann, S. (2016). Noninvasive color Doppler sonography of uterine blood flow throughout pregnancy in sheep and goats. Theriogenology 85, 1070–1079. doi:10.1016/J.THERIOGENOLOGY.2015.11.018

Ghidini, A., and Salafia, C. M. (2005). Gender differences of placental dysfunction in severe prematurity. BJOG 112, 140–144. doi:10.1111/J. 1471-0528.2004.00308.X

Giussani, D. A. (2011). The vulnerable developing brain. Proc. Natl Acad. Sci. USA 108, 2641–2642. doi:10.1073/PNAS.1019726108

Górecki, M. T. (2003). Sex ratio in litters of domestic pigs (Sus scrofa f. domestica Linnaeus, 1758). Biol. Lett. 40, 111–118.

Hall, L. W., and Clarke, K. W. (1991). Chapter 14: Anaesthesia of the pig. In 'Veterinary Anaesthesia.' 9th Edn. (Eds L. W. Hall and K. W. Clarke.) pp. 275–289. (Baillie`re Tindall: London.)

Harris, E. K., Berg, E. P., Berg, E. L., and Vonnahme, K. A. (2013). Effect of maternal activity during gestation on maternal behavior, fetal growth, umbilical blood flow, and farrowing characteristics in pigs. J. Anim. Sci. 91, 734–744. doi:10.2527/JAS.2012-5769

Hodgkinson, O. (2007). Practical sedation and anaesthesia in pigs. In Pract. 29, 34–39. doi:10.1136/INPRACT.29.1.34

Kalisch-Smith, J. I., Simmons, D. G., Dickinson, H., and Moritz, K. M. (2017). Review: sexual dimorphism in the formation, function and adaptation of the placenta. Placenta 54, 10–16. doi:10.1016/J.PLACEN TA.2016.12.008

Klemcke, H. G. (2003). 11-Hydroxysteroid dehydrogenase and glucocorticoid receptor messenger RNA expression in porcine placentae: effects of stage of gestation, breed, and uterine environment. Biol. Reprod. 69, 1945–1950. doi:10.1095/BIOLREPROD.103.018150

Klemcke, H. G., and Christenson, R. K. (1997). Porcine fetal and maternal adrenocorticotropic hormone and corticosteroid concentrations during gestation and their relation to fetal size. Biol. Reprod. 57, 99–106. doi:10.1095/BIOLREPROD57.1.99

Lillico, S. G., Proudfoot, C., Carlson, D. F., Stverakova, D., Neil, C., Blain, C., King, T. J., Ritchie, W. A., Tan, W., Mileham, A. J., McLaren, D. G., Fahrenkrug, S. C., and Whitelaw, C. B. A. (2013). Live pigs produced from genome edited zygotes. Sci. Rep. 3, 2847. doi:10.1038/SREP02847

McDicken, W. N. (1991). 'Diagnostic Ultrasonics – Principles and Use of Instruments.' 3rd edn. (Churchill Livingstone: Edinburgh.) Muralimanoharan, S., Maloyan, A., and Myatt, L. (2013). Evidence of sexual dimorphism in the placental function with severe preeclampsia. Placenta 34, 1183–1189. doi:10.1016/J.PLACENTA.2013.09.015

Oliver, G., Novak, S. A., Patterson, J. L. A., Pasternak, J. A. A., and Paradis, F. A. (2011). Restricted feed intake in lactating primiparous sows. II. Effects on subsequent litter sex ratio and embryonic gene expression. Reprod. Fertil. Dev. 23, 899–911. doi:10.1071/RD11013

Panarace, M., Garnil, C., Marfil, M., Jauregui, G., Lagioia, J., Luther, E., and Medina, M. (2006). Transrectal Doppler sonography for evaluation of uterine blood flow throughout pregnancy in 13 cows. Theriogenology 66, 2113–2119. doi:10.1016/J.THERIOGENOLOGY.2006.03.040

Serin, G., Gokdal, O., Tarimcilar, T., and Atay, O. (2010). Umbilical artery Doppler sonography in Saanen goat fetuses during singleton and multiple pregnancies. Theriogenology 74, 1082–1087. doi:10.1016/J.THERIOGENOLOGY.2010.05.005

Silva, L. A., and Ginther, O. J. (2010). Local effect of the conceptus on uterine vascular perfusion during early pregnancy in heifers. Reproduction 139, 453–463. doi:10.1530/REP-09-0363

Thompson, R. S., Trudinger, B. J., and Cook, C. M. (1988). Doppler ultrasound waveform indices: A/B ratio, pulsatility index and Pourcelot ratio. Br J Obstet Gynaecol 95, 581–588. doi:10.1111/J.1471-0528.1988.TB09487.X

Trudinger, B. J., Giles, W. B., Cook, C. M., Bombardieri, J., and Collins, L. (1985). Fetal umbilical artery flow velocity waveforms and placental resistance: clinical significance. Br J Obstet Gynaecol 92, 23–30. doi:10.1111/J.1471-0528.1985.TB01044.X

Vallet, J. L., McNeel, A. K., Miles, J. R., and Freking, B. A. (2014). Placental accommodations for transport and metabolism during intrauterine crowding in pigs. J. Anim. Sci. Technol. 5, 55. doi:10.1186/2049-1891-5-55

Widnes, C., Flo, K., and Acharya, G. (2017). Exploring sexual dimorphism in placental circulation at 22–24 weeks of gestation: a cross-sectional observational study. Placenta 49, 16–22. doi:10.1016/J.PLACENTA. 2016.11.005

van Woerkens, L. J., Duncker, D. J., Huigen, R. J., Van Der Giessen, W. J., and Verdouw, P. D. (1990). Redistribution of cardiac output caused by opening of arteriovenous anastomoses by a combination of azaperone and metomidate. Br. J. Anaesth. 65, 393–399. doi:10.1093/BJA/65.3.393

Wu, G., Bazer, F. W., Wallace, J. M., and Spencer, T. E. (2006). Board-invited review: intrauterine growth retardation: implications for the animal sciences. J. Anim. Sci. 84, 2316–2337. doi:10.2527/JAS.2006-156

Yuan, T. L., Zhu, Y., Shi, M., Li, T., Li, N., Wu, G., Bazer, F. W., Zang, J., Wang, F., and Wang, J. (2015). Within-litter variation in birth weight: impact of nutritional status in the sow. J. Zhejiang Univ. Sci. B 16, 417– 435. doi:10.1631/JZUS.B1500010

6.4 Chapter Discussion

The placenta is vital in regulating foetal growth and development, and mediating pregnancy outcome. In clinical settings, Doppler-derived parameters describing placental circulation are widely used to assess placental function and monitor compromised pregnancies. The broad objective of this study was to determine if UA blood flow could be investigated using a non-invasive approach in pregnant gilts under light sedation. To date, very few studies have investigated UA blood flow in the pig (Brüssow *et al.*, 2012; Harris *et al.*, 2013). To our knowledge, this is the first report of the use of Doppler ultrasound to monitor UA blood flow as early as GD30. This method was used to successfully obtain traces at all GD and highlighted interesting temporal changes in all parameters investigated. The length of the sedation period influenced FHR at GD60 and 90, but not earlier in gestation, suggesting that foetuses in late gestation may be more affected by maternal sedation. Pregnant gilts were subjected to a SSR procedure to allow measurements on two days of gestation within the same litter. Interestingly, the most striking finding from this experiment was that approximately 30 minutes of light sedation in early gestation decreased foetal weight in later gestation, highlighting surprising potential long-term programming effects which warrant further investigation.

6.4.1 Doppler ultrasound was successfully used to monitor umbilical arterial blood flow at GD30, 45, 60 and 90, and revealed temporal changes in all parameters investigated.

This experiment successfully demonstrated that Doppler ultrasound can be used to monitor umbilical blood flow in pregnant gilts as early as GD30. Temporal changes in all parameters investigated were observed, with FHR, A/B Ratio and RI decreasing, and PSV and EDV increasing with advancing gestation, with the most extreme differences observed between GD60 and 90. Similar findings have been reported in sheep and goat, with FHR, A/B Ratio,

PI and RI decreasing with advancing gestation (Newnham *et al.*, 1987; Carr *et al.*, 2012).

Brüssow *et al.*, (2012) investigated umbilical blood flow at GD36, 42 and 51 in the pig, reporting a decrease in FHR at GD42 when compared with GD36, with no temporal changes observed in RI or the flow velocity parameters investigated. Harris *et al.*, (2013) investigated umbilical blood flow at GD39, 55, 66 and 81 in the pig, and demonstrated a progressive decline in FHR with advancing gestation, with a significant decrease at GD55 and 66 compared with 39, followed by a further decrease at GD81. However, in contrast to Brüssow *et al.*, (2012) temporal changes in RI and PI were observed, with an increase at GD55 and 66 when compared with GD39 and 81. The temporal changes observed in RI in the current study follow a similar pattern to Harris *et al.*, (2013), with a marked decrease in RI between GD66 and 81. The changes in FHR observed in both studies follow a similar pattern to those observed in the current experiment. The two published studies and the current experiment were performed under differing sedation conditions, with Harris *et al.*, (2013) using non-sedated gilts, 'rubbing' the udder of the gilts to produce a 'calming' effect in the animals whereas Brüssow *et al.*, (2012) performed the procedure under GA. To determine if the results of the current experiment could be compared with the published studies, considering the striking effect of sedation observed in this experiment, the mean FHR from the three studies were plotted against GD (Figure 6.2). This demonstrated that whilst there are similarities in the direction of change in FHR with advancing gestation, the level of sedation appears to influence FHR at all GD. The light sedation used in the current study induced an intermediate decrease in FHR compared to that of the animals subjected to GA. This suggests that to determine the baseline FHR and UA blood flow at all GD it may be more appropriate to train pregnant gilts to allow scanning without the use of sedation, or to optimise the use of alternative sedatives which do not influence UA blood flow.

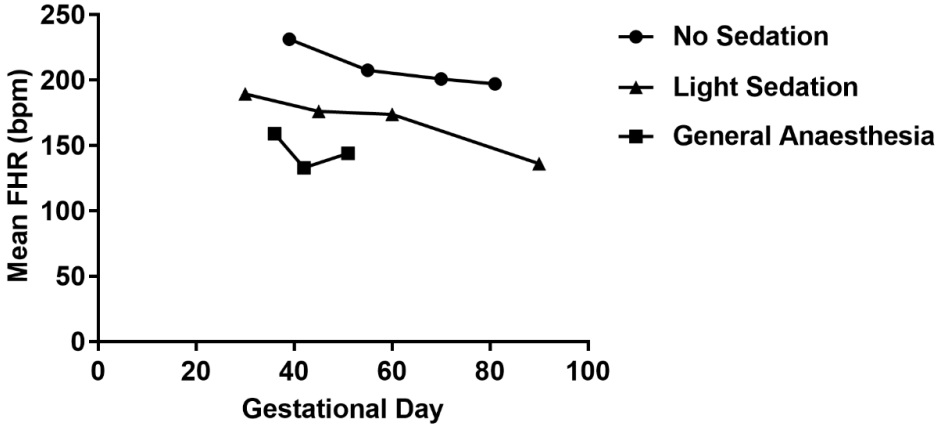

Figure 6.2: Level of Sedation Appears to Influence FHR throughout Gestation.

FHR was plotted against GD investigated for the three pig studies. Circles: represents the mean FHR from Harris *et al.*, (2013), which was performed without the use of sedation. Triangles: represents the mean FHR from the current experiment, which was performed under light sedation. Squares: represents the mean FHR from Brüssow *et al.*, (2012), which was performed under general anaesthesia. Abbreviations used: FHR = Foetal Heart Rate; bpm = beats per minute; GD = Gestational Day.

6.4.2 The number of foetuses in the whole uterus, in the right uterine horn and the percentage of males in the litter had minimal effects on FHR, PSV, EDV, A/B Ratio and RI.

The number of foetuses in the whole uterus and the right uterine horn did not influence any of the parameters investigated. However, a positive relationship between the percentage of males in the litter and A/B Ratio and RI at GD30, and trends towards relationships with EDV and PSV were observed.

The published Doppler ultrasound papers in the pig (Brüssow *et al.*, 2012; Harris *et al.*, 2013) did not discuss the influence of the number of foetuses or the sex ratio of the litter on UA blood flow. Père and Etienne, (2000) investigated uterine blood flow in pregnant pigs using ultrasonic transit time flow probes and demonstrated that as litter size increased, uterine blood flow per foetus decreased. However, this study investigated uterine blood flow and not UA blood flow. Similarly, investigations into UA blood flow in other litter

bearing species (dog, cat, rabbit) have not reported whether litter size or the sex ratio within the litter influence blood flow parameters (Di Salvo *et al.*, 2006; Scotti *et al.*, 2008; Miranda and Domingues, 2010; Polisca *et al.*, 2010). In the goat however it has been suggested that the number of foetuses did not influence FHR, UA PI or RI (Serin *et al.*, 2010).

Reynolds *et al.*, (1985) investigated uterine and umbilical blood flow in Yorkshire sows at GD70, 90 and 110 under GA (Surital (sodium thiamylal); maintained with an oxygen and halothane (fluothane) mixture. This study utilised an invasive method (Ford and Christenson, 1979) whereby midventral laparotomy was performed and electromagnetic transducers were placed around the uterine artery and vein and the umbilical cord. The results of their investigations suggest a negative relationship exists between umbilical blood flow and foetal number. The suggestion by Père and Etienne, (2000) and Reynolds *et al.*, (1985) that uterine and umbilical blood flow is negatively correlated with the number of foetuses contradict the findings of the current study however, different methods were used to monitor blood flow. Additionally, Reynolds *et al.*, (1985) performed the procedure under GA using alternative drugs to the current study, which may account for the differences observed. In the study presented in this chapter, gilts were utilised whereas Reynolds *et al.*, (1985) used sows. Considering the marked differences in reproductive performance observed between sows and gilts (Yoder *et al.*, 2014; Koketsu *et al.*, 2017), it could be hypothesised that UA blood flow may be influenced by parity.

Recent studies have revealed that sexual dimorphism exists in human placentas (reviewed by Kalisch-Smith *et al.*, (2016); Adibi *et al.*, (2017)), and it is proposed that male foetuses are disadvantaged, with increased perinatal mortality and morbidity on occasions where the pregnancy is complicated by preeclampsia and IUGR (Challis *et al.*, 2013; Muralimanoharan *et al.*, 2013). Similarly, foetal sex has been shown to influence the expression of placental genes and the inflammatory response in humans, which is thought to be attributed to sexual dimorphism in placental function (Ghidini and Salafia, 2005; Challis *et al.*, 2013). Throughout this thesis, a number of incidences of

sexual dimorphism in gene expression and tissue structure in the placenta and endometrium have been described the first time in the pig. Widnes *et al.*, (2017) reported that in humans UA PI is increased in females compared to males although, they did not suggest that foetal sex influenced any of the other parameters investigated. Therefore, if differences are observed in placental and endometrial tissue supplying foetuses of different sex, this may indicate that the uterine environment of a male biased litter would be very different to that of a female biased litter; which may explain the relationships between sex ratio of the litter and the UA blood flow parameters measured in this study.

6.4.3 The length of the sedation period influenced FHR at GD60 and 90 but not 30 and 45.

The results of the current study suggest that the length of the sedation period has an influence on foetuses in late but not early gestation, with a significant decrease in FHR as the duration of sedation period increased. In this study, the uterine horn was consistently scanned from the cervical end of the uterine horn towards the ovary. This was consistent throughout the experiment therefore, it is not possible to determine if the decrease in FHR is due to the length of the sedation period or whether this could be influenced by the position within the uterine horn. These two factors cannot be disentangled from one another in this study. To address this problem in future studies, it would be useful to repeat the Doppler ultrasound process on a subset of animals, scanning from the ovarian end of the right uterine horn towards the cervix to determine if the decrease in FHR over the sedation period was still present. Preliminary data from one GD90 gilt suggest the same relationship exists between length of sedation and FHR when performing the procedure in an ovarian to cervix direction. In addition, when dissecting the pregnant tract, it would be of interest to note the position of any large uterine arteries in relation to foetal position, and to include this in the analysis of the data.

It has been suggested from sheep studies that, although Ketamine readily crosses the placenta (Musk *et al.*, 2012), it does not influence uterine blood

flow (Craft *et al.*, 1983; Strümper *et al.*, 2004). To date, there has been little investigation into the action of Azaperone during pregnancy in large animals, although it is considered safe to use. Azaperone has been administered to pregnant rats, mice, golden hamsters and rabbits (http://www.inchem.org/documents/jecfa/jecmono/v29je09.htm accessed 4th May 2017) however, it was felt that these studies were inadequate to determine the influence of Azaperone on reproduction and fertility.

Brüssow *et al.*, (2012) also used Azaperone and Ketamine however, the doses administered resulted in GA, in contrast to the light levels of sedation observed in the current experiment. Whilst they acknowledge that the administration of these drugs may have an influence on the results obtained, they do not account for this. In addition, they report that the examinations were 45-90 minutes in duration which is much greater than the duration of scanning in the current experiment. Considering the large sedation effects observed in the current experiment, it could be expected that by 45 minutes FHR and umbilical blood flow may be drastically altered compared to the baseline non-sedated levels, therefore questioning the relevance of these results to real-life situations.

As described previously in this thesis, in mid-late gestation there is an increase in the width of the folded bilayer of the placenta to increase the efficiency of the placenta to cope with the increasing demand from the exponentially growing foetus (Vallet and Freking, 2007). This may suggest that if the drugs can pass the placenta, there will be greater transport in late pregnancy than in earlier pregnancy. This, in combination with the foetuses perhaps being more susceptible to sedation due to being more developed, may explain the decrease in FHR with increasing length of sedation observed.

6.4.4 Umbilical arterial blood flow traces were successfully obtained from all the foetuses in the right uterine horn in four GD90 litters, allowing relation of the parameters to foetal size and sex.

In four GD90 gilts, UA traces were obtained from all the foetuses in the right uterine horn, allowing relation of the results to foetal size and sex. In this experiment, foetal sex was not associated with any of the parameters investigated. However, an inverse relationship between foetal weight and FHR, A/B Ratio and RI was observed. Unfortunately, the sample size to determine the relationship between foetal weight, sex, and UA parameters was small (n=4 litters) and restricted to one GD. Considering this, the findings of these analyses should not be over-interpreted.

Previous studies have investigated the association between foetal sex and umbilical blood flow in humans. Prior *et al.*, (2013) suggested that the umbilical venous velocity was decreased in males compared to females immediately prior to parturition. Additionally, Widnes *et al.*, (2017) investigated UA blood flow in human foetuses at 22-24 weeks gestation and suggested that FHR was not associated with foetal sex but PI was increased in female foetuses compared to male foetuses. PI is a proxy for placental resistance in humans, therefore this may indicate sex differences in the placental vasculature. Also, Panarace *et al.*, (2006) found that in pregnant cows, foetal sex did not influence uterine arterial blood flow when investigated on GD30-270.

Carr *et al.*, (2012) investigated UA blood flow in a sheep model of foetal growth restriction from GD80 to 130 (gestation = 145 days). PI, RI, and A/B Ratio were all increased in growth restricted foetuses compared to controls throughout the period investigated. Additionally, Panarace *et al.*, (2006) demonstrated that calf birth weight had a positive correlation with the volume of uterine blood flow and a negative relationship with RI throughout gestation. It is thought that in human IUGR pregnancies, there is a temporal sequence in the changes in blood flow observed (Baschat *et al.*, 2001; Ferrazzi *et al.*, 2002). These changes can be categorised into ‘early’ and ‘late’ whereby ‘early’ changes reflect alterations in the middle cerebral artery and the UA and ‘late’ changes reflect UA reverse diastolic blood flow and abnormalities in the ductus venosus

and aortic blood flow. The reduction, complete absence, or reversal of end diastolic blood flow results in increased RI, PI, and A/B ratios. Following further optimisation of the technique of using Doppler ultrasound in the pregnant pig, it would be interesting to determine if similar changes can be observed in this species.

The current study indicates that foetal size has a minimal effect on UA blood flow, reinforcing the findings of Brüssow *et al.*, (2012), where foetal size did not influence FHR, PSV, timed average velocity, RI or PI in the pig. Interestingly, at GD36 the largest foetuses (upper 25%) tended to have increased systolic pulse duration compared with the smallest foetuses (lower 25%). This difference was not significant between the smallest and normal-sized (mean 50%) foetuses) and did not persist throughout gestation. Brüssow *et al.*, (2012) utilised a laparoscopic approach to allow relation of the data to foetal size. Whilst this appears to be an effective method to relate umbilical blood flow to foetal size, considering the influence of GA on blood flow, discussed in 6.4.3, care must be taken not to extrapolate the significance of these results.

Although the results presented in relation to foetal size and sex are intriguing, further studies are required to optimise a protocol to allow the relation of UA blood flow to foetal size and sex throughout gestation, ensuring that any sedation performed does not influence UA blood flow.

6.4.5 SSR can be used to perform Doppler ultrasound at multiple points during gestation in the pig, however light sedation in early gestation influenced foetal weight in late gestation.

The aim of the SSR experiment was to obtain repeated UA blood flow measurements within the same gilt. This experiment revealed that the same temporal changes in vascular parameters with advancing gestation were observed within litter as were observed when all the litters were combined. Surprisingly, the light, short-duration sedation in early gestation decreased foetal weight in later gestation. This, alongside the decrease in FHR over the

sedation period, as discussed in 6.4.3, suggests that sedation during gestation could have significant effects on foetal development. The mechanisms behind this decrease in foetal weight warrant much further investigation.

It has previously been suggested that Azaperone has a vasodilatory effect, and can therefore result in a decrease in blood pressure and body temperature (Van Woerkens *et al.*, 1990; Hall and Clarke, 1991; Brodbelt and Taylor, 1999; Hodgkinson, 2007). Although care was taken to ensure that the gilts were kept warm throughout the process, temperature and blood pressure were not monitored. In addition, there is some evidence to suggest that Azaperone can promote activation of the hypothalamus pituitary adrenal cortex (HPA) axis (Daş *et al.*, 2016). Daş *et al.*, (2016) investigated the effects of Azaperone-, Xylazine- and Ketamine-induced GA on plasma metabolites in non-pregnant female pigs. Administration of Azaperone led to a prolonged and significant increase in plasma cortisol within 15 minutes of drug administration. This effect was augmented further with the addition of Ketamine, which may indicate that cortisol mediates the observed physiological effects of Azaperone; suggesting that Azaperone may promote an increased stress response in pigs (Figure 6.3).

Although the doses of the drugs administered in our study were very different to the doses administered by Daş *et al.*, (2016) (2mg/kg and 1mg/kg compared with 0.68mg/kg and 13.5 mg/kg for Azaperone and Ketamine respectively), the route of administration was also different. Daş *et al.*, (2016) administered the drugs via jugular catheter, which is a very unusual method for administration of these drugs and potentially would lead to increased circulating levels of both drugs compared to the current study where intra-muscular injection was used for drug administration. In the Daş *et al.*, (2016) paper, Ketamine did not appear to influence the physiological parameters investigated therefore it is unlikely that it would have had an effect in our animals. Azaperone appears to have substantial effects on the stress response, which is augmented by the addition of Ketamine. The current study used 2.5 times the amount of Azaperone per kg body weight which, with the differing method of

administration, could be expected to be present at a similar maternal plasma concentration.

Interestingly, Blatchford *et al.*, (1978) investigated the responses of the porcine HPA axis in relation to environmental effects (extreme treatments) and the administration of drugs. They reported a 52% increase in plasma corticosteroids 15 minutes after intramuscular injection with Azaperone (2mg/kg), which considering the same method of administration and dose was used this could be reflective of the circulating plasma corticosteroids present in the current study. However, these studies were not performed on pregnant animals and therefore did not investigate the transport of these drugs across the placenta.

The proposed mechanism of action that may explain the decreased foetal weight observed is that as Azaperone is a potent vasodilator, administration with the drug may have unwanted side effects of decreased surface and core body temperature and/or alterations in blood pressure. These changes would then activate the maternal HPA axis, promoting increased production of cortisol by the adrenal cortex. Cortisol is metabolised by 11β-Hydroxysteroid dehydrogenase 2 (11βHSD2) into inactive corticosterone at the placenta from GD24 in the pig (Klemcke *et al.*, 2003). All the available cortisol would not be converted into inactive corticosterone, leading to an increase in the amount of maternal cortisol crossing the placenta to affect the foetus. This in turn would act as a stressful environment for the foetus, ultimately leading to the decreased foetal weight observed in late gestation and potential other programming effects, e.g. increased baseline cortisol levels in the offspring postnatally. To test the proposed mechanism of action in the future, it would be useful to monitor maternal rectal and surface temperature, blood pressure and salivary cortisol at regular intervals throughout the Doppler process.

Alternatively, the decrease in foetal weight may be due to Azaperone and Ketamine crossing the placenta themselves, as may be indicated by the observed decrease in FHR over the sedation period (discussed in 6.4.3). As stated previously, very little investigation has been carried out into the effects

of Ketamine and Azaperone at the porcine placenta. It has been suggested that Ketamine can cross the placenta in pregnant ewes (Musk *et al.*, 2012), and in humans most anaesthetic drugs cross the placenta readily by diffusion (Horta and Lemonica, 2002). In humans, Ketamine is not used routinely during the first trimester of pregnancy as it can trigger uterine contractions (Oats *et al.*, 1979) and a number of studies have suggested that exposure to Ketamine *in utero* can impact upon brain development (Brambrink *et al.*, 2012; Zhao *et al.*, 2016). To date, there is little evidence in humans to suggest that prenatal Ketamine exposure decreases foetal weight however, Lantz-McPeak *et al.*, (2015) suggest that it can restrict growth in zebrafish embryos.

There has been little investigation into the action of Azaperone during gestation in large animals, although it is considered safe to use. As described in 6.4.3, the results from pregnant rats, mice, golden hamsters and rabbits were inadequate to determine the influence of Azaperone on reproduction and fertility. In these experiments, a notable decrease in foetal weight was recorded in rats and golden hamsters however, the doses used in these experiments were extremely high (40mg/kg/day) and therefore would not be reflective of the use of the drug in a real-life situation.

6.4.6 Conclusion

In conclusion, this study has demonstrated that Doppler ultrasound can be used to monitor UA blood flow throughout gestation in sedated pregnant gilts. Novel temporal changes in all parameters investigated were observed and, to our knowledge, this is the first report of using the technique as early as GD30 in the pig. The sedation process can be manipulated to allow litters to be scanned at multiple points in gestation to investigate changes within the same litter. Novel and intriguing effects of the sedation process on foetal weight in late gestation were revealed and further investigations should be performed to investigate the proposed mechanisms behind this. It is hoped that further optimisation of the technique would improve the knowledge and understanding of UA blood flow in the pig, especially in relation to foetal growth.

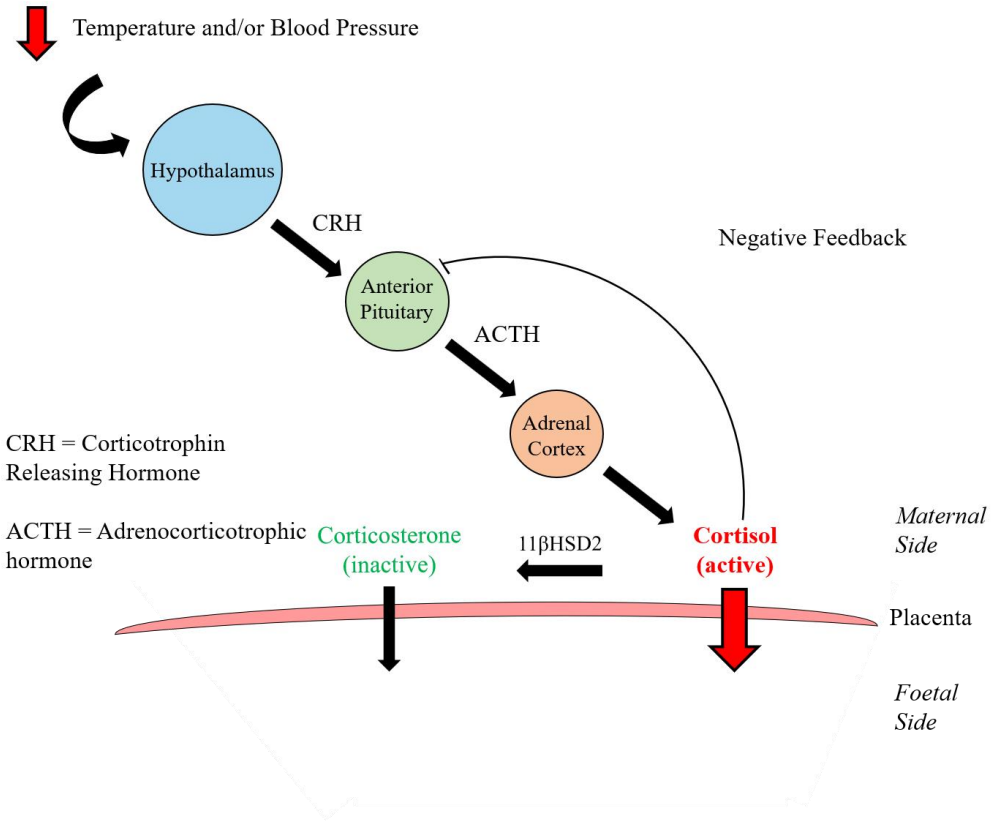

Figure 6.3: Proposed mechanism to explain how light sedation in early gestation with Azaperone and Ketamine may influence foetal weight in late gestation.

Azaperone is a potent vasodilator which may cause a decreased in surface and core body temperature and/or blood pressure. These side effects then could influence the maternal hypothalamus pituitary adrenal (HPA) axis, leading to increased production of cortisol. Although cortisol can be metabolised by 11β-Hydroxysteroid dehydrogenase 2 (11βHSD2) into inactive corticosterone at the placenta, and 11βHSD2 placental expression increases in response to maternal stress, all the cortisol will not be converted into corticosterone which will lead to increased maternal cortisol crossing the placenta to affect the foetus. This in turn will act as a stressful environment for the foetus, ultimately leading to the decreased foetal weight observed in late gestation and potential other programming effects.

7 Assessment of Placental and Endometrial Vascularity

7.1 Introduction

As described in the general introduction, uterine and placental angiogenesis are essential for foetal and placental development and have been shown to be inappropriately regulated in instances of pregnancy complications in humans. Therefore, it is essential to improve the understanding of the regulation of vascularity at the feto-maternal interface. In the experiments performed in this chapter, candidate genes which are associated with quantitative trait loci (QTL) for prenatal survival and litter size and/or have a suggested role in angiogenesis and foetal development were investigated. These include Uteroferrin (ACP5), Platelet and Endothelial Cell Adhesion Molecule 1 (CD31), Hypoxia Inducible Factor 1 Alpha Subunit (HIF1A), Heparanase (HPSE), Prostaglandin F2α Receptor (PTGFR) and Vascular Endothelial Growth Factor a (VEGFA). The proposed functions and rationale for selecting these genes are described below.

7.1.1 ACP5

ACP5, also known as Tartrate-resistant acid phosphatase (TRAP), is a glycoprotein which is secreted by the glandular epithelium (GE) of the porcine endometrium in response to progesterone (P4) (Roberts *et al.*, 1986). Fluid phase pinocytosis allows the areolae of the placenta (tall columnar epithelial cells) to take up ACP5, where it can then be released into the feto-placental circulation (Renegar *et al.*, 1982).

ACP5 is thought to have two central roles at the porcine feto-maternal interface: 1) to transfer iron to the developing foetus (Buhi *et al.*, 1982; Ducsay *et al.*, 1982, 1984, 1986; Roberts *et al.*, 1986), and 2) to act as a haematopoietic growth factor (Bazer *et al.*, 1991). The rate of synthesis of ACP5 increases continuously from gestational day (GD) 30 to 75, reaching a maximum secretion of approximately 2g per day, to keep pace with the

demand for iron from the developing foetus. However, in late gestation ACP5 secretion decreases, whilst the foetal demand for iron increases due to the exponential growth of the foetus. It is therefore proposed that an alternative method of iron transport is present in the late stages of gestation. It is known that piglets are commonly born anaemic, often requiring iron supplementation post-natally (Lipiński *et al.*, 2010), suggesting that the alternative mechanism of iron transport in late gestation is not sufficient to meet the demands of the foetus.

It has been previously shown that the haemocrit, plasma iron and folate levels are correlated with the efficiency of the placenta (foetal weight/placental weight). Additionally, a positive relationship between foetal weight and haemocrit has been reported, indicating that smaller foetuses may have impaired erythropoiesis (Pearson *et al.*, 1998; Vallet *et al.*, 2002, 2003). Erythropoiesis describes the production of red blood cells, which are essential for the transport of oxygen around the body. Therefore, if impaired this would indicate that oxygen transport in these foetuses may be hindered (Gump *et al.*, 1968). This in turn may influence both offspring health and survival (pre- and post-natally), alongside placental efficiency. It has been suggested that the increased hypoxia of foetal tissues can promote increased erythropoiesis in instances of growth restriction (Snijders *et al.*, 1993). In human IUGR, it has been demonstrated that the foetal to maternal ratio of ferritin, which would indicate the availability of iron in the body, is reduced between 26 and 36 weeks of gestation (Abbas and Nicolaides, 1994); potentially indicating aberrant iron transport to the foetus. Overall, this makes ACP5 an interesting candidate to investigate at the feto-maternal interface in the pig.

7.1.2 CD31

CD31 is an endothelial cell marker, expressed at the junctions between endothelial cells (Mamdouh *et al.*, 2003; Kim *et al.*, 2013a). It also functions as an inhibitory receptor composed of six immunoglobulin-like homology domains (~100 amino acids each), two immunoreceptor tyrosine-based inhibitory motifs

(ITIMs) and a transmembrane domain (Kim *et al.*, 2015; Lertkiatmongkol *et al.*, 2016). In response to phosphorylation, SHP-2 (protein-tyrosine phosphatase) is bound to the ITIMs (O'Brien, 2004; Wang and Sheibani, 2006), and the actions of this complex inhibits phosphorylated signal transducer and activator of transcription 3 (p-STAT3) (Xu and Qu, 2008). In addition, CD31 has been suggested to be involved in angiogenesis by regulating endothelial cell migration (DeLisser *et al.*, 1997; Matsumura *et al.*, 1997; Yang *et al.*, 1999; Zhou *et al.*, 1999; Cao *et al.*, 2002, 2009).

Lee *et al.*, (2017) utilised $CD31^{-/-}$ mice to investigate the role of CD31 in early gestation. They demonstrated that litters produced by mating $CD31^{-/-}$ females with $CD31^{+/+}$ males had an increased litter size, increased pregnancy rate, increased weight of the uterus at 3.5 days post coitum (dpc) and dramatically improved development of the uterine glands compared to $CD31^{+/+}$ females. In contrast to the previously referenced literature that suggest CD31 influences angiogenesis, there appeared to be no alterations in blood vessel density at implantation sites at 7.5dpc. Intriguingly, the $CD31^{-/-}$ mice had increased uterine LIF (Leukaemia Inhibitory Factor) mRNA and protein expression, which is known to play an essential role in regulating the receptivity of the uterus and implantation (Stewart *et al.*, 1992). P4 increases the expression of Heart- and Neural Crest Derivatives-Expressed Protein 2 (Hand2) which then increases LIF expression (Stewart *et al.*, 1992; Li *et al.*, 2011). Following administration of oestradiol (E2) and P4, LIF expression remained elevated for longer in the $CD31^{-/-}$ mice compared to $CD31^{+/+}$ mice, indicating that CD31 may have a central role in implantation by regulating LIF expression. In the uterus, E2 promotes protein synthesis by extracellular signal–regulated kinases (ERK) 1/2 signalling, activating the mechanistic target of rapamycin (mTOR) pathway (Wang *et al.*, 2015). This protein synthesis was not inhibited by P4 in the $CD31^{-/-}$ mice in contrast to the inhibition observed in the $CD31^{+/+}$ mice. Additionally, proliferation was increased in the $CD31^{-/-}$ mice in response to treatment with E2 and P4. The authors of this paper performed a comprehensive analysis of the potential mechanisms of action of CD31 in the uterus and suggested that CD31 acts to inhibit the proliferation of epithelial cells in response to E2 in the

uterus in response to the increase in P4 observed in early gestation (Figure 7.1).

Endothelial cells have been isolated from the porcine endometrium using magnetic beads for CD31 (Kaczynski *et al.*, 2016), demonstrating that CD31 is expressed in the blood vessels of the pig reproductive tract. However, to date a similar study to that described in the mouse (Lee *et al.*, 2017) has not been performed in the pig, limiting our understanding of the role of CD31 in the pig uterus.

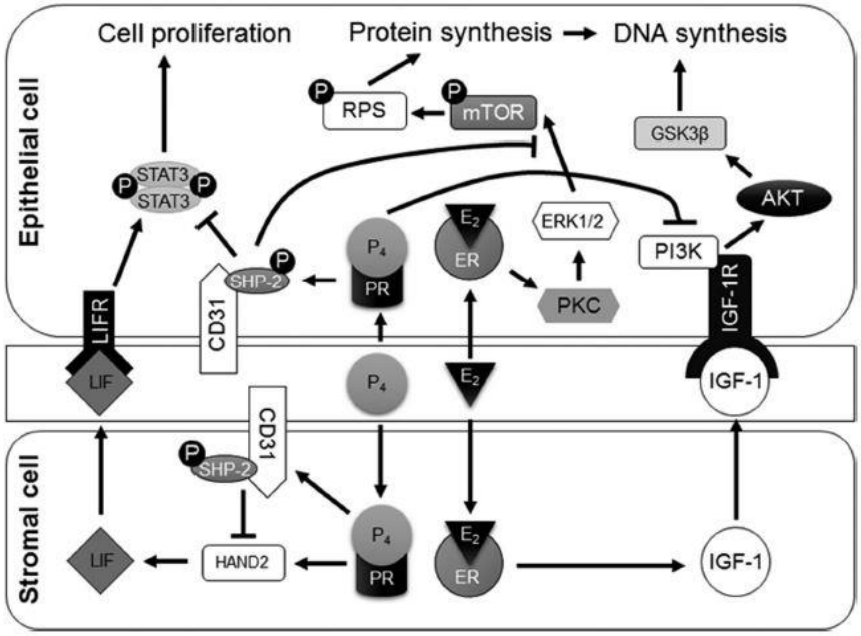

Figure 7.1: Proposed mechanism of CD31 action on the uterus in early gestation.

Progesterone (P4) inhibits the proliferation of epithelial cells via the action of CD31, which phosphorylates SHP-2 that it is bound to the immunoreceptor tyrosine-based inhibitory motifs (ITIMS) on CD31. Oestradiol (E2) regulates cell cycle machinery by IGF-1 (Insulin Growth Factor-1) and cell proliferation by LIF (Leukaemia Inhibitory Factor), alongside promoting protein synthesis by activating mammalian target of rapamycin (mTOR) signalling. Taken from Lee *et al.*, (2017).

7.1.3 HIF1A

Hypoxia-inducible factor 1 (HIF-1) is central in the maintenance of oxygen homeostasis *in vivo*, regulating the response of the cell to low oxygen levels (Charnock-Jones *et al.*, 2004). It is a heterodimer, composed of the HIF-1α (HIF1A) and HIF1-β (HIF1B) subunits. The HIF1B subunit is constitutively active in the cell whereas the HIF1A subunit is oxygen sensitive and is inactivated and degraded in response to normoxic conditions (Tal, 2012). Due to its activity in hypoxic conditions, and the placenta being a hypoxic environment (Fajersztajn and Veras, 2017), HIF1A is thought to play a central role in the regulation of placental angiogenesis (Macklin *et al.*, 2017) and foetal programming (Sookoian *et al.*, 2013; Fajersztajn and Veras, 2017).

In response to hypoxia, HIF1A accumulates in the cell which then is translocated to the nucleus to form a transcriptional complex with HIF1B and the transcriptional coactivator CBP/p300. The transcriptional complex then binds to the Hypoxia Response Element (HRE) in the promotor region of target genes that respond to hypoxia, for example genes that are involved in angiogenesis e.g. VEGF and VEGFR-1. Activation of these genes then promotes angiogenesis.

Recently it has been proposed that an imbalance between pro- and anti-angiogenic factors is responsible for the development of preeclampsia (Tal, 2012). Similarly, it has been suggested that hypoxia and HIF1A could play a central role in the development of the condition. In preeclamptic pregnancies, a 50% decline in utero-placental blood flow has been observed (Lunell *et al.*, 1982), suggesting that oxygen availability will be lower in preeclamptic placentas. HIF1A (Caniggia and Winter, 2002; Iwagaki *et al.*, 2004) and genes that are known to be regulated by HIF1 (Soleymanlou *et al.*, 2005) have been shown to have altered expression in placental samples from preeclamptic pregnancies and in *in vitro* models of preeclampsia, highlighting the importance of appropriate HIF1 signalling for foetal and placental development.

Tal *et al.*, (2010) injected mice on GD8 with an adenovirus expressing HIF1A to examine the influence of this on foetal and placental development at GD18. Several differences were observed in the group injected with the HIF1A vector compared to the controls including growth restriction of the foetuses, decreased placental weight, pregnancy complications, calcification of the labyrinth region of the placenta, extensive vascular damage to the placenta, increased maternal blood pressure, proteinuria and glomerular endotheliosis. These observed features have striking similarities to the phenotypes observed in IUGR and preeclamptic pregnancies in humans, highlighting the potential dysregulation of this gene in compromised pregnancies. Further, when investigating the use of an inflammation based experimental rat model of foetal growth restriction, an increase in HIF1A protein expression was observed (Robb *et al.*, 2017).

Minimal investigation into the role of HIF1A at the porcine feto-maternal interface has been performed. It has been shown that in the feto-placental units of arresting foetuses there is minimal *HIF1A* expression compared with normal littermates (Tayade *et al.*, 2006, 2007b), highlighting the importance of appropriate HIF1A expression to allow the establishment of a functional placenta. Chen *et al.*, (2015) demonstrated that placentas supplying IUGR foetuses have increased HIF1A protein expression compared to those supplying their normal-sized littermates at GD60, 90 and 110, suggesting that the vascularity of the placentas supplying foetuses of growth restricted foetuses may be altered in late gestation.

7.1.4 HPSE

The extracellular matrix (ECM) of the pig placenta is comprised of glycosaminoglycans (Steele and Froseth, 1980) and undergoes significant remodelling during gestation to meet the demands of the developing foetus. Heparan sulphate (HS) is the major glycosaminoglycan of the placenta ECM in early and mid-gestation although it decreases in abundance in late gestation (Steele and Froseth, 1980). HPSE is an endoglycosidase that degrades HS at

specific sites, and it has been implicated in tumour metastasis, and tissue remodelling (Vlodavsky and Friedmann, 2001). Due to the action of HPSE, and the decrease in HS in late gestation in the pig, it has been suggested that HPSE degrades HS to allow remodelling of the ECM structure of the placenta to meet the ever-increasing demands of the exponentially growing foetus.

Due to the extensive role of HPSE in tissue remodelling, several studies have investigated the role of HPSE in regulating tumour angiogenesis, both *in vitro* and *in vivo* (reviewed by Vlodavsky *et al.*, 2002). HPSE is expressed in the endothelium of the blood vessels which are undergoing angiogenesis but is not expressed in mature vessels (Elkin *et al.*, 2001). This preferential expression in smaller vessels could suggest that HPSE functions to allow endothelial cells to pass through the basement membrane and extracellular matrix whilst the vessels are undergoing angiogenesis. Elkin *et al.*, (2001) and Vlodavsky *et al.*, (2002) proposed a mechanism whereby HPSE affects angiogenesis (Figure 7.2). They suggest HPSE induces endothelial cell migration and proliferation by degrading the basement membrane to allow the invasion and migration of endothelial cells. It also has an additional angiogenic role as, when degrading the extracellular matrix and basement membrane, it releases the angiogenic factors basic fibroblast growth factor (bFGF) and VEGF which are bound to HS and generate fragments of HS which can potentiate receptor binding, dimerisation and signalling of bFGF, promoting angiogenesis. Use of both the mouse Matrigel plug angiogenesis assay, using HPSE transfected T lymphoma cells, and a mouse wound-healing model, in response to a topical administration of recombinant HPSE demonstrated that HPSE promoted an angiogenic response *in vivo* (Elkin *et al.*, 2001).

In humans, during the first trimester HPSE has been shown to be expressed in cytotrophoblast, intermediate trophoblast and synctiotrophoblast cells (Haimov-Kochman *et al.*, 2002). Additionally, it is expressed in the endothelium of developing foetal capillaries, with much lower expression observed in larger vessels, suggesting a potential role in angiogenesis. Throughout the second and third trimesters, HPSE continued to be expressed in the villous cytotrophoblasts and extravillous trophoblasts however, its expression in the

synctiotrophoblasts is highly variable. A different study investigated the expression in the term human placenta, and they observed expression in both the synctiotrophoblasts and invasive extravillous trophoblasts (Dempsey *et al.*, 2000). Haimov-Kochman *et al.*, (2002) compared normal and preeclamptic placentas, and revealed similar temporal expression and localisation of HPSE.

In mice, it has been demonstrated that HPSE is highly expressed on both an mRNA and protein level at the primary decidual zone (the site of implantation) during early pregnancy (D'Souza *et al.*, 2007). A decrease in the number of implantation sites present following *in vivo* treatment with an inhibitor of HPSE (PI-88) was observed (D'Souza *et al.*, 2007), suggesting that HPSE plays a central role in the implantation in the mouse. Revel *et al.*, (2005) investigated the role of HPSE in mouse implantation further by flushing morulae and culturing them with HPSE *in vitro* for 24 hours before transferring them to pseudopregnant recipient mice. This treatment resulted in a significant increase in the number of implantation sites present, suggesting a pivotal role of HPSE in implantation in the mouse.

HPSE has been successfully cloned from the bovine placenta (Kizaki *et al.*, 2001, 2003) and transcripts have been detected in the cotyledon throughout gestation, and in the intercotyledonary foetal membranes and caruncle at GD60, 120 and 260 (Kizaki *et al.*, 2001). Like the mouse, HPSE was expressed at a low level in the conceptus prior to implantation. Expression increased significantly between GD27-34, the time of implantation. In addition to this, *HPSE* was expressed in the cotyledon, intercotyledonary foetal membrane and caruncle after GD60–64, but its expression was absent in the intercaruncular endometrium throughout gestation (Kizaki *et al.*, 2001). The results of these experiments suggest that HPSE is expressed in the bovine uterus at stages which would indicate that HPSE plays a central role in implantation, and the development of a functional placenta.

To improve the understanding of the role of HPSE in the pig uterus, Miles *et al.*, (2009) cloned HPSE cDNA and investigated the expression and localisation throughout gestation in the placenta. *HPSE* was localised

specifically to the trophoblast cells which were in immediate proximity to the underlying endometrium. *HPSE* expression was increased at GD25, suggesting a role in placental development. Its expression then decreased before significantly increasing towards the end of gestation (GD85 and 105), implicating HPSE in placental remodelling to increase the surface area available for nutrient transfer to the exponentially growing foetus. Miles *et al.*, (2009) mapped the HPSE gene to chromosome 8, near the QTL for litter size and prenatal survival. Hong *et al.*, (2014) compared the expression of HPSE mRNA and protein at the feto-maternal interface between Meishan (MS) and Yorkshire pigs throughout gestation. They demonstrated that in late gestation, MS pigs have increased placental HPSE mRNA and protein expression compared with Yorkshire pigs. Breed specific differences were observed in the expression of HPSE, with all trophoblast cells in MS pigs expressing *HPSE* mRNA, and HPSE protein was present in both the trophoblast and luminal epithelial (LE) cells in late gestation. In contrast to this, only trophoblast cells located at the bottom and sides of the placental folds in Yorkshire pigs expressed HPSE mRNA and protein. These results heavily implicate HPSE in the remodelling of the bilayer to increase the available area for exchange at the feto-maternal interface, with breed specific differences potentially explaining the differences in placental efficiency (foetal weight/placental weight) observed between breeds. HPSE is suggested to have a central role at the feto-maternal interface, making it an interesting candidate to investigate in relation to the regulation of foetal growth.

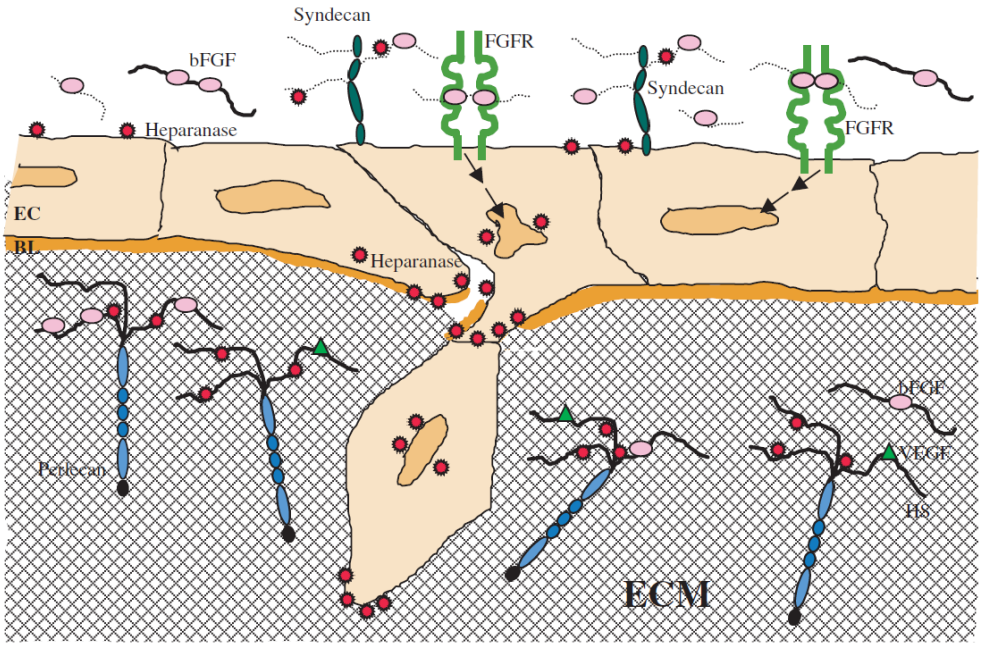

Figure 7.2: Proposed Mechanism of the Mechanism of HPSE Action on Angiogenesis.

HPSE promotes the migration of endothelial cells (EC) and degradation of the subendothelial basal lamina (BL) and extracellular matrix (ECM). This degradation of the ECM releases the active heparan sulphate (HS) bound bFGF and VEGF. The release of the HS degradation fragments promotes FGF-receptor (FGFR) binding and signalling (black arrows), which induces endothelial cell migration and proliferation. Taken from Elkin *et al.*, (2001); Vlodavsky *et al.*, (2002).

7.1.5 PGF2α/PTGFR

Prostaglandins (PGs) belong to the prostanoid group and are 20-carbon molecules derived from aracadonic or di-homo-γ-linolenic acid (Weems *et al.*, 2006). They have a central role in regulating reproduction in female livestock species and are fundamental in the processes of luteolysis and pregnancy establishment in the pig (Bazer and Thatcher, 1977; McCracken *et al.*, 1999; Waclawik *et al.*, 2009; Kaczynski *et al.*, 2016).

The development and maintenance of the *corpora lutea* (CL) is dependent upon a delicate balance in the supply of luteolytic and luteotropic factors. As described in the general introduction, prostaglandin F2α (PGF2α) is essential for luteolysis, the establishment of pregnancy and uterine angiogenesis in the pig. A peak in endometrial secretion of PGF2α occurs at days 15 and 16 of the oestrous cycle (Moeljono *et al.*, 1977), and is thought to be the driver of regression of the CL in the absence of conceptuses (McCracken *et al.*, 1999). PGF2α binds to the PGF2α receptor (PTGFR) on luteal cells which activates the luteolytic cascade, resulting in loss of P4 synthesis, followed by degeneration of the CL structure (Reviewed by Geisert and Bazer, 2015; Ziecik *et al.*, 2017). Conceptus secreted E2 during the preimplantation period allows maintenance of the CL by inducing a switch in the mode of PGF2α secretion from an endocrine approach (uterine venous drainage), to an exocrine approach (uterine luminal secretion) (Bazer and Thatcher, 1977). This allows it to act directly on the uterus, preventing CL regression and allowing the establishment of pregnancy. Further, PGF2α from uterine venous blood and lymph can be transferred into the uterine lumen, which leads to accumulation of PGF2α in the veins and arterial walls of the uterus, preventing luteal regression and allowing the establishment and maintenance of a pregnancy (Krzymowski and Stefańczyk-Krzymowska, 2004).

An alternative “two-signal switch hypothesis” has recently been proposed to describe the involvement of PGF2α in regression or rescue of the porcine CL (Przygrodzka *et al.*, 2015, 2016; Waclawik *et al.*, 2017; Ziecik *et al.*, 2017). In brief, luteolytic sensitivity (LS) is acquired at approximately day 12-13 of the

oestrous cycle. Prior to this stage, PGF2α can bind to PTGFR on luteal cells, allowing accumulation of cyclic adenosine monophosphate (cAMP), which is sufficient to maintain the function of the CL. The acquisition of LS alters the signalling that occurs following binding to the PTGFR, inhibiting the production of cAMP, which allows luteolysis to occur. In contrast to this, in the presence of conceptus secreted E2 (and PGE2 produced by the endometrium), the CL are rescued by activation of protein kinase A. This blocks Raf-1 proto-oncogene, serine/threonine kinase activity, allowing the LS to be “switched off”, and allowing the angiogenic and steroidogenesis pathways required for adequate CL function to occur.

Conceptus secreted E2 upregulates the expression of PTGFR in the porcine endometrium (Kaczynski and Waclawik, 2013; Kaczynski *et al.*, 2016), with its expression localised to the blood vessels, LE and GE (Kaczynski *et al.*, 2016). PGF2α is synthesised by both the porcine endometrium and conceptus during the period of implantation (Waclawik *et al.*, 2006; Waclawik and Ziecik, 2007). It binds to the PTGFR on the endometrium, which in turn induces phosphorylation of MAPK1/3 kinases, resulting in increased production and expression of VEGFA by the endometrium. VEGFA binds to the VEGF receptors in the endometrium (discussed in 1.1.1), which increases angiogenesis in the endometrium by inducing proliferation of the endothelial cells (Kaczynski *et al.*, 2016).

Further evidence for the role of PGF2α binding to PTGFR on angiogenesis was provided by Sales *et al.*, (2005) by investigating human endometrial adenocarcinomas. Following treatment with PGF2α, transphosphorylation of epidermal growth factor receptor and extracellular signal-regulated kinase (ERK) 1/2 via binding to the PTGFR in Ishikawa cells was observed. PGF2α was found to upregulate the ERK1/2 signalling pathway, enhancing VEGF mRNA expression and protein production. PTGFR expression was found to be co-localized with VEGF and CD31 expression on endothelial cells, further suggesting a potential role of this pathway in uterine angiogenesis.

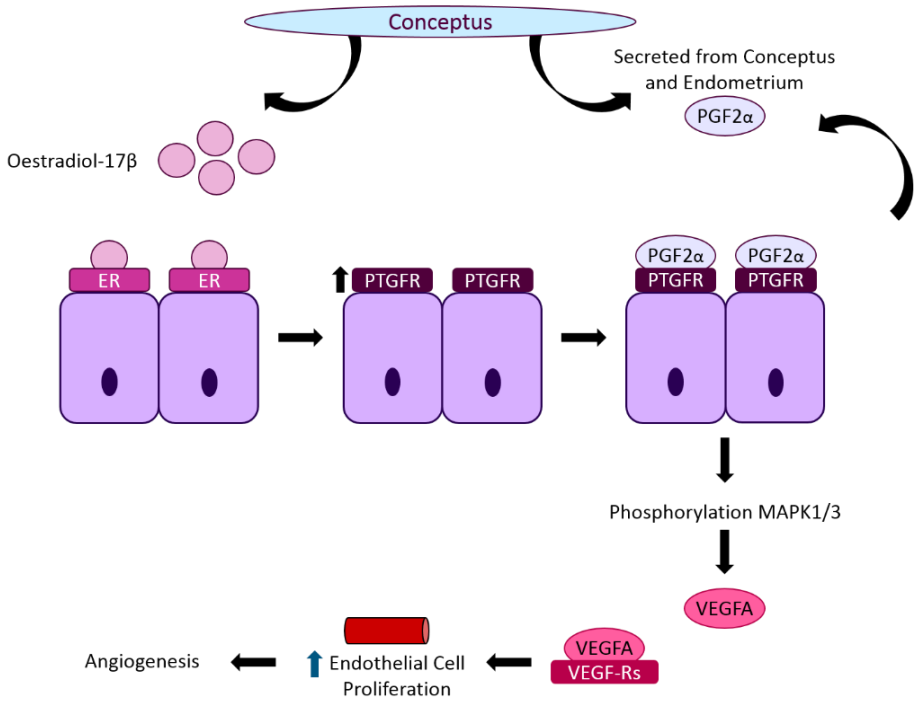

Figure 7.3: Proposed mechanism of action: PGF2α effects Angiogenesis through Binding to Endometrial PTGFR.

During the period of implantation, oestradiol-17β (E2) is secreted by the conceptus and binds to the oestrogen receptor (ER), upregulating Prostaglandin F2α Receptor (PTGFR) expression in the blood vessels, LE and GE of the endometrium. Prostaglandin F2α (PGF2α) is synthesised by both the porcine endometrium and conceptus during the period of implantation, which binds to the PTGFR on the endometrium. This induces phosphorylation of Mitogen-Activated Protein Kinase (MAPK) 1/3 kinases, resulting in increased production and expression of Vascular Endothelial Cell Growth Factor A (VEGFA) by the endometrium. VEGFA binds to VEGF receptors (VEGF-Rs) in the endometrium, which results in increased angiogenesis in the endometrium by inducing endothelial cell proliferation.

7.1.6 VEGFA

Vascular Endothelial Growth Factors (VEGFs) and their receptors (VEGFRs) have a crucial role in the regulation of physiological and pathological angiogenesis (Ferrara *et al.*, 2003; Hoeben *et al.*, 2004; Shibuya, 2011) and are rate-limiting components in angiogenesis (Otrock *et al.*, 2007). VEGF has also been suggested to function as a survival factor, promoting increased expression of anti-apoptotic proteins (Gerber *et al.*, 1998). The VEGF family is composed of several members including VEGFA, VEGFB, VEGFC, VEGFD and Placental Growth Factor (PlGF) (Koch and Claesson-Welsh, 2012). VEGFA has been extensively analysed and is known to bind to the membrane bound tyrosine-kinase receptors VEGFR1 (Flt1) and VEGFR2 (KDR/Flk1) which are located on monocytes, macrophages, and vascular endothelial cells (Koch and Claesson-Welsh, 2012). VEGFR2 is thought to act as the major mediator of the proliferation and angiogenic effects of VEGFA (Ferrara and Kerbel, 2005). Binding of VEGFA to VEGFRs promotes proliferation and migration of endothelial cells by activating several pathways (Neufeld *et al.*, 1999; Ferrara *et al.*, 2003). This leads to increased proliferation, survival, permeability, and migration of endothelial cells.

Onteru *et al.*, (2012) identified a QTL linked to gestation length, and in this are several genes associated with angiogenesis and haematopoiesis, including VEGFA. Similarly, Sell-Kubiak *et al.*, (2015) identified a novel single nucleotide polymorphism (SNP) for VEGFA which was linked to variation in litter size, highlighting the potential role of VEGFA not only in angiogenesis within the reproductive system but also its close relationship with reproductive traits that are under selection within the population. VEGFA has been extensively investigated in the female reproductive tract due to the importance of angiogenesis in regulating normal foetal and placental development. In mice, single allelic knock out of the VEGFA gene ($VEGFA^{+/-}$) is embryonic lethal due to the aberrant formation of the circulatory system (Carmeliet *et al.*, 1996), highlighting its essential role in development.

It has been demonstrated that VEGF mRNA and protein are expressed at the feto-maternal interface in the pig (Winther *et al.*, 1999; Charnock-Jones *et al.*, 2001; Vonnahme *et al.*, 2001; Vonnahme and Ford, 2004; Wu *et al.*, 2009; Novak *et al.*, 2012). In the endometrium, VEGF and VEGF receptors have low protein expression in the LE from GD13.5 to 21, after which they have intense expression until GD100 (Winther *et al.*, 1999). In the placenta, the foetal vessels expressed VEGF and VEGF receptors and, from GD30 onwards, intense protein expression has been observed in trophoblast cells (Winther *et al.*, 1999). Charnock-Jones *et al.*, (2001) found *VEGF* was expressed in both maternal and foetal epithelial cells at the interface and was expressed at a low level in the GE of the endometrium. However, on a protein level VEGF was highly expressed by the GE. They demonstrated that VEGF binds to VEGF receptors in the endothelial cells of the endometrium, and to the small capillaries found in the bilayer, suggesting that VEGF may promote angiogenesis of the small capillaries in the bilayer.

Vonnahme *et al.*, (2001) investigated VEGF mRNA and protein expression in placental and endometrial samples throughout gestation and demonstrated a positive relationship between VEGF expression and the number of blood vessels present. Placental *VEGF* expression was positively correlated with foetal weight and placental efficiency (foetal weight/placental weight). A similar analysis was performed by Vonnahme and Ford, (2004), who found an increase in the density of blood vessels in the placenta from GD70 to 90, corresponding to increased *VEGF* expression. Similarly, at GD90 *VEGF* expression was increased in a group of sows selected for increased placental efficiency. Wu *et al.*, (2009) demonstrated that breed influenced *VEGF* expression at GD90, with Erhualian pigs that have a large litter size having increased *VEGF* expression compared to Landrace pigs. The influence of breed on placental vascularity has been suggested previously (Biensen *et al.*, 1998; Vonnahme and Ford, 2004). Biensen *et al.*, (1998) reported that, compared to Yorkshire pigs, MS pigs had increased placental vascular density between GD70 and 110. This alteration in vascularity to improve placental efficiency is the proposed mechanism by which MS pigs overcome the problem

of uterine crowding to successfully have an increased number of live born piglets which are more uniform in size than observed in more commonly used commercial pig breeds.

Altered expression of VEGF and VEGF receptors in placental and endometrial samples has been associated with embryo loss in early gestation (GD20-32) in the pig (Tayade *et al.*, 2006; Han *et al.*, 2014; García Fernández *et al.*, 2015); highlighting the importance of appropriate VEGF expression to allow the establishment of a functional placenta. VEGF and endothelial nitric oxide synthase (eNOS) are essential in altering blood flow rates in the placenta (Vonnahme *et al.*, 2001; Reynolds *et al.*, 2006). Placentas from human preeclamptic pregnancies, the placentas have been shown to have elevated VEGFR-1 protein expression (Ahmad and Ahmed, 2005). Term IUGR placentas have been shown to have increased von Willebrand Factor (vWF; produced by endothelial cells) staining (Çelik *et al.*, 2017), and decreased vascularity of the villi than placentas supplying normally-grown infants, (Junaid *et al.*, 2014). Further, term human IUGR placentas have been suggested to have increased VEGFA, b-FGF and eNOS protein expression compared to normal placentas (Barut *et al.*, 2010). When investigating the vascularity of pig placentas supplying IUGR foetuses, it has been shown that VEGF and VEGFR-1 protein expression is decreased in IUGR placentas compared to those supplying their 'normal' sized littermates at GD60, 90 and 110 (Chen *et al.*, 2015). Intriguingly, *eNOS* expression has been shown to be increased in IUGR placentas at GD50 compared to control placentas (Blomberg *et al.*, 2010), which may suggest that at this stage of gestation the placentas supplying IUGR foetuses are trying to compensate for having a decreased nutrient supply. In addition, alterations in VEGF signalling have also been reported in experimentally induced IUGR models in the sheep (reviewed by Reynolds *et al.*, (2006).

7.2 Hypotheses

It is hypothesised that placental and endometrial samples associated with the lightest conceptuses or foetuses will have impaired angiogenesis and vascularity compared to their normal-sized littermates throughout gestation. In addition, it is hypothesised that placental and endometrial samples supplying male foetuses will have decreased vascularity compared to those supplying their female littermates.

7.3 Aims

The aims of the research described in this chapter were:

i. To investigate the vascularity of the feto-maternal interface by analysing CD31 stained placental and endometrial samples at GD18, 30, 45, 60 and 90.
ii. To investigate if foetal size is related to the vascularity of the feto-maternal interface by analysing CD31 stained placental and endometrial samples supplying the lightest and closest to mean litter weight (CTMLW) conceptuses or foetuses at GD18, 30, 45, 60 and 90.
iii. To investigate if foetal sex is related to the vascularity of the feto-maternal interface by analysing CD31 stained placental and endometrial samples supplying male and female foetuses at GD30, 45, 60 and 90.
iv. To investigate the mRNA expression of candidate genes which are associated with QTL for litter size and prenatal survival and/or have a central role in angiogenesis and foetal development in placental and endometrial samples at GD18, 30, 45, 60 and 90.
v. To investigate if foetal size influences the mRNA expression of candidate genes which are QTL associated and/or have a central role in angiogenesis and foetal development in placental and endometrial samples supplying the lightest and CTMLW conceptuses or foetuses at GD18, 30, 45, 60 and 90.

vi. To investigate if foetal sex influences the mRNA expression of candidate genes which are QTL associated and/or have a central role in angiogenesis and foetal development in placental and endometrial samples supplying male and female foetuses at GD30, 45, 60 and 90.

7.4 Materials and Methods

7.4.1 Analysis of Placental and Endometrial Vascularity by Immunohistochemistry for CD31

7.4.1.1 Staining of Placental and Endometrial Samples for CD31

For this experiment placental samples from GD45, 60 and 90 (n=6, 7 and 5 litters respectively), and endometrial samples from GD18, 30, 45, 60 and 90 (n=5, 9, 6, 7 and 7 litters respectively) were used. GD30 placental samples were not used for this analysis due to the heterogeneity in the tissue observed at this early stage of gestation making the samples very difficult to compare. In addition their vascularity was not directly comparable with the other GD investigated. The samples were fixed with Bouin's fixative (Sigma Aldrich), processed, embedded, and sectioned (2.3).

The sections were stained for the endothelial cell marker CD31 (1:100 dilution; ab28364; Abcam, Cambridge, U.K.) using the Vectastain Elite ABC Kit (2.3.3). The slides were imaged using the NanoZoomer slide scanner (Hamamatsu, Welwyn Garden City, U.K.).

7.4.1.2 Image Analysis of CD31 Stained Placental and Endometrial Samples

All image analyses were performed using ImageJ (Fiji). When analysing the CD31 stained placentas, the chorioallantoic membrane (CAM) region and the stroma were not directly comparable with one another. Therefore, the two regions were imaged and analysed separately (Figure 7.4).

The stromal regions of the GD45 and 60 stained placentas were analysed in a similar way to one another. It was decided to not analyse the stromal regions of the GD90 placentas due to the CAM regions being so highly prevalent in

these samples, making the stromal regions not comparable with the GD45 and 60 analyses performed. At GD45, 6 images were taken from the slide scans of stromal regions, which did not contain CAM regions, at x20 magnification from 2 sections. At GD60, 4 images were taken at x10 magnification of stromal regions which did not contain CAM regions from 2 sections. The number of blood vessels (BV) present was quantified for each image and a grid (21500μm^2) was superimposed on the image (Figure 7.5). The internal and external BV diameters were measured for the BV present in every second square. Due to the difference in image magnification, this translated to 33 squares per image at GD60 and 8 squares per image at GD45. Each measurement was performed in triplicate for each vessel and the mean value was taken to account for the vessel not being cut through directly at right angles to the vessel lumen. The internal diameter was subtracted from the external to give the vessel wall thickness. The images were split into red, green, and blue channels and the percentage staining was quantified using the green channel at a threshold of 136.

To investigate the percentage staining of the CAM at GD45, 60 and 90, 3 images at x10 magnification were taken from 2 sections. The images were split into red, green, and blue channels and, using the freehand drawing tool on the green channel the CAM area was selected. The percentage staining was quantified at 136 threshold using ImageJ (Fiji).

For the analysis of the stained endometrial samples, 3 images at x10 magnification were taken from 2 sections. The number of BV and uterine glands were measured. The images were split into red, green, and blue channels and, the green channel was selected. The percentage staining was quantified at 136 threshold using ImageJ (Fiji).

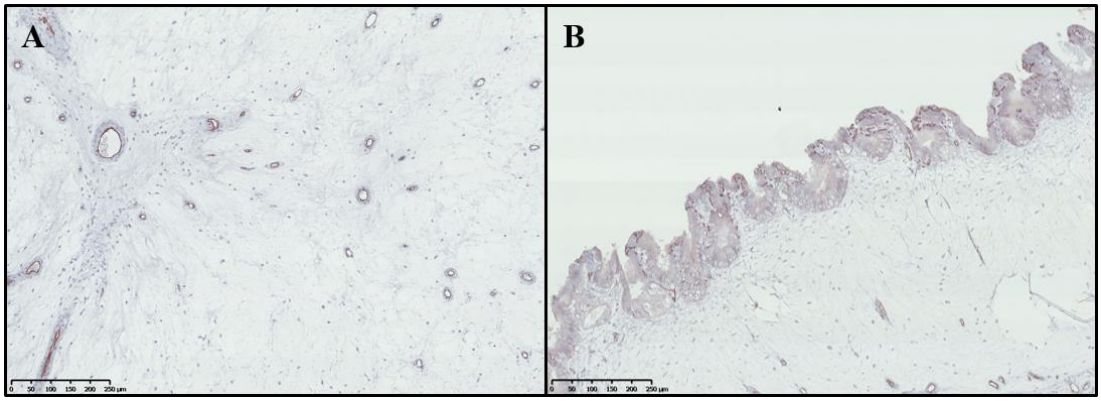

Figure 7.4: Representative Stromal and CAM Regions of a GD60 Placenta.

Images taken from a representative CD31 stained GD60 placenta. Placental stromal and chorioallantoic membrane (CAM) regions were not directly comparable with one another throughout gestation. Scale bar represents 250μm. Image taken at x10 magnification from slide scans (NanoZoomer slide scanner, Hamamatsu).

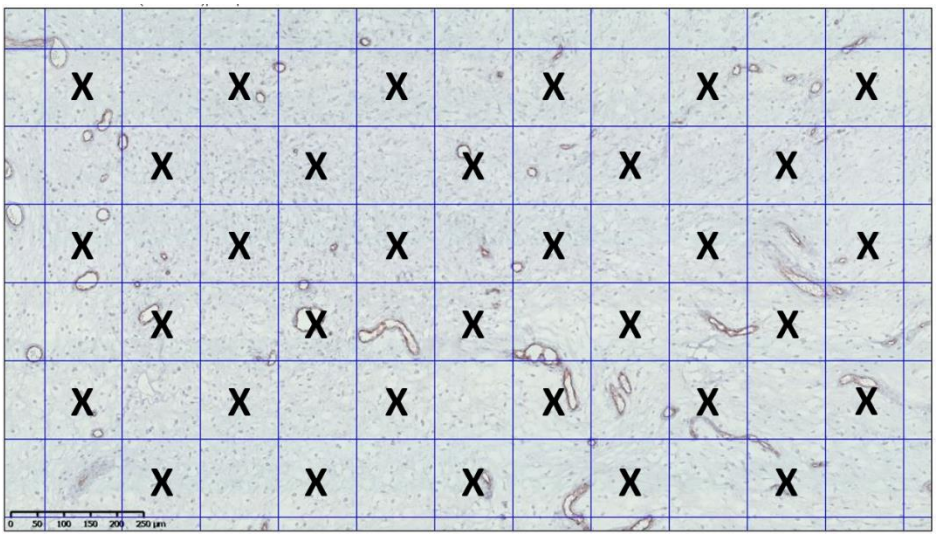

Figure 7.5: Illustration of the Grid Used for BV Measurements.

CD31 stained GD60 placenta with a 21500μm^2 grid superimposed. The internal and external BV diameters were measured in every second square. Each measurement was performed in triplicate for each vessel and the mean value was taken. The mean internal diameter was subtracted from the mean external diameter to give the mean vessel wall thickness. Scale bar represents 250μm. Image taken at x10 magnification from slide scans (NanoZoomer slide scanner, Hamamatsu).

7.4.2 mRNA Expression of Candidates Associated with Vascularity, Angiogenesis and linked to prenatal-survival and/or litter size by qPCR

The RNA extracted from placental (GD30, 45, 60 and 90; n=6, 6, 6 and 8 litters respectively), and endometrial (GD18, 30, 45, 60 and 90; n=5, 5, 6, 6 and 6 litters respectively) samples described in 2.2.3 were utilised. Complementary DNA was synthesised as described in 2.2.7 and diluted 1:25 with nuclease free water. The candidates of interest were *ACP5*, *CD31, HIF1A*, *HPSE*, *PTGFR* and *VEGFA*. The primer sequences for these candidates are detailed in Table 7.1. All qPCRs were performed for 40 cycles with an annealing temperature of 60^{o}C (2.2.8.2).

The GeNorm experiment (2.2.8.4) identified that multiple genes were stable in both tissues and that the optimal number of reference genes for each tissue based on use of the most stable reference genes was two. The most stable reference genes for this experiment were *TBP1* (TATA box binding protein) and *HPRT1* (Hypoxanthine phosphoribosyltransferase 1) for the placenta and *TBP1* and *YWHAZ* (Tyrosine 3-monooxygenase/tryptophan 5-monooxygenase activation protein, zeta polypeptide) for the endometrium. These reference genes were run for all samples; the primer sequences are detailed in Table 2.4. All data were scaled to the minimum sample and were imported into qBase+ (Biogazelle) and data for each candidate gene were normalised to the reference gene expression.

Gene Symbol	Gene Name	Accession Number	Function	Primer Sequence (5'→ 3')		Amplicon Size (bp)	Reference
ACP5	Uteroferrin	NM_214209.1	Transports iron to the foetus. Haematopoietic growth factor.	Fwd	GCAGCCAAGGAGGACTATGT	130	Hernandez *et al.*, 2013
				Rev	GGTAGGCAGTGACCTTGTGT		
CD31	Platelet and Endothelial Cell Adhesion Molecule 1	NM_213907.1	Acts as an adhesion receptor molecule by its role in leukocyte trafficking across the endothelial layer.	Fwd	CCGAGGTCTGGGAACAAAGG	98	n/a
				Rev	AGCCTTCCGTTCTAGAATATCTGTT		
HIF1A	Hypoxia Inducible Factor 1 Alpha Subunit	NM_001123124	Regulator of cellular and systemic homeostatic response to hypoxia. Induces angiogenesis.	Fwd	CCATGCCCCAGATTCAAGAT	64	Oliver *et al.*, 2011
				Rev	GGTGAACTCTGTCTAGTGCTTCCA		
HPSE	Heparanase	NM_001146130.2	Endoglycosidase that degrades heparan sulphate, in the pig placenta.	Fwd	CAGACCCCACAAGAAGGTGT	170	Miles *et al.*, 2009
				Rev	GTTCCAGCTCCAAAGAGCAC		
PTGFR	Prostaglandin F2α Receptor	NM_214059	Receptor for PGF2α, which plays a key role in angiogenesis and the establishment of pregnancy.	Fwd	TCAGCAGCACAGACAAGG	151	Kaczynski and Waclawik, 2013
				Rev	TTCACAGGCATCCAGATAATC		

VEGFA	Vascular Endothelial Growth Factor A	NM_214084	Growth factor active in angiogenesis, vasculogenesis and endothelial cell growth.	Fwd	GCCCACTGAGGAGTTCAACATC	59	Oliver *et al.*, 2011
				Rev	GGCCTTGGTGAGGTTTGATC		

Table 7.1: Primer Sequences for qPCR of Candidate Genes.

This table summarises the gene abbreviation and name, accession number, gene function, primer sequences (Fwd = Forward, Rev = Reverse), amplicon size (bp=base pairs) and the source of the primer sequences. n/a indicates that the primer pair were designed specifically for this experiment using NCBI Primer Blast.

7.4.3 Statistical Analysis

Statistical analyses were performed following the general protocol outlined in 2.5. Mean values were taken for each parameter and the normality of the data was assessed and transformations performed as required.

7.4.3.1 Analysis of Placental Vascularity by Immunohistochemistry for CD31

7.4.3.1.1 Analysis of the GD45 and 60 Placental Stroma

At GD45, total number of BV, percentage CD31 staining, internal BV diameter and BV wall thickness were all normally distributed without transformation, and external BV diameter was normally distributed following log10 transformation. At GD60 internal BV diameter, external BV diameter and BV wall thickness were all normally distributed without transformation, and BV number and percentage CD31 staining had a normal distribution following log10 transformation.

Statistical analyses to assess the influence of size (GD45 and 60) and sex (GD60 only) were performed as outlined in 2.5. A two-way ANOVA for sex x size, with and without a block for gilt was performed to investigate the presence of sex x size interactions at GD60. However, it could not be performed at GD45 due to the small sample size in the lightest male group.

7.4.3.1.2 Analysis of the Percentage CD31 Staining in the Chorioallantoic Membrane at GD45, 60 and 90

Statistical analyses to assess the influence of GD, size (GD45 and 60) and sex (GD60 only) were performed as outlined in 2.5. Log10 transformation was required at GD60 and 90 but not GD45. A two-way ANOVA for sex x size, with and without a block for gilt was performed to investigate the presence of sex x size interactions at GD60 and 90. However, it could not be performed at GD45 due to the small sample size in the lightest male group.

7.4.3.2 Analysis of Endometrial Vascularity by Immunohistochemistry for CD31

The normality of the distribution of the endometrial data, and any transformations required, are summarised in Table 7.2. Statistical analyses to assess the influence of foetal size and sex were performed as outlined in 2.5. A two-way ANOVA for sex x size, with and without a block for gilt was performed to investigate the presence of sex x size interactions on all GD except for GD18 and 45.

7.4.3.3 Analysis of mRNA Expression Data for Candidates Associated with Vascularity, Angiogenesis and linked to prenatal-survival and/or litter size

Statistical analyses to assess the influence of GD, size and sex were performed as outlined in 2.5. The normality of the distribution of the data obtained from the placental and endometrial qPCRs and any transformations required are summarised in Table 7.3 and Table 7.4 respectively. To investigate the presence of sex x size interactions in the expression of the candidate genes, two-way ANOVA for sex x size with and without a block for gilt within GD was performed on the data with a normal distribution at GD30, 60 and 90.

GD	Total Number of Glandular Epithelium Uterine Glands	Total Number of Blood Vessels	Mean Number of Uterine Glands	Mean Number of Blood Vessels	Mean Percentage CD31 Staining
18	Normal	Normal	Normal	Normal	Normal
30	Normal	Normal	Normal	Normal	Normal
45	Log10	Normal	Normal	Normal	Normal
60	Log10	Normal	Log10	Normal	Sqrt
90	Normal	Normal	Normal	Normal	Normal

Table 7.2: Summary of Normality of Endometrial CD31 Data.

Log10 and Square Root (Sqrt) transformations were carried out where appropriate, with the aim of improving the normality of the distribution of the data. Abbreviations: GD=Gestational day, Sqrt=Square Root.

	All GD	30	45	60	90
ACP5	Log10				
CD31	Not Normal		Normal		
HIF1A	Log10		Normal		
HPSE	Log10				
PTGFR	Not Normal	Normal	Log10	Not Normal	Normal
VEGFA	Log10				

Table 7.3: Summary of Normality Distributions of Placental qPCR Data.

Log10 transformations were carried out where appropriate, with the aim of improving the normality of the distribution of the data. Abbreviations: GD=Gestational day; ACP5=Uteroferrin, CD31=Platelet and Endothelial Cell Adhesion Molecule 1, HIF1A=Hypoxia Inducible Factor 1 Alpha Subunit, HPSE=Heparanase, PTGFR=Prostaglandin F2α Receptor and VEGFA=Vascular Endothelial Growth Factor A.

	All GD	18	30	45	60	90
ACP5	Not Normal	Log10	Normal		Log10	
CD31	Not Normal	Log10				
HIF1A	Log10					
HPSE	Log10					
PTGFR	Not Normal	Log10				
VEGFA	Normal	Log10	Normal			

Table 7.4: Summary of Normality Distributions of Endometrial qPCR Data.

Log10 transformations were carried out where appropriate, with the aim of improving the normality of the distribution of the data. Abbreviations: GD=Gestational day; ACP5=Uteroferrin, CD31=Platelet and Endothelial Cell Adhesion Molecule 1, HIF1A=Hypoxia Inducible Factor 1 Alpha Subunit, HPSE=Heparanase, PTGFR=Prostaglandin F2α Receptor and VEGFA=Vascular Endothelial Growth Factor A.

7.5 Results

7.5.1 Assessment of Placental Vascularity by IHC for CD31

7.5.1.1 Placental Stroma

7.5.1.1.1 No Association between Foetal Size and Placental Stromal Vascularity was observed at GD45 or 60

To determine if there was an association between foetal size and placental stromal vascularity at GD45 or 60, the total number of BV, percentage CD31 staining, internal BV diameter, external BV diameter and BV wall thickness were quantified. No associations between foetal size and the total number of BV, percentage CD31 staining, internal BV diameter or external BV diameter were observed at either GD investigated (Table 7.5). An indication towards the BV in placentas supplying the lightest foetuses having decreased BV wall thickness at GD45 (ANOVA without Gilt Block FPr=0.057) was observed. However, this was only a trend towards statistical significance, which was lost with the addition of a block for gilt in the analysis (Table 7.5).

7.5.1.1.2 No Association between Foetal Sex and Placental Stromal Vascularity was observed at GD45 or 60

As described in the general introduction, recent investigations have suggested that sexual dimorphism may exist in the development of the human placenta. To investigate whether foetal sex may be associated with placental vascular development, the same data set from 7.5.1.1.1 was analysed in relation to foetal sex. No associations between foetal sex and the total number of BV, percentage CD31 staining, internal BV diameter, external BV diameter or BV wall thickness were observed at GD45 or 60 (Table 7.5).

To investigate the presence of sex x size interactions in placental vascularity, two-way ANOVA for sex x size, with and without a block for gilt for each parameter for the lightest and CTMLW foetuses was performed. No statistically significant interactions were observed in this analysis for total number of BV, percentage CD31 staining, internal BV diameter, external BV diameter or BV wall thickness were observed at GD60 (data not presented). Due to the

limitation of the GD45 samples only containing one litter where the overall lightest foetus was a male, a sex x size analysis to investigate the presence of sex x size interactions in the parameters investigated was not performed.

7.5.1.2 Placental Chorioallantoic Membrane Analysis – GD45, 60 and 90

7.5.1.2.1 Temporal Changes were observed in CD31 Expression in the Chorioallantoic Membrane

As described in 7.2, one of the broad objectives of this chapter was to investigate gestational changes in the vasculature of the pig placenta. The mean values obtained for percentage CD31 staining in the CAM for GD45, 60 and 90 are illustrated in Figure 7.6A. An overall GD effect in CD31 expression was observed (Kruskal-Wallis $P \leq 0.001$), with a decrease in CD31 staining observed at GD60 compared to GD45, before increasing significantly between GD60 and 90.

7.5.1.2.2 Associations between Foetal Size and Placental CAM CD31 Protein Expression were observed

To determine if there was an association between foetal size and placental CAM CD31 expression, placentas supplying the lightest and CTMLW foetuses were compared within GD. Foetal size was not associated with CD31 percentage staining in the CAM at GD45 (Figure 7.6B). Intriguingly, placentas supplying the lightest foetuses at GD60 had increased percentage CD31 staining in the CAM compared to those supplying the CTMLW foetuses (ANOVA with Gilt Block FPr=0.055; Figure 7.6B). However, the direction of this relationship was switched at GD90, with placentas supplying the lightest foetuses having decreased CD31 staining in the CAM compared to those supplying the CTMLW foetuses (ANOVA with Gilt Block FPr=0.05; Figure 7.6B).

7.5.1.2.3 No Association between Foetal Sex and Placental CAM CD31 Protein Expression was observed at GD45, 60 or 90

To investigate the relationship between foetal sex and CD31 CAM staining existed, the data set from 7.5.1.2.1 was analysed in relation to foetal sex. No associations between foetal sex and CAM CD31 staining were observed at GD45, 60 or 90 (Figure 7.6C).

7.5.1.2.4 No Statistically Significant Sex X Size Interactions were observed in Placental Chorioallantoic CD31 Protein Staining at GD60 or 90

To investigate the presence of sex x size interactions in CD31 staining of the CAM, two-way ANOVA for sex x size with a block for gilt for the lightest and CTMLW foetuses was performed at GD60 and 90. As stated previously, this analysis could not be performed at GD45. No statistically significant interactions were observed in this analysis (Figure 7.6D and E).

7.5.2 Assessment of Endometrial Vascularity by IHC for CD31

7.5.2.1.1 Temporal Changes were observed in the Structure of the Endometrium

As described in 7.2, one of the broad objectives of this chapter was to investigate gestational changes in the vasculature of the pig endometrium. The total and mean number of uterine glands, total and mean number of BV and the percentage CD31 staining of endometrial stromal images were analysed at GD18, 30, 45, 60 and 90.

An overall GD effect was observed in total number of uterine glands (Kruskal-Wallis $P \leq 0.001$; Figure 7.7A), with the number of uterine glands fluctuating substantially throughout gestation. The mean number of uterine glands (Kruskal-Wallis $P \leq 0.001$) and percentage CD31 staining (Kruskal-Wallis $P=0.028$) both followed a similar profile to the total number of uterine glands. Both the total and mean number of BV (ANOVA with and without Gilt Block

FPr≤0.001 for both parameters) gradually decreased with advancing gestation, with the significant decrease occurring between GD30 and 45 (Figure 7.7B and D).

Parameter	GD45 (mean±S.E.M; (number of foetuses))				GD60 (mean±S.E.M; (number of foetuses))			
	CTMLW	Lightest	Male	Female	CTMLW	Lightest	Male	Female
Mean Total BV Number	30.065 ± 5.481 (6)	37.083 ± 5.356 (4)	32.944 ± 4.798 (11)	31.947 ± 4.449 (11)	54.196 ± 9.649 (7)	50.429 ± 9.180 (7)	50.804 ± 4.766 (14)	46.741 ± 5.767 (14)
Mean Percentage CD31 Staining (%)	0.977 ± 0.135 (6)	0.948 ± 0.170 (4)	0.875 ± 0.071 (10)	1.040 ± 0.095 (11)	0.470 ± 0.210 (7)	0.576 ± 0.159 (7)	0.464 ± 0.111 (14)	0.449 ± 0.091 (14)
Mean Internal BV Diameter (μm)	9.587 ± 2.685 (6)	6.080 ± 0.879 (4)	10.861 ± 3.151 (11)	9.236 ± 1.609 (11)	15.290 ± 3.159 (7)	12.413 ± 1.624 (7)	13.874 ± 1.300 (14)	15.115 ± 2.135 (14)
Mean External BV Diameter (μm)	18.983 ± 3.394 (6)	13.043 ± 1.014 (4)	21.103 ± 4.937(11)	18.257 ± 2.212(11)	22.615 ± 2.301 (6)	25.306 ± 2.819 (7)	28.238 ± 2.076 (14)	25.507 ± 2.610 (13)
Mean BV Wall Thickness (μm)	9.395 ± 0.858 (6)	6.963 ± 0.278 (4)	10.242 ± 2.142 (11)	9.021 ± 0.713 (11)	12.411 ± 2.347 (7)	12.893 ± 1.592 (7)	14.364 ± 1.156 (14)	12.728 ± 1.338 (14)

Table 7.5: Foetal Size or Sex were not associated with BV Number, Percentage CD31 Staining or BV diameter at GD45 or 60 in the Placental Stroma.

Abbreviations: BV=Blood Vessel; GD=Gestational Day; CTMLW=Closest to Mean Litter Weight; S.E.M.=Standard Error of the Mean.

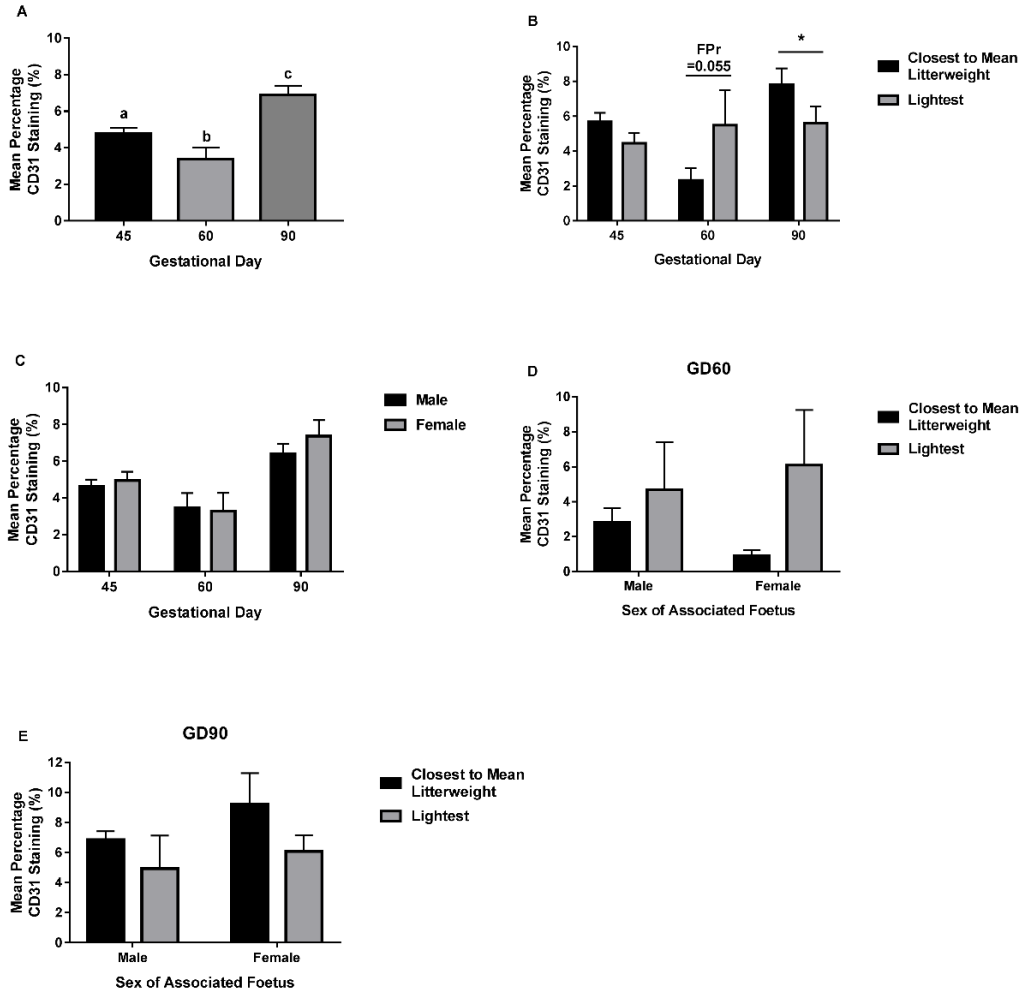

Figure 7.6: Analysis of CD31 Staining in the Chorioallantoic Membrane of the Placenta at GD45, 60 and 90.

Analysis of the percentage CD31 staining in the chorioallantoic membrane (CAM) region of the placenta was performed at gestational day (GD) 45, 60 and 90. A: An overall GD effect was observed, with CD31 staining decreasing at GD60 compared to GD45 before increasing significantly between GD60 and 90 (Kruskal-Wallis P≤0.001). B: No associations between foetal size and CAM CD31 staining was observed at GD45. At GD60, the percentage staining in the CAM of placentas supplying the lightest foetuses was increased compared to those supplying the CTMLW foetuses (ANOVA with Gilt Block FPr=0.055). The direction of this relationship switched at GD90, with placentas supplying the lightest foetuses having decreased percentage CD31 staining in the CAM compared to those supplying the CTMLW foetuses (ANOVA with Gilt Block FPr=0.05). C: No association between foetal sex and CD31 staining of the placental CAM was observed at GD45, 60 or 90. No sex x size interactions were observed in the percentage CD31 staining at GD60 (D) or 90 (E). Mean values presented. Error bars represent S.E.M. Letters indicate group means differ (Mann-Whitney). *FPr≤0.05. ***FPr≤0.001.

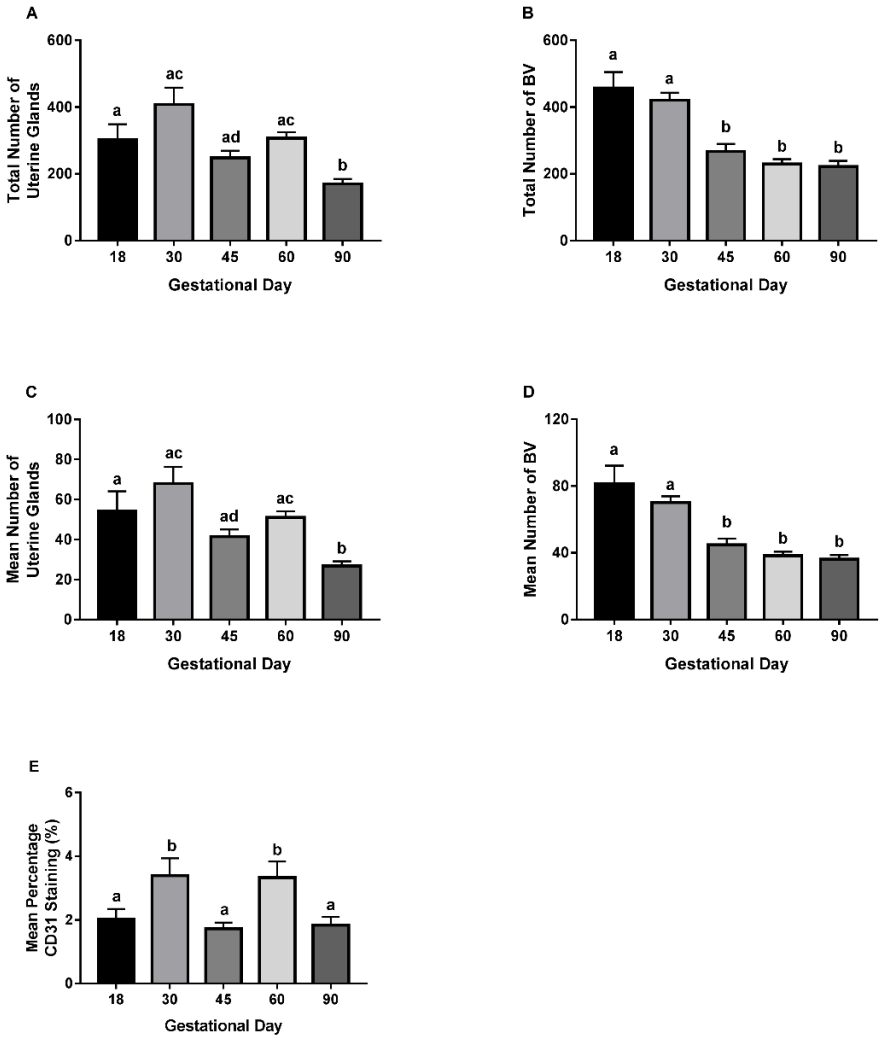

Figure 7.7: Gestational Changes in all Parameters Investigated were observed in the CD31 Stained Endometrium.

A: An overall gestational day (GD) effect was observed in total number of uterine glands (Kruskal-Wallis P≤0.001); with the number of uterine glands fluctuating substantially throughout gestation. B: The total number of blood vessels (BV) (ANOVA with and without Gilt Block FPr≤0.001) gradually decreased with advancing gestation, with the significant decrease occurring between GD30 and 45. C: An overall GD effect was observed in mean number of uterine glands (Kruskal-Wallis P≤0.001); with the number of uterine glands fluctuating substantially throughout gestation D: The mean number of BV (ANOVA with and without Gilt Block FPr≤0.001) gradually decreased with advancing gestation, with a significant decrease occurring between GD30 and 45. E: The percentage CD31 staining also fluctuated substantially throughout gestation (Kruskal-Wallis P=0.028), following a similar profile to the total and mean number of uterine glands. Mean values presented. Error bars represent S.E.M. *P/FPr≤0.05. ** P/FPr≤0.01. *** P/FPr≤0.001. Letters indicate that group means differ from one another (Tukey/Mann-Whitney).

7.5.2.1.2 Indications of Relationships between Foetal Size and the Mean and Total Number of BV at GD60, and the Mean Number of Uterine Glands at GD90 in CD31 Stained Endometrial Samples.

To determine if there was an association between foetal size and endometrial stromal vascularity, the total and mean number of uterine glands and BV, and the percentage CD31 staining were quantified in endometrial samples associated with the lightest and CTMLW conceptuses or foetuses at GD18, 30, 45, 60 and 90 (Figure 7.8). No statistically significant relationships between conceptus or foetal size and the mean total number of uterine glands (Figure 7.8A) or percentage CD31 staining (Figure 7.8E) were observed. At GD60, a trend for both the total number of BV (ANOVA without Gilt Block FPr=0.086; with Gilt Block FPr=0.071; Figure 7.8B) and mean number of BV (ANOVA without Gilt Block FPr=0.086; Gilt Block FPr=0.071; Figure 7.8C) to be decreased in endometrial samples supplying the lightest foetuses compared to the CTMLW foetuses was observed. Similarly, a trend towards a decrease in the mean number of uterine glands in endometrial samples supplying the lightest compared to the CTMLW foetuses was observed at GD90 (ANOVA with Gilt Block FPr=0.082; Figure 7.8D).

7.5.2.1.3 Foetal Sex Influenced Endometrial Structure

To determine if there was an association between foetal sex and endometrial vascularity, the data set from 7.5.1.2.1 was analysed in relation to foetal sex at GD30, 45, 60 and 90. The total number of uterine glands (ANOVA without Gilt Block FPr=0.047; with Gilt Block FPr=0.04; Figure 7.9A), total number of BV (ANOVA without Gilt Block FPr=0.034; with Gilt Block FPr=0.035; Figure 7.9B) and mean number of BV (ANOVA without Gilt Block FPr=0.037; with Gilt Block FPr=0.041; Figure 7.9D) were increased in endometrial samples supplying female foetuses compared to male foetuses at GD45. No associations between foetal sex and the mean number of uterine glands (Figure 7.9C) or percentage CD31 staining (Figure 7.9E) were observed.

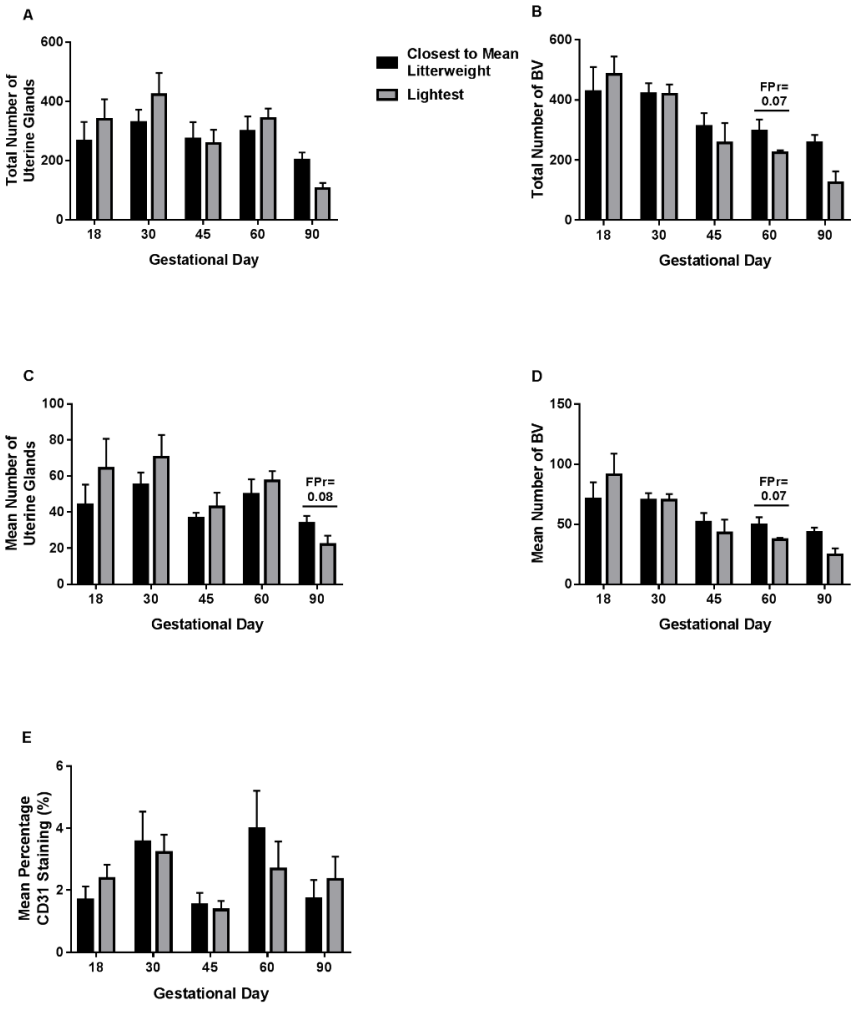

Figure 7.8: Indications of Relationships between Foetal Size and the Mean and Total Number of BV at GD60, and the Mean Number of Uterine Glands at GD90 in CD31 Stained Endometrial Samples.

To determine if there was an association between foetal size and endometrial stromal vascularity, the total number of uterine glands, total number of blood vessels (BV), mean number of uterine glands, mean number of BV and the percentage CD31 staining was quantified for the lightest and closest to mean litter weight (CTMLW) conceptuses or foetuses at gestational day (GD) 18, 30, 45, 60 and 90. No statistically significant relationships between foetal size and total number of uterine glands (A) or percentage CD31 staining (E) were observed. At GD60, a trend for both the total number of BV (ANOVA without Gilt Block FPr=0.086; with Gilt Block FPr=0.07; B) and mean number of BV (C) to be decreased in endometrial samples supplying the lightest foetuses compared to the CTMLW foetuses was observed. A trend towards decreased mean number of uterine glands was observed in endometrial samples supplying the lightest compared to the CTMLW foetuses was observed at GD90 (ANOVA with Gilt Block FPr=0.08; D). Mean values presented. Error bars represent S.E.M.

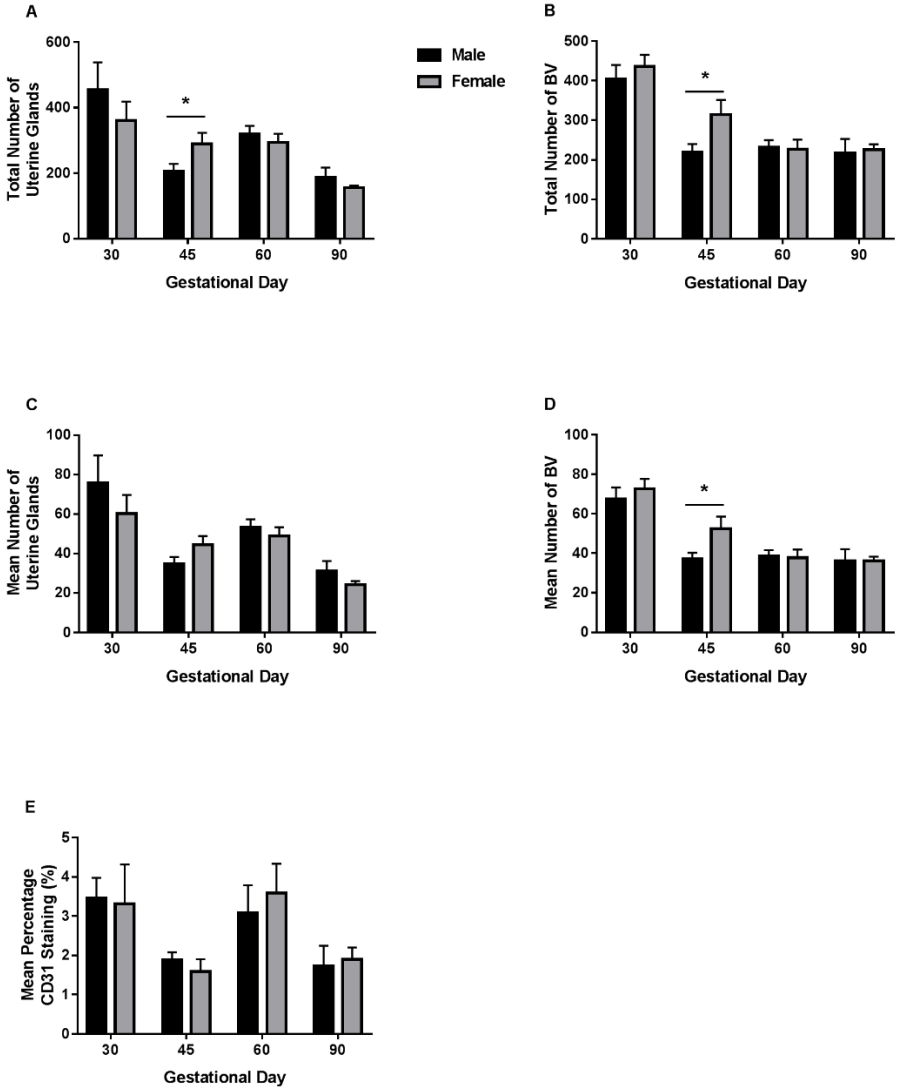

Figure 7.9: Females had an Increased Total Number of Uterine Glands, and Total and Mean Number of BV at GD45 Compared to Male Foetuses in CD31 Stained Endometrial Samples.

To determine if there was an association between foetal sex and endometrial vascularity, the total number of uterine glands, total number of blood vessels (BV), mean number of uterine glands, mean number of BV and the percentage CD31 staining were quantified in endometrial samples supplying male and female foetuses at gestational day (GD) 30, 45, 60 and 90. The total number of uterine glands (ANOVA with and without Gilt Block FPr≤0.05; A), total number of BV (ANOVA with and without Gilt Block FPr≤0.05; B) and mean number of BV (ANOVA with and without Gilt Block FPr≤0.05; D) were increased in endometrial samples supplying female foetuses compared to male foetuses at GD45. No associations between foetal sex and the mean number of uterine glands (C) or percentage CD31 staining (E) were observed. Mean values presented. Error bars represent S.E.M. *FPr/P≤0.05.

7.5.2.1.4 Sex x Size Interactions were not observed in Endometrial Structure

To investigate the presence of sex x size interactions in the vascularity of the endometrium, a two-way ANOVA for sex x size, with and without a block for gilt for the lightest and CTMLW foetuses was performed at GD30, 60 and 90. As stated previously, this analysis could not be performed at GD45 due to the small sample size, and GD18 as the sex of the conceptuses is not known. No sex x size interactions were observed in any of the parameters investigated at GD30, 60 or 90 (data not presented).

7.5.3 Assessment of Placental mRNA Expression by qPCR

7.5.3.1.1 Quantitative Polymerase Chain Reaction Calibration Curve Data for Placental qPCRs

qPCR was performed for the candidates of interest *ACP5*, *CD31*, *HIF1A*, *HPSE*, *PTGFR* and *VEGFA* alongside the reference genes *TBP1* and *HPRT1*. The amplification efficiencies, RSq, slope and intercept values for each gene are detailed in Table 7.6.

7.5.3.1.2 Temporal Changes in Placental mRNA Expression were observed

As described in 7.2, one of the broad objectives of this chapter was to investigate gestational changes in the expression of candidate genes in placental samples. Temporal changes were observed in all the candidates investigated (Figure 7.10). *ACP5* (ANOVA without Gilt Block FPr=0.078, Figure 7.10A) and *PTGFR* (Kruskal-Wallis P≤0.001; Figure 7.10B) had low expression at GD30 which increased at GD45, and remained elevated for the remainder of gestation. *CD31* (P=0.003 Kruskal-Wallis, Figure 7.10B), *HIF1A* (ANOVA without Gilt Block FPr≤0.001, with Gilt Block FPr=0.008; Figure 7.10C) and *HPSE* (ANOVA without Gilt Block FPr≤0.001, with Gilt Block FPr=0.003; Figure 7.10D) all had a similar temporal profile with expression remaining constant between GD30, 45 and 60 before increasing dramatically

towards GD90. *VEGFA* expression followed a different profile, where expression increased gradually throughout gestation (Figure 7.10F). *VEGFA* expression increased between GD30 and 45, where it plateaued until increasing substantially between GD60 and 90 (ANOVA with and without Gilt Block FPr≤0.001).

7.5.3.1.3 Foetal Size is Associated with Altered Placental *ACP5* and *CD31* Expression

To address the question of whether there is a relationship between foetal size and the placental expression of the candidate genes, placentas supplying the lightest foetuses were compared with those supplying the CTMLW foetuses within GD (Figure 7.11). *ACP5* expression was increased in placentas supplying the lightest foetuses compared to those supplying the CTMLW foetuses at GD60 (ANOVA with Gilt Block FPr≤0.05; Figure 7.11A). *CD31* expression was decreased in placentas supplying the lightest foetuses compared to those supplying the CTMLW foetuses at GD45 (ANOVA GD45 without gilt block FPr=0.006; with gilt block FPr=0.033; Figure 7.11B). The direction of this difference was switched at GD60, with placentas supplying the lightest foetuses having increased *CD31* expression compared to those supplying the CTMLW foetuses (ANOVA with Gilt Block FPr=0.052). This switched again at GD90 (ANOVA without Gilt Block FPr=0.08), although this difference was not statistically significant with the addition of a block for gilt. No significant size associations were observed in *HIF1A*, *HPSE*, *PTGFR* (ANOVA GD90 without gilt block FPr=0.056), or *VEGFA* expression (Figure 7.11C, D, E, and F respectively).

Gene	Amplification Efficiency (%)	RSq	Slope	Intercept
ACP5	94.9	0.997	-3.451	23.705
CD31	97.2	0.999	-3.390	24.097
HIF1A	97.8	0.994	-3.375	24.911
HPSE	107.7	0.992	-3.088	26.124
PTGFR	102	0.991	-3.275	24.062
VEGFA	104.4	0.992	-3.222	24.462
TBP1	102.9	0.990	-3.402	27.002
HPRT1	96.8	0.991	-3.254	27.211

Table 7.6: Quantitative Polymerase Chain Reaction Calibration Curve Data for Placental qPCRs.

Abbreviations used: *ACP5*=Uteroferrin, *CD31*=Platelet and Endothelial Cell Adhesion Molecule 1, *HIF1A*=Hypoxia Inducible Factor 1 Alpha Subunit, *HPSE*=Heparanase, *PTGFR*=Prostaglandin F2α Receptor, *VEGFA*=Vascular Endothelial Growth Factor A, *TBP1*=TATA box binding protein, and *HPRT1*=Hypoxanthine phosphoribosyltransferase 1.

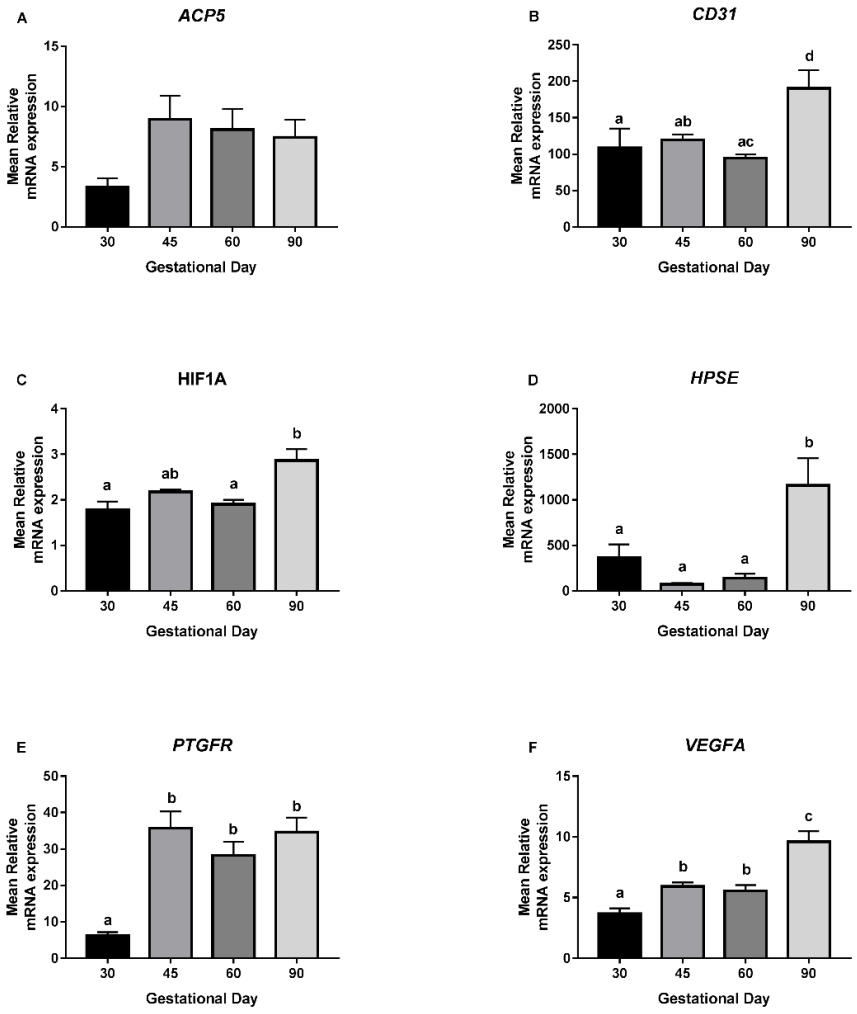

Figure 7.10: Gestational Changes were observed in the Placental Expression of All the Candidate Genes Investigated.

The mean values, normalised to the expression of stable reference genes are plotted here. A: *ACP5* expression increased between gestational day (GD) 30 and 45 where it remained elevated for the remainder of gestation (ANOVA without Gilt Block FPr=0.078). B: *CD31* expression remained constant between GD30, 45 and 60 before increasing dramatically towards GD90 (P=0.003 Kruskal-Wallis). C: *HIF1A* expression remained constant between GD30, 45 and 60 before increasing dramatically towards GD90 (ANOVA without Gilt Block FPr≤0.001, with Gilt Block FPr=0.008). D: *HPSE* (ANOVA without Gilt Block FPr≤0.001, with Gilt Block FPr=0.003). E: *PTGFR* had low expression at GD30 which increased at GD45 and remained elevated for the remainder of gestation (Kruskal-Wallis P≤0.001). F: *VEGFA* expression increased gradually throughout gestation, with a moderate increase between GD30 and 45, where it plateaued until increasing substantially between GD60 and 90 (ANOVA with and without Gilt Block FPr≤0.001). Error bars represent S.E.M. Letters indicate that group means differ from one another (Tukey/Mann-Whitney).

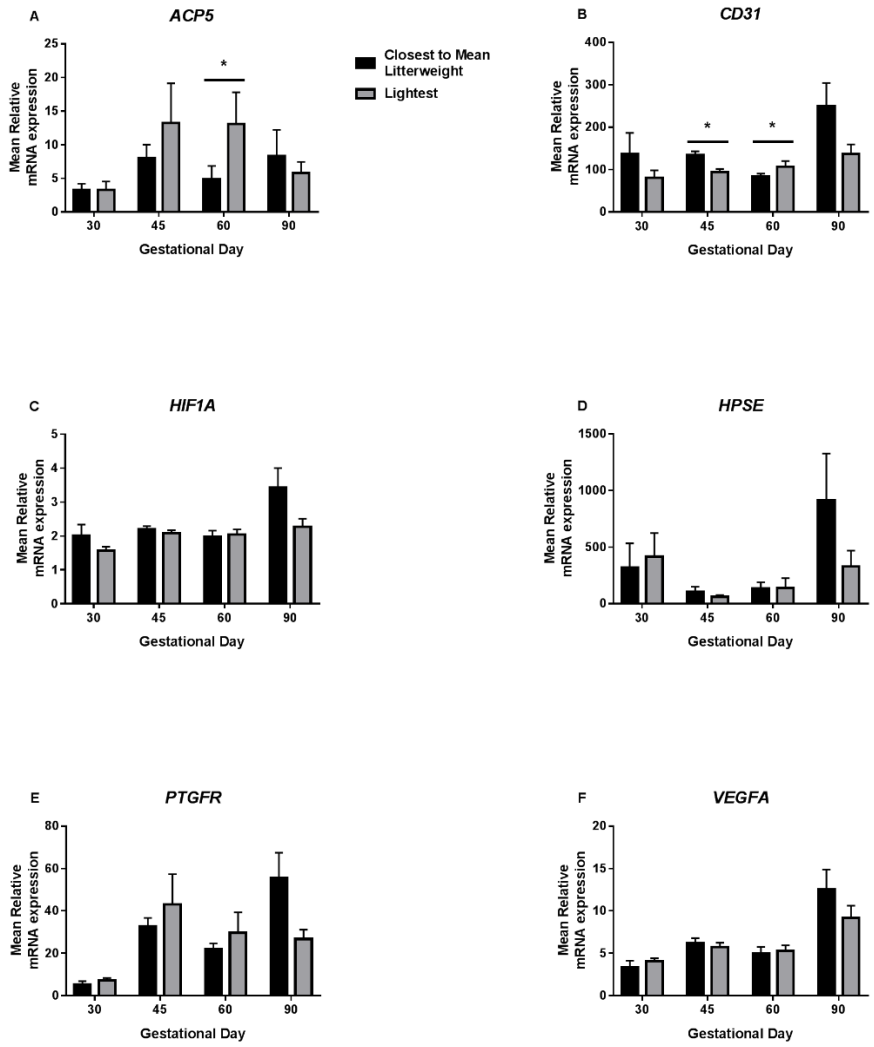

Figure 7.11: Foetal Size is Associated with Altered Placental *ACP5* and *CD31* Expression.

The mean values, normalised to the expression of stable reference genes are plotted here. A: *ACP5* expression was increased in placentas supplying the lightest foetuses compared to those supplying the closest to mean litter weight (CTMLW) foetuses at gestational day (GD) 60 (ANOVA with Gilt Block FPr≤0.05) B: *CD31* expression was decreased in placentas supplying the lightest foetuses compared to those supplying the CTMLW foetuses at GD45 (ANOVA without Gilt Block FPr=0.006; with Gilt Block FPr=0.033). The direction of this difference was switched at GD60, with placentas supplying the lightest foetuses having increased *CD31* expression compared to those supplying the CTMLW foetuses at GD60 (ANOVA with Gilt Block FPr=0.052). The direction of this difference switched again at GD90 (ANOVA without Gilt Block FPr=0.08), although it was not statistically significant with the addition a block for gilt. No significant size associations were observed in *HIF1A* (C), *HPSE* (D), *PTGFR* (ANOVA GD90 without Gilt Block FPr=0.056; E) or *VEGFA* expression (F). Error bars represent S.E.M. *FPr/P≤0.05.

7.5.3.1.4 No Statistically Significant Associations between Foetal Sex and Placental mRNA Expression were observed.

The influence of foetal sex on placental mRNA expression was investigated within GD by comparing the mean expression of samples supplying males with those supplying females (Figure 7.12). No associations between foetal sex and placental mRNA expression were observed in *ACP5* (Figure 7.12A), *CD31* (Figure 7.12B), *HPSE* (ANOVA without Gilt Block GD90 FPr=0.079; Figure 7.12D), *PTGFR* (Figure 7.12E) or *VEGFA* (Figure 7.12F) expression. At GD90, a trend towards increased *HIF1A* expression was observed in placental samples supplying females compared to those supplying male foetuses (ANOVA without Gilt Block FPr=0.066; with Gilt Block FPr=0.073; Figure 7.12C).

7.5.3.1.5 No Statistically Significant Sex X Size Interactions were observed in Placental mRNA Expression at GD30, 60 or 90

To investigate the presence of sex x size interactions in placental mRNA expression, a two-way ANOVA for sex x size, with and without a block for gilt were performed at GD30, 60 and 90 for each candidate for the lightest and CTMLW foetus. As described previously this was not performed at GD45 due to the small sample size available for the male comparison.

No significant sex x size interactions were observed in the mRNA expression of the candidates at GD30 or 90 when a block for gilt was added to the analysis. Intriguingly, at GD60 a sex x size interaction was observed in VEGFA expression (ANOVA with Gilt Block FPr=0.008; Figure 7.13) with the placentas supplying the CTMLW females having lower expression than the other 3 groups.

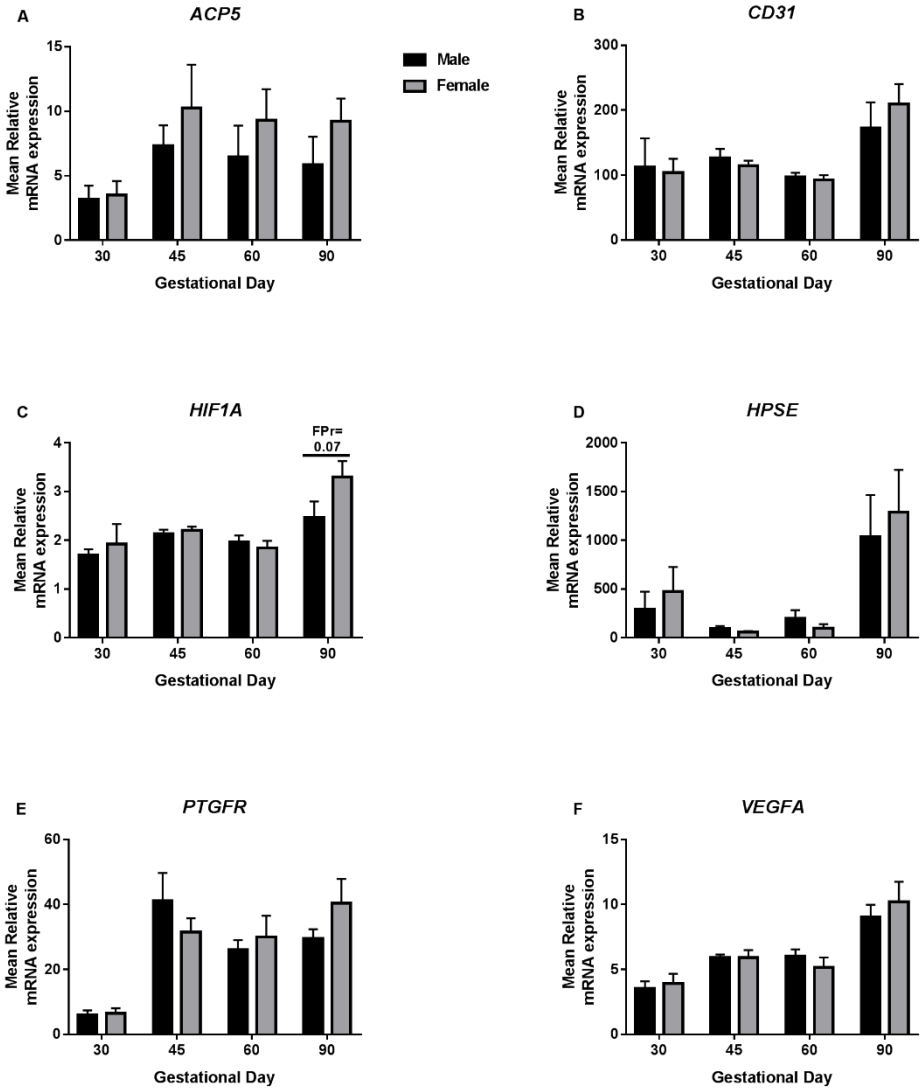

Figure 7.12: No Statistically Significant Associations between Foetal Sex and Placental mRNA Expression were observed.

The mean values, normalised to the expression of stable reference genes are plotted here. No associations between foetal sex and placental expression of *ACP5* (A), *CD31* (B), *HPSE* (D), *PTGFR* (E) or *VEGFA* (F) were observed. A trend towards increased *HIF1A* expression at gestational day (GD) 90 was observed in placental samples supplying females compared to those supplying male foetuses (ANOVA without Gilt Block FPr=0.066; with Gilt Block FPr=0.073; C). Error bars represent S.E.M.

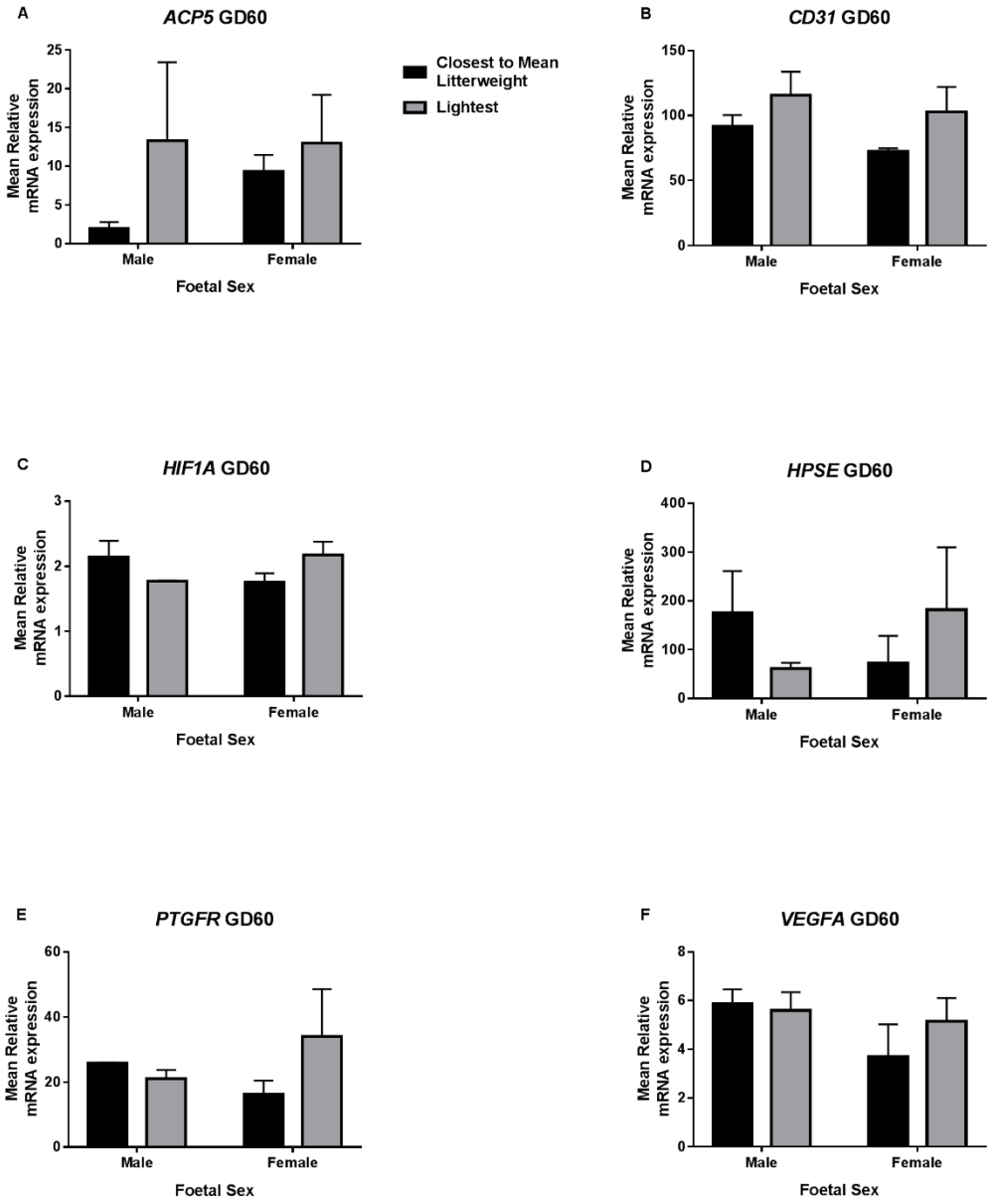

Figure 7.13: A Sex X Size Interaction in Placental VEGFA Expression was observed at GD60.

qPCR was performed on cDNA from porcine placental samples supplying the lightest and CTMLW male and female foetuses at gestational day (GD) 60. The mean values, normalised to the expression of the reference genes *TBP1* and *HPRT1* are plotted here. No sex x size interactions in placental expression of *ACP5* (A), *CD31* (B), *HIF1A* (C), *HPSE* (D) or *PTGFR* (E) were observed. A sex x size interaction in *VEGFA* expression was observed (ANOVA with Gilt Block FPr≤0.01; F), with the CTMLW females having lower expression that the other 3 groups. Error bars represent S.E.M.

7.5.4 Assessment of Endometrial mRNA Expression by qPCR

7.5.4.1.1 Quantitative Polymerase Chain Reaction Calibration Curve Data for Endometrial qPCRs

qPCR was performed for the candidates of interest *ACP5*, *CD31*, *HIF1A*, *HPSE*, *PTGFR* and *VEGFA* alongside the reference genes *TBP1* and *YWHAZ*. The amplification efficiencies, RSq, slope, and intercept values for each gene are detailed in

Table 7.7, and were all within the acceptable criteria (2.2.8.3).

7.5.4.1.2 Temporal Changes in Endometrial mRNA Expression were observed

As described in 7.2, one of the broad objectives of this chapter was to investigate gestational changes in the expression of candidate genes in endometrial samples. Temporal changes were observed in almost all the candidates investigated (Figure 7.14). A gradual increase in *ACP5* expression was observed between GD18 and 60, before decreasing between GD60 and 90 (ANOVA with and without Gilt Block FPr≤0.001; Figure 7.14A). *CD31* expression fluctuated slightly throughout gestation although no statistically significant GD effect was observed (Figure 7.14B). A significant decrease in *HIF1A* expression occurred between GD45 and 60 (overall GD effect ANOVA without Gilt Block FPr=0.023, with Gilt Block FPr=0.052; Figure 7.14C). Temporal changes were observed in *HPSE* (ANOVA with and without Gilt Block FPr≤0.001; Figure 7.14D) and *PTGFR* (ANOVA without Gilt Block FPr≤0.001, with Gilt Block FPr=0.004; Figure 7.14E) expression, with similar temporal profiles observed until between GD60 and 90. The expression of both genes was low at GD18 before increasing by GD30, then decreasing sharply to plateau between GD45 and 60. *PTGFR* expression remained constant between GD60 and 90, whereas *HPSE* expression significantly increased. In contrast, *VEGFA* expression increased between GD18 and 30, before modestly increasing between GD30 and 45, and then remained constant for the remainder of gestation (P≤0.001, Kruskal-Wallis).

7.5.4.1.3 An Association between Foetal Size and Endometrial *CD31*, *HIF1A*, *HPSE* and *VEGFA* Expression was observed

To address the question of whether there is a relationship between foetal size and the endometrial expression of the candidate genes, endometrial expression in samples associated with the lightest conceptuses or foetuses were compared with the CTMLW conceptuses or foetuses within GD (Figure 7.15). No associations between conceptus or foetal size and endometrial *ACP5* (Figure 7.15A) or *PTGFR* (Figure 7.15E) expression were observed. An increase in *CD31* expression (Figure 7.15B) was observed in endometrial samples supplying the lightest foetuses compared to the CTMLW foetuses at GD60 (ANOVA without Gilt Block FPr=0.018; with Gilt Block FPr=0.06). Intriguingly, *HIF1A* expression was found to be increased in endometrial samples supplying the lightest foetuses compared to the CTMLW foetuses at GD45 (ANOVA with Gilt Block FPr=0.016; Figure 7.15C). The direction of this difference was reversed at GD60, with endometrial samples supplying the lightest foetuses having decreased expression (ANOVA without Gilt Block FPr=0.066; with Gilt Block FPr=0.079) compared to the CTMLW foetuses. Both *HPSE* (ANOVA without Gilt Block FPr=0.019; with Gilt Block FPr=0.04; Figure 7.15D) and *VEGFA* (ANOVA without Gilt Block FPr=0.046; with Gilt Block FPr=0.057; Figure 7.15F) endometrial expression were decreased in samples supplying the lightest foetuses compared to the CTMLW foetuses at GD90.

Gene	Amplification Efficiency (%)	RSq	Slope	Intercept
ACP5	95.5	0.991	-3.434	18.279
CD31	102.0	0.990	-3.274	25.097
HIF1A	103.3	0.990	-3.246	24.940
HPSE	99.1	0.991	-3.344	27.719
PTGFR	108.8	0.990	-3.127	26.503
VEGFA	99.5	0.990	-3.334	23.538
TBP1	105.6	0.991	-3.194	28.209
YWHAZ	92.6	0.991	-3.513	21.871

Table 7.7: Quantitative Polymerase Chain Reaction Calibration Curve Data for Endometrial qPCRs.

Abbreviations used: *ACP5*=Uteroferrin, *CD31*=Platelet and Endothelial Cell Adhesion Molecule 1, *HIF1A*=Hypoxia Inducible Factor 1 Alpha Subunit, *HPSE*=Heparanase, *PTGFR*=Prostaglandin F2α Receptor, *VEGFA*=Vascular Endothelial Growth Factor A, *TBP1*=TATA box binding protein, and *YWHAZ*=Tyrosine 3-monooxygenase/tryptophan 5-monooxygenase activation protein, zeta polypeptide.

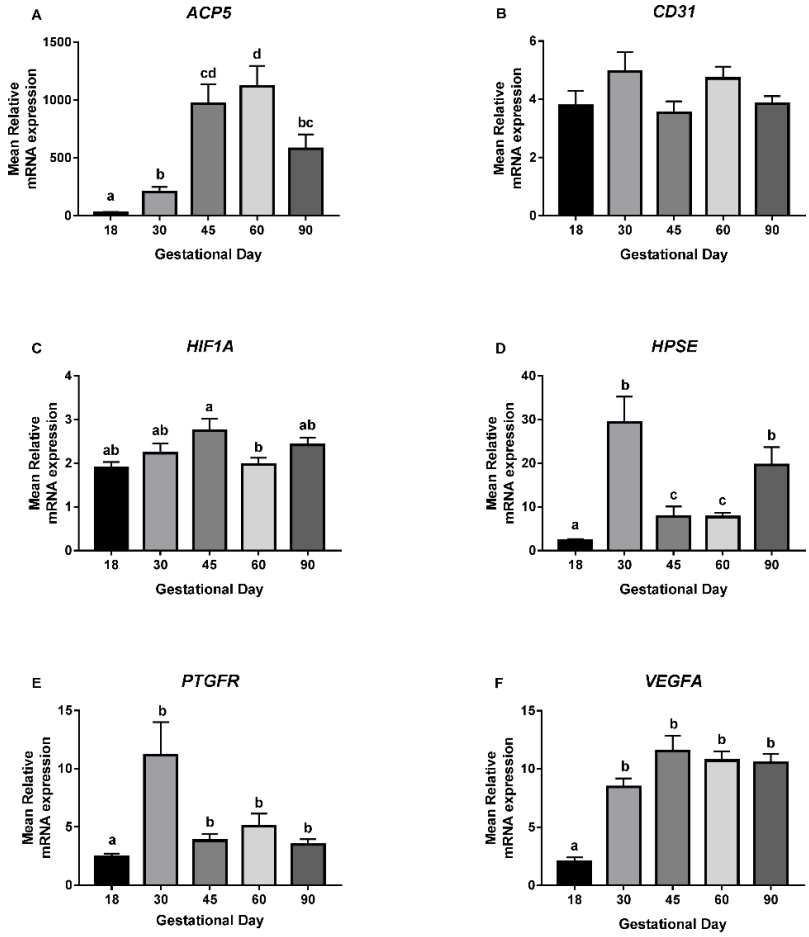

Figure 7.14: Gestational Changes were observed in the Endometrial Expression of 5 of the 6 Candidate Genes Investigated.

The mean values, normalised to the expression of stable reference genes are plotted here. A: *ACP5* expression increased from gestational day (GD) 18 to 60, before a large decrease in expression was observed between GD60 and 90 (ANOVA with and without Gilt Block FPr≤0.001). B: *CD31* expression fluctuated slightly throughout gestation although no significant GD effect was observed. C: A decrease in *HIF1A* expression between GD45 and 60 (overall GD effect ANOVA without Gilt Block FPr=0.023, with Gilt Block FPr=0.052) was observed. D: *HPSE* expression was low at GD18 before increasing dramatically at GD30. Following this it decreased sharply at GD45 and 60, before increasing towards GD90 (ANOVA with and without Gilt Block FPr≤0.001). E: A large increase in *PTGFR* expression was observed between GD18 and 30, following which it decreased to a constant level for the remainder of gestation (ANOVA without Gilt Block FPr≤0.001, with Gilt Block FPr=0.004). F: *VEGFA* expression increased between GD18 and 30, where it slightly increased between GD30 and 45, and remained constant for the remainder of gestation (P≤0.001, Kruskal-Wallis). Error bars represent S.E.M. Letters indicate that group means differ from one another (Tukey/Mann-Whitney).

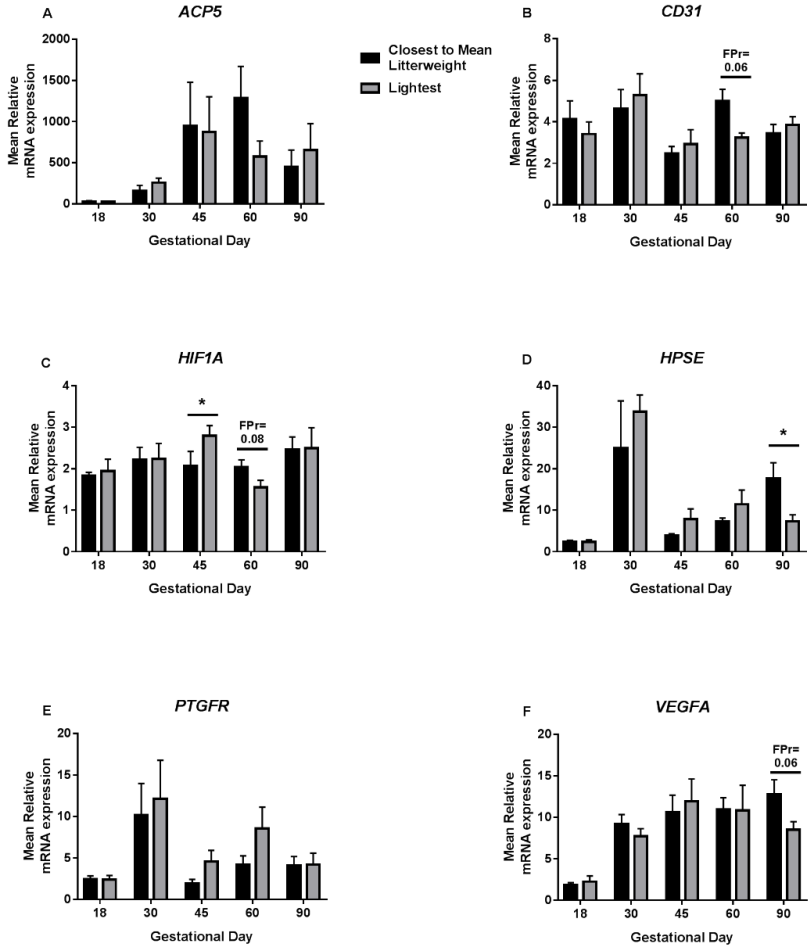

Figure 7.15: An Association between Foetal Size and Endometrial *CD31*, *HIF1A*, *HPSE* and *VEGFA* Expression was observed

The mean values, normalised to the expression of stable reference genes are plotted here. A: No associations between conceptus or foetal size and endometrial *ACP5* expression were observed. B: An increase in *CD31* expression was observed in endometrial samples supplying the lightest compared to the closest to mean litter weight (CTMLW) foetuses at gestational day (GD60) (ANOVA without Gilt Block FPr=0.018; with Gilt Block FPr=0.06). C: *HIF1A* expression was increased in endometrial samples supplying the lightest foetuses compared to the CTMLW foetuses at GD45 (ANOVA with Gilt Block FPr=0.016). The direction of this difference was reversed at GD60, with endometrial samples supplying the lightest foetuses having decreased expression (ANOVA without Gilt Block FPr=0.066; with Gilt Block FPr=0.079) compared to the CTMLW foetuses. Both *HPSE* (ANOVA without Gilt Block FPr=0.019; with Gilt Block FPr=0.04; D) and *VEGFA* (ANOVA without Gilt Block FPr=0.046; with Gilt Block FPr=0.057; F) endometrial expression was found to be decreased in samples supplying the lightest foetuses compared to the CTMLW foetuses at GD90. E: No associations between foetal size and *PTGFR* (E) expression were observed. Error bars represent S.E.M. *FPr/P≤0.05.

7.5.4.1.4 An Association between Foetal Sex and Endometrial *ACP5*, *CD31*, *HIF1A*, *HPSE*, *PTGFR* and *VEGFA* Expression was observed.

The influence of foetal sex on endometrial mRNA expression was investigated within GD by comparing the mean expression of samples supplying males with those supplying females (Figure 7.16). As the GD18 conceptuses were not sexed, this analysis could not be performed at this stage.

Endometrial samples supplying female foetuses had decreased *ACP5* expression compared to male foetuses at GD60 (ANOVA with Gilt Block FPr=0.05; Figure 7.16A). Both *CD31* (ANOVA without Gilt Block FPr=0.051; with Gilt Block FPr=0.012; Figure 7.16B) and *VEGFA* (ANOVA with Gilt Block FPr= 0.018; Figure 7.16F) endometrial expression was increased in samples supplying female foetuses at GD30 compared to samples supplying male foetuses. Intriguingly, the direction of this difference in expression was switched at GD60 in both *CD31* (ANOVA without Gilt Block FPr=0.009; with Gilt Block FPr=0.006) and *VEGFA* (ANOVA without Gilt Block FPr=0.022; with Gilt Block FPr=0.035) expression, with samples supplying females having decreased expression compared to samples supplying male foetuses. A trend towards decreased *HIF1A* expression in endometrial samples supplying female foetuses compared to those supplying their male foetuses was observed at both GD60 (ANOVA with Gilt Block FPr=0.061) and 90 (ANOVA without Gilt Block FPr=0.07; with Gilt Block FPr=0.061; Figure 7.16C). Similarly, at GD45 a trend towards decreased *HPSE* expression (ANOVA with Gilt Block FPr=0.071; Figure 7.16D) was observed in endometrial samples supplying female foetuses compared to those supplying male foetuses. Additionally, *PTGFR* expression was increased in endometrial samples supplying female foetuses compared to those supplying male foetuses at GD30 (ANOVA without Gilt Block FPr=0.084; with Gilt Block FPr=0.032; Figure 7.16E).

7.5.4.1.5 No Statistically Significant Sex X Size Interactions in Endometrial mRNA Expression at GD30, 60 or 90 were observed

To investigate the presence of sex x size interactions in endometrial mRNA expression, two-way ANOVA for sex x size, with and without a block for gilt were performed at GD30, 60 and 90 for each candidate for the lightest and CTMLW foetuses. As stated previously, this was not performed at GD45 due to the low sample size. No statistically significant sex x size interactions were observed in any of the candidates at any of the three GD investigated (data not presented).

Figure 7.16: An Association between Foetal Sex and Endometrial *ACP5, CD31, HIF1A, HPSE*, *PTGFR* and *VEGFA* Expression was observed.

The mean values, normalised to the expression of stable reference genes are plotted here. A: *ACP5* expression was decreased in endometrial samples supplying female foetuses compared to male foetuses at gestational day (GD) 60 (ANOVA with Gilt Block FPr=0.05). Both *CD31* (ANOVA without Gilt Block FPr=0.051; with Gilt Block FPr=0.012; B) and *VEGFA* (ANOVA with Gilt Block FPr= 0.018; F) endometrial expression was increased in samples supplying female foetuses at GD30 compared to endometrial samples supplying male foetuses. The direction of this difference in expression was switched at GD60 in both *CD31* (ANOVA without Gilt Block FPr=0.009; with Gilt Block FPr=0.006) and *VEGFA* (ANOVA without Gilt Block FPr=0.022; with Gilt Block FPr=0.035), with females having decreased expression compared to samples supplying male foetuses. C: A trend towards decreased endometrial *HIF1A* expression in endometrial samples supplying female foetuses compared to those supplying male foetuses was observed at both GD60 (ANOVA with Gilt Block FPr=0.061) and 90 (ANOVA without Gilt Block FPr=0.07; with Gilt Block FPr=0.061). D: A trend towards decreased *HPSE* expression (ANOVA with Gilt Block FPr=0.071) at GD45 was observed in endometrial samples supplying female foetuses compared to those supplying male foetuses. E: *PTGFR* expression was increased in endometrial samples supplying female foetuses compared to those supplying male foetuses at GD30 (ANOVA without Gilt Block FPr=0.084; with Gilt Block FPr=0.032). Error bars represent S.E.M. *FPr/P≤0.05. ** FPr/P≤0.01.

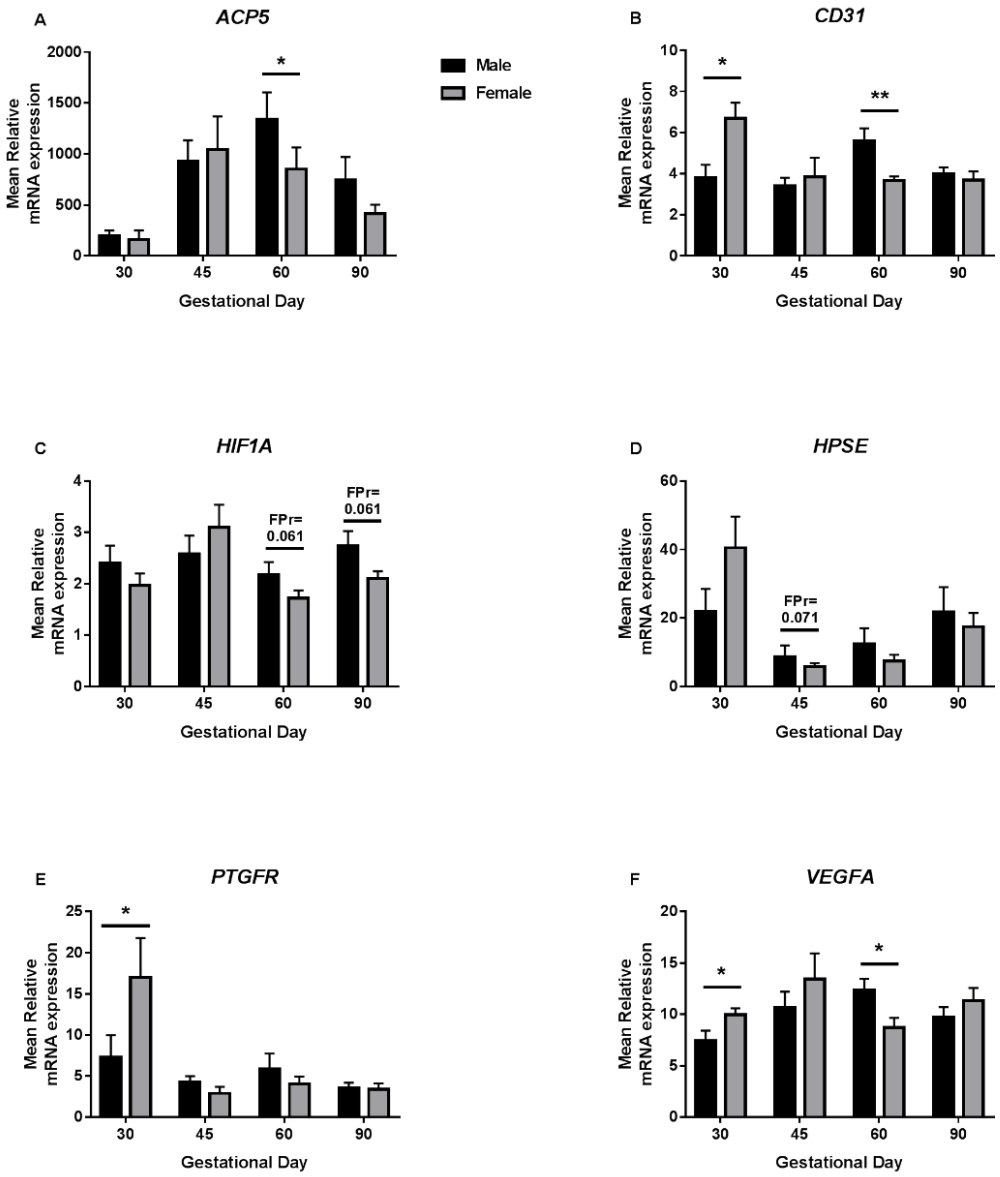

Figure 7.16: An Association between Foetal Sex and Endometrial *ACP5*, *CD31*, *HIF1A*, *HPSE*, *PTGFR* and *VEGFA* Expression was observed.

7.6 Discussion

The experiments described in this chapter have demonstrated novel associations between foetal size, sex and the vascularity and mRNA expression of candidate genes which have a central role in angiogenesis and foetal development, at the feto-maternal interface in the pig (Table 7.8 and Table 7.9). Currently, this is the first suggestion in the literature that foetal sex may have a strong influence on the activity of the porcine endometrium, and the mechanisms behind this warrant much further investigation.

7.6.1 Temporal Changes were observed in both Placental and Endometrial Samples

As described in 7.1.1, it has previously been demonstrated in the pig that endometrial ACP5 secretion decreases in late gestation, after which alternative methods are thought to regulate iron transport. A gradual increase in endometrial *ACP5* expression was observed between GD18 and 60, before decreasing between GD60 and 90, reinforcing the previous literature. In this chapter, no statistically significant GD effect was observed in placental *ACP5* expression, although expression was low at GD30, before increasing at towards GD45, after which point its expression level was stable for the reminder of gestation. Steinhauser *et al.*, (2017) demonstrated that ACP5 protein is expressed in the areolae throughout gestation, which adds confidence to the data presented in this thesis.

The function of CD31 in the pig uterus remains poorly understood and the temporal profile of CD31 has not been reported previously. Reassuringly, the temporal changes observed in percentage CD31 staining in the CAM and in the endometrial stroma follow the same temporal profile observed in the mRNA expression data. In the placenta, it is known that remodelling of the bilayer occurs to increase the surface area available for exchange with the developing foetus, with the width of the bilayer increasing from GD65 to 105 (Vallet and Freking, 2007). Similarly, it is known that there is an increase in the density of blood vessels present in the placenta in late pregnancy to increase the transfer

of nutrients from the mother to the exponentially growing foetus (Tayade *et al.*, 2007b), which may reflect the increase in the expression of the endothelial cell marker CD31 between GD60 and 90 in the placenta. In the endometrium, a decrease in the number of BVs quantified was observed with advancing gestation. This presumably reflects that BVs increase in size with advancing gestation, as it is known that uterine blood flow increases with advancing gestation in the pig (Père and Etienne, 2000). Similarly, the temporal changes in uterine gland number observed were expected and are thought to reflect the dynamic nature of the endometrium and the changes in secretion of the histotroph throughout gestation.

In contrast to Novak *et al.*, (2012), who reported that *HIF1A* decreased gradually from GD16 to 50, *HIF1A* placental expression remained constant between GD30, 45 and 60 before increasing dramatically towards GD90. Biologically, the observed increase in *HIF1A* expression towards GD90 could be explained by the increasing foetal demands being placed upon the placenta resulting in a more hypoxic environment towards the end of gestation. In the endometrium, a significant decrease in *HIF1A* expression occurred between GD45 and 60. This has not been reported previously in the literature however, this may reflect that the uterus is hypoxic in early pregnancy and the expression of HIF1A at GD45 induces angiogenesis in the uterus, as detailed in 7.1.3, leading to decreased expression being observed at GD60, after initiation of the second wave of angiogenesis,

Temporal changes were observed in both endometrial and placental *HPSE* expression in this chapter. Previously Miles *et al.*, (2009) demonstrated an increase in *HPSE* expression at GD25, implying that HPSE has a role in placental development, and an increase in expression towards the end of gestation (GD85 and 105), implicating HPSE in placental remodelling in the phase of exponential foetal growth. Hong *et al.*, (2014) also demonstrated that HPSE plays a pivotal role in placental bilayer remodelling. They demonstrated the HPSE expression was high on GD26, before decreasing at GD50, and increased at GD90 in both MS and Yorkshire pig placentas. The expression levels and localisation of both mRNA and protein were different in late

gestation between the two breeds. MS pigs had increased HPSE mRNA and protein expression compared with Yorkshire pigs, with all trophoblast cells in MS pigs expressing *HPSE* mRNA, and HPSE protein was present in both the trophoblast and LE cells in late gestation. In contrast to this, only trophoblast cells located at the bottom and sides of the folds in Yorkshire pigs expressed HPSE mRNA and protein. In the current study, placental *HPSE* expression was increased at GD30 compared to GD45 and 60, although this was not statistically significant. However, a significant increase was observed in *HPSE* expression at GD90 compared to the other GD investigated, reinforcing the results of both Miles *et al.*, (2009) and Hong *et al.*, (2014). To date there is little information regarding the endometrial expression of HPSE although, as described above, it has been suggested that LE expression of HPSE varies between breeds. In the current study, temporal changes were observed in *HPSE* expression, with GD18 having the lowest expression of all GD investigated, suggesting that HPSE is not involved in the attachment process itself. HPSE expression was increased at GD30 and 90 compared to GD45 and 60, suggesting that it may play a role at the feto-maternal interface in assisting with placental development, and for remodelling of the interface in late gestation to facilitate increased nutrient transport. Localisation of the mRNA and protein at the feto-maternal interface in the pigs used in this study would improve our understanding of the role of HPSE in the endometrium.

Endometrial *PTGFR* expression was found to significantly increase between GD18 and 30, which reinforces the previous literature describing how PGF2α is central in regulating the establishment of pregnancy (Bazer and Thatcher, 1977; McCracken *et al.*, 1999; Spencer *et al.*, 2004; Waclawik *et al.*, 2009; Kaczynski *et al.*, 2016).

Winther *et al.*, (1999) demonstrated that VEGF and VEGF receptors have decreased protein expression in the LE until GD21, after which they have intense expression until GD100. The qPCR results presented in this chapter reinforce this, with decreased endometrial *VEGFA* at GD18 compared to the other GD investigated. Similarly, Vonnahme and Ford, (2004) suggested that placental *VEGF* expression increases between GD70 and 90, reflecting the

increase in vascular density of the placenta to increase the nutrient supply to the exponentially growing foetus. The qPCR results presented in this chapter found a similar increase in *VEGF* expression between GD60 and 90. Overall, the temporal changes in *VEGFA* expression observed in this chapter are supported by the previous literature describing placental and endometrial expression at the porcine feto-maternal interface, adding confidence to the other results obtained in this chapter.

7.6.2 Foetal Size was Associated with Alterations in Vascularity and mRNA Expression at the Feto-Maternal Interface

Foetal size was associated with altered mRNA expression in both placental and endometrial samples. Intriguingly, more associations between foetal size and mRNA expression were observed in the endometrium than the placenta.

Foetal size was not associated with the parameters investigated in the CD31 stained placental and endometrial stromal tissue. However, a temporal association between foetal size and CAM CD31 staining was observed, which was reinforced by the CD31 qPCR data. The consistency in the findings of these two experiments reinforces the significance of this finding and highlights the dynamic nature of the relationship between the foetus and the placenta throughout gestation.

At GD90, a decrease in *HPSE* expression was observed in endometrial samples associated with the lightest foetuses compared to the CTMLW foetuses. This difference was also observed in the placenta, although it was not statistically significant. Due to the role of HPSE in remodelling of the feto-maternal interface in late gestation, it could be hypothesised that this decrease in expression is due to the HS in the ECM being degraded in the preceding period to allow remodelling of the CAM. This in turn, would allow an increased surface area for exchange with the mother. Vallet and Freking, (2007) previously investigated the remodelling of the CAM, or folded bilayer, throughout gestation in the pig. In this experiment, it was demonstrated that the width of the bilayer was increased significantly at GD65, 85 and 105 in

placentas supplying the smallest foetuses in the litter compared to the largest. They also demonstrated that the stroma above the CAM decreased in size at a faster rate in the placentas supplying the smallest foetuses compared to the largest foetuses. Considering this, it is thought that to compensate for having smaller placentas, the width of the bilayers of placentas supplying small foetuses increase at a faster rate to form larger folds, thereby providing a larger area for nutrient transfer and improving the efficiency of the placenta to attempt to rescue the phenotype. The results of this chapter may reinforce these observations as at GD60, the placental CAM may have an increased density of endothelial cells in the smaller area of CAM available due to the placenta having initiated the second wave of angiogenesis. If the folds were beginning to increase in width, the density of endothelial cells would decrease, therefore by GD90 the percentage staining is decreased in the placentas supplying the small foetuses compared to the CTMLW foetuses. To test this theory, whole uterine samples should be taken at GD of interest and the width of the bilayer, percentage CD31 staining and area of the stroma above the bilayer should be measured. Additionally, as laser microdissection technology continues to improve, it may eventually be possible to perform RNASeq on angiogenic candidates of interest in the CAM specifically and isolate endothelial cells specifically from the CAM region to investigate their angiogenic potential. A more feasible alternative would be to isolate cell types of interest (trophoblast, LE, GE) and perform RNASeq on them.

ACP5 expression was increased in placentas supplying the lightest foetuses compared to those supplying the CTMLW foetuses at GD60 however, no associations between foetal size and endometrial *ACP5* expression were observed. As described in 7.1.1, it is known that in response to P4, the GE secrete ACP5, which is transported across the placenta and enters the feto–placental circulation (Renegar *et al.*, 1982). Therefore, as no association between foetal size and *ACP5* expression was observed in the endometrium, this may indicate that the placental transport of ACP5 is increased in placentas supplying the lightest foetuses compared to the CTMLW foetuses at GD60. This would be hypothesised to increase iron transport to the foetus. As the

transport of iron from the uterine GE in late gestation is not thought to be through ACP5, investigation into the alternative methods may reveal related pathways which should be investigated in relation to foetal size at GD90. One potential alternative method is thought to be transferrin.

Chen *et al.*, (2015) demonstrated that at GD60, 90 and 110, HIF1A protein expression was increased, whilst VEGFA expression was decreased in placentas supplying IUGR foetuses compared to normal sized foetuses. In this chapter, *HIF1A* expression was increased in endometrial samples supplying the lightest foetuses compared to CTMLW foetuses at GD45. However, at GD60 the direction of this difference was switched. *VEGFA* expression was decreased at GD90 in the endometrium (statistically significant) and placenta (not statistically significant). There are several potential reasons for the observed differences. Whilst at the time of performing the experiments in this thesis, there was only 1 sequenced transcript for HIF1A in the pig, there may be splice variants of HIF1A in the pig which are not yet known. Similarly, when performing these types of experiments, it is important to remember that the mRNA expression levels do not necessarily translate to the observed protein levels (Maier *et al.*, 2009; Koussounadis *et al.*, 2015). Attempts were made to validate the *VEGFA* and *HIF1A* results on a protein level however the antibodies available in the laboratory for these proteins were not successfully validated. Chen *et al.*, (2015) did not provide information regarding litter size, ovulation rate or prenatal survival. However, the values provided for mean foetal weight in the IUGR and normal weight classifications are considerably heavier than observed in our litters at the same GD, which may indicate the litters produced were smaller, therefore allowing more space for foetal growth.

In both tissues, switches were observed in gene expression between the feto-placental units of the lightest foetuses compared with the CTMLW foetuses between GD45 and 60. This may indicate that the tissues associated with small foetuses are attempting to rescue foetal growth by transcriptionally altering the expression of candidate genes important in regulating placental and foetal development. *eNOS* expression has previously been shown to be increased in IUGR placentas at GD50 compared to control placentas (Blomberg *et al.*,

2010), providing further evidence for the potential presence of a mechanism in placentas supplying small foetuses to compensate for having a disadvantaged blood supply. The switches observed at different stages of gestation highlight the dynamic nature of the interaction between the foetus and the feto-maternal interface and reinforce that to fully understand the mechanisms governing foetal growth, multiple GDs and tissues need to be investigated.

7.6.3 Foetal Sex was Associated with Alterations in Vascularity and mRNA Expression at the Feto-Maternal Interface

Whilst recent literature indicates that there is sexual dimorphism in placental development and the placental response to stress, this area remains poorly understood in the pig. However, the experiments detailed in this chapter did not find any significant association between foetal sex and the placental histological and mRNA expression results.

The data presented in this chapter suggest that foetal sex may influence the endometrial transcriptome to a greater degree than that of the placenta. Associations between foetal sex and endometrial, but not placental, gene expression were observed early in gestation (GD30). Based on these findings, it could be hypothesised that male and female conceptuses communicate differently with the endometrium in the pre-implantation period, when the conceptuses are migrating around the uterus, and at the point of implantation itself (discussed further in general discussion).

7.7 Conclusion

The experiments detailed in this chapter have highlighted novel and intriguing findings that foetal size and sex influence vascularity and mRNA expression of candidate genes which are associated with QTL linked to prenatal survival and litter size and/or have a central role in angiogenesis and foetal development at the feto-maternal interface. Currently, this is the first suggestion in the literature that foetal sex may have a strong influence on the activity of the porcine

endometrium. Switches were observed throughout gestation, notably between GD45 and 60, suggesting this is a key period of change at the feto-maternal interface supplying foetuses of different size and sex.

For future work investigating this area, it will be essential to investigate both tissues and multiple stages of pregnancy to get the full picture of how foetuses of different size and sex interact with the placenta and endometrium. Whilst these results have provided interesting preliminary data in this field, investigation into additional candidates on both an mRNA and protein level, as well as the use of *in vitro* and *in vivo* angiogenic assays would vastly improve our understanding of the mechanisms governing angiogenesis, foetal and placental development.

Tissue	Gestational Day				
	18	30	45	60	90
Placenta	n/a	ns	*CD31*	*ACP5* *CD31* CD31 CAM Staining	*HIF1A* CD31 CAM Staining
Endometrium	ns	ns	*HIF1A*	*HIF1A* Total and Mean BV Number *CD31*	*HPSE* *VEGFA* Mean Number of Uterine Glands

Table 7.8: Summary of Results which showed statistically significant effects of foetal size.

Green=Increased; Red=Decreased in samples associated with the lightest foetuses compared to their Closest to Mean Litter Weight (CTMLW) littermates. Abbreviations: CD31=Platelet and Endothelial Cell Adhesion Molecule 1, ACP5=Uteroferrin, HIF1A=Hypoxia Inducible Factor 1 Alpha Subunit, HPSE=Heparanase, VEGFA=Vascular Endothelial Growth Factor A, BV=Blood Vessel; CAM=Chorioallantoic Membrane, ns=not significant, n/a=not applicable.

Tissue	Gestational Day			
	30	45	60	90
Placenta	ns	ns	ns	*HIF1A*
Endometrium	*CD31* *PTGFR* *VEGFA*	Total Number of Uterine Glands Total and Mean Number of BV *HPSE*	*ACP5* *CD31* *VEGFA* *HIF1A*	*HIF1A*

Table 7.9: Summary of Results which showed statistically significant effects of foetal sex.

Green=Increased; Red=Decreased in samples associated with the male foetuses compared to their female littermates. Abbreviations: CD31= Platelet and Endothelial Cell Adhesion Molecule 1, ACP5=Uteroferrin, VEGFA=Vascular Endothelial Growth Factor A, PTGFR=Prostaglandin F2α Receptor, BV=Blood Vessel, ns=not significant, n/a=not applicable.

8 *In Vitro* Assessment of Angiogenic Potential

8.1 Introduction

In Chapter 7, placental and endometrial vascularity were investigated using qPCR to measure mRNA expression of candidate genes, and immunohistochemistry for the endothelial cell marker Platelet and Endothelial Cell Adhesion Molecule 1 (CD31). These experiments highlighted some interesting temporal changes and associations between foetal size and sex, and placental and endometrial vascularity. Whilst these differences are novel and interesting, it would be beneficial to attempt to investigate the results further to place them in a more biological context. Several *in vitro* and *in vivo* techniques have been developed to assess the angiogenic potential of cells, molecules and tissue samples. Some examples of commonly used validated angiogenic assays are described in detail below, with advantages and disadvantages of these techniques summarised in Table 8.1.

8.1.1 Matrigel Plug Assay

Matrigel is composed of extracellular matrix (ECM) components and growth factors, and solidifies following injection into a mouse. In this assay, the test substance is mixed with Matrigel and injected subcutaneously into the ventral region of a mouse where it solidifies, forming the “Matrigel plug”. The Matrigel is left in the mouse for 1 to 3 weeks, after which the plug and surrounding granulation tissue is removed, and the vascularity of the plug can be assessed. Angiogenesis in the plug can be quantified by paraffin embedding the Matrigel plugs and performing immunohistochemical staining for CD31 or vascular endothelial growth factor (VEGF) (Al-Khaldi *et al.*, 2003) or staining sections with Masson’s Trichrome (Al-Khaldi *et al.*, 2003; Malinda, 2009). Alternatively, the haemoglobin content in the plug can be quantified using the Drabkin method (Johns *et al.*, 1996; Kim *et al.*, 2000; Lee *et al.*, 2005). The Matrigel plug assay is commonly used to test if a substance stimulates or inhibits angiogenesis. However, despite it being relatively simple to set up, it is expensive to run and may be considered to have more ethical concerns, due

to the invasive nature of the assay in live animals, than some of the alternative methods discussed in this chapter.

8.1.2 Corneal Angiogenesis Assay

This method has been used in rats, mice and rabbits and operates on the principle that the cornea is an avascular tissue composed of fine parallel collagen fibres embedded in ECM (Norrby, 2006). To perform this assay, micropockets are created in the cornea and the test substance is injected into the pocket in a slow-release polymer or polyvinyl sponge. Multiple micropockets can be created within the same cornea to allow within animal replicates to be performed. Monitoring of angiogenesis is usually performed daily, allowing multiple measurements within the same animal, and can be recorded non-invasively (Conrad *et al.*, 1994), or by intra-venous injection with a high-molecular weight FITC-labelled dextran (Cole *et al.*, 2010).

8.1.3 Rat Aortic Ring Model

This method is based on the principle that rat aortic rings can be embedded in gels composed of collagen, fibrin or basement membrane and produce new vessels *in vitro* (West and Burbridge, 2009). The aortic cultures have a mixed population of cells including endothelial cells, fibroblasts, pericytes and macrophages. This is a major advantage of the model over other assays as it gives a complete overview of the processes involved in angiogenesis including cell proliferation, migration, tube formation and perivascular recruitment, over a physiologically comparable timescale (Baker *et al.*, 2012) (Table 8.1).

Nicosia, (2009) and West and Burbridge, (2009) review the protocol in detail. In brief, the aorta is dissected from the rat and flushed to remove any remaining blood. The aorta is cut into rings and embedded in a three-dimensional matrix (e.g. collagen) which can be cultured with media containing test substances. Endothelial cells from the rat aortic rings begin to sprout from the explants approximately 2–3 days into the culture period. This process is initiated by

producing cut edges on the explants while setting up the assay and the aorta produces growth factors which allow its maintenance in culture (Villaschi and Nicosia, 1993; Nicosia *et al.*, 1997). The growth of the vessels continues, and the newly formed vessels begin to form lumen (Nicosia *et al.*, 2012; De Rossi *et al.*, 2013). The new vessels are surrounded by pericytes, which interact with the endothelial cells, migrating and proliferating along them. The cultures can be maintained for approximately 2 weeks before the gel begins to degrade, allowing long-term investigation.

Since the original development of the technique (Nicosia and Ottinetti, 1990), the protocol has been modified to allow analysis of the angiogenic abilities of different tissues and vessels. From a reproductive perspective, human placental vein discs (Jung *et al.*, 2001) and human amnion discs (Niknejad *et al.*, 2013, 2014) have been successfully analysed using this method.

8.1.4 Chick Chorioallantoic Membrane (CAM) assays

The developing chick embryo is an easily accessible model for the study of embryonic development (Stern, 2005). Within the incubating fertile egg, there is a large, non-innervated, highly vascular and easily accessible extraembryonic chorioallantoic membrane (CAM; Ribatti *et al.*, 2001). The capillaries of the CAM undergo extensive proliferation until incubation day 8, following which they continue to grow until incubation day 11 (Ausprunk *et al.*, 1974), after which the rate of proliferation decreases significantly. During this period, the inflammatory system is relatively immature (Leene *et al.*, 1973), which minimises the risk of graft rejection.

In the chick chorioallantoic membrane assay, fertile chicken eggs are incubated at 37ºC under constant humidity. On incubation day 3 (approximately stage 20 (Hamburger and Hamilton, 1951)), 2-3ml albumen is aspirated from the egg and a small window is cut into the shell to reveal the underlying developing embryo and CAM. This is sealed with Sellotape and incubated until the desired stage to set up the assay. The developmental stage when the graft is performed varies between studies but frequently is around

incubation day 8, due to the development of the vasculature detailed above (Ribatti *et al.*, 2006; Ribatti, 2015; Esteves *et al.*, 2017). At this stage, the piece of tissue or cells are grafted onto the chorioallantoic membrane, usually at a branching point, and the egg is resealed with Sellotape. The eggs are incubated for between 24 and 72 hours, and imaging is performed to allow quantification of the influence of the graft on angiogenesis.

This assay is an established experimental system for tumour angiogenesis research and investigation into angiogenic properties of compounds (reviewed by Ribatti, (2010, 2016)). In addition to this, it can be used to investigate angiogenesis in tissue grafts. From a mammalian reproductive perspective, the chick CAM assay has been utilised to investigate bovine *corpus luteal* (Redmer *et al.*, 1988) and the endometrial caruncular and cotyledonary angiogenesis (Reynolds and Ferrell, 1987) with some success. Reynolds and Ferrell, (1987) reported that the caruncular region promoted angiogenesis, whereas the cotyledon did not induce angiogenesis in this model. Reynolds and Redmer, (1988) furthered this work by assessing the proliferative ability of conditioned media from the caruncle and cotyledon and observed similar results, indicating that the caruncle region is the main source of placental angiogenic activity in the cow. The human endometrium (Peek *et al.*, 1995; Maas *et al.*, 1999) and placenta (Stallmach *et al.*, 2001) have been investigated using this method. Although this method is quick and inexpensive to perform, it is highly labour intensive, and many replicates and controls are required to account for the between egg variation (Table 8.1).

8.1.5 *In vitro* tube formation assay (Matrigel Branching Assay)

To investigate the ability of human endothelial cells to make vessel-like structures *in vitro*, a tube formation assay was devised which used collagen gel coated 24 well plates (Kubota *et al.*, 1988). This method has continued to be optimised over the past 30 years for use with a wide range of primary and immortalised cell lines to investigate the angiogenic potential of substances and cells, and to improve the understanding of cell-cell organization *in vitro*

(Arnaoutova *et al.*, 2009, 2012; Arnaoutova and Kleinman, 2010; DeCicco-Skinner *et al.*, 2014; Guo *et al.*, 2014). This method operates on the principle that in culture, endothelial cells form cobble-stone like patterns and maintain their ability to proliferate, synthesise protein and migrate towards pro- but not anti-angiogenic stimuli (Arnaoutova *et al.*, 2009; Arnaoutova and Kleinman, 2010). When added to a basement membrane, endothelial cells will form vessel-like structures *in vitro*, with a visible 'lumen'.

Several basement membrane gels are commercially available, and generally contain high concentrations of collagen-IV, proteoglycans and laminin-1. Depending on the requirements of the assay, the basement membrane can contain growth factors or be growth factor reduced, as was the case in the experiment described in this chapter, with both approaches allow the development of vessel-like structures when performing the assay (Xie *et al.*, 2016). This method has a few advantages over the detailed methods above (Table 8.1) and has previously been utilised with porcine endothelial cells (Chrusciel *et al.*, 2011; Marquez-Curtis *et al.*, 2017).

8.1.6 Deciding the Appropriate Assay to Use

To further the knowledge of the association between foetal size, sex, and placental and endometrial angiogenesis, an angiogenic assay needed to be performed. The information detailed in the introduction was used, in combination with optimising the use of the available samples and resources, to determine which assay was appropriate to use. It was decided that the Matrigel branching assay would be utilised.

Method	Advantages	Disadvantages
Matrigel Plug Assay	Easy to perform, can get quantifiable data in the form of haemoglobin measurements or vessel quantification, suitable for large-scale experiments.	Expensive assay due to the use of live animals, not suitable for tissue or tumour grafts.
Corneal Angiogenesis Assay	Easy to identify and quantify vessel formation, can be used in rabbits, rats, or mice, can monitor long-term non-invasively.	Expensive assay due to the use of live animals, not easy to upscale, introduction of the substance to a tissue which does not normally undergo angiogenesis, very invasive to the animal, technically challenging, non-specific inflammatory responses can be observed.
Rat Aortic Ring Assay	Easy to identify and quantify vessel formation, can be used in rats or mice, can investigate over a 2-week period, closely related to *in vivo* angiogenesis as have a mixed population of cells	Lack of blood flow, variation between rats, technical.
Chick Chorioallantoic Membrane Assay	Quick, inexpensive, easy to perform, can monitor non-invasively, can perform on a large scale.	Highly variable results obtained therefore large numbers required, labour intensive, difficult to monitor vessel formation, non-specific inflammatory responses can be observed, time restrictions due to embryo development.
Tube Formation Assays	Quick, reliable, reproducible, easy to perform, can be up scaled to perform large analyses, flexible use.	Basement membranes can be expensive, if using primary cells must be performed at a low passage number, lack of blood flow.

Table 8.1: Summary of Advantages and Disadvantages of Commonly Used Angiogenesis Assays.

8.2 Hypotheses

Based on the results presented in previous chapters, it was hypothesised that conditioned media from placental and endometrial samples supplying the lightest foetus and male foetuses will have impaired *in vitro* branching ability compared to those supplying closest to mean litter weight (CTMLW) and female foetuses respectively.

8.3 Aims

The aims of the research described in this chapter were:

i. To investigate the influence of placental and endometrial conditioned media from Gestational Day (GD) 45 and 60 on endothelial cell branching.
ii. To investigate the influence of foetal size on endothelial cell branching at GD45 and 60 in response to placental and endometrial conditioned media.
iii. To investigate the influence of foetal sex on endothelial cell branching at GD60 in response to placental and endometrial conditioned media.

8.4 Materials and Methods

8.4.1 Media Used

The compositions of the media used are described in the general materials and methods.

8.4.2 Generation of Conditioned Medium from Placental and Endometrial Samples

To allow the assessment of the angiogenic potential of placental and endometrial samples, conditioned media was generated from the feto-placental units of interest. Following dissection of the uterus, the remainder of the whole uterus was placed in a jar containing sterile phosphate buffered

saline (PBS) with Penicillin-Streptomycin (PenStrep) for transport to the laboratory. Following this, the uterus was removed, and the placenta and endometrium were dissected from the underlying myometrium (Figure 8.1). To cut equally sized pieces of tissue, a 17mm corer was used and a minimum of 4 pieces of tissue were weighed to ensure that the cutting of the tissue was consistent. The tissue was placed in a 6 well plate (NUNC, ThermoFisher Scientific) containing 8ml of medium (DMEM-F12 + 10% NBCS + PenStrep). The pieces of tissue were cultured for 2, 8, 18 or 24 hours, at which point the medium was removed and stored at -80^{o}C until required.

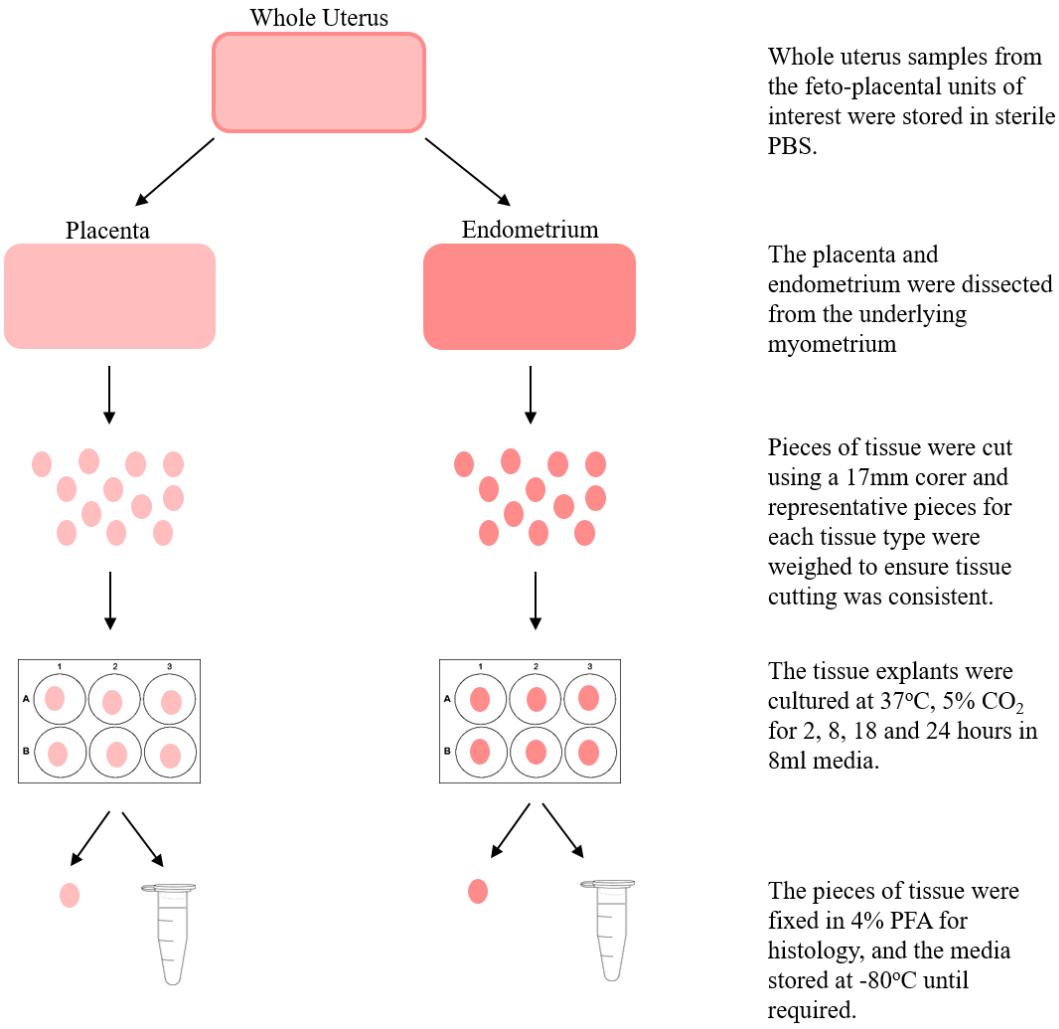

Figure 8.1: Workflow for the Generation of Conditioned Media.

Whole uterus samples were taken from the anti-mesometrial side of the feto-placental units of interest at the time of dissection. They were placed in sterile PBS and transported back to the lab. The placenta and endometrium were dissected from the underlying myometrium. The tissue was cut into equally sized pieces using a 17mm corer and cultured at 37ºC with 5% CO2 for 2, 8, 18 or 24 hours in 8ml of medium. At the end of the culture, the tissue pieces were fixed in 4% paraformaldehyde (PFA), processed and embedded for histology and the conditioned media was frozen and stored at -80ºC until required.

8.4.3 Tissue Processing, Embedding, Ki67 Staining

The cultured tissue explants were removed from the 6 well plates at the end of the culture period and fixed overnight at 4°C in 4% paraformaldehyde (PFA) (2.3.5.1). Following this, the samples were processed, embedded and sectioned (2.3.1. and 2.3.2.).

To ensure that the cultured samples were proliferating, the samples from the 18 hour time point were stained for the proliferation marker Ki67 (1:200 dilution; ab15580; Abcam, Cambridge, U.K.) using the Vectastain Elite ABC Kit, as described in (2.3.3). The slides were imaged using the NanoZoomer slide scanner (Hamamatsu, Welwyn Garden City, U.K.).

8.4.4 Culture and Validation of G-1410 Immortalised Endothelial Cell Line

Dr Aneta Andronowska (Institute of Animal Reproduction and Food Research, Polish Academy of Science, Olsztyn, Poland) kindly provided cells from the G-1410 immortalised cell line. The generation of this cell line using the Simian virus 40 T-antigen (SV40 T-ag), to overcome the problem of premature senescence associated with primary cells, is described in detail by Chrusciel *et al.*, (2011).

To ensure that the immortalised endothelial cells provided expressed markers of endothelial cells on both a protein and mRNA level, immunocytochemistry and PCR using cDNA isolated from the cells was performed. Immunocytochemistry was performed (2.3.5) or CD31 (1:20 dilution; ab28364, Abcam) and von Willebrand factor (vWF) (1:400 dilution; ab6994, Abcam), using the fluorescent secondary antibody Alexa Fluor® 488 goat anti-rabbit (H+L) (1:1000 dilution for both; ThermoFisher Scientific). RNA was extracted from the endothelial cells (2.2.4), cDNA synthesised (2.2.7) and PCR was performed (2.1.3), for the endothelial cell markers *CD31*, two isoforms of *VEGF-A* (*VEGF-120* and *VEGF-164*) and *VEGF-R1* (primer sequences detailed in Table 8.2). The products underwent electrophoresis on a TAE gel (2.1.4).

Gene Symbol	Primer Sequence (5'→ 3')		Amplicon Size (bp)	Accession Number	Source
B2M1	F	CAAGATAGTTAAGTGGGATCGAGAC	161	DQ845172	Nygard *et al.*, (2007)
	R	TGGTAACATCAATACGATTTCTGA			
CD31	F	CCGAGGTCTGGGAACAAAGG	98	NM213907.1	n/a
	R	AGCCTTCCGTTCTAGAATATCTGTT			
VEGF-120	F	AAGGCCAGCACATAGGAGAG	101	XM013977975.1	Chrusciel *et al.*, (2011)
	R	CCTCGGCTTGTCACATTTTT			
VEGF-164	F	GAGGCAAGAAAATCCCTGTG	150	NM214084.1	Chrusciel *et al.*, (2011)
	R	TCACATCTGCAAGTACGTTCG			
VEGF-R1	F	CACCCCGGAAATCTATCAGATC	180	XM021065524.1	Chrusciel *et al.*, (2011)
	R	GAGTACGTGAAGCCGCTGTTG			

Table 8.2: Primer Sequences Used for Amplification of Endothelial Cell cDNA by PCR.

This table summarises the gene abbreviation and name, primer sequences, amplicon size, accession number and the source where the primer sequence tested were obtained from. Abbreviations: *B2M1*=Beta-2-microglobulin; *CD31*=Platelet and Endothelial Cell Adhesion Molecule 1; *VEGF* =Vascular Endothelial Growth Factor; *VEGFR-1* = VEGF Receptor 1; n/a=not applicable; F=forward primer; R=reverse primer; bp=base pairs.

8.4.5 Matrigel Branching Assay

Approximately 18 hours before the assay was performed, T75 flasks (Eppendorf) at ~80% confluency were serum starved (M199 + PenStrep). The bottom of wells of a 24 well tissue culture plate (Eppendorf) were coated with 300µl Growth Factor Reduced Matrigel Basement Membrane (Corning, Wiesbaden, Germany), which had been thawed overnight at 4^{o}C. This step was performed on wet ice in a sterile tissue culture hood using chilled pipette tips and plates to prevent the Matrigel prematurely solidifying. The plate was incubated at 37°C and 5% CO_2 for a minimum of 30 minutes to solidify the Matrigel.

The serum starved endothelial cells were washed with PBS without calcium and magnesium (Life Technologies, ThermoFisher Scientific). TryPLE (Life Technologies, ThermoFisher Scientific) (10ml) was added to the flask for 6 minutes, with gentle agitation, to dissociate the cells from the flask. After the incubation, 10ml of medium (DMEM-F12 + 10% NBCS + PenStrep) was added to the flask. The solution was transferred to a 50ml falcon tube and centrifuged for 5 minutes at 400g at room temperature (Sorvall RT7, ThermoFisher Scientific). The waste medium was discarded, and the cell pellet was resuspended in 1ml of branching assay medium (DMEM-F12 + 10% NBCS + PenStrep). A cell count was performed in duplicate and the mean number of cells was taken. The cells were centrifuged again, and the pellet resuspended in the desired volume of medium which would allow 50,000 cells to be added to the well in a 10µl volume.

Due to the observed differences detailed in Chapter 7, it was decided to focus on conditioned media samples from GD45 and 60. At both GD, the lightest foetus, and the CTMLW foetus of the same sex were used. Due to limitations in sample availability, samples were used from three GD45 litters, only focussing on female samples. At GD60, 6 litters were used for the experiment, making comparisons of males in 3 litters and females in the remaining 3 litters. Conditioned media collected at the 18 hour time point was used for the Matrigel branching assay, as the tissue was shown to be still proliferating at this point

(Figure 8.3) and the placental media promoted endothelial cell branching effectively in the initial trials.

The conditioned media was thawed immediately prior to use and prepared by mixing 200µl of the conditioned media with 100µl of branching assay media (DMEM-F12 + 10% NBCS + PenStrep). To this, the 10µl cell suspension (50,000 cells) was added and the cells were gently mixed by pipetting. The cells were added to the wells of interest, with each sample being analysed in duplicate. In addition to the conditioned media of interest, a medium only control (300µl DMEM-F12 + 10% NBCS + PenStrep) and a positive control (300µl DMEM-F12 + 10% NBCS + PenStrep containing Recombinant Human EG-VEGF (20ng/ml) (Peprotech, Rocky Hill, New Jersey, U.S.A.) were set up in duplicate. The cells were allowed to adhere to the plate for approximately 30 minutes prior to setting up the imaging.

The Zeiss Live Cell Observer system (AxioObserver Z1, Zeiss, Cambridge, U.K.) was used to image the cells at 37^{o}C with 5% CO_2. Within each well, 6 different positions around the centre of the well set up. The wells were imaged at x5 magnification every 10 minutes from approximately 90 minutes post seeding for 10 hours.

Images taken at 2 hours, for every hour until 10 hours post-seeding were used for analysis. The images were exported from Zen Blue (Zeiss) and analysed using AngioTool (Zudaire *et al.*, 2011). AngioTool computes several morphological and spatial parameters including the explant area, vessel area, vessels as a percentage of area, number of junctions (branching points), junction density, average vessel length, total vessel length, the number of end points and the lacunarity (which describes the distribution of the gaps).

8.4.6 Statistical Analysis

Statistical analyses were performed following the general protocol outlined in 2.5. In brief, for each placental and endometrial sample, there were 6 images taken per well at each time point of interest. As the experiment was performed

in duplicate, the mean value for each parameter was calculated per well, and then the mean value of the two wells was calculated. For each parameter for each sample, the value obtained was divided by the value of the medium only control to account for any angiogenic effects observed due to the medium itself.

The normality of the data was assessed, and transformations performed as required (Table 8.3) to improve the normality of the data distribution. Statistical analyses to assess the influence of GD, size (GD45 and 60) and sex (GD60 only) were performed as outlined in 2.5. This was performed using the data from the nine time points combined and within time point.

Placenta	Normality of Data		
Parameter	**Both GD Combined**	**GD45**	**GD60**
Explant area	Not Normal	Not Normal	Not Normal
Vessel area	Not Normal	Normal	Not Normal
Vessels as a percentage of area	Not Normal	Normal	Not Normal
Total number of junctions	Normal	Normal	Normal
Junction density	Normal	Normal	Normal
Total vessel length	Not Normal	Normal	Not Normal
Average vessel length	Not Normal	Normal with Log10 Transformation	Not Normal
Total number of end points	Not Normal	Normal	Not Normal
Lacunarity	Normal	Normal	Normal
Endometrium	**Normality of Data**		
Parameter	**Both GD Combined**	**GD45**	**GD60**
Explant area	Not Normal	Not Normal	Not Normal
Vessel area	Not Normal	Not Normal	Not Normal
Vessels as a percentage of area	Not Normal	Not Normal	Not Normal
Total number of junctions	Not Normal	Log10	Not Normal
Junction density	Not Normal	Log10	Not Normal
Total vessel length	Not Normal	Not Normal	Not Normal
Average vessel length	Not Normal	Not Normal	Not Normal
Total number of end points	Not Normal	Normal	Not Normal
Lacunarity	Normal	Normal	Normal

Table 8.3: Summary of Normality of the Matrigel Branching Assay Data.

Log10 transformations were carried out where appropriate, with the aim of improving the normality of the distribution of the data. GD=Gestational Day.

8.5 Results

8.5.1 Placental and Endometrial Samples Proliferate Following 18 hours in Culture

Ki67 staining was observed in both placental (Figure 8.2) and endometrial (Figure 8.3) samples following 18 hours in culture, suggesting that both tissues were still proliferating.

8.5.2 G-1410 Immortalised Endothelial Cells express Endothelial Cell Markers

G-1410 immortalised endothelial cells retained their endothelial cell identity in culture, expressing CD31 and vWF at a protein level (Figure 8.4A) and *CD31*, two splice variants of *VEGF-A* (*VEGF-120* and *VEGF-164*) and *VEGF-R1* on an mRNA level (Figure 8.4B).

8.5.3 Matrigel Branching Assays can be used to investigate the Angiogenic Potential of Placental and Endometrial Samples

Conditioned media from placentas (Figure 8.5) and endometrial samples (Figure 8.6) supplying foetuses at both GD45 and 60 were used to investigate endothelial cell branching ability *in vitro*. Interestingly, when cultured with endometrial (Figure 8.6) conditioned media the cells appear to aggregate together more than when cultured with placental (Figure 8.5) conditioned media.

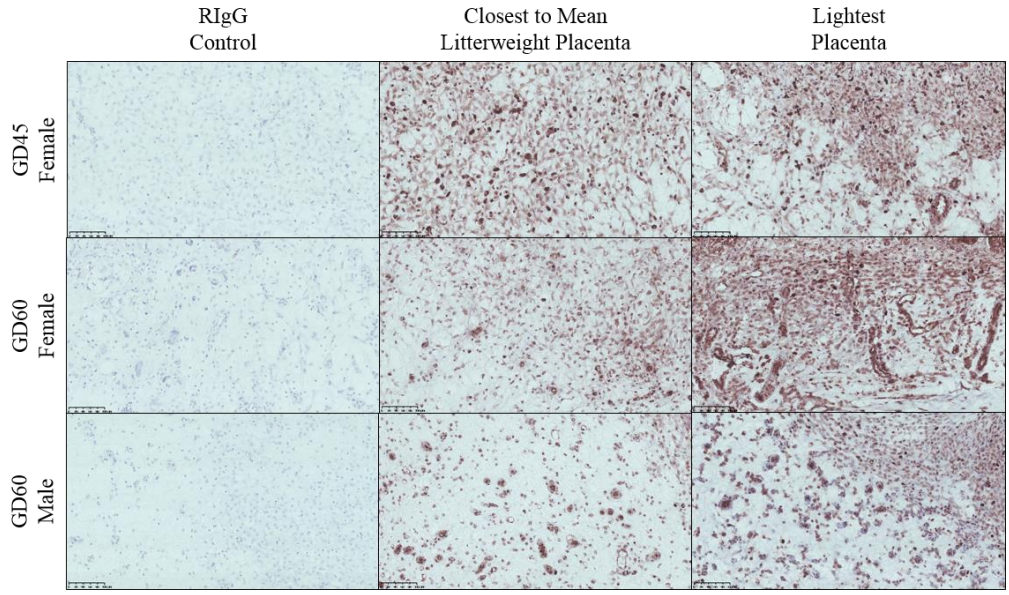

Figure 8.2: Cultured Placental Samples are Proliferating after 18 hours in Culture.

Representative placental samples cultured for 18 hours. Immunohistochemistry performed for rabbit immunoglobulin G (RIgG) (column 1) and the proliferation marker Ki67 (columns 2 and 3). Imaged using the NanoZoomer slide scanner (Hamamatsu). Scale bar represents 250μm.

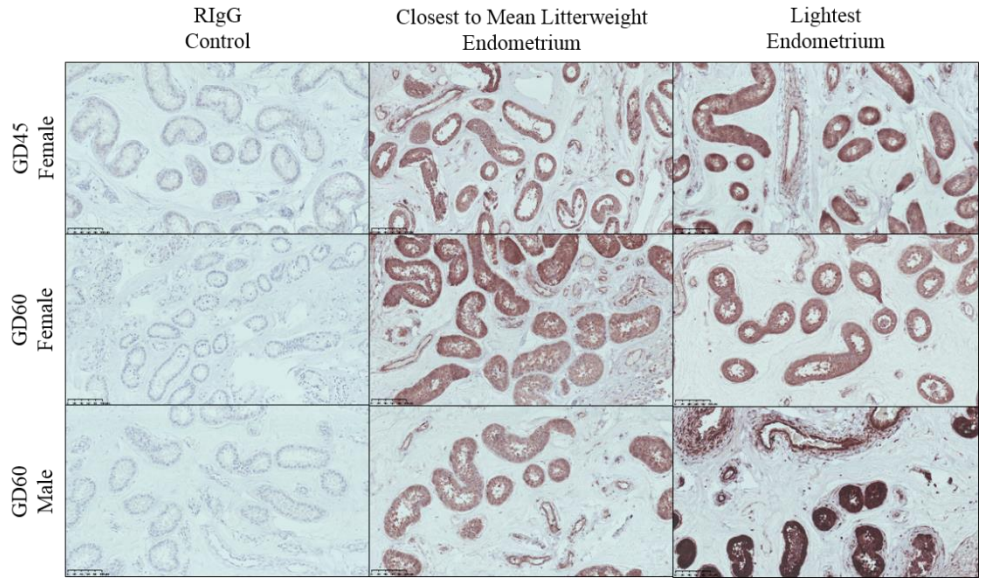

Figure 8.3: Cultured Endometrial Samples are still Proliferating after 18 hours in Culture.

Representative endometrial samples cultured for 18 hours. Immunohistochemistry performed for rabbit immunoglobulin G (RIgG) (column 1) and the proliferation marker Ki67 (columns 2 and 3). Imaged using the NanoZoomer slide scanner (Hamamatsu). Scale bar represents 250μm.

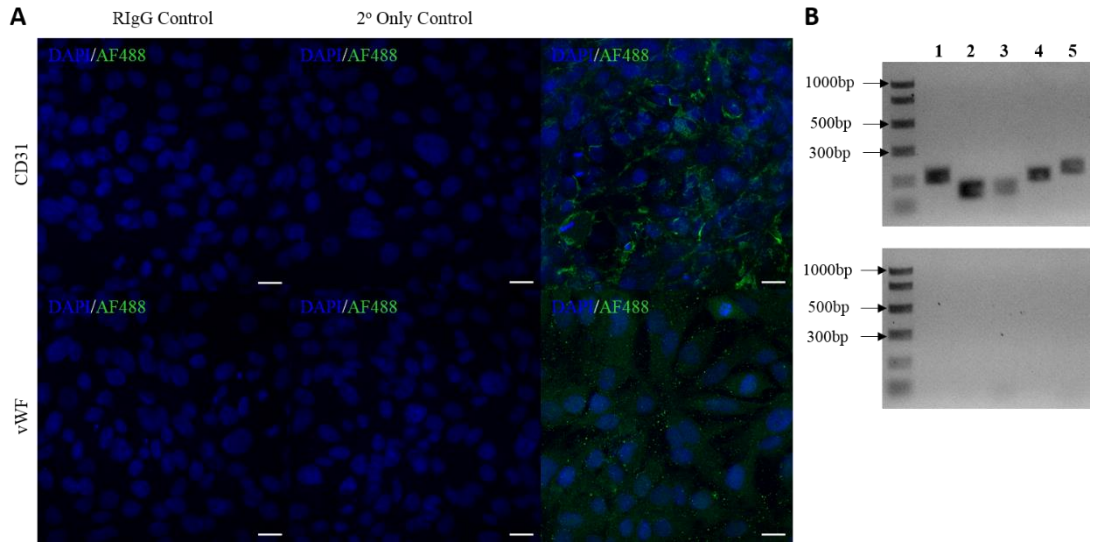

Figure 8.4: G-1410 Cells Express Endothelial Cell Markers.

A: Immunocytochemistry was performed for the endothelial cell markers CD31 and vWF. First column: Cells were stained with an equivocal protein concentration of RIgG to that of the primary antibody. Second column: cells were stained with only the secondary antibody. Third column: positive staining was observed for CD31 (top panel) and vWF (bottom panel). Scale bar represents 20µm. B: RNA was extracted from the endothelial cells and a PCR was performed for 1) *B2M1* (reference gene control) 2) *CD31*, two splice-variants of VEGFA 3) *VEGF-120* and 4) *VEGF-164*, and 5) *VEGF-R1*. Top panel: PCR with template cDNA. Bottom panel: PCR with NRT control. Electrophoresis performed using a TAE gel stained with SYBR Safe. PCR markers (Promega) used as ladder. Abbreviations: CD31 = Platelet and Endothelial Cell Adhesion Molecule 1; vWF = von Willebrand Factor; RIgG = Rabbit Immunoglobulin G; *B2M1* = Beta-2-microglobulin; *VEGFA* = Vascular Endothelial Growth Factor A; *VEGFR-1* = VEGF Receptor 1.

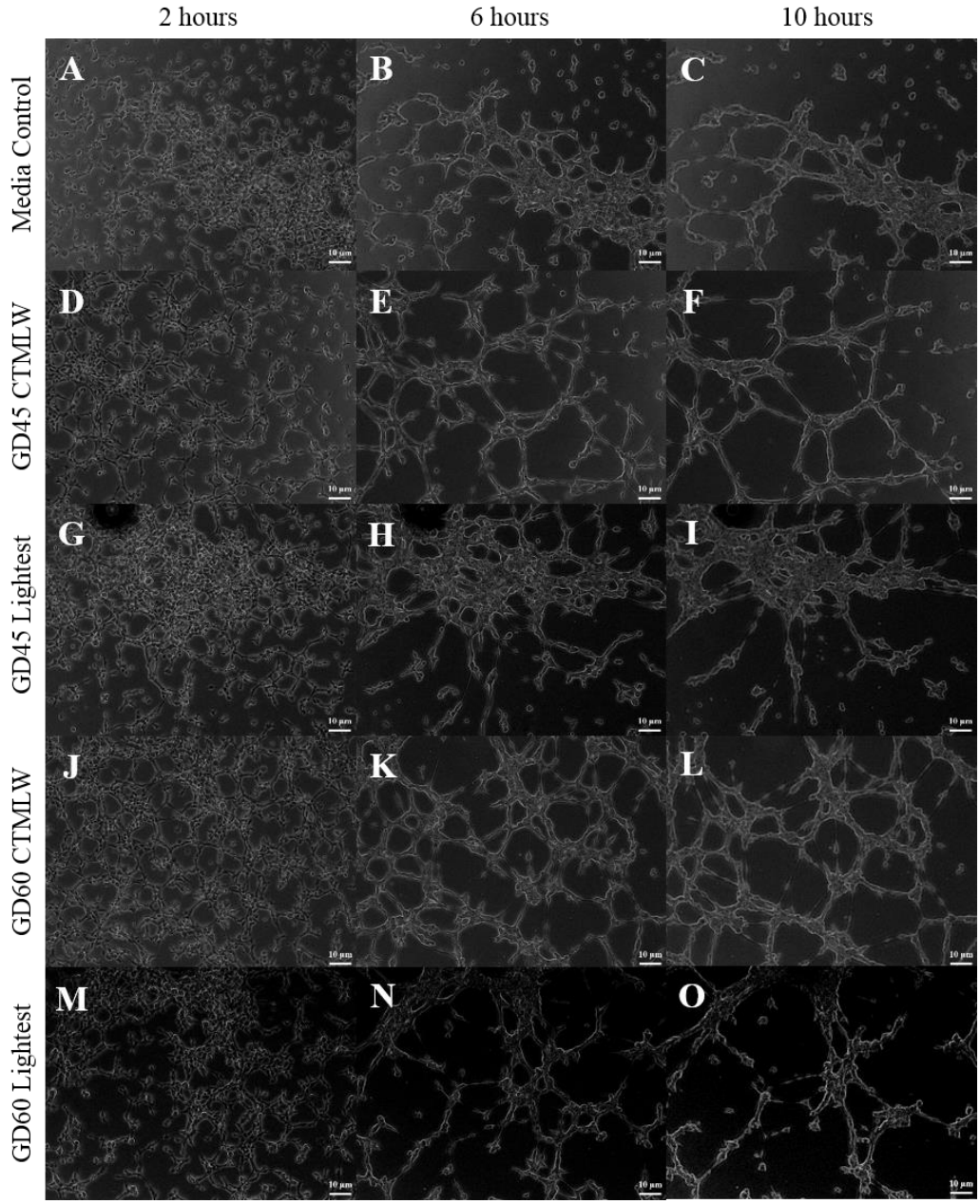

Figure 8.5: Matrigel Branching Assays were successfully used to Investigate Endothelial Cell Branching when cultured with Conditioned Media from Placental Samples.

A, B and C: Media only control. Cells treated with conditioned media from a placenta supplying the closest to mean litter weight foetus (CTMLW) (D, E and F) and lightest foetus (G H, and I) at gestational day (GD) 45. Cells treated with conditioned media from a placenta supplying the CTMLW (J, K and L) or lightest foetus (M, N and O) at GD60.All conditioned media collected after 18 hours of tissue explant culture. The CTMLW and lightest foetuses within GD were from the same litter. Scale bars represent 10μM. Representative images taken using the Zeiss AxioObserver Z1 at x5 magnification at 2, 6 and 10 hours post-seeding of the endothelial cells.

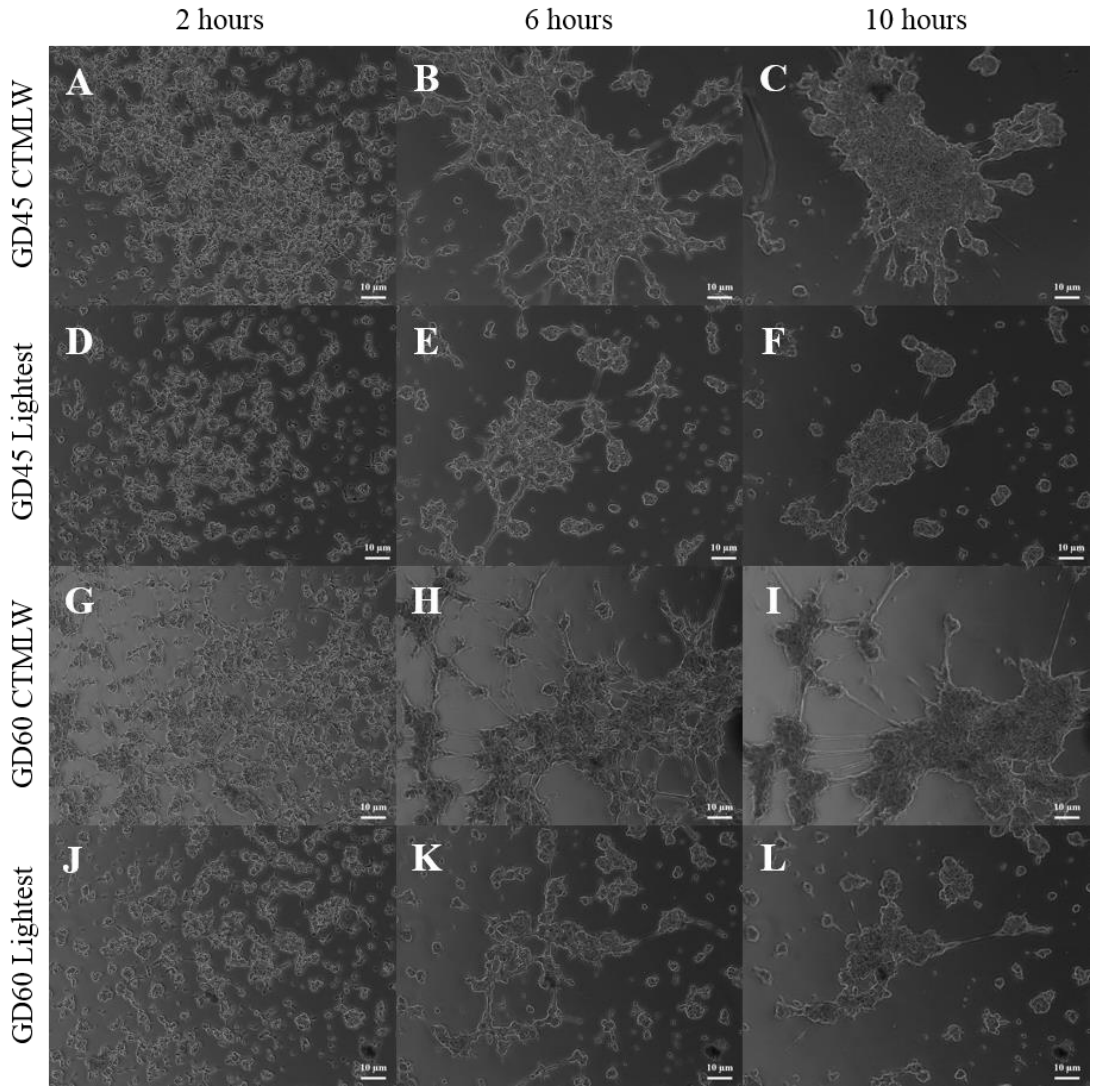

Figure 8.6: Matrigel Branching Assays were successfully used to Investigate Endothelial Cell Branching when cultured with Conditioned Media from Endometrial Samples.

Cells treated with conditioned media from endometrial tissue supplying the closest to mean litter weight (CTMLW) (A, B and C) and lightest (D, E and F) foetus at gestational day (GD) 45. Cells treated with conditioned media from endometrial tissue supplying the CTMLW (G, H and I) and lightest (J, K and L) foetus at GD60. All conditioned media collected after 18 hours of tissue explant culture. The CTMLW and lightest foetuses within GD were from the same litter. Scale bars represent 10μM. Representative images taken using the Zeiss AxioObserver Z1 at x5 magnification at 2, 6 and 10 hours post-seeding of the endothelial cells.

8.5.4 Matrigel Branching Assays can be used to investigate the Angiogenic Potential of Placental Samples

8.5.4.1 The GD of a Placental Sample Influences Endothelial Cell Branching *in vitro*

The results of chapter 7 highlighted large temporal changes in the expression of angiogenesis related genes throughout gestation, in both tissue types. Due to this, and Vonnahme *et al.*, (2001) describing a second wave of angiogenesis in the pig uterus around GD50, placental samples from GD45 and 60 were utilised for this experiment. Figure 8.7 illustrates the temporal changes in the nine parameters of interest over the course of the experiment (2-10 hours post-seeding).

No statistically significant differences in the response of the cells cultured with conditioned media from placentas at the two GD were observed in explant area (Figure 8.7A), total number of junctions (Figure 8.7D), junction density (Figure 8.7E), or total vessel length (Figure 8.7F). Interestingly, endothelial cells cultured with the GD45 conditioned media had an increased vessel area at 2, 3, 5 and 6 hours post-seeding ($P \leq 0.05$) compared to culture with conditioned media from GD60. This was observed when investigating the vessels as a percentage of the total area at 2-6 ($P \leq 0.05$) and 8 hours ($P = 0.08$) post-seeding. The average vessel length observed was increased throughout the culture period in response to the conditioned media from the GD45 placentas compared to the GD60 placentas ($P = 0.08$ at 2 hours, $P = 0.07$ at 3 hours, $P \leq 0.05$ at 5 and 6 hours, and $P \leq 0.01$ at 6-10 hours post-seeding). Between 2 and 7 hours post-seeding, an increase in the number of end points in response to the GD45 media was observed, which was statistically significant at 6 and 7 hours post-seeding ($P \leq 0.01$).

An overall statistically significant GD effect was observed when comparing the effect over the course of the experiment (ANOVA without Gilt Block $FPr \leq 0.001$; with Gilt Block $FPr \leq 0.01$; Figure 8.7I), with endothelial cells treated with the GD45 conditioned media having decreased lacunarity compared with those that had been treated with conditioned media from GD60 placentas. This was

statistically significant at 2-6 hours post-seeding (ANOVA with Gilt Block FPr≤0.01 at 2 and 5 hours, FPr≤0.05 at 3, 4 and 6 hours post-seeding).

Figure 8.7: The GD of Placental Samples Influences Endothelial Cell Branching *in vitro*.

Matrigel branching assays were performed where endothelial cells were cultured with conditioned media from porcine placentas at gestational day (GD) 45 and 60. Nine parameters of interest were investigated, from 2-10 hours post-seeding of the cells. The mean values for each GD are presented here relative to the media only control. A: No statistically significant differences in total explant area were observed between the two GD investigated. B: Vessel area was increased in response to the GD45 media compared to the GD60 media at 2, 3, 5 and 6 hours post-seeding. C: Vessels as a percentage of area was increased in response to the GD45 media compared to the GD60 media between 2-6 hours post-seeding, and this trend was also observed at 10 hours post-seeding (P=0.08). No statistically significant differences in response to the conditioned media from the two GD investigated were observed in total number of junctions (D), junction density (E) or total vessel length (F). G: Average vessel length was increased in response to the conditioned media from GD45 compared to the GD60 media throughout the experiment (trending towards significant at 2 (P=0.08) and 3 hours (P=0.07), statistically significant at 5-10 hours post-seeding). H: Total number of end points was increased in response to culture with GD45 media compared to the GD60 media between 2 and 7 hours post-seeding, which was statistically significant at 6 and 7 hours post-seeding. I: An overall GD effect in lacunarity was observed, with cells cultured with the GD45 media having decreased lacunarity compared to those cultured with the GD60 media. (ANOVA without Gilt Block FPr≤0.001; with Gilt Block FPr=0.01). This was statistically significant between 2 and 6 hours post-seeding. Error bars represent S.E.M. *FPr/P≤0.05. **FPr/P≤0.01.

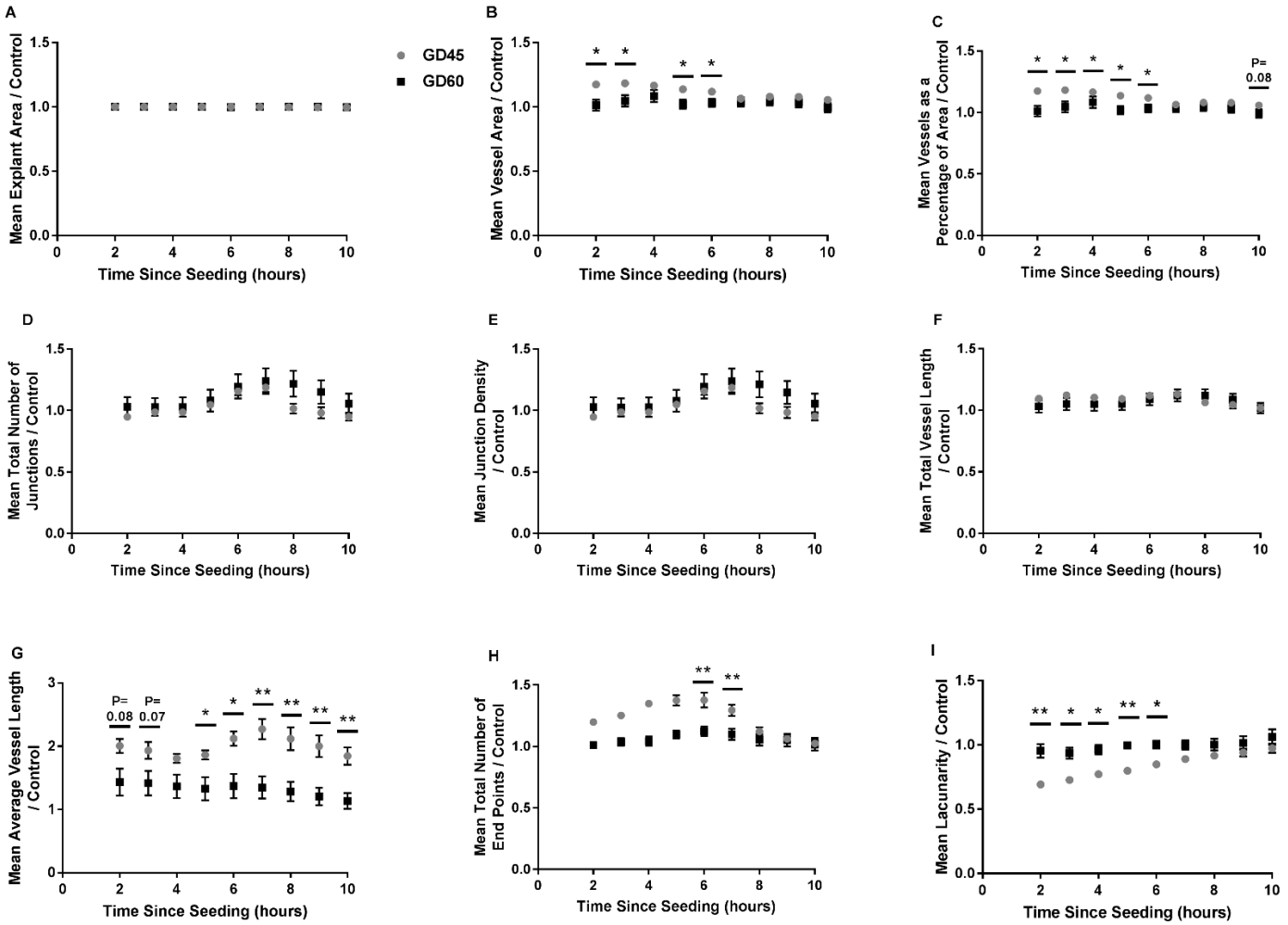

Figure 8.7: The GD of Placental Samples Influences Endothelial Cell Branching *in vitro*.

8.5.4.2 Foetal Size Influences Endothelial Cell Branching in Response to Placental Conditioned Media at GD45

To test the hypothesis that placentas supplying the lightest foetuses will have decreased ability to induce endothelial cell branching *in vitro* compared to placentas supplying the CTMLW foetuses, conditioned media was generated from these samples at GD45. Figure 8.8 illustrates the relationship between foetal size and changes in the nine parameters of interest over the course of the experiment (2-10 hours post-seeding).

Whilst no relationship between foetal size and explant area (Figure 8.8A) or total number of end points (Figure 8.8H) was observed, foetal size was associated with the remaining parameters investigated. An overall size effect was observed in vessel area (ANOVA without Gilt Block FPr=0.018; with Gilt Block FPr=0.007), with conditioned media from the lightest foetuses having a decreased vessel area compared to endothelial cells treated with media from the CTMLW foetuses (Figure 8.8B). This decrease was statistically significant at 3 and 4 hours post-seeding (ANOVA with Gilt Block FPr≤0.05). The same pattern was observed in vessels as a percentage of area (Figure 8.8C), with an overall size effect observed (ANOVA without Gilt Block FPr=0.019; with Gilt Block FPr=0.007), which was statistically significant at 3 and 4 hours post-seeding (ANOVA with Gilt Block FPr≤0.05). Culture with the conditioned media supplying the lightest foetuses compared to the CTMLW foetuses decreased the total number of junctions (Figure 8.8D) at 4 hours post-seeding (ANOVA with Gilt Block FPr≤0.05). This also resulted in a decrease in the density of the junctions (Figure 8.8E) at 3 and 4 hours post-seeding (ANOVA with Gilt Block FPr≤0.05).

When investigating the influence of foetal size on the length of the vessels produced, an overall decrease was observed in both total vessel length (Figure 8.8F; ANOVA without Gilt Block FPr=0.02; with Gilt Block FPr=0.004) and average vessel length (Figure 8.8G with and without Gilt Block FPr≤0.001) in response to culture with conditioned media from the lightest foetuses compared to the CTMLW foetuses. This decrease in vessel length was statistically significant in total vessel length at 3 (ANOVA with Gilt Block

FPr≤0.05) and 4 hours (ANOVA with Gilt Block FPr≤0.01), and average vessel length at 3 hours (ANOVA with Gilt Block FPr≤0.05) post-seeding. Lacunarity was increased following culture with conditioned media from the lightest foetuses compared to the CTMLW foetuses at 4 (ANOVA with Gilt Block FPr≤0.01), 5 and 6 (ANOVA with Gilt Block FPr=0.07 and 0.08 respectively) hours post-seeding (Figure 8.8I).

Figure 8.8: Endothelial Cell Branching is impaired in Response to Conditioned Media from Placentas Supplying the Lightest Foetuses at GD45.

Matrigel branching assays were performed where endothelial cells were cultured with conditioned media from porcine placentas supplying the lightest and closest to mean litter weight (CTMLW) foetuses at gestational day (GD) 45. Nine parameters of interest were investigated, from 2-10 hours post-seeding of the cells. The mean values for each treatment are presented here. A: No relationship between foetal size and explant area was observed. B: An overall size effect was observed in vessel area (ANOVA without Gilt Block FPr≤0.05; with Gilt Block FPr≤0.01); with culture with conditioned media from the lightest foetuses resulting in a decreased vessel area. This was statistically significant at 3 and 4 hours post-seeding. C: Vessels as a percentage of area was decreased in response to conditioned media for the lightest compared to the CTMLW foetuses (overall effect ANOVA without Gilt Block FPr≤0.05; with Gilt Block FPr≤0.01), which was statistically significant at 3 and 4 hours post-seeding. D: The total number of junctions was decreased at 4 hours post-seeding in response to conditioned media supplying the lightest compared to the CTMLW foetuses. E: Junction density was decreased following treatment with the lightest compared to the CTMLW foetuses at 3 and 4 hours post-seeding. F: Total vessel length was decreased in response to conditioned media from placentas supplying the lightest foetuses compared to the CTMLW foetuses (overall effect ANOVA without Gilt Block FPr≤0.05; with Gilt Block FPr≤0.01), which was statistically significant at 3 and 4 hours post-seeding. G: Average vessel length was decreased in response to conditioned media from the lightest compared to the CTMLW foetuses (ANOVA with and without Gilt Block FPr≤0.001); which was statistically significant at 3 post-seeding. H: No statistically significant relationships between foetal size and the total number of end points was observed. I: Lacunarity was increased following treatment with conditioned media from the lightest foetuses compared to the CTMLW foetuses at 4, 5 (ANOVA with Gilt Block FPr=0.07) and 6 (ANOVA with Gilt Block FPr=0.08) hours post-seeding. Error bars represent S.E.M. *FPr/P≤0.05. **FPr/P≤0.01.

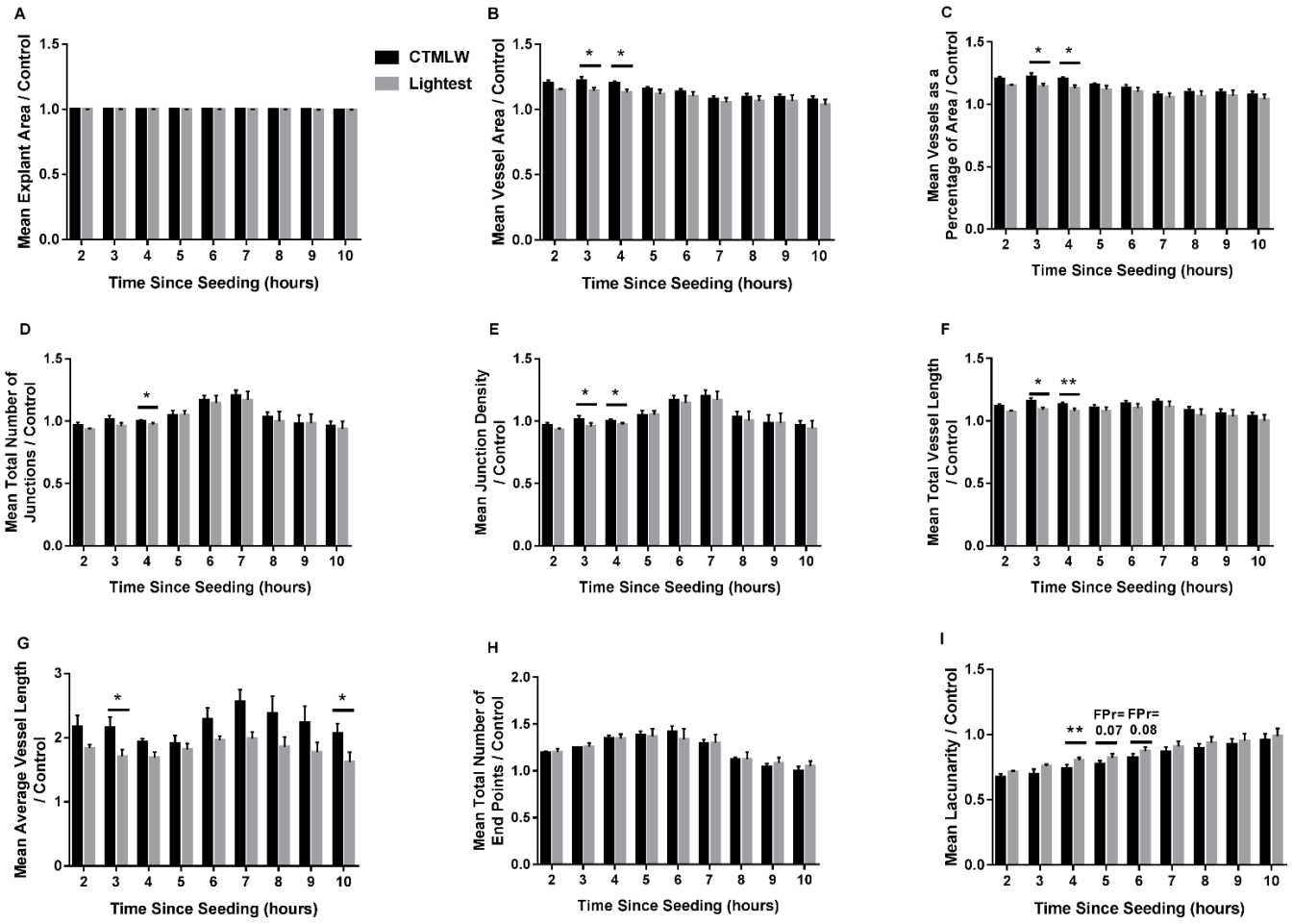

Figure 8.8: Endothelial Cell Branching is impaired in Response to Conditioned Media from Placentas Supplying the Lightest Foetuses at GD45.

8.5.4.3 Foetal Size Influences Endothelial Cell Branching in Response to Placental Conditioned Media at GD60

To test the hypothesis that placentas supplying the lightest foetuses will have a decreased ability to induce endothelial cell branching *in vitro* compared to placentas supplying the CTMLW foetuses, conditioned media was generated from these samples at GD60. Figure 8.9 illustrates the relationship between foetal size and changes in the nine parameters of interest over the course of the experiment (2-10 hours post-seeding).

Overall size effects were observed, with a decrease in explant area ($P \leq 0.001$; Figure 8.9A), vessel area ($P \leq 0.01$; Figure 8.9B), vessels as a percentage of area ($P \leq 0.01$; Figure 8.9C), the total number of junctions (ANOVA without Gilt Block FPr=0.017; with Gilt Block FPr≤0.001; Figure 8.9D), junction density (ANOVA without Gilt Block FPr=0.021; with Gilt Block FPr≤0.001; Figure 8.9E), total vessel length ($P \leq 0.001$; Figure 8.9F) in response to culture with conditioned media from the lightest foetuses compared to the CTMLW foetuses. An increase in the total number of end points ($P \leq 0.001$, Figure 8.9H) and lacunarity (ANOVA without Gilt Block FPr=0.002; with Gilt Block FPr≤0.001, Figure 8.9I) was observed in response to treatment with conditioned media from the lightest foetuses compared to the CTMLW foetuses. Foetal size was not associated with average vessel length (Figure 8.9G).

These differences were then investigated within time point. The decrease in mean explant area was statistically significant at 4 ($P=0.06$), 5, 7, 8 (all $P \leq 0.05$) and 10 ($P=0.07$) hours post-seeding (Figure 8.9A). No statistically significant differences were observed within time point for vessel area (Figure 8.9B), vessels as a percentage of area (Figure 8.9C), average vessel length (Figure 8.9G) or total number of end points (Figure 8.9H). The decrease in the total number of junctions in response to culture with conditioned media from the lightest foetuses compared to the CTMLW foetuses was statistically significant at 8 hours post-seeding (ANOVA with Gilt Block FPr≤0.05; Figure 8.9D). The observed decrease in junction density was statistically significant at 7 and 8 hours post-seeding (ANOVA with Gilt Block FPr≤0.05; Figure 8.9E). Culture

with conditioned media from the lightest foetuses induced a statistically significant decrease in total vessel length at 8 hours post-seeding (ANOVA with Gilt Block P≤0.05; Figure 8.9F) compared to cells cultured with conditioned media from the CTMLW foetuses. The increase in lacunarity observed was statistically significant at 6, 7 and 8 hours (ANOVA with Gilt Block FPr≤0.05; Figure 8.9I) post-seeding.

8.5.4.4 Foetal Sex Influences Endothelial Cell Branching at GD60

Due to the sex differences observed in chapter 7, conditioned media from placentas supplying foetuses of different sex at GD60 were used in the Matrigel branching assays to determine if foetal sex influenced endothelial cell branching *in vitro*. Figure 8.10 illustrates the relationship between foetal sex and the nine parameters of interest over the course of the experiment (2-10 hours post-seeding).

An overall sex effect was observed for explant area (P≤0.05; Figure 8.10A); vessel area (P≤0.001; Figure 8.10B); vessels as a percentage of area (P≤0.001; Figure 8.10C); total number of junctions (without Gilt Block FPr≤0.001; with Gilt Block FPr=0.028; Figure 8.10D); junction density (without Gilt Block FPr≤0.001; with Gilt Block FPr=0.027; Figure 8.10E); total vessel length (P≤0.001; Figure 8.10F) and average vessel length (P≤0.001; Figure 8.10G), with conditioned media from placentas supplying female foetuses having an increased effect on endothelial cell branching compared to those supplying male foetuses.

When investigating the influence of foetal sex within time point, no statistically significant effects were observed in explant area (Figure 8.10A) or total number of end points (Figure 8.10H). Mean vessel area and vessels as a percentage of area were increased in response to conditioned media from placentas supplying female foetuses at 2, 3, 4, 5 (all P≤0.05) and 6 (P=0.07) hours post-seeding (Figure 8.10B and C) when compared with conditioned media from placentas supplying male foetuses.

The total number of junctions (Figure 8.10D), junction density (Figure 8.10E) and average vessel length (Figure 8.10G) were increased in response to culture with conditioned media from placentas supplying female foetuses compared with conditioned media from placentas supplying male foetuses at all time points investigated (FPr/P≤0.05). Total vessel length was increased in response to treatment with conditioned media from placentas supplying female foetuses at 2, 3, 4 (all P≤0.01), 5, 6 (both P≤0.05) and 7 (P=0.07) hours post-seeding (Figure 8.10F). A trend towards decreased lacunarity (FPr=0.07) was observed in response to conditioned media from placentas supplying female foetuses compared to male foetuses at 2 hours post-seeding.

Figure 8.9: Endothelial Cell Branching Impaired in Response to Conditioned Media from Placentas Supplying the Lightest Foetuses at GD60.

Matrigel branching assays were performed where endothelial cells were cultured with conditioned media from porcine placentas supplying the lightest and closest to mean litter weight (CTMLW) foetuses at gestational day (GD) 60. Nine parameters of interest were investigated, from 2-10 hours post-seeding of the cells. The mean values for each treatment are presented here. A: Conditioned media from placentas supplying the lightest foetuses induced an overall decrease in explant area ($P \leq 0.001$), which was statistically significant at 5, 7 and 8 hours post-seeding, and was trending towards significant at 4 ($P=0.06$) and 10 ($P=0.07$) hours compared to culture with conditioned media from placentas supplying the CTMLW foetuses. B: An overall decrease in vessel area in response to culture with conditioned media from placentas supplying the lightest foetuses compared to the CTMLW foetuses was observed ($P \leq 0.01$). C: An overall decrease in vessels as a percentage of area in response to conditioned media from placentas supplying the lightest foetuses compared to the CTMLW foetuses ($P \leq 0.01$) was observed. D: The total number of junctions was decreased in response to culture with conditioned media from placentas supplying the lightest foetuses compared to the CTMLW foetuses (without Gilt Block FPr=0.017; with Gilt Block FPr≤0.001), which was statistically significant at 8 hours post-seeding. E: Culture with conditioned media from placentas supplying the lightest foetuses promoted an overall decrease in junction density (without Gilt Block FPr=0.021; with Gilt Block FPr≤0.001) compared to the CTMLW foetuses, which was statistically significant at 7 and 8 hours post-seeding. F: An overall decrease in total vessel length in response to conditioned media from placentas supplying the lightest foetuses ($P \leq 0.001$) was observed, which was statistically significant at 8 hours post-seeding. G: Foetal size did not influence average vessel length. H: The total number of end points increased ($P \leq 0.001$) following culture with conditioned media from placentas supplying the lightest foetuses compared to the CTMLW foetuses. I: An overall increase in lacunarity (without Gilt Block FPr=0.002; with Gilt Block FPr≤0.001) was observed in response to culture with conditioned media from the lightest foetuses compared to the CTMLW foetuses, which was statistically significant at 6, 7 and 8 hours post-seeding. Error bars represent S.E.M. *FPr/$P \leq 0.05$. **FPr/$P \leq 0.01$.

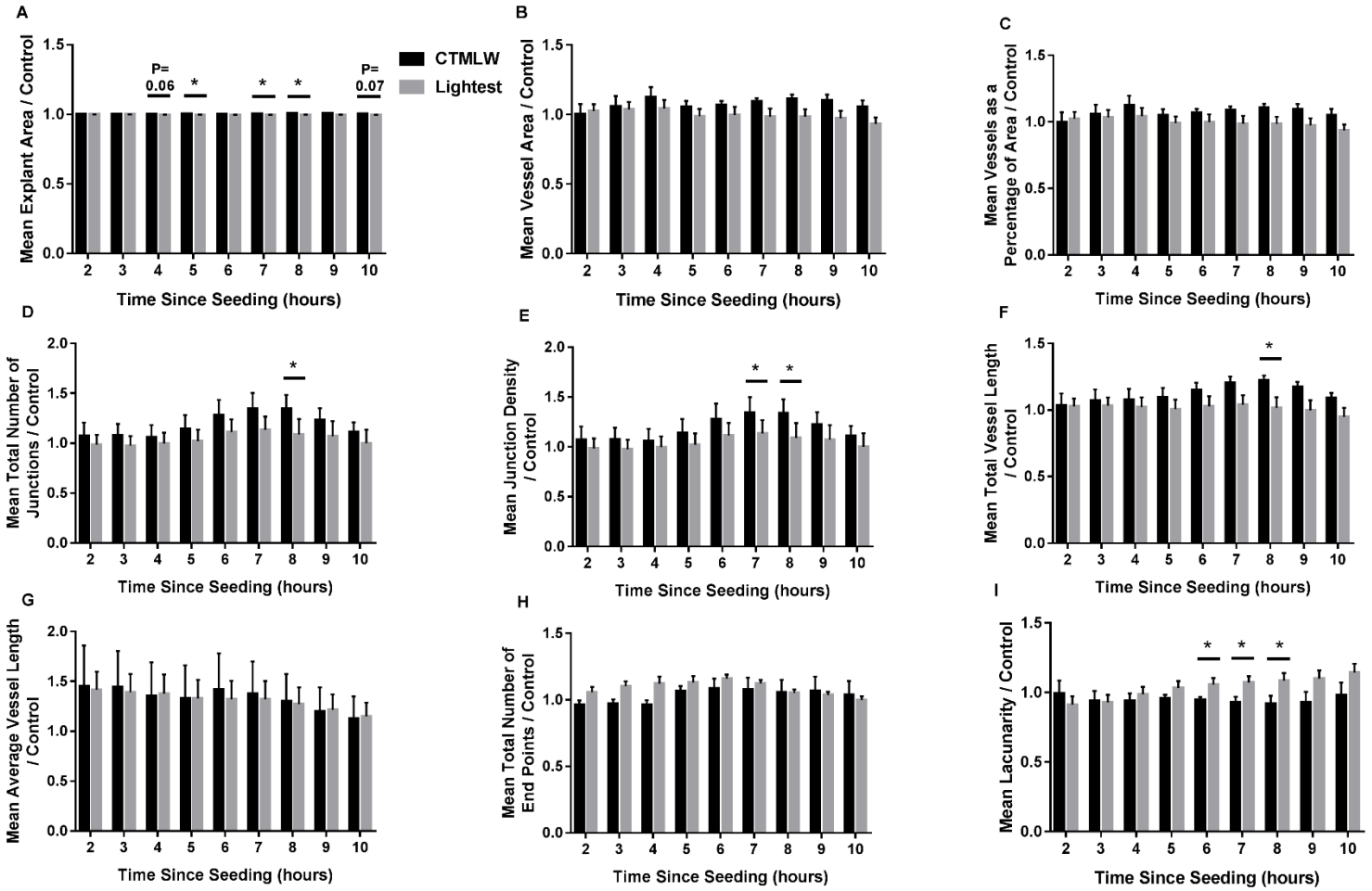

Figure 8.9: Endothelial Cell Branching Impaired in Response to Conditioned Media from Placentas Supplying the Lightest Foetuses at GD60.

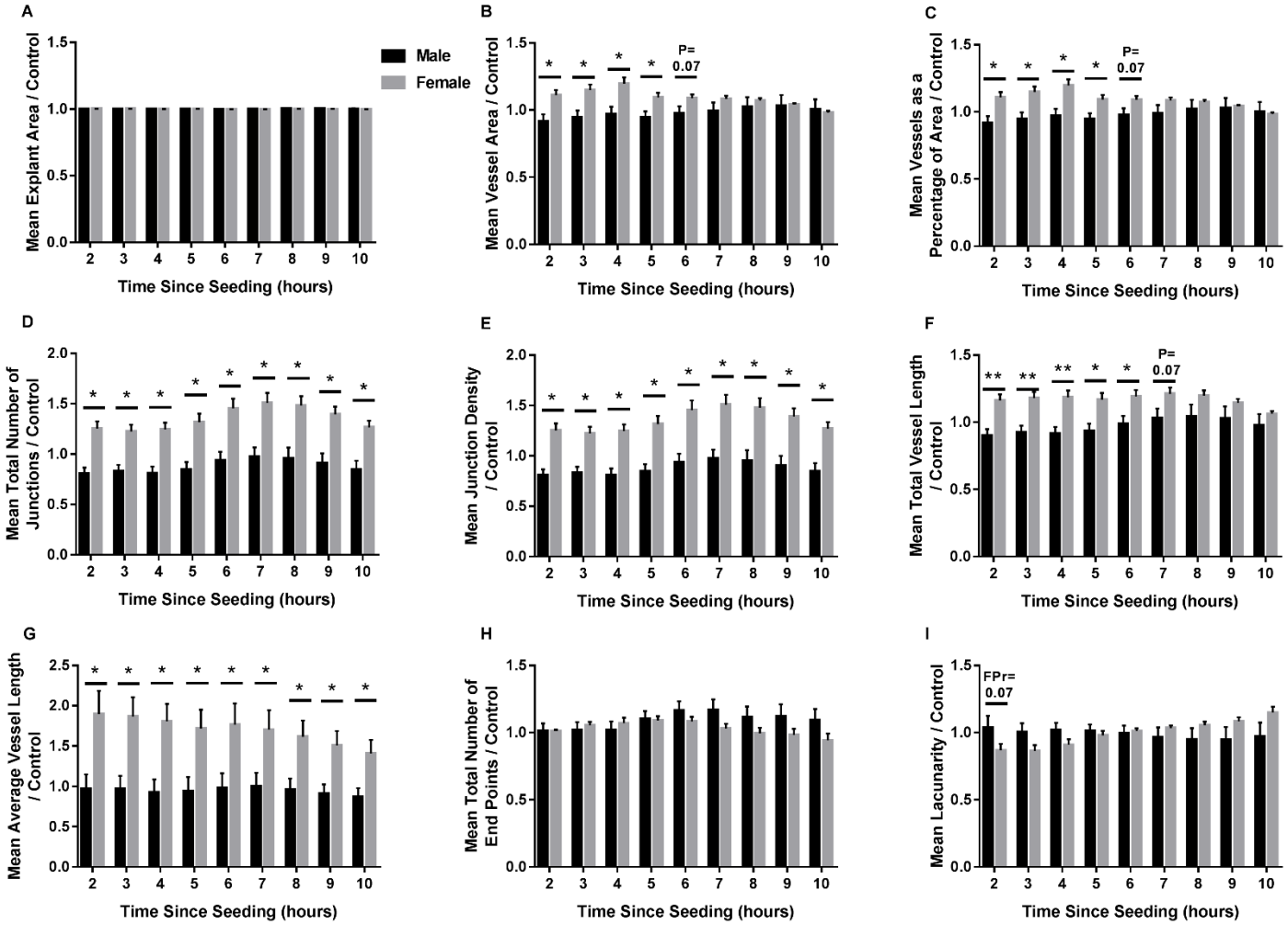

Figure 8.10: Foetal Sex Influences Endothelial Cell Branching in Response to Placental Conditioned Media at GD60.

Figure 8.10: Foetal Sex Influences Endothelial Cell Branching in Response to Placental Conditioned Media at GD60.

Matrigel branching assays were performed where endothelial cells were cultured with conditioned media from porcine placentas supplying foetuses of both sex at gestational day (GD) 60. Nine parameters of interest were investigated, from 2-10 hours post-seeding of the cells. The mean values for each sex are presented here. A: An overall sex effect was observed for explant area ($P \leq 0.05$), although no statistically significant effects were observed when the analysis was performed within time point. B: Culture with conditioned media from placentas supplying female foetuses promoted an overall increase in vessel area ($P \leq 0.001$) compared to culture with media from placentas supplying male foetuses, which was statistically significant at 2-5 hours post-seeding. C: An overall increase in vessels as a percentage of area ($P \leq 0.001$), which was statistically significant at 2-5 hours post-seeding, was observed in response to conditioned media supplying female foetuses compared to media supplying male foetuses. The total number of junctions (overall effect without Gilt Block $FPr \leq 0.001$; with Gilt Block $FPr = 0.028$; D), junction density (overall effect without Gilt Block $FPr \leq 0.001$; with Gilt Block $FPr = 0.027$; E), and average vessel length ($P \leq 0.001$; G), were all increased in response to treatment with conditioned media from placentas supplying female foetuses compared to media supplying male foetuses at all time points investigated. F: Total vessel length was increased overall ($P \leq 0.001$) in response to culture with conditioned media from placentas supplying female foetuses compared to male foetuses, with this difference being statistically significant at 2-6 hours post-seeding. H: No relationships between foetal sex and the total number of end points were observed. I: A trend towards a decrease in lacunarity ($P = 0.07$) was observed in response to conditioned media from placentas supplying female foetuses compared to male foetuses at 2 hours post-seeding. Error bars represent S.E.M. *$FPr/P \leq 0.05$. **$FPr/P \leq 0.01$.

8.5.4.5 Conditioned Media from Placentas Supplying the CTMLW Male has Differential Branching Ability to the Other Three Groups at GD60.

Following the observation that both foetal size and sex influence endothelial cell branching in response to culture with placental conditioned media, at GD60 sex x size interactions were investigated. The mean value for each treatment group (placenta samples supplying the lightest and CTMLW, male and female foetuses) were plotted over the course of the experiment (Figure 8.11).

The influence of foetal sex on endothelial cell branching described in 8.5.4.4 can be observed again in Figure 8.11. In addition to this, there was an indication that the CTMLW males had a different branching ability compared to the other three treatment groups in the following parameters investigated. In vessel area (Figure 8.11B), vessels as a percentage of area (Figure 8.11C), total vessel length (Figure 8.11F) and total number of end points (Figure 8.11H), the CTMLW males has a different profile, with a lag behind the other three groups during the initial hours of the experiment before their branching ability overtook the other three groups in the later stages of the experiment. The inverse of this was observed in the lacunarity parameter (Figure 8.11I), with the CTMLW males having decreased lacunarity initially before having increased lacunarity towards the end of the experiment compared with the other three treatment groups. Average vessel length consistently was the shortest in the CTMLW male group (Figure 8.11G).

Due to the data for 8 of the 9 parameters at GD60 not having a normal distribution, a two-way ANOVA for sex x size could only be performed for lacunarity (Figure 8.11I) to test statistically for the presence of sex x size interactions. This analysis revealed a sex x size interaction at 2 (ANOVA without Gilt Block FPr = 0.052), 7 (ANOVA with Gilt Block FPr=0.059), 8 (ANOVA with Gilt Block FPr=0.045) and 9 (ANOVA with Gilt Block FPr=0.027) hours post-seeding.

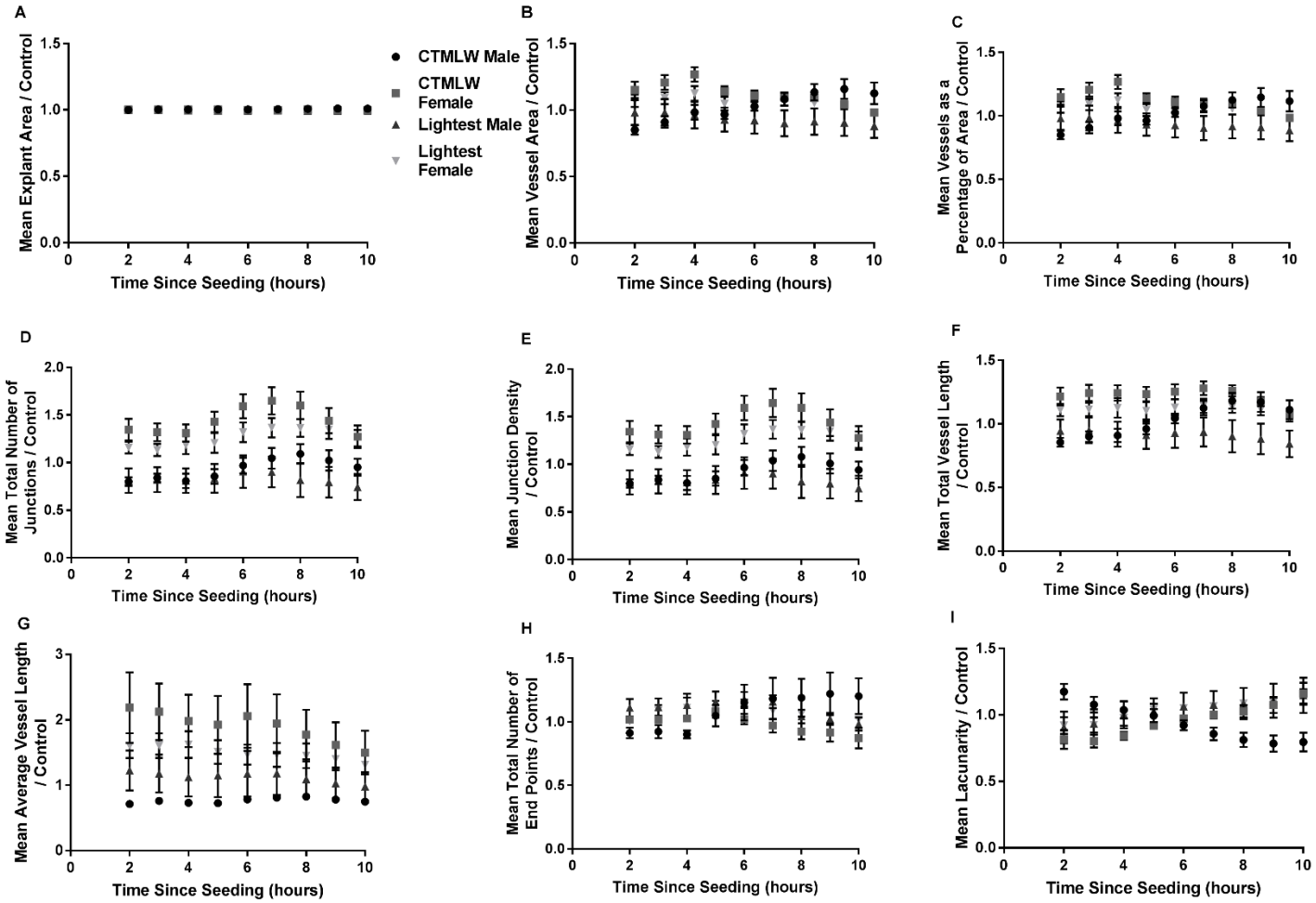

Figure 8.11: Conditioned Media from Placentas Supplying the CTMLW Male has Differential Branching Ability to the Other Three Groups.

Figure 8.11: Conditioned Media from Placentas Supplying the CTMLW Male has Differential Branching Ability to the Other Three Groups.

Matrigel branching assays were performed where endothelial cells were cultured with conditioned media from porcine placentas supplying the lightest and closest to mean litter weight (CTMLW) foetuses of both sex at gestational day (GD) 60. Nine parameters of interest were investigated, from 2-10 hours post-seeding of the cells. The mean values for each group are presented here. No sex x size interactions were observed in explant area (A). In vessel area (B), vessels as a percentage of area (C), total vessel length (F) and total number of end points (H), the CTMLW males lag behind the other three groups during the initial hours of the experiment before their branching ability overtook the other three groups in the later stages of the experiment. The inverse of this was observed in lacunarity (I), with the CTMLW males having decreased lacunarity in the early stages before having increased lacunarity in the late stages of the experiment compared with the other three groups. A significant sex x size interaction at 2 (without Gilt Block FPr=0.052), 7 (with Gilt Block FPr=0.059), 8 (with Gilt Block FPr=0.045) and 9 (with Gilt Block FPr=0.027) hours post-seeding was observed in lacunarity. In both the total number of junctions (D) and junction density (E), the effect of foetal sex was observed however there were no indications of a sex x size interaction. Average vessel length consistently was the shortest in the CTMLW group (G). Error bars represent S.E.M.

8.5.5 Matrigel Branching Assays can be used to investigate the Angiogenic Potential of Endometrial Samples

8.5.5.1 The GD of an Endometrial Sample Influences Endothelial Cell Branching *in vitro*

The results of chapter 7 demonstrated that there are large temporal changes in the expression of angiogenesis related genes throughout gestation in the endometrium. The results of the placental Matrigel branching assays demonstrated that conditioned media from placental samples at GD45 promote increased endothelial cell branching compared to conditioned media from GD60 placentas. Considering this, the same experiment was performed on endometrial samples associated with the same foetuses used in the placental experiment. Figure 8.12 illustrates the temporal changes in the nine parameters of interest over the course of the experiment (2-10 hours post-seeding).

In response to culture with conditioned media from GD45 endometrium, explant area (Figure 8.12A) was decreased at 8 of the 9 time points investigated (2 and 4 hours $P=0.06$, 5-10 hours post-seeding $P\leq0.05$), when compared with the GD60 endometrial conditioned media. Total vessel area was decreased in response the GD45 endometrial conditioned media at 9 and 10 hours post-seeding ($P=0.07$ and $P\leq0.05$ respectively; Figure 8.12B). Vessels as a percentage of area was decreased at 10 hours post-seeding ($P\leq0.05$) following culture with GD45 endometrial conditioned media compared to GD60 conditioned media (Figure 8.12C). No statistically significant effect of GD was observed in the parameters of total number of junctions (Figure 8.12D), junction density (Figure 8.12E) or average vessel length (Figure 8.12G). A trend towards a decrease in total vessel length ($P=0.08$; Figure 8.12F) and total number of end points ($P=0.07$; Figure 8.12H) at 10 hours post-seeding was observed following culture with conditioned media from GD45 endometrial samples compared with GD60 endometrial samples. An overall GD effect was observed in lacunarity (without Gilt Block $FPr\leq0.001$; with Gilt Block $FPr=0.01$; Figure 8.12I) with the GD45 endometrial samples having increased lacunarity compared with the GD60 samples. This

was statistically significant within time point at 6-10 hours post-seeding (6 hours FPr=0.07; 7-10 hours FPr≤0.01).

Figure 8.12: The GD of Endometrial Samples Influences Endothelial Cell Branching *in vitro*.

Matrigel branching assays were performed where endothelial cells were cultured with conditioned media from porcine endometrial samples at gestational day (GD) 45 and 60. Nine parameters of interest were investigated, from 2-10 hours post-seeding of the cells. The mean values for each GD are presented here. A: Total explant area was decreased in response to the GD45 conditioned media in 8 of the 9 time points investigated (trending towards significant at 2 and 4 hours P=0.06, 5-10 hours was statistically significant), when compared with culture with the GD60 endometrial conditioned media. B: A decrease in total vessel area in response the GD45 endometrial conditioned media was observed at 9 (P=0.07) and 10 hours post-seeding when compared with the GD60 endometrial conditioned media. C: Vessels as a percentage of area was decreased at 10 hours post-seeding following culture with GD45 endometrial conditioned media compared to GD60 conditioned media. No statistically significant effect of GD was observed in total number of junctions (D) or junction density (E). F: A trend towards a decrease in total vessel length (P=0.08) was observed following culture with conditioned media from GD45 endometrial conditioned media compared to conditioned media from GD60 endometrial samples. G: No statistically significant effect of GD was observed in average vessel length. H: Total number of end points was decreased at 10 hours post-seeding (P=0.07) following culture with conditioned media from GD45 endometrial samples compared with GD60 endometrial samples. I: An overall GD effect was observed in lacunarity (without Gilt Block FPr≤0.001; with Gilt Block FPr=0.01) with GD45 endometrial samples promoting an increase in lacunarity. This was statistically significant within time point at 7-10 hours post-seeding (trend at 6 hours FPr=0.07). Error bars represent S.E.M. *FPr/P≤0.05. **FPr/P≤0.01.

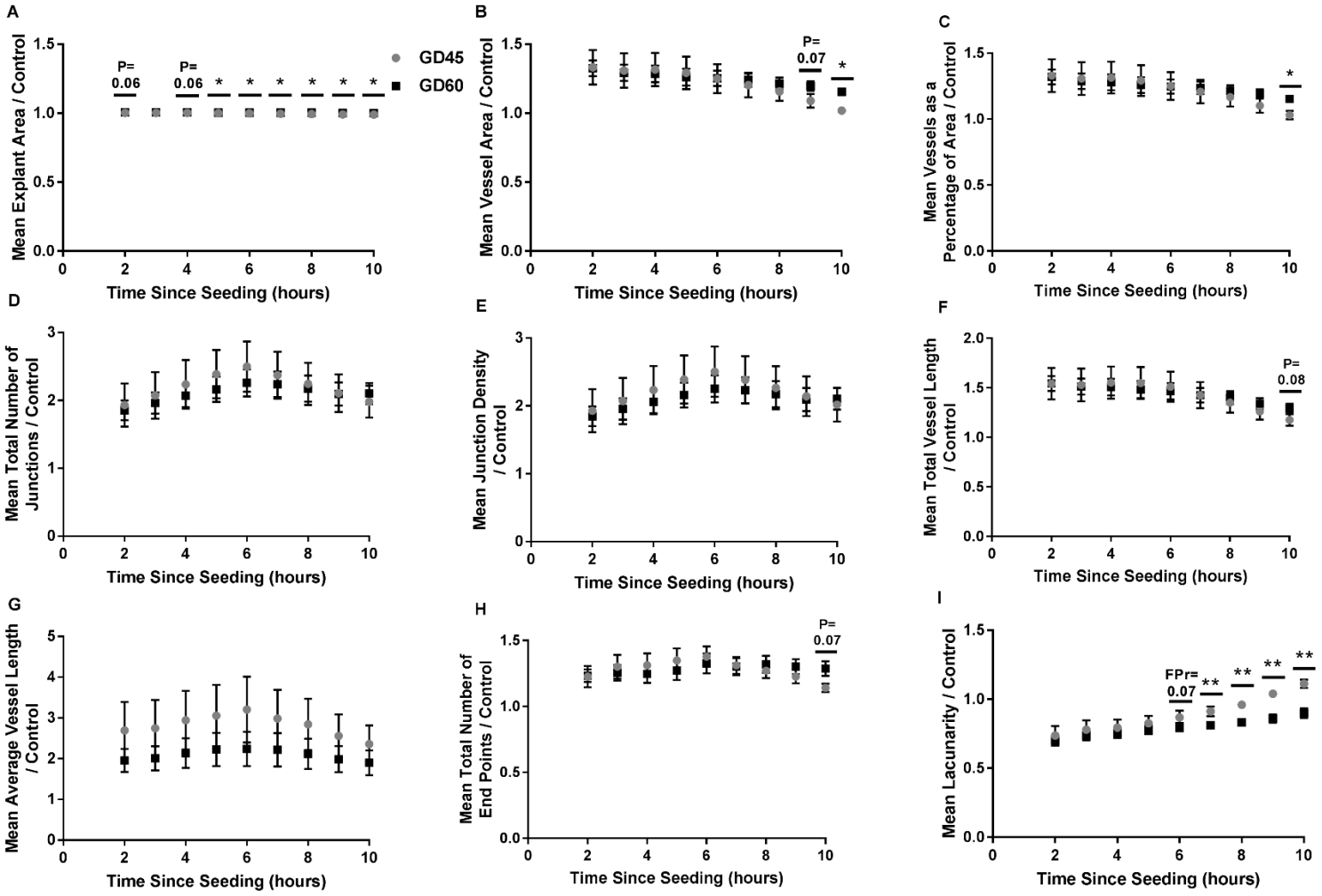

Figure 8.12: The GD of Endometrial Samples Influences Endothelial Cell Branching *in vitro*.

8.5.5.2 Foetal Size Influences Endothelial Cell Branching in Response to Endometrial Conditioned Media at GD45

To test the hypothesis that endometrial samples supplying the lightest foetuses will have a decreased ability to induce endothelial cell branching *in vitro* compared to those supplying the CTMLW foetuses, conditioned media was generated from these samples at GD45. Figure 8.13 illustrates the relationship between foetal size and changes in the nine parameters of interest over the course of the experiment (2-10 hours post-seeding).

Overall size effects (with all-time points combined) were observed in many of the parameters investigated, with a decrease observed in response to conditioned media from endometrial samples associated with the lightest compared to the CTMLW foetuses unless otherwise stated. An overall size effect was observed in explant area (P=0.02; Figure 8.13A), with a trend towards a significant decrease in response to culture with conditioned media from endometrial samples associated with the lightest compared to the CTMLW foetuses observed at 5 and 6 hours post-seeding (P=0.08). An overall size effect, with a decrease observed in response to culture with the conditioned media associated with the lightest foetuses was observed in vessel area (P=0.004; Figure 8.13B), vessels as a percentage of area (P=0.005; Figure 8.13C), total number of junctions and junction density (with and without Gilt Block FPr≤0.001; Figure 8.13D and E), compared to the CTMLW foetuses. An overall size effect was also observed in total vessel length (P=0.015; Figure 8.13F) and average vessel length (P=0.002; Figure 8.13G), with a shorter vessel length observed following culture with conditioned media from endometrial samples associated with the lightest compared to the CTMLW foetuses. Whilst no size effect was observed in total number of end points (Figure 8.13H), an overall size effect for increased lacunarity was observed (with and without gilt block FPr=0.039). Within time point, a trend towards an increase in lacunarity in response to conditioned media from endometrial samples associated with the lightest compared to the CTMLW foetuses was present at 8 hours post-seeding (FPr=0.07).

8.5.5.3 Foetal Size Influences Endothelial Cell Branching in Response to Endometrial Conditioned Media at GD60

To test the hypothesis that endometrial samples supplying the lightest foetuses will have decreased ability to induce endothelial cell branching *in vitro* compared to those supplying the CTMLW foetuses, conditioned media was generated from these samples at GD60. Figure 8.14 illustrates the relationship between foetal size and changes in the nine parameters of interest over the course of the experiment (2-10 hours post-seeding).

Overall size effects (with all-time points combined) were observed in many the parameters investigated, with a decrease observed in response to conditioned media from endometrial samples associated with the lightest compared to the CTMLW foetuses unless otherwise stated. Foetal size did not influence explant area (Figure 8.14A) or total number of end points (Figure 8.14H). An overall size effect was observed for vessel area ($P \leq 0.001$; Figure 8.14B), vessels as a percentage of area ($P \leq 0.001$; Figure 8.14C), total number of junctions ($P \leq 0.001$; Figure 8.14D) and junction density (with and without Gilt Block $FPr \leq 0.001$; Figure 8.14E). An overall size effect was observed for total vessel length ($P \leq 0.05$; Figure 8.14F) and average vessel length ($P \leq 0.01$; Figure 8.14G), with conditioned media from endometrial samples associated with the lightest foetuses promoting a decrease in vessel length compared to the CTMLW foetuses. An overall size effect in lacunarity (with and without Gilt Block $FPr \leq 0.001$; Figure 8.14I) was observed, with conditioned media from endometrial samples associated with the lightest foetuses promoting an increase in lacunarity compared to the CTMLW foetuses. Whilst an overall size effect was present in 7 of the 9 parameters investigated, none of these differences were statistically significant within time point.

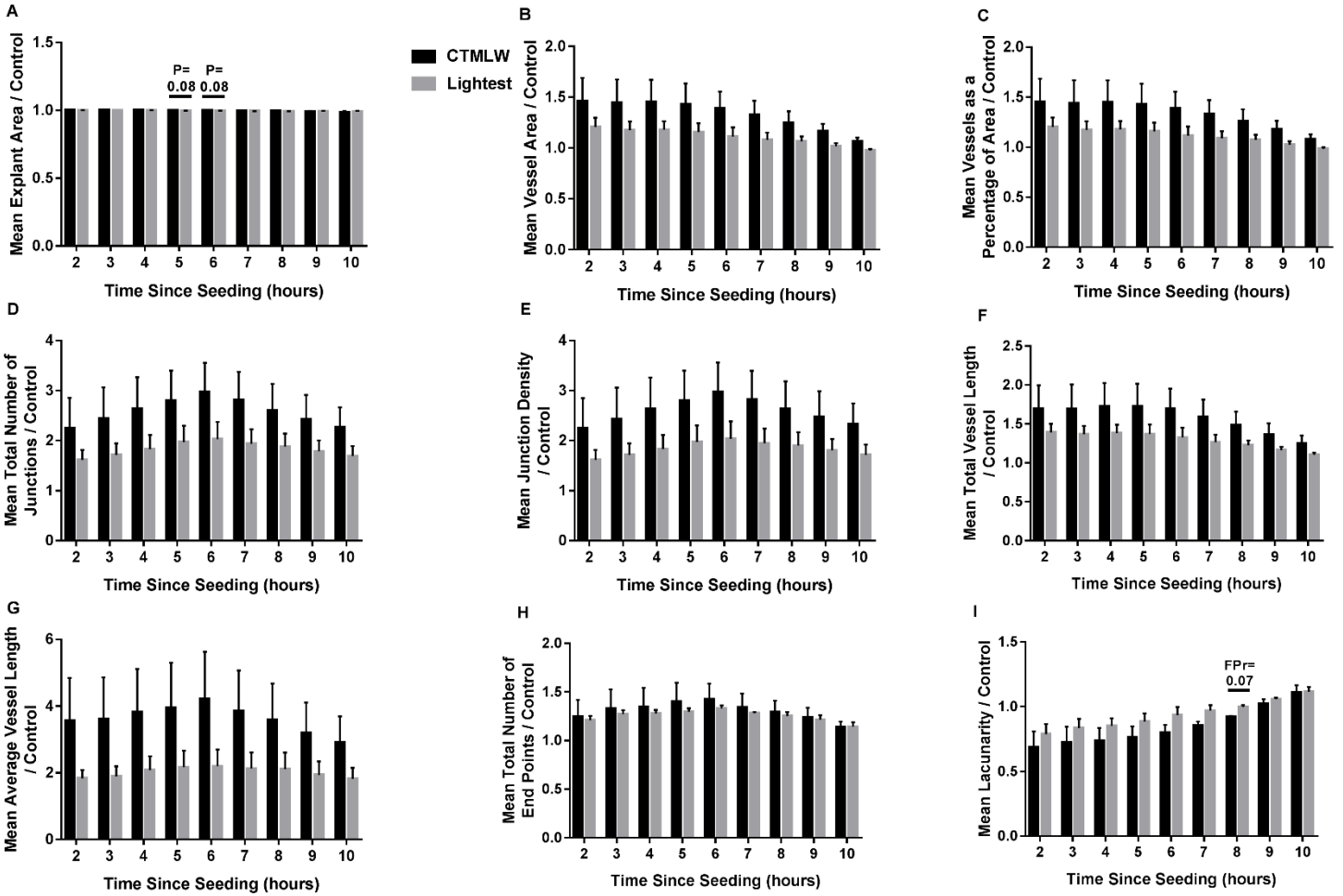

Figure 8.13: Endothelial Cell Branching was impaired in Response to Conditioned Media from Endometrium Supplying the Lightest Foetuses at GD45.

Figure 8.13: Endothelial Cell Branching was impaired in Response to Conditioned Media from Endometrium Supplying the Lightest Foetuses at GD45.

Matrigel branching assays were performed where endothelial cells were culture with conditioned media from porcine endometrial samples supplying the lightest and closest to mean litter weight (CTMLW) foetuses at gestational day (GD) 45. Nine parameters of interest were investigated, from 2-10 hours post-seeding of the cells. The mean values for each treatment are presented here. A: An overall decrease in explant area (P=0.02) was observed in response to culture with conditioned media from endometrial samples associated with the lightest compared to the CTMLW foetuses. Within time point a trend towards significance was observed in this parameter at 5 and 6 hours post-seeding (P=0.08). An overall size effect, with a decrease in response to culture with the conditioned media associated with the lightest foetuses was observed in vessel area (P=0.004; B); vessels as a percentage of area (P=0.005; C); total number of junctions (with and without Gilt Block FPr≤0.001; D) and junction density (with and without Gilt Block FPr≤0.001; E). Both total vessel length (P=0.015; F) and average vessel length (P=0.002; G) were decreased overall following culture with conditioned media from endometrial samples associated with the lightest compared to the CTMLW foetuses. H: Foetal size did not influence the total number of end points. I: An overall size effect in lacunarity was observed (with and without gilt block FPr=0.039), with a trend towards an increase in lacunarity in response to conditioned media from endometrial samples associated with the lightest compared to the CTMLW foetuses at 8 hours post-seeding (FPr=0.07). Error bars represent S.E.M. *FPr/P≤0.05. **FPr/P≤0.01.

Figure 8.14: Endothelial Cell Branching Impaired in Response to Conditioned Media from Endometrium Supplying the Lightest Foetuses at GD60.

Matrigel branching assays were performed where endothelial cells were cultured with conditioned media from porcine endometrial samples supplying the lightest and closest to mean litter weight (CTMLW) foetuses at gestational day (GD) 60. Nine parameters of interest were investigated, from 2-10 hours post-seeding of the cells. The mean values for each treatment are presented here. A: Foetal size did not influence explant area overall or at any time point investigated. An overall size effect was observed for vessel area ($P \leq 0.001$; B) and vessels as a percentage area ($P \leq 0.001$; C), with a decrease observed in response to conditioned media from endometrial samples associated with the lightest compared to the CTMLW foetuses. A decrease in the total number of junctions ($P \leq 0.001$; D) and junction density (with and without Gilt Block FPr≤ 0.001; E) was observed in response to conditioned media from endometrial samples associated with the lightest compared to the CTMLW foetuses. An overall size effect was observed for both the total vessel length ($P \leq 0.05$; F) and average vessel length ($P \leq 0.01$; G), with conditioned media from endometrial samples associated with the lightest foetuses having shorter vessels compared to the CTMLW foetuses. Foetal size did not influence total number of end points (H) overall or at any time point investigated. An overall size effect in lacunarity was observed (with and without Gilt Block FPr≤ 0.001; I), with conditioned media from endometrial samples associated with the lightest promoting an increase in lacunarity compared to the CTMLW foetuses. Error bars represent S.E.M.

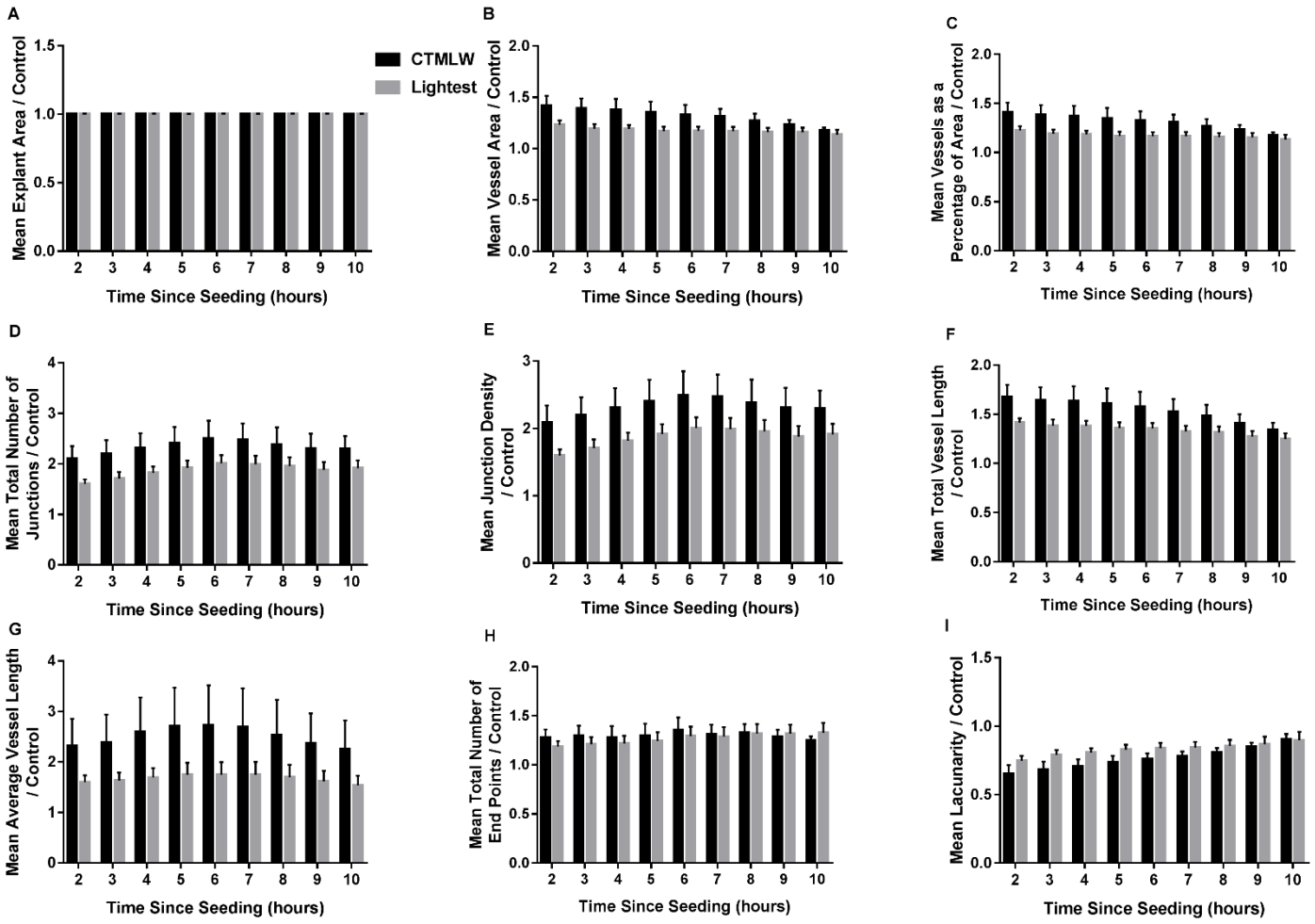

Figure 8.14: Endothelial Cell Branching Impaired in Response to Conditioned Media from Endometrium Supplying the Lightest Foetuses at GD60.

8.5.5.4 Foetal Sex Influences Endothelial Cell Branching in Response to GD60 Endometrial Conditioned Media

Due to the striking sex differences observed in chapter 7, and the results obtained from the placental Matrigel branching assays (8.5.4.4), the Matrigel branching assays were performed using conditioned media from endometrial samples supplying foetuses of different sex at GD60. Figure 8.15 illustrates the relationship between foetal sex and the nine parameters of interest over the course of the experiment (2-10 hours post-seeding).

An overall sex effect was observed for explant area ($P \leq 0.05$; Figure 8.15A); vessel area ($P \leq 0.05$; Figure 8.15B); vessels as a percentage of area ($P \leq 0.05$; Figure 8.15C); total number of junctions ($P \leq 0.001$; Figure 8.15D) junction density ($P \leq 0.001$; Figure 8.15E); total vessel length ($P \leq 0.01$; Figure 8.15F), average vessel length ($P \leq 0.001$; Figure 8.15G) and total number of end points ($P \leq 0.001$; Figure 8.15H), with conditioned media from endometrial samples supplying female foetuses having a decreased effect on endothelial cell branching compared to male foetuses. Sex did not influence lacunarity overall or within time point (Figure 8.15I).

When investigating the influence of foetal sex within time point on the nine parameters, foetal sex did not have a significant effect on any parameters except for average vessel length. Average vessel length was shorter in response to treatment with conditioned media from endometrial samples supplying female foetuses compared to male foetuses at 2 ($P=0.07$), 8 ($P \leq 0.05$), 9 ($P=0.07$) and 10 ($P=0.07$) hours post-seeding (Figure 8.15G).

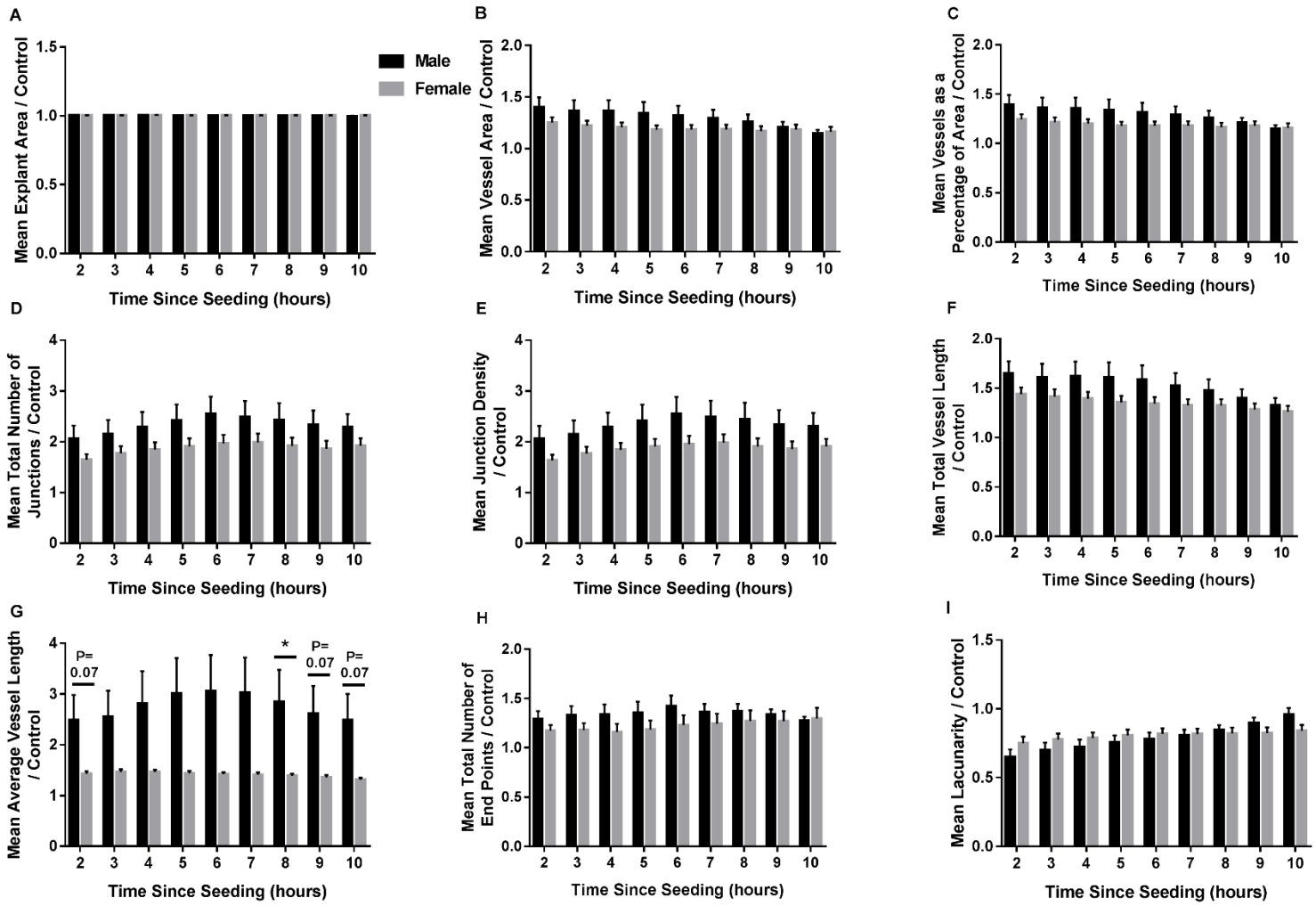

Figure 8.15: Foetal Sex Influences Endothelial Cell Branching in Response to Endometrial Conditioned Media at GD60.

Figure 8.15: Foetal Sex Influences Endothelial Cell Branching in Response to Endometrial Conditioned Media at GD60.

Matrigel branching assays were performed where endothelial cells were treated with conditioned media from porcine endometrial samples supplying foetuses of both sex at gestational day (GD) 60. Nine parameters of interest were investigated, from 2-10 hours post-seeding of the cells. The mean values for each sex are presented here. An overall sex effect, with conditioned media from endometrial samples supplying female foetuses promoting a decrease compared to conditioned media from those supplying male foetuses, was observed for explant area ($P \leq 0.05$; A), vessel area ($P \leq 0.05$; B), vessels as a percentage of area ($P \leq 0.05$; C), total number of junctions ($P \leq 0.001$; D), junction density ($P \leq 0.001$; E), and total vessel length ($P \leq 0.01$; F). G: An overall sex effect was observed in average vessel length ($P \leq 0.001$) with a decreased length observed in response to treatment with conditioned media from endometrial samples supplying female foetuses compared to male foetuses. This was significant within time point at 2 ($P=0.07$), 8 ($P \leq 0.05$), 9 ($P=0.07$) and 10 ($P=0.07$) hours post-seeding (G). H: The total number of end points ($P \leq 0.001$) was decreased in response to treatment with conditioned media from endometrial samples supplying female foetuses having an increased effect on endothelial cell branching compared to those supplying male foetuses. I: Lacunarity was not influenced by foetal sex overall or within time point. Error bars represent S.E.M. *FPr/$P \leq 0.05$. **FPr/$P \leq 0.01$.

Figure 8.16: Conditioned Media from Endometrial Samples Supplying the CTMLW Male has Differential Branching Ability to the Other Three Groups.

Matrigel branching assays were performed where endothelial cells were treated with conditioned media from porcine endometrial samples supplying the lightest and closest to mean litter weight (CTMLW) foetuses of both sex at gestational day (GD) 60. Nine parameters of interest were investigated, from 2-10 hours post-seeding of the cells. The mean values for each group are presented here. No sex x size interactions were visible in explant area (A). In vessel area (B), vessels as a percentage of area (C), total number of junctions (D), junction density (E), total vessel length (F), and average vessel length (G), the CTMLW males had an increased branching ability compared to the other three groups. CTMLW males had the largest number of end points (H) but there was no obvious sex x size interaction in this parameter. CTMLW males had the lowest lacunarity (I) until the last couple of hours of the experiment. Unfortunately, as with the placental analysis, due to the issues with the normality of the data for 8 of the 9 parameters, a two-way ANOVA for sex x size could only be performed for lacunarity to test statistically for the presence of sex x size interactions. This analysis did not indicate the presence of sex x size interactions. Error bars represent S.E.M.

8.5.5.5 Conditioned Media from Endometrial Samples Supplying the CTMLW Male has Differential Branching Ability to the Other Three Groups at GD60.

Following the observation that both foetal size and sex influence endothelial cell branching in response to culture with endometrial conditioned media, at GD60 sex x size interactions were investigated. The mean value for each treatment group (endometrial samples supplying the lightest and CTMLW, male and female foetuses) was plotted over the 9 hours of the experiment (Figure 8.16).

As with the placental analysis, in many the parameters investigated there was an indication that the CTMLW males had a different branching ability compared to the other three treatment groups. In vessel area (Figure 8.16B), vessels as a percentage of area (Figure 8.16C), total number of junctions (Figure 8.16D), junction density (Figure 8.16E), total vessel length (Figure 8.16F), and average vessel length (Figure 8.16G), the CTMLW males have an increased branching ability compared to the other three groups.

Unfortunately, as with the placental analysis, the data for 8 of the 9 parameters at GD60 did not have a normal distribution at GD60, therefore a two-way ANOVA for sex x size could only be performed for lacunarity (Figure 8.16I) to test statistically for the presence of sex x size interactions. This analysis did not indicate the presence of sex x size interactions.

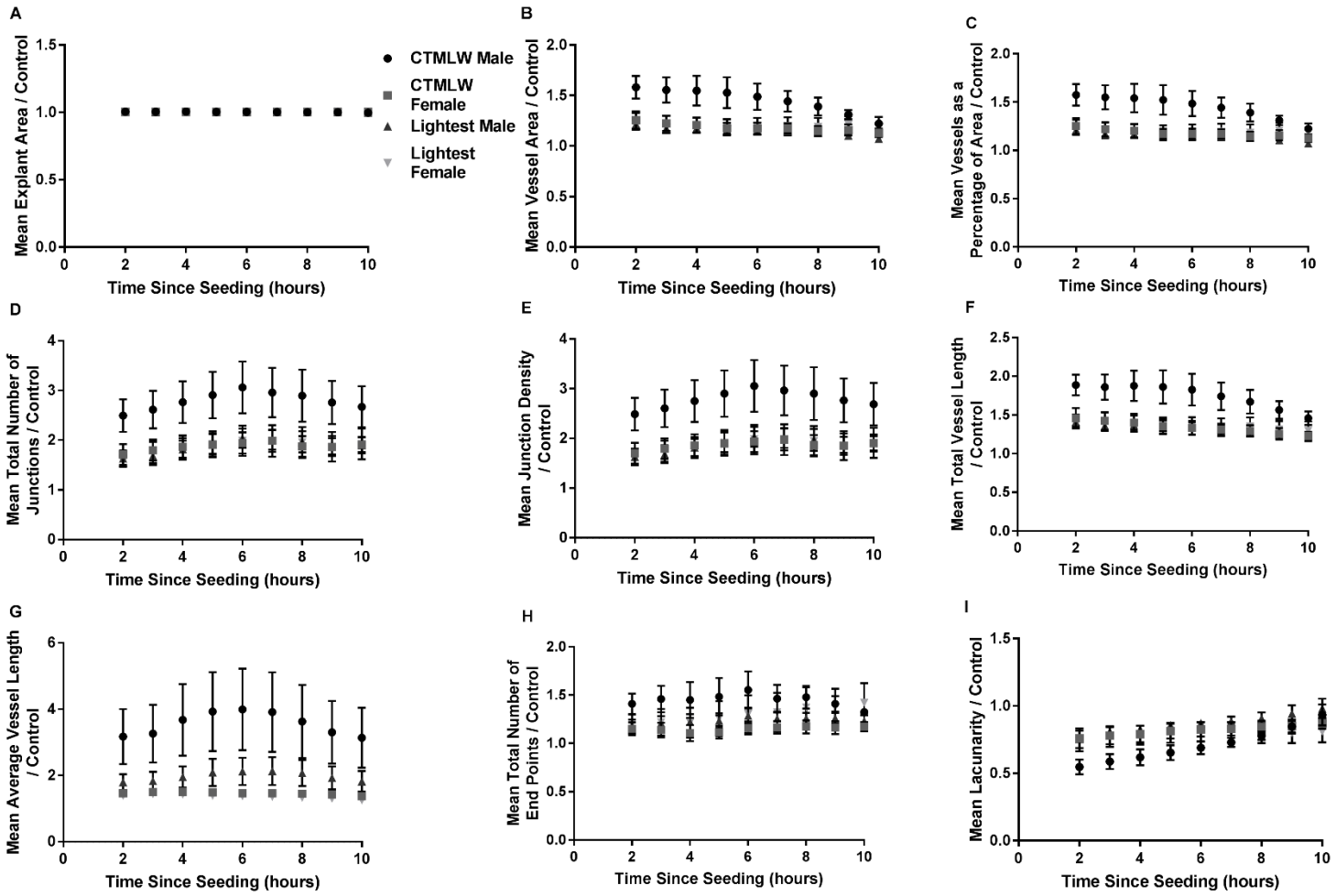

Figure 8.16: Conditioned Media from Endometrial Samples Supplying the CTMLW Male has Differential Branching Ability to the Other Three Groups.

8.6 Discussion

This chapter investigated the potential of using conditioned media from placental and endometrial samples supplying foetuses of different size and sex at GD45 and 60 to investigate endothelial cell branching *in vitro*. GD of placental conditioned media was associated with endothelial cell branching ability *in vitro*, with conditioned media from GD45 placentas having an increased effect on endothelial cell branching compared to media from GD60 placentas. GD of endometrial conditioned media did influence endothelial cell branching *in vitro* however, the influence was not as striking as that observed in the placenta. Conditioned media from the lightest foetuses at both GD45 and 60 had a decreased ability to induce endothelial cell branching *in vitro* compared to the CTMLW conditioned media. At GD60, conditioned media from female placentas had an increased effect on endothelial cell branching compared to those supplying males. Interestingly, the inverse of this was observed in the endometrium, with conditioned media from endometrial samples supplying females having a decreased ability to induce endothelial cell branching compared with those supplying males.

This chapter has presented novel findings which suggest that conditioned media from porcine placental and endometrial samples of different size, and more intriguingly sex, can influence endothelial cell branching *in vitro*. It is hoped that the conditioned media generated reflects the proteins secreted by the placental and endometrial tissues *in vivo*.

8.6.1 Conditioned Media from Placental Samples has an Increased Ability to Induce Endothelial Cell Branching *in vitro* Compared to Endometrial Samples

Conditioned media from placental samples successfully induced endothelial cell branching *in vitro.* However, increased aggregation or ‘clumping’ of the cells was observed in response to treatment with the endometrial conditioned media. This may indicate that the endometrium does not have as great a stimulatory effect on endothelial cell branching as the placenta *in vitro* which,

considering it has been suggested in the cow that the caruncle and cotyledon have differential angiogenic potential (Reynolds and Ferrell, 1987; Reynolds and Redmer, 1988), may not be unexpected. Alternatively, it may be that the assay is suboptimal for use with the endometrial compared to the placental conditioned media. Conditioned media was used from the same time point in both tissues to allow comparison between both tissues in the feto-maternal interface. And whilst it has been demonstrated that both tissues are undergoing proliferation (Figure 8.2 and Figure 8.3), it may be that a different volume of conditioned media is required or conditioned media from a different time point during the tissue culture period may be more appropriate. It has been shown that the structural integrity of stromal cells in human endometrial explant cultures begins to decline following 6 hours in culture (Bersinger *et al.*, 2010) and that the culture itself reduces the expression of progesterone, oestrogen and leukaemia inhibitory factor (LIF) receptors (Schäfer *et al.*, 2011). This was not observed in the current study however, comparison with the media from earlier in the culture period should be performed.

As described in the general introduction and Chapter 4, it is known that the secretion of glycoproteins, for example secreted phosphoprotein 1 (SPP1), and the expression of their receptors is essential to act as a bridge at the feto-maternal interface in the pig (White *et al.*, 2005; Erikson *et al.*, 2009a; Hernández *et al.*, 2013), to allow the establishment and maintenance of a successful pregnancy. Therefore, it could be that the endometrium is secreting an increased abundance of proteins like SPP1 into the conditioned media than the placenta; thereby inducing the endothelial cells to aggregate together rather than forming the vessel structures observed in the placental experiment.

8.6.2 Conditioned Media from GD45 Feto-Placental Units had an Increased Influence on Endothelial Cell Branching *in vitro* compared to GD60 Conditioned Media

The ability of endothelial cells to make ‘vessel-like’ structures *in vitro* was decreased in response to culture with conditioned media from the GD60 feto-

maternal interface compared to the GD45. This switch between GD45 and 60 has been observed in gene expression data in previous chapters and reflects the dynamic changes in placental structure and function at this stage of gestation. As discussed in Chapter 7, it is believed that there are two distinct waves of angiogenesis in the pig uterus during gestation. The decreased branching ability in response to the conditioned media at GD60 presumably reflects that the placenta has already initiated the second wave of angiogenesis. Around this stage of gestation, angiogenesis and extensive remodelling of the placenta occur to allow an increase in both the available attachment area and the density of the vascular supply available. This occurs to meet the increasing requirements of the growing foetuses (Tayade *et al.*, 2007a). Whilst this is interesting and the results throughout this thesis have consistently highlighted the dynamic nature of the feto-maternal interface at this period, to understand fully the temporal changes in the angiogenic potential of the feto-maternal interface additional GD should be investigated. If this was to be performed on the GD30 and 90 samples, the data could be related to the gene expression data, providing a comprehensive overview of angiogenesis at the feto-maternal interface throughout gestation.

8.6.3 Conditioned Media from Placental and Endometrial Samples Supplying the Lightest Foetuses has decreased Angiogenic Potential to the CTMLW Foetuses

The overall objective of performing the *in vitro* branching assays was to attempt to validate the GD45 and 60 results from Chapter 7. In summary, the CD31 staining of the CAM was increased in placentas supplying the lightest foetuses compared to the CTMLW foetuses at GD60. In the placenta and endometrium, the expression of *ACP5* and *CD31*, and *HIF1A* and *CD31* respectively were influenced by foetal size. *CD31* placental expression was decreased in placentas supplying the lightest foetuses at GD45, and increased at GD60 compared to the CTMLW foetuses. Interestingly, *HIF1A* endometrial expression was increased in endometrial samples supplying the lightest foetuses compared to the CTMLW foetuses at GD45 and the direction of this

difference was switched at GD60. At GD60, *CD31* expression was also decreased in the placentas supplying the lightest foetuses compared to the CTMLW foetuses.

Generally, in the *in vitro* branching experiments a decrease in endothelial cell branching was observed in response to the conditioned media from the placental and endometrial samples supplying the lightest foetuses compared to the CTMLW foetuses. In response to the placental conditioned media, this was observed at both GD investigated. However, the influence of foetal size was more pronounced at GD45 than at GD60. This to a certain extent would reinforce the CD31 expression data and the additional evidence in previous chapters and papers (Blomberg *et al.*, 2010) to suggest the presence of a compensation mechanism developing around this stage of gestation. Whilst the differences in the angiogenic ability at GD60 are not as pronounced as at GD45, they are still present. This may potentially indicate that the attempt of the placentas supplying the lightest foetuses to 'catch up' through increased angiogenesis is ultimately not going to be successful in rescuing the foetal growth restriction.

In the endometrial assays, foetal size influenced endothelial cell branching, with conditioned media from the small feto-placental units decreasing the branching ability compared to the CTMLW foetuses. Whilst the influence of foetal size was not as pronounced as that observed in the placental samples, the direction of the difference was the same, with the lightest foetuses inducing less endothelial cell branching at both GD.

8.6.4 Foetal Sex Influenced Endothelial Cell Branching in Response to both Placental and Endometrial Conditioned Media

In Chapter 7, the influence of foetal sex on placental and endometrial vascularity and angiogenesis were assessed by immunohistochemistry and qPCR. As discussed in previous chapters, recent literature has suggested sexual dimorphism in placental development (Clifton, 2010; Buckberry *et al.*, 2014; Rosenfeld, 2015; Kalisch-Smith *et al.*, 2017b) therefore it was

hypothesised that foetal sex may influence placental gene expression. Intriguingly, in Chapter 7 foetal sex was shown to have a minimal influence on placental gene expression and no relationships between the CD31 immunohistochemistry analysis and foetal sex were observed. Despite this, striking differences were observed the endometrium, with foetal sex influencing the expression of all the genes investigated by qPCR and the number of blood vessels in the endometrial stroma at GD45.

As stated previously, the *in vitro* branching assays were performed in this chapter to attempt to validate the results from Chapter 7. Unfortunately, due to the same limitations at GD45 discussed previously in this thesis, it was not possible to assess the influence of foetal sex on *in vitro* branching ability at this stage of gestation. The results from this chapter support those presented in Chapter 7, showing that foetal sex had a striking effect on endothelial cell branching. In the current chapter endometrial conditioned media from male foetuses had a greater effect on branching compared to media from females at GD60. The reverse of this was observed in the placenta, with increased endothelial cell branching observed in response to conditioned media from placentas supplying female foetuses compared to male foetuses. This intriguing finding that foetal sex influences endothelial cell branching *in vitro* in response to placental conditioned media which was not observed in Chapter 7 warrants much further investigation. This may suggest that other parts of the angiogenic pathway are altered by foetal sex that have not been investigated in this thesis. Conditioned media has been utilised in these experiments, which had the advantage of allowing direct comparison of the influence of the proteins secreted by each tissue on endothelial cell branching. However, it is important to recognise that despite this the experimental conditions used are biologically removed from the *in vivo* function of the placenta and therefore the significance of these findings should not be over-exaggerated.

These novel and exciting findings relating foetal sex to angiogenesis and vascularity at the feto-maternal interface need to be investigated thoroughly. Initially, repeating the current experiment with conditioned media from placentas supplying foetuses of different sex should be performed throughout

gestation in both tissues to allow the mRNA, immunohistochemistry, and *in vitro* branching assays to be directly compared with one another. Considering these findings, it would also be advisable to investigate other parts of the angiogenic pathways, for example endothelial nitric oxide synthase (eNOS) and placental growth factor (PlGF), to attempt to determine if other points of the pathways of interest are altered.

8.6.5 Additional issues which should be addressed

The short-term tissue culture experiments to generate the conditioned media were carried out in advance of deciding to perform the branching assays detailed in this chapter. Because of this, serum was added to the media to attempt to ensure that the integrity of the tissues was maintained throughout the culture period. However, serum itself contains a variety of molecules which may themselves be angiogenic therefore, this may influence the angiogenic ability of the cells. In this chapter, this has been addressed, with all parameters investigated being expressed relative to the media only control, which contained the same percentage of serum. However, if this experiment was to be repeated in the future, minimising, or eliminating the serum from the cultures may be advisable.

As described in 4.1, there are several different *in vitro* and *in vivo* assays available to assess angiogenesis, each of which has a series of advantages and disadvantages. For this chapter, the decision was made to use the *in vitro* Matrigel branching assay, due to the availability of resources and the advantages and disadvantages detailed in 4.1. However, the results of these *in vitro* assays should not be extrapolated to the *in vivo* potential as this two-dimensional culture system cannot fully reflect the process *in vivo* (Xie *et al.*, 2016). Therefore, it would be advisable to perform an additional assay to compare the results obtained.

The chick CAM assay was attempted to investigate the angiogenic potential of placental and endometrial samples (results not shown in this thesis). This assay offered several advantages, including ease of use and ability to upscale,

detailed in 4.1. However, the results obtained using this approach were extremely variable within all groups, and it was felt that the technique was not robust enough to identify what were expected to be quite subtle differences between the groups of interest. An alternative approach which may be more appropriate to address the questions of interest would be the use of the rat aortic ring model which has more similarities with the *in vivo* conditions, and would allow investigation into pericyte recruitment in the angiogenesis process (Nicosia, 2009).

8.6.6 Future Studies

To further improve the knowledge and understanding of the relationship between foetal size and sex and placental and endometrial angiogenesis, several additional experiments should be performed. Additional experiments could be performed using the conditioned media generated from the short-term cultures (Figure 8.1). Mass spectrometry could be performed to identify: 1) which molecules were secreted by the tissues of interest and 2) differential secretion of the molecules, over the culture period between tissues supplying foetuses of different size and sex. These results could then be validated by ELISA and any candidates of interest could also be investigated by qPCR on the placental and endometrial samples that were used in Chapter 7. To improve the understanding of what happens to endothelial cells in response to treatment with conditioned media, RNA could be extracted from the cells following completion of the assay and qPCR or RNASeq could be used to identify pathways which are up or down regulated. Based on these results, the experiments could be repeated with the addition of a candidate molecule or siRNAs to determine if the observed effects on branching ability could be rescued or inhibited.

To overcome some of the limitations discussed and to further improve the understanding of the mechanisms governing angiogenesis at the feto-maternal interface in pigs, it would be useful to isolate primary endothelial cells from placental and endometrial samples supplying foetuses of different size and sex

throughout gestation by Fluorescent Activated Cell Sorting (FACS) or the use of magnetic beads (van Beijnum *et al.*, 2008; Kaczynski *et al.*, 2016). The Matrigel branching assays could then be repeated using these cells. However, due to common limitations associated with culturing primary cells, including loss of expression of markers and concerns over the duration of culture this should be performed between passages 2 and 6 (DeCicco-Skinner *et al.*, 2014). This would provide an exciting and novel opportunity to investigate whether it is the endothelial cells themselves that have differential branching abilities or whether it is the secretion/expression of factors by the placenta or endometrium that is causing the differences in angiogenesis and vascularity observed in this thesis. This would allow direct comparison between the tissue perspective (the use of conditioned media as described in this chapter) and the cellular perspective. Additionally, this would provide an exciting opportunity to attempt to rescue the phenotype/branching ability of these cells, either by the addition of specific molecules or by addition of the conditioned media generated from the other treatment groups.

8.6.7 Conclusion

The results of the *in vitro* endothelial cell branching assays described in this chapter have demonstrated that porcine placental and endometrial conditioned media can be successfully used to investigate endothelial cell branching *in vitro*. The novel finding of an association between foetal size, and more intriguingly foetal sex, and endothelial cell branching ability in response to conditioned media from both placental and endometrial samples is exciting and warrants much further investigation into the mechanisms behind these differences.

9 General Discussion

Genetic selection has successfully increased the number of piglets weaned per sow per year. However, this increase has unfortunately been accompanied by increased within-litter variation in piglet size and an increased prevalence of growth restricted piglets (Quiniou *et al.*, 2002). The phenotype of these piglets cannot be rescued post-natally, making them a significant burden to the industry (Wu *et al.*, 2006). It is therefore essential to improve the understanding of the mechanisms governing foetal growth in the pig, with a long-term aim to increase the within-litter uniformity in piglet weight at birth, whilst maintaining healthy birthweights and thereby increasing the number of piglets weaned per sow per year (Bee, 2007).

Male new-born piglets have a survival disadvantage compared to their female littermates (Baxter *et al.*, 2012) which is a significant problem to the pork industry. Considering the recent evidence to suggest sexual dimorphism in human placental development (Rosenfeld, 2015; Kalisch-Smith *et al.*, 2017a), it could be hypothesised that sexual dimorphism in gene expression and vascularity of the feto-maternal interface in the pig may lead to this survival disadvantage post-natally.

The research presented in this thesis has utilised complementary analytical approaches to improve the knowledge of the relationship between foetal size, sex, and integrin signalling, apoptosis and proliferation, umbilical arterial (UA) blood flow, and angiogenesis and vascularity at the feto-maternal interface at five key stages of gestation (gestational day (GD) 18, 30, 45, 60 and 90).

9.1 Discussion Points and Limitations of the Study

All the pigs that provided samples used in this thesis were gilts, to eliminate variations associated with different parities. The gilts used were of the same genotype from the same herd, which provided an additional level of control in the experiment. Similar effects would be expected in sows. However, the experiments should be repeated to confirm this. The use of only gilts was

effective when investigating the general litter characteristics, as discussed in chapter 3. Unfortunately, it was not possible to obtain semen from the same desired sire throughout the three sample collections and multiple sires had to be used. Whilst this is undesirable, the sires used were from the same herd and were often related to one another therefore a similar degree of heterosis would be expected. In addition, their use was distributed between the GD investigated where possible to further limit the influence of sire on the results obtained. Similarly, it would have been preferable not to use pregnant mare serum gonadotrophin (PMSG) to induce ovulation however, this was not within our control. Despite the use of PMSG, litter size (LS), percentage prenatal survival (PPS) and ovulation rate (OR) were not statistically different between animals which were treated with PMSG and those that were not at GD30-90 (data not presented), which suggests that the PMSG treatment would have had very little influence on the data presented throughout this thesis. As only one animal had PMSG treatment at GD18, it was not possible to statistically analyse the data however, considering it did not have an effect at GD30-90, it would not be anticipated to have an effect.

The sample collections performed at GD18 were extremely challenging and had not been optimised in the Ashworth laboratory previously. In one animal, an exceptionally large ovulation rate was recorded however, there is a possibility that we are not confident in this result due to it being the first occasion where the individual who recorded the number had dissected c*orpora lutea* (CL) from ovaries. Although the high ovulation rate obtained from this animal did skew the PPS and OR statistics, the animal was included in the analyses detailed in this thesis. Consistently, outliers were tested for in the data set. The samples obtained from this animal were not seen as outliers in the analyses performed and therefore, considering the small number of litters obtained at GD18, they were included in the experiments performed in this thesis. In addition, in the first two sample collections at GD18, the number of conceptuses present exceeded the number of CL present on the ovaries. This has been previously described in the pig (Ashworth *et al.*, 1990, 1997, 1998; Ashworth and Antipatis, 1999) and a number of potential explanations for this

exist. Multi-oocyte follicles are known to be present in the pig (Ashworth *et al.*, 2016) and arise from incomplete breakdown of the germ cell nests (Tingen *et al.*, 2009). This could lead to release of multiple oocytes during ovulation, leading to increased fertilisation compared to the number of CL present. Alternatively, mono-zygotic twins have been observed in the pigs to occur in the pig (Ashworth *et al.*, 1998) which again could explain this difference. More likely, this difference arose due to technical issues when isolating the porcine conceptuses from the uterine lumen. The porcine conceptuses are extremely delicate and difficult to handle at this stage of gestation, therefore it is possible that individual conceptuses were fragmented during recovery from the uterus. In the future, nucleic acids should be isolated from these conceptuses to ensure that the conceptuses collected are individuals by sequencing or the use of technologies such as DNA fingerprinting (Ashworth *et al.*, 1998). In addition, this would allow the conceptuses to be sexed, which in turn would allow investigation into the signalling between conceptuses of different sex and the endometrium during implantation. Another potential limitation of the results presented in this study is that at GD45 in only one of the six litters investigated was the lightest foetus a male. This was a significant limitation to the analysis of potential sex x size interactions throughout this thesis.

Isolating RNA of an acceptable quality from porcine placentas is extremely challenging compared to other tissues, such as the endometrium (Hernández, 2012). Whilst an optimised method for obtaining high quality RNA was utilised (Hernández *et al.*, 2013), the GD90 placentas proved particularly challenging to obtain RNA of sufficient quality from. The porcine placenta has a high lipophilic content which can make RNA extractions particularly challenging (McNeil *et al.*, 2007). Further, the porcine placenta is rich in endogenous RNases which, over the course of the dissection period, will begin degrading the placental RNA. Whilst the placental and endometrial samples were snap-frozen for RNA as soon as possible, the sample collection process was quite lengthy (1-2.5 hours after maternal barbiturate overdose) due to the large numbers of samples collected and the measurements made. This was especially true at GD90 as foetal cardiac injection with sodium pentobarbitone

had to be performed, which further increased the time between maternal death and preservation of the samples for RNA. Considering this, throughout this thesis the RNA samples utilised were limited and again particularly limited the sex x size interactions possible.

In this thesis, angiogenesis, cell proliferation and apoptosis, and integrins were analysed as distinct biological phenomena. It is important to note however that due to the dynamic nature of the feto-maternal interface, these pathways interact with one another. For example, it has previously been suggested that endometrial stromal secreted phosphoprotein 1 protein (SPP1) expression is positively related to von Willebrand factor staining, and SPP1 can induce endothelial cell angiogenesis *in vitro* in the sheep (Dunlap *et al.*, 2008). Analysis of GD9, 12 and 15 porcine endometrial samples identified the presence of a 32kDA fragment of SPP1, which is known to bind to the cell surface of endothelial cells (Erikson *et al.*, 2009b; Bayless *et al.*, 2010). *In vitro* experiments using blood samples from newborn piglets demonstrated that SPP1 has a positive effect on the migration and adhesion of endothelial cells, suggesting a potential role in regulating placental and endometrial angiogenesis. Further, the receptor for SPP1, Integrin αVβ3, interacts with the endothelial cell marker Platelet and Endothelial Cell Adhesion Molecule 1 (CD31) (Wong *et al.*, 2000; Humphries, 2006), providing an additional link between integrin signalling and angiogenesis.

Table 9.1 and Table 9.2 summarise some of the central results of interest within GD and tissue presented in this thesis from the different aspects investigated.

9.2 Points for Discussion - Size

One of the broad objectives of this thesis was to investigate the relationship between foetal size and gene expression at the feto-maternal interface. From GD18, large variation in conceptus weight was observed within-litter, supporting the previous literature which suggests that large variation in conceptus size can be observed early in gestation. However, considering

these large differences, conceptus size had limited associations with gene expression at GD18. To date, RNA has not been isolated from the GD18 conceptuses as they are part of a larger project. However, considering associations between foetal size and gene expression observed in mid and late gestation (

Table 9.1), it could be hypothesised that foetal size would be associated with conceptus gene expression, presumably in the trophectoderm cells which go on to form the placenta (Figure 9.1). Alternatively, as a candidate gene approach was utilised in the current study, additional genes which have not been investigated may have impaired expression at the feto-maternal interface.

Considering this large variation in size observed from early in gestation, it could be hypothesised that there is a large range in developmental stage at the time of attachment, which could be attributed to a large range in timing of fertilisation and/or the variation in the rate of development between fertilisation and attachment. This may suggest that ovulation in these pigs is occurring over a long period of time therefore, if interventions were performed to ensure uniformity in the timing of ovulation, this may be a successful method in decreasing the within-litter variation in foetal size.

Whilst foetal size has previously been demonstrated to be associated with placental development and gene/protein expression (discussed in previous chapters), limited investigations have been performed on the associated endometrial tissue. Chen *et al.*, (2015) demonstrated that both placental and endometrial samples associated with growth restricted porcine foetuses had impaired expression of proteins involved in energy metabolism, proliferation, cellular structure, nutrient metabolism and transport at GD60, 90 and 100. The results presented in this thesis suggest that the endometrium is highly associated with foetal size from GD30 of gestation and intriguingly does not necessarily mirror the findings observed in the placenta. Considering this, and the association between foetal size and endometrial gene expression from as early as GD30, this may suggest the presence of differential signalling early in gestation (for example in the peri-implantation period) between conceptuses of differing size and the endometrium (Figure 9.1).

Importantly, in both placental and endometrial samples, switches in the direction of differences in gene expression were observed (Table 9.1). The temporal changes in the relationship between foetal size and gene expression highlight the dynamic nature of the feto-maternal interface. Importantly, the temporal changes in gene expression often occurred between GD45 and 60, which presumably reflects the extensive remodelling of the feto-maternal interface during this period of gestation discussed in previous chapters. Further, the differences in gene expression observed in one tissue may not necessarily be observed in the other e.g. P53 expression was decreased in placental samples associated with the lightest foetuses compared to the CTMLW foetuses at GD45 but the reverse was observed in the endometrium. These findings highlight the importance of investigating multiple periods of gestation and the placenta and endometrium separately when investigating the relationship between aberrant foetal growth and the feto-maternal interface.

Considering the association between foetal size and vascularity during this period, interventions such as the administration of Viagra (Sildenafil citrate) to the gilt/sow during placental development and this period of remodelling and initiation of the second wave of angiogenesis may be a successful intervention to increase blood flow and nutrient supply. Similar experiments in the rat (Dilworth *et al.*, 2013) and sheep (Satterfield *et al.*, 2010) have reported increased foetal weights in models of growth restriction therefore it would be hypothesised to minimise the within-litter variation in piglet size, whilst improving the post-natal outcome for the growth restricted piglets.

As described above, Dunlap *et al.*, (2008) has suggested that a positive relationship exists between SPP1 and uterine vascularity in the sheep. At GD60, *SPP1* and *CD31* expression, blood vessel number and endothelial cell branching were all decreased in endometrial samples associated with the lightest foetuses compared to the Closest to Mean Litter Weight (CTMLW) foetuses (

Table 9.1). The results presented in this thesis have provided novel and intriguing insights into the feto-maternal interface in foetuses of differing size.

Although, further investigations of other candidate genes in the pathways investigated and validation on a protein level should be performed.

9.3 Points for Discussion - Sex

As described in the general introduction, recent investigations have suggested that sexual dimorphism in placental development may explain sexual dimorphism in disease susceptibility postnatally in humans. However, despite the intriguing data to suggest sexual dimorphism in placental development in humans, this area remains poorly understood in the pig. The results presented in this thesis support the findings in other species and suggest that sexual dimorphism exists in placental gene expression (Table 9.2). In addition, the novel finding that foetal sex is associated with endometrial gene expression furthers the suggestion of sexual dimorphism in the development of the feto-maternal interface (Table 9.2). Interestingly, foetal sex was associated with endometrial expression of *CD31*, Prostaglandin F2α Receptor (*PTGFR*), Vascular Endothelial Growth Factor A (*VEGFA*), Fibronectin (*FN*) and Bcl-2-associated X protein (*Bax*), with endometrial samples supplying male foetuses having decreased expression. These candidate genes are involved in angiogenesis, integrin signalling and apoptosis suggesting that foetal sex is not simply altering the expression of one pathway. Foetal sex was demonstrated to be associated with endometrial, but not placental, gene expression at GD30 which is an intriguing finding that warrants further investigation. At this stage, based on the information available, the proposed mechanisms behind these differences are purely speculative.

In bovine GD19 conceptuses, Forde *et al.*, (2016) demonstrated that >5000 transcripts were differentially expressed in conceptuses of different sex, highlighting the early development of sexual dimorphism in foetal development. Considering this, and the demonstration that porcine male conceptuses have an increased growth rate compared to female conceptuses from GD10 (Cassar *et al.*, 1994), it would be highly likely that sexual dimorphism in conceptus gene expression/protein secretion would be

observed during implantation in the pig. This would be proposed to ‘prime’ the uterus differently for foetuses of different sex, resulting in differential gene and protein expression. Alternatively, it could be proposed that male and female conceptuses ‘prefer’ different areas of the uterus however, the sex of the neighbour results (chapter 3) suggest that male and female foetuses do not cluster together which would not support this theory.

In this study, a suggestion of SPP1 regulating endometrial angiogenesis at GD60 was described above. This was also observed in the foetal sex analysis, with endometrial samples associated with male foetuses having increased Uteroferrin (*ACP5*), *CD31*, *VEGFA* and *SPP1* expression at GD60, again supporting the interaction between SPP1/integrin signalling and angiogenesis (Wong *et al.*, 2000; Humphries, 2006; Dunlap *et al.*, 2008).

Considering the intriguing and novel finding of the association between foetal sex and both endometrial gene expression and angiogenic ability, further investigations should be performed to investigate early interactions between the conceptus and the endometrium. To investigate this further, sexed semen could be utilised (Johnson *et al.*, 2005; Rath and Johnson, 2008). Semen carrying an X or Y could be used to fertilise oocytes *in vitro,* with the embryos allowed to mature to the blastocyst stage (Figure 9.2). Following this, embryos of different sex could then be transferred to each uterine horn, with the horn separated using ligatures to prevent embryo migration. The embryos would be allowed to mature *in vivo* until the desired GD of interest. Initially it may be interesting the flush embryos from each uterine horn at GD10, 12 and 14 and investigate sexual dimorphism in conceptus gene expression in early migration. Additionally, at GD18 the uterine tract could be dissected as described in the current study and RNA sequencing could be performed on the endometrial and conceptus samples. These experiments would not only allow assessment of sexual dimorphism in early embryo development, but it would also allow assessment of sexual dimorphism of the endometrial transcriptome.

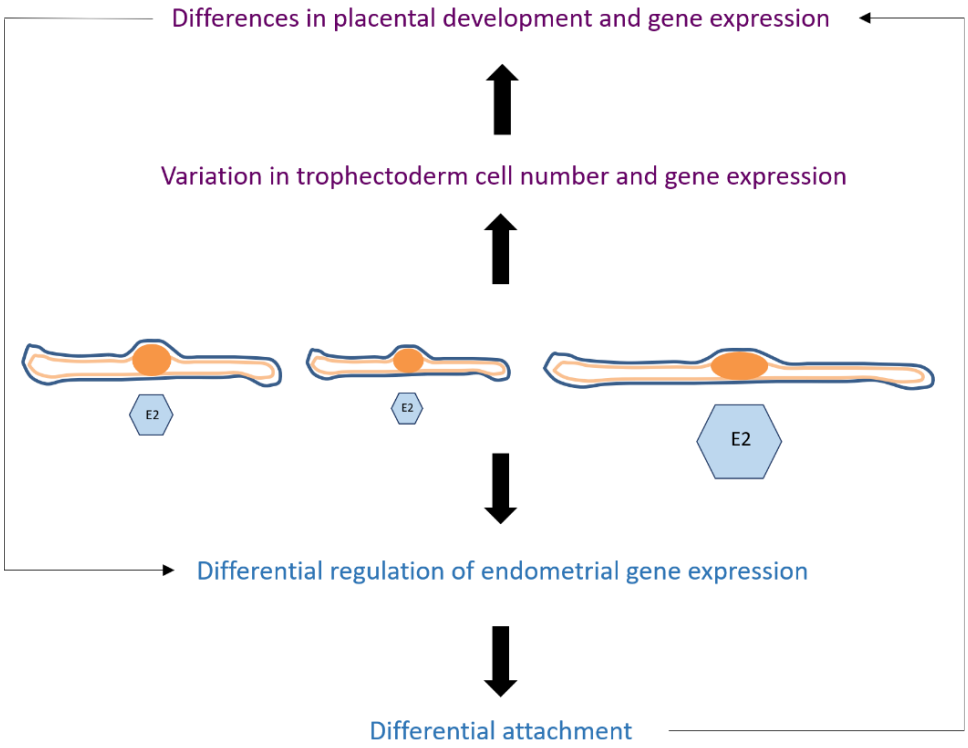

Figure 9.1: Proposed Mechanisms to Explain the Relationship between Conceptus Size and Gene Expression at the Feto-Maternal Interface.

Variation in conceptus size exists during the peri-implantation period which results in differential secretion of oestradiol-17β (E2) (and potentially other molecules) by the conceptuses. E2 is known to regulate endometrial gene expression during implantation and this would therefore result in differential gene expression in endometrial tissue associated with the lightest conceptuses compared to the closest to mean litter weight (CTMLW) conceptuses. In turn, this would result in impaired attachment, which would result in impaired placental development and altered placental gene expression. Alternatively, the smaller conceptuses would have fewer trophectoderm cells during implantation than larger conceptuses and, considering the difference in developmental stage, would not have optimal gene expression. As the trophectoderm proceeds to form the placenta this would result in impaired placental development which, due to the cross talk between the conceptus and the endometrium, may result in altered gene expression in the endometrial samples associated with the lightest foetuses compared to the CTMLW foetuses during and after placental development.

Tissue	Gestational Day				
	18	30	45	60	90
Placenta	n/a	ns	*ITGα2* *P53* *Ki67* *CD31* Branching	*P53* *ACP5* *CD31* CD31 CAM Staining Branching	*ITGα2* *HIF1A* CD31 CAM Staining
Endometrium	ns	*ITGB5*	*P53* *HIF1A* *ITGβ1* Branching	*SPP1* *HIF1A* Total and Mean BV Number *CD31* Branching	*HPSE* *VEGFA* Mean Number of Uterine Glands

Table 9.1: Summary of Results which showed statistically significant effects of foetal size.

Green=Increased; Red=Decreased in samples associated with the lightest foetuses compared to their Closest to Mean Litter Weight (CTMLW) littermates. Abbreviations: ITG=Integrin Subunit, P53=tumour suppressor protein 53, CD31=Platelet and Endothelial Cell Adhesion Molecule 1, ACP5=Uteroferrin, HIF1A=Hypoxia Inducible Factor 1 Alpha Subunit, HPSE=Heparanase, SPP1=Secreted Phosphoprotein 1, VEGFA=Vascular Endothelial Growth Factor A, BV=Blood Vessel; CAM=Chorioallantoic Membrane, ns=not significant, n/a=not applicable.

Tissue	Gestational Day			
	30	45	60	90
Placenta	ns	*Bax* *ITGβ6*	*Bcl2* *P53* *Ki67* Branching	*FN* *HIF1A*
Endometrium	*CD31* *PTGFR* *VEGFA* *FN* *Bax*	Total Number of Uterine Glands Total and Mean Number of BV *HPSE*	*Bcl2* *P53* *Ki67* *SPP1* *ACP5* *CD31* *VEGFA* *HIF1A* Branching *ITGβ3*	*HIF1A*

Table 9.2: Summary of Results which showed statistically significant effects of foetal sex.

Green=Increased; Red=Decreased in samples associated with the male foetuses compared to their female littermates. Abbreviations: ITG=Integrin Subunit, P53=tumour suppressor protein 53, CD31= Platelet and Endothelial Cell Adhesion Molecule 1, ACP5=Uteroferrin, SPP1=Secreted Phosphoprotein 1, VEGFA=Vascular Endothelial Growth Factor A, PTGFR=Prostaglandin F2α Receptor, FN=Fibronectin, Bax=Bcl-2-associated X protein, Bcl2= B-cell lymphoma 2, BV=Blood Vessel, ns=not significant, n/a=not applicable.

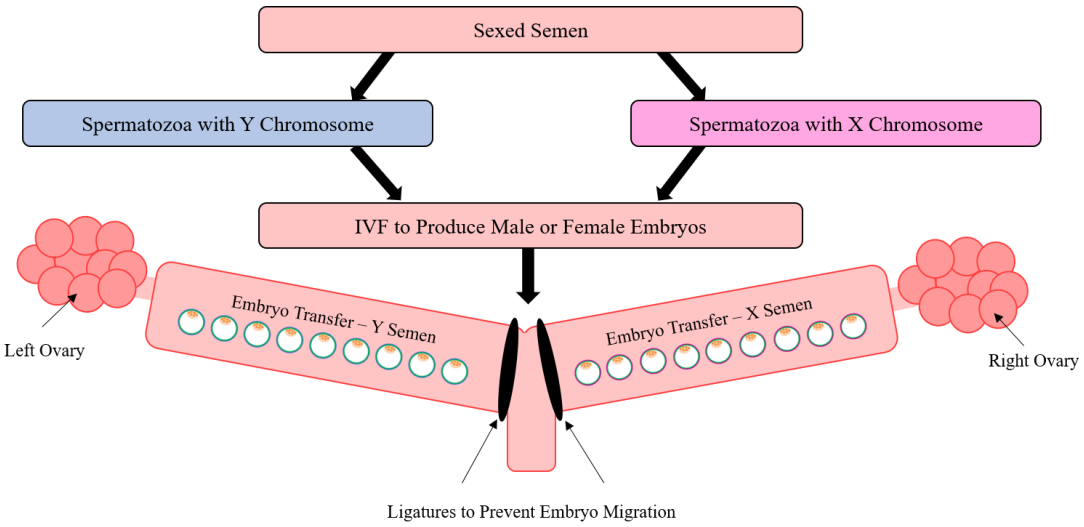

Figure 9.2: Use of Sexed Semen to Investigate the Relationship between Conceptus Sex and Endometrial Gene Expression.

Sexed semen could be utilised to fertilise oocytes *in vitro* (IVF) to produce male or female embryos of known sex. These embryos could then be transferred to the recipient female pig, with foetuses of different sex in separate uterine horns, and sexual dimorphism in conceptus gene expression and endometrial transcriptome could be investigated.

9.4 Future Investigations

9.4.1 RNA Sequencing

The results presented in this thesis have demonstrated temporal, foetal size and sex associated changes in both placental and endometrial mRNA expression. Whilst these results are novel and interesting, they have involved the investigation of the expression of genes have been selected based on their function. An alternative approach would be to perform RNA sequencing on the same samples throughout gestation to investigate temporal changes, alongside the association between foetal size and sex on mRNA expression. This would be a hypothesis generating approach whereby differentially expressed genes and pathways would be identified which could be investigated further.

9.4.2 MicroRNAs

MicroRNAs (miRNAs) are short 18-22 nucleotide long RNA molecules which regulate mRNA activity by repressing translation or destabilising the mRNA (Bidarimath *et al.*, 2014). It is estimated that miRNAs regulate the translation of approximately 60% of mRNAs and are therefore under considerable scientific interest (Friedman *et al.*, 2009), with miRNAs playing a central role in the regulation of angiogenesis and cell death and proliferation (Hwang and Mendell, 2006; Caporali and Emanueli, 2011). Importantly, miRNAs have been demonstrated to play a central role in the establishment and maintenance of pregnancy in mice and humans (Morales-Prieto and Markert, 2011; Morales-Prieto *et al.*, 2012, 2013; Bidarimath *et al.*, 2014). Further, aberrant placental miRNA expression has been heavily implicated in pregnancy pathologies including intrauterine growth restriction (IUGR) and pre-eclampsia (Pineles *et al.*, 2007; Zhang *et al.*, 2012; Guo *et al.*, 2013; Higashijima *et al.*, 2013; Huang *et al.*, 2013; Chiofalo *et al.*, 2017; Thamotharan *et al.*, 2017). Similarly, aberrant miRNA expression has been observed in endometrial samples from women suffering from recurrent implantation failure (Revel *et al.*, 2011), endometriosis, dysfunctional bleeding and endometrial cancer (reviewed by Pan and Chegini,

2008). As discussed in the general introduction, it has been suggested that sexual dimorphism in placental development contributes to sexual dimorphism in postnatal disease susceptibility in response to adverse prenatal conditions. This has also been suggested in relation to miRNA expression, with differential placental miRNA expression in response to maternal obesity reported, leading to inhibition of mitochondrial respiration and placental dysfunction in females compared to males (Muralimanoharan *et al.*, 2015).

Whilst considerable investigations have been performed in the role of miRNAs in pregnancy in humans and mice, limited investigations have been performed in the pig. A potential role of miRNAs in the establishment of pregnancy has been suggested in the pig (Wessels *et al.*, 2013; Su *et al.*, 2014; Krawczynski *et al.*, 2015a, b). Angiogenesis associated miRNAs have been reported to be present in extracellular vesicles which mediate intracellular communication at the feto-maternal interface in the pig at GD20 (Bidarimath *et al.*, 2017). Recent investigations have identified that specific miRNAs can be identified in the serum of pregnant gilts at GD16 that are the result of interactions occurring between the conceptus and the endometrium during attachment (Reliszko *et al.*, 2017). In addition to the role in the establishment of pregnancy, Su *et al.*, (2010) have observed temporal changes in porcine placental miRNA expression at GD30 and 90 which, considering the temporal changes in mRNA expression observed in the current study, is not surprising. The role of miRNAs at the feto-maternal interface in foetal growth has not been determined in the pig although, differential conceptus and endometrial miRNA expression has been observed between arresting and viable conceptuses.

Based on the results described in the recent studies in the pig, miRNAs should be considered to have a central role of regulating mRNA expression at the feto-maternal interface. A comprehensive miRNA sequencing experiment should be performed at multiple GD to improve the understanding of the dynamics and temporal changes in miRNA expression during gestation. Further, the sequencing experiment could be performed using placental and endometrial samples associated with the lightest compared to the CTMLW, male and female foetuses throughout gestation to identify differentially

expressed miRNAs. Whilst this analysis would improve the understanding of the relationship between foetal size, sex and the expression of miRNAs at the feto-maternal interface, the mRNA targets of these miRNAs could also be investigated. If both mRNA and miRNA sequencing was performed on the same RNA samples, the data sets could be compared to identify target genes and pathways to investigate further.

9.4.3 Epigenetics

The preimplantation embryo undergoes high levels of epigenetic modifications (Seisenberger *et al.*, 2013), making the epigenetic modification of DNA at the feto-maternal interface another potential avenue for future investigation (epigenetic modifications reviewed by Golbabapour *et al.*, 2011). DNA methylation (an epigenetic modification) has been highly implicated in trophoblast cell migration and invasion in humans (Rahnama *et al.*, 2006). Similarly in the rat, DNA methylation has been suggested to regulate placental development and be associated with pregnancy outcome (Šerman *et al.*, 2007).

A number of recent studies have investigated the relationship between placental DNA methylation and foetal size. Investigations in monozygotic monochorionic twins using genome wide methylation analyses have revealed impaired lipid metabolism, Wingless-type MMTV integration site family (Wnt) and cadherin signalling in placentas associated with growth restricted offspring compared to their normally-grown twin (Roifman *et al.*, 2016). In addition to the genome wide analysis performed, Xiao *et al.*, (2016) investigated DNA methylation levels of genes that play a central role in placental function. Interestingly, a positive relationship between DNA methylation of Insulin Growth Factor 2 (IGF2) and Aryl-Hydrocarbon Receptor Repressor (AHRR), and birth weight was observed. In contrast, a negative relationship between 11 β-hydroxysteroid dehydrogenase type 2 (11βHSD2) and Wingless-type MMTV integration site family, member 2 (WNT2) DNA methylation levels, and birth weight was observed. Impaired DNA methylation has also been observed

in human placentas complicated by IUGR (Bourque *et al.*, 2010; Tabano *et al.*, 2010), highlighting the role of DNA methylation of this gene in foetal development. In addition to DNA methylation in the placenta, it has been suggested that epigenetic changes regulate the menstrual cycle in humans (Munro *et al.*, 2010). Further, it has been reported that DNA methylation of e-cadherin is important in the regulation of endometrial receptivity (Rahnama *et al.*, 2009). As it is hypothesised that IUGR in the pig can be attributed to impaired conceptus attachment, this would be an interesting avenue to investigate further.

In addition to a relationship between placental epigenetic modifications and foetal size, it has recently been suggested that sexual dimorphism in DNA methylation and the expression of enzymes involved in epigenetic modifications (Kdm5x, Kdm5d and Dnmt3l) exists in the mouse (Gallou-Kabani *et al.*, 2010; Gabory *et al.*, 2012). Considering the proposed relationship between foetal size, sex and placental DNA methylation in other species, it could be hypothesised that similar findings would be observed at the porcine feto-maternal interface.

9.5 Conclusion

The research presented in this thesis has utilised complementary analytical approaches to gain a more integrated understanding of the relationship between foetal size and sex, and the feto-maternal interface throughout gestation in the pig. This thesis has presented novel findings of associations between foetal size and sex, and placental and endometrial integrin signalling, apoptosis and proliferation, and angiogenesis and vascularity. This is the first suggestion in the literature that foetal size, and more intriguingly foetal sex, may have a strong influence on the activity of the endometrium however, the mechanisms behind these findings are not fully understood and warrant further investigation. Switches in the direction of differences at the feto-maternal interface between foetuses of different size were observed throughout gestation, notably between GD45 and 60, highlighting the dynamic nature of

the feto-maternal interface; suggesting this as a potential window that could be manipulated by the industry to attempt to rescue the postnatal phenotype of IUGR piglets.

References

Abbas A and Nicolaides KH (1994) Serum ferritin and cobalamin in growth retarded fetuses. *British Journal of Obstetrics and Gynaecology* **101** 215–219.

Abi-Nader KN, Mehta V, Wigley V, Filippi E, Tezcan B, Boyd M, Peebles DM and David AL (2010) Doppler ultrasonography for the noninvasive measurement of uterine artery volume blood flow through gestation in the pregnant sheep. *Reproductive Sciences* **17** 13–19.

Acharya G, Erkinaro T, Mäkikallio K, Lappalainen T and Rasanen J (2004) Relationships among Doppler-derived umbilical artery absolute velocities, cardiac function, and placental volume blood flow and resistance in fetal sheep. *American Journal of Physiology. Heart and Circulatory Physiology* **286** H1266–H1272.

Acharya G, Sitras V, Erkinaro T, Mäkikallio K, Kavasmaa T, Päkkilä M, Huhta JC and Räsänen J (2007) Experimental validation of uterine artery volume blood flow measurement by Doppler ultrasonography in pregnant sheep. *Ultrasound in Obstetrics and Gynecology* **29** 401–406.

Adibi JJ, Lee MK, Saha S, Boscardin WJ, Apfel A and Currier RJ (2015) Fetal sex differences in human chorionic gonadotropin fluctuate by maternal race, age, weight and by gestational age. *Journal of Developmental Origins of Health and Disease* **6** 493–500.

Adibi J, Burton GJ, Clifton V, Collins S, Frias AE, Gierman L, Grigsby P, Jones H, Lee C, Maloyan A *et al.* (2017) IFPA meeting 2016 workshop report II: Placental imaging, placenta and development of other organs, sexual dimorphism in placental function and trophoblast cell lines. *Placenta* **xxx** 1–5.

Ahmad S and Ahmed A (2005) Antiangiogenic Effect of Soluble Vascular Endothelial Growth Factor Receptor-1 in Placental Angiogenesis. *Endothelium* **12** 89–95.

Albertini DF, Overstrom EW and Ebert KM (1987) Changes in the Organization of the Actin Cytoskeleton during Preimplantation Development of the Pig Embryo. *Biology of Reproduction* **37** 441–451.

Al-Khaldi A, Eliopoulos N, Martineau D, Lejeune L, Lachapelle K and Galipeau J (2003) Postnatal bone marrow stromal cells elicit a potent VEGF-dependent neoangiogenic response in vivo. *Gene Therapy* **10** 621–629.

Allaire AD, Ballenger KA, Wells SR, McMahon MJ and Lessey BA (2000) Placental apoptosis in preeclampsia. *Obstetrics and Gynecology* **96** 271–276.

Ananth C V and Vintzileos AM (2009) Distinguishing pathological from constitutional small for gestational age births in population-based studies. *Early Human Development* **85** 653–658.

Anderson LL and Parker RO (1976) Distribution and development of embryos in the pig. *Journal of Reproduction and Fertility* **46** 363–368.

Anegon I, Cuturi MC, Godard A, Moreau M, Terqui M, Martinat-Botté F and Soulillou JP (1994) Presence of leukaemia inhibitory factor and interleukin 6 in porcine uterine secretions prior to conceptus attachment. *Cytokine* **6** 493–499.

Ansari B, Coates PJ, Greenstein BD and Hall PA (1993) In situ end-labelling detects

DNA strand breaks in apoptosis and other physiological and pathological states. *Journal of Pathology* **170** 1–8.

Ao A, Erickson RP, Winston RML and Handyside AH (1994) Transcription of Paternal Y-Linked Genes in the Human Zygote as Early as the Pronucleate Stage. *Zygote* **2** 281–287.

Aplin JD (1997) Adhesion molecules and implantation. *Reviews of Reproduction* **2** 84–93.

Aplin JD, Seif MW, Graham RA, Hey NA, Behzad F and Campbell S (1994) The Endometrial Cell Surface and Implantation: Expression of the Polymorphic Mucin MUC-1 and Adhesion Molecules during the Endometrial Cycle. *Annals of the New York Academy of Sciences* **734** 103–121.

Apparao KBC, Illera MJ, Beyler SA, Olson GE, Osteen KG, Corjay MH, Boggess K and Lessey BA (2003) Regulated Expression of Osteopontin in the Peri-Implantation Rabbit Uterus. *Biology of Reproduction* **68** 1484–1490.

Arnaoutova I and Kleinman HK (2010) In vitro angiogenesis: Endothelial cell tube formation on gelled basement membrane extract. *Nature Protocols* **5** 628–635.

Arnaoutova I, George J, Kleinman HK and Benton G (2009) The endothelial cell tube formation assay on basement membrane turns 20: state of the science and the art. *Angiogenesis* **12** 267–274.

Arnaoutova I, George J, Kleinman HK and Benton G (2012) Basement Membrane Matrix (BME) has Multiple Uses with Stem Cells. *Stem Cell Reviews and Reports* **8** 163–169.

Ashdown RR and Marrable AW (1967) Adherence and fusion between the extremities of adjacent embryonic sacs in the pig. *Journal of Anatomy* **101** 269–275.

Ashkenazi A and Dixit VM (1998) Death Receptors: Signaling and Modulation. *Science* **281** 1305–1308.

Ashworth CJ (1991) Effect of pre-mating nutritional status and post-mating progesterone supplementation on embryo survival and conceptus growth in gilts. *Animal Reproduction Science* **26** 311–321.

Ashworth CJ (2006) Chapter 4: Reproduction. In *Whittemore's Science and Practice of Pig Reproduction*, Third Edit, pp 104–147. Eds I Kyriazakis and C Whittemore. Blackwell Publishing Ltd.

Ashworth CJ and Antipatis C (1999) Effects of Pre- and Post-Mating Nutrition on Embryo Survival in Gilts. *Reproduction in Domestic Animals* **34** 103–108.

Ashworth CJ, Haley CS, Aitken RP and Wilmut I (1990) Embryo survival and conceptus growth after reciprocal embryo transfer between Chinese Meishan and Landrace x Large White gilts. *Journal of Reproduction and Fertility* **90** 595–603.

Ashworth CJ, Pickard AR, Miller SJ, Flint APF and Diehl JR (1997) Comparative studies of conceptus–endometrial interactions in Large White X Landrace and Meishan gilts. *Reproduction, Fertility and Development* **9** 217–225.

Ashworth CJ, Ross AW and Barrett P (1998) The use of DNA fingerprinting to

assess monozygotic twinning in Meishan and Landrace x large white pigs. *Reproduction, Fertility and Development* **10** 487–490.

Ashworth CJ, Finch AM, Page KR, Nwagwu MO and McArdle HJ (2001) Causes and consequences of fetal growth retardation in pigs. *Reproduction Supplement* **58** 233–246.

Ashworth MD, Ross JW, Stein DR, Allen DT, Spicer LJ and Geisert RD (2005) Endocrine disruption of uterine insulin-like growth factor expression in the pregnant gilt. *Reproduction* **130** 545–551.

Ashworth CJ, Nwagwu MO and McArdle HJ (2013) Genotype and fetal size affect maternal- fetal amino acid status and fetal endocrinology in Large White X Landrace and Meishan pigs. *Reproduction, Fertility and Development* **25** 439–445.

Ashworth CJ, Avey B, Stenhouse C, Sauter K, Waddell L, Hogg C, Lisowski Z and Hume D (2016) The effect of macrophage colony-stimulating factor (CSF1) on piglet gonad development. *Reproduction Abstracts* **3** P051.

Ausprunk DH, Knighton DR and Folkman J (1974) Differentiation of Vascular Endothelium in the Chick Chorioallantois: A Structural and Autoradiographic Study. *Developmental Biology* **38** 237–248.

Avagliano L, Garò C and Marconi AM (2012) Placental Amino Acids Transport in Intrauterine Growth Restriction. *Journal of Pregnancy* 1–6.

Bachman H, Nicosia J, Dysart M and Barker TH (2015) Utilizing Fibronectin Integrin-Binding Specificity to Control Cellular Responses. *Advances in Wound Care* **4** 501–511.

Bailey DW, Dunlap KA, Frank JW, Erikson DW, White BG, Bazer FW, Burghardt RC and Johnson GA (2010) Effects of long-term progesterone on developmental and functional aspects of porcine uterine epithelia and vasculature: Progesterone alone does not support development of uterine glands comparable to that of pregnancy. *Reproduction* **140** 583–594.

Baker M, Robinson SD, Lechertier T, Barber PR, Tavora B, D'Amico G, Jones DT, Vojnovic B and Hodivala-Dilke K (2012) Use of the mouse aortic ring assay to study angiogenesis. *Nature Protocols* **7** 89–104.

Bamfo JEAK and Odibo AO (2011) Diagnosis and Management of Fetal Growth Restriction. *Journal of Pregnancy* 1–15.

Barker DJP (2004) The Developmental Origins of Adult Disease. *Journal of the American College of Nutrition* **23** 588S – 595S.

Barker DJP (2006) Adult Consequences of Fetal Growth Restriction. *Clinical Obstetrics and Gynecology* **49** 270–283.

Barr M and Brent RL (1970) The Relation of the Uterine Vasculature to Fetal Growth and the Intrauterine Position Effect in Rats. *Teratology* **3** 251–260.

Barr M, Jensh RP and Brent RL (1969) Fetal Weight and Intrauterine Position in Rats. *Teratology* **2** 241–246.

Barr M, Jensh RP and Brent RL (1970) Prenatal Growth in the Albino Rat: Effects of Number, Intrauterine Position and Resorptions. *American Journal of Anatomy*

128 413–428.

Barrio E, Calvo MT, Romo A, Alvarez R, Gutierrez JI and Longás F (2003) Restricted intrauterine growth: study of apoptosis in the placenta. *Anales de Pediatria* **58** 51–54.

Barry JS and Anthony R V (2008) The Pregnant Sheep as a Model for Human Pregnancy. *Theriogenology* **69** 55–67.

Barut F, Barut A, Gun BD, Kandemir NO, Harma MI, Harma M, Aktunc E and Ozdamar SO (2010) Intrauterine growth restriction and placental angiogenesis. *Diagnostic Pathology* **5** 1–7.

Baschat AA, Gembruch U and Harman CR (2001) The sequence of changes in Doppler and biophysical parameters as severe fetal growth restriction worsens. *Ultrasound in Obstetrics and Gynecology* **18** 571–577.

Bauer R, Walter B, Hoppe A, Gaser E, Lampe V, Kauf E and Zwiener U (1998) Body weight distribution and organ size in newborn swine (sus scrofa domestica) - A study describing an animal model for asymmetrical intrauterine growth retardation. *Experimental and Toxicologic Pathology* **50** 59–65.

Bauer R, Walter B, Ihring W, Kluge H, Lampe V and Zwiener U (2000) Altered renal function in growth-restricted newborn piglets. *Paediatric Nephrology* **14** 735–739.

Bauer R, Walter B, Brust P, Füchtner F and Zwiener U (2003) Impact of asymmetric intrauterine growth restriction on organ function in newborn piglets. *European Journal of Obstetrics Gynecology and Reproductive Biology* **110** S40–S49.

Bauer R, Walter B and Brandl U (2007) Intrauterine growth restriction improves cerebral O2 utilization during hypercapnic hypoxia in newborn piglets. *The Journal of Physiology* **584** 693–704.

Bautista A, Rödel HG, Monclús R, Juárez-Romero M, Cruz-Sánchez E, Martínez-Gómez M and Hudson R (2015) Intrauterine position as a predictor of postnatal growth and survival in the rabbit. *Physiology and Behavior* **138** 101–106.

Baxter EM, Jarvis S, Palarea-Albaladejo J and Edwards SA (2012) The weaker sex? the propensity for male-biased piglet mortality. *PLoS ONE* **7** e30318.

Bayless KJ, Erikson DW, Frank JW, Joyce MM, Burghardt RC, Bazer FW and Johnson GA (2010) Recruitment and Modulation of Porcine Endothelial Progenitor Cells by Secreted Phosphoprotein 1 (SPP1, Osteopontin). *Biology of Reproduction* **83** 94.

Bazer FW (2013) Pregnancy recognition signaling mechanisms in ruminants and pigs. *Journal of Animal Science and Biotechnology* **4** 1–10.

Bazer FW and Thatcher WW (1977) Theory of maternal recognition of pregnancy in swine based on estrogen controlled endocrine versus exocrine secretion of prostaglandin F2α by the uterine endometrium. *Prostaglandins* **14** 397–401.

Bazer FW, Worthington-White D, Fliss MF V and Gross S (1991) Uteroferrin: A progesterone-induced hematopoietic growth factor of uterine origin. *Experimental Hematology* **19** 910–915.

Bazer FW, Ford JJ and Kensinger RS (2001) Reproductive Physiology. In *Biology of the Domestic Pig*, pp 150–224. Eds WG Pond and HJ Mersmann. Cornell University.

Bazer FW, Spencer TE, Johnson GA, Burghardt RC and Wu G (2009) Comparative aspects of implantation. *Reproduction* **138** 195–209.

Bazer FW, Song G, Kim J, Dunlap KA, Satterfield MC, Johnson GA, Burghardt RC and Wu G (2012a) Uterine biology in pigs and sheep. *Journal of Animal Science and Biotechnology* **3** 1.

Bazer FW, Song G, Kim J, Erikson DW, Johnson GA, Burghardt RC, Gao H, Satterfield MC, Spencer TE and Wu G (2012b) Mechanistic mammalian target of rapamycin (MTOR) cell signaling: Effects of select nutrients and secreted phosphoprotein 1 on development of mammalian conceptuses. *Molecular and Cellular Endocrinology* **354** 22–33.

Beach FA (1976) Sexual Attractivity, Proceptivity, and Receptivity in Female Mammals. *Hormones and Behavior* **7** 105–138.

Von Beckerath AK, Kollmann M, Rotky-Fast C, Karpf E, Lang U and Klaritsch P (2013) Perinatal complications and long-term neurodevelopmental outcome of infants with intrauterine growth restriction. *American Journal of Obstetrics and Gynecology* **208** 130.e1–e130.e6.

Bee G (2004) Effect of early gestation feeding, birth weight, and gender of progeny on muscle fiber characteristics of pigs at slaughter. *Journal of Animal Science* **82** 826–836.

Bee G (2007) Birth Weight of Litters as a Source of Variation in Postnatal Growth, and Carcass and Meat Quality. *Advances in Pork Production* **18** 191–196.

van Beijnum JR, Rousch M, Castermans K, van der Linden E and Griffioen AW (2008) Isolation of endothelial cells from fresh tissues. *Nature Protocols* **3** 1085–1091.

Bell AW and Ehrhardt RA (2002) Regulation of placental nutrient transport and implications for fetal growth. *Nutrition Research Reviews* **15** 211.

Bell AW, Kennaugh JM, Battaglia FC, Makowski EL and Meschia G (1986) Metabolic and circulatory studies of fetal lamb at midgestation. *The American Journal of Physiology* **250** E538–E544.

Bellahcène A, Castronovo V, Ogbureke KUE, Fisher LW and Fedarko NS (2008) Small integrin-binding ligand N-linked glycoproteins (SIBLINGs): Multifunctional proteins in cancer. *Nature Reviews Cancer* **8** 212–226.

Bérard J and Bee G (2010) Effects of dietary L-arginine supplementation to gilts during early gestation on foetal survival, growth and myofiber formation. *Animal* **4** 1680–1687.

Bermejo-Alvarez P, Rizos D, Rath D, Lonergan P and Gutierrez-Adan A (2009) Micro-Array Analysis Reveals That One Third of the Genes Actively Expressed Are Differentially Expressed Between Male and Female Bovine Blastocysts. *Biology of Reproduction* **81** 40.

Berridge M (2014) Module 9: Cell Cycle and Proliferation. *Cell Signalling Biology* 1–45.

Bersinger NA, Genewein EM, Müller O, Altermatt HJ, McKinnon B and Mueller MD (2010) Morphology of human endometrial explants and secretion of stromal marker proteins in short-and long-term cultures. *Gynecological Surgery* **7** 75–80.

Bhasin KKS, van Nas A, Martin LJ, Davis RC, Devaskar SU and Lusis AJ (2009) Maternal Low-Protein Diet or Hypercholesterolemia Reduces Circulating Essential Amino Acids and Leads to Intrauterine Growth Restriction. *Diabetes* **58** 559–566.

Bidarimath M and Tayade C (2017) Pregnancy and spontaneous fetal loss: A pig perspective. *Molecular Reproduction and Development* **84** 856–869.

Bidarimath M, Khalaj K, Wessels JM and Tayade C (2014) MicroRNAs, immune cells and pregnancy. *Cellular & Molecular Immunology* **11** 1–10.

Bidarimath M, Khalaj K, Kridli RT, Kan FWK, Koti M and Tayade C (2017) Extracellular vesicle mediated intercellular communication at the porcine maternal-fetal interface: A new paradigm for conceptus-endometrial cross-talk. *Scientific Reports* **7** 1–14.

Biensen NJ, Wilson ME and Ford SP (1998) The Impact of Either a Meishan or Yorkshire Uterus on Meishan or Yorkshire Fetal and Placental Development to Days 70, 90, and 110 of Gestation. *Journal of Animal Science* **76** 2169–2176.

Biswas D, Jung EM, Jeung EB and Hyun SH (2011) Effects of vascular endothelial growth factor on porcine preimplantation embryos produced by in vitro fertilization and somatic cell nuclear transfer. *Theriogenology* **75** 256–267.

Black R (2015) Global Prevalence of Small for Gestational Age Births. *Nestle Nutrition Institute Workshop Series* **81** 1–7.

Blatchford D, Holzbauer M, Ingram DL and Sharman DF (1978) Responses of the Pituitary-Adrenal System of the Pig To Environmental Changes and Drugs. *British Journal of Pharmacology* **62** 241–254.

Blitek A, Morawska E and Ziecik AJ (2012) Regulation of expression and role of leukemia inhibitory factor and interleukin-6 in the uterus of early pregnant pigs. *Theriogenology* **78** 951–964.

Blitek A, Morawaska-Pucinska E, Szymanska M, Kiewisz J and Waclawik A (2013) Effects of Conceptus on Transforming Growth Factor (TGF) β1 mRNA and Protein Concentration in the Porcine Endometrium - In Vivo and In Vitro Studies. *Journal of Reproduction and Development* **59** 512–519.

Blomberg LA, Garrett WM, Guillomot M, Miles JR, Sonstegard TS, Van Tassell CP and Zuelke KA (2006) Transcriptomic Profiling of the Tubular Porcine Conceptus Identifies the Differential Regulation of Growth and Developmentally Associated Genes. *Molecular Reproduction and Development* **73** 1491–1502.

Blomberg LA, Schreier LL, Guthrie HD, Sample GL, Vallet J, Caperna T and Ramsay T (2010) The effect of intrauterine growth retardation on the expression of developmental factors in porcine placenta subsequent to the initiation of placentation. *Placenta* **31** 549–552.

Bloor DJ, Metcalfe AD, Rutherford A, Brison DR and Kimber SJ (2002) Expression of cell adhesion molecules during human preimplantation embryo development. *Molecular Human Reproduction* **8** 237–245.

Boehlert GW, Kusakari M and Yamada J (1991) Oxygen consumption of gestating female Sebastes schlegeli: Estimating the reproductive costs of livebearing. *Environmental Biology of Fishes* **30** 81–89.

Boklage CE (2005) The epigenetic environment: Secondary sex ratio depends on differential survival in embryogenesis. *Human Reproduction* **20** 583–587.

Bollwein H, Maierl J, Mayer R and Stolla R (1998) Transrectal Color Doppler Sonography of the A. Uterina in Cyclic Mares. *Theriogenology* **49** 1483–1488.

Bollwein H, Meyer HHD, Maierl J, Weber F, Baumgartner U and Stolla R (2000) Transrectal Doppler sonography of uterine blood flow in cows during the estrous cycle. *Theriogenology* **53** 1541–1552.

Bollwein H, Baumgartner U and Stolla R (2002) Transrectal Doppler sonography of uterine blood flow in cows during pregnancy. *Theriogenology* **57** 2053–2061.

Bollwein H, Mayer R and Stolla R (2003) Transrectal Doppler sonography of uterine blood flow during early pregnancy in mares. *Theriogenology* **60** 597–605.

Bollwein H, Weber F, Woschée I and Stolla R (2004) Transrectal Doppler sonography of uterine and umbilical blood flow during pregnancy in mares. *Theriogenology* **61** 499–509.

Bologna-Molina R, Mosqueda-Taylor A, Molina-Frechero N, Mori-Estevez AD and Sánchez-Acuña G (2013) Comparison of the value of PCNA and Ki-67 as markers of cell proliferation in ameloblastic tumors. *Medicina Oral, Patologia Oral Y Cirugia Bucal* **18** e174–e179.

Börzsönyi B, Demendi C, Rigó J, Szentpéteri I, Rab A and Joó JG (2013) The regulation of apoptosis in intrauterine growth restriction: a study of Bcl-2 and Bax gene expression in human placenta. *The Journal of Maternal-Fetal & Neonatal Medicine* **26** 347–350.

Bourdon A, Parnet P, Nowak C, Tran NT, Winer N and Darmaun D (2016) L-Citrulline Supplementation Enhances Fetal Growth and Protein Synthesis in Rats with Intrauterine Growth Restriction. *The Journal of Nutrition and Disease* **146** 532–541.

Bourque DK, Avila L, Peñaherrera M, von Dadelszen P and Robinson WP (2010) Decreased Placental Methylation at the H19/IGF2 Imprinting Control Region is Associated with Normotensive Intrauterine Growth Restriction but not Preeclampsia. *Placenta* **31** 197–202.

Bowen JA, Bazer FW and Burghardt RC (1996) Spatial and Temporal Analyses of Integrin and Muc-1 Expression in Porcine Uterine Epithelium and Trophectoderm In Vivo. *Biology of Reproduction* **55** 1098–1106.

Brambrink AM, Evers AS, Avidan MS, Farber NB, Smith DJ, Martin LD, Dissen GA, Creeley CE and Olney JW (2012) Ketamine-induced Neuroapoptosis in the Fetal and Neonatal Rhesus Macaque Brain. *Anesthesiology* **116** 372–384.

Bratton SB, Walker G, Srinivasula SM, Sun XM, Butterworth M, Alnemri ES and Cohen GM (2001) Recruitment, activation and retention of caspases-9 and-3 by Apaf-1 apoptosome and associated XIAP complexes. *EMBO Journal* **20** 998–1009.

Bredbacka K and Bredbacka P (1996) Glucose controls sex-related growth rate

differences of bovine embryos produced in vitro. *Journal of Reproduction and Fertility* **106** 169–172.

Brodbelt DC and Taylor PM (1999) Comparison of two combinations of sedatives before anaesthetising pigs with halothane and nitrous oxide. *The Veterinary Record* **145** 283–287.

Brüssow KP, Kurth J, Vernunft A, Becker F, Tuchscherer A and Kanitz W (2012) Laparoscopy Guided Doppler Ultrasound Measurement of Fetal Blood Flow Indices During Early to Mid-Gestation in Pigs. *Journal of Reproduction and Development* **58** 243–247.

Buckberry S, Bianco-Miotto T, Bent SJ, Dekker GA and Roberts CT (2014) Integrative transcriptome metaanalysis reveals widespread sex-biased gene expression at the human fetal-maternal interface. *Molecular Human Reproduction* **20** 810–819.

Buhi WC, Ducsay CA, Bazer FW and Roberts RM (1982) Iron Transfer between the Purple Phosphatase Uteroferrin and Transferrin and Its Possible Role in Iron Metabolism of the Fetal Pig. *Journal of Biological Chemistry* **257** 1712–1723.

Burghardt RC, Johnson GA, Jaeger LA, Ka H, Garlow JE, Spencer TE and Bazer FW (2002) Integrins and extracellular matrix proteins at the maternal-fetal interface in domestic animals. *Cells Tissues Organs* **172** 202–217.

Burghardt RC, Burghardt JR, Taylor JD, Reeder AT, Nguen BT, Spencer TE, Bayless KJ and Johnson GA (2009) Enhanced focal adhesion assembly reflects increased mechanosensation and mechanotransduction at maternal-conceptus interface and uterine wall during ovine pregnancy. *Reproduction* **137** 567–582.

Cali U, Cavkaytar S, Sirvan L and Danisman N (2013) Placental apoptosis in preeclampsia, intrauterine growth retardation, and HELLP syndrome: An immunohistochemical study with caspase-3 and bcl-2. *Clinical and Experimental Obstetrics and Gynecology* **40** 45–48.

Calkins K, Devaskar SU and Angeles L (2011) Fetal Origins of Adult Disease. *Current Problems in Pediatric Adolescent Health Care* **41** 158–176.

Campbell S, Swann HR, Seif MW, Kimber SJ and Aplin JD (1995) Cell adhesion molecules on the oocyte and preimplantation human embryo. *Human Reproduction* **10** 1571–1578.

Can M, Guven B, Bektas S and Arikan I (2014) Oxidative stress and apoptosis in preeclampsia. *Tissue and Cell* **46** 477–481.

Caniggia I and Winter JL (2002) Adriana and Luisa Castellucci Award Lecture 2001 Hypoxia Inducible Factor-1: Oxygen Regulation of Trophoblast Differentiation in Normal and Pre-eclamptic Pregnancies - A Review. *Placenta* **16** S47–S57.

Cao G, O'Brien CD, Zhou Z, Sanders SM, Greenbaum JN, Makrigiannakis A and DeLisser HM (2002) Involvement of human PECAM-1 in angiogenesis and in vitro endothelial cell migration. *American Journal of Cell Physiology* **282** C1181–C1190.

Cao G, Fehrenbach ML, Williams JT, Finklestein JM, Zhu JX and DeLisser HM (2009) Angiogenesis in platelet endothelial cell adhesion molecule-1-null mice.

American Journal of Pathology **175** 903–915.

Caporali A and Emanueli C (2011) MicroRNA regulation in angiogenesis. *Vascular Pharmacology* **55** 79–86.

Cárdenas H and Pope WF (2002) Control of ovulation rate in swine. *Journal of Animal Science* **80** E36–E46.

Carmeliet P (2000) Mechanisms of angiogenesis and arteriogenesis. *Nature Medicine* **6** 389–395.

Carmeliet P, Ferreira V, Breier G, Pollefeyt S, Kieckens L, Gertsenstein M, Fahrig M, Vandenhoeck A, Harpal K, Eberhardt C *et al.* (1996) Abnormal blood vessel development and lethality in embryos lacking a single VEGF allele. *Nature* **380** 435–439.

Carr DJ, Aitken RP, Milne JS, David AL and Wallace JM (2012) Fetoplacental biometry and umbilical artery Doppler velocimetry in the overnourished adolescent model of fetal growth restriction. *American Journal of Obstetrics and Gynecology* **207** e6–e15.

Carson DD, Bagchi I, Dey SK, Enders AC, Fazleabas AT, Lessey BA and Yoshinaga K (2000) Embryo Implantation. *Developmental Biology* **223** 217–237.

Carter AM, Kingston MJ, Han KK, Mazzuca DM, Nygard K and Han VKM (2005) Altered expression of IGFs and IGF-binding proteins during intrauterine growth restriction in guinea pigs. *Journal of Endocrinology* **184** 179–189.

Cassar G, King WA and King GJ (1994) Influence of sex on early growth of pig conceptuses. *Journal of Reproduction and Fertility* **101** 317–320.

Caulfield AJ and Lathem WW (2014) Disruption of Fas-Fas Ligand Signaling, Apoptosis, and Innate Immunity by Bacterial Pathogens. *PLoS Pathogens* **10** e1004252 1–4.

Çelik HG, Uhri M and Yildirim G (2017) Expression of von Willebrand factor and caldesmon in the placental tissues of pregnancies complicated with intrauterine growth restriction. *The Journal of Maternal-Fetal & Neonatal Medicine* 1–6.

Chaddha V, Viero S, Huppertz B and Kingdom J (2004) Developmental biology of the placenta and the origins of placental insufficiency. *Seminars in Fetal & Neonatal Medicine* **9** 357–369.

Chaen T, Konno T, Egashira M, Bai R, Nomura N, Nomura S, Hirota Y, Sakurai T and Imakawa K (2012) Estrogen-Dependent Uterine Secretion of Osteopontin Activates Blastocyst Adhesion Competence. *PLoS ONE* **7** e48933 1–12.

Chahoud I and Paumgartten FJR (2005) Relationships between fetal body weight of Wistar rats at term and the extent of skeletal ossification. *Brazilian Journal of Medical and Biological Research* **38** 565–575.

Chahoud I and Paumgartten FJR (2009) Influence of litter size on the postnatal growth of rat pups: is there a rationale for litter-size standardization in toxicity studies? *Environmental Research* **109** 1021–1027.

Challis J, Newnham J, Petraglia F, Yeganegi M and Bocking A (2013) Fetal sex and preterm birth. *Placenta* **34** 95–99.

Charnock-Jones DS, Clark DE, Licence D, Day K, Wooding FBP and Smith SK (2001) Distribution of vascular endothelial growth factor (VEGF) and its binding sites at the maternal–fetal interface during gestation in pigs. *Reproduction* **122** 753–760.

Charnock-Jones DS, Kaufmann P and Mayhew TM (2004) Aspects of human fetoplacental vasculogenesis and angiogenesis. I. Molecular regulation. *Placenta* **25** 103–113.

Chauhan S and Magann E (2006) Screening for Fetal Growth Restriction. *Clinical Obstetrics and Gynecology* **49** 284–294.

Chen L, Willis SN, Wei A, Smith BJ, Fletcher JI, Hinds MG, Colman PM, Day CL, Adams JM and Huang DCS (2005) Differential Targeting of Prosurvival Bcl-2 Proteins by Their BH3-Only Ligands Allows Complementary Apoptotic Function. *Molecular Cell* **17** 393–403.

Chen HY, Chauhan SP, Salm Ward TC, Mori N, Gass ET and Cisler RA (2011) Aberrant fetal growth and early, late, and postneonatal mortality: An analysis of Milwaukee births, 1996-2007. *American Journal of Obstetrics and Gynecology* **204** 1–10.

Chen F, Wang T, Feng C, Lin G, Zhu Y, Wu G, Johnson G and Wang J (2015) Proteome differences in placenta and endometrium between normal and intrauterine growth restricted pig fetuses. *PLoS ONE* **10** E0142396 1–18.

Chiavaroli V, Castorani V, Guidone P, Derraik JGB, Liberati M, Chiarelli F and Mohn A (2016) Incidence of infants born small- and large-for-gestational-age in an Italian cohort over a 20-year period and associated risk factors. *Italian Journal of Pediatrics* **42** 1–7.

Chiofalo B, Laganà AS, Vaiarelli A, La Rosa VL, Rossetti D, Palmara V, Valenti G, Rapisarda AMC, Granese R, Sapia F *et al.* (2017) Do miRNAs play a role in fetal growth restriction? A fresh look to a busy corner. *BioMed Research International* 1–8.

Chiu PM, Ngan YS, Khoo US and Cheung ANY (2001) Apoptotic activity in gestational trophoblastic disease correlates with clinical outcome: Assessment by the caspase-related M30 CytoDeath antibody. *Histopathology* **38** 243–249.

Christenson RK (1993) Ovulation Rate and Embryonic Survival in Chinese Meishan and White Crossbred Pigs. *Journal of Animal Science* **71** 3060–3066.

Chrusciel M, Bodek G, Kirtiklis L, Lewczuk B, Hyder CL, Blitek A, Kaczmarek MM, Ziecik AJ and Andronowska A (2011) Immortalization of Swine Umbilical Vein Endothelial Cells (SUVECs) with the Simian Virus 40 Large-T Antigen. *Molecular Reproduction and Development* **78** 597–610.

Clark MM, Crews D and Galef BG (1991) Concentrations of Sex Steroid Hormones in Pregnant and Fetal Mongolian Gerbils. *Physiology and Behavior* **49** 239–243.

Clark MM, vom Saal FS and Galef BG (1992) Intrauterine positions and testosterone levels of adult male gerbils are correlated. *Physiology and Behavior* **51** 957–960.

Clemens G, Gladue BA and Coniglio LP (1978) Prenatal Endogenous Androgenic Influences Masculine Sexual Behavior and Genital Morphology in Male and Female Rats. *Hormones and Behavior* **10** 40–53.

Clifton VL (2010) Review: Sex and the Human Placenta: Mediating Differential Strategies of Fetal Growth and Survival. *Placenta* **31** S33–S39.

Coe BL, Kirkpatrick JR, Taylor JA and Vom Saal FS (2008) A New 'Crowded Uterine Horn' Mouse Model for Examining the Relationship Between Foetal Growth and Adult Obesity. *Basic and Clinical Pharmacology and Toxicology* **102** 162–167.

Cohen E, Baerts W and Van Bel F (2015) Brain-Sparing in Intrauterine Growth Restriction: Considerations for the Neonatologist. *Neonatology* **108** 269–276.

Cole RW, Liu F and Herron BJ (2010) Imaging of angiogenesis: past , present and future. In *Microscopy: Science, Technology, Applications and Education*, pp 885–896. Eds A Méndez-Vilas and J Diaz. Formatex.

Colenbrander B, van Rossum-Kok C, Van Straaten HWM and Wensing CJG (1979) The Effect of Fetal Decapitation on the Testis and Other Endocrine Organs in the Pig. *Biology of Reproduction* **20** 198–204.

Conrad TJ, Chandler DB, Corless JM and Klintworth GK (1994) in vivo measurement of corneal angiogenesis with video data acquisition and computerized image analysis. *Laboratory Investigation* **70** 426–434.

Constância M, Hemberger M, Hughes J, Dean W, Ferguson-Smith A, Fundele R, Stewart F, Kelsey G, Fowden A, Sibley C *et al.* (2002) Placental-specific IGF-II is a major modulator of placental and fetal growth. *Nature* **417** 945–948.

Cory S and Adams JM (2002) The BCL2 family: Regulators of the cellular Life-Or-Death Switch. *Nature Reviews Cancer* **2** 647–656.

Coutelle C and Rodeck C (2002) On the scientific and ethical issues of fetal somatic gene therapy. *Gene Therapy* **9** 670–673.

Craft JB, Coaldrake LA, Yonekura ML, Dao SD, Co EG, Roizen MF, Mazel P, Gilman R, Shokes L and Trevor AJ (1983) Ketamine, Catecholamines, and Uterine Tone in Pregnant Ewes. *American Journal of Obstetrics and Gynecology* **146** 429–434.

Cristofolini A, Sanchis G, Moliva M, Alonso L, Chanique A, Koncurat M and Merkis C (2013) Cellular remodelling by apoptosis during porcine placentation. *Reproduction in Domestic Animals* **48** 584–590.

D'Souza SS, Daikoku T, Farach-Carson MC and Carson DD (2007) Heparanase Expression and Function During Early Pregnancy in Mice. *Biology of Reproduction* **77** 433–441.

Dai J, Peng L, Fan K, Wang H, Wei R, Ji G, Cai J, Lu B, Li B, Zhang D *et al.* (2009) Osteopontin induces angiogenesis through activation of PI3K/AKT and ERK1/2 in endothelial cells. *Oncogene* **28** 3412–3422.

Dalçik H, Yardimoglu M, Vural B, Dalçik C, Filiz S, Gonca S, Kokö ktörk S and Ceylan S (2001) Expression of insulin-like growth factor in the placenta of intrauterine growth-retarded human fetuses. *Acta Histochemica* **103** 195–207.

Dallanora D, Marcon J, Walter MP, Biondo N, Bernardi ML, Wentz I and Bortolozzo FP (2017) Effect of dietary amino acid supplementation during gestation on placental efficiency and litter birth weight in gestating gilts. *Livestock Science* **197** 30–35.

Dantzer V (1985) Electron microscopy of the initial stages of placentation in the pig. *Anatomy and Embryology* **172** 281–293.

Daş G, Vernunft A, Görs S, Kanitz E, Weitzel JM, Brüssow KP and Metges CC (2016) Effects of general anesthesia with ketamine in combination with the neuroleptic sedatives xylazine or azaperone on plasma metabolites and hormones in pigs. *Journal of Animal Science* **94** 3229–3239.

Dean A and Sharpe RM (2013) Anogenital Distance or Digit Length Ratio as Measures of Fetal Androgen Exposure: Relationship to Male Reproductive Development and Its Disorders. *Journal of Clinical Endocrinology and Metabolism* **98** 2230–2238.

DeChiara TM, Efstratiadis A and Robertson EJ (1990) A growth-deficiency phenotype in heterozygous mice carrying an insulin-like growth factor II gene disrupted by targeting. *Nature* **345** 78–80.

DeCicco-Skinner KL, Henry GH, Cataisson C, Tabib T, Gwilliam JC, Watson NJ, Bullwinkle EM, Falkenburg L, O'Neill RC, Morin A *et al.* (2014) Endothelial Cell Tube Formation Assay for the In Vitro Study of Angiogenesis. *Journal of Visualized Experiments* **91** 1–8.

Dekel N, Gnainsky Y, Granot I and Mor G (2010) Inflammation and Implantation. *American Journal of Reproductive Immunology* **63** 17–21.

Dekel N, Gnainsky Y, Granot I, Racicot K and Mor G (2014) The Role of Inflammation for a Successful Implantation. *American Journal of Reproductive Immunology* **72** 141–147.

DeLisser HM, Christofidou-Solomidou M, Strieter RM, Burdick MD, Robinson CS, Wexler RS, Kerr JS, Garlanda C, Merwin JR, Madri JA *et al.* (1997) Involvement of Endothelial PECAM-1/CD31 in Angiogenesis. *The American Journal of Pathology* **151** 671–677.

Delon I and Brown NH (2007) Integrins and the actin cytoskeleton. *Current Opinion in Cell Biology* **19** 43–50.

Demicheva E and Crispi F (2014) Long-Term Follow-Up of Intrauterine Growth Restriction: Cardiovascular Disorders. *Fetal Diagnosis and Therapy* **36** 143–153.

Dempsey LA, Plummer TB, Coombes SL and Platt JL (2000) Heparanase expression in invasive trophoblasts and acute vascular damage. *Glycobiology* **10** 467–475.

Denker HW (1993) Implantation: a cell biological paradox. *Journal of Experimental Zoology* **266** 541–558.

Detti L, Akiyama M and Mari G (2002) Doppler blood flow in obstetrics. *Current Opinion in Obstetrics & Gynecology* **14** 587–593.

Díaz-Cueto L and Gerton GL (2001) The Influence of Growth Factors on the Development of Preimplantation Mammalian Embryos. *Archives of Medical Research* **32** 619–626.

Dickey RP (1997) Doppler ultrasound investigation of uterine and ovarian blood flow in infertility and early pregnancy. *Human Reproduction Update* **3** 467–503.

Didenko V V (2011) *DNA Damage Detection In Situ, Ex Vivo, and In Vivo. Methods*

and Protocols. Humana Press.

Dilworth MR, Andersson I, Renshall LJ, Cowley E, Baker P, Greenwood S, Sibley CP and Wareing M (2013) Sildenafil Citrate Increases Fetal Weight in a Mouse Model of Fetal Growth Restriction with a Normal Vascular Phenotype. *PLoS ONE* **8** e77748 1–8.

v. Domarus H, Louton T and Lange-Wühlisch F (1986) The position effect in mice on day 14. *Teratology* **34** 73–80.

Downing J (2010) Sildenafil for the Treatment of Preeclampsia. *Hypertension in Pregnancy* **29** 248–250.

Drickamer LC (1996) Intra-uterine position and anogenital distance in house mice: Consequences under field conditions. *Animal Behaviour* **51** 925–934.

Drickamer LC, Arthur RD and Rosenthal TL (1997) Conception Failure in Swine: Importance of the Sex Ratio of a Female's Birth Litter and Tests of Other Factors. *Journal of Animal Science* **75** 2192–2196.

Drickamer LC, Rosenthal TL and Arthur RD (1999) Factors affecting the number of teats in pigs. *Journal of Reproduction and Fertility* **115** 97–100.

Ducsay CA, Buhi WC, Bazer FW and Roberts RM (1982) Role of Uteroferrin in Iron Transport and Macromolecular Uptake by Allantoic Epithelium of the Porcine Conceptus. *Biology of Reproduction* **26** 729–743.

Ducsay CA, Buhi WC, Bazer FW, Roberts RM and Combs GE (1984) Role of Uteroferrin in Placental Iron Transport : Effect of Maternal Iron Treatment on Fetal Iron and Uteroferrin Content and Neonatal Hemoglobin. *Journal of Animal Science* **59** 1303–1308.

Ducsay CA, Buhi WC, Bazer FW and Roberts RM (1986) Role of Uteroferrin in Placental Iron Transport in Swine: Relationship between Uteroferrin Levels and Iron Deposition in the Conceptus During Gestation. *Journal of Animal Science* **62** 706–716.

Dunlap KA, Erikson DW, Burghardt RC, White FJ, Reed KM, Farmer JL, Spencer TE, Magness RR, Bazer FW, Bayless KJ *et al.* (2008) Progesterone and Placentation Increase Secreted Phosphoprotein One (SPP1 or osteopontin) in Uterine Glands and Stroma for Histotrophic and Hematotrophic Support of Ovine Pregnancy. *Biology of Reproduction* **79** 983–990.

Dyce KM, Sack WO and Wesing CJG (1996) *Textbook of Veterinary Anatomy*. Philadelphia: W. B. Saunders Co.

Dzierzak E and Robin C (2010) Placenta as a source of hematopoietic stem cells. *Trends in Molecular Medicine* **16** 361–367.

Einspanier R, Schönfelder M, Müller K, Stojkovic M, Kosmann M, Wolf E and Schams D (2002) Expression of the Vascular Endothelial Growth Factor and its Receptors and Effects of VEGF During In Vitro Maturation of Bovine Cumulus-Oocyte Complexes (COC). *Molecular Reproduction and Development* **62** 29–36.

Eixarch E, Hernandez-Andrade E, Crispi F, Illa M, Torre I, Figueras F and Gratacos E (2011) Impact on fetal mortality and cardiovascular Doppler of selective ligature of uteroplacental vessels compared with undernutrition in a rabbit model of intrauterine growth restriction. *Placenta* **32** 304–309.

Elias AA, Ghaly A, Matushewski B, Regnault TRH and Richardson BS (2016) Maternal Nutrient Restriction in Guinea Pigs as an Animal Model for Inducing Fetal Growth Restriction. *Reproductive Sciences* **23** 219–227.

Elkin M, Ilan N, Ishai-Michaeli R, Friedmann Y, Papo O, Pecker I and Vlodavsky I (2001) Heparanase as a mediator of angiogenesis: mode of action. *Federation of American Societies for Experimental Biology Journal* **15** 1661–1663.

Elmetwally M, Rohn K and Meinecke-Tillmann S (2016) Noninvasive color Doppler sonography of uterine blood flow throughout pregnancy in sheep and goats. *Theriogenology* **85** 1070–1079.e1.

Elmore S (2007) Apoptosis: A Review of Programmed Cell Death. *Toxicologic Pathology* **35** 495–516.

Enders AC and Blankenship TN (1999) Comparative Placental Structure. *Advanced Drug Delivery Reviews* **38** 3–15.

Enders AC and Carter AM (2004) What Can Comparative Studies of Placental Structure Tell Us? - A Review. *Placenta* **25** S3–S9.

Erikson DW, Burghardt RC, Bayless KJ and Johnson GA (2009a) Secreted Phosphoprotein 1 (SPP1, osteopontin) Binds to Integrin Alphavbeta 6 on Porcine Trophectoderm Cells and Integrin Alphavbeta3 on Uterine Luminal Epithelial Cells, and Promotes Trophectoderm Cell Adhesion and Migration. *Biology of Reproduction* **81** 814–825.

Erikson DW, Burghardt RC, Bazer FW, Johnson GA and Bayless KJ (2009b) Secreted Phosphoprotein 1 (SPP1, Osteopontin) Stimulates Adhesion and Migration of Circulating Endothelial Cells in Pigs. *Biology of Reproduction* **81** 91.

Eriksson JG, Kajantie E, Osmond C, Thornburgh K and Barker DJP (2010) Boys Live Dangerously in the Womb. *American Journal of Human Biology* **22** 330–335.

Erkens T, Van Poucke M, Vandesompele J, Goossens K, Van Zeveren A and Peelman LJ (2006) Development of a new set of reference genes for normalization of real-time RT-PCR data of porcine backfat and longissimus dorsi muscle, and evaluation with PPARGC1A. *BioMed Central Biotechnology* **6** 1–8.

Esteves CL, Sheldrake TA, Mesquita SP, Pesántez JJ, Menghini T, Dawson L, Péault B and Donadeu FX (2017) Isolation and characterization of equine native MSC populations. *Stem Cell Research and Therapy* **8** 1–12.

Even MD, Dhar MG and vom Saal FS (1992) Transport of steroids between fetuses via amniotic fluid in relation to the intrauterine position phenomenon in rats. *Journal of Reproduction and Fertility* **96** 709–716.

Fajersztajn L and Veras MM (2017) Hypoxia: From Placental Development to Fetal Programming. *Birth Defects Research* **109** 1377–1385.

Fassler R and Meyer M (1995) Consequences of lack of beta 1 integrin gene expression in mice. *Genes and Development* **9** 1896–1908.

Fazleabas AT, Bell SC, Fleming S, Sun J and Lessey BA (1997) Distribution of Integrins and the Extracellular Matrix Proteins in the Baboon Endometrium during the Menstrual Cycle and Early Pregnancy. *Biology of Reproduction* **56** 348–356.

Feinberg RF, Kliman HJ and Lockwood CJ (1991) Is Oncofetal Fibronectin a Trophoblast Glue for Human Implantation? *The American Journal of Pathology* **138** 537–543.

Fernandez-Rodriguez A, Munoz M, Fernandez A, Pena RN, Tomas A, Noguera JL, Ovilo C and Fernandez AI (2011) Differential Gene Expression in Ovaries of Pregnant Pigs with High and Low Prolificacy Levels and Identification of Candidate Genes for Litter Size. *Biology of Reproduction* **84** 299–307.

Ferrara N and Kerbel RS (2005) Angiogenesis as a therapeutic target. *Nature* **438** 967–974.

Ferrara N, Gerber HP and LeCouter J (2003) The biology of VEGF and its receptors. *Nature Medicine* **9** 669–676.

Ferrazzi E, Bozzo M, Rigano S, Bellotti M, Morabito A, Pardi G, Battaglia FC and Galan HL (2002) Temporal sequence of abnormal Doppler changes in the peripheral and central circulatory systems of the severely growth-restricted fetus. *Ultrasound in Obstetrics and Gynecology* **19** 140–146.

Finch AM, Anitpatis C, Pickard AR and Ashworth CJ (2002) Patterns of fetal growth within Large White X Landrace and Chinese Meishan gilt litters at three stages of gestation. *Reproduction, Fertility and Development* **14** 419–425.

Finch AM, Yang LG, Nwagwu MO, Page KR, McArdle HJ and Ashworth CJ (2004) Placental transport of leucine in a porcine model of low birth weight. *Reproduction* **128** 229–235.

Fisher LW, Stubbs JT and Young MF (1995) Antisera and cDNA probes to human and certain animal model bone matrix noncollagenous proteins. *Acta Orthopaedica* **66** 61–65.

Fisher LW, Torchia DA, Fohr B, Young MF and Fedarko NS (2001) Flexible Structures of SIBLING Proteins, Bone Sialoprotein, and Osteopontin. *Biochemical and Biophysical Research Communications* **280** 460–465.

Fléchon JE, Degrouard J and Fléchon B (2004) Gastrulation Events in the Prestreak Pig Embryo: Ultrastructure and Cell Markers. *Genesis* **38** 13–25.

Flood PF (1973) Endometrial Differentiation in the Pregnant Sow and the Necrotic Tips of the Allantochorion. *Journal of Reproduction and Development* **32** 539–543.

Ford JJ (1985) Reevaluation of the Role of Progesterone in Stimulating Sexual Receptivity in Estrogen-Treated Gilts. *Journal of Animal Science* **61** 36–43.

Ford SP and Christenson RK (1979) Blood Flow to Uteri of Sows During the Estrous Cycle and Early Pregnancy: Local Effect of the Conceptus on the Uterine Blood Supply. *Biology of Reproduction* **21** 617–624.

Ford SP, Vonnahme KA and Wilson ME (2002) Uterine capacity in the pig reflects a combination of uterine environment and conceptus genotype effects. *Journal of Animal Science* **80** E66–E73.

Forde N, Maillo V, O'Gaora P, Simintiras CA, Sturmey RG, Ealy AD, Spencer TE, Gutierrez-Adan A, Rizos D and Lonergan P (2016) Sexually Dimorphic Gene Expression in Bovine Conceptuses at the Initiation of Implantation. *Biology of Reproduction* **95** 92 1–8.

Fowden AL (2003) The Insulin-Like Growth Factors and Feto-Placental Growth. *Placenta* **24** 803–812.

Foxcroft GR and Town SC (2004) Prenatal Programming of Postnatal Performance – the Unseen Cause of Variance. *Advances in Pork Production* **15** 4–10.

Foxcroft GR, Dixon WT, Novak S, Putman CT, Town SC and Vinsky MDA (2006) The biological basis for prenatal programming of postnatal performance in pigs. *Journal of Animal Science* **84** E105–E112.

Foxcroft GR, Dixon WT, Dyck MK, Novak S, Harding JCS and Almeida FCRL (2009) Prenatal programming of postnatal development in the pig. *Society of Reproduction and Fertility Supplement* **66** 213–231.

Frank JW, Seo H, Burghardt RC, Bayless KJ and Johnson GA (2017) ITGAV (alpha v integrins) bind SPP1 (osteopontin) to support trophoblast cell adhesion. *Reproduction* **153** 695–706.

Friedman RC, Farh KKH, Burge CB and Bartel DP (2009) Most mammalian mRNAs are conserved targets of microRNAs. *Genome Research* **19** 92–105.

Friess AE, Sinowatz F, Skolek-Winnisch R and Träutner W (1981) The Placenta of the Pig II The Ultrasound of the Areolae. *Anatomy and Embryology* **163** 43–53.

Fuchs Y and Steller H (2011) Programmed Cell Death in Animal Development and Disease. *Cell* **147** 742–758.

Fuentes-Prior P and Salvesen GS (2004) The protein structures that shape caspase activity, specificity, activation and inhibition. *The Biochemical Journal* **384** 201–232.

Gabory A, Ferry L, Fajardy I, Jouneau L, Gothié JD, Vigé A, Fleur C, Mayeur S, Gallou-Kabani C, Gross MS *et al.* (2012) Maternal Diets Trigger Sex-Specific Divergent Trajectories of Gene Expression and Epigenetic Systems in Mouse Placenta. *PLoS ONE* **7** e47986 1–14.

Gabory A, Roseboom TJ, Moore T, Moore LG and Junien C (2013) Placental contribution to the origins of sexual dimorphism in health and diseases: Sex chromosomes and epigenetics. *Biology of Sex Differences* **4** 1–14.

Galan HL, Hussey MJ, Barbera A, Ferrazzi E, Chung M, Hobbins JC and Battaglia FC (1999) Relationship of fetal growth to duration of heat stress in an ovine model of placental insufficiency. *American Journal of Obstetrics and Gynecology* **180** 1278–1282.

Gallant ND, Michael KE and García AJ (2005) Cell Adhesion Strenthening: Contributions of Adhesive Area, Integrin Binding, and Focal Adhesion Assembly. *Molecular Biology of the Cell* **16** 4329–4340.

Gallou-Kabani C, Gabory A, Tost J, Karimi M, Mayeur S, Lesage J, Boudadi E, Gross MS, Taurelle J, Vigé A *et al.* (2010) Sex- and Diet-Specific Changes of Imprinted Gene Expression and DNA Methylation in Mouse Placenta under a High-Fat Diet. *PLoS ONE* **5** e14398 1–13.

Gandelman R, vom Saal FS and Reinisch JM (1977) Contiguity to male foetuses affects morphology and behaviour of female mice. *Nature* **266** 722–724.

Gao K, Jiang Z, Lin Y, Zheng C, Zhou G, Chen F, Yang L and Wu G (2012) Dietary l-arginine supplementation enhances placental growth and reproductive performance in sows. *Amino Acids* **42** 2207–2214.

García Fernández RA, Sánchez Pérez MA, Sánchez Maldonado B, García-Palencia P, Naranjo Freixa C, Palomo Yagüe A and Flores JM (2015) Iberian pig early pregnancy: Vascular endothelial growth factor receptor system expression in the maternofetal interface in healthy and arresting conceptuses. *Theriogenology* **83** 334–343.

Gardosi J (2011) Clinical Strategies for Improving the Detection of Fetal Growth Restriction. *Clinics in Perinatology* **38** 21–31.

Garlow JE, Ka H, Johnson GA, Burghardt RC, Jaeger LA and Bazer FW (2002) Analysis of Osteopontin at the Maternal-Placental Interface in Pigs. *Biology of Reproduction* **66** 718–725.

Geisert RD and Bazer FW (2015) *Regulation of Implantation and Establishment of Pregnancy in Mammals*.

Geisert RD and Schmitt RAM (2002) Early embryonic survival in the pig: Can it be improved? *Journal of Animal Science* **80** E54–E65.

Geisert RD, Brookbank JW, Roberts RM and Bazer FW (1982) Establishment of Pregnancy in the Pig: II. Cellular Remodeling of the Porcine Blastocyst During Elongation on Day 12 of Pregnancy. *Biology of Reproduction* **27** 941–955.

Geisert RD, Whyte JJ, Meyer AE, Mathew DJ, Juárez MR, Lucy MC, Prather RS and Spencer TE (2017) Rapid conceptus elongation in the pig: An interleukin 1 beta 2 and estrogen-regulated phenomenon. *Molecular Reproduction and Development* **84** 760–774.

Gekas C, Dieterlen-Lièvre F, Orkin SH and Mikkola HKA (2005) The Placenta is a Niche for Hematopoietic Stem Cells. *Developmental Cell* **8** 365–375.

George EL, Georges-Labouesse EN, Patel-King RS, Rayburn H and Hynes RO (1993) Defects in mesoderm, neural tube and vascular development in mouse embryos lacking fibronectin. *Development* **119** 1079–1091.

Gerber HP, Dixit VM and Ferrara N (1998) Vascular Endothelial Growth Factor Induces Expression of the Antiapoptotic Proteins Bcl-2 and A1 in Vascular Endothelial Cells. *Journal of Biological Chemistry* **273** 13313–13316.

Germeyer A, Savaris RF, Jauckus J and Lessey B (2014) Endometrial beta3 Integrin profile reflects endometrial receptivity defects in women with unexplained recurrent pregnancy loss. *Reproductive Biology and Endocrinology* **12** 1–5.

Ghidini A and Salafia CM (2005) Gender differences of placental dysfunction in severe prematurity. *British Journal of Obstetrics and Gynaecology* **112** 140–144.

Giancotti FG and Ruoslahti E (1999) Integrin Signaling. *Science* **285** 1028–1032.

Gibson TC, Phernetton TM, Wiltbank MC and Magness RR (2004) Development and Use of an Ovarian Synchronization Model to Study the Effects of Endogenous Estrogen and Nitric Oxide on Uterine Blood Flow During Ovarian Cycles in Sheep. *Biology of Reproduction* **70** 1886–1894.

Girard JR, Ferre P, Gilbert M, Kervran A, Assan R and Marliss EB (1977) Fetal metabolic response to maternal fasting in the rat. *American Journal of Physiology* **232** E456–E463.

Girotti M and Zingg HH (2003) Gene Expression Profiling of Rat Uterus at Different Stages of Parturition. *Endocrinology* **144** 2254–2265.

Giussani DA (2011) The vulnerable developing brain. *Proceedings of the National Academy of Sciences* **108** 2641–2642.

Godfrey KM (2002) The Role of the Placenta in Fetal Programming - A Review. *Placenta* **23** S20–S27.

Gol M and Tuna B (2009) Effect of Fetal Sex on Apoptosis- Regulating Proteins in Trophoblasts of Full-Term Human Placenta. *Gynecologic and Obstetric Investigation* **67** 53–56.

Golbabapour S, Abdulla MA and Hajrezaei M (2011) A Concise Review on Epigenetic Regulation: Insight into Molecular Mechanisms. *International Journal of Molecular Sciences* **12** 8661–8694.

Goldstein MH, Bazer FW and Barron DH (1980) Characterization of Changes in Volume, Osmolarity and Electrolyte Composition of Porcine Fetal Fluids During Gestation. *Biology of Reproduction* **22** 1168–1180.

Golias CH, Charalabopoulos A and Charalabopoulos K (2004) Cell proliferation and cell cycle control : a mini review. *International Journal of Clinical Practice* **58** 1134–1141.

Gonzalez TL, Sun T, Koeppel AF, Lee B, Wang ET, Farber CR, Rich SS, Sundheimer LW, Buttle RA, Chen YI *et al.* (2018) Sex differences in the late first trimester human placenta transcriptome. *Biology of Sex Differences* **9** 1–23.

Górecki MT (2003) Sex ratio in litters of domestic pigs (Sus scrofa f. domestica Linnaeus, 1758). *Biology Letters* **40** 111–118.

Green ML, Simmen RCM and Simmen FA (1995) Developmental Regulation of Steroidogenic Enzyme Gene Expression in the Periimplantation Porcine Conceptus: A Paracrine Role for Insulin-Like Growth Factor 1. *Endocrinology* **136** 3961–3970.

Greenwood PL, Hunt AS, Hermanson JW and Bell AW (2000) Effects of birth weight and postnatal nutrition on neonatal sheep: II. Skeletal muscle growth and development. *Journal of Animal Science* **78** 50–61.

Guillomot M (1999) Changes in Extracellular Matrix Components and Cytokeratins in the Endometrium During Goat Implantation. *Placenta* **20** 339–345.

Gump FE, Butler H and Kinney JM (1968) Oxygen Transport and Consumption during Acute Hemodilution. *Annals of Surgery* **168** 54–60.

Guo L, Tsai SQ, Hardison NE, James AH, Motsinger-Reif AA, Thames B, Stone EA, Deng C and Piedrahita JA (2013) Differentially expressed microRNAs and affected biological pathways revealed by modulated modularity clustering (MMC) analysis of human preeclamptic and IUGR placentas. *Placenta* **34** 599–605.

Guo S, Lok J, Liu Y, Hayakawa K, Leung W, Xing C, Ji X and Lo EH (2014) Assays to Examine Endothelial Cell Migration, Tube Formation, and Gene Expression

Profiles. *Methods in Molecular Biology* **1135** 393–402.

Gupta A, Bazer FW and Jaeger LA (1996) Differential expression of beta transforming growth factors (TGF beta 1, TGF beta 2, and TGF beta 3) and their receptors (type I and type II) in peri-implantation porcine conceptuses. *Biology of Reproduction* **55** 796–802.

Gupta A, Ing NH, Bazer FW, Bustamante LS and Jaeger LA (1998) Beta transforming growth factors (TGFss) at the porcine conceptus-maternal interface. Part I: expression of TGFbeta1, TGFbeta2, and TGFbeta3 messenger ribonucleic acids. *Biology of Reproduction* **59** 905–910.

Gutiérrez-Adán A, Oter M, Martínez-Madrid B, Pintado B and De La Fuente J (2000) Differential Expression of Two Genes Located on the X Chromosome Between Male and Female In Vitro-Produced Bovine Embryos at the Blastocyst Stage. *Molecular Reproduction and Development* **55** 146–151.

Gutiérrez-Adán A, Granados J, Pintado B and Fuente JDL (2001) Influence of glucose on the sex ratio of bovine IVM/IVF embyros cultured in vitro. *Reproduction, Fertility and Development* **13** 361–365.

Haimov-Kochman R, Friedmann Y, Prus D, Goldman-Wohl DS, Greenfield C, Anteby EY, Aviv A, Vlodavsky I and Yagel S (2002) Localization of heparanase in normal and pathological human placenta. *Molecular Human Reproduction* **8** 566–573.

Hall LW and Clarke KW (1991) *Veterinary Anaesthesia 9th Edition*.

Halperin R, Peller S, Sandbank J, Bukovsky I and Schneider D (2000) Expression of the p53 Gene and Apoptosis in Gestational Trophoblast Disease. *Placenta* **21** 58–62.

Hamburger V and Hamilton H (1951) A Series of Normal Stages in the Development of the Chick Embryo. *Developmental Dynamics* **88** 49–92.

Han SH, Shin KY, Lee SS, Ko MS, Oh HS and Cho IC (2012) Porcine SPP1 gene polymorphism association with phenotypic traits in the Landrace × Jeju (Korea) black pig F2 population. *Molecular Biology Reports* **39** 7705–7709.

Han Y, Ouyang H, Che D, Chen X, Huang Y, Elfakielhag I, Pang D and Li Z (2014) Elevated expression of vascular endothelial growth factor (VEGF) 120 in parthenogenetic porcine placentas. *Biotechnology Letters* **36** 913–917.

Hannan NJ, Paiva P, Meehan KL, Rombauts LJF, Gardner DK and Salamonsen LA (2011) Analysis of fertility-related soluble mediators in human uterine fluid identifies VEGF as a key regulator of embryo implantation. *Endocrinology* **152** 4948–4956.

Hannan NJ, Beard S, Binder NK, Onda K, Kaitu'u-Lino TJ, Chen Q, Tuohey L, De Silva M and Tong S (2017) Key players of the necroptosis pathway RIPK1 and SIRT2 are altered in placenta from preeclampsia and fetal growth restriction. *Placenta* **51** 1–9.

Hao Y, Murphy CN, Spate L, Wax D, Zhong Z, Samuel M, Mathialagan N, Schatten H and Prather RS (2008) Osteopontin Improves In Vitro Development of Porcine Embryos and Decreases Apoptosis. *Molecular Reproduction and Development* **75** 291–298.

Harris EK, Berg EP, Berg EL and Vonnahme KA (2013) Effect of maternal activity during gestation on maternal behavior, fetal growth, umbilical blood flow, and farrowing characteristics in pigs. *Journal of Animal Science* **91** 734–744.

Harville EW, Savitz DA, Dole N, Herring AH, Thorp JM and Light KC (2008) Stress and placental resistance measured by Doppler ultrasound in early and mid-pregnancy. *Ultrasound in Obstetrics and Gynecology* **32** 23–30.

Hayashi M, Ingram DI and Dauncey MJ (1987) Heat production and respiratory enzymes in normal and runt newborn piglets . *Biology of the Neonate* **51** 324–331.

Hazeleger W, Soede NM and Kemp B (2005) The effect of feeding strategy during the pre-follicular phase on subsequent follicular development in the pig. *Domestic Animal Endocrinology* **29** 362–370.

Healy MJR, McLaren A and Michie D (1961) Foetal Growth in the Mouse. *Proceedings of the Royal Society London Biological Sciences* **153** 367–379.

Heazell AEP and Crocker IP (2008) Live and Let Die - Regulation of Villous Trophoblast Apoptosis in Normal and Abnormal Pregnancies. *Placenta* **29** 772–783.

Heazell AEP, Sharp AN, Baker PN and Crocker IP (2011) Intra-uterine growth restriction is associated with increased apoptosis and altered expression of proteins in the p53 pathway in villous trophoblast. *Apoptosis* **16** 135–144.

Hennington BS and Alexander BT (2013) Linking IUGR and Blood Pressure: Insight into the Human Origins of Cardiovascular Disease. *Circulation* **128** 2179–2180.

Hernández SC V (2012) Genetics of litter size and prenatal survival in pigs. University of Edinburgh.

Hernández SC, Hogg CO, Billon Y, Sanchez MP, Bidanel JP, Haley CS, Archibald AL and Ashworth CJ (2013) Secreted Phosphoprotein 1 Expression in Endometrium and Placental Tissues of Hyperprolific Large White and Meishan Gilts. *Biology of Reproduction* **88** 1–7.

Hernández SC, Finlayson HA, Ashworth CJ, Haley CS and Archibald AL (2014) A genome-wide linkage analysis for reproductive traits in F2 Large White × Meishan cross gilts. *Animal Genetics* **45** 191–197.

Herrera EA, Alegría R, Farias M, Díaz-López F, Hernández C, Uauy R, Regnault TRH, Casanello P and Krause BJ (2016a) Assessment of in vivo fetal growth and placental vascular function in a novel intrauterine growth restriction model of progressive uterine artery occlusion in guinea pigs. *The Journal of Physiology* **594** 1553–1561.

Herrera EA, Rojas RT, Krause BJ, Ebensperger G, Reyes R V, Giussani DA, Parer JT and Llanos AJ (2016b) Cardiovascular function in term fetal sheep conceived, gestated and studied in the hypobaric hypoxia of the Andean altiplano. *Journal of Physiology* **594** 1231–1245.

Higashijima A, Miura K, Mishima H, Kinoshita A, Jo O, Abe S, Hasegawa Y, Miura S, Yamasaki K, Yoshida A *et al.* (2013) Characterization of placenta-specific microRNAs in fetal growth restriction pregnancy. *Prenatal Diagnosis* **33** 214–222.

Hirota Y, Daikoku T, Tranguch S, Xie H, Bradshaw HB and Dey SK (2010) Uterine-specific p53 deficiency confers premature uterine senescence and promotes preterm birth in mice. *Journal of Clinical Investigation* **120** 803–815.

Hodgkinson O (2007) Practical sedation and anaesthesia in pigs. *In Practice* **29** 34–39.

Hodivala-Dilke KM, Mchugh KP, Tsakiris DA, Rayburn H, Crowley D, Ullman-Cullere M, Ross FP, Coller BS, Teitelbaum S and Hynes RO (1999) β3-integrin-deficient mice are a model for Glanzmann thromboasthenia showing placental defects and reduced survival. *Journal of Clinical Investigation* **103** 229–238.

Hoeben A, Landuyt B, Highley MS, Wildiers H, Oosterom ATVAN, Bruijn EADE, Van Oosterom AT and De Bruijn EA (2004) Vascular endothelial growth factor and angiogenesis. *Pharmacological Reviews* **56** 549–580.

Hong L, Hou C, Li X, Li C, Zhao S and Yu M (2014) Expression of Heparanase Is Associated with Breed-Specific Morphological Characters of Placental Folded Bilayer Between Yorkshire and Meishan Pigs. *Biology of Reproduction* **90** 1–9.

Horta ML and Lemonica IP (2002) Placental Transfer and Embryo-Fetal Effects of Drugs Used in Anesthesia. *Brazilian Journal of Anestesiology* **52** 101–113.

Hu W, Feng Z, Teresky AK and Levine AJ (2007) p53 regulates maternal reproduction through LIF. *Nature* **450** 721–724.

Huang L, Shen Z, Xu Q, Huang X, Chen Q and Li D (2013) Increased levels of microRNA-424 are associated with the pathogenesis of fetal growth restriction. *Placenta* **34** 624–627.

Huerta S, Goulet EJ, Huerta-Yepez S and Livingston EH (2007) Screening and Detection of Apoptosis. *Journal of Surgical Research* **139** 143–156.

Huhn R, Tuchscherer A, Breite L, Grodzycki M and Huhn U (2002) Influence of base litter sex ratio of gilts on their subsequent reproductive performances. *Zuchtungskunde* **74** 56–69.

Humphries JD (2006) Integrin ligands at a glance. *Journal of Cell Science* **119** 3901–3903.

Huppertz B and Kaufmann P (1999) The apoptosis cascade in human villous trophoblast. *Trophoblast Research* **13** 215–242.

Huppertz B, Kadyrov M and Kingdom JCP (2006) Apoptosis and its role in the trophoblast. *American Journal of Obstetrics and Gynecology* **195** 29–39.

Hwang HW and Mendell JT (2006) MicroRNAs in cell proliferation, cell death, and tumorigenesis. *British Journal of Cancer* **94** 776–780.

Hynes RO (1996) Targeted Mutations in Cell Adhesion Genes: What Have We Learned from Them? *Developmental Biology* **180** 402–412.

Hyttel P, Kamstrup KM and Hyldig S (2011) From Hatching into Fetal Life in the Pig. *Acta Scientiae Veterinariae* **39** S203–S221.

Illera MJ, Cullinan E, Gui Y, Yuan L, Beyler SA and Lessey BA (2000) Blockade of the αvβ3 Integrin Adversely Affects Implantation in the Mouse1. *Biology of*

Reproduction **62** 1285–1290.

Illera MJ, Lorenzo PL, Gui Y, Beyler SA, Apparao KBC and Lessey BA (2003) A role for αvβ3 integrin during implantation in the rabbit model. *Biology of Reproduction* **68** 766–771.

Imakawa K, Imai M, Sakai A, Suzuki M, Nagaoka K, Sakai S, Lee SR, Chang KT, Echternkamp SE and Christenson RK (2006) Regulation of Conceptus Adhesion by Endometrial CXC Chemokines During the Implantation Period in Sheep. *Molecular Reproduction and Development* **73** 850–858.

Ingemarsson I (2003) Gender aspects of preterm birth. *British Journal of Obstetrics and Gynaecology* **110** 34–38.

Irving JA and Lala PK (1995) Functional role of cell surface integrins on human trophoblast cell migration: Regulation by TGF-β, IGF-II, and IGFBP-1. *Experimental Cell Research* **217** 419–427.

Ishihara N, Matsuo H, Murakoshi H, Laoag-Fernandez JB, Samoto T and Maruo T (2002) Increased apoptosis in the syncytiotrophoblast in human term placentas complicated by either preeclampsia or intrauterine growth retardation. *American Journal of Obstetrics and Gynecology* **186** 158–166.

Ishikawa H, Rattigan A, Fundele R and Burgoyne PS (2003) Effects of Sex Chromosome Dosage on Placental Size in Mice. *Biology of Reproduction* **69** 483–488.

Ishikawa H, Seki R, Yokonishi S, Yamauchi T and Yokoyama K (2006) Relationship between fetal weight, placental growth and litter size in mice from mid- to late-gestation. *Reproductive Toxicology* **21** 267–270.

Iwagaki S, Yokohama Y, Tang L, Takahashi Y, Nakagawa Y and Tamaya T (2004) Augmentation of leptin and hypoxia-inducible factor 1α mRNAs in the pre-eclamptic placenta. *Gynecological Endocrinology* **18** 263–268.

Jang YD, Ma YL and Lindemann MD (2014) Intrauterine position affects fetal weight and crown-rump length throughout gestation. *Journal of Animal Science* **92** 4400–4406.

Janot M, Cortes-Dubly ML, Rodriguez S and Huynh-Do U (2014) Bilateral uterine vessel ligation as a model of intrauterine growth restriction in mice. *Reproductive Biology and Endocrinology* **12** 1–11.

Jeffers JR, Parganas E, Lee Y, Yang C, Wang JL, Brennan J, MacLean KH, Han J, Chittenden T, Ihle JN *et al.* (2003) Puma is an essential mediator of p53-dependent and -independent apoptotic pathways. *Cancer Cell* **4** 321–328.

Jensh RP, Brent RL and Barr Jr M (1970) The Litter Effect as a Variable in Teratologic Studies of the Albino Rat. *American Journal of Anatomy* **128** 185–192.

Jeong W and Song G (2014) EGF, IGF-I, VEGF and CSF2: Effects on Trophectoderm of Porcine Conceptus. *Reproductive & Developmental Biology* **38** 21–34.

Jeong W, Kim J, Bazer FW and Song G (2013) Epidermal Growth Factor Stimulates Proliferation and Migration of Porcine Trophectoderm Cells Through Protooncogenic Protein Kinase 1 and Extracellular-Signal-Regulated Kinases

1/2 Mitogen-Activated Protein Kinase Signal Transduction Cascades During Early. *Molecular and Cellular Endocrinology* **381** 302–311.

Jeong W, Kim J, Bazer FW and Song G (2014a) Proliferation-Stimulating Effect of Colony Stimulating Factor 2 on Porcine Trophectoderm Cells is Mediated by Activation of Phosphatidylinositol 3-Kinase and Extracellular Signal-Regulated Kinase 1/2 Mitogen-Activated Protein Kinase. *PLoS ONE* **9** e88731 1–9.

Jeong W, Song G, Bazer FW and Kim J (2014b) Insulin-like growth factor I induces proliferation and migration of porcine trophectoderm cells through multiple cell signaling pathways, including protooncogenic protein kinase 1 and mitogen-activated protein kinase. *Molecular and Cellular Endocrinology* **384** 175–184.

Jeschke U, Schiessl B, Mylonas I, Kunze S, Kuhn C, Schulze S, Friese K and Mayr D (2006) Expression of the Proliferation Marker Ki-67 and of p53 Tumor Protein in Trophoblastic Tissue of Preeclamptic, HELLP, and Intrauterine Growth-Restricted Pregnancies. *International Journal of Gynecological Pathology* **25** 354–360.

Ji F, Wu G, Blanton JR and Kim SW (2005) Changes in weight and composition in various tissues of pregnant gilts and their nutritional implications. *Journal of Animal Science* **83** 366–375.

Jiménez A, Madrid-Bury N, Fernandez R, Pérez-Garnelo S, Moreira P, Pintado B, De La Fuente J and Gutiérrez-Adan A (2003) Hyperglycemia-Induced Apoptosis Affects Sex Ratio of Bovine and Murine Preimplantation Embryos. *Molecular Reproduction and Development* **65** 180–187.

Jogee M, Myatt L and Elder MG (1983) Decreased prostacyclin production by placental cells in culture from pregnancies complicated by fetal growth retardation. *British Journal of Obstetrics and Gynaecology* **90** 247–250.

Johns A, Freay AD, Fraser W, Korach KS and Rubanyi GM (1996) Disruption of Estrogen Receptor Gene Prevents 17B Estradiol-Induced Angiogenesis in Transgenic Mice. *Endocrinology* **137** 4511–4513.

Johnson GA, Burghardt RC, Spencer TE, Newton GR, Ott TL and Bazer FW (1999a) Ovine Osteopontin: II. Osteopontin and αVβ3 Integrin Expression in the Uterus and Conceptus During the Periimplantation Period. *Biology of Reproduction* **61** 892–899.

Johnson GA, Spencer TE, Burghardt RC and Bazer FW (1999b) Ovine Osteopontin: I. Cloning and Expression of Messenger Ribonucleic Acid in the Uterus During the Periimplantation Period. *Biology of Reproduction* **61** 884–891.

Johnson GA, Bazer FW, Jaeger LA, Ka H, Garlow JE, Pfarrer C, Spencer TE and Burghardt RC (2001a) Muc-1, Integrin, and Osteopontin Expression During the Implantation Cascade in Sheep. *Biology of Reproduction* **65** 820–828.

Johnson P, Stojilkovic T and Sarkar P (2001b) Middle cerebral artery Doppler in severe intrauterine growth restriction. *Ultrasound in Obstetrics and Gynecology* **17** 416–420.

Johnson GA, Burghardt RC, Bazer FW and Spencer TE (2003a) Osteopontin: Roles in Implantation and Placentation. *Biology of Reproduction* **69** 1458–1471.

Johnson GA, Burghardt RC, Joyce MM, Spencer TE, Bazer FW, Gray CA and

Pfarrer C (2003b) Osteopontin is Synthesized by Uterine Glands and a 45-kDa Cleavage Fragment is Localized at the Uterine-Placental Interface Throughout Ovine Pregnancy. *Biology of Reproduction* **69** 92–98.

Johnson LA, Rath D, Vazquez JM, Maxwell WMC and Dobrinsky JR (2005) Preselection of sex of offspring in swine for production: Current status of the process and its application. *Theriogenology* **63** 615–624.

Jones CT and Parer JT (1983) The Effect of Alterations in Placental Blood Flow on the Growth of and Nutrient Supply to the Fetal Guinea-Pig. *The Journal of Physiology* **343** 525–537.

Jones Jr M, Sheldon RE, Peeters LL, Meschia G, Battaglia FC and Makowski EL (1977) Fetal cerebral oxygen consumption at different levels of oxygenation. *Journal of Applied Physiology* **43** 1080–1084.

Junaid TO, Brownbill P, Chalmers N, Johnstone ED and Aplin JD (2014) Fetoplacental vascular alterations associated with fetal growth restriction. *Placenta* **35** 808–815.

Jung SP, Siegrist B, Wade MR, Anthony CT and Woltering EA (2001) Inhibition of human angiogenesis with heparin and hydrocortisone. *Angiogenesis* **4** 175–186.

Ka H and Hunt JS (2006) FLICE-inhibitory Protein: Expression in Early and Late Gestation Human Placentas. *Placenta* **27** 626–634.

Ka H, Spencer TE, Johnson GA and Bazer FW (2000) Keratinocyte growth factor: Expression by Endometrial Epithelia of the Porcine Uterus. *Biology of Reproduction* **62** 1772–1778.

Ka H, Jaeger LA, Johnson GA, Spencer TE and Bazer FW (2001) Keratinocyte Growth Factor Is Up-Regulated by Estrogen in the Porcine Uterine Endometrium and Functions in Trophectoderm Cell Proliferation and Differentiation. *Endocrinology* **142** 2303–2310.

Ka H, Al-Ramadan S, Erikson DW, Johnson GA, Burghardt RC, Spencer TE, Jaeger LA and Bazer FW (2007) Regulation of Expression of Fibroblast Growth Factor 7 in the Pig Uterus by Progesterone and Estradiol. *Biology of Reproduction* **77** 172–180.

Kaczynski P and Waclawik A (2013) Effect of conceptus on expression of prostaglandin F2α receptor in the porcine endometrium. *Theriogenology* **79** 784–790.

Kaczynski P, Kowalewski MP and Waclawik A (2016) Prostaglandin F2α promotes angiogenesis and embryo-maternal interactions during implantation. *Reproduction* **151** 539–552.

Kalisch-Smith J, Simmons DG, Dickinson H and Moritz KM (2017a) Review: Sexual dimorphism in the formation, function and adaptation of the placenta. *Placenta* **54** 10–16.

Kalisch-Smith JI, Simmons DG, Pantaleon M and Moritz KM (2017b) Sex differences in rat placental development: from pre-implantation to late gestation. *Biology of Sex Differences* **8** 1–13.

Kang HJ and Rosenwaks Z (2018) P53 and Reproduction. *Fertility and Sterility* **109** 39–43.

Kang YJ, Forbes K, Carver J and Aplin JD (2014) The role of the osteopontin-integrin αvβ3 interaction at implantation: Functional analysis using three different in vitro models. *Human Reproduction* **29** 739–749.

Kanoh M, Takemura G, Misao J, Hayakawa Y, Aoyama T, Nishigaki K, Noda T, Fujiwara T, Fukuda K, Minatoguchi S *et al.* (1999) Significance of Myocytes With Positive DNA In Situ Nick End Labeling (TUNEL) in Hearts with Dilated Cardiomyopathy. Not Apoptosis but DNA Repair. *Circulation* **99** 2757–2764.

Kao LC, Tulac S, Lobo S and Imani B (2002) Global Gene Profiling in Human Endometrium During the Window of Implantation. *Endocrinology* **143** 2119–2138.

Karowicz-Bilińska A, Szczerba A, Kowalska-Koprek U and Nawrocka-Kunecka A (2007) The evaluation of selected indices of apoptosis in placentas from pregnancies complicated by fetal growth restriction. *Ginekologia Polska* **78** 521–526.

Kaufmann P, Mayhew TM and Charnock-Jones DS (2004) Aspects of Human Fetoplacental Vasculogenesis and Angiogenesis. II. Changes During Normal Pregnancy. *Placenta* **25** 114–126.

Ke B, Tia M, Li J, Liu B and He G (2016) Targeting Programmed Cell Death Using Small-Molecule Compounds to Improve Potential Cancer Therapy. *Medicinal Research Reviews* **36** 938–1035.

Kearney J (2010) Food consumption trends and drivers. *Philosophical Transactions of the Royal Society B: Biological Sciences* **365** 2793–2807.

Keys JL, King GJ and Kennedy TG (1986) Increased Uterine Permeability at the Time of Embryonic Attachment in the Pig. *Biology of Reproduction* **34** 405–411.

Khoury MJ, Berg CJ and Calle EE (1990) The Ponderal Index in Term Newborn Siblings. *American Journal of Epidemiology* **132** 576–583.

Kiewisz J, Krawczynski K, Lisowski P, Blitek A, Zwierzchowski L, Ziecik AJ and Kaczmarek MM (2014) Global gene expression profiling of porcine endometria on Days 12 and 16 of the estrous cycle and pregnancy. *Theriogenology* **82** 897–909.

Kim MS, Lee YM, Moon EJ, Kim SE, Lee JJ and Kim KW (2000) Anti-Angiogenic Activity of Torilin, A Sesquiterpene Compound Isolated from Torilis Japonica. *International Journal of Cancer* **87** 269–275.

Kim J, Song G, Wu G and Bazer FW (2012) Functional roles of fructose. *Proceedings of the National Academy of Sciences* **109** E1619–E1628.

Kim M, Park HJ, Seol JW, Jang JY, Cho YS, Kim KR, Choi Y, Lydon JP, Demayo FJ, Shibuya M *et al.* (2013a) VEGF-A regulated by progesterone governs uterine angiogenesis and vascular remodelling during pregnancy. *EMBO Molecular Medicine* **5** 1415–1430.

Kim J, Song G, Wu G, Gao H, Johnson GA and Bazer FW (2013b) Arginine, Leucine, and Glutamine Stimulate Proliferation of Porcine Trophectoderm Cells Through the MTOR-RPS6K-RPS6-EIF4EBP1 Signal Transduction Pathway. *Biology of Reproduction* **88** 1–9.

Kim BJ, Park DR, Nam TS, Lee SH and Kim UH (2015) Seminal CD38 Enhances

Human Sperm Capacitation Through Its Interaction with CD31. *PLoS ONE* **10** e0139110 1–11.

Kimmins S and MacLaren LA (1999) Cyclic Modulation of Integrin Expression in Bovine Endometrium. *Biology of Reproduction* **61** 1267–1274.

King AH, Jiang Z, Gibson JP, Haley CS and Archibald AL (2003) Mapping Quantitative Trait Loci Affecting Female Reproductive Traits on Porcine Chromosome 8. *Biology of Reproduction* **68** 2172–2179.

King DP, Burman A, Gold S, Shaw AE, Jackson T and Ferris NP (2011) Integrin sub-unit expression in cell cultures used for the diagnosis of foot-and-mouth disease. *Veterinary Immunology and Immunopathology* **140** 259–265.

Kinsley C, Miele J, Wagner CK, Ghiraldi L, Broida J and Svare B (1986) Prior Intrauterine Position Influences Body Weight in Male and Female Mice. *Hormones and Behavior* **20** 201–211.

Kizaki K, Nakano H, Nakano H, Takahashi T, Imai K and Hashizume K (2001) Expression of heparanase mRNA in bovine placenta during gestation. *Reproduction* **121** 573–580.

Kizaki K, Yamada O, Nakano H, Takahashi T, Yamauchi N, Imai K and Hashizume K (2003) Cloning and Localization of Heparanase in Bovine Placenta. *Placenta* **24** 424–430.

Klemcke HG, Kumar RS, Yang K, Vallet JL and Christenson RK (2003) 11-Hydroxysteroid Dehydrogenase and Glucocorticoid Receptor Messenger RNA Expression in Porcine Placentae: Effects of Stage of Gestation, Breed, and Uterine Environment. *Biology of Reproduction* **69** 1945–1950.

Klinger S, Turgeon B, Levesque K, Wood GA, Aagaard-Tillery KM and Meloche S (2009) Loss of Erk3 function in mice leads to intrauterine growth restriction, pulmonary immaturity, and neonatal lethality. *Proceedings of the National Academy of Sciences* **106** 16710–16715.

Knight JW, Bazer FW and Wallace HD (1973) Hormonal Regulation of Porcine Uterine Protein Secretion. *Journal of Animal Science* **36** 546–553.

Knight JW, Bazer FW, Wallace HD and Wilcox CJ (1974a) Dose-Response Relationships between Exogenous Progesterone and Estradiol and Porcine Uterine Protein Secretions. *Journal of Animal Science* **39** 747–751.

Knight JW, Bazer FW and Wallace HD (1974b) Effect of Progesterone Induced Increase in Uterine Secretory Activity on Development of the Porcine Conceptus. *Journal of Animal Science* **39** 743–746.

Knight JW, Bazer FW, Thatcher WW, Franke DE and Wallace D (1977) Conceptus Development in Intact and Unilaterally Hysterectomized-Ovariectomized Gilts : Interrelations among Hormonal Status , Placental Development , Fetal Fluids and Fetal Growth. *Journal of Animal Science* **44** 620–637.

Knudson CM, Tung KSK, Tourtellotte WG, Brown GAJ and Korsmeyer SJ (1995) Bax-Deficient Mice with Lymphoid Hyperplasia and Male Germ Cell Death. *Science* **270** 96–99.

Koch S and Claesson-Welsh L (2012) Signal transduction by vascular endothelial growth factor receptors. *Cold Spring Harbor Perspectives in Medicine* **2** 1–21.

Koketsu Y, Tani S and Iida R (2017) Factors for improving reproductive performance of sows and herd productivity in commercial breeding herds. *Porcine Health Management* **3** 1–10.

Konje JC, Howarth ES, Kaufmann P and Taylor DJ (2003) Longitudinal quantification of uterine artery blood volume flow changes during gestation in pregnancies complicated by intrauterine growth restriction. *British Journal of Obstetrics and Gynaecology* **110** 301–305.

Korwin-Kossakowska A, Goluch D, Kapelanski W, Bocian M and Sender G (2013) Polymorphisms of the Osteopontin Gene and Level of its Expression in the Reproductive Tract of Sows. *Annals of Animal Science* **13** 241–252.

Koussounadis A, Langdon SP, Um IH, Harrison DJ and Smith VA (2015) Relationship between differentially expressed mRNA and mRNA-protein correlations in a xenograft model system. *Scientific Reports* **5** 1–9.

Kraemer S (2000) The Fragile Male. *British Medical Journal* **321** 1609–1612.

Krawczynski K, Bauersachs S, Reliszko ZP, Graf A and Kaczmarek MM (2015a) Expression of microRNAs and isomiRs in the porcine endometrium: Implications for gene regulation at the maternal-conceptus interface. *BioMed Central Genomics* **16** 1–19.

Krawczynski K, Najmula J, Bauersachs S and Kaczmarek MM (2015b) MicroRNAome of Porcine Conceptuses and Trophoblasts: Expression Profile of microRNAs and Their Potential to Regulate Genes Crucial for Establishment of Pregnancy. *Biology of Reproduction* **92** 1–13.

Krietsch WKG, Fundele R, Kuntz GWK, Fehlau M, Bürki K and Illmensee K (1982) The Expression of X-Linked Phosphoglycerate Kinase in the Early Mouse Embryo. *Differentiation* **23** 141–144.

Krohmer RW and Baum MJ (1989) Effect of Sex, Intrauterine Position and Androgen Manipulation on the Development of Brain Aromatase Activity in Fetal Ferrets. *Journal of Neuroendocrinology* **1** 265–271.

Krzymowski T and Stefańczyk-Krzymowska S (2004) The oestrous cycle and early pregnancy - a new concept of local endocrine regulation. *Veterinary Journal* **168** 285–296.

Kubota Y, Kleinman HK, Marin GR and Lawley TJ (1988) Role of Laminin and Basement Membrane in the Morphological Differentiation of Human Endothelial Cells into Capillary Like Structures. *Journal of Cell Biology* **107** 1589–1598.

Kusinski LC, Stanley JL, Dilworth MR, Hirt CJ, Andersson IJ, Renshall LJ, Baker BC, Baker PN, Sibley CP, Wareing M *et al.* (2012) eNOS knockout mouse as a model of fetal growth restriction with an impaired uterine artery function and placental transport phenotype. *American Journal of Physiology. Regulatory, Integrative and Comparative Physiology* **303** R86–R93.

Lamberson WR, Blair RM, Rohde Parfet KA, Day BN and Johnson RK (1988) Effect of Sex Ratio of the Birth Litter on Subsequent Reproductive Performance of Gilts. *Journal of Animal Science* **66** 595–598.

Lane M and Gardner DK (1996) Selection of viable mouse blastocysts prior to transfer using a metabolic criterion. *Human Reproduction* **11** 1975–1978.

Lantz-McPeak S, Guo X, Cuevas E, Dumas M, Newport GD, Ali SF, Paule MG and Kanungo J (2015) Developmental toxicity assay using high content screening of zebrafish embryos. *Journal of Applied Toxicology* **35** 261–272.

Larson MA, Kimura K, Kubisch HM and Roberts RM (2001) Sexual dimorphism among bovine embryos in their ability to make the transition to expanded blastocyst and in the expression of the signaling molecule IFN-τ. *Proceedings of the National Academy of Sciences* **98** 9677–9682.

Laughlin TD, Miles JR, Wright-Johnson EC, Rempel LA, Lents CA and Pannier AK (2017) Development of pre-implantation porcine blastocysts cultured within alginate hydrogel systems either supplemented with secreted phosphoprotein 1 or conjugated with Arg-Gly-Asp Peptide. *Reproduction, Fertility and Development* **29** 2345–2356.

Lee KH, Choi HR and Kim CH (2005) Anti-angiogenic effect of the seed extract of Benincasa hispida Cogniaux. *Journal of Ethnopharmacology* **97** 509–513.

Lee SH, Kim BJ and Kim UH (2017) The critical role of uterine CD31 as a post-progesterone signal in early pregnancy. *Reproduction* **154** 595–605.

Leene W, Duyzings MJM and van Steeg C (1973) Lymphoid Stem Cell Identification in the Developing Thymus and Bursa of Fabricius of the Chick. *Zeitschrift Für Zellforschung Und Mikroskopische Anatomie* **136** 521–533.

Leiser R and Dantzer V (1994) Initial Vascularisation in the Pig Placenta: II. Demonstration of Gland and Areola-Gland Subunits by Histology and Corrosion Casts. *The Anatomical Record* **238** 326–334.

van der Lende T, Hazeleger W and de Jager D (1990) Weight distribution within litters at the early foetal stage and at birth in relation to embryonic mortality in the pig. *Livestock Production Science* **26** 53–65.

Lertkiatmongkol P, Liao D, Mei H, Hu Y and Newman PJ (2016) Endothelial functions of PECAM-1 (CD31). *Current Opinion in Hematology* **23** 253–259.

Lessey BA, Castelbaum AJ, Buck CA, Lei Y, Yowell CW and Sun J (1994) Further characterization of endometrial integrins during the menstrual cycle and in pregnancy. *Fertility and Sterility* **62** 497–506.

Lessey BA, Yeh IT, Castelbaum AJ, Fritz MA, Ilesanmi AO, Korzeniowski P, Sun J and Chwalisż K (1996) Endometrial progesterone receptors and markers of uterine receptivity in the window of implantation. *Fertility and Sterility* **65** 477–483.

Letcher R, Simmen RCM, Bazer FW and Simmen FA (1989) Insulin-Like Growth Factor-1 Expression during Early Conceptus in the Pig. *Biology of Reproduction* **41** 1143–1151.

Leung DN, Smith SC, To KF, Sahota DS and Baker PN (2001) Increased placental apoptosis in pregnancies complicated by preeclampsia. *American Journal of Obstetrics and Gynecology* **184** 1249–1250.

Levy R (2005) The Role of Apoptosis in Preeclampsia. *Israel Medical Association Journal* **7** 178–181.

Levy R, Smith SD, Chandler K, Sadovsky Y and Nelson DM (2000) Apoptosis in human cultured trophoblasts is enhanced by hypoxia and diminished by

epidermal growth factor. *American Journal of Physiology. Cell Physiology* **278** C982–C988.

Leymaster KA and Jenkins TG (1993) Comparison of Texel- and Suffolk-Sired Crossbred Lambs for Survival, Growth, and Compositional Traits. *Journal of Animal Science* **71** 859–869.

Li Q, Kannan A, DeMayo FJ, Lydon JP, Cooke PS, Yamagishi H, Srivastave D, Bagchi MK and Bagchi IC (2011) The antiproliferative action of Progesterone in uterine epithelium is mediated by Hand2. *Science* **331** 912–916.

Li MC, Fang Q, He ZM, Gao Y and Zhou Y (2013) Placental expression of osteopontin (OPN) in monochorionic twins with discordant growth. *Placenta* **34** 288–290.

Li X, Bazer FW, Johnson GA, Burghardt RC, Frank JW, Dai Z, Wang J, Wu Z, Shinzato I and Wu G (2014) Dietary supplementation with L-arginine between days 14 and 25 of gestation enhances embryonic development and survival in gilts. *Amino Acids* **46** 375–384.

Lillico SG, Proudfoot C, Carlson DF, Stverakova D, Neil C, Blain C, King TJ, Ritchie WA, Tan W, Mileham AJ *et al.* (2013) Live pigs produced from genome edited zygotes. *Scientific Reports* **3** 1–4.

Lim W, Bae H, Bazer FW and Song G (2017) Stimulatory effects of fibroblast growth factor 2 on proliferation and migration of uterine luminal epithelial cells during early pregnancy. *Biology of Reproduction* **96** 185–198.

Lim W, Bae H, Bazer FW and Song G (2018) Fibroblast growth factor 2 induces proliferation and distribution of G2/M phase of bovine endometrial cells involving activation of PI3K/AKT and MAPK cell signaling and prevention of effects of ER stress. *Journal of Cellular Physiology* **233** 3295–3305.

Lin H, Wang X, Liu G, Fu J and Wang A (2007) Expression of αV and β3 Integrin Subunits During Implantation in Pig. *Molecular Reproduction and Development* **74** 1379–1385.

Lin Y, Cheng X, Sutovsky P, Wu D, Che LQ, Fang ZF, Xu SY, Ren B and Dong HJ (2017) Effect of intra-uterine growth restriction on long-term fertility in boars. *Reproduction, Fertility and Development* **29** 374–382.

Lindsten T, Aj R, King A, Wx Z, Jc R and Ha S (2000) The Combined Functions of Proapoptotic Bcl-2 Family Members Bax and Bak are Essential for Normal Development of Multiple Tissues. *Molecular Cell* **6** 1389–1399.

Lingas R, Dean F and Matthews SG (1999) Maternal nutrient restriction (48 h) modifies brain corticosteroid receptor expression and endocrine function in the fetal guinea pig. *Brain Research* **846** 236–242.

Lipiński P, Starzyński RR, Canonne-Hergaux F, Tudek B, Oliński R, Kowalczyk P, Dziaman T, Thibaudeau O, Gralak MA, Smuda E *et al.* (2010) Benefits and Risks of Iron Supplementation in Anemic Neonatal Pigs. *American Journal of Pathology* **177** 1233–1243.

Liu JP, Baker J, Perkins AS, Robertson EJ and Efstratiadis A (1993) Mice Carrying Null Mutations of the Genes Encoding Insulin-Like Growth Factor I (Igf-1) and Type 1 IGF Receptor (Igf1r). *Cell* **75** 59–72.

Liu R, Wang M, Su L, Li X, Zhao S and Yu M (2015) The Expression Pattern of microRNAs and the Associated Pathways Involved in the Development of Porcine Placental Folds That Contribute to the Expansion of the Exchange Surface Area. *Biology of Reproduction* **93** 1–13.

Locksley RM, Killeen N and Lenardo MJ (2001) The TNF and TNF Receptor Superfamilies: Integrating Mammalian Biology. *Cell* **104** 487–501.

Longtine MS, Chen B, Odibo AO, Zhong Y and Nelson DM (2012) Villous trophoblast apoptosis is elevated and restricted to cytotrophoblasts in pregnancies complicated by preeclampsia, IUGR, or preeclampsia with IUGR. *Placenta* **33** 352–359.

Lorenzen E, Follmann F, Jungersen G and Agerholm JS (2015) A review of the human vs. porcine female genital tract and associated immune system in the perspective of using minipigs as a model of human genital Chlamydia infection. *Veterinary Research* **46** 1–13.

Louton T, v. Domarus H and Hartmann P (1988) The Position Effect in Mice on Day 19. *Teratology* **38** 67–74.

Lubchenco LO, Hansman C, Dressler M and Boyd E (1963) Intrauterine Growth as Estimated from Liveborn Birth-Weight Data at 24 to 42 Weeks of Gestation. *Pediatrics* **32** 793–800.

Lunell NO, Nylund LE, Lewander R and Sarby B (1982) Uteroplacental blood flow in pre-eclampsia measurements with indium-113m and a computer-linked gamma camera. *Clinical and Experimental Hypertension Part B* **1** 105–117.

Maas JWM, Le Noble FAC, Dunselman GAJ, de Goeij AFPM, Boudier HAJS and Evers JLH (1999) The Chick Embryo Chorioallantoic Membrane as a Model to Investigate the Angiogenic Properties of Human Endometrium. *Gynecologic and Obstetric Investigation* **48** 108–112.

Macklin PS, Mcauliffe J, Pugh CW and Yamamoto A (2017) Hypoxia and HIF pathway in cancer and the placenta. *Placenta* **56** 8–13.

Magness RR (1998) Chapter 18: Maternal Cardiovascular and Other Physiological Responses to the Endocrinology of Pregnancy. In *The Endocrinology of Pregnancy*, pp 507–539. Ed F Bazer. Humana Press.

Maier T, Güell M and Serrano L (2009) Correlation of mRNA and protein in complex biological samples. *FEBS Letters* **583** 3966–3973.

Malinda KM (2009) Chapter 17: In Vivo Matrigel Migration and Angiogenesis Assay. In *Angiogenesis Protocols, Methods in Molecular Biology*, pp 287–294. Eds S Martin and C Murray. Humana Press.

Maltepe E and Fisher SJ (2015) Placenta: The Forgotten Organ. *Annual Review of Cell and Developmental Biology* **31** 523–552.

Mamdouh Z, Chen X, Plerini LM, Maxfield FR and Muller WA (2003) Targeted recycling of PECAM from endothelial surface-connected compartments during diapedesis. *Nature* **421** 748–753.

Manning FA, Platt LD and Sipos L (1980) Antepartum fetal evaluation: Development of a fetal biophysical profile. *American Journal of Obstetrics and Gynecology* **136** 787–795.

Manning FA, Harman CR, Morrison I, Menticoglou SM, Lange IR and Johnson JM (1990) Fetal assessment based on fetal biophysical profile scoring. IV. An analysis of perinatal morbidity and mortality. *American Journal of Obstetrics and Gynecology* **162** 703–709.

Marquez-Curtis LA, McGann LE and Elliott JAW (2017) Expansion and cryopreservation of porcine and human corneal endothelial cells. *Cryobiology* **77** 1–13.

Marrable AW (1971) *The Embryonic Pig: A Chronological Account*. London: Pitman Medical.

Martins VM V, Marques AP, Vasconcelos AC, Martins E, Santos RL and Lima FPC (2004) Placental maturation and expulsion in Holstein and Nelore cows. *Arquivo Brasileiro de Medicina Veterinaria E Zootecnia* **56** 157–167.

Marzusch K, Ruckh P, Hornyb P, Dietl J and Kaiserling E (1995) Short Communication : Expression of the p53 Tumour Suppressor Gene in Human Placenta: An Immunohistochemical Study. *Placenta* **16** 101–104.

Matsumura T, Wolff K and Petzelbauer P (1997) Endothelial cell tube formation depends on cadherin 5 and CD31 interactions with filamentous actin. *Journal of Immunology* **158** 3408–3416.

Mattson BA, Overstrom EW and Albertini DF (1990) Transitions in Trophectoderm Cellular Shape and Cytoskeletal Organization in the Elongating Pig Blastocyst. *Biology of Reproduction* **42** 195–205.

Mayhew TM, Leach L, McGee R, Wan Ismail W, Myklebust R and Lammiman MJ (1999) Proliferation, Differentiation and Apoptosis in Villous Trophoblast at 13-41 Weeks of Gestation (Including Observations on Annulate Lamellae and Nuclear Pore Complexes). *Placenta* **20** 407–422.

McCance RA and Dickerson JWT (1957) The Composition and Origin of the Foetal Fluids of the Pig. *Journal of Embryology and Experimental Morphology* **5** 43–50.

McCracken JA, Custer EE and Lamsa JC (1999) Luteolysis : A Neuroendocrine-Mediated Event. *Physiological Reviews* **79** 263–324.

McDermott NJ, Gandelman R and Reinisch JM (1978) Contiguity to Male Fetuses Influences Ano-Genital Distance and Time of Vaginal Opening in Mice. *Physiology and Behavior* **20** 661–663.

McDicken W (1991) *Diagnostic Ultrasonics - Principles And Use Of Instruments.* Churchill Livingstone.

McGeady TA, Quinn PJ, FitzPatrick ES, Ryan MT, Kilroy D and Lonergan P (2018) Chapter 13 Embryo mortality in domestic species. In *Veterinary Embryology Second Edition*, Second Edi, pp 112–118. John Wiley & Sons, Ltd.

McIntire DD, Bloom SL, Casey BM and Leveno KJ (1999) Birth Weight in Relation to Morbidity and Mortality Among Newborn Infants. *The New England Journal of Medicine* **340** 1234–1238.

McLaurin KA and Mactutus CF (2015) Polytocus Focus: Uterine Position Effect is Dependent Upon Horn Size. *International Journal of Developmental Neuroscience* **40** 85–91.

McMillen IC, Adams MB, Ross JT, Coulter CL, Simonetta G, Owens JA, Robinson JS and Edwards LJ (2001) Fetal growth restriction: adaptations and consequences. *Reproduction* **122** 195–204.

McNeil CJ, Nwagwu MO, Finch AM, Page KR, Thain A, McArdle HJ and Ashworth CJ (2007) Glucocorticoid exposure and tissue gene expression of 11β HSD-1, 11β HSD-2, and glucocorticoid receptor in a porcine model of differential fetal growth. *Reproduction* **133** 653–661.

McPherson RL, Ji F, Wu G, Blanton Jr. JR and Kim SW (2004) Growth and compositional changes of fetal tissues in pigs. *Journal of Animal Science* **82** 2534–2540.

Mellor DJ and Matheson IC (1979) Daily Changes in the Curved Crown-Rump Length of Individual Sheep Fetuses During the Last 60 Days of Pregnancy and Effects of Different Levels of Maternal Nutrition. *Quarterly Journal of Experimental Physiology* **64** 119–131.

Merkis C, Cristofolini A, Sanchis E and Koncurat M (2010) Expression of Death Cellular Receptors FAS / CD95 and DR4 During Porcine Placentation. *International Journal of Morphology* **28** 829–834.

Mesa H, Cammack KM, Safranski TJ, Green JA and Lamberson WR (2012) Selection for placental efficiency in swine: Conceptus development. *Journal of Animal Science* **90** 4217–4222.

Michael K, Ward BS and Moore WMO (1983) Relationship of fetal to placental size: the pig model. *European Journal of Obstetrics and Gynecology and Reproductive Biology* **16** 53–62.

Michael DD, Wagner SK, Ocón OM, Talbot NC, Rooke JA and Ealy AD (2006) Granulocyte-Macrophage Colony-Stimulating-Factor Increases Interferon-τ Protein Secretion in Bovine Trophectoderm Cells. *American Journal of Reproductive Immunology* **56** 63–67.

Mikawa T, Poh AM, Kelly KA, Ishii Y and Reese DE (2004) Induction and Patterning of the Primitive Streak, an Organizing Center of Glastrulation in the Amniote. *Developmental Dynamics* **229** 422–432.

Miles JR, Vallet JL, Freking BA and Nonneman DJ (2009) Molecular cloning and characterisation of heparanase mRNA in the porcine placenta throughout gestation. *Reproduction, Fertility and Development* **21** 757–772.

Miller SL, Huppi PS and Mallard C (2016) The consequences of fetal growth restriction on brain structure and neurodevelopmental outcome. *Journal of Physiology* **594** 807–823.

Miranda SA and Domingues SFS (2010) Conceptus ecobiometry and triplex Doppler ultrasonography of uterine and umbilical arteries for assessment of fetal viability in dogs. *Theriogenology* **74** 608–617.

Mirkin S, Arslan M, Churikov D, Corica A, Diaz JI, Williams S, Bocca S and Oehninger S (2005) In search of candidate genes critically expressed in the human endometrium during the window of implantation. *Human Reproduction* **20** 2104–2117.

Moeljono MP, Thatcher WW, Bazer FW, Frank M, Owens LJ and Wilcox CJ (1977)

A study of prostaglandin F2alpha as the luteolysin in swine: II Characterization and comparison of prostaglandin F, estrogens and progestin concentrations in utero-ovarian vein plasma of nonpregnant and pregnant gilts. *Prostaglandins* **14** 543–555.

Molina RD, Meschia G, Battaglia FC and Hay WW (1991) Gestational maturation of placental glucose transfer capacity in sheep. *The American Journal of Physiology* **261** R697–R704.

Montiel JF, Kaune H and Maliqueo M (2013) Maternal-fetal unit interactions and eutherian neocortical development and evolution. *Frontiers in Neuroanatomy* **7** 1–14.

Morales-Prieto DM and Markert UR (2011) MicroRNAs in pregnancy. *Journal of Reproductive Immunology* **88** 106–111.

Morales-Prieto DM, Chaiwangyen W, Ospina-Prieto S, Schneider U, Herrmann J, Gruhn B and Markert UR (2012) MicroRNA expression profiles of trophoblastic cells. *Placenta* **33** 725–734.

Morales-Prieto DM, Ospina-Prieto S, Chaiwangyen W, Schoenleben M and Markert UR (2013) Pregnancy-associated miRNA-clusters. *Journal of Reproductive Immunology* **97** 51–61.

Morawska-Pucinska E, Szymanska M and Blitek A (2014) Expression profile and role of prostacyclin receptor (PTGIR) in peri-implantation porcine conceptuses. *Theriogenology* **82** 546–556.

Morris SS, Victora CG, Barros FC, Halpern R, Menezes AMB, César JA, Horta BL and Tomasi E (1998) Length and ponderal index at birth: Associations with mortality, hospitalizations, development and post natal growth in Brazilian infants. *International Journal of Epidemiology* **27** 242–247.

Munro SK, Farquhar CM, Mitchell MD and Ponnampalam AP (2010) Epigenetic regulation of endometrium during the menstrual cycle. *Molecular Human Reproduction* **16** 297–310.

Muralimanoharan S, Maloyan A and Myatt L (2013) Evidence of sexual dimorphism in the placental function with severe preeclampsia. *Placenta* **34** 1183–1189.

Muralimanoharan S, Guo C, Myatt L and Maloyan A (2015) Sexual dimorphism in miR-210 expression and mitochondrial dysfunction in the placenta with maternal obesity. *International Journal of Obesity* **39** 1–8.

Murray E, Fernandes M, Fazel M, Kennedy S, Villar J and Stein A (2015) Differential effect of intrauterine growth restriction on childhood neurodevelopment: A systematic review. *British Journal of Obstetrics and Gynaecology* **122** 1062–1072.

Musk GC, Netto JD, Maker GL and Trengove R (2012) Transplacental transfer of medetomidine and ketamine in pregnant ewes. *Laboratory Animals* **46** 46–50.

Myers DL, Harmon KJ, Lindner V and Liaw L (2003) Alterations of Arterial Physiology in Osteopontin-Null Mice. *Arteriosclerosis, Thrombosis, and Vascular Biology* **23** 1021–1028.

Nagai T, Shimokawa O, Harada N, Sakazume S, Ohashi H, Matsumoto N, Obata K, Yoshino A, Murakami N, Murai T *et al.* (2002) Postnatal overgrowth by 15q-

Trisomy and Intrauterine Growth Retardation by 15q-Monosomy Due to Familial Translocation t(13;15): Dosage Effect of IGF1R? *American Journal of Medical Genetics* **113** 173–177.

Nagata S (1997) Apoptosis by Death Factor. *Cell* **88** 355–365.

Nagata S and Golstein P (1995) The Fas Death Factor. *Science* **267** 1449–1456.

Nakada D, Oguro H, Levi BP, Ryan N, Kitano A, Saitoh Y, Takeichi M, Wendt GR and Morrison SJ (2014) Oestrogen increases haematopoietic stem-cell self-renewal in females and during pregnancy. *Nature* **505** 555–558.

Nakayama K, Nakayama K, Negishi I, Kuida K, Shinkai Y, Louie M, Fields L, Lucas P, Stewart V, Alt F *et al.* (1993) Disappearance of the Lymphoid System in Bcl-2 Homozygous Mutant Chimeric Mice. *Science* **261** 1584–1588.

Neufeld G, Cohen T, Gengrinovitch S and Poltorak Z (1999) Vascular endothelial growth factor (VEGF) and its receptors. *Federation of American Societies for Experimental Biology Journal* **13** 9–22.

Newnham JP, Kelly RW, Roberts R V, Macintyre M, Speijers J, Johnson T and Reid SE (1987) Fetal and Maternal Doppler Flow Velocity Waveforms in Normal Sheep Pregnancy. *Placenta* **8** 467–476.

Nicosia RF (2009) The aortic ring model of angiogenesis: A quarter century of search and discovery. *Journal of Cellular and Molecular Medicine* **13** 4113–4136.

Nicosia RF and Ottinetti A (1990) Growth of microvessels in serum-free matrix culture of rat aorta. A quantitative assay of angiogenesis in vitro. *Laboratory Investigation* **63** 115–122.

Nicosia RF, Lin YJ, Hazelton D and Qian X (1997) Endogenous Regulation of Angiogenesis in the Rat Aorta Model. Role of Vascular Endothelial Growth Factor. *American Journal of Pathology* **151** 1379–1386.

Nicosia RF, Ligresti G and Aplin AC (2012) Preparation and Analysis of Aortic Ring Cultures for the Study of Angiogenesis Ex Vivo. In *The Textbook of Angiogenesis and Lymphangiogenesis: Methods and Applications*, pp 127–148.

Nielsen PR, Mortensen PB, Dalman C, Henriksen TB, Pedersen MG, Pedersen CB and Agerbo E (2013) Fetal Growth and Schizophrenia: A Nested Case-Control and Case-Sibling Study. *Schizophrenia Bulletin* **39** 1337–1342.

Niknejad H, Paeini-Vayghan G, Tehrani F, Khayat-Khoei M and Peirovi H (2013) Side dependent effects of the human amnion on angiogenesis. *Placenta* **34** 340–345.

Niknejad H, Khayat-Khoei M, Peirovi H and Abolghasemi H (2014) Human amniotic epithelial cells induce apoptosis of cancer cells: a new anti-tumor therapeutic strategy. *Cytotherapy* **16** 33–40.

Nilsson SK, Johnston HM, Whitty GA, Williams B, Webb RJ, Denhardt DT, Bertoncello I, Bendall LJ, Simmons PJ and Haylock DN (2005) Osteopontin, a key component of the hematopoietic stem cell niche and regulator of primitive hematopoietic progenitor cells. *Blood* **106** 1232–1239.

Norrby K (2006) In vivo models of angiogenesis. *Journal of Cellular and Molecular Medicine* **10** 588–612.

Novak SA, Paradis FA, Patterson JLA, Pasternak JAA and Oxtoby KA (2012) Temporal candidate gene expression in the sow placenta and embryo during early gestation and effect of maternal Progenos supplementation on embryonic and placental development. *Reproduction, Fertility and Development* **24** 550–558.

Nygard AB, Jørgensen CB, Cirera S and Fredholm M (2007) Selection of reference genes for gene expression studies in pig tissues using SYBR green qPCR. *BioMed Central Molecular Biology* **8** 1–6.

O'Brien CD (2004) Role of immunoreceptor tyrosine-based inhibitory motifs of PECAM-1 in PECAM-1-dependent cell migration. *American Journal of Physiology. Cell Physiology* **287** C1103–C1113.

Oats JN, Vasey DP and Waldron BA (1979) Effects of Ketamine on the Pregnant Uterus. *British Journal of Anaesthesia* **51** 1163–1166.

Okano A, Ogawa H, Takahashi H and Geshi M (2007) Apoptosis in the Porcine Uterine Endometrium During the Estrous Cycle, Early Pregnancy and Post Partum. *Journal of Reproduction and Development* **53** 923–930.

Okubo Y, Siddle K, Firth H, O'Rahilly S, Wilson LC, Willatt L, Fukushima T, Takahashi SI, Petry CJ, Saukkonen T *et al.* (2003) Cell Proliferation Activities on Skin Fibroblasts from a Short Child with Absence of One Copy of the Type 1 Insulin-Like Growth Factor Receptor (IGF1R) Gene and a Tall Child with Three Copies of the IGF1R Gene. *Journal of Clinical Endocrinology and Metabolism* **88** 5981–5988.

Oliver GA, Novak SA, Patterson JLA, Pasternak JAA and Paradis FA (2011) Restricted feed intake in lactating primiparous sows . II . Effects on subsequent litter sex ratio and embryonic gene expression. *Reproduction, Fertility and Development* **23** 899–911.

Onteru SK, Fan B, Du ZQ, Garrick DJ, Stalder KJ and Rothschild MF (2012) A whole-genome association study for pig reproductive traits. *Animal Genetics* **43** 18–26.

Østrup E, Bauersachs S, Blum H, Wolf E and Hyttel P (2010) Differential Endometrial Gene Expression in Pregnant and Nonpregnant Sows. *Biology of Reproduction* **83** 277–285.

Otrock ZK, Makarem JA and Shamseddine AI (2007) Vascular endothelial growth factor family of ligands and receptors: Review. *Blood Cells, Molecules, and Diseases* **38** 258–268.

Owens JA, Falconer J, Robinson JS and Inson SROB (1986) Effect of restriction of placental growth on umbilical and uterine blood flows. *American Journal of Physiology* **250** R427–R434.

Paauw ND, Terstappen F, Ganzevoort W, Joles JA, Gremmels H and Lely AT (2017) Sildenafil During Pregnancy: A Preclinical Meta-Analysis on Fetal Growth and Maternal Blood Pressure. *Hypertension* **70** 998–1006.

Pálos J, Szendrő ZS and Kustos K (1996) The Effect of Number and Position of Embryos in the Uterine Horns on their Weight at 30 Days of Pregnancy. *6th World Rabbit Congress* **2** 97–102.

Pan Q and Chegini N (2008) MicroRNA Signature and Regulatory Functions in the Endometrium during Normal and Disease States. *Seminars in Reproductive Medicine* **26** 479–493.

Panarace M, Garnil C, Marfil M, Jauregui G, Lagioia J, Luther E and Medina M (2006) Transrectal Doppler sonography for evaluation of uterine blood flow throughout pregnancy in 13 cows. *Theriogenology* **66** 2113–2119.

Panda S, Das A and Md Nowroz HM (2014) Sildenafil Citrate in Fetal Growth Restriction. *Journal of Reproduction & Infertility* **15** 168–169.

Parr RA, Williams AH, Campbell IP, Witcombe GF and Roberts AM (1986) Low nutrition of ewes in early pregnancy and the residual effect on the offspring. *The Journal of Agricultural Science* **106** 81–87.

Pearson PL, Klemcke HG, Christenson RK and Vallet JL (1998) Uterine Environment and Breed Effects on Erythropoiesis and Liver Protein Secretion in Late Embryonic and Early Fetal Swine. *Biology of Reproduction* **58** 911–918.

Pedersen JF (1980) Ultrasound evidence of sexual difference in fetal size in first trimester. *Obstetrical and Gynecological Survey* **281** 1253.

Peek MJ, Markham R and Fraser IS (1995) Angiogenic activity in normal and dysfunctional uterine bleeding human endometrium; as measured by the chick chorioallantoic membrane assay. *Experimental and Toxicologic Pathology* **47** 397–402.

Père MC and Etienne M (2000) Uterine blood flow in sows: effects of pregnancy stage and litter size. *Reproduction Nutrition Development* **40** 369–382.

Pérez-Crespo M, Ramírez MA, Fernández-González R, Rizos D, Lonergan P, Pintado B and Gutiérrez-Adán A (2005) Differential Sensitivity of Male and Female Mouse Embryos to Oxidative Induced Heat-Stress is Mediated by Glucose-6-Phosphate Dehydrogenase Gene Expression. *Molecular Reproduction and Development* **72** 502–510.

Perry JS (1981) The mammalian fetal membranes. *Journal of Reproduction and Fertility* **62** 321–335.

Perry JS and Rowell JG (1969) Variations in Foetal Weight and Vascular Supply Along the Uterine Horn in the Pig. *Journal of Reproduction and Fertility* **19** 527–534.

Perry JS and Rowlands IW (1962) Early Pregnancy In The Pig. *Journal of Reproduction and Fertility* **4** 175–188.

Pettigrew J, Cornelius S, Moser R, Heeg T, Hanke H, Miller K and Hagen C (1986) Effects of oral doses of corn oil and other factors on preweaning survival and growth of piglets . *Journal of Animal Science* **62** 601–612.

Phillips ID, Anthony R V, Simonetta G, Owens JA, Robinson JS, McMillen IC and Schwartz J (2001) Restriction of Fetal Growth has a Differential Impact on Fetal Prolactin and Prolactin Receptor mRNA Expression. *Journal of Neuroendocrinology* **13** 175–181.

Pineles BL, Romero R, Montenegro D, Tarca AL, Han YM, Kim YM, Draghici S, Espinoza J, Kusanovic JP, Mittal P *et al.* (2007) Distinct subsets of microRNAs are expressed differentially in the human placentas of patients with

preeclampsia. *American Journal of Obstetrics and Gynecology* **196** 1–6.

Ploner C, Kofler R and Villunger A (2008) Noxa: at the tip of the balance between life and death. *Oncogene* **27** S84–S92.

Poggi SH, Spong C, Ghidini A and Ossandon M (2004) Gender differences in amniotic fluid cytokine levels. *Journal of Maternal-Fetal and Neonatal Medicine* **15** 367–371.

Poigner J, Szendrõ ZS, Lévai A, Radnai I and Biró-Németh E (2010) Effect of Birth Weight and Litter Size on Growth and Mortality in Rabbits. *World Rabbit Science* **8** 17–22.

Polisca A, Scotti L, Orlandi R, Brecchia G and Boiti C (2010) Doppler evaluation of maternal and fetal vessels during normal gestation in rabbits. *Theriogenology* **73** 358–366.

Pontelo TP, Miranda JR, Felix MAR, Pereira BA, da Silva WE, Avelar GF, Mariano FCMQ, Guimarães GC and Zangeronimo MG (2018) Histological characteristics of the gonads of pig fetuses and their relationship with fetal anatomical measurements. *Research in Veterinary Science* **117** 28–36.

Poore KR and Fowden AL (2004) The effects of birth weight and postnatal growth patterns on fat depth and plasma leptin concentrations in juvenile and adult pigs. *Journal of Physiology* **558** 295–304.

Pope WF (1994) Chapter 3: Embryonic Mortality in Swine. In *Embryonic Mortality in Domestic Species*, pp 53–78. Eds M Zavy and RD Geisert. CRC Press.

Prast J, Saleh L, Husslein H, Sonderegger S, Helmer H and Kno M (2008) Human Chorionic Gonadotropin Stimulates Trophoblast Invasion through Extracellularly Regulated Kinase and AKT Signaling. *Endocrinology* **149** 979–987.

Prayaga KC and Eady SJ (2001) Factors Affecting Litter Size and Birth Weight in Rabbits. *Proceedings for the Advancement of Animal Breeding and Genetics* **14** 59–62.

Prior T, Wild M, Mullins E, Bennett P and Kumar S (2013) Sex Specific Differences in Fetal Middle Cerebral Artery and Umbilical Venous Doppler. *PLoS ONE* **8** e56933 1–5.

Prunier A and Quesnel H (2000) Influence of the nutritional status on ovarian development in female pigs. *Animal Reproduction Science* **60-61** 185–197.

Przygrodzka E, Witek KJ, Kaczmarek MM, Andronowska A and Ziecik AJ (2015) Expression of factors associated with apoptosis in the porcine corpus luteum throughout the luteal phase of the estrous cycle and early pregnancy: Their possible involvement in acquisition of luteolytic sensitivity. *Theriogenology* **83** 535–545.

Przygrodzka E, Kaczmarek MM, Kaczynski P and Ziecik AJ (2016) Steroid hormones, prostanoids, and angiogenic systems during rescue of the corpus luteum in pigs. *Reproduction* **151** 135–147.

Qi QR, Xie QZ, Liu XL and Zhou Y (2014) Osteopontin is Expressed in the Mouse Uterus During Early Pregnancy and Promotes Mouse Blastocyst Attachment and Invasion In Vitro. *PLoS ONE* **9** e104955 1–12.

Qin L, Wang YL, Bai SX, Ji SH, Qiu W, Tang S and Piao YS (2003) Temporal and Spatial Expression of Integrins and their Extracellular Matrix Ligands at the Maternal-Fetal Interface in the Rhesus Monkey During Pregnancy. *Biology of Reproduction* **69** 563–571.

Quadagno DM, McQuitty C, McKee J, Koelliker L, Wolfe G and Johnson DC (1987) The Effects of Intrauterine Position on Competition and Behavior in the Mouse. *Physiology and Behavior* **41** 639–642.

Qualls CP and Shine R (1995) Matemal body-volume as a constraint on reproductive output in lizards: evidence from the evolution of viviparity. *Oecologia* **103** 73–78.

Quiniou N, Dagorn J and Gaudré D (2002) Variation of piglets' birth weight and consequences on subsequent performance. *Livestock Production Science* **78** 63–70.

Rab A, Szentpéteri I, Kornya L, Börzsönyi B, Demendi C and Joó JG (2013) Placental gene expression patterns of epidermal growth factor in intrauterine growth restriction. *European Journal of Obstetrics Gynecology and Reproductive Biology* **170** 96–99.

Rahnama F, Shafiei F, Gluckman PD, Mitchell MD and Lobie PE (2006) Epigenetic Regulation of Human Trophoblastic Cell Migration and Invasion. *Endocrinology* **147** 5275–5283.

Rahnama F, Thompson B, Steiner M, Shafiei F, Lobie PE and Mitchell MD (2009) Epigenetic Regulation of E-Cadherin Controls Endometrial Receptivity. *Endocrinology* **150** 1466–1472.

Ramaekers P, Kemp B and van der Lende T (2006) Progenos in Sows Increases Number of Piglets Born. *Journal of Animal Science* **84** 394.

Rashev P, Georgieva R and Rees D (2005) Expression of α5β1 integrin and fibronectin during early pregnancy in pigs. *Folia Biologica* **51** 121–125.

Rath D and Johnson LA (2008) Application and Commercialization of Flow Cytometrically Sex-Sorted Semen. *Reproduction in Domestic Animals* **43** 338–346.

Redmer DA, Grazul AT, Kirsch JD and Reynolds LP (1988) Angiogenic activity of bovine corpora lutea at several stages of luteal development. *Journal of Reproduction and Fertility* **82** 627–634.

Reeves S and Galan HL (2017) Chapter 45: Fetal Growth Restriction. In *Maternal-Fetal Evidence Based Guidelines*, pp 412–431. Ed V BERGHELLA. CRC Press, Taylor & Francis.

Regnault TRH, Marconi AM, Smith CH, Glazier JD, Novak DA, Sibley CP and Jansson T (2005) Placental amino acid transport systems and fetal growth restriction - A workshop report. *Placenta* **26** S76–S80.

Reliszko ZP, Gajewski Z and Kaczmarek MM (2017) Signs of embryo-maternal communication: miRNAs in the maternal serum of pregnant pigs. *Reproduction* **154** 217–228.

Renegar RH, Bazer FW and Roberts RM (1982) Placental Transport and Distribution of Uteroferrin in the Fetal Pig. *Biology of Reproduction* **27** 1247–1260.

van Rens BTTM and van der Lende T (2004) Parturition in gilts: duration of farrowing, birth intervals and placenta expulsion in relation to maternal, piglet and placental traits. *Theriogenology* **62** 331–352.

Di Renzo GC, Rosati A, Sarti RD, Cruciani L and Cutuli AM (2007) Does Fetal Sex Affect Pregnancy Outcome? *Gender Medicine* **4** 19–30.

Resnick O, Morgane PJ, Hasson R and Miller M (1982) Overt and Hidden Forms of Chronic Malnutrition in the Rat and Their Relevance to Man. *Neuroscience and Biobehavioral Reviews* **6** 55–75.

Revel A, Helman A, Koler M, Shushan A, Goldshmidt O, Zcharia E, Aingorn H and Vlodavsky I (2005) Heparanase improves mouse embryo implantation. *Fertility and Sterility* **83** 580–586.

Revel A, Achache H, Stevens J, Smith Y and Reich R (2011) MicroRNAs are associated with human embryo implantation defects. *Human Reproduction* **26** 2830–2840.

Reynolds LP and Ferrell CL (1987) Transplacental clearance and blood flows of bovine gravid uterus at several stages of gestation. *American Journal of Physiology* **253** 735–739.

Reynolds LP and Redmer DA (1988) Secretion of angiogenic activity by placental tissues of cows at several stages of gestation. *Journal of Reproduction and Fertility* **83** 497–502.

Reynolds LP and Redmer DA (1995) Utero-placental vascular development and placental function. *Journal of Animal Science* **73** 1839–1851.

Reynolds LP, Ford SP and Ferrell CL (1985) Blood Flow and Steroid and Nutrient Uptake of the Gravid Uterus and Fetus of Sows. *Journal of Animal Science* **61** 968–974.

Reynolds LP, Ferrell CL, Robertson DA and Ford SP (1986) Metabolism of the gravid uterus, foetus and utero-placenta at several stages of gestation in cows. *Journal of Agricultural Science* **106** 437–444.

Reynolds LP, Borowicz PP, Vonnahme KA, Johnson ML, Grazul-Bilska AT, Redmer DA and Caton J (2005a) Placental angiogenesis in sheep models of compromised pregnancy. *Journal of Physiology* **565** 43–58.

Reynolds LP, Borowicz PP, Vonnahme KA, Johnson ML, Grazul-Bilska AT, Wallace JM, Caton JS and Redmer DA (2005b) Animal Models of Placental Angiogenesis. *Placenta* **26** 689–708.

Reynolds LP, Caton JS, Redmer DA, Grazul-Bilska AT, Vonnahme KA, Borowicz PP, Luther JS, Wallace JM, Wu G and Spencer TE (2006) Evidence for altered placental blood flow and vascularity in compromised pregnancies. *Journal of Physiology* **572** 51–58.

Ribatti D (2010) The Chick Embryo Chorioallantoic Membrane as an In Vivo Assay to Study Antiangiogenesis. *Pharmaceuticals* **3** 482–513.

Ribatti D (2015) Chapter 12: The Chick Embryo Chorioallantoic Membrane Assay. In *Handbook of Vascular Biology Techniques*, Springer N, pp 141–148. Eds M Slevin and G McDowell.

Ribatti D (2016) The chick embryo chorioallantoic membrane (CAM). A multifaceted experimental model. *Mechanisms of Development* **141** 70–77.

Ribatti D, Nico B, Vacca A, Roncali L, Burri PH and Djonov V (2001) Chorioallantoic Membrane Capillary Bed: A Useful Target for Studying Angiogenesis and Anti-Angiogenesis In Vivo. *The Anatomical Record* **264** 317–324.

Ribatti D, Nico B, Vacca A and Presta M (2006) The gelatin sponge-chorioallantoic membrane assay. *Nature Protocols* **1** 85–91.

Rice GE, Dantzer V, Madsen MT and Skadhauge E (1991) Gestational changes in electrolyte transport, electrical activity, and permeability of the porcine placenta. *Journal of Comparative Physiology B* **161** 189–198.

Rider V, Carlone DL, Witrock D, Cai C and Oliver N (1992) Uterine Fibronectin mRNA Content and Localization are Modulated During Implantation. *Developmental Dynamics* **195** 1–14.

Rines JP and vom Saal FS (1984) Fetal Effects on Sexual Behaviour and Agression in Young and Old Female Mice. *Hormones and Behavior* **18** 117–129.

Ritacco G, Radecki S V and Schoknecht PA (1997) Compensatory Growth in Runt Pigs Is Not Mediated by Insulin-Like Growth Factor I. *Journal of Animal Science* **75** 1237–1243.

Robb KP, Cotechini T, Allaire C, Sperou A and Graham CH (2017) Inflammation-induced fetal growth restriction in rats is associated with increased placental HIF-1α accumulation. *PLoS ONE* **12** e0175805 1–15.

Roberts RM and Bazer FW (1988) The functions of uterine secretions. *Journal of Reproduction and Fertility* **82** 875–892.

Roberts RM, Raub TJ and Bazer FW (1986) Role of uteroferrin in transplacental iron transport in the pig. *Federation Proceedings* **45** 2513–2518.

Roberts CT, Sohlstrom A, Kind KL, Earl RA, Khong TY, Robinson JS, Owens PC and Owens JA (2001) Maternal Food Restriction Reduces the Exchange Surface Area and Increases the Barrier Thickness of the Placenta in the Guinea-Pig. *Placenta* **22** 177–185.

Robertson SA (2007) GM-CSF regulation of embryo development and pregnancy. *Cytokine and Growth Factor Reviews* **18** 287–298.

Robertson SA, Roberts CT, Farr KL, Dunn AR and Seamark RF (1999) Fertility Impairment in Granulocyte-Macrophage Colony-Stimulating Factor-Deficient Mice. *Biology of Reproduction* **60** 251–261.

Robertson SA, Sjöblom C, Jasper MJ, Norman RJ and Seamark RF (2001) Granulocyte-Macrophage Colony-Stimulating Factor Promotes Glucose Transport and Blastomere Viability in Murine Preimplantation Embryos. *Biology of Reproduction* **64** 1206–1215.

Rohde Parfet KA, Ganjam VK, Lamberson WR, Rieke AR, vom Saal FS and Day BN (1988) Effects of Intrauterine Position on Reproductive Behavior and Performance of Gilts. *Journal of Animal Science* **66** 234.

Rohde Parfet KA, Lamberson WR, Rieke AR, Cantley TC, Ganjam VK, vom Saal

FS and Day BN (1990a) Intrauterine Position Effects in Male and Female Swine: Subsequent Survivability, Growth Rate, Morphology and Semen Characteristics. *Journal of Animal Science* **68** 179–185.

Rohde Parfet KA, Ganjam VK, Lamberson WR and Rieke AR (1990b) Intrauterine Position Effects in Female Swine: Subsequent Reproductive Performance, and Social and Sexual Behavior. *Applied Animal Behaviour Science* **26** 349–362.

Roifman M, Choufani S, Turinsky AL, Drewlo S, Keating S, Brudno M, Kingdom J and Weksberg R (2016) Genome-wide placental DNA methylation analysis of severely growth-discordant monochorionic twins reveals novel epigenetic targets for intrauterine growth restriction. *Clinical Epigenetics* **8** 1–13.

Romar GA, Kupper TS and Divito SJ (2016) Research techniques made simple: Techniques to assess cell proliferation. *Journal of Investigative Dermatology* **136** e1–e7.

Romo A, Carceller R and Tobajas J (2009) Intrauterine growth retardation (IUGR): epidemiology and etiology. *Paediatric Endocrinology Reviews* **6** 332–336.

Rootwelt V, Reksen O, Farstad W and Framstad T (2012) Associations between intrapartum death and piglet, placental, and umbilical characteristics. *Journal of Animal Science* **90** 4289–4296.

Rootwelt V, Reksen O, Farstad W and Framstad T (2013) Postpartum deaths: Piglet, placental, and umbilical characteristics. *Journal of Animal Science* **91** 2647–2656.

Rosenfeld CS (2015) Sex-Specific Placental Responses in Fetal Development. *Endocrinology* **156** 3422–3434.

Ross JW, Malayer JR, Ritchey JW and Geisert RD (2003) Characterization of the Interleukin-1 System During Porcine Trophoblastic Elongation and Early Placental Attachment. *Biology of Reproduction* **69** 1251–1259.

Ross JW, Ashworth MD, Stein DR, Couture OP, Tuggle CK and Geisert RD (2009) Identification of differential gene expression during porcine conceptus rapid trophoblastic elongation and attachment to uterine luminal epithelium. *Physiological Genomics* **36** 140–148.

De Rossi G, Scotland RS and Whiteford JR (2013) Critical Factors in Measuring Angiogenesis Using the Aortic Ring Model. *Journal of Genetic Syndromes & Gene Therapy* **4** 1–8.

Royston JP, Flecknewww PA and Wootton R (1982) New Evidence that the Intra-Uterine Growth Retarded Piglet is a Member of a Discrete Subpopulation. *Biology of the Neonate* **42** 100–104.

Ruck P, Marzusch K, Kaiserling E, Horny HP, Dietl J, Geiselhart A, Handgretinger R and Redman CW (1994) Distribution of cell adhesion molecules in decidua of early human pregnancy. An immunohistochemical study. *Laboratory Investigation* **71** 94–101.

Rudolph AM and Heymann MA (1970) Circulatory changes during growth in the fetal lamb. *Circulation Research* **26** 289–299.

Rutherford KMD, Baxter EM, D'Eath RB, Turner SP, Arnott G, Roehe R, Ask B, Sandøe P, Moustsen VA, Thorup F *et al.* (2013) The welfare implications of

large litter size in the domestic pig I: biologicaL factors. *Animal Welfare* **22** 199–218.

Ryan BC and Vandenbergh JG (2002) Intrauterine position effects. *Neuroscience and Biobehavioral Reviews* **26** 665–678.

vom Saal FS (1981) Variation in phenotype due to random intrauterine positioning of male and female fetuses in rodents. *Journal of Reproduction and Fertility* **62** 633–650.

vom Saal FS (1983) Variation in infanticide and parental behavior in male mice due to prior intrauterine proximity to female fetuses: Elimination by prenatal stress. *Physiology and Behavior* **30** 675–681.

vom Saal FS (1988) *Perinatal Testosterone Exposure Has Opposite Effects on Adult Intermale Aggression and Infanticide in Mice*.

vom Saal FS (1989) Sexual differentiation in litter-bearing mammals: influence of sex of adjacent fetuses in utero. *Journal of Animal Science* **67** 1824–1840.

Vom Saal FS (1989) The production of and sensitivity to cues that delay puberty and prolong subsequent oestrous cycles in female mice are influenced by prior intrauterine position. *Journal of Reproduction and Fertility* 457–471.

vom Saal FS and Bronson FH (1978) In Utero Proximity of Female Mouse Fetuses to Males: Effect on Reproductive Performance during Later Life. *Biology of Reproduction* **19** 842–853.

vom Saal FS and Bronson FH (1980a) Sexual Characteristics of Adult Female Mice Are Correlated with Their Blood Testosterone Levels During Prenatal Development. *Science* **208** 597–599.

vom Saal FS and Bronson FH (1980b) Variation in Length of the Estrous Cycle in Mice Due to Former Intrauterine Proximity to Male Fetuses. *Biology of Reproduction* **22** 777–780.

vom Saal FS and Dhar M (1992) Blood Flow in the Uterine Loop Artery and Loop Vein is Bidirectional in the Mouse: Implications for Transport of Steroids between Fetuses. *Physiology and Behavior* **52** 163–171.

vom Saal FS, Quadagno M, Keisler DH, Even MD, Khan S and Keisler LW (1990) Paradoxical Effects of Maternal Stress on Fetal Steroids and Postnatal Reproductive Traits in Female Mice from Different Intrauterine of Biological of Biological of Animal. *Biology of Reproduction* **43** 751–761.

vom Saal FS, Clark MM, Galef Jr. BG, Drickamer LC and Vandenbergh JG (1999) Intrauterine Position Phenomenon. *Encyclopedia of Reproduction Volume 2* 893–900.

Safa AR (2012) c-FLIP, A Master Anti-Apoptotic Regulator. *Experimental Oncology* **34** 176–184.

Sales KJ, List T, Boddy SC, Williams ARW, Anderson RA, Naor Z and Jabbour HN (2005) A Novel Angiogenic Role for Prostaglandin F2α-FP Receptor Interaction in Human Endometrial Adenocarcinomas. *Cancer Research* **65** 7707–7716.

Di Salvo P, Bocci F, Zelli R and Polisca A (2006) Doppler evaluation of maternal

and fetal vessels during normal gestation in the bitch. *Theriogenology* **81** 382–388.

Samborski A, Graf A, Krebs S, Kessler B and Bauersachs S (2013a) Deep Sequencing of the Porcine Endometrial Transcriptome on Day 14 of Pregnancy. *Biology of Reproduction* **88** 1–13.

Samborski A, Graf A, Krebs S, Kessler B, Reichenbach M, Reichenbach HD, Ulbrich SE and Bauersachs S (2013b) Transcriptome Changes in the Porcine Endometrium During the Preattachment Phase. *Biology of Reproduction* **89** 1–16.

Sandman CA, Glynn LM and Davis EP (2013) Is there a viability-vulnerability tradeoff? Sex differences in fetal programming. *Journal of Psychosomatic Research* **75** 327–335.

Sangamam R (2015) Perinatal mortality and morbidity among low birth weight babies. *International Journal of Community Medicine and Public Health* **2** 51–58.

Sasser JM and Baylis C (2010) Effects of sildenafil on maternal hemodynamics and fetal growth in normal rat pregnancy. *American Journal of Physiology. Regulatory, Integrative and Comparative Physiology* **298** R433–R438.

Satterfield MC, Bazer FW, Spencer TE and Wu G (2010) Sildenafil Citrate Treatment Enhances Amino Acid Availability in the Conceptus and Fetal Growth in an Ovine Model of Intrauterine Growth Restriction. *Journal of Nutrition* **140** 251–258.

Schäfer WR, Fischer L, Roth K, Jüllig AK, Stuckenschneider JE, Schwartz P, Weimer M, Orlowska-Volk M, Hanjalic-Beck A, Kranz I *et al.* (2011) Critical evaluation of human endometrial explants as an ex vivo model system: a molecular approach. *Molecular Human Reproduction* **17** 255–265.

Schultz JF and Armant DR (1995) β1- and β3-Class Integrins Mediate Fibronectin Binding Activity at the Surface of Developing Mouse Peri-implantation Blastocysts. *Journal of Biological Chemistry* **270** 11522–11531.

Schultz JF, Mayernik L, Rout UK and Armant DR (1997) Integrin Trafficking Regulates Adhesion to Fibronectin During Differentiation of Mouse Peri-Implantation Blastocysts. *Developmental Genetics* **21** 31–43.

Schwartz MA and Assoian RK (2001) Integrins and cell proliferation: regulation of cyclin-dependent kinases via cytoplasmic signaling pathways. *Journal of Cell Science* **114** 2553–2560.

Scifres CM and Nelson DM (2009) Intrauterine growth restriction, human placental development and trophoblast cell death. *Journal of Physiology* **587** 3453–3458.

Scott FL, Stec B, Pop C, Dobaczewska MK, Lee JJ, Monosov E, Robinson H, Salvesen GS, Schwarzenbacher R and Riedl SJ (2009) The Fas-FADD death domain complex structure unravels signalling by receptor clustering. *Nature* **457** 1019–1022.

Scotti L, Di Salvo P, Bocci F, Pieramati C and Polisca A (2008) Doppler evaluation of maternal and foetal vessels during normal gestation in queen. *Theriogenology* **69** 1111–1119.

Seeds JW and Peng T (1998) Impaired growth and risk of fetal death: Is the tenth

percentile the appropriate standard? *American Journal of Obstetrics and Gynecology* **178** 658–669.

Seisenberger S, Peat JR and Reik W (2013) Conceptual links between DNA methylation reprogramming in the early embryo and primordial germ cells. *Current Opinion in Cell Biology* **25** 281–288.

Sell-Kubiak E, Duijvesteijn N, Lopes MS, Janss LLG, Knol EF, Bijma P and Mulder HA (2015) Genome-wide association study reveals novel loci for litter size and its variability in a Large White pig population. *BioMed Central Genomics* **16** 1–13.

Seo HW, Li XL, Bayless KJ, Bazer FW, Wu G and Johnson GA (2014) Supplementation of pregnant pigs with arginine increases folding at the uterine-placental interface of pigs: A mechanism to increase nutrient transport from mother to fetus to improve fetal development and survival. In *Society of the Study of Reproduction Annual Meeting*, pp 19–23.

Serin G, Gökdal Ö, Tarimcilar T and Atay O (2010) Umbilical artery doppler sonography in Saanen goat fetuses during singleton and multiple pregnancies. *Theriogenology* **74** 1082–1087.

Šerman L, Vlahović M, Šijan M, Bulić-Jakuš F, Šerman A, Sinčić N, Matijević R, Jurić-Lekić G and Katušić A (2007) The Impact of 5-Azacytidine on Placental Weight, Glycoprotein Pattern and Proliferating Cell Nuclear Antigen Expression in Rat Placenta. *Placenta* **28** 803–811.

Seymour JF, Lieschke GJ, Grail D, Quilici C, Hodgson G and Dunn AR (1997) Mice Lacking Both Granulocyte Colony-Stimulating Factor (CSF) and Granulocyte-Macrophage CSF have Impaired Reproductive Capacity, Perturbed Neonatal Granulopoiesis, Lung Disease, Amyloidosis, and Reduced Long-Term Survival. *Blood* **90** 3037–3049.

Sferruzzi-Perri AN, Macpherson AM, Roberts CT and Robertson SA (2009) Csf2 Null Mutation Alters Placental Gene Expression and Trophoblast Glycogen Cell and Giant Cell Abundance in Mice. *Biology of Reproduction* **81** 207–221.

Sferruzzi-Perri AN, Owens JA, Pringle KG and Roberts CT (2011) The neglected role of insulin-like growth factors in the maternal circulation regulating fetal growth. *Journal of Physiology* **589** 7–20.

Sharma D, Shastri S and Sharma P (2016) Intrauterine Growth Restriction: Antenatal and Postnatal Aspects. *Clinical Medical Insights: Pediatrics* **10** 67–83.

Shibuya M (2011) Vascular Endothelial Growth Factor (VEGF) and Its Receptor (VEGFR) Signaling in Angiogenesis: A Crucial Target for Anti- and Pro-Angiogenic Therapies. *Genes and Cancer* **2** 1097–1105.

Shiokawa S, Yoshimura Y, Nagamatsu S, Sawa H, Hanashi H, Koyama N, Katsumata Y, Nagai A and Nakamura Y (1996) Function of β1 Integrins on Human Decidual Cells During Implantation. *Biology of Reproduction* **54** 745–752.

Shiokawa S, Yoshimura Y, Sawa H, Nagamatsu S, Hanashi H, Sakai K, Ando M and Nakamura Y (1999) Functional Role of Arg-Gly-Asp (RGD)-Binding Sites on β1 Integrin in Embryo Implantation Using Mouse Blastocysts and Human Decidua. *Biology of Reproduction* **60** 1468–1474.

Signoret JP (1971) The Mating Behavior of the Sow. In *Pig Production*, pp 295–313.

Silva LA and Ginther OJ (2010) Local effect of the conceptus on uterine vascular perfusion during early pregnancy in heifers. *Reproduction* **139** 453–463.

Da Silva-Buttkus P, Hurk RVD, Velde ER and Taverne MAM (2003) Ovarian development in intrauterine growth-retarded and normally developed piglets originating from the same litter. *Reproduction* **126** 249–258.

Simmen RCM, Simmen FA, Hofig A, Farmer SJ and Bazer FW (1990) Hormonal Regulation of Insulin-Like Growth Factor Gene Expression in Pig Uterus. *Endocrinology* **127** 2166–2174.

Singh P, Carraher C and Schwarzbauer JE (2010) Assembly of Fibronectin into Extracellular Matrix. *Annual Review of Cell and Developmental Biology* **26** 397–419.

Sjöblom C, Wikland M and Robertson SA (1999) Granulocyte-macrophage colony-stimulating factor promotes human blastocyst development in vitro. *Human Reproduction* **14** 3069–3076.

Sjöblom C, Roberts CT, Wikland M and Robertson SA (2005) Granulocyte-Macrophage Colony-Stimulating Factor Alleviates Adverse Consequences of Embryo Culture on Fetal Growth Trajectory and Placental Morphogenesis. *Endocrinology* **146** 2142–2153.

Sloop GD, Roa JC, Delgado AG, Balart JT, Hines MO and Hill JM (1999) Histologic sectioning produces TUNEL reactivity: A potential cause of false-positive staining. *Archives of Pathology and Laboratory Medicine* **123** 529–532.

Smit MN, Spencer JD, Almeida FRCL, Patterson JL, Chiarini-Garcia H, Dyck MK and Foxcroft GR (2013) Consequences of a low litter birth weight phenotype for postnatal lean growth performance and neonatal testicular morphology in the pig. *Animal* **7** 1681–1689.

Smith CA, Farmh T and Goodwin R (1994) The TNF Receptor Superfamily of Cellular and Viral Proteins : Activation & stimulation and Death. *Cell* **76** 959–962.

Smith SC, Baker PN and Symonds EM (1997) Increased placental apoptosis in intrauterine growth restriction. *American Journal of Obstetrics and Gynecology* **177** 1395–1401.

Snegovskikh V, Hodgson E, Wehrum M, Luo G, Funai E, Ma Y, Rahman M and Norwitz E (2007) Human chorionic gonadotrophin (hcg) is produced by both synctiotrophoblast and cytotrophoblast cells: a paradigm shift. *American Journal of Obstetrics and Gynecology* **Suppl Dece** S120.

Snijders RJ, Abbas A, Melby O, Ireland RM and Nicolaides KH (1993) Fetal plasma erythropoietin concentration in severe growth retardation. *American Journal of Obstetrics and Gynecology* **168** 615–619.

Soede NM, Wetzels CCH, Zondag W, de Koning MA and Kemp B (1995) Effects of time of insemination relative to ovulation, as determined by ultrasonography, on fertilization rate and accessory sperm count in sows. *Journal of Reproduction and Fertility* **104** 99–106.

Soede NM, Langendijk P and Kemp B (2011) Reproductive cycles in pigs. *Animal Reproduction Science* **124** 251–258.

Soleymanlou N, Jurisica I, Nevo O, Ietta F, Zhang X, Zamudio S, Post M and Caniggia I (2005) Molecular Evidence of Placental Hypoxia in Preeclampsia. *Journal of Clinical Endocrinology and Metabolism* **90** 4299–4308.

Solnica-Krezel L and Sepich DS (2012) Gastrulation: Making and Shaping Germ Layers. *Annual Review of Cell and Developmental Biology* **28** 687–717.

Sookoian S, Gianotti TF, Burgueño AL and Pirola CJ (2013) Fetal metabolic programming and epigenetic modifications: A systems biology approach. *Pediatric Research* **73** 531–542.

Spencer TE and Bazer FW (2004) Conceptus signals for establishing and maintenance of pregnancy. *Reproductive Biology and Endocrinology* **2** 1–15.

Spencer TE, Johnson GA, Burghardt RC and Bazer FW (2004) Progesterone and Placental Hormone Actions on the Uterus: Insights from Domestic Animals. *Biology of Reproduction* **71** 2–10.

Sprague BJ, Phernetton TM, Magness RR and Chesler NC (2009) The effects of the ovarian cycle and pregnancy on uterine vascular impedance and uterine artery mechanics. *European Journal of Obstetrics & Gynecology and Reproductive Biology* **144S** S170–S178.

Srichai MB and Zent R (2010) Chapter 2: Integrin Structure and Function. In *Cell-Extracellular Matrix Interactions in Cancer*, pp 19–41.

Staines KA, MacRae V and Farquharson C (2012) The importance of the SIBLING family of proteins on skeletal mineralisation and bone remodelling. *Journal of Endocrinology* **214** 241–255.

Stallmach T, Duc C, Van Praag E, Mumenthaler C, Ott C, Kolb SA, Hebisch G and Steiner R (2001) Feto-maternal interface of human placenta inhibits angiogenesis in the chick chorioallantoic membrane (CAM) assay. *Angiogenesis* **4** 79–84.

Steele VS and Froseth JA (1980) Effect of Gestational Age on the Biochemical Composition of Porcine Placental Glycosaminoglycans. *Processings of the Society for Experimental Biology and Medicine* **165** 480–485.

Steinhauser CB, Bazer FW, Burghardt RC and Johnson GA (2017) Expression of progesterone receptor in the porcine uterus and placenta throughout gestation: correlation with expression of uteroferrin and osteopontin. *Domestic Animal Endocrinology* **58** 19–29.

Stephens L, Sutherland A and Klimanskaya I (1995) Deletion of β1 integrins in mice results in inner cell mass failure and peri-implantation lethality. *Genes and Development* **9** 1883–1895.

Stephens AS, Bentley JP, Taylor LK and Arbuckle SM (2015) Diagnosis of fetal growth restriction in perinatal deaths using brain to liver weight ratios. *Pathology* **47** 51–57.

Stern CD (2005) The Chick: A Great Model System Becomes Even Greater. *Developmental Cell* **8** 9–17.

Stewart CL, Kaspar P, Brunet LJ, Bhatt H, Gadi I, Kontgen F and Abbondanzo SJ (1992) Blastocyst implantation depends on maternal expression of leukaemia inhibitory factor. *Nature* **359** 76–79.

Stier S, Ko Y, Forkert R, Lutz C, Neuhaus T, Grünewald E, Cheng T, Dombkowski D, Calvi LM, Rittling SR *et al.* (2005) Osteopontin is a hematopoietic stem cell niche component that negatively regulates stem cell pool size. *The Journal of Experimental Medicine* **201** 1781–1791.

Straszewski-Chavez SL, Abrahams VM and Mor G (2005) The Role of Apoptosis in the Regulation of Trophoblast Survival and Differentiation During Pregnancy. *Endocrine Reviews* **26** 877–897.

Stroband HW and Van der Lende T (1990) Embryonic and uterine development during early pregnancy in pigs. *Journal of Reproduction Supplement* **40** 261–277.

Strümper D, Gogarten W, Durieux ME, Hartleb K, Van Aken H and Marcus MAE (2004) The Effects of S+-Ketamine and Racemic Ketamine on Uterine Blood Flow in Chronically Instrumented Pregnant Sheep. *Anesthesia and Analgesia* **98** 497–502.

Sturmey RG, Bermejo-Alvarez P, Gutierrez-Adan A, Rizos D, Leese HJ and Lonergan P (2010) Amino Acid Metabolism of Bovine Blastocysts: A Biomarker of Sex and Viability. *Molecular Reproduction and Development* **77** 285–296.

Su L, Zhao S, Zhu M and Yu M (2010) Differential expression of microRNAs in porcine placentas on Days 30 and 90 of gestation. *Reproduction, Fertility and Development* **22** 1175–1182.

Su L, Liu R, Cheng W, Zhu M, Li X, Zhao S and Yu M (2014) Expression Patterns of MicroRNAs in Porcine Endometrium and Their Potential Roles in Embryo Implantation and Placentation. *PloS ONE* **9** e87867 1–10.

Suhag A and Berghella V (2013) Intrauterine Growth Restriction (IUGR): Etiology and Diagnosis. *Current Obstetrics and Gynecology Reports* **2** 102–111.

Sutherland AE, Calarco PG and Damsky CH (1993) Developmental regulation of integrin expression at the time of implantation in the mouse embryo. *Development* **119** 1175–1186.

Swanson AM and David AL (2015) Animal models of fetal growth restriction: Considerations for translational medicine. *Placenta* **36** 623–630.

Swindle MM, Makin A, Herron AJ, Clubb FJ and Frazier KS (2012) Swine as Models in Biomedical Research and Toxicology Testing. *Veterinary Pathology* **49** 344–356.

Tabano S, Colapietro P, Cetin I, Grati FR, Zanutto S, Mandò C, Antonazzo P, Pileri P, Rossella F, Larizza L *et al.* (2010) Epigenetic modulation of the IGF2/H19 imprinted domain in human embryonic and extra-embryonic compartments and its possible role in fetal growth restriction. *Epigenetics* **5** 313–324.

Tait SWG, Ichim G and Green DR (2014) Die another way – non-apoptotic mechanisms of cell death. *Journal of Cell Science* **127** 2135–2144.

Tal R (2012) The Role of Hypoxia and Hypoxia-Inducible Factor-1Alpha in Preeclampsia Pathogenesis. *Biology of Reproduction* **87** 1–8.

Tal R, Shaish A, Barshack I, Polak-Charcon S, Afek A, Volkov A, Feldman B, Avivi C and Harats D (2010) Effects of Hypoxia-Inducible Factor-1α

Overexpression in Pregnant Mice: Possible Implications for Preeclampsia and Intrauterine Growth Restriction. *American Journal of Pathology* **177** 2950–2962.

Tanaka M, Natori M, Ishimoto H, Miyazaki T, Kobayashi T and Nozawa S (1994) Experimental growth retardation produced by transient period of uteroplacental ischemia in pregnant Sprague-Dawley rats. *American Journal of Obstetrics and Gynecology* **171** 1231–1234.

Tarraf CG and Knight JW (1995) Effect of intrauterine position on conceptus development, placental and endometrial release of progesterone and estrone in vitro, and concentration of steroid hormones in fetal fluids throughout gestation in swine. *Domestic Animal Endocrinology* **12** 179–187.

Tayade C, Black GP, Fang Y and Croy BA (2006) Differential Gene Expression in Endometrium, Endometrial Lymphocytes, and Trophoblasts During Successful and Abortive Embryo Implantation. *Journal of Immunology* **176** 148–156.

Tayade C, Fang Y and Croy BA (2007a) A Review of Gene Expression in Porcine Endometrial Lymphocytes , Endothelium and Trophoblast During Pregnancy Success and Failure. *Journal of Reproduction and Development* **53** 455–463.

Tayade C, Fang Y, Hilchie D and Croy BA (2007b) Lymphocyte contributions to altered endometrial angiogenesis during early and midgestation fetal loss. *Journal of Leukocyte Biology* **82** 877–886.

Tchirikov M, Hecher K, Deprest J, Zikulnig L, Devlieger R and Schröder HJ (2001) Doppler ultrasound measurements in the central circulation of anesthetized fetal sheep during obstruction of umbilical-placental blood flow. *Ultrasound in Obstetrics and Gynecology* **18** 656–661.

Thamotharan S, Chu A, Kempf K, Janzen C, Grogan T, Elashoff DA and Devaskar SU (2017) Differential microRNA expression in human placentas of term intra-uterine growth restriction that regulates target genes mediating angiogenesis and amino acid transport. *PLoS ONE* **12** e0176493 1–26.

Thankamony A, Pasterski V, Ong KK, Acerini CL and Hughes IA (2016) Anogenital distance as a marker of androgen exposure in humans. *Andrology* **4** 616–625.

Thompson RS, Trudinger BJ and Cook CM (1988) Doppler ultrasound waveform indices: A/B ratio, pulsatility index and Pourcelot ratio. *British Journal of Obstetrics and Gynaecology* **95** 581–588.

Tilley RE, McNeil CJ, Ashworth CJ, Page KR and McArdle HJ (2007) Altered muscle development and expression of the insulin-like growth factor system in growth retarded fetal pigs. *Domestic Animal Endocrinology* **32** 167–177.

Tingen C, Kim A and Woodruff TK (2009) The primordial pool of follicles and nest breakdown in mammalian ovaries. *Molecular Human Reproduction* **15** 795–803.

Todros T, Marzioni D, Lorenzi T, Piccoli E, Capparuccia L, Perugini V, Cardaropoli S, Romagnoli R, Gesuita R, Rolfo A *et al.* (2007) Evidence for a Role of TGF-β1 in the Expression and Regulation of α-SMA in Fetal Growth Restricted Placentae. *Placenta* **28** 1123–1132.

Tolcos M and Rees S (1997) Chronic placental insufficiency in the fetal guinea pig affects neurochemical and neuroglial development but not neuronal numbers in

the brainstem: A new method for combined stereology and immunohistochemistry. *Journal of Comparative Neurology* **379** 99–112.

Torres-Rovira L, Tarrade A, Astiz S, Mourier E, Perez-Solana M, de la Cruz P, Gomez-Fidalgo E, Sanchez-Sanchez R, Chavatte-Palmer P and Gonzalez-Bulnes A (2013) Sex and Breed-Dependent Organ Development and Metabolic Responses in Foetuses from Lean and Obese/Leptin Resistant Swine. *PLoS ONE* **8** e66728 1–9.

Toshiyuki M and Reed JC (1995) Tumor suppressor p53 is a direct transcriptional activator of the human bax gene. *Cell* **80** 293–299.

Town SC, Putman CT, Turchinsky NJ, Dixon WT and Foxcroft GR (2004) Number of conceptuses in utero affects porcine fetal muscle development. *Reproduction* **128** 443–454.

Tummaruk P, Lundeheim N, Einarsson S and Dalin AM (2000) Factors influencing age at first mating in purebred Swedish Landrace and Swedish Yorkshire gilts. *Animal Reproduction Science* **63** 241–253.

Unterscheider J, O'Donoghue K, Daly S, Geary MP, Kennelly MM, McAuliffe FM, Hunter A, Morrison JJ, Burke G, Dicker P *et al.* (2014) Fetal growth restriction and the risk of perinatal mortality-case studies from the multicentre PORTO study. *BioMed Central Pregnancy and Childbirth* **14** 2–7.

Usha K and Sarita B (2011) Placental Insufficiency and Fetal Growth Restriction. *Journal of Obstetrics and Gynecology of India* **61** 505–511.

Vailhé B, Vittet D and Feige JJ (2001) In vitro Models of Vasculogenesis and Angiogenesis. *Laboratory Investigation* **81** 439–452.

Vallet JL and Freking BA (2007) Differences in placental structure during gestation associated with large and small pig fetuses. *Journal of Animal Science* **85** 3267–3275.

Vallet JL, Klemcke HG and Christenson RK (2002) Interrelationships among conceptus size, uterine protein secretion, fetal erythropoiesis, and uterine capacity. *Journal of Animal Science* **80** 729–737.

Vallet JL, Klemcke HG, Christenson RK and Pearson PL (2003) The effect of breed and intrauterine crowding on fetal erythropoiesis on day 35 of gestation in swine. *Journal of Animal Science* **81** 2352–2356.

Vallet JL, Freking BA and Miles JR (2011) Effect of empty uterine space on birth intervals and fetal and placental development in pigs. *Animal Reproduction Science* **125** 158–164.

Vandenbergh JG and Huggett CL (1995) The anogenital distance index, a predictor of the intrauterine position effects on reproduction in female house mice. *Laboratory Animal Science* **45** 567–573.

Vandesompele J, Preter KD, Poppe B, Roy N V and Paepe AD (2002) Accurate normalization of real-time quantitative RT -PCR data by geometric averaging of multiple internal control genes. *Genome Biology* **3** 1–12.

Vatten LJ and Skjærven R (2004) Offspring sex and pregnancy outcome by length of gestation. *Early Human Development* **76** 47–54.

Vaughan TJ, James PS, Pascall JC, Brown KD, Varley JM, Klagsbrun M, Andrews GK and Dey SK (1992) Expression of the genes for TGF alpha, EGF and the EGF receptor during early pig development. *Development* **116** 663–669.

Veis DJ, Sorenson CM, Shutter JR and Korsmeyer SJ (1993) Bcl-2-deficient mice demonstrate fulminant lymphoid apoptosis, polycystic kidneys, and hypopigmented hair. *Cell* **75** 229–240.

Vélez C, Williamson D, Riesco O, Martín P, García M, Yaful G and Koncurat M (2015) Estrogens, progesterone and integrin-fibronectin interaction during porcine placentation. *Placenta* **36** 500.

Vélez C, Barbeito C and Koncurat M (2017) αvβ3 Integrin and fibronectin expressions and their relation to estrogen and progesterone during placentation in swine. *Biotechnic and Histochemistry* **7** 1–7.

Vernunft A, Ivell R, Heng K and Anand-Ivell R (2016) The male fetal biomarker INSL3 reveals substantial hormone exchange between fetuses in early pig gestation. *PLoS ONE* **11** 1–14.

Vickers MH, Clayton ZE, Yap C and Sloboda DM (2011) Maternal fructose intake during pregnancy and lactation alters placental growth and leads to sex-specific changes in fetal and neonatal endocrine function. *Endocrinology* **152** 1378–1387.

Villaschi S and Nicosia RF (1993) Angiogenic role of endogenous basic fibroblast growth factor released by rat aorta after injury. *The American Journal of Pathology* **143** 181–190.

Vincent IC, Williams HL and Hill R (1985) The influence of a low-nutrient intake after mating on gestation and perinatal survival of lambs. *British Veterinary Journal* **141** 611–617.

Vlodavsky I and Friedmann Y (2001) Heparan sulfate proteoglycans Molecular properties and involvement of heparanase in cancer metastasis and angiogenesis. *Journal of Clinical Investigation* **108** 341–347.

Vlodavsky I, Goldshmidt O, Zcharia E, Atzmon R, Rangini-Guatta Z, Elkin M, Peretz T and Friedmann Y (2002) Mammalian heparanase: Involvement in cancer metastasis, angiogenesis and normal development. *Seminars in Cancer Biology* **12** 121–129.

Vomachka AJ and Lisk RD (1986) Androgen and estradiol levels in plasma and amniotic fluid of late gestational male and female hamsters: Uterine position effects. *Hormones and Behavior* **20** 181–193.

Vonnahme KA and Ford SP (2004) Placental vascular endothelial growth factor receptor system mRNA expression in pigs selected for placental efficiency. *The Journal of Physiology* **554** 194–201.

Vonnahme KA, Wilson ME and Ford SP (2001) Relationship between placental vascular endothelial growth factor expression and placental/endometrial vascularity in the pig. *Biology of Reproduction* **64** 1821–1825.

Vonnahme K a, Wilson ME, Foxcroft GR and Ford SP (2002) Impacts on conceptus survival in a commercial swine herd. *Journal of Animal Science* **80** 553–559.

Vonnahme KA, Hess BW, Hansen TR, McCormick RJ, Rule DC, Moss GE,

Murdoch WJ, Nijland MJ, Skinner DC, Nathanielsz PW *et al.* (2003) Maternal Undernutrition from Early- to Mid-Gestation Leads to Growth Retardation, Cardiac Ventricular Hypertrophy, and Increased Liver Weight in the Fetal Sheep. *Biology of Reproduction* **69** 133–140.

van Vorstenbosch CJAH V, Colenbrander B and Wensing CJG (1982) Leydig Cell Development of Pig Testis in the Early Fetal Period: an Ultrastructural Study. *American Journal of Anatomy* **165** 305–318.

Vuguin PM (2007) Animal Models for Small for Gestational Age and Fetal Programing of Adult Disease. *Hormone Research* **68** 113–123.

Waclawik A and Ziecik AJ (2007) Differential expression of prostaglandin (PG) synthesis enzymes in conceptus during peri-implantation period and endometrial expression of carbonyl reductase/PG 9-ketoreductase in the pig. *Journal of Endocrinology* **194** 499–510.

Waclawik A, Rivero-Muller A, Blitek A, Kaczmarek MM, Brokken LJS, Watanabe K, Rahman NA and Ziecik AJ (2006) Molecular cloning and spatiotemporal expression of prostaglandin F synthase and microsomal prostaglandin E synthase-1 in porcine endometrium. *Endocrinology* **147** 210–221.

Waclawik A, Blitek A, Kaczmarek M, Kiewisz J and Ziecik A (2009) Antiluteolytic mechanisms and the establishment of pregnancy in the pig. In *Control of Pig Reproduction VIII*, pp 307–320. Eds H Rodriguez-Martinez, J Vallet and AJ Ziecik. Nottingham University Press.

Waclawik A, Kaczmarek MM, Blitek A, Kaczynski P and Ziecik AJ (2017) Embryo-maternal dialogue during pregnancy establishment and implantation in the pig. *Molecular Reproduction and Development* **84** 842–855.

Waldorf DP, Self HL and Chapman AB (1957) Factors Affecting Fetal Pig Weight Late in Gestation. *Journal of Animal Science* **16** 976–985.

Walenkamp MJE, Karperien M, Pereira AM, Hilhorst-Hofstee Y, Van Doorn J, Chen JW, Mohan S, Denley A, Forbes B, Van Duyvenvoorde HA *et al.* (2005) Homozygous and heterozygous expression of a novel insulin-like growth factor-I mutation. *Journal of Clinical Endocrinology and Metabolism* **90** 2855–2864.

Wallace JM, Aitken RP and Cheyne MA (1996) Nutrient partitioning and fetal growth in rapidly growing adolescent ewes. *Journal of Reproduction and Fertility* **107** 183–190.

Wallner W, Sengenberger R, Strick R, Strissel PL, Meurer B, Beckmann MW and Schlembach D (2007) Angiogenic growth factors in maternal and fetal serum in pregnancies complicated by intrauterine growth restriction. *Clinical Science* **112** 51–57.

Wang Y and Sheibani N (2006) PECAM-1 isoform-specific activation of MAPK/ERKs and small GTPases: Implications in inflammation and angiogenesis. *Journal of Cellular Biochemistry* **98** 451–468.

Wang G, Johnson GA., Spencer TE. and Bazer FW. (2000) Isolation , Immortalization , and Initial Characterization of Uterine Cell Lines : An in vitro Model System for the Porcine Uterus. *In Vitro Cellular and Developmental Biology. Animal.* **36** 650–656.

Wang J, Chen L, Li D, Yin Y, Wang X, Li P, Dangott LJ, Hu W and Wu G (2008) Intrauterine growth restriction affects the proteomes of the small intestine, liver, and skeletal muscle in newborn pigs. *The Journal of Nutrition* **138** 60–66.

Wang Y, Yan W, Lu X, Qian C, Zhang J, Li P, Shi L, Zhao P, Fu Z, Pu P *et al.* (2011) Overexpression of osteopontin induces angiogenesis of endothelial progenitor cells via the avβ3/PI3K/AKT/eNOS/NO signaling pathway in glioma cells. *European Journal of Cell Biology* **90** 642–648.

Wang Y, Zhu L, Kuokkanen S and Pollard JW (2015) Activation of protein synthesis in mouse uterine epithelial cells by estradiol-17β is mediated by a PKC–ERK1/2–mTOR signaling pathway. *Proceedings of the National Academy of Sciences* **112** E1382–E1391.

Wareing M, Myers JE, O'Hara M and Baker PN (2005) Sildenafil citrate (viagra) enhances vasodilatation in fetal growth restriction. *Journal of Clinical Endocrinology and Metabolism* **90** 2550–2555.

Webel S and Dziuk P (1974) Effect of Stage of Gestation and Uterine Space on Prenatal Survival in the Pig. *Journal of Animal Science* **38** 960–963.

Weems CW, Weems YS and Randel RD (2006) Prostaglandins and reproduction in female farm animals. *Veterinary Journal* **171** 206–228.

Weintraub AS, Lin X, Itskovich V V., Aguinaldo JGS, Chaplin WF, Denhardt DT and Fayad ZA (2004) Prenatal Detection of Embryo Resorption in Osteopontin-Deficient Mice Using Serial Noninvasive Magnetic Resonance Microscopy. *Pediatric Research* **55** 419–424.

Wen HY, Abbasi S, Kellems RE and Xia Y (2005) mTOR: A placental growth signaling sensor. *Placenta* **26**.

Wessels JM, Edwards AK, Khalaj K, Kridli RT, Bidarimath M and Tayade C (2013) The microRNAome of pregnancy: deciphering miRNA networks at the maternal-fetal interface. *PloS ONE* **8** e72264.

West DC and Burbridge MF (2009) Chapter 11: Three-Dimensional In Vitro Angiogenesis in the Rat Aortic RIng Model. In *Angiogenesis Protocols, Methods in Molecular Biology*, pp 189–210. Eds S Martin and C Murray. Humana Press.

Westphal D, Dewson G, Czabotar PE and Kluck RM (2011) Molecular biology of Bax and Bak activation and action. *Biochimica et Biophysica Acta* **1813** 521–531.

White FJ, Ross JW, Joyce MM, Geisert RD, Burghardt RC and Johnson GA (2005) Steroid Regulation of Cell Specific Secreted Phosphoprotein 1 (Osteopontin) Expression in the Pregnant Porcine Uterus. *Biology of Reproduction* **73** 1294–1301.

White FJ, Burghardt RC, Hu J, Joyce MM, Spencer TE and Johnson GA (2006) Secreted phosphoprotein 1 (osteopontin) is expressed by stromal macrophages in cyclic and pregnant endometrium of mice, but is induced by estrogen in luminal epithelium during conceptus attachment for implantation. *Reproduction* **132** 919–929.

Widdowson EM (1971) Intra-Uterine Growth Retardation in the Pig I Organ Size and Cellular Development at Birth and after Growth to Maturity. *Biology of the*

Neonate **19** 329–340.

Widnes C, Flo K and Acharya G (2017) Exploring sexual dimorphism in placental circulation at 22-24 weeks of gestation: a cross-sectional observational study. *Placenta* **49** 16–22.

Wigglesworth JS (1974) Fetal Growth Retardation. Animal Model: Uterine Vessel Ligation in the Pregnant Rat. *American Journal of Pathology* **77** 347–350.

Wigmore PMC and Stickland NC (1983) Muscle development in large and small pig fetuses. *Journal of Anatomy* **137** 235–245.

Williams TJ (1986) A Technique for Sexing Mouse Embryos by a Visual Colorimetric Assay of the X-Linked Enzyme, Glucose 6-Phosphate Dehydrogenase. *Theriogenology* **25** 733–739.

Wilson ME and Ford P (2001) Comparative Aspects of Placenta Efficiency. *Reproduction Supplement* **58** 223–232.

Wilson ME, Biensen NJ, Youngs CR and Ford SP (1998) Development of Meishan and Yorkshire Littermate Conceptuses in Either a Meishan or Yorkshire Uterine Environment to Day 90 of Gestation and to Term. *Biology of Reproduction* **58** 905–910.

Winther H, Ahmed A and Dantzer V (1999) Immunohistochemical Localization of Vascular Endothelial Growth Factor (VEGF) and its Two Receptors, Flt-I and KDR, in the Porcine Placenta and Non-pregnant Uterus. *Placenta* **20** 35–43.

Wise TH and Christenson RK (1992) Relationship of Fetal Position Within the Uterus to Fetal Weight, Placental Weight, Testosterone, Estrogens, and Thymosin β4 Concentrations at 70 and 104 Days of Gestation in Swine. *Journal of Animal Science* **70** 2787–2793.

Wise T, Roberts AJ and Christenson RK (1997) Relationships of Light and Heavy Fetuses to Uterine Position , Placental Weight , Gestational Age , and Fetal Cholesterol Concentrations. *Journal of Animal Science* **75** 2197–2207.

Van Woerkens LJ, Duncker DJ, Huigen RJ, Van Der Giessen WJ and Verdouw PD (1990) Redistribution of cardiac output caused by opening of arteriovenous anastomoses by a combination of azaperone and metomidate. *British Journal of Anaesthesia* **65** 393–399.

Wolf XA, Serup P and Hyttel P (2011) Three-Dimensional Immunohistochemical Characterization of Lineage Commitment by Localization of T and FOXA2 in Porcine Peri-Implantation Embryos. *Developmental Dynamics* **240** 890–897.

Wong CW, Wiedle G, Ballestrem C, Wehrle-Haller B, Etteldorf S, Bruckner M, Engelhardt B, Gisler RH and Imhof BA (2000) PECAM-1/CD31 Trans-Homophilic Binding at the Intercellular Junctions is Independent of its Cytoplasmic Domain; Evidence for Heterophilic Interaction with Integrin αVβ3 in Cis. *Molecular Biology of the Cell* **11** 3109–3121.

Woodall SM, Breier BH, Johnston BM and Gluckman PD (1996) A model of intrauterine growth retardation caused by chronic maternal undernutrition in the rat: effects on the somatotrophic axis and postnatal growth. *Journal of Endocrinology* **150** 231–242.

Woodall SM, Breier BH, Johnston BM, Bassett NS, Barnard R and Gluckman PD

(1999) Administration of growth hormone or IGF-I to pregnant rats on a reduced diet throughout pregnancy does not prevent fetal intrauterine growth retardation and elevated blood pressure in adult offspring. *Journal of Endocrinology* **163** 69–77.

Wooding P and Burton G (2008) *Comparative Placentation. Structures, Functions and Evolution*. Springer.

Wootton R, McFadyen IR and Cooper JE (1977) Measurement of Placental Blood Flow in the Pig and Its Relation to Placental and Fetal Weight. *Biology of the Neonate* **31** 333–339.

World Health Organisation (2006) Neonatal and Perinatal Mortality: country, regional and global estimates.

Wright RW, Grammer J, Bondioli K, Kuzan F and Menino A (1983) Protein Content and Volume of Early Porcine Blastocysts. *Animal Reproduction Science* **5** 207–212.

Wright EC, Miles JR, Lents CA and Rempel LA (2016) Uterine and placenta characteristics during early vascular development in the pig from day 22 to 42 of gestation. *Animal Reproduction Science* **164** 14–22.

Wu G, Bazer FW, Tuo W and Flynn SP (1996) Unusual Abundance of Arginine and Ornithine in Porcine Allantoic Fluid. *Biology of Reproduction* **54** 1261–1265.

Wu G, Ott TL, Knabe DA and Bazer FW (1999) Amino acid composition of the fetal pig. *Journal of Nutrition* **129** 1031–1038.

Wu G, Bazer FW, Cudd TA, Meininger CJ and Spencer TE (2004) Maternal Nutrition and Fetal Development. *Journal of Nutrition* **134** 2169–2172.

Wu G, Bazer FW, Hu J, Johnson GA and Spencer TE (2005) Polyamine Synthesis from Proline in the Developing Porcine Placenta. *Biology of Reproduction* **72** 842–850.

Wu G, Bazer FW, Wallace JM and Spencer TE (2006) Board-Invited Review: Intrauterine Growth Retardation: Implications for the Animal Sciences. *Journal of Animal Science* **84** 2316–2337.

Wu G, Bazer FW, Datta S, Johnson GA, Li P, Satterfield MC and Spencer TE (2008) Proline metabolism in the conceptus: Implications for fetal growth and development. *Amino Acids* **35** 691–702.

Wu SP, Xu XW, Li CC, Mei Y and Zhao SH (2009) Six placenta permeability-related genes: molecular characterization and expression analysis in pigs. *Animal* **3** 408–414.

Wu G, Bazer FW, Burghardt RC, Johnson GA, Kim SW, Li XL, Satterfield MC and Spencer TE (2010) Impacts of amino acid nutrition on pregnancy outcome in pigs: mechanisms and implications for swine production. *Journal of Animal Science* **88** E195–E204.

Wu G, Bazer FW, Johnson GA, Herring C, Seo H, Dai Z, Wang J, Wu Z and Wang X (2017) Functional amino acids in the development of the pig placenta. *Molecular Reproduction and Development* **84** 870–882.

Wyness L (2016) The role of red meat in the diet: Nutrition and health benefits.

Proceedings of the Nutrition Society **75** 227–232.

Xiao X, Zhao Y, Jin R, Chen J, Wang X, Baccarelli A and Zhang Y (2016) Fetal growth restriction and methylation of growth-related genes in the placenta. *Epigenomics* **8** 33–42.

Xie D, Ju D, Speyer C, Gorski D and Kosir MA (2016) Strategic Endothelial Cell Tube Formation Assay: Comparing Extracellular Matrix and Growth Factor Reduced Extracellular Matrix. *Journal of Visualized Experiments* 1–6.

Xu D and Qu CK (2008) Protein tyrosine phosphatases in the JAK/STAT pathway. *Frontiers in Bioscience* **13** 4925–4932.

Yang S, Graham J, Kahn JW, Schwartz EA and Gerritsen ME (1999) Functional Roles for PECAM-1 (CD31) and VE-Cadherin (CD144) in Tube Assembly and Lumen Formation in Three-Dimensional Collagen Gels. *American Journal of Pathology* **155** 887–895.

Yelian FD, Yang Y, Hirata JD, Schultz JF and Armant DR (1995) Molecular Interactions Between Fibronectin and Integrins During Mouse Blastocyst Outgrowth. *Molecular Reproduction and Development* **41** 435–448.

Yelich J V, Pomp D and Geisert RD (1997) Detection of Transcripts for Retinoic Acid Receptors, Retinol-Binding Protein, and Transforming Growth Factors During Rapid Trophoblastic Elongation in the Porcine Conceptus. *Biology of Reproduction* **57** 286–294.

Yoder C, Lawrence S, Duttlinger V and J CS (2014) Parity differences in reproductive performance and progeny - performance. *American Association of Swine Veterinarians* 243–246.

Yoshimura Y, Shiokawa S, Nagamatsu S, Hanashi H, Sawa H, Koyama N, Katsumata Y and Nakamura Y (1995) Effects of beta-1 integrins in the process of implantation. *Hormone Research* **44** 36–41.

Yu J and Zhang L (2003) No PUMA, no death: Implications for p53-dependent apoptosis. *Cancer Cell* **4** 248–249.

Yu J and Zhang L (2009) PUMA, a potent killer with or without p53. *Oncogene* **27** S71–S83.

Yuan TL, Zhu YH, Shi M, Li TT, Li N, Wu G, Bazer FW, Zang JJ, Wang FL and Wang JJ (2015) Within-litter variation in birth weight: impact of nutritional status in the sow. *Journal of Zhejiang University-SCIENCE B* **16** 417–435.

Zegher FD, Devlieger H and Eeckels R (1999) Fetal Growth: Boys before Girls. *Hormone Research* **51** 258–259.

Zhang Q, Wrana JL and Sodek J (1992) Characterization of the promoter region of the porcine opn (osteopontin, secreted phosphoprotein 1) gene: Identification of positive and negative regulatory elements and a ‘silent’ second promoter. *European Journal of Biochemistry* **207** 649–659.

Zhang Y, Fei M, Xue G, Zhou Q, Jia Y, Li L, Xin H and Sun S (2012) Elevated levels of hypoxia-inducible microRNA-210 in pre-eclampsia: new insights into molecular mechanisms for the disease. *Journal of Cellular and Molecular Medicine* **16** 249–259.

Zhang H, Wang S, Liu M, Zhang A, Wu Z, Zhang Z and Li J (2013) Differential gene expression in the endometrium on gestation day 12 provides insight into sow prolificacy. *BioMed Central Genomics* **14** 1–10.

Zhao YY, Wang W, Li XX, Chen X, Yu P, Wang JJ and Xu YX (2014) Effect of BMPRIB gene silencing by siRNA on apoptosis and steroidogenesis of porcine granulosa cells. *Genetics and Molecular Research* **13** 9964–9975.

Zhao T, Li C, Wei W, Zhang H, Ma D, Song X and Zhou L (2016) Prenatal ketamine exposure causes abnormal development of prefrontal cortex in rat. *Scientific Reports* **6** 1–12.

Zheng J, Wen YX, Austin JL and Chen DB (2006) Exogenous Nitric Oxide Stimulates Cell Proliferation via Activation of a Mitogen-Activated Protein Kinase Pathway in Ovine Fetoplacental Artery Endothelial Cells. *Biology of Reproduction* **74** 375–382.

Zhou Z, Christofidou-Solomidou M, Garlanda C and DeLisser HM (1999) Antibody against murine PECAM-1 inhibits tumor angiogenesis in mice. *Angiogenesis* **3** 181–188.

Zhu J, Motejlek K, Wang D, Zang K, Schmidt A and Reichardt LF (2002) β8 Integrins Are Required for Vascular Morphogenesis in Mouse Embryos. *Development* **129** 2891–2903.

Ziecik AJ, Przygrodzka E and Kaczmarek MM (2017) Chapter 12: Corpus Luteum Regresstion and Early Pregnancy Maintenance in Pigs. In *The Life Cycle of the Corpus Luteum*, pp 227–248.

Zou H, Henzel WJ, Liu X, Lutschg A and Wang X (1997) Apaf-1 , a Human Protein Homologous to C . elegans CED-4, Participates in Cytochrome c-Dependent Activation of Caspase-3. *Cell* **90** 405–413.

Zudaire E, Gambardella L, Kurcz C and Vermeren S (2011) A Computational Tool for Quantitative Analysis of Vascular Networks. *PLoS ONE* **6** e27385 1–12.

Zygmunt M, Boving B, Wienhard J, Münstedt K, Braems G, Bohle RM and Lang U (1997) Expression of cell adhesion molecules in the extravillous trophoblast is altered in IUGR. *American Journal of Reproductive Immunology* **38** 295–301.

Zygmunt M, Herr F, Münstedt K, Lang U and Liang OD (2003) Angiogenesis and vasculogenesis in pregnancy. *European Journal of Obstetrics Gynecology and Reproductive Biology* **110** S10–S18.

Appendices

Within-Litter Ranges for Foetal Weight, CRL, PI, Allantoic and Amniotic Fluid Volumes

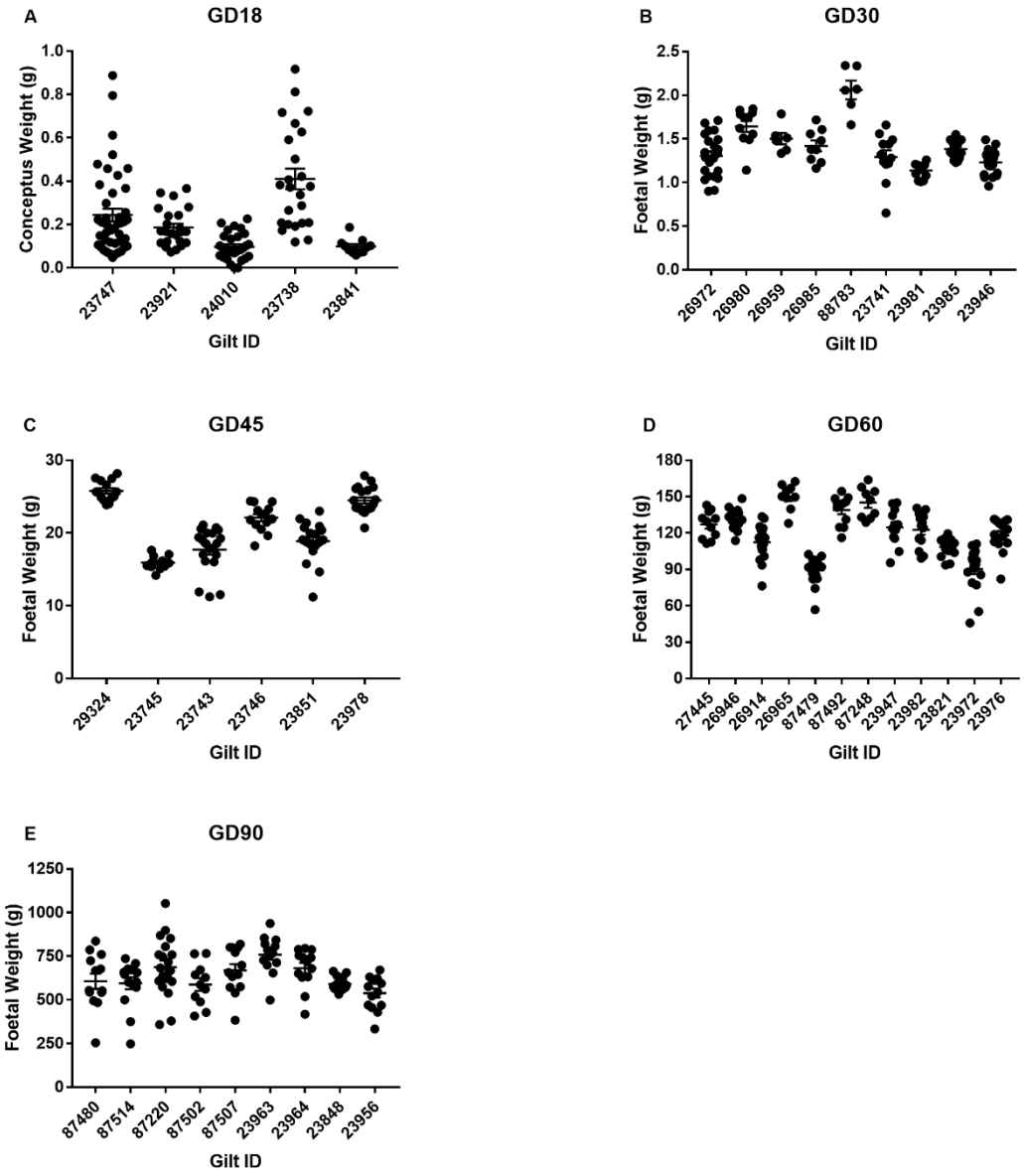

Supplementary Figure 1: Within Litter Range in Conceptus/Foetal Weight.

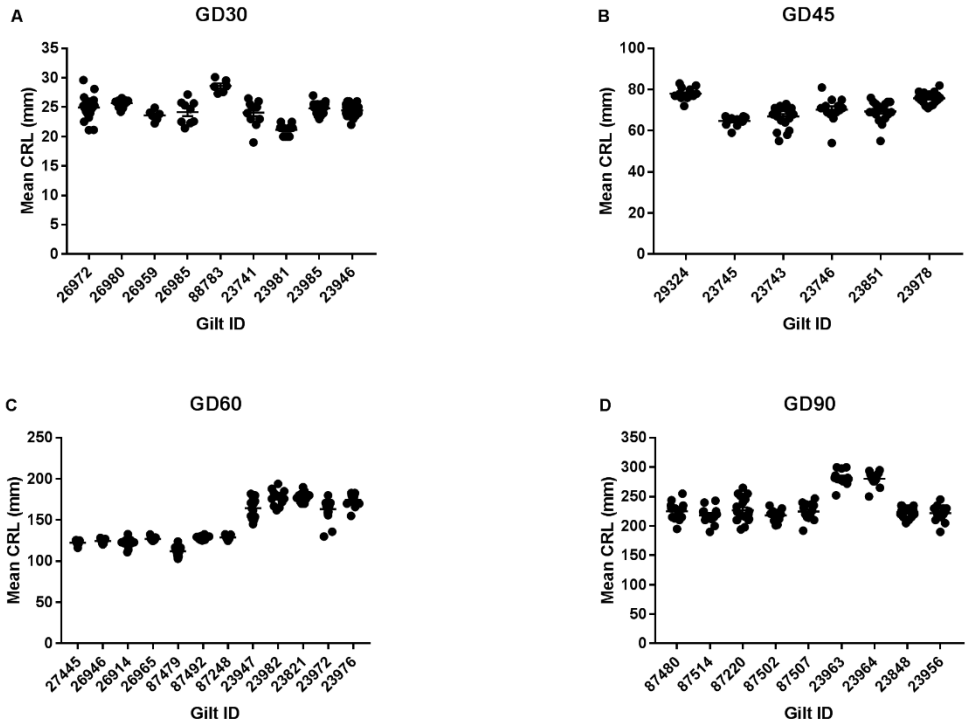

Supplementary Figure 2: Within Litter Range in CRL.

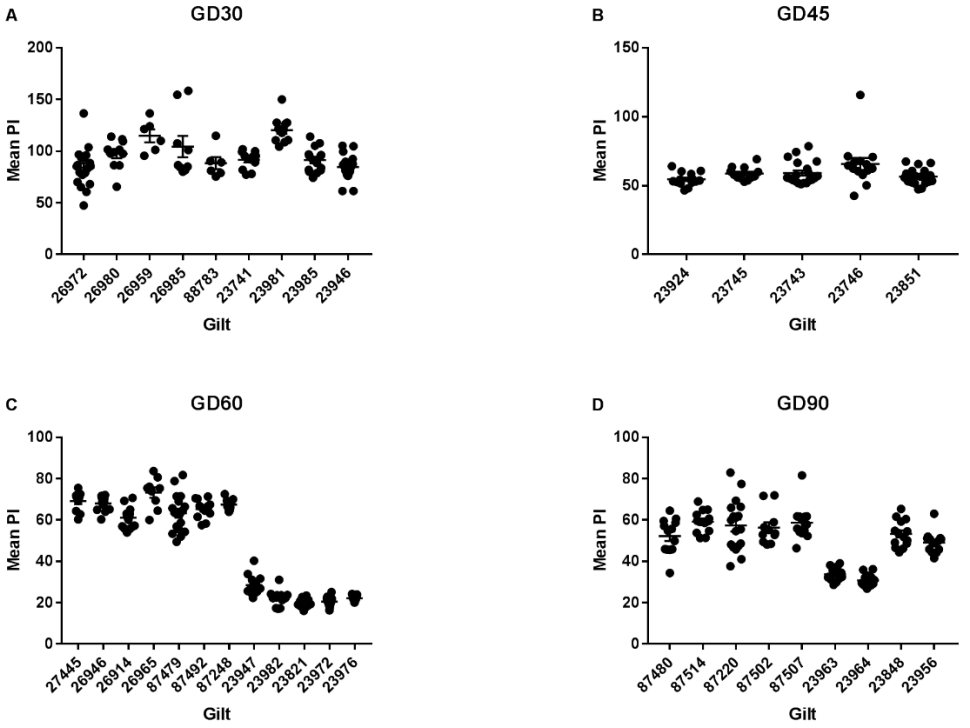

Supplementary Figure 3: Within Litter Range in PI.

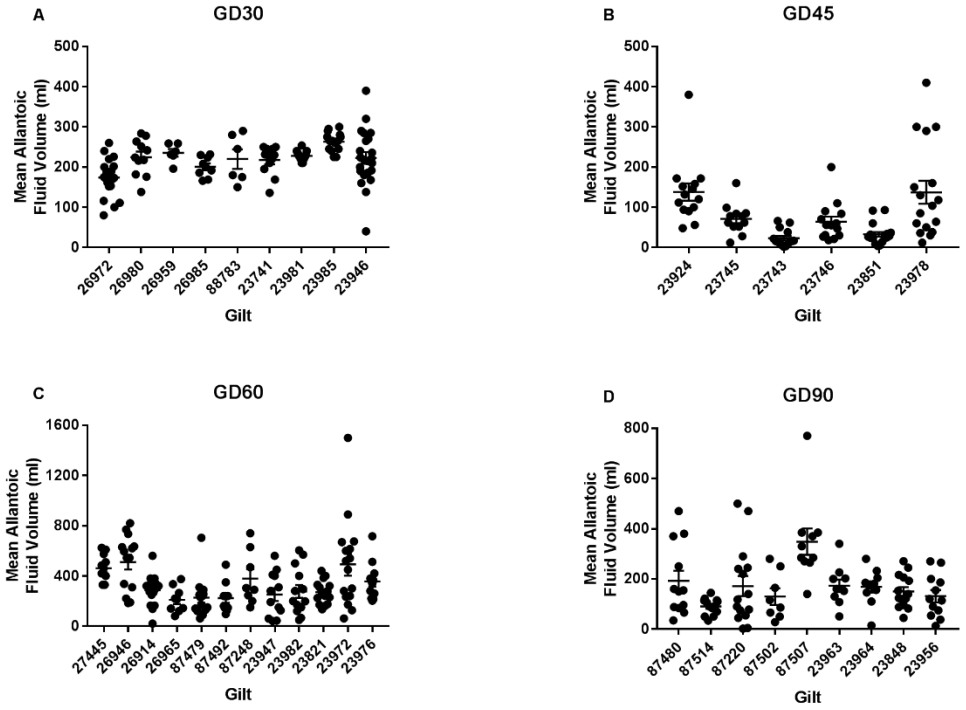

Supplementary Figure 4: Within Litter Range in Allantoic Fluid Volume.

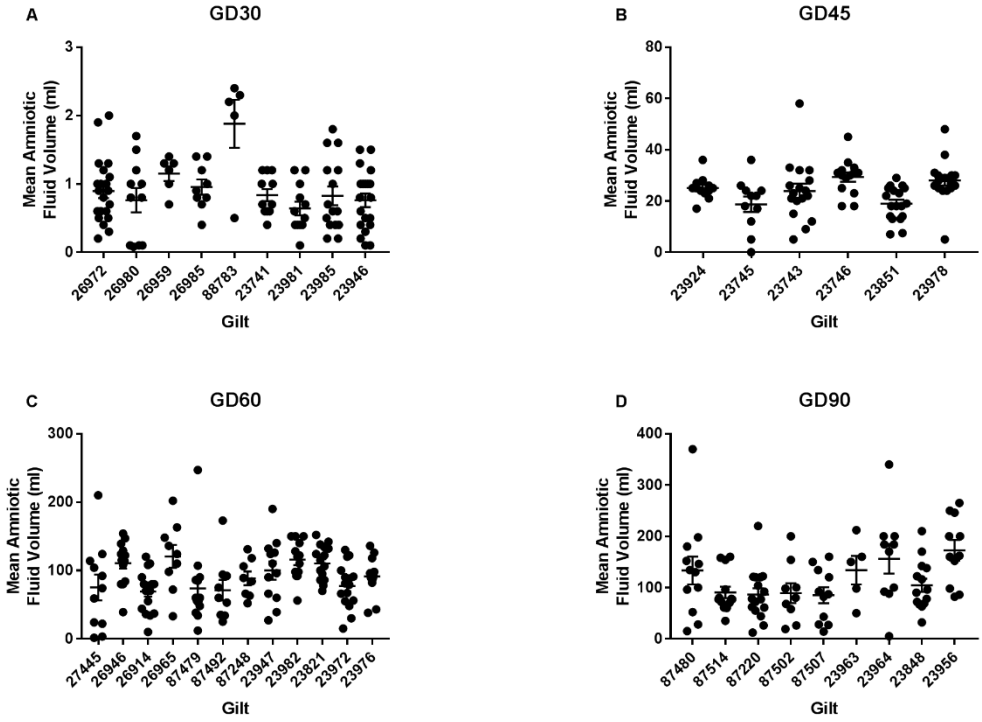

Supplementary Figure 5: Within Litter Range in Amniotic Fluid Volume.

Correlation between Maternal Weight at Sample Collection and the Number of Foetuses, Percentage Prenatal Survival, Mean and Total Litter Weight within GD.

Parameter	Maternal Weight									
	GD18		GD30		GD45		GD60		GD90	
	RSq (%)	P	RSq (%)	P	RSq (%)	P	RSq (%)	P	RSq (%)	P
Number of Foetuses	76.7	0.052	1.3	0.887	6.0	0.639	92.5	0.038	27.8	0.145
Percentage Prenatal Survival	1.7	0.835	17.0	0.588	37.4	0.197	37.1	0.391	20.3	0.224
Mean Litter Weight	1.5	0.517	90.9	0.046	16.5	0.425	98.9	0.005	2.2	0.701
Total Litter Weight	64.3	0.103	3.4	0.817	0.0	0.996	1.1	0.897	0.4	0.886

Supplementary Table 1: Summary of Pearson's Correlation Values between Maternal Weight and Number of Conceptuses/Foetuses, Percentage Prenatal Survival, Mean Litter Weight, and Total Litter Weight within Gestational Day.

Uterine Position

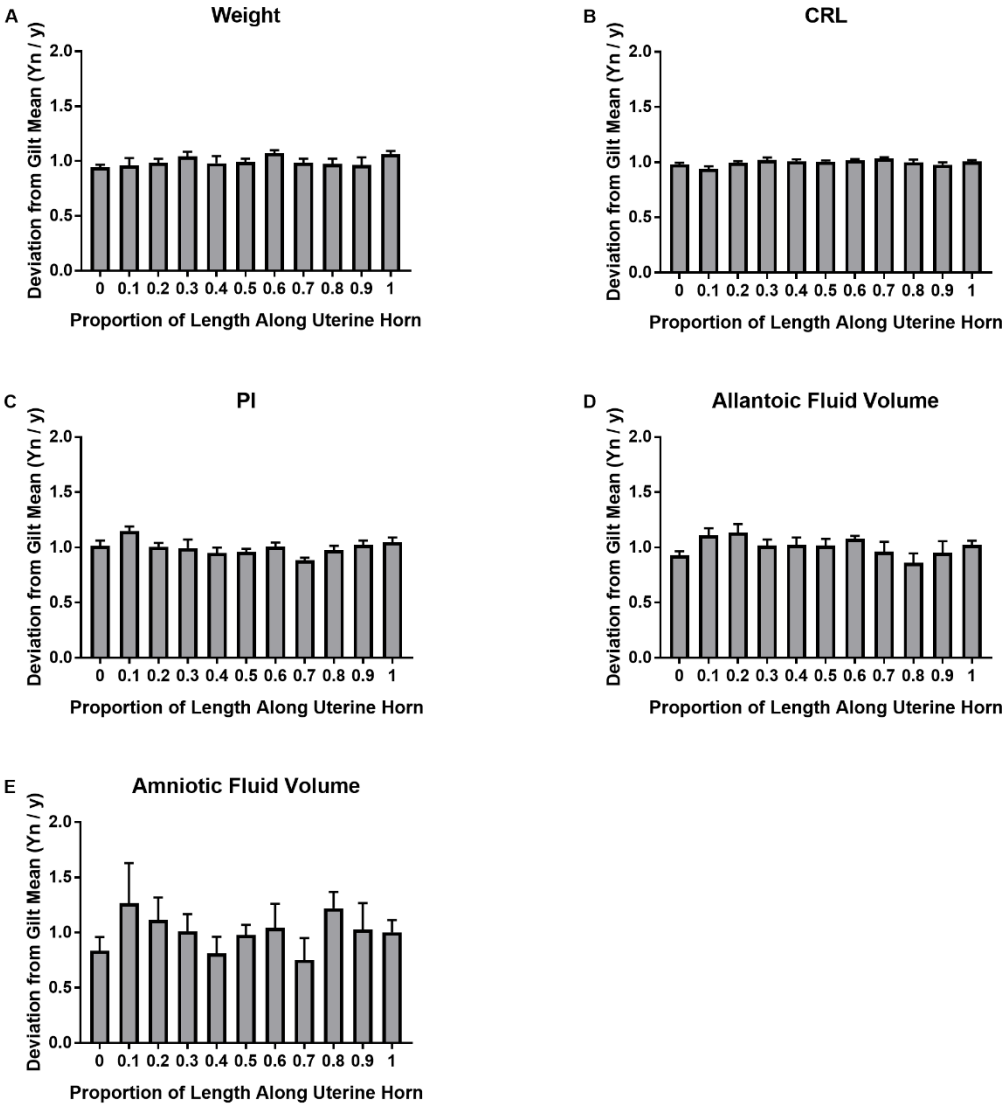

Supplementary Figure 6: Influence of Uterine Position on Foetal Weight, CRL, PI, Allantoic and Amniotic Fluid Volume at GD30.

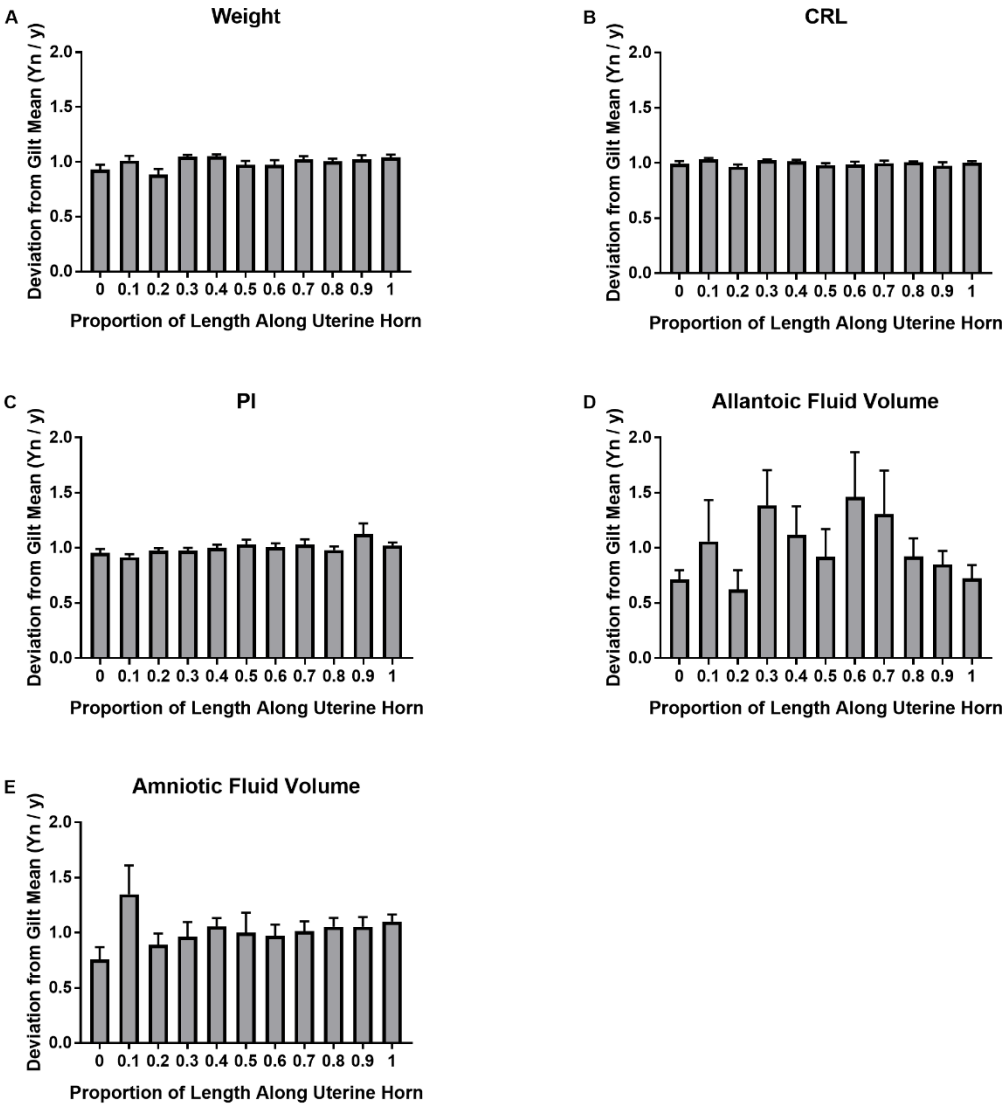

Supplementary Figure 7: Influence of Uterine Position on Foetal Weight, CRL, PI, Allantoic and Amniotic Fluid Volume at GD45.

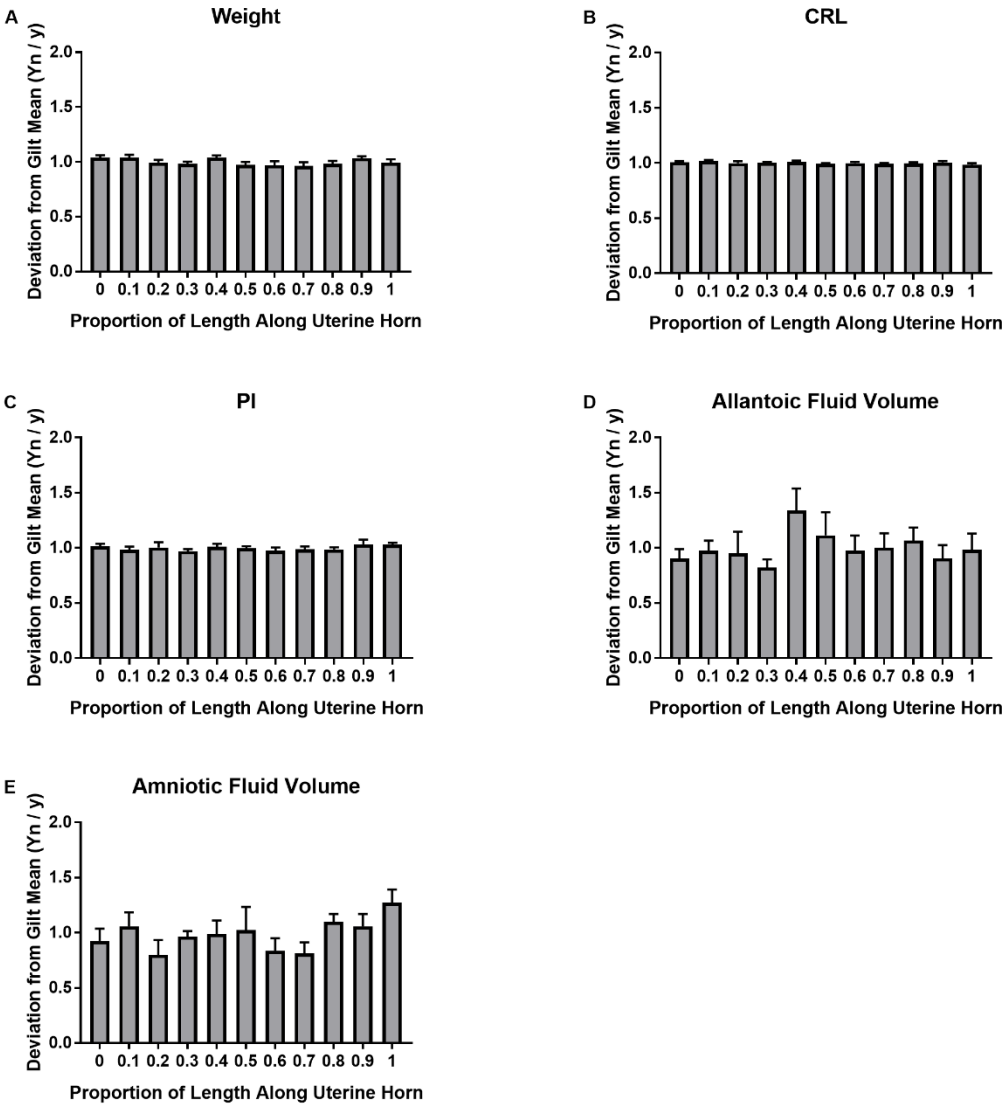

Supplementary Figure 8: Influence of Uterine Position on Foetal Weight, CRL, PI, Allantoic and Amniotic Fluid Volume at GD60.

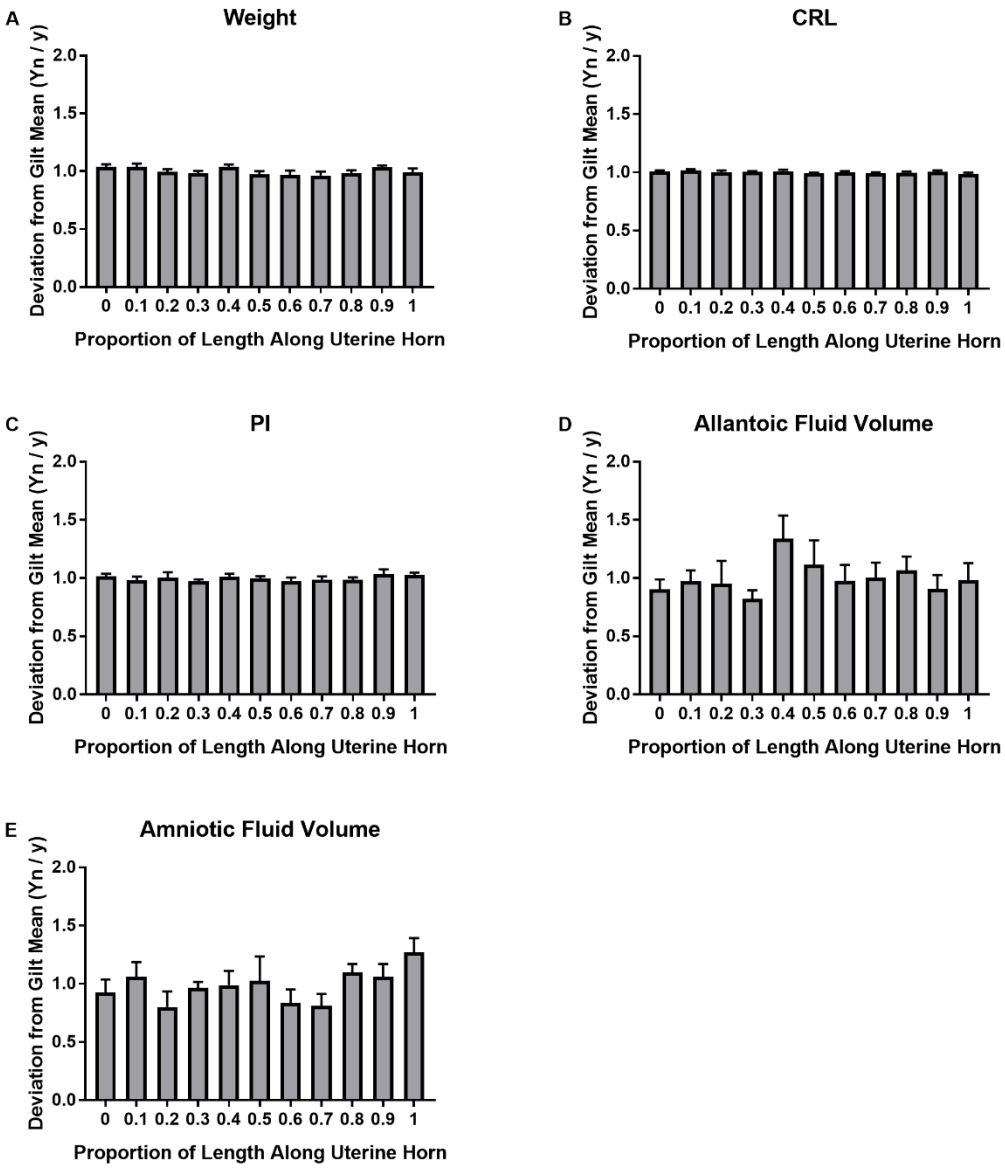

Supplementary Figure 9: Influence of Uterine Position on Foetal Weight, CRL, PI, Allantoic and Amniotic Fluid Volume at GD90.

All End Foetuses Compared with All Middle Foetuses

The values and deviation from gilt mean for each variable for the foetuses at the end of the uterine horns were compared with the foetuses at the middle of the uterine horn (Supplementary Table 2 and Supplementary Table 3). At GD30, no relationship between uterine position and ALF and AMF volumes, CRL or weight were observed. Similarly, there was no association between uterine position and deviation from gilt mean for any of the five variables investigated. An indication of foetuses at the end of the uterine horns having increased PI compared to those in the middle of the horn at GD30 was observed (ANOVA without Gilt Block FPr=0.034) however, this was not observed with the addition of a block for gilt. At GD45, no association between uterine position and the variables, or deviation from mean for each of the five variables were observed. At GD60, no association between uterine position and ALF and AMF volumes, CRL, and PI were observed. Similarly, no relationship between uterine position and deviation from gilt mean for ALF volume, CRL, and weight were observed. At GD60, there was an indication that foetuses at the end of the uterine horn were heavier than those in the middle of the uterine horn (ANOVA without Gilt Block FPr=0.027) however, this was not significant following the addition of a block for gilt. In addition, the deviation from gilt mean for AMF volume (ANOVA without Gilt Block FPr=0.065; with Gilt Block FPr=0.09), and PI (Mann-Whitney P=0.06) was increased in foetuses at the end of the uterine horn compared to those in the middle of the uterine horn. At GD90, foetuses located at the end of the uterine horn had a decreased ALF volume (variable: ANOVA with Gilt Block FPr=0.052; deviation from gilt mean: ANOVA without Gilt Block FPr=0.068, with Gilt Block FPr=0.061). A trend towards increased weight of foetuses at the end of the uterine horn compared to the middle of the uterine horn was observed at GD90 (variable: ANOVA with Gilt Block FPr=0.057; deviation from gilt mean: Mann Whitney P=0.057). PI was increased in foetuses at the end of the uterine horn compared to those in the middle of the uterine horn at GD90 (ANOVA without Gilt Block FPr=0.009; with Gilt Block FPr=0.012).

Variable	GD30			GD45			GD60			GD90		
	Middle	End	FPr/P	Middle	End	FPr/P	Middle	End	FPr/P	Middle	End	FPr/P
ALF Volume (ml)	219.848 ± 6.364	215.686 ± 6.155	ns	84.373 ± 10.771	56.609 ± 8.521	ns	344.5 ± 20.595	308.439 ± 29.258	ns	179.662 ± 15.036	149.182 ± 19.844	+ Gilt 0.052
AMF Volume (ml)	0.876 ± 0.056	0.882 ± 0.097	ns	24.718 ± 1.047	23.341 ± 2.044	ns	88.894 ± 3.793	99.261 ± 7.344	ns	111.377 ± 7.771	119.344 ± 13.585	ns
CRL (mm)	24.469 ± 0.225	24.462 ± 0.381	ns	70.963 ± 0.683	70.771 ± 1.408	ns	145.134 ± 2.406	143.025 ± 3.538	ns	234.644 ± 3.099	236.914 ± 4.395	ns
Weight (g)	1.335 ± 0.027	1.399 ± 0.043	ns	20.856 ± 0.448	20.603 ± 0.959	ns	115.367 ± 1.886	123.681 ± 3.499	- Gilt 0.027	628.316 ± 15.060	670.660 ± 17.577	+ Gilt 0.057
PI	91.805 ± 1.987	100.245 ± 3.573	- Gilt 0.034	58.485 ± 1.060	57.720 ± 1.439	ns	45.121 ± 2.032	49.245 ± 3.296	ns	49.458 ± 1.277	52.372 ± 2.251	ns

Supplementary Table 2: Association between Uterine Position (Both End vs Middle of Uterine Horn) on Allantoic and Amniotic Fluid Volume, CRL, Weight and PI.

To determine the relationship between uterine position and the five variables of interest, the mean values for each variable for foetuses located in the middle of the uterine horn and the end of the uterine horn within GD was calculated. Mean values presented here ± standard error of the mean (S.E.M). Abbreviations: ALF=Allantoic Fluid, AMF=Amniotic Fluid, CRL=Crown-Rump Length, PI=Ponderal Index, + Gilt = with Gilt Block, - Gilt = without Gilt Block, ns=not significant, FPr/P=Probability value, ns=not significant, FPr/P=Probability value.

Variable Deviation from Gilt Mean	GD30			GD45			GD60			GD90		
	Middle	End	FPr/P	Middle	End	FPr/P	Middle	End	FPr/P	Middle	End	FPr/P
ALF Volume	1.013 ± 0.192	0.974 ± 0.027	ns	1.096 ± 0.099	0.720 ± 0.072	0.081	1.022 ± 0.050	0.940 ± 0.081	ns	1.057 ± 0.069	0.865 ± 0.104	- Gilt 0.068; + Gilt 0.061
AMF Volume	1.034 ± 0.062	0.924 ± 0.084	ns	1.034 ± 0.043	0.945 ± 0.071	ns	0.946 ± 0.033	1.086 ± 0.086	- Gilt 0.065; + Gilt 0.090	0.988 ± 0.059	1.027 ± 0.108	ns
CRL	1.006 ± 0.006	0.994 ± 0.009	ns	1.001 ± 0.007	0.998 ± 0.014	ns	1.001 ± 0.004	0.997 ± 0.008	ns	0.998 ± 0.007	1.004 ± 0.009	ns
Weight	0.998 ± 0.016	1.005 ± 0.020	ns	1.004 ± 0.012	0.986 ± 0.027	ns	0.994 ± 0.009	1.016 ± 0.019	ns	0.979 ± 0.021	1.052 ± 0.023	0.057
PI	0.979 ± 0.015	1.014 ± 0.027	ns	1.004 ± 0.016	0.988 ± 0.023	ns	0.991 ± 0.009	1.022 ± 0.015	0.06	0.979 ± 0.014	1.051 ± 0.024	- Gilt 0.009; + Gilt 0.012

Supplementary Table 3: Association between Uterine Position (End vs Middle of Uterine Horn) on Deviation from Gilt Mean and Allantoic and Amniotic Fluid Volume, CRL, Weight and PI.

To determine the relationship between uterine position and the five variables of interest, the deviation from gilt mean for each of the variables of interest was calculated. The mean values were calculated for foetuses located in the middle of the uterine horn and the end of the uterine horn within GD. Mean values presented here ± standard error of the mean (S.E.M). Abbreviations: ALF=Allantoic Fluid, AMF=Amniotic Fluid, CRL=Crown-Rump Length, PI=Ponderal Index, + Gilt = with Gilt Block, - Gilt = without Gilt Block, ns=not significant, FPr/P=Probability value.

Semi-Quantitative Analysis of GD60 and 90 SPP1 Stained Luminal Epithelial Images

Whilst foetal size and sex were not found to influence uterine gland SPP1 staining, they may influence uterine LE or placental protein staining. A semi-quantitative approach was used by four researchers (Charis Hogg, Claire Stenhouse, Kaitlyn Patterson and Cheryl Ashworth) to attempt to quantify LE staining at GD60 and 90. Charis Hogg performed her analysis in duplicate to determine how consistent the analysis is by a single researcher. The intensity, distribution of staining along the LE, distribution of staining throughout the LE, and how punctate the staining was, were assessed. This was carried out using a scale of 0-4 (y-axis) from four images from two sections for the lightest and CTMLW foetus of both sex at GD60 and GD90 (n=6 and 7 litters respectively). All images were blinded. Heat maps were generated to determine how consistent this analysis was between researchers, with each column on the heat maps representing a researcher. Supplementary Figure 10 illustrates the GD60 data and Supplementary Figure 11 illustrates the GD90 data. This analysis demonstrated that the assessment of LE staining in these four criteria appears to be subjective, even between the duplicate analysis performed by the same researcher (Columns A and B). In light of this, this analysis was not taken any further. In the future, a different approach may allow more accurate quantification SPP1 protein levels in the LE of endometrial samples supplying foetuses of different size and sex throughout gestation.

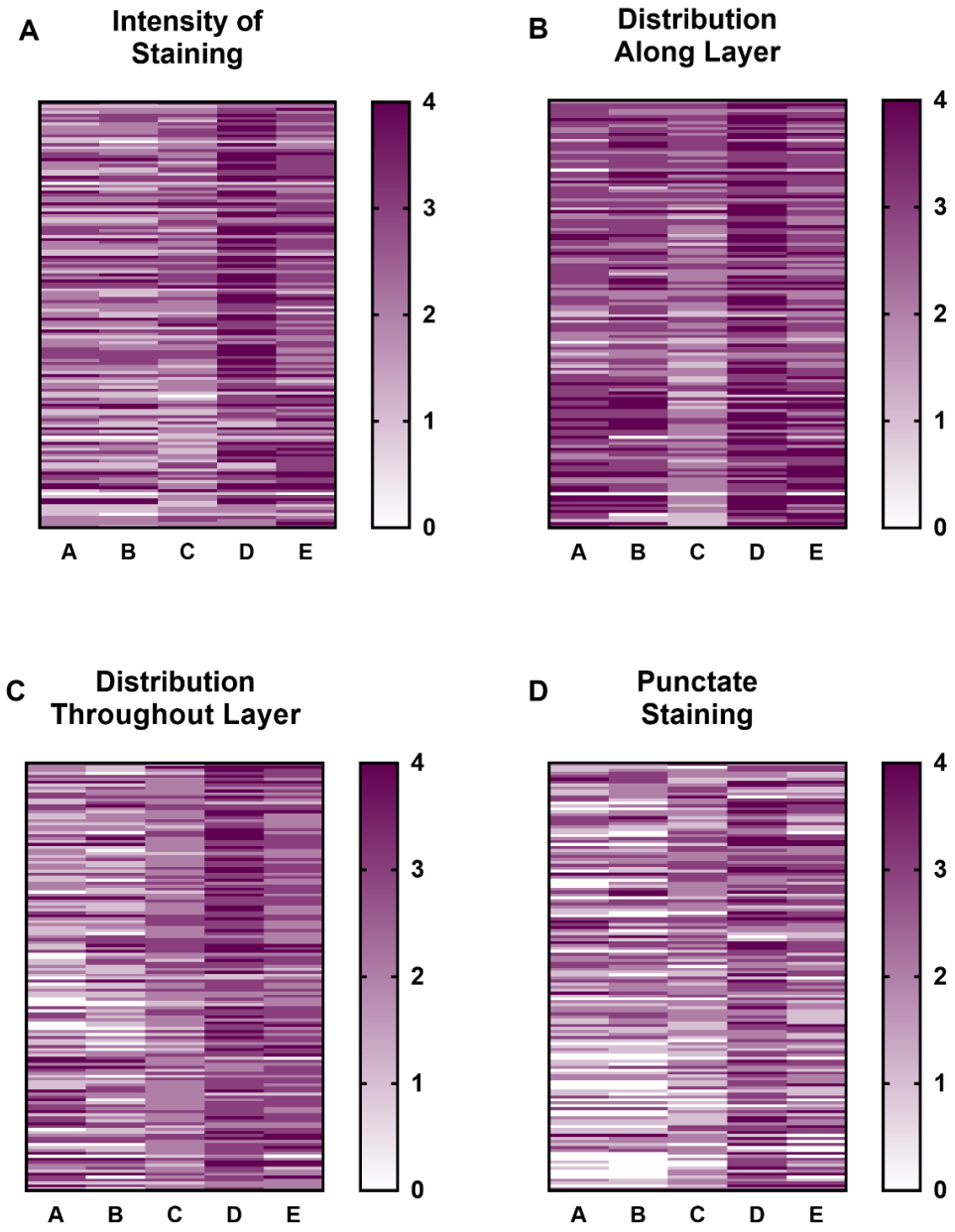

Supplementary Figure 10: Heat maps Illustrating the Subjectivity of SPP1 Uterine LE Protein Staining at GD60.

To investigate the uterine luminal epithelial (LE) SPP1 staining at gestational day (GD) 60, blinded images were analysed by 4 independent researchers (indicated by different letters along the axis), with one researcher performing the analysis in duplicate (Columns A and B). The intensity (A), distribution of staining along the LE (B), distribution of staining throughout the LE (C), and how punctate the staining was (D), were assessed. This was carried out using a scale of 0-4 (y axis). The results of this preliminary analysis suggest that this analysis is subjective between researchers.

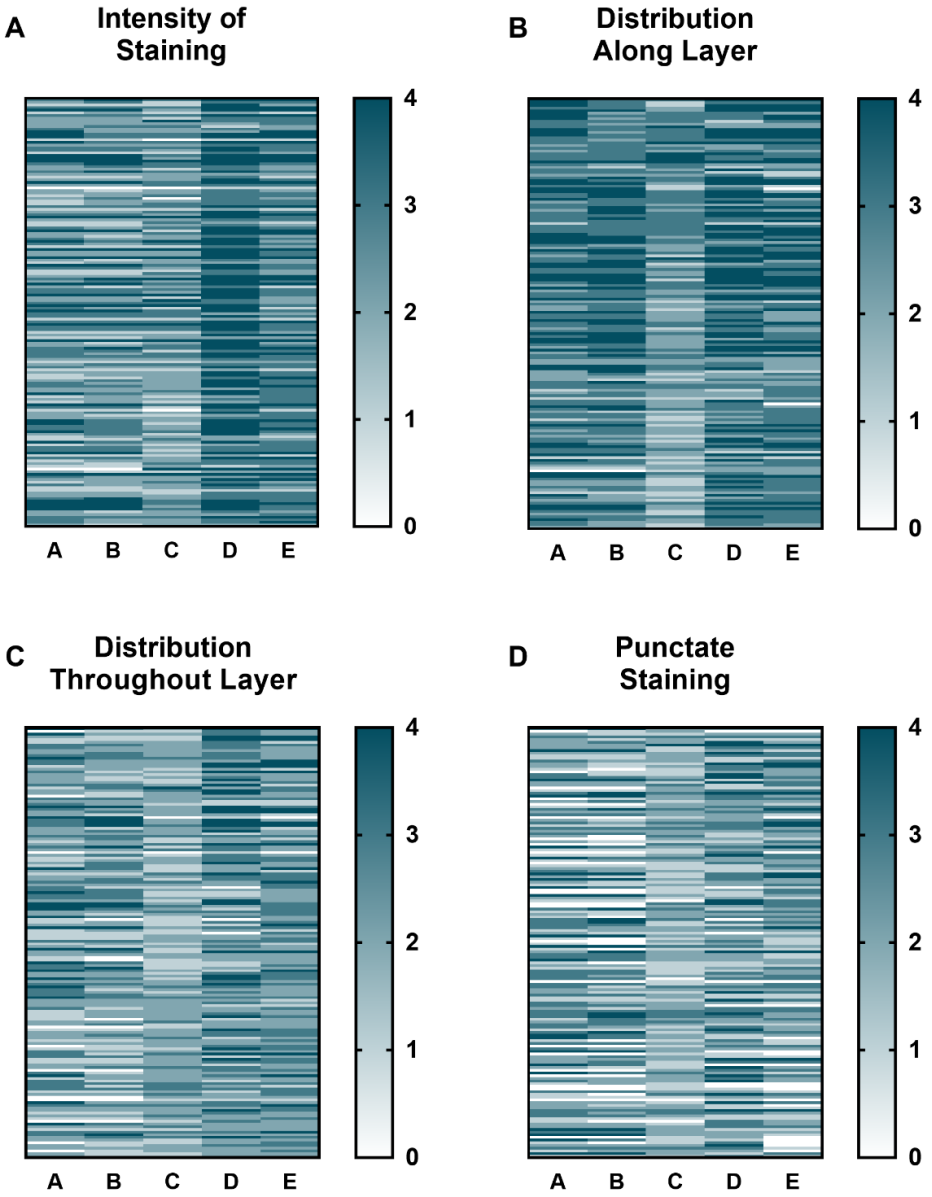

Supplementary Figure 11: Heat maps Illustrating the Subjectivity of SPP1 Uterine LE Protein Staining at GD90.

To investigate the uterine luminal epithelial (LE) SPP1 staining at gestational day (GD) 90, blinded images were analysed by 4 independent researchers (indicated by different letters along the axis), with one researcher performing the analysis in duplicate (Columns A and B). The intensity (A), distribution of staining along the LE (B), distribution of staining throughout the LE (C), and how punctate the staining was (D), were assessed. This was carried out using a scale of 0-4 (y axis). The results of this preliminary analysis suggest that this analysis is subjective between researchers.

Analysis of Uterine LE Thickness in SPP1 Stained Samples

A preliminary experiment was carried out using endometrial samples supplying the lightest and CTMLW conceptuses or foetuses at GD18 and 30 (n=5 and 6 litters respectively), and the lightest and CTMLW foetuses of both sex at GD45, 60 and 90 (n=6, 6, and 7 litters respectively). From each sample, two sections were stained for SPP1, and four images analysed per section. Using ImageJ, 3 measurements of LE thickness were taken per image, and the mean calculated per image. These values were used to calculate the mean LE thickness per section, which was used to calculate the mean per foetus.

Statistical analysis was performed as detailed in 2.5. The LE thickness data had a normal distribution at GD18, 60 and 90 but the GD30 and 45 data did not have a normal distribution. The data from each endometrial sample of interest within a litter was used to calculate a gilt mean, and this was used to perform regressions against litter size and percentage prenatal survival within GD (GD30-90). Regressions were performed to assess the relationship between individual foetal weight and uterine LE thickness within GD (GD30-90). Temporal changes in uterine LE thickness was assessed by Kruskal-Wallis. ANOVA was performed to determine if foetal sex (GD60 and 90) or size (GD18, 60 and 90) influenced uterine LE thickness, and Kruskal-Wallis was performed to assess the relationship between foetal sex and size on uterine LE thickness at GD30 and 45.

Temporal changes in uterine LE thickness were observed ($P \leq 0.001$), with an increase in LE thickness observed between GD18 and 30, after which uterine LE thickness decreased with advancing GD (Supplementary Figure 12A). The LE thickness was increased in endometrial samples supplying the lightest conceptuses compared to the CTMLW conceptuses at GD18 (FPr=0.043 without Gilt Block) however, this was not statistically significant with the addition of a block for gilt (Supplementary Figure 12B). At GD45, a trend towards endometrial samples supplying female foetuses having a decreased LE thickness compared to males was observed (P=0.079) (Supplementary

Figure 12C). Intriguingly, a positive relationship was observed between foetal weight and uterine LE thickness was observed at GD30 (P=0.04; RSq=34.56%) (Supplementary Figure 12D). A trend towards a negative relationship between percentage survival and mean LE thickness was observed at GD60 (P=0.07; RSq=59.71%) (Supplementary Figure 12E). No other statistically significant results were observed.

Supplementary Figure 12: Summary of the Results of Interest from the Uterine LE Thickness Analysis.

SPP1 stained endometrial samples supplying the lightest and CTMLW (GD18, 30, 45, 60 and 90) and male and female (GD30, 45, 60 and 90) conceptuses or foetuses were used to assess temporal changes in luminal epithelial (LE) thickness (A) and the association between uterine LE thickness and foetal size and sex (B and C). A: Temporal changes in uterine LE thickness were observed (P≤0.001), with an increase in LE thickness observed between GD18 and 30, after which uterine LE thickness decreased with advancing GD. B: The LE thickness was increased in endometrial samples supplying the lightest compared to the CTMLW conceptuses at GD18 (FPr=0.043 without Gilt Block) however, this was not statistically significant with the addition of a block for gilt. C: At GD45, a trend towards endometrial samples supplying female foetuses having a decreased LE thickness compared to those supplying males was observed (P=0.079). The data from each endometrial sample of interest within a litter was used to calculate a gilt mean, and this was used to perform regressions against litter size and percentage prenatal survival within GD (GD30-90). Regressions were performed to assess the relationship between individual foetal weight and uterine LE thickness within GD (GD30-90) (D and E). D: A positive relationship was observed between foetal weight and uterine LE thickness was observed at GD30 (P=0.04; RSq=34.56%). E: A trend towards a negative relationship between percentage survival and mean LE thickness was observed at GD60 (P=0.07; RSq=59.71%). No other statistically significant results were observed. Error bars represent S.E.M.

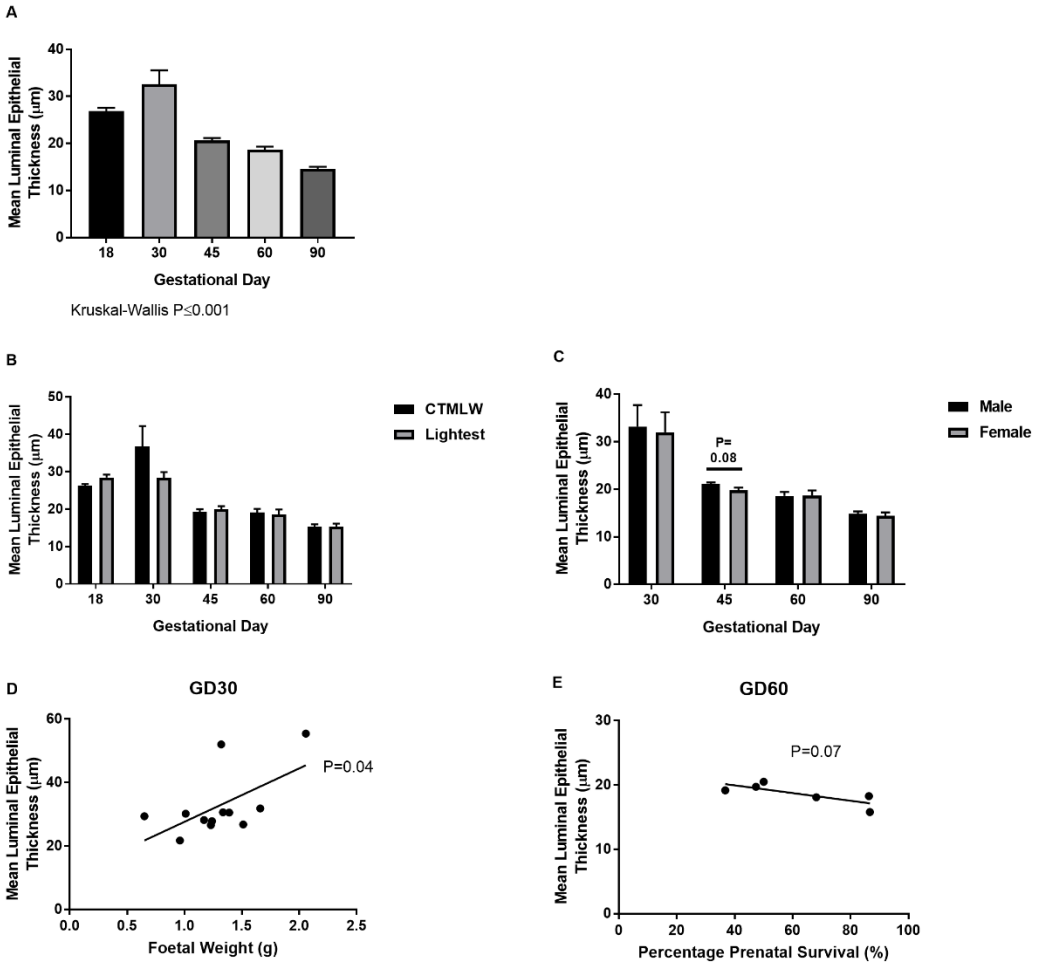

Supplementary Figure 12: Summary of the Results of Interest from the Uterine LE Thickness Analysis.

Supplementary Table 4: Growth Factors that Induce Cell Proliferation at the Porcine Feto-Maternal Interface which should be investigated in Relation to IUGR.

Abbreviation	Factor Name	Suggested Role in Proliferation at the Feto-Maternal Interface.	Known to be altered in IUGR Placentas/Endometrium?	References
CSF2/GM-CSF	Colony Stimulating Factor 2	Activates PI3K and ERK1/2 MAPK-dependent signalling to induce trophectoderm proliferation. Conceptus expression during peri-implantation (~GD10-12). CSF2 null mouse placentas have altered expression of genes involved in placental development, and trophoblast glycogen cell and giant cell abundance. Addition of CSF2 to mouse blastocyst cultures increases rate of development. Demonstrated that CSF2 can promote proliferation of bovine conceptus trophectoderm cells.	CSF2 null mice have decreased blastocyst cell number, decreased litter sizes, due to increased prenatal loss in late gestation; increased incidence of developmental abnormalities, and decreased foetal weight, with an increased incidence of very small foetuses.	Seymour *et al.*, (1997); Sjöblom *et al.*, (2005); Robertson *et al.*, (1999), (2001); Sjöblom *et al.*, (1999); Díaz-Cueto and Gerton, (2001); Michael *et al.*, (2006); Robertson, (2007); Sferruzzi-Perri *et al.*, (2009); Jeong and Song, (2014); Jeong *et al.*, (2014)
IGF1	Insulin-like Growth Factor 1	Conceptus gene expression of IGF1 and its receptors increases during early development, peaking during elongation. Endometrial expression is observed at ~GD10-12. Acts through multiple signalling pathways to increase the proliferation and migration of trophectoderm cells through MAPK, ERK1/2 and PI3K signalling pathways.	The IGFs are known to play a central role in IUGR, with mutations in associated with IUGR in humans. Mouse models ablating IGF1 and -2, and IGF1R found a significant decrease in foetal weight, alongside a permanently impaired growth rate whereas, over-expression of IGF-II leads to foetal overgrowth. Deletion of IGF1 results in an increased cell cycle	Letcher *et al.*, (1989); Simmen *et al.*, (1990); DeChiara *et al.*, (1990); Liu *et al.*, (1993); Green *et al.*, (1995); Dalçik *et al.*, (2001); Nagai *et al.*, (2002); Okubo *et al.*, (2003); Fowden, (2003); Carter *et al.*, (2005); Walenkamp *et*

			length, thereby decreasing the rate of new cell generation. In humans, a dose-response of IGF1 copy number on foetal growth has been observed. IUGR guinea pigs had increased *IGFBPs* expression in their amniotic fluid, and increased *IGFBP-4* placental expression compared to those supplying their normal-sized littermates. In human term placentas, high IGF1 protein staining was observed in placentas associated with IUGR foetuses compared to normal-sized foetuses.	*al.*, (2005); Sferruzzi-Perri *et al.*, (2011); Jeong and Song, (2014); Jeong *et al.*, (2014b)
TGFβ	Transforming Growth Factor β	TGFβ1, 2 and 3 expressed during implantation. Porcine conceptus regulated TGFβ1 synthesis during peri-implantation, and that TGFβ1 can induce proliferation of the endometrium during implantation and can influence trophoblast proliferation and therefore conceptus development.	Increased TGFβ1 protein expression has been observed in human term placentas associated with IUGR foetuses compared to those supplying normal-sized foetuses at ~31 weeks.	Gupta *et al.*, (1996, 1998); Yelich *et al.*, (1997); Todros *et al.*, (2007); Blitek *et al.*, (2013)
VEGF	Vascular Endothelial Growth Factor	VEGF and VEGFR are expressed by trophoblast cells in the preimplantation conceptus, where VEGF is not playing an angiogenic role; suggesting an alternative role. Addition of VEGF to *in vitro* embryo cultures increases both outgrowth and blastocyst cell numbers.	Placental *VEGF* expression was positively correlated with porcine foetal weight and placental efficiency (foetal weight/placental weight). VEGF is an angiogenic factor and aberrant placental angiogenesis has been associated with IUGR (discussed in chapters 6-8).	Vonnahme *et al.*, (2001); Einspanier *et al.*, (2002); Barut *et al.*, (2010); Biswas *et al.*, (2011); Hannan *et al.*, (2011); Jeong and Song, (2014); Chen *et al.*, (2015)

			Increased protein expression of VEGFA, was observed in term human IUGR placentas compared to normal placentas. In contrast in the pig it has been shown that VEGF and VEGFR1 protein expression is decreased in IUGR placentas compared to those supplying their normal sized littermates at GD60, 90 and 110.	
Arg, Leu, Gln	Arginine, Leucine, and Glutamine	Stimulate trophectoderm cell proliferation and migration by MTOR pathway activation.	Placental transport of amino acids is crucial in the regulation of foetal growth. Pregnancies complicated with IUGR are associated with aberrant amino acid transport. It has been demonstrated that treatment of rats with L-Citrulline (precursor of L-arginine and nitric oxide) and l-arginine can increase foetal weight in growth restricted rats. Evidence that supplementation of amino acids during gestation can increase birth weight, decrease within litter variation in birth weight, and decrease the incidence of growth restriction.	Regnault *et al.*, (2005); Wu *et al.*, (2006, 2010), (2017); Avagliano *et al.*, (2012); Kim *et al.*, (2013); Bourdon *et al.*, (2016)
PG	Prostaglandins	PGI2-dependent activation of PTGIR increases trophoblast cells proliferation and attachment. PGF2α through the receptor PTGFR activates MAPK1/3 kinase signalling in LE cells; stimulates VEGFA expression and secretion by the	IUGR human placental cells have decreased production of PGI2 in vitro compared to those supplying normal-sized foetuses. PTGFR investigated in relation to foetal size in chapter 7.	Jogee *et al.*, (1983); Morawska-Pucinska *et al.*, (2014); Kaczynski *et al.*, (2016)

		endometrium which stimulates proliferation of endometrial endothelial cells.		
EGF	Epidermal Growth Factor	EGF protein and mRNA expressed by endometrium and trophectoderm during implantation. Stimulates trophectoderm cell proliferation and migration by ERK1/2, MAPK and PI3K-dependent signalling	Decreased EGF expression has been observed in human placentas supplying IUGR foetuses compared to those supplying normal-sized foetuses at term.	Vaughan *et al.*, (1992); Jeong *et al.*, (2013); Rab *et al.*, (2013); Jeong and Song, (2014)
KGF	Keratinocyte Growth Factor	High expression in the porcine endometrium at GD12. The uterine expression of KGF is upregulated in response to conceptus secreted E2 during peri-implantation. Increased expression in endometrial samples in Erhulian (highly prolific) compared to Large White X Landrace at GD12.	N/A	Ka *et al.*, (2001); Zhang *et al.*, (2013)
FGF2/bFGF	Fibroblast Growth Factor 2	FGF2 and FGFR1 and 2 are expressed in porcine conceptuses and endometrial tissue during peri-implantation. Supplementing uterine LE cells with FGF2 increases proliferation and migration through PI3K/AKT and MAPK pathways.	FGF2 is an angiogenic factor and aberrant placental angiogenesis has been associated with IUGR (discussed in chapters 6-8). In human pregnancies complicated by IUGR it has been demonstrated that FGF2 is increased in both umbilical vein serum and the placenta.	Reynolds *et al.*, (2005); Wallner *et al.*, (2007); Barut *et al.*, (2010); Lim *et al.*, (2017, 2018)

Undefined abbreviations used: MAPK=Mitogen-Activated Protein Kinase; ERK1/2=Extracellular Signal-Regulated Kinase 1/2; PI3K=Phosphatidylinositol-3 Kinase; AKT=protein kinase B; mTOR=mechanistic Target of Rapamycin; GD=Gestational Day; IUGR=Intrauterine Growth Restriction; IGFBP=Insulin-Like Growth Factor Binding Protein.